Engineering microbial hosts for the production of aromatic compounds

Saez Saez, Javier

Publication date:
2023

Document Version
Publisher's PDF, also known as Version of record

Engineering microbial hosts for the production of aromatic compounds

PhD Thesis

Javier Sáez Sáez

DTU

The Novo Nordisk Foundation
Center for Biosustainability

Engineering microbial hosts for the production of aromatic compounds

PhD thesis by Javier Sáez Sáez

Main supervisor: Prof. Irina Borodina

Co-supervisors: Dr. Mahsa Babaei, Dr. Sheila Ingemann Jensen

The Novo Nordisk Foundation Center for Biosustainability

Technical University of Denmark

Preface

This PhD thesis serves as a partial fulfilment of the requirements for obtaining a PhD degree at the Technical University of Denmark. The works included in the thesis were carried out at the Novo Nordisk Foundation Center for Biosustainability in the period from March 1st, 2020 to May 31st, 2023 under the supervision of Prof. Irina Borodina, along with co-supervision of Dr. Mahsa Babaei and Dr. Sheila Ingemann Jensen. The thesis also entailed an external stay at DSM Food Specialties B.V. in Delft, the Netherlands, from September 5th, 2022 to December 15th, 2022 under the supervision of Dr. Joep Schmitz. This PhD project has been funded by the European Union's Horizon 2020 Framework Programme SHIKIFACTORY100 (grant agreement ID: 814408).

Javier Sáez Sáez

Kongens Lyngby, May 2023

Abstract

With the global population surpassing 8 billion individuals, there has been a parallel increase in demand for indispensable commodities like fuels, food, and consumer goods. Aromatic compounds play an integral role in these essential commodities, as they are widely utilized in pharmaceuticals, food ingredients, flavorings, cosmetics, and plastic precursors. However, aromatic compounds are typically sourced from non-sustainable sources, causing environmental destruction and contributing to climate change.

Biotechnological production utilizing microbial cell factories has emerged as a promising alternative for manufacturing aromatic compounds, enabling the conversion of renewable substrates into a diverse array of high-value aromatics. However, this approach faces certain limitations that hinder its widespread implementation for larger-scale production of compounds. This thesis focuses on investigating and addressing some of these challenges, aiming to provide solutions for improved utilization of biotechnological systems in aromatic compound production.

We first explore the use of the oleaginous yeast *Yarrowia lipolytica* for the production of aromatic compounds, as an alternative to *Escherichia coli* and the baker's yeast *Saccharomyces cerevisiae*, the conventional hosts typically engineered for the production of aromatics in literature. We demonstrate high-level production of the plant antioxidant resveratrol with limited genetic engineering, showing the potential of *Y. lipolytica* for the production of these compounds.

Next, we investigate *in vivo* halogenation of the aromatic amino acid L-tryptophan by the expression of tryptophan halogenases. We show how L-tryptophan can be halogenated at different positions of the molecule with either chlorine or bromine, and how these can be decarboxylated into halogenated tryptamine, precursor for a wide range of compounds with pharmaceutical applications.

Another topic researched is the toxicity of aromatic compounds against common production hosts, as many of these products are naturally produced by plants as a defense mechanism against microbes. We perform a systematic analysis of the toxicity of over 50 aromatics in multiple production hosts and use a transporter deletion library to investigate transporters that affect product tolerance and might be involved in transport mechanisms.

These findings present avenues for further exploration and innovation in developing sustainable and efficient microbial cell factories to produce valuable aromatic compounds.

Dansk resumé

Med en global befolkning på over 8 milliarder mennesker er der sket en parallel stigning i efterspørgslen af uundværlige råvarer som brændstof, fødevarer og forbrugsgoder. Aromatiske forbindelser spiller en integreret rolle i disse vigtige råvarer, da de i vid udstrækning anvendes i lægemidler, fødevareingredienser, smagsstoffer, kosmetik og som forløbere til plastik. Aromatiske forbindelser stammer imidlertid typisk fra ikke-bæredygtige kilder, hvilket forårsager miljøødelæggelse og bidrager til klimaændringer.

Bioteknologisk produktion ved hjælp af mikrobielle cellefabrikker har vist sig at være et lovende alternativ til fremstilling af aromatiske forbindelser, der gør det muligt at omdanne vedvarende substrater til en bred vifte af aromatiske stoffer af høj værdi. Denne fremgangsmåde er imidlertid underlagt visse begrænsninger, som hindrer dens udbredte anvendelse til produktion af forbindelserne i større skala. Denne afhandling fokuserer på at undersøge og løse nogle af disse udfordringer med henblik på at finde løsninger til bedre udnyttelse af bioteknologiske systemer til fremstilling af aromatiske forbindelser.

Vi undersøger først brugen af den olieholdige gær *Yarrowia lipolytica* til produktion af aromatiske forbindelser som et alternativ til *Escherichia coli* og bagegær *Saccharomyces cerevisiae*, begge konventionelle værter, der typisk er benyttet til produktion af aromatiske forbindelser i litteraturen. Vi demonstrerer produktion på højt niveau af plante antioxidanten resveratrol med minimal genmodificering, hvilket viser *Y. lipolyticas* potentiale til produktion af disse forbindelser.

Dernæst undersøger vi *in vivo* halogenering af den aromatiske aminosyre L-tryptophan ved ekspression af tryptophanhalogenaser. Vi viser, hvordan L-tryptofan kan halogeneres ved forskellige positioner i molekylet med enten klor eller brom, og hvordan disse kan decarboxyleres til halogeneret tryptamin, som er forløber for en lang række forbindelser med farmaceutiske anvendelser.

Et andet emne, der undersøges, er de aromatiske forbindelsers toksicitet over for almindelige produktionsværter, da mange af disse forbindelser produceres naturligt af planter som en forsvarsmekanisme mod mikrober. Vi udfører en systematisk analyse af toksiciteten af over 50 aromatiske stoffer i flere produktionsværter og anvender et transportordeletionsbibliotek for at undersøge transporterer, der påvirker tolerance for produktet og som kan være involveret i transportmekanismer.

Disse resultater viser muligheder for yderligere forskning og innovation i forbindelse med udvikling af bæredygtige og effektive mikrobielle cellefabrikker til produktion af værdifulde aromatiske forbindelser.

Acknowledgements

It's (finally) over. The past three years of my PhD journey have been intense and demanding, and I couldn't have made it through without the support, encouragement (and brainpower) from my circle of colleagues, friends and family. I hope not to leave anyone off the list, and if I do, may my oversights go unnoticed.

First and foremost, I am sincerely thankful to Irina for offering me the opportunity and believing in me to pursue a PhD. Your guidance, expertise, and support throughout this research journey have been instrumental in shaping the direction and quality of this thesis. I want to extend my gratitude to my co-supervisors, Mahsa and Sheila, for being always there for me whenever I needed help. Thank you Sheila for training a newcomer like myself on the basics of *E. coli*.

Most of my time during the PhD was spent alongside the team members of the Yeast Metabolic Engineering group, who were responsible for making the PhD not so burdensome and more enjoyable and manageable. Roy, even though you left CfB right after my PhD began, you have always been present throughout these years. Thank you for having smart and insightful answers to all my (stupid) scientific and non-scientific questions, and for taking the time to listen to all my complaints. Jonathan D, I greatly admire your infinite patience and your brilliant brain that consistently generates creative ideas and suggestions for all our projects. Thank you for always caring and offering valuable insights and innovative solutions, especially during moments of stress and panic. Wei, you're an absolute legend! I can't thank you enough for your jokes, sharing a bit of Chinese culture with me, and being there during moments of frustration. Guokun, your varied expertise was very valued during the early steps of my thesis. Iben, Lyubo, and Steven, thank you for taking care of the yeast transporters deletion library. Jane, thank you for always caring about how things were going. The *Dansk resumé* is also there thanks to you. Philip, thank you for being a helpful, kind-hearted and patient YME member. By the way, I hereby bestow upon you the title of *most senior PhD student*. Kiki, thank you for your efforts to make our group more social. Pawel, thank you for listening to my wave of negativity, especially during these past months of writing that seemed to be never ending. Shengbao, Daniel, and Christina, I will really miss the environment we had in the office these past months. Marc, you hold a special place in the overlapping section of the Venn diagram that represents *YME colleagues* and *friends*. As a result, you will receive most of the recognition in the corresponding section below. I have to thank you here, however, for our work-unrelated activities we enjoyed in the office during working hours.

Besides the YME team, my PhD has also been shaped by many different collaborations and support from other groups at CfB. Viktor, my Biolector comrade, thank you for suffering all the experimental struggles of the project with me and for being available for sampling at the most inconvenient times. I envy your excellent data analysis skills, and our meetings always leave me with a refreshed perspective. Paulina, thank you for being flexible in accommodating our sophisticated ideas for Biolector/ambr. Lachlan, thank you for introducing me to the magic world of Opentrons and automation. Suresh, thank you for keeping a watchful eye on my bioreactors, ensuring their well-being even during the late-night hours. Daniela, thank you for always finding time to assist me with my endless LC-MS requests.

As part of my PhD, I had the opportunity to spend nearly 4 months in Delft, the Netherlands, for my external stay at DSM. I am immensely grateful to Joep and Priscilla for accepting me and making it possible, even at the eleventh hour. Priscilla, I also extend my thanks for showing me around Delft and Koen, you were the perfect supervisor during my time there.

While these years have been mostly dedicated to science, there has also been time for activities beyond the confines of the lab. Marc, thank you for introducing me to climbing and for our *cenas de lords* that I hope will continue in the future. Thank you also for always being the one suggesting plans to drag me out of CfB. Vero, thank you for the *chokolade* breaks, for providing constructive critique to improve the aesthetics of my ugly figures, and for being there whenever needed. Marc, Vero, Paulina, Marcos, Mykha, Ari, Matt thank you for being friends outside the lab and for all the experiences and adventures we have shared together. To my friends from UPV: it's been nearly seven years since I left Valencia, and although we only get to see each other a few times a year, whenever we do, it feels as if time hasn't passed at all.

Por último, no puedo olvidarme de mi familia. Gracias por hacer posible el venir a estudiar a Dinamarca y el apoyo en la distancia durante todos estos años. Aunque no tengáis mucha idea de lo que hago, siempre he valorado vuestro interés y respaldo. Vuestra presencia y cariño han sido fundamentales en mi trayectoria y estoy eternamente agradecido por todo. Papá, espero que te leas la tesis y a partir de ahora, cuando la gente te pregunte sobre qué hago, el porcentaje de magia y fantasía disminuya y aportes datos objetivos.

List of publications

The following manuscripts constitute the primary work of this thesis:

1. Sáez-Sáez J, Wang G, Marella ER, Sudarsan S, Cernuda Pastor M, Borodina I. Engineering the oleaginous yeast *Yarrowia lipolytica* for high-level resveratrol production. *Metabolic Engineering* 2020;62:51–61.
2. Milne N, Sáez-Sáez J, Nielsen AM, Dyekjær JD, Rago D, Kristensen M, Wulff T, Borodina I.
   Engineering *Saccharomyces cerevisiae* for the *de novo* Production of Halogenated Tryptophan and Tryptamine Derivatives. *ChemistryOpen* 2023;12.
3. Sáez-Sáez J, Munro LJ, Møller-Hansen I, Kell DB, Borodina I.
   Identification of transporters involved in aromatic compounds tolerance through a deletion library screening. *Manuscript in preparation*.
4. Sáez-Sáez J†, Hesselberg-Thomsen V†, Babaei M, Borodina I.
   Understanding the physiology of *p*-coumaric acid production in *Saccharomyces cerevisiae*. *Manuscript in preparation*.

   †These authors contributed equally.

Table of contents

CHAPTER 1

Introduction

The current state of production of chemicals

The world population has increased fourfold over the past century, surpassing 8 billion inhabitants in early 2023. The global need of energy, fuels, and consumer goods has grown concomitantly, largely reliant on non-renewable resources for their production and manufacturing (Ahmad and Zhang, 2020). Coal, oil, and gas are still the main sources of energy, accounting for almost 80% of the global energy mix (International Energy Agency, 2021). Likewise, the manufacturing of fuels and consumer goods is inextricably tied to the production of a vast assortment of chemicals, which in turn are largely obtained from unsustainable resources (Meyers, 2005; Osbourn and Lanzotti, 2009).

The shift towards renewable energy sources, including solar, wind, water, and geothermal power, is gaining momentum as a sustainable alternative to non-renewable sources. Many countries have already begun transitioning to an energy mix where sustainable energies dominate (Bhattarai et al., 2022). However, while renewable energy sources provide energy, they do not supply the carbon or mass necessary to produce the chemicals used in fuels and consumer goods. The base chemicals that serve as the foundation for many everyday products are primarily derived from petrochemicals, which are produced through the refining of crude oil (Speight, 2016).

At every stage of the process, from crude oil extraction to petrochemical processing, significant environmental impacts occur. The extraction of crude oil directly disrupts the earth's natural carbon cycle equilibrium by transferring carbon sinks from the geosphere to the biosphere (Reichle, 2023). Furthermore, oil exploration, drilling, and extraction are harmful to wildlife and can reduce the quality of soil, air, and water in nearby areas (Cordes et al., 2016; Johnston et al., 2019). The drilling and extraction of oil also result in gas venting and flaring, which releases greenhouse gases and contributes to climate change (Soltanieh et al., 2016). Occasional oil spills during these steps and during transportation can have devastating effects on ecosystems (Asif et al., 2022).

Refining crude oil generates additional greenhouse and hazardous gases, consumes significant amounts of energy, and produces substantial quantities of wastewaters and hazardous solid wastes that are challenging to dispose of (Bleckmann et al., 1995;

Wake, 2005). The chemical industry, which converts petrochemicals into a variety of compounds, poses similar environmental risks (Pleissner and Kümmerer, 2018).

Despite the prevalence of chemicals derived from crude oil, plant-based alternatives such as resins, waxes, oils, dyes, flavors, fragrances, and drugs are frequently utilized for various industrial and commercial purposes (Osbourn and Lanzotti, 2009). Plant-based chemicals are often viewed as inherently sustainable, but this is not always the case. In reality, several practices used in the cultivation of crops for chemical production may result in unsustainable practices that are on par with petrochemical production. Cultivating crops for chemical production may require deforestation or land-use changes, which reduce carbon absorption and biodiversity (Cazzolla Gatti and Velichevskaya, 2020; Lawrence et al., 2022; Tanaka et al., 2021). Additionally, heavy use of fertilizers can cause eutrophication, toxic algae blooms, and habitat destruction (Chakraborty et al., 2017; Huang et al., 2017). Inadequate disposal of plant waste can lead to the release of uncontrolled amounts of methane, a potent greenhouse gas (Bakkaloglu et al., 2022).

Recent advances in biotechnology have enabled the production of a wide range of chemicals through microbial fermentation. This process involves the use of genetically modified microorganisms to convert renewable feedstocks, such as plant-based sugars and waste biomass, into high-value chemicals, including biofuels, biopolymers, and specialty chemicals (Hatti-Kaul et al., 2007; Nielsen et al., 2022). Unlike petrochemicals, which are derived from finite fossil resources, and some plant-based chemicals, which can have negative environmental impacts due to their production methods, biobased chemicals offer a sustainable and eco-friendly alternative that can help reduce our reliance on non-renewable resources and mitigate climate change (Figure 1) (Lammens et al., 2011; Broeren et al., 2017; Grasa et al., 2021).

One of the key advantages of biobased chemicals is their ability to be produced through fermentation in microbial cell factories. This process offers several benefits over traditional chemical synthesis, including high specificity and efficiency, and the ability to produce complex molecules that are difficult to produce through chemical synthesis (Du et al., 2011; Zhang et al., 2022). Additionally, microbial cell factories can be scaled up to commercial production levels, allowing for the efficient and cost-effective production of biobased chemicals at large volumes (Delvigne and Noorman, 2017; Du et al., 2022). Furthermore, the use of renewable feedstocks in fermentation reduces

the carbon footprint of biobased chemical production, making it a sustainable alternative to petrochemicals and some plant-based chemicals (Francois et al., 2020).

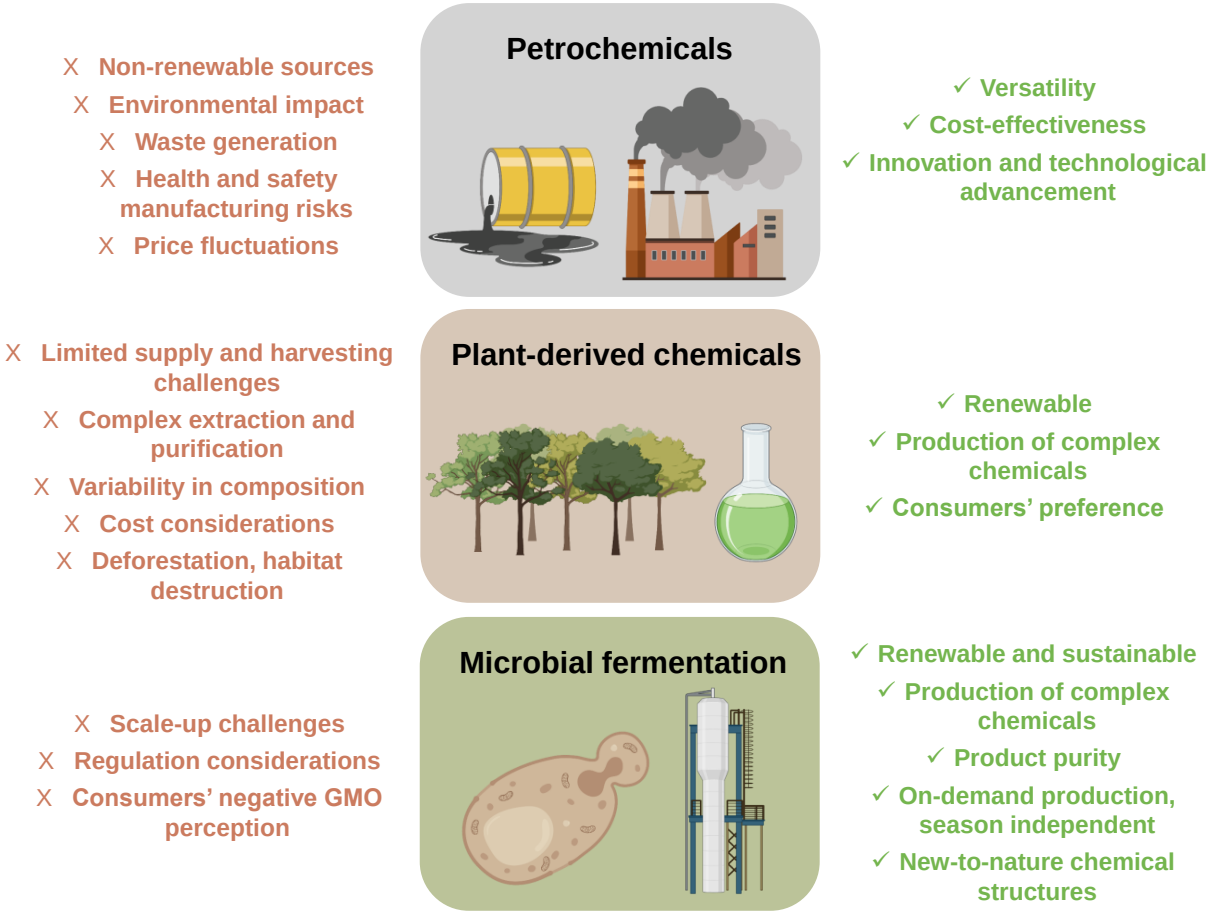

Figure 1. Current production methods for chemicals: an overview.

In spite of these benefits, there are still challenges associated with the production of biobased chemicals through fermentation, including the optimization of microbial strains, the development of robust fermentation processes, and the cost competitiveness compared to their petrochemical counterparts (Formenti et al., 2014; Liu and Nielsen, 2019; Francois et al., 2020). Nevertheless, the potential benefits of biobased chemicals make them a promising area of research that has attracted significant attention from industry, academia, and policymakers alike (Ewing et al., 2022).

From ancient times to modern applications: a brief history of microbial biomanufacturing

Microbial biotechnology has a rich history that dates back to prehistoric times (Figure 2). Before the emergence of microbiology as a scientific discipline, humans had already been using microbes for the production of fermented foods and beverages for several millennia. Evidence from archaeobotanical studies shows that bread-like products were already being consumed over 14,000 years ago in northeastern Jordan (Arranz-Otaegui et al., 2018). The production of mixed fermented beverages of rice, honey, and fruit in China or wine in Georgia can be traced back to around 6000-7000 BC according to chemical analyses in pottery fragments (McGovern et al., 2004, 2017).

In recorded history, the documentation of brewing techniques by the Sumerians in 3200-3000 BC coincided with the rise of beer as a common product and a crucial component of the economy (Damerow, 2012). Similarly, in ancient China, the process of soya fermentation was documented and played a significant economic role, as evidenced in historical records (Han et al., 2001).

Microorganisms had been utilized for thousands of years, but their existence was not officially discovered until 1674, when Antonie van Leeuwenhoek used his self-built microscope to observe and document what he called *animalcules* (Toledo-Pereyra, 2009). However, initially microbes were not credited with playing a role in fermentation processes. Over the following centuries, a number of discoveries contributed to the initial understanding of the relationship between fermentation and microorganisms.

By the beginning of the 19th century, Gay-Lussac established numerical associations for alcoholic fermentation, yet he did not provide any explanations for the underlying mechanism responsible for the process (Gay-Lussac, 1815). In the mid-1830s, a growing body of evidence suggested that yeast fermentation was a biological process. In 1837, Schwann and in 1838, Cagniard-Latour, independently demonstrated by microscopic studies that yeast is a microorganism and that alcoholic fermentation is associated with living yeast (Schwann, 1837; Cagniard-Latour, 1838). Louis Pasteur's experiments validated these findings, demonstrating the role of microorganisms in fermentation and establishing it as a biological process caused by living organisms. He developed techniques for controlling the growth of microorganisms and preventing

spoilage, which were crucial for the development of the food and beverage industry (Buchholz and Collins, 2010).

Around that time, Moritz Traube's 1858 study challenged the belief that living organisms were solely responsible for fermentation, with preliminary evidence of enzymes' role (Traube, 1858). Eduard Buchner, awarded the 1907 Nobel Prize in Chemistry, later showed that fermentation could occur in cell-free yeast extracts, thanks to enzymes, revolutionizing biochemistry and proving their significance in biological processes (Buchner, 1897).

By the end of the 19th century, industrial fermentation had emerged as a vital contributor to the economies of Europe, Asia, and North America, due to its established processes for the production of diverse food and beverage products, such as beer, wine, sake, soy sauce, and cheese (Buchholz and Collins, 2013). Simultaneously, the production of enzymes as ferments for the food industry had commenced (Fernandes, 2010). The significance of industrial fermentation was further expanded at the beginning of the 20th century with the initial development of processes for bulk chemicals production, including citric acid, gluconic acid, lactic acid, glycerol, acetone, and butanol (Garrett, 1930; May and Herrick, 1930; Sauer, 2016). The urgency of chemicals for various applications during the First World War led to improvements in fermentation processes.

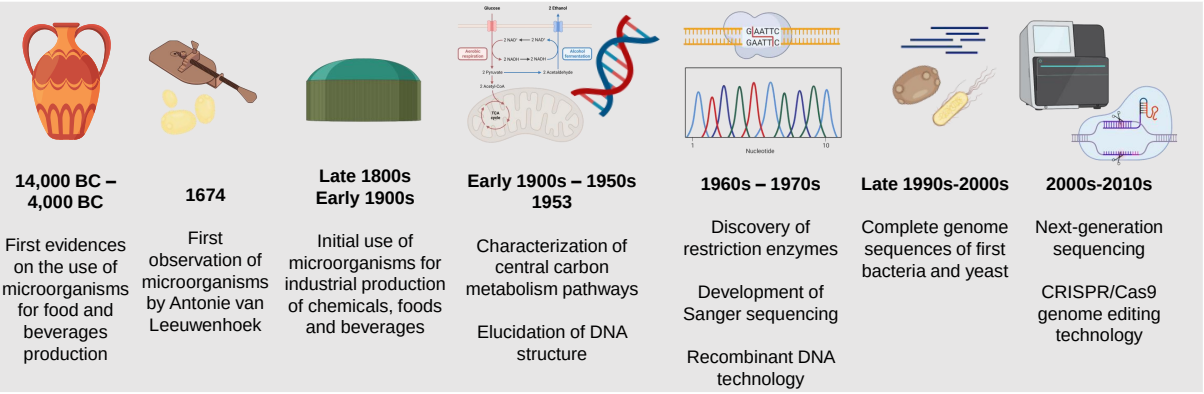

Figure 2. Milestones in the history of industrial microbiology.

In the early days of industrial fermentation, most of the products manufactured were relatively simple metabolites derived from the central carbon metabolism or closely

related pathways. However, the discovery of penicillin in 1928 marked a major milestone in the history of industrial microbiology, as it was the first complex structure to be produced using microbial fermentation (Fleming, 1929). Despite the discovery, it took until the late 1930s for the industrial production of penicillin to begin (Barreiro and García-Estrada, 2019). The outbreak of the Second World War created a global need for antibiotics, leading to the discovery and production of other antibiotics such as actinomycin, streptothricin, and streptomycin (Boruff and Lanen, 1947; Bud, 2011; Buchholz and Collins, 2013).

By the 1950s, industrial production of multiple chemicals, including antibiotics, enzymes, and food products, had become well established (Buchholz and Collins, 2013). However, from the perspective of strain engineering, there were limited methods to improve production since the knowledge of metabolic pathways was deficient, and the structure and functions of DNA had not yet been elucidated. The potential for improvement was therefore limited to the native capabilities of microorganisms, and only rudimentary mutagenesis techniques, such as those involving UV, X-rays, or chemicals, could be employed to enhance their performance (Bonner, 1946; Muñiz et al., 2007).

During the first half of the 20th century, a number of central metabolic pathways like glycolysis or the tricarboxylic acid (TCA) cycle were characterized, providing a better understanding of cellular metabolism (Krebs and Johnson, 1937a, 1937b; Krebs, 1940; Barnett, 2003). Another milestone was the elucidation of the DNA structure in 1953 by Watson and Crick, which paved the way for significant advances in our understanding of genetic information (Watson and Crick, 1953). Early work in the 1950s and 1960s then revealed the central dogma of molecular biology, describing the flow of genetic information from DNA to RNA to protein (Crick, 1970). The discovery of restriction enzymes in the late 1960s and early 1970s enabled the progress on procedures for DNA manipulation, while the development of DNA sequencing techniques in the early 1970s allowed researchers to read the nucleotide sequence of DNA directly (Kelly and Smith, 1970; Sanger et al., 1977; Loenen et al., 2014). These advancements culminated in the development of recombinant DNA technology, which revolutionized the field of genetic engineering. With this new technology, it became possible to create genetically modified microbes that could produce compounds heterologous to the host. The production of insulin in 1978 was the first successful

application of recombinant DNA technology, followed by many other biologically active substances like interferon or the human growth hormone (Goeddel et al., 1979a, 1979b; Nagata et al., 1980).

At the end of the 1990s, the first whole genome sequences became available, including the genomes of *Haemophilus influenzae*, baker's yeast *Saccharomyces cerevisiae*, and *Escherichia coli* (Fleischmann et al., 1995; Goffeau et al., 1996; Blattner et al., 1997). Since then, there has been an explosion in genome sequencing technologies, resulting in the availability of whole-genome sequences for a vast range of organisms (Giani et al., 2020). The detailed knowledge of metabolic pathways and genomes, together with genetic modification techniques, led to the development of metabolic engineering as a research area in the late 1990s (Bailey, 1991).

Metabolic engineering is a discipline that involves the optimization of cellular processes and the development of new biological systems. It applies genetic engineering techniques to modify metabolic pathways, regulatory networks, and transport systems to produce desired compounds by improving the efficiency of metabolic pathways (Woolston et al., 2013; García-Granados et al., 2019). The complexity of genomes and metabolic networks has also spurred the development of genomics, systems biology, and synthetic biology, which integrate experimental biology with mathematical modeling (Ko et al., 2020). Furthermore, the advent of targeted strain engineering has revolutionized metabolic engineering. With the identification of the Cas9 endonuclease and its versatile use as a precise, fast, and multi-target genome editing tool, researchers are now able to make targeted and accurate modifications to the genome of an organism (Jinek et al., 2012; Wright et al., 2016). These modifications have been crucial in optimizing metabolic pathways and producing a vast number of compounds with potential applications in several industries, including agriculture, energy, and pharmaceuticals (Lee et al., 2019).

Strain engineering in the modern age: insights from the DBTL cycle

In recent years, the use of microorganisms in biomanufacturing has gained significant ground, resulting in a surge of biobased products in the chemical market (Philp et al., 2013; European Commission - Joint Research Centre and BTG Biomass Technology Group B.V., 2019). However, there are challenges that hinder the widespread adoption

of microbial biomanufacturing for a broader number of products. Developing microbial cell factories is a complex and time-consuming process. In 2016, it was estimated that the cost of bringing a product to the market from a proof-of-principle strain was over 50 million USD, and could take 6-8 years to complete (Nielsen and Keasling, 2016). Biological systems have complex metabolic pathways and regulatory mechanisms that have evolved over millions of years. Our understanding of these mechanisms is still limited, and redirecting carbon flux towards the desired pathways can be challenging due to the intricate interplay between cellular, metabolic, and regulatory processes.

Strain engineering programs employ a diverse range of tools, technologies, and methodologies to overcome the hurdles in developing microbial cell factories. The Design-Build-Test-Learn (DBTL) cycle has been adopted as a typical framework in metabolic engineering to accommodate these strategies. The DBTL cycle is a four step workflow that is run in an iterative fashion until a strain design that satisfies a set of desired specifications, typically in terms of titer, rate and yield is achieved (Volk et al., 2023) (Figure 3). Beyond its utility in systematizing metabolic engineering, the DBTL cycle is also valuable in enhancing efficacy and generalizability (Check Hayden, 2015).

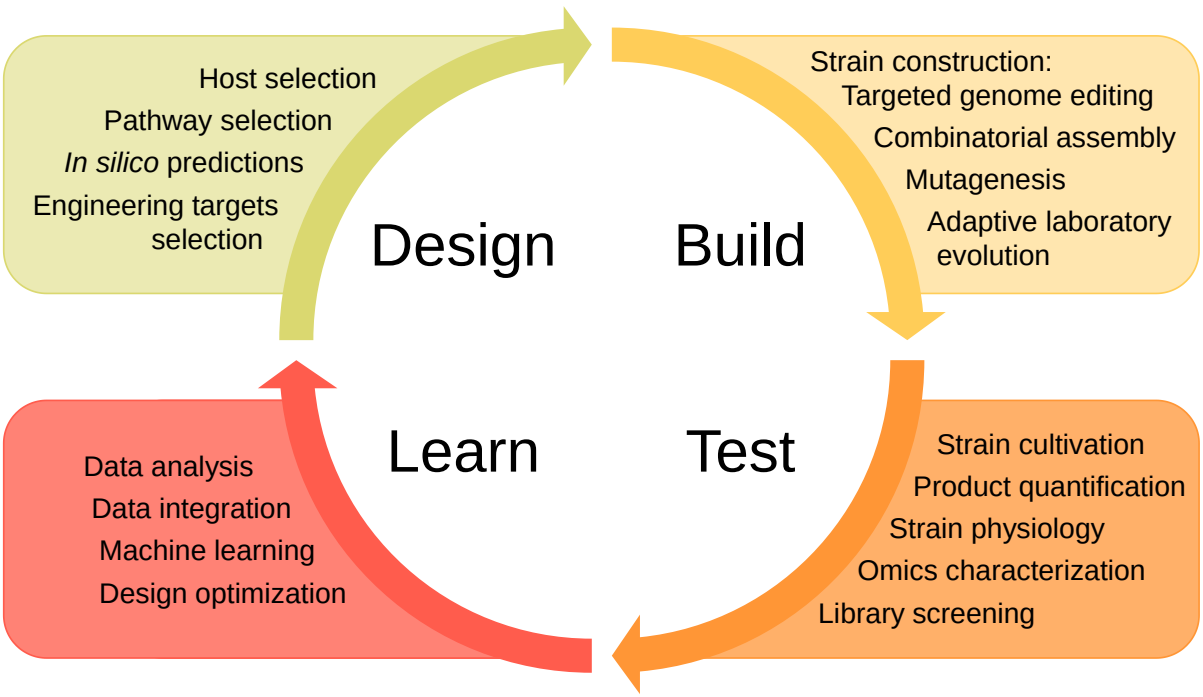

Figure 3. The Design-Build-Test-Learn (DBTL) cycle in metabolic engineering.

Design: engineering the blueprint

In the design phase of the DBTL cycle, the goal is to identify and optimize the metabolic pathway required for the production of a desired target product. The initial step in bioproduction of a desired compound is the selection of a host organism, capable of expressing the necessary metabolic pathway. Currently, the prevalent trend in metabolic engineering is to choose a host organism from a limited pool of well-established options, such as *Escherichia coli*, *Corynebacterium glutamicum*, *Saccharomyces cerevisiae* or *Yarrowia lipolytica*. These organisms have been thoroughly studied, and their genetic, metabolic and physiological characteristics are well-known. In addition, the availability of efficient genetic engineering and expression systems make them more favorable candidates than newer or exotic organisms (Lian et al., 2018; Löbs et al., 2017; Pontrelli et al., 2018; Wolf et al., 2021). The selection of a host organism is influenced by various factors such as the substrate for the bioprocess, product tolerance, or endogenous metabolic traits, including precursor availability and ease in functional expression of specific enzymes in the metabolic pathway (Pujari et al., 2021).

Conventionally, the selection of pathways and other engineering targets has been a manual process that relies on prior knowledge and data acquired from the host organism or the production of similar products derived from related or analogous pathways (Davy et al., 2017).

In the recent years, a number of computational tools have facilitated a significant part of the design process. Retrosynthesis tools enable the linking of native metabolic precursors to the target product, and generate enzymatic steps for performing all reactions in the pathway. Several tools such as RetroPath 2.0, ReactPred, Selenzyme, or recently ARBRE, specifically purposed for aromatic compounds, assist with this process (Delépine et al., 2018; Sivakumar et al., 2016; Carbonell et al., 2018; Sveshnikova et al., 2022). In cases where a putative biosynthetic pathway is missing any steps, enzyme discovery is required, which could dramatically hinder the workflow (Srinivasan and Smolke, 2020).

In addition, genome-scale metabolic models have enabled the representation of cellular metabolism in a mathematical format (Thiele and Palsson, 2010). While the initial models were purely stoichiometric and simplistic, they proved useful in

estimating maximum theoretical yields and ranking potential designs (Borodina et al., 2015; Gu et al., 2019). Subsequent algorithms have successfully predicted engineering outcomes and growth-coupled strain designs (Banerjee et al., 2020; Choi et al., 2010; Jensen et al., 2019). The latest models incorporate a range of additional constraints, including enzyme kinetics parameters, transcriptional regulations, and multi-omics data to improve the accuracy of predictions (Domenzain et al., 2022; Khodayari and Maranas, 2016; Lu et al., 2018; Niu et al., 2021).

Membrane transporters are often neglected in the design phase of engineering, mainly due to the limited knowledge of how metabolites are transported across cell membranes. However, transporter engineering has emerged as a valuable strategy for improving the performance of microbial cell factories, as demonstrated by various studies (Kell et al., 2015; van der Hoek and Borodina, 2020; Zhu et al., 2020). By manipulating transporter activity, alternative substrates can be utilized more effectively, leading to improved substrate uptake rates and volumetric productivity (Thomik et al., 2017). Moreover, transporter engineering can prevent biosynthetic intermediates from leaking out of the cell and enable the export of potentially toxic or inhibitory products, thereby improving the process economics and simplifying downstream processing (Hu et al., 2018; Korosh et al., 2017; Li et al., 2019; Wu et al., 2019).

The design phase outputs a set of *in silico* strain designs that include the expression of heterologous genes and the modulation of native gene expression through upregulation, downregulation, or complete deletion. For well-characterized and annotated production hosts, *in silico* design of DNA parts can be standardized and automated using bioinformatics tools.

Build: constructing the foundation

During the build phase, the *in silico* strain designs generated in the previous phase are translated into actual strains that can be experimentally evaluated. This process involves selecting the appropriate genetic tools and techniques for introducing the desired genetic modifications into the target organism.

For popular production hosts, like the yeasts *S. cerevisiae* and *Y. lipolytica* employed in this thesis, transformation methods as well as genetic engineering toolboxes –

especially for *S. cerevisiae*– have been well-established for a number of years (Besada-Lombana et al., 2018; Larroude et al., 2018). Genomic modifications are usually preferred over plasmid-based expression methods due to the potential for heterogeneity in expression levels within a population or loss of expression over generations (Zhang et al., 1996; Karim et al., 2013).

Traditionally, selection markers such as auxotrophic or antibiotic resistance genes were required within the genetic construct for the selection of genetically modified cells (Siewers, 2014; Larroude et al., 2018). However, the limited availability of different markers restricted the number of potential genetic modifications. An alternative strategy is to introduce loxP sites flanking the marker gene, allowing for its excision through the Cre-lox system (Gueldener, 2002). However, this approach may result in occasional genome rearrangements over multiple rounds of engineering, possibly leading to unintended effects on cell fitness. In recent years, the CRISPR/Cas9 technology has revolutionized the field by enabling marker-free genetic edits, thus allowing for a greater number of genomic modifications and the incorporation of long biosynthetic pathways (Wright et al., 2016; Zhang et al., 2022).

Genome editing toolboxes not only facilitate genetic engineering but also provide a repertoire of well-characterized genetic components, such as promoters and terminators, to precisely modulate the expression of target genes. Although complete gene deletion or strong constitutive expression are often the ultimate goals, certain applications demand a range of expression levels. In this regard, numerous yeast promoters have been thoroughly investigated to achieve precise control over gene expression or to restrict the expression to specific conditions (Madzak et al., 2000; Blazeck et al., 2012; Trassaert et al., 2017). Alternative strategies for regulating gene expression include the use of RNA-guided regulatory proteins like RNA interference (RNAi) and dead Cas9 (dCas9). RNAi exerts its action at the RNA level by cleaving targeted mRNA and has been demonstrated to modulate gene expression effectively in *S. cerevisiae* (Y. Chen et al., 2020). In contrast, dCas9 is an inactive version of the Cas9 endonuclease that operates at the DNA level by binding to specific target genes and obstructing their accessibility. However, the current level of transcriptional control achieved through this approach is limited (Deaner et al., 2017; Jensen et al., 2017).

Besides targeted genome editing, a number of approaches aim at generating genetic diversity within a population and subsequently selecting for desired phenotypes. These strategies include random mutagenesis, site-directed mutagenesis, combinatorial assembly, and adaptive laboratory evolution (ALE). Random mutagenesis involves inducing random mutations in the genome of an organism to generate new phenotypic traits (Wang et al., 2020). Site-directed mutagenesis, on the other hand, is a more precise approach that involves the targeted introduction of specific mutations into the genome (Biot-Pelletier and Martin, 2016). Combinatorial assembly is yet another strategy that allows the creation of diverse genetic sequences by combining smaller DNA fragments in various ways (Zhang et al., 2021).

ALE involves subjecting a population of microorganisms to a specific selective pressure over multiple generations to drive the evolution of a desired phenotype. By subjecting an organism to a specific selection pressure, such as a nutrient limitation or exposure to a toxic compound, the population will naturally undergo mutations that confer an advantage in that environment. Over time, these beneficial mutations become fixed in the population, leading to the evolution of a desired phenotype. Reverse engineering of non-evolved strains then enables the identification of causal mutations responsible for the evolved phenotype (Dragosits and Mattanovich, 2013; Sandberg et al., 2019). In the field of metabolic engineering, tolerance adaptive evolution (TALE) is particularly useful when the target product is toxic for the host organism (Lennen et al., 2023). A number of studies have shown how beneficial mutations for product tolerance have improved the production capabilities of a biosynthetic system. For instance, engineering tolerance to isobutyl acetate or L-phenylalanine in *E. coli* has been shown to improve production metrics in producing strains (Matson et al., 2022; Radi et al., 2022).

Among the four phases of the DBTL cycle, the build phase is particularly time-consuming. However, advancements in robotic lab automation have demonstrated significant potential in streamlining and accelerating the build phase, offering a promising avenue for more efficient strain construction (Gurdo et al., 2022).

Test: evaluating performance

The test phase of the DBTL cycle involves evaluating the constructed strains experimentally to analyze their performance. Typically, the primary parameter evaluated is product formation, which can be assessed in terms of titer (product concentration), rate (product per unit of time), and yield (product per substrate). In addition, quantification of any intermediate metabolites or by-products enables the identification of potential carbon loss or bottlenecks that could hinder optimal production efficiency. Moreover, monitoring the biomass yield and growth rate provides insights into the impact of genetic modifications and product formation on cellular physiology (Nielsen and Keasling, 2016).

Commonly used quantification methods include analytical chemistry techniques such as HPLC coupled with DAD, RI, or MS detectors and GC-MS. NMR is mainly utilized to confirm the product structure (Petzold et al., 2015; Khanijou et al., 2022). These methods might be sufficient for the number of strain designs generated in academic settings, but could become a bottleneck in industrial applications with higher throughput requirements.

High-throughput quantification of products containing chromophores or fluorophores can be achieved through absorbance or fluorescence measurements in plate readers, or by applying fluorescence-activated cell sorting (FACS) in the latter case (Rienzo et al., 2021). High-throughput chromogenic assays have been applied for the quantification of colored compounds such as violacein or carotenoids, while some non-chromogenic products have been quantified through chemical reactions with other compounds that yield a colored compound (Hui et al., 2022a, 2022b; Kozaeva et al., 2022). Likewise, FACS quantification has been applied to the efficient quantification of fluorescent molecules like riboflavin or astaxanthin in acetone (Ukibe et al., 2008; Wagner et al., 2018a).

In the case of fluorescence, moreover, biosensor-aided metabolic engineering has emerged as a promising tool for high-throughput screenings. Biosensors couple the intracellular concentration of a metabolite, typically the target product, with the expression of a fluorescent protein (Teng et al., 2022). Genetic diversity resulting from random mutagenesis, directed evolution, or combinatorial library approaches can lead to different levels of production, which can be quantified by measuring the

corresponding fluorescence signals. FACS can then be used to sort single cells with specific fluorescence features (D'Ambrosio and Jensen, 2017). Biosensors have been developed for a variety of products, with promising results when applied to strain engineering. For example, random mutagenesis and directed-evolution in combination with biosensor-guided engineering has been successfully employed to improve the production of *cis*,*cis*-muconic acid in *S. cerevisiae* (Wang et al., 2020; Jensen et al., 2021).

In addition to measuring product formation, there are instances where a comprehensive understanding of the cell factory is necessary. Multi-omics analyses, encompassing transcriptomics, proteomics, metabolomics, and fluxomics, have proven to be valuable in identifying metabolic bottlenecks or pathway sinks underlying low production efficiency. Furthermore, it assists in the comprehension of how engineered biological systems operate (Hansen et al., 2017; Kim et al., 2021).

Transcriptomics has been recognized as the most widely used omic technology in metabolic engineering due to the advancement of quantitative RNA-sequencing technologies (Hansen et al., 2017). It provides established experimental protocols, enables easy acquisition of genome-wide data, and allows for straightforward interpretation. Through comparing gene expression levels between contrasting experimental conditions or strains exhibiting different degrees of engineering, differentially expressed genes (DEGs) can be revealed and used to pinpoint the observed phenotypic differences (Kim et al., 2018). Typically, a subset of these DEGs is selected for experimental testing based on their expression levels or existing knowledge of their function. For instance, this approach has proven successful in identifying candidate genes to improve the production of polyketides or the tolerance to *n*-butanol in *E. coli* (Meng et al., 2016; Si et al., 2016). Recently, there has been an increasing interest in the integration of transcriptomics with computational tools to gain a more comprehensive understanding of cellular regulatory networks. iModulons are defined as sets of genes that are co-regulated by a common set of transcription factors, providing insight into the global regulatory architecture of cells (Sastry et al., 2019). iModulon analysis can be applied to identify regulatory modules that are relevant to a specific phenotype or condition, and can be used to predict how changes in gene expression or perturbations to the regulatory network will affect cellular behavior (Rychel et al., 2021; Lim et al., 2022).

Transcriptomics serves as an indicator of gene expression levels, but the primary effectors in cellular processes are the proteins. Several studies have highlighted the lack of strong correlation between transcripts and the corresponding protein levels for many genes (Redding-Johanson et al., 2011; Bai et al., 2015). Consequently, proteomics is increasingly preferred over transcriptomics, whenever feasible, due to its ability to provide direct measurements of proteins (Yunus and Lee, 2022). Multiple studies have applied proteomics for a number of applications, including debottlenecking pathways (Redding-Johanson et al., 2011), pathway discovery (Gregson et al., 2020) or constraining genome-scale metabolic models (Sánchez et al., 2017). Moreover, phosphoproteomics has proven to be a valuable tool for investigating the role of protein phosphorylation as a regulatory mechanism. This is exemplified by its application in the study of the effects of nitrogen limitation on the dynamics of phosphorylation of regulatory proteins in *Y. lipolytica* (Pomraning et al., 2016). Proteomics research presents several challenges, including the absolute quantification of proteins in a label-free manner, addressing the large variations in protein abundance within samples, accurately quantifying membrane-bound proteins, and analyzing post-translational modifications (Schubert et al., 2017; Chang et al., 2019; Yang et al., 2023).

Metabolomics involves the comprehensive identification and quantification of small-molecule metabolites, both intracellular and extracellular, in a biological system. This approach is valuable for gaining a broad overview of the metabolic activity within a biological sample (Iman et al., 2022). However, intracellular quantification of metabolites can be challenging in certain cultivation settings due to the need for a sub-second arrest of metabolism, faster than the turnover rates of the metabolites being investigated, which in some cases is on the order of 2-3 seconds or less (Canelas et al., 2008; Vasilakou et al., 2020). To this end, a quenching solution is typically used to rapidly halt metabolic processes, inactivate enzymes, and maintain membrane integrity, thereby avoiding leakage of intracellular metabolites (Canelas et al., 2008; Pinu et al., 2017; Kapoore and Vaidyanathan, 2018). Intracellular quantification can be a tricky methodology, requiring careful optimization to ensure accurate and reliable measurements. Despite these challenges, metabolomics remains a valuable tool for understanding the metabolic activity within biological systems and identifying potential targets for metabolic engineering (Iman et al., 2022). Metabolomics-guided approaches have successfully identified suboptimal enzymatic steps as targets for

engineering, resulting in improved production of desired compounds (Teoh et al., 2015; Ohtake et al., 2017).

Fluxomics is a powerful approach that aims to quantitatively assess the flow of carbon through metabolic pathways. This method involves the use of stable isotope tracing techniques, such as ^{13}C-based metabolic flux analysis (MFA), to track the flow of carbon derived from isotopically labeled substrates through the metabolism of cells (Buescher et al., 2015). Metabolites that have been labelled can be directly measured using LC-MS or NMR techniques to gain insights into the distribution of ^{13}C in the metabolic pathways (Sauer, 2006; Zamboni et al., 2009). Another commonly used strategy in fluxomics involves using GC-MS to analyze the incorporation of labelled carbon into proteinogenic amino acids (Long and Antoniewicz, 2019). This is particularly useful as the carbon building blocks for proteins are derived from central carbon metabolism. By combining these approaches with mathematical modeling of metabolism, fluxomics provides a powerful tool for determining the rate and direction of metabolic fluxes, allowing for a detailed understanding of the metabolic network and its regulation (Buescher et al., 2015). While fluxomics has been applied in a number of studies to improve production, such as acetol in *E. coli* (Yao et al., 2019) or to compare the metabolism of multiple yeast species (Christen and Sauer, 2011), it is currently the least used omic technology in metabolic engineering (Hansen et al., 2017). The high costs associated with labelled substrates and the advanced expertise required for data acquisition and analysis limits its broader use.

In general, omics technologies for characterizing engineered strains are not routinely used during the test phase. Instead, it is typically reserved for a limited number of strains that show promise and require a systems-level understanding for engineering or troubleshooting. The associated costs of omics techniques and the insufficient automation in data processing and analysis often hinder their widespread adoption, particularly in academic settings where resources are limited.

Learn: iterative improvement

In the final stage of the DBTL cycle, the objective is to analyze the data obtained in the previous step, summarize it, and extract insights that can be translated into a set of ideas or engineering targets for the next iteration of the DBTL cycle. However, in

practice, this stage often lacks a systematic method and instead relies on the intuition of researchers, their previous experience, and *ad hoc* observations. Moreover, negative outcomes are commonly disregarded or remain inaccessible to data mining. This can lead to researchers pursuing strategies that have a low probability of success, thereby wasting valuable time and resources (Nielsen and Keasling, 2016).

The incorporation of a standardized computational and statistical methodology could significantly improve the learn phase (Yáñez Feliú et al., 2021). With datasets continuously growing in terms of variety and intricacy, it is becoming progressively difficult for researchers to consider all the relevant aspects of the data generated. Several studies have demonstrated how computational tools can be utilized to integrate data and derive meaningful insights from it (Ramon et al., 2018; Lakrisenko and Weindl, 2021). As an example, genome-scale metabolic models have incorporated layers of information from omics datasets, including proteomics, metabolomics and transcriptomics (Lahtvee et al., 2017; Sánchez et al., 2017; Tian and Reed, 2018).

Machine learning holds great potential in the learn phase of the DBTL cycle (Lawson et al., 2021). Despite being a relatively new field, early studies have demonstrated its capacity to accelerate bioengineering in various domains, such as bioretrosynthesis (Koch et al., 2020), the prediction of enzyme commission (EC) numbers from proteomics data (Ryu et al., 2019), promoter strength (Meng et al., 2013) or production titers (Zhang et al., 2020).

Yeast as production host in biomanufacturing

As detailed in previous sections the tendency in metabolic engineering is to select a host from a reduced pool of well-characterized microorganisms and engineer them for the specific needs of the bioprocess. Among these candidates, the baker's yeast *Saccharomyces cerevisiae* is the most frequently employed eukaryotic host in metabolic engineering projects (Cho et al., 2022).

Saccharomyces cerevisiae, or budding yeast, is a versatile microorganism widely used in fermentation processes. Initially used for producing fermented foods and beverages such as bread, beer, and wine, *S. cerevisiae* is now a popular host for the production of diverse chemicals and proteins (Lian et al., 2018; Parapouli et al., 2020). It has many desirable features, including fast growth rate, ease of cultivation and

engineering, and the ability to utilize a wide range of substrates (Kavšček et al., 2015b). Many strains of *S. cerevisiae* have been recognized as generally regarded as safe (GRAS) by regulatory agencies, facilitating the approval of new processes by governmental organizations (FDA, 2023). Moreover, *S. cerevisiae* is the most extensively studied eukaryote, with research covering its cell biology, metabolism, physiology in industrial settings, and use as a model organism to study human diseases (Karathia et al., 2011; Rodrigues et al., 2021).

From a metabolic perspective, *S. cerevisiae* can grow rapidly on a diverse range of carbon sources. These include glucose, galactose, fructose, maltose, ethanol, and glycerol. Cultivation on glucose supports a relatively short doubling time of 1.25 to 2 hours at 30°C. Furthermore, *S. cerevisiae* possesses a remarkable tolerance to a range of environmental conditions, including low pH levels, which makes it well-suited for the production and downstream processing of acidic compounds. Baker's yeast can also withstand a variety of stresses commonly encountered in industrial settings, further adding to its appeal as an industrial production host. However, a metabolic limitation of *S. cerevisiae* is the Crabtree effect, which describes the tendency of the yeast to, in the excess of glucose, preferentially ferment glucose to ethanol, even under aerobic conditions, instead of completely oxidizing glucose to carbon dioxide and water via the TCA cycle (Piskur et al., 2006; Pfeiffer and Morley, 2014). Therefore, precise control of fermentation feeding profiles is necessary to prevent the carbon flux from being directed towards ethanol formation.

The genome of *S. cerevisiae* is approximately 12 Mb in size and is arranged into 16 linear chromosomes, named I to XVI. The genome sequence was completed in 1996 and found to contain 5,570 protein-encoding genes (Goffeau et al., 1996; Mackiewicz et al., 2002; Wood et al., 2001). The mitochondria of *S. cerevisiae* contain their own circular genome of approximately 85 kb in size, which encodes a number of essential genes involved in oxidative phosphorylation and energy metabolism (Osman et al., 2015; Malina et al., 2018). *S. cerevisiae* also harbors a distinct extra-chromosomal DNA genetic element called 2μ plasmid. This plasmid has a length of approximately 6.3 kb and a copy number of approximately 60 per cell (Chan et al., 2013). Although it has little phenotypic consequence for its host, it has been instrumental in the development of genetic manipulation techniques in *S. cerevisiae*.

Since the genetic modification barrier was overcome for S. cerevisiae in 1978, making it the first eukaryotic organism to be modified, a wide range of genetic engineering tools have been developed (Hinnen et al., 1978). The ease with which *S. cerevisiae* natively performs homologous recombination facilitated the integration of exogenous DNA containing homology arms to the target region. More recently, the development of advanced genome editing tools, with CRISPR-Cas9 being the most commonly adopted system, has enabled rapid, simple, low-cost, marker-free, and multiplexed genome editing of yeast. The Cas9 endonuclease, guided by a sequence-specific guide RNA (gRNA), induces a double-strand break (DSB) at the target DNA sequence, which is lethal unless repaired. The lethality is used as a negative selection marker so that transformants are obtained only when the DNA DSB is repaired. This repair is facilitated by providing a DNA construct containing sequences homologous to the target region. Besides genomic integrations and deletions using the CRISPR-Cas9 system, targeted repression or activation of gene transcription using gRNA and dCas9 has also been applied in *S. cerevisiae*, achieving different degrees of expression (Deaner et al., 2017).

Moreover, a number of genetic engineering toolboxes have facilitated the identification of integration sites with optimal expression levels and the characterization of a range promoters and terminators with varying expression levels (Jessop-Fabre et al., 2016; Lee et al., 2015). Among the commonly used promoters are *TDH3*, *TEF1*, *PGK1*, and, *TEF2* which are known for their strong and constitutive activity (Lee et al., 2013, 2015). Alternatively, inducible promoters such as *GAL1*, *CUP1*, and *MET3* have been used to control the expression of downstream genes in response to the presence or absence of galactose, Cu^{2+}, and methionine, respectively (Rönicke et al., 1997; Labbé and Thiele, 1999).

The popularity of *S. cerevisiae* as a producing host led to the reconstruction of multiple genome-scale metabolic models to guide metabolic engineering efforts. The most updated model, Yeast8, harbors data from enzymatic constraints and protein 3D structures to improve accuracy and predictability (Lu et al., 2019).

The production of chemicals and biofuels in *S. cerevisiae* through metabolic engineering has been extensively documented in the literature, with several of these products successfully reaching industrial-scale production and commercialization. (Nielsen et al., 2013; Becker et al., 2015; Zhang et al., 2017; Liu et al., 2020). Initially,

the commercialized chemicals were mostly metabolically simple bulk chemicala, such as isobutanol and lactic acid produced by GEVO and Natureworks LLC, respectively (GEVO, 2022; Rajgarhia et al., 2004). However, with the emergence of novel genetic engineering methods, more complex natural products like farnesene or plant-based compounds such as resveratrol are now being produced (Evolva, 2019; Amyris, 2023). The eukaryotic cell structure of *S. cerevisiae* is advantageous in this regard, as it enables the expression of membrane-bound proteins like cytochromes P450s that are commonly found in biosynthetic pathways for natural products (R. Chen et al., 2020; Naseri, 2023). These proteins are difficult to functionally express in bacteria, making *S. cerevisiae* an attractive host for the production of complex natural products (Zelasko et al., 2013).

Non-conventional yeasts in metabolic engineering: *Yarrowia lipolytica*

In addition to *S. cerevisiae*, several other yeasts have gained attention in the field of metabolic engineering due to their interesting metabolic traits. Among them, the oleaginous yeast *Yarrowia lipolytica* is a popular choice for the production of lipids, polyunsaturated fatty acids, and organic acids (Abdel-Mawgoud et al., 2018).

Yarrowia lipoytica is a heterothallic ascomycetous yeast commonly found in lipid and/or protein-rich substrates, such as processed meat, dairy products, or oil-polluted environments (Roostita and Fleet, 1996; Hassanshahian et al., 2012; Groenewald et al., 2014). Unlike other yeasts, *Y. lipolytica* possesses a unique set of characteristics that make it more similar to higher eukaryotes, like filamentous fungi. Consequently, it has been categorized as a non-conventional yeast. One of its most notable features is its remarkable dimorphism, as it can exist in both yeast and pseudo-hyphae forms, which depend on environmental and nutrient conditions (Barth and Gaillardin, 1997). Transition from the yeast to pseudo-hyphae form is usually triggered as a stress response to these factors (Kawasse et al., 2003). Under microscopic examination, *Y. lipolytica* cells display a spherical, ellipsoidal, or elongated structure (Kurtzman, 1998), with lipid bodies being a striking feature that can be visualized using fluorescence microscopy (Athenstaedt, 2010). These structures consist primarily of triacylglycerides (TAG) in the inner core and steryl esters (SE) in the outer core, encased by a protein-embedded phospholipid monolayer (Athenstaedt et al., 2006).

The formation of lipid bodies is induced under nitrogen or oxygen limitation, whereas demands for biomass and energy production trigger TAG and SE degradation (Abghari and Chen, 2014).

Y. lipolytica is a non-fermentative, obligate aerobe exhibiting optimal growth under well-oxygenated conditions and a cultivation temperature ranging between 25-30 °C. Most Y. lipolytica strains are unable to grow above 34 °C, which is one of the reasons why this organism is considered safe for use in various applications (Kurtzman, 1998; Groenewald et al., 2014). *Y. lipolytica* exhibits broad pH tolerance and can survive in pH values as low as 2.5; however, the metabolic profile of this yeast is highly dependent on the pH conditions (Egermeier et al., 2017).

Y. lipolytica displays a remarkable ability to utilize diverse carbon sources, including both hydrophilic and hydrophobic compounds. The hydrophilic compounds assimilated by *Y. lipolytica* include glucose, fructose, glycerol, ethanol, lactate, acetate, succinate, or citrate, as well as uncommon polyols like erythritol, mannitol, or glucitol (Barth and Gaillardin, 1996). The hydrophobic substrates that can be utilized by *Y. lipolytica* are triglycerides, fatty acids, fatty acid methyl esters, and C12-C16 alkanes (Michely et al., 2013).

The genetic information of *Y. lipolytica* is distributed across six nuclear chromosomes named A to F and one mitochondrial chromosome (Pomraning and Baker, 2015; Kerscher et al., 2001). The genomes of the most extensively studied strains, CLIB122, W29 (CLIB89), and PO1f, have been sequenced and are publicly available (Liu and Alper, 2014; Pomraning and Baker, 2015; Dujon et al., 2004). *Y. lipolytica* W29 has a total genome size of 20.3 Mb, with a G-C content of around 49.0%. These values are 1.7 and 1.3 times larger than those of the model yeast, *S. cerevisiae*, respectively (Dujon et al., 2004). However, despite its larger genome size, *Y. lipolytica* W29 has only 7,949 protein-coding genes, with a lower gene density of 0.33 genes/kb, compared to 0.5 genes/kb in *S. cerevisiae* (Dujon et al., 2004).

Yarrowia lipolytica is known for its unique ability to store large amounts of triacylglycerols (TAGs) in lipid bodies, often comprising up to 50% of the cell's dry weight (Ratledge, 2010). This impressive lipid accumulation is due to the redirection of 75-80% of the metabolic flux from glycolysis towards pyruvate dehydrogenase (PDH), which produces acetyl-CoA, a crucial precursor not only for fatty acids but also

for terpenoids and organic acids from the TCA cycle (Morgunov et al., 2004) (Figure 4).

Acetyl-CoA is primarily synthesized in the mitochondria, whereas lipid biosynthesis takes place in the cytosol. To address this spatial separation of acetyl-CoA synthesis and lipid biosynthesis, *Y. lipolytica* uses a citrate-malate antiport system dependent on nitrogen availability to mediate the bidirectional flow of acetyl-CoA between mitochondrial and cytosolic pools (Evans et al., 2005; Wasylenko et al., 2015).

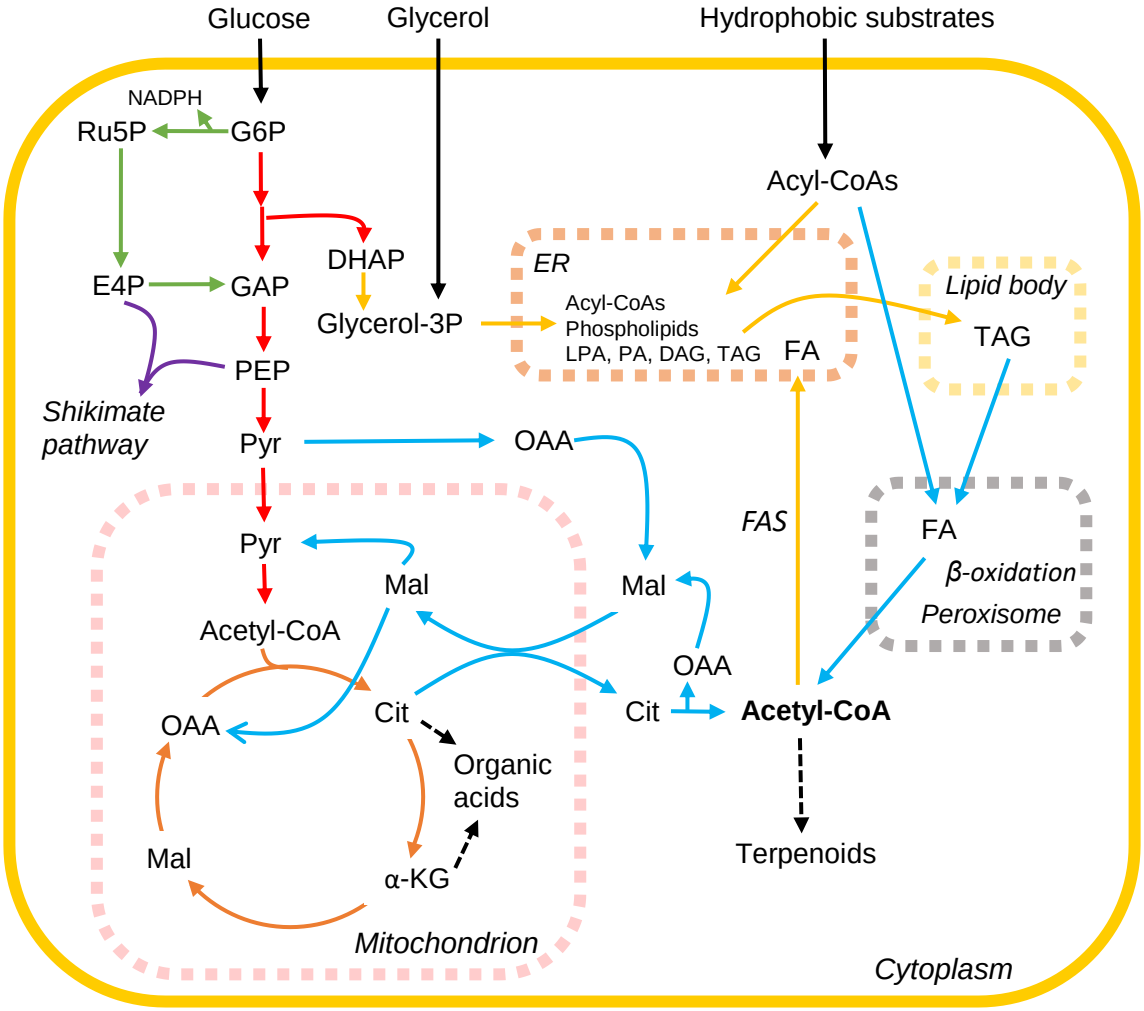

Figure 4. Main metabolic network of *Yarrowia lipolytica*. Glycolysis (red); pentose phosphate pathway (green); tricarboxylic acid cycle (orange); lipids biosynthesis (yellow); anaplerotic reactions for acetyl-CoA biosynthesis; shikimate pathway (purple).

When nitrogen is present, energy demands from protein and DNA biosynthesis stimulate high activity in the TCA cycle for ATP biosynthesis, consuming mitochondrial acetyl-CoA. Conversely, when nitrogen is depleted, AMP levels decrease and the TCA cycle is halted upon the inactivation of isocitrate dehydrogenase, an AMP-dependent enzyme. This results in an accumulation of citrate (Botham and Ratledge, 1979), which is subsequently shuttled out to the cytosol via the citrate-malate antiport. In the cytosol, ATP:citrate-lyase converts citrate back to acetyl-CoA, which serves as the two-carbon building block for the production of fatty acids (Zhang et al., 2014).

In the biosynthesis of fatty acids, acetyl-CoA is first carboxylated by acetyl-CoA carboxylase (ACC1) to yield malonyl-CoA, which serves as the extender unit in the iterative process of fatty acid elongation. In each extension round, malonyl-CoA is coupled to the growing fatty acid chain, increasing its length by two carbons. These steps are catalyzed by the enzymatic complex fatty acid synthase (FAS) and require one molecule of NADPH in each iteration round (Tai and Stephanopoulos, 2013; Tehlivets et al., 2007). In *Y. lipolytica*, the synthesis of triacylglycerols (TAGs) from fatty acids requires the coupling of three fatty acid units with glycerol-3-phosphate. Typically, these fatty acid units consist of 16 or 18 carbons in length. (Qiao et al., 2015).

NADPH, which is an essential redox cofactor required for lipid biosynthesis, is primarily synthesized through the oxidative phase of the pentose phosphate pathway (PPP) in *Y. lipolytica*. This differs from other yeasts, where the malic enzyme serves as the primary source of NADPH (Wasylenko et al., 2015; Zhang et al., 2007).

Acetyl-CoA serves not only as a fundamental constituent for the biosynthesis of fatty acids, but also as a vital precursor for TCA cycle intermediates and terpenoids. The significant metabolic flux towards acetyl-CoA in *Y. lipolytica* renders it a prospective host for the production of various compounds using it as a precursor (Abdel-Mawgoud et al., 2018; Madzak, 2021).

Y. lipolytica, as an emerging cell factory, has seen the development of several synthetic biology tools over the past few decades. Plasmids, the basic element in the engineering of any organism, were the first tools investigated. Although *Y. lipolytica* can support episomal plasmid expression, stability is a significant limitation since native plasmids have not been documented (Heslot, 1990). Episomal plasmids require both CEN and ARS elements, which cannot be separated, resulting in low-copy plasmids as the sole

type of replicative element for the oleaginous yeast (Fournier et al., 1993). Transformation of foreign DNA into *Y. lipolytica* cells can be achieved using a heat shock lithium acetate-based method that shares similarities with the transformation protocol utilized for *S. cerevisiae* (Chen et al., 1997). A broad range of markers are available to select for transformed cells, including both auxotrophic and antibiotics-based markers. Commonly employed auxotrophic markers include *leu2* and *ura3* (Madzak et al., 2000), while nourseothricin, hygromycin, and phleomycin are among the frequently used antibiotic-based selection markers (Wagner et al., 2018b). These have also been applied in transposon mutagenesis systems (Patterson et al., 2018; Wagner et al., 2018b).

In recent years, the focus has shifted towards the development of advanced tools that allow for the modulation of gene expression, rapid genetic engineering (such as the CRISPR/Cas9-based system), and the use of computational tools for rational strain design. The tuning of gene expression was initially accomplished by the identification of various native promoters that exhibit varying levels of expression (Damude et al., 2011). Subsequently, the fusion of core upstream regions from various genes resulted in the development of hybrid promoters with improved activity (Blazeck et al., 2013). Inducible promoters have also been investigated for temporal control of gene expression, with alkanes or erythritol serving as inducers (Sumita et al., 2002; Trassaert et al., 2017). The CRISPR/Cas9-based system has enabled efficient genome editing, allowing for manipulation of up to three genes simultaneously (Gao et al., 2016). Furthermore, several toolboxes based on this system have been developed, facilitatin the integration of genetic material at specific loci, deletions of genomic regions, and providing different genetic components for engineering (Holkenbrink et al., 2018; Larroude et al., 2020; Wong et al., 2017).

Lastly, in terms of computational modeling, seven genome-scale metabolic models have been reconstructed, differing in complexity and thereby producing varying levels of accuracy in their predictions (Loira et al., 2012; Pan and Hua, 2012; Kavšček et al., 2015a; Kerkhoven et al., 2016; Wei et al., 2017; Mishra et al., 2018; Guo et al., 2022; Xu et al., 2020).

Y. lipolytica has found industrial applications for over 70 years, initially using proprietary wild-type isolates or traditionally improved strains. In the 1950s, British Petroleum (BP) used *Y. lipolytica* to produce single-cell protein for livestock feed using

crude oil, resulting in the first GRAS (generally recognized as safe) notification for a process using the oleaginous yeast (Bamberg, 2000; Groenewald et al., 2014; Madzak, 2021). In the 1970s, Pfizer, Inc (USA) developed a process for the production of citric acid, later purchased to Archer Daniels Midland Company (ADM, USA) (Fried, 1972; Nubel et al., 1979; Barth et al., 2003). Nowadays, companies like Baolingbao Biology Co. (China) use proprietary wild-type strains or traditionally improved strains to produce erythritol. Similarly, Skotan SA (Poland) sells fodder yeast for farm and pet animals (Groenewald et al., 2014; Rywińska et al., 2013).

Genetic engineering allowed the production of more complex products, like the technology for carotenoids, commercialized by Microbia, Inc (USA) and later acquired by Royal DSM N.V. (the Netherlands) (Sibirny et al., 2015). DuPont created a genetically modified strain of *Y. lipolytica* to produce single-cell oils (SCOs) that are rich in eicosapentaenoic acid (EPA) (Xue et al., 2009, 2013). This technology was utilized to manufacture two products: EPA-rich SCO for human consumption and EPA-rich *Y. lipolytica* biomass for animal feed. The EPA-rich SCO was briefly marketed from 2010-2013 as New Harvest™, a vegetarian alternative to fish-based omega-3 oils. EPA-rich *Y. lipolytica* biomass produced by DuPont has been used since 2010 as an omega-3 supplement for Verlasso™, a high-quality salmon farmed by the Chilean company AquaChile (Madzak, 2021). Recently, DuPont has modified *Y. lipolytica* to produce 2'-fucosyllactose (2′FL), a major human milk oligosaccharide (HMO) and possibly other HMOs for use in infant formulas (Hollands et al., 2019).

In addition to the aforementioned examples of industrial production and commercialized products, over the past decade there has been a significant increase in the number of proof-of-principle strains, as documented in the literature (Abdel-Mawgoud et al., 2018; Madzak, 2021). Metabolic engineering of *Y. lipolytica* has focused primarily on acetyl-CoA derived products, such as terpenoids, fatty acids, and organic acids from the TCA cycle (Arnesen and Borodina, 2022; Liu et al., 2021; Ledesma-Amaro et al., 2016).

Aromatic compounds: an interesting family for biobased production

Aromatic compounds have long been of interest in both chemistry and industry due to their unique chemical properties and applications (Franck and Stadelhofer, 1988). The

term *aromatic* was first coined by August Wilhelm Hofmann in 1855 to describe organic compounds with strong, pleasant aromas (Rocke, 2015). However, it was later discovered that not all aromatic compounds have a distinct smell. Instead, they are characterized by a specific ring of atoms with delocalized electrons, known as an *aromatic ring*. These compounds follow the Hückel's rule, which states that a compound is aromatic if it is cyclic, planar, and has (4n+2) π electrons (Schleyer, 2001).

Crude oil is the most common source of bulk aromatic compounds, with benzene, toluene, and xylene (collectively referred to as BTX) being among the most commercially important. These chemicals can be extracted from petroleum by fractional distillation and further processed to create a wide range of materials, including plastics, synthetic fibers, solvents, and resins (Meyers, 2005). In fact, BTX serve as the building blocks for a plethora of other aromatics, such as phenol and styrene, which are used in the manufacture of numerous consumer goods (Sweeney and Bryan, 2000).

Plants are also a major source of aromatic compounds. These natural compounds can be found in a variety of plant parts such as leaves, stems, flowers, roots, and fruits (Talapatra and Talapatra, 2015). Aromatic compounds in plants serve a range of functions such as attracting pollinators, protecting against herbivores and pathogens, and helping with plant communication (Makkar et al., 2007). Aromatic compounds from plants have a wide range of applications in various industries, including the food, cosmetic, pharmaceutical, and fragrance industries (Barrales-Cureño et al., 2021). For example, they are used as flavors and fragrances in food, skincare products and perfumes, as well as for their medicinal properties that make them useful in drugs (Kliszcz et al., 2021; Nasim et al., 2022).

While plants are a good source of valuable aromatic compounds, economically feasible production of these chemicals from plant biomass is hindered by several factors. Firstly, due to the low concentration of bioactive compounds in plants, a significant amount of biomass must be harvested, which is further compounded by their slow growth rate (Hostetler et al., 2017; Rodriguez et al., 2017b). Secondly, the levels of relevant compounds in plants are influenced by several factors such as environmental, seasonal and geographical variation, as well as plant species and tissue (Dong and Lin,

2021). Furthermore, plants often produce a range of structurally related compounds, which complicates the purification of individual products (Jiang et al., 2005).

Although chemical synthesis provides an alternative for the extraction of compounds with simple structures, it becomes challenging for more complex compounds such as phenylpropanoids, which contain multiple active functional groups and modifications at specific positions (Zha et al., 2019). Additionally, chemical synthesis often requires the use of toxic chemical solvents and extreme reaction conditions, which adversely affect the yield and scalability of production processes (Chemler and Koffas, 2008). Furthermore, the use of chemically produced food additives is restricted by European and US legislation, and consumers are increasingly demanding natural sources for applications such as food coloring (European Parliament, 2008; Cortez et al., 2017). These challenges highlight the need for biobased production using engineered microbial cell factories as an alternative (Averesch and Krömer, 2018; Huccetogullari et al., 2019; Liu et al., 2020).

The shikimate pathway as source of aromatic precursors

Most aromatic compounds produced by microbial cell factories are biosynthesized via the shikimate pathway, which is exclusive to plants, algae, fungi, bacteria, and archaea. This pathway yields the three aromatic amino acids L-tryptophan, L-phenylalanine, and L-tyrosine, serving as a key source of aromatic precursors for the implementation of heterologous pathways to produce high-value aromatics (Mir et al., 2015) (Figure 5).

The shikimate pathway commences with the condensation of two intermediates from the Embden-Meyerhof-Parnas glycolysis (EMP) and the Pentose Phosphate Pathway (PPP): phosphoenolpyruvate (PEP) and erythrose 4-phosphate (E4P), respectively, resulting in the production of 3-deoxy-D-arabino-heptulosonic acid 7-phosphate (DAHP) (Jossek et al., 2001). DAHP is subjected to a redox reaction that leads to the formation of 3-dehydroquinate synthase (DHQ), which is then followed by a dehydration process, producing 3-dehydroshikimate (DHS) (Tzin and Galili, 2010a). Next, shikimate (SHK) is synthesized from DHS through a reducing reaction utilizing NADPH as a cofactor. The pathway then involves two consecutive phosphorylation reactions: firstly, ATP is incorporated to produce shikimate 3-phosphate (SHK-3P),

followed by the coupling of a second molecule of PEP, leading to the formation of 5-enolpyruvylshikimate-3-phosphate (EPSP) (Tzin and Galili, 2010b). Lastly, the removal of a phosphate group in EPSP leads to the synthesis of chorismate (Herrmann, 1995). From chorismate, the shikimate pathway bifurcates to produce the aromatic amino acid precursors anthranilate and prephenate, which ultimately lead to the biosynthesis of L-tryptophan (TRP) and the aromatic amino acids L-phenylalanine (PHE) and L-tyrosine (TYR), respectively (Pittard and Yang, 2008).

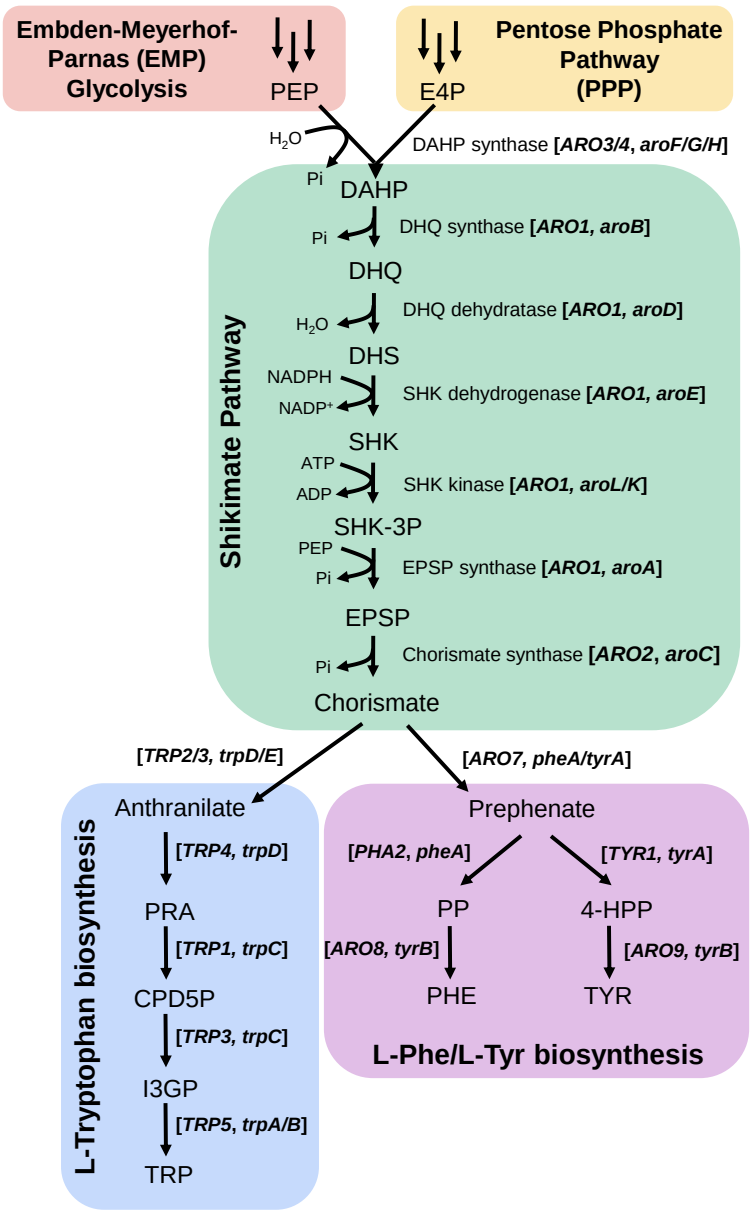

Figure 5. Shikimate and aromatic amino acids biosynthetic pathways. Enzymes and cofactors are only detailed for the shikimate pathway. Multiple arrows denote multiple enzymatic steps. *S. cerevisiae* and *E. coli* genes are described within brackets.

The shikimate pathway, its enzymes, and its regulation have been extensively studied in model organisms. The initial condensation of PEP and E4P is catalyzed by DAHP synthase, which is feedback inhibited by aromatic amino acids in both *E. coli* and *S. cerevisiae*. In *E. coli*, three isozymes (encoded by *aroF*, *aroG*, and *aroH*) perform this reaction, with each isozyme being inhibited by one of the aromatic amino acids (TYR, PHE, and TRP, respectively). Similarly, two isozymes (encoded by *ARO3* and *ARO4*) carry out the reaction in *S. cerevisiae*, with each being feedback inhibited by a different aromatic amino acid (PHE and TYR, respectively) (Brown, 1968; Helmstaedt et al., 2005). In contrast, no feedback regulation for DAHP synthases has been reported in plants (Herrmann, 1995). In *S. cerevisiae*, the next five steps of the pathway are catalyzed by the pentafunctional protein Aro1p (encoded by *ARO1*), which contains monofunctional domains responsible for each of the five reactions. However, in plants and bacteria, each step is catalyzed by a monofunctional protein encoded by a single gene. For example, in *E. coli*, AroB, AroD, AroE, AroL/K, and AroA are the enzymes responsible for these reactions, each sharing a high degree of homology with a monofunctional domain of Aro1p (Duncan et al., 1987; Rodriguez et al., 2015). The last step of the shikimate pathway, along with the reactions leading to the synthesis of TRP, TYR, and PHE, are conserved in all model organisms (Mir et al., 2015). In *S. cerevisiae*, chorismate synthase (Aro2p) catalyzes this final last step, converting EPSP into chorismate.

TRP biosynthesis comprises five enzymatic steps (Trp1-5p), commencing with the conversion of chorismate into anthranilate. Subsequently, a series of reactions generate 5-phosphoribosyl-anthranilate (PRA), 1-(2-carboxyphenylamino)-1-deoxy-D-ribulose 5-phosphate (CPD5P), indole-3-glycerol-P (I3GP) and ultimately TRP. On the other hand, PHE and TYR are biosynthesized from prephenate, produced by chorismate mutase (Aro7p). TYR has been shown to feedback-inhibit the action of Aro7p (Luttik et al., 2008). From prephenate, the pathway bifurcates, leading to the biosynthesis of phenylpyruvate (PP) and 4-hydroxyphenylpyruvate (4-HPP), catalyzed by prephenate dehydratase (Pha2p) and prephenate dehydrogenase (Tyr1p), respectively. Lastly, PHE and TYR are produced by coupling an amine group to PP and 4-HPP using two different aromatic amino transferases (Aro8p and Aro9p) (Braus, 1991).

In *Y. lipolytica*, most of the enzymatic steps from the shikimate pathway and the biosynthesis of aromatic amino acids appear to be conserved compared to *S. cerevisiae*, with one notable exception being the presence of a third DAHP synthase, named *ARO5* (Gu et al., 2020).

Products derived from the shikimate pathway: examples of biobased production

The inherent structure of the metabolites found in the shikimate pathway and its derived aromatic amino acids have been extensively leveraged as entry points for the heterologous biosynthesis of a vast array of aromatic compounds in yeast and bacteria. These compounds can be broadly categorized into three groups: (i) phenylpropanoids, (ii) alkaloids, and (iii) benzyl derivatives (Figure 6). In the following sections, examples of these families of aromatic compounds produced in *S. cerevisiae* and *Y. lipolytica*, the main hosts engineered in this PhD thesis, will be reviewed, along with the most remarkable metabolic engineering strategies pursued.

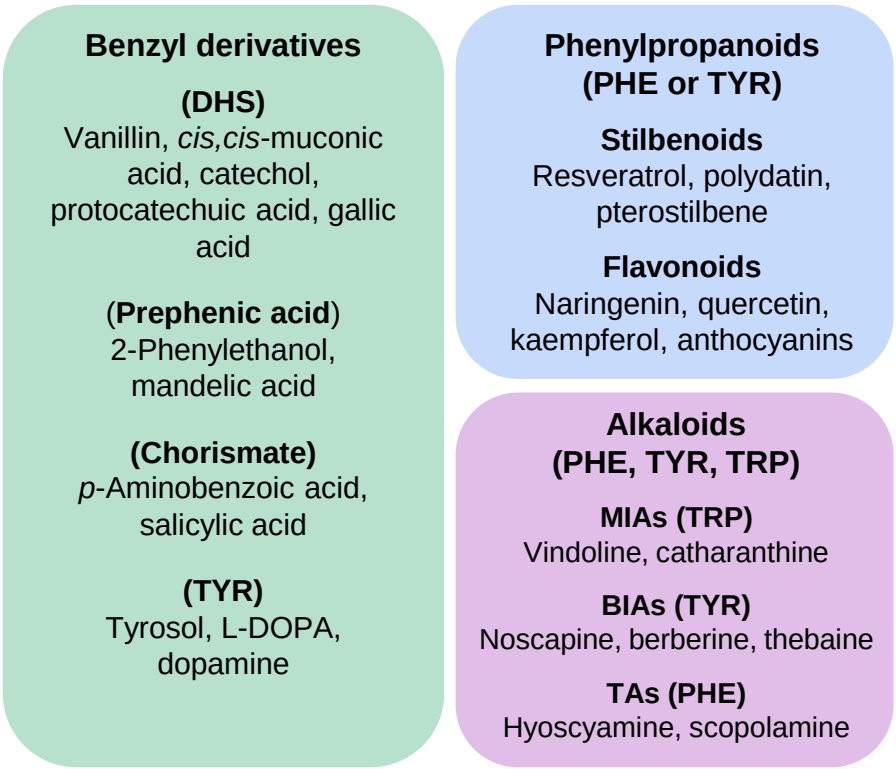

Figure 6. Major aromatic compound families produced in microbial hosts. The compounds in parentheses represent the precursor compounds for each respective family.

(i) Phenylpropanoids

The phenylpropanoid pathway in plants serves as a source of various bioactive aromatic compounds. It originates with the transamination of either PHE or TYR, leading to the production of cinnamic or *p*-coumaric acid, respectively. *p*-Coumaric acid can further be utilized to synthesize a variety of phenylpropanoids, including stilbenoids, flavonoids, condensed tannins, coumarins or hydroxyl-cinnamic acids (Vogt, 2010).

p-Coumaric acid, as a precursor for such an important array of compounds, is one of the most studied heterologous aromatics in yeast. The highest reported titer, 12.5 g/L was achieved in *S. cerevisiae* in an extensively engineered strain (Liu et al., 2019). To optimize production of *p*-coumaric acid, a series of engineering strategies were implemented to increase and balance the flux through the glycolysis, the pentose phosphate pathway, the shikimate pathway, and the aromatic amino acid (AAA) biosynthesis. Specifically, within the shikimate and AAA biosynthesis pathways, the expression of feedback-insensitive variants of Aro4p and Aro7p (*ARO4*^{K221L}, *ARO7*^{G141S}), the (over)expression of multiple key genes (*ARO1/2/3/8*, *EcaroL*, *PHA2*, *MtPHD1*), and the deletion of competing pathways (*ARO10*, *PDC5*) yielded positive outcomes. Additionally, the PHE and TYR routes for *p*-coumaric acid production were integrated to achieve a synergistic effect. To increase the supply of the limiting precursor E4P, a phosphoketalose-based approach was utilized, balancing the flux between the glycolysis and PPP. The flux between these two pathways was further fine-tuned through promoter engineering and inducible promoters.

Other studies have engineered yeast to product *p*-coumaric acid from xylose or used omic technologies, including metabolomics, transcriptomics and proteomics, to characterize or guide metabolic engineering efforts (Borja et al., 2019; Chen et al., 2021; Ciamponi et al., 2022; Rodriguez et al., 2017a). Since *p*-coumaric acid may cause toxicity to yeast cells, particularly in low pH environments, adaptive laboratory evolution (TALE) has also been implemented to identify potential engineering targets that could improve the production and secretion of the aromatic compound, with the exporter Esbp6p being one such target (Pereira et al., 2020).

Amongst the stilbenoids, resveratrol has been the most popular compound for heterologous biosynthesis in yeast (Feng et al., 2022). Resveratrol has a number of

different health-promoting properties, including antioxidant, anti-inflammatory, and anti-cancer activities, as well as cardioprotective effects (Gambini et al., 2015). In *S. cerevisiae*, production from both TYR and PHE has been investigated, with the highest titers achieved in a fed-batch fermentation using the PHE pathway (0.8 g/L) (Li et al., 2015, 2016). To improve *p*-coumaric acid production, feedback insensitive versions of *ARO4* and *ARO7* (*ARO4*^{K221L}, *ARO7*^{G141S}) were expressed, while *ARO10* was deleted to prevent the channeling of PHE into competing pathways. Since phenylpropanoid biosynthesis requires three molecules of malonyl-CoA per molecule of p-coumaric acid, the malonyl-CoA supply was also improved by expressing a feedback-resistant allele of ACC1 (acetyl-CoA carboxylase) and a post-translational modification-insensitive allele of ACS (acetyl-CoA synthase) from *Salmonella enterica*, which had a positive effect on production levels. Lastly, to address the poor catalytic activity often observed when plant-derived biosynthetic pathways are expressed in yeast, multiple copies of the biosynthetic genes were integrated to improve production.

The use of *Y. lipolytica* as a host for the production of resveratrol is the subject of Chapter 2 in this thesis (Sáez-Sáez et al., 2020). The metabolic engineering employed were similar to those used in *S. cerevisiae*, but the titers and yields obtained were significantly higher (12.4 g/L and 54.4 mg/g). Subsequent studies have also investigated the use of *Y. lipolytica* for resveratrol production, with optimization in the fermentation process resulting in even higher metrics (22.5 g/L and 65.5 mg/g) (Palmer et al., 2020; He et al., 2020; M. Liu et al., 2022). Recently, resveratrol-derivatives like polydatin, a glycosylated form, has also been successfully produced in *Y. lipolytica* with high titers (Shang et al., 2023).

Lastly, naringenin represents the most remarkable molecule within the flavonoids family. A recent study reported the highest titer of 1.18 g/L of naringenin in *S. cerevisiae*, utilizing metabolic engineering strategies similar to those employed for resveratrol production (Li et al., 2021). In addition, a glycosylation engineering approach was employed to enhance the solubility and secretion of the product out of the cell (Li et al., 2021, 2022). *Y. lipolytica* has also been engineered for naringenin production, achieving titers close to the gram-per-liter range with minimal engineering efforts. (Lv et al., 2019; Palmer et al., 2020; Wei et al., 2020).

Other flavonoids of interest produced in engineered *S. cerevisiae* are anthocyanins, water-soluble pigments responsible for the red, purple, and blue colors of many fruits,

vegetables, and flowers, including grapes, blueberries, and red cabbage (Alappat and Alappat, 2020). The complex biosynthetic pathway, which requires up to 21 heterologous genes, was successfully assembled in neochromosomes, demonstrating the feasibility of this system for long biosynthetic pathways (Postma et al., 2022).

(ii) Alkaloids

Alkaloids are naturally occurring bioactive compounds that contain at least one heterocyclic nitrogen atom, and are produced by plants, fungi, and some animals. These compounds have been used in traditional medicine for a long time, and are of interest due to their potential pharmaceutical properties (Schläger and Dräger, 2016; Heinrich et al., 2021). The primary precursors for alkaloid biosynthesis are the aromatic amino acids PHE, TYR, and TRP, as well as other amino acids. The three primary superfamilies of alkaloids produced in engineered yeast are the monoterpene indole alkaloids (MIAs), the benzylisoquinoline alkaloids (BIAs), and the tropane alkaloids (TAs).

The biosynthesis of MIAs involves the utilization of geranyl pyrophosphate and tryptophan as precursors, natively produced in yeast via the isoprenoid and shikimate pathways, respectively. However, the heterologous pathways required for the biosynthesis of MIAs involve numerous enzymatic steps, often extending into the order of tens of steps (R. Chen et al., 2020). Consequently, the process necessitates the expression of a large number of genes, along with the optimization of host endogenous pathways. Moreover, several of the heterologous enzymes require compartmentalization, further complicating the process. As a result, the DBTL cycle requires extensive troubleshooting to identify and debottleneck rate-limiting steps, making the production of MIAs a challenging endeavor in yeast. Despite the significant challenges posed by the complex biosynthesis of MIAs in yeast, recent advances have led to the successful production of several compounds, including vindoline and catharanthine (Brown et al., 2015; Qu et al., 2015; Kulagina et al., 2021; T. Liu et al., 2022; Zhang et al., 2022). Notably, this represents the longest pathway ever refactored in yeast, and offers a promising alternative to traditional plant extraction and purification processes (Ishikawa et al., 2009).

The biosynthetic pathways for benzylisoquinoline alkaloids (BIAs) and tropane alkaloids (TAs) are similarly complex, requiring extensive engineering efforts in yeast. This includes the use of functional genomics, protein engineering, and transport engineering to identify and optimize each step of the pathway, as well as achieve proper spatial organization between enzymes and substrates. Despite these challenges, recent successes have been achieved in producing various alkaloids, including noscapine, berberine, thebaine, hyoscyamine and scopolamine (Galanie et al., 2015; Li et al., 2018; Srinivasan and Smolke, 2020; Payne et al., 2021; Srinivasan and Smolke, 2021; Han and Li, 2023).

Shorter pathways, such as those of tryptamine alkaloids like psilocybin or melatonin, can be produced in yeast with fewer engineering efforts compared to more complex molecules such as MIAs, BIAs, and TAs (Germann et al., 2016; Milne et al., 2020).

Halogenation is a highly desirable feature in plant natural products and other chemicals with pharmaceutical properties, including alkaloids. The stereospecific halogenation of a molecule can have a significant impact on its properties, such as increased membrane permeability and enhanced blood-brain barrier transport (Gentry et al., 1999; Gerebtzoff et al., 2004). Halogenation can also lead to stronger binding interactions between the ligand and its target, resulting in increased ligand potency and altered pharmacokinetics (Prieto-Díaz et al., 2023; Xu et al., 2014). As a result, halogenation is a common strategy employed in the development of new pharmaceuticals, with approximately 25% of licensed drugs and 40% of new drugs in development containing halogenated moieties (Xu et al., 2014; Fejzagić et al., 2019). Despite its utility, halogenation of specific atoms within complex organic molecules like alkaloids presents a significant challenge in synthetic chemistry. The structural complexity of these molecules often makes site-specific substitution difficult to achieve, requiring directing groups, heavy metals as catalysts, and generates hazardous waste streams (Chung and Vanderwal, 2016; Maddox et al., 2015; Petrone et al., 2016; Taskesenligil et al., 2023). As an alternative, biotransformation of halogenated pathway precursors that can be taken up by the downstream enzymes in the pathway has been shown to work for multiple products. For instance, 3-iodo/chloro-L-tyrosine is successfully processed into a range of halogenated BIAs when implementing the heterologous pathway in yeast (Li et al., 2018). The high cost of halogenated precursors can impede their use in biotransformation processes,

emphasizing the necessity for alternative methodologies. *In vivo* halogenation of precursors via flavin-dependent tryptophan halogenases is one such approach. These enzymes can selectively introduce halogen atoms onto the indole ring of tryptophan, presenting a promising avenue for *de novo* biosynthesis of halogenated molecules in microbial cell factories (Bradley et al., 2020).

(iii) Benzyl derivatives

Benzyl derivatives are a class of relatively simple aromatic compounds that are commonly derived from the shikimate or the aromatic amino acid biosynthesis pathways. Examples of these products, which will be discussed below, include 2-phenylethanol, *cis*,*cis*-muconic acid, vanillin, tyrosol, and mandelic acid.

cis,*cis*-Muconic acid has various applications in the production of bioplastics and synthetic fibers (Rorrer et al., 2016; Vardon et al., 2016). The heterologous pathway branches off from DHS in three enzymatic steps that result in the cleavage of catechol, resulting in the formation of the dicarboxylic acid *cis*,*cis*-muconic acid (Xie et al., 2014; Choi et al., 2020). Since the first report on *S. cerevisiae* engineering for *cis*,*cis*-muconic acid production, various studies have been conducted until the most recent publications resulting in the production of 22.5 g/L (Wang et al., 2022). Early research revealed limitations in the heterologous pathway and metabolic imbalances, which prompted exploration of strategies such as biosensor-aided metabolic engineering, random mutagenesis, directed evolution, protein engineering, and promoter engineering (Curran et al., 2013; Johnson et al., 2016; Leavitt et al., 2017; Skjoedt et al., 2016; Snoek et al., 2018; Suástegui et al., 2017; Brückner et al., 2018; Wang et al., 2022; Jensen et al., 2021; Wang et al., 2020).

S. cerevisiae natively produces 2-phenylethanol via the Ehrlich pathway using phenylalanine as a precursor. This compound has a floral/rose scent and is utilized in the food and fragrance industries. Additionally, it can alter the sensory properties of wine and other alcoholic beverages (Hua and Xu, 2011; Cordente et al., 2021). Despite its natural production, native titers are typically low, requiring the supplementation of costly PHE to achieve high titers (Mitri et al., 2022). Consequently, metabolic engineering of *S. cerevisiae* has been explored to develop an alternative approach to bioconversion. Similar engineering targets to those utilized for *p*-coumaric acid

production have been pursued, resulting in over 1.5 g/L of 2-phenylethanol (Hassing et al., 2019).

Other benzyl/phenyl derivatives include vanillin, tyrosol, and mandelic acid. Vanillin is s commonly used as a flavoring agent in foods, beverages, and cosmetics (Olatunde et al., 2022). The toxicity of vanillin in yeast cells has led to its glycosylation to mitigate cytotoxicity and implementing biosensors to couple production to essential cellular functions (Brochado et al., 2010; D'Ambrosio et al., 2020). Tyrosol has been reported to possess various biological activities such as antioxidant, anti-inflammatory, and neuroprotective effects (Karković Marković et al., 2019). Despite being a native metabolite produced through the bioconversion of tyrosine, some metabolic engineering strategies have aimed to enhance its *de novo* production (Guo et al., 2020). Lastly, mandelic acid, a common constituent of skincare products, has been synthesized by modifying the shikimate pathway and blocking the Ehrlich apthway (Reifenrath and Boles, 2018).

The scope of this thesis

This PhD thesis is framed within the production of aromatics in microbial hosts, primarily the yeasts *S. cerevisiae* and *Y. lipolytica*. The current **Chapter 1** has provided an overview of several aspects of microbial production of aromatic compounds that are addressed in the experimental chapters described below.

In **Chapter 2**, we explore the use of *Y. lipolytica* for the production of various aromatic compounds, including resveratrol, which we demonstrate can be produced with high performance metrics. While research on the use of *Y. lipolytica* for aromatics production was limited when this PhD thesis was first defined, numerous studies over the past 3-4 years have confirmed its potential for producing a wide range of aromatic compounds.

Chapter 3 is a proof-of-principle study demonstrating the potential of *S. cerevisiae* for the production of new-to-nature halogenated aromatics. Throughout the functional expression of tryptophan halogenases, we demonstrate *in vivo* halogenation of the indole ring of tryptophan at different positions with both chlorine and bromine. Halogenated tryptophan can be further converted into halogenated

tryptamine, building block for a myriad of molecules with pharmaceutical potential within the monoterpene indole alkaloids family.

Chapter 4 addresses the issue of cytotoxicity often observed when engineering microbial hosts for the production of plant natural products, including aromatics. We perform a systematic analysis of the toxicity of tens of aromatic compounds in *E. coli*, *S. cerevisiae* and *Y. lipolytica*. Next, we screen a transporter deletion library against a subset of toxic aromatics, identifying a number of transporter-encoding genes whose deletion increases or reduces product tolerance. Finally, we demonstrate how some of the identified transporters can be used as engineering targets to improve 2-phenylethanol bioconversion in *S. cerevisiae*.

Chapter 5 reports the initial results of an ongoing study aimed at conducting a comprehensive multi-omics analysis of several *S. cerevisiae* strains that produce varying levels of *p*-coumaric acid, a fundamental precursor for phenylpropanoids.

Finally, **Chapter 6** covers the perspectives and future directions for research in this area. This chapter summarizes the main findings and contributions of the thesis, discusses their significance in the context of current knowledge, and identifies the limitations and potential avenues for future research.

References

Abdel-Mawgoud, A.M., Markham, K.A., Palmer, C.M., Liu, N., Stephanopoulos, G., Alper, H.S., 2018. Metabolic engineering in the host Yarrowia lipolytica. Metab. Eng., Metabolic Engineering Host Organism Special Issue 50, 192–208. https://doi.org/10.1016/j.ymben.2018.07.016

Abghari, A., Chen, S., 2014. Yarrowia lipolytica as an Oleaginous Cell Factory Platform for Production of Fatty Acid-Based Biofuel and Bioproducts. Front. Energy Res. 2. https://doi.org/10.3389/fenrg.2014.00021

Ahmad, T., Zhang, D., 2020. A critical review of comparative global historical energy consumption and future demand: The story told so far. Energy Rep. 6, 1973–1991. https://doi.org/10.1016/j.egyr.2020.07.020

Alappat, B., Alappat, J., 2020. Anthocyanin Pigments: Beyond Aesthetics. Molecules 25, 5500. https://doi.org/10.3390/molecules25235500

Amyris, 2023. Biofene® (or trans-β-farnesene) is a scaffold for specialty chemical applications. [WWW Document]. URL https://amyris.com/ingredient/fene

Arnesen, J.A., Borodina, I., 2022. Engineering of Yarrowia lipolytica for terpenoid production. Metab. Eng. Commun. 15, e00213. https://doi.org/10.1016/j.mec.2022.e00213

Arranz-Otaegui, A., Gonzalez Carretero, L., Ramsey, M.N., Fuller, D.Q., Richter, T., 2018. Archaeobotanical evidence reveals the origins of bread 14,400 years ago in northeastern Jordan. Proc. Natl. Acad. Sci. 115, 7925–7930. https://doi.org/10.1073/pnas.1801071115

Asif, Z., Chen, Z., An, C., Dong, J., 2022. Environmental Impacts and Challenges Associated with Oil Spills on Shorelines. J. Mar. Sci. Eng. 10, 762. https://doi.org/10.3390/jmse10060762

Athenstaedt, K., 2010. Neutral Lipids in Yeast: Synthesis, Storage and Degradation, in: Timmis, K.N. (Ed.), Handbook of Hydrocarbon and Lipid Microbiology. Springer Berlin Heidelberg, Berlin, Heidelberg, pp. 471–480. https://doi.org/10.1007/978-3-540-77587-4_35

Athenstaedt, K., Jolivet, P., Boulard, C., Zivy, M., Negroni, L., Nicaud, J.-M., Chardot, T., 2006. Lipid particle composition of the yeast Yarrowia lipolytica depends on the carbon source. PROTEOMICS 6, 1450–1459. https://doi.org/10.1002/pmic.200500339

Averesch, N.J.H., Krömer, J.O., 2018. Metabolic Engineering of the Shikimate Pathway for Production of Aromatics and Derived Compounds—Present and Future Strain Construction Strategies. Front. Bioeng. Biotechnol. 6. https://doi.org/10.3389/fbioe.2018.00032

Bai, Y., Wang, Sen, Zhong, H., Yang, Q., Zhang, F., Zhuang, Z., Yuan, J., Nie, X., Wang, Shihua, 2015. Integrative analyses reveal transcriptome-proteome correlation in biological pathways and secondary metabolism clusters in A. flavus in response to temperature. Sci. Rep. 5, 14582. https://doi.org/10.1038/srep14582

Bailey, J.E., 1991. Toward a Science of Metabolic Engineering. Science 252, 1668–1675. https://doi.org/10.1126/science.2047876

Bakkaloglu, S., Cooper, J., Hawkes, A., 2022. Life cycle environmental impact assessment of methane emissions from the biowaste management strategy of the United Kingdom: Towards net zero emissions. J. Clean. Prod. 376, 134229. https://doi.org/10.1016/j.jclepro.2022.134229

Bamberg, J.H., 2000. British Petroleum and Global Oil, 1950-1975: the challenge of nationalism. Cambridge University Press, Cambridge, UK ; New York.

Banerjee, D., Eng, T., Lau, A.K., Sasaki, Y., Wang, B., Chen, Y., Prahl, J.-P., Singan, V.R., Herbert, R.A., Liu, Y., Tanjore, D., Petzold, C.J., Keasling, J.D., Mukhopadhyay, A., 2020. Genome-scale metabolic rewiring improves titers rates and yields of the non-native product indigoidine at scale. Nat. Commun. 11, 5385. https://doi.org/10.1038/s41467-020-19171-4

Barnett, J.A., 2003. A history of research on yeasts 5: the fermentation pathway. Yeast 20, 509–543. https://doi.org/10.1002/yea.986

Barrales-Cureño, H.J., Salgado-Garciglia, R., López-Valdez, L.G., Reynoso-López, R., Herrera-Cabrera, B.E., Lucho-Constantino, G.G., Zaragoza-Martínez, F., Reyes-Reyes, C., Aftab, T., 2021. Use of Secondary Metabolites from Medicinal and Aromatic Plants in the Fragrance Industry, in: Aftab, T., Hakeem, K.R. (Eds.), Medicinal and Aromatic Plants. Springer International Publishing, Cham, pp. 669–690. https://doi.org/10.1007/978-3-030-58975-2_26

Barreiro, C., García-Estrada, C., 2019. Proteomics and Penicillium chrysogenum: Unveiling the secrets behind penicillin production. J. Proteomics 198, 119–131. https://doi.org/10.1016/j.jprot.2018.11.006

Barth, G., Beckerich, J.-M., Dominguez, A., Kerscher, S., Ogrydziak, D., Titorenko, V., Gaillardin, C., 2003. Functional genetics of Yarrowia lipolytica, in: de Winde, J.H. (Ed.), Functional Genetics of Industrial Yeasts, Topics in Current Genetics. Springer Berlin Heidelberg, Berlin, Heidelberg, pp. 227–271. https://doi.org/10.1007/3-540-37003-X_8

Barth, G., Gaillardin, C., 1997. Physiology and genetics of the dimorphic fungus *Yarrowia lipolytica*. FEMS Microbiol. Rev. 19, 219–237. https://doi.org/10.1111/j.1574-6976.1997.tb00299.x

Barth, G., Gaillardin, C., 1996. Yarrowia lipolytica, in: Nonconventional Yeasts in Biotechnology. Springer Berlin Heidelberg, Berlin, Heidelberg, pp. 313–388. https://doi.org/10.1007/978-3-642-79856-6_10

Becker, J., Lange, A., Fabarius, J., Wittmann, C., 2015. Top value platform chemicals: bio-based production of organic acids. Curr. Opin. Biotechnol. 36, 168–175. https://doi.org/10.1016/j.copbio.2015.08.022

Besada-Lombana, P.B., McTaggart, T.L., Da Silva, N.A., 2018. Molecular tools for pathway engineering in Saccharomyces cerevisiae. Curr. Opin. Biotechnol. 53, 39–49. https://doi.org/10.1016/j.copbio.2017.12.002

Bhattarai, U., Maraseni, T., Apan, A., 2022. Assay of renewable energy transition: A systematic literature review. Sci. Total Environ. 833, 155159. https://doi.org/10.1016/j.scitotenv.2022.155159

Biot-Pelletier, D., Martin, V.J.J., 2016. Seamless site-directed mutagenesis of the Saccharomyces cerevisiae genome using CRISPR-Cas9. J. Biol. Eng. 10, 6. https://doi.org/10.1186/s13036-016-0028-1

Blattner, F.R., Plunkett, G., Bloch, C.A., Perna, N.T., Burland, V., Riley, M., Collado-Vides, J., Glasner, J.D., Rode, C.K., Mayhew, G.F., Gregor, J., Davis, N.W., Kirkpatrick, H.A., Goeden, M.A., Rose, D.J., Mau, B., Shao, Y., 1997. The Complete Genome Sequence of *Escherichia coli* K-12. Science 277, 1453–1462. https://doi.org/10.1126/science.277.5331.1453

Blazeck, J., Garg, R., Reed, B., Alper, H.S., 2012. Controlling promoter strength and regulation in *Saccharomyces cerevisiae* using synthetic hybrid promoters. Biotechnol. Bioeng. 109, 2884–2895. https://doi.org/10.1002/bit.24552

Blazeck, J., Reed, B., Garg, R., Gerstner, R., Pan, A., Agarwala, V., Alper, H.S., 2013. Generalizing a hybrid synthetic promoter approach in Yarrowia lipolytica. Appl. Microbiol. Biotechnol. 97, 3037–3052. https://doi.org/10.1007/s00253-012-4421-5

Bleckmann, C.A., Rabe, B., Edgmon, S.J., Fillingame, D., 1995. Aquatic toxicity variability for fresh- and saltwater species in refinery wastewater effluent. Environ. Toxicol. Chem. 14, 1219–1223. https://doi.org/10.1002/etc.5620140714

Bonner, D., 1946. Production of biochemical mutations in Penicillium. Am. J. Bot. 33, 788–791. https://doi.org/10.1002/j.1537-2197.1946.tb12942.x

Borja, G.M., Rodriguez, A., Campbell, K., Borodina, I., Chen, Y., Nielsen, J., 2019. Metabolic engineering and transcriptomic analysis of Saccharomyces cerevisiae producing p-coumaric acid from xylose. Microb. Cell Factories 18, 191. https://doi.org/10.1186/s12934-019-1244-4

Borodina, I., Kildegaard, K.R., Jensen, N.B., Blicher, T.H., Maury, J., Sherstyk, S., Schneider, K., Lamosa, P., Herrgård, M.J., Rosenstand, I., Öberg, F., Forster, J., Nielsen, J., 2015. Establishing a synthetic pathway for high-level production of 3-hydroxypropionic acid in Saccharomyces cerevisiae via β-alanine. Metab. Eng. 27, 57–64. https://doi.org/10.1016/j.ymben.2014.10.003

Boruff, C.S., Lanen, J.M.V., 1947. The Fermentation Industry during World War II. Ind. Eng. Chem. 39, 934–937. https://doi.org/10.1021/ie50452a002

Botham, P.A., Ratledge, C., 1979. A Biochemical Explanation for Lipid Accumulation in Candida 107 and Other Oleaginous Micro-organisms. J. Gen. Microbiol. 114, 361–375. https://doi.org/10.1099/00221287-114-2-361

Bradley, S.A., Zhang, J., Jensen, M.K., 2020. Deploying Microbial Synthesis for Halogenating and Diversifying Medicinal Alkaloid Scaffolds. Front. Bioeng. Biotechnol. 8, 594126. https://doi.org/10.3389/fbioe.2020.594126

Braus, G.H., 1991. Aromatic amino acid biosynthesis in the yeast Saccharomyces cerevisiae: a model system for the regulation of a eukaryotic biosynthetic pathway. Microbiol. Rev. 55, 349–370. https://doi.org/10.1128/mr.55.3.349-370.1991

Brochado, A.R., Matos, C., Møller, B.L., Hansen, J., Mortensen, U.H., Patil, K.R., 2010. Improved vanillin production in baker's yeast through in silico design. Microb. Cell Factories 9, 84. https://doi.org/10.1186/1475-2859-9-84

Broeren, M.L.M., Zijp, M.C., Waaijers-van der Loop, S.L., Heugens, E.H.W., Posthuma, L., Worrell, E., Shen, L., 2017. Environmental assessment of bio-based chemicals in early-stage development: a review of methods and indicators. Biofuels Bioprod. Biorefining 11, 701–718. https://doi.org/10.1002/bbb.1772

Brown, K.D., 1968. Regulation of aromatic amino acid biosynthesis in *Escherichia coli* K12. Genetics 60, 31–48. https://doi.org/10.1093/genetics/60.1.31

Brown, S., Clastre, M., Courdavault, V., O'Connor, S.E., 2015. De novo production of the plant-derived alkaloid strictosidine in yeast. Proc. Natl. Acad. Sci. 112, 3205–3210. https://doi.org/10.1073/pnas.1423555112

Brückner, C., Oreb, M., Kunze, G., Boles, E., Tripp, J., 2018. An expanded enzyme toolbox for production of cis, cis-muconic acid and other shikimate pathway derivatives in Saccharomyces cerevisiae. FEMS Yeast Res. 18. https://doi.org/10.1093/femsyr/foy017

Buchholz, K., Collins, J., 2013. The roots—a short history of industrial microbiology and biotechnology. Appl. Microbiol. Biotechnol. 97, 3747–3762. https://doi.org/10.1007/s00253-013-4768-2

Buchholz, K., Collins, J., 2010. Concepts in biotechnology: history, science and business. Wiley-VCH, Weinheim, Germany.

Buchner, E., 1897. Alkoholische Gärung ohne Hefezellen. Berichte Dtsch. Chem. Ges. 30, 1110–1113. https://doi.org/10.1002/cber.189703001215

Bud, R., 2011. Innovators, deep fermentation and antibiotics: promoting applied science before and after the Second World War. Dynamis 31, 323–341. https://doi.org/10.4321/S0211-95362011000200004

Buescher, J.M., Antoniewicz, M.R., Boros, L.G., Burgess, S.C., Brunengraber, H., Clish, C.B., DeBerardinis, R.J., Feron, O., Frezza, C., Ghesquiere, B., Gottlieb, E., Hiller, K., Jones, R.G., Kamphorst, J.J., Kibbey, R.G., Kimmelman, A.C., Locasale, J.W., Lunt, S.Y., Maddocks, O.D., Malloy, C., Metallo, C.M., Meuillet, E.J., Munger, J., Nöh, K., Rabinowitz, J.D., Ralser, M., Sauer, U., Stephanopoulos, G., St-Pierre, J., Tennant, D.A., Wittmann, C., Vander Heiden, M.G., Vazquez, A., Vousden, K., Young, J.D., Zamboni, N., Fendt, S.-M., 2015. A roadmap for interpreting 13 C metabolite labeling patterns from cells. Curr. Opin. Biotechnol. 34, 189–201. https://doi.org/10.1016/j.copbio.2015.02.003

Cagniard-Latour, C., 1838. Mémoire sur la fermentation vineuse. Ann. Chim. 68.

Canelas, A.B., Ras, C., ten Pierick, A., van Dam, J.C., Heijnen, J.J., van Gulik, W.M., 2008. Leakage-free rapid quenching technique for yeast metabolomics. Metabolomics 4, 226–239. https://doi.org/10.1007/s11306-008-0116-4

Carbonell, P., Wong, J., Swainston, N., Takano, E., Turner, N.J., Scrutton, N.S., Kell, D.B., Breitling, R., Faulon, J.-L., 2018. Selenzyme: enzyme selection tool for pathway design. Bioinformatics 34, 2153–2154. https://doi.org/10.1093/bioinformatics/bty065

Cazzolla Gatti, R., Velichevskaya, A., 2020. Certified "sustainable" palm oil took the place of endangered Bornean and Sumatran large mammals habitat and tropical forests in the last 30 years. Sci. Total Environ. 742, 140712. https://doi.org/10.1016/j.scitotenv.2020.140712

Chakraborty, S., Tiwari, P.K., Sasmal, S.K., Misra, A.K., Chattopadhyay, J., 2017. Effects of fertilizers used in agricultural fields on algal blooms. Eur. Phys. J. Spec. Top. 226, 2119–2133. https://doi.org/10.1140/epjst/e2017-70031-7

Chan, K.-M., Liu, Y.-T., Ma, C.-H., Jayaram, M., Sau, S., 2013. The 2 micron plasmid of Saccharomyces cerevisiae: A miniaturized selfish genome with optimized functional competence. Plasmid 70, 2–17. https://doi.org/10.1016/j.plasmid.2013.03.001

Chang, C., Gao, Z., Ying, W., Fu, Y., Zhao, Y., Wu, S., Li, M., Wang, G., Qian, X., Zhu, Y., He, F., 2019. LFAQ: Toward Unbiased Label-Free Absolute Protein Quantification by Predicting Peptide Quantitative Factors. Anal. Chem. 91, 1335–1343. https://doi.org/10.1021/acs.analchem.8b03267

Check Hayden, E., 2015. Synthetic biologists seek standards for nascent field. Nature 520, 141–142. https://doi.org/10.1038/520141a

Chemler, J.A., Koffas, M.A., 2008. Metabolic engineering for plant natural product biosynthesis in microbes. Curr. Opin. Biotechnol. 19, 597–605. https://doi.org/10.1016/j.copbio.2008.10.011

Chen, D.-C., Beckerich, J.-M., Gaillardin, C., 1997. One-step transformation of the dimorphic yeast Yarrowia lipolytica. Appl. Microbiol. Biotechnol. 48, 232–235. https://doi.org/10.1007/s002530051043

Chen, R., Yang, S., Zhang, L., Zhou, Y.J., 2020. Advanced Strategies for Production of Natural Products in Yeast. iScience 23, 100879. https://doi.org/10.1016/j.isci.2020.100879

Chen, Y., Guo, E., Zhang, J., Si, T., 2020. Advances in RNAi-Assisted Strain Engineering in Saccharomyces cerevisiae. Front. Bioeng. Biotechnol. 8, 731. https://doi.org/10.3389/fbioe.2020.00731

Chen, Yu, Li, F., Mao, J., Chen, Yun, Nielsen, J., 2021. Yeast optimizes metal utilization based on metabolic network and enzyme kinetics. Proc. Natl. Acad. Sci. 118, e2020154118. https://doi.org/10.1073/pnas.2020154118

Cho, J.S., Kim, G.B., Eun, H., Moon, C.W., Lee, S.Y., 2022. Designing Microbial Cell Factories for the Production of Chemicals. JACS Au 2, 1781–1799. https://doi.org/10.1021/jacsau.2c00344

Choi, H.S., Lee, S.Y., Kim, T.Y., Woo, H.M., 2010. *In Silico* Identification of Gene Amplification Targets for Improvement of Lycopene Production. Appl. Environ. Microbiol. 76, 3097–3105. https://doi.org/10.1128/AEM.00115-10

Choi, S., Lee, H.-N., Park, E., Lee, S.-J., Kim, E.-S., 2020. Recent Advances in Microbial Production of cis,cis-Muconic Acid. Biomolecules 10, 1238. https://doi.org/10.3390/biom10091238

Christen, S., Sauer, U., 2011. Intracellular characterization of aerobic glucose metabolism in seven yeast species by 13C flux analysis and metabolomics: Flux response to Crabtree effect in yeast species. FEMS Yeast Res. 11, 263–272. https://doi.org/10.1111/j.1567-1364.2010.00713.x

Chung, W., Vanderwal, C.D., 2016. Stereoselective Halogenation in Natural Product Synthesis. Angew. Chem. Int. Ed. 55, 4396–4434. https://doi.org/10.1002/anie.201506388

Ciamponi, F.E., Procópio, D.P., Murad, N.F., Franco, T.T., Basso, T.O., Brandão, M.M., 2022. Multi-omics network model reveals key genes associated with p-coumaric acid stress response in an industrial yeast strain. Sci. Rep. 12, 22466. https://doi.org/10.1038/s41598-022-26843-2

Cordente, A.G., Espinase Nandorfy, D., Solomon, M., Schulkin, A., Kolouchova, R., Francis, I.L., Schmidt, S.A., 2021. Aromatic Higher Alcohols in Wine: Implication on Aroma and Palate Attributes during Chardonnay Aging. Molecules 26, 4979. https://doi.org/10.3390/molecules26164979

Cordes, E.E., Jones, D.O.B., Schlacher, T.A., Amon, D.J., Bernardino, A.F., Brooke, S., Carney, R., DeLeo, D.M., Dunlop, K.M., Escobar-Briones, E.G., Gates, A.R., Génio, L., Gobin, J., Henry, L.-A., Herrera, S., Hoyt, S., Joye, M., Kark, S., Mestre, N.C., Metaxas, A., Pfeifer, S., Sink, K., Sweetman, A.K., Witte, U., 2016. Environmental Impacts of the Deep-Water Oil and Gas Industry: A Review to Guide Management Strategies. Front. Environ. Sci. 4. https://doi.org/10.3389/fenvs.2016.00058

Cortez, R., Luna-Vital, D.A., Margulis, D., Gonzalez de Mejia, E., 2017. Natural Pigments: Stabilization Methods of Anthocyanins for Food Applications: Stabilization of natural pigments…. Compr. Rev. Food Sci. Food Saf. 16, 180–198. https://doi.org/10.1111/1541-4337.12244

Crick, F., 1970. Central Dogma of Molecular Biology. Nature 227, 561–563. https://doi.org/10.1038/227561a0

Curran, K.A., Leavitt, J.M., Karim, A.S., Alper, H.S., 2013. Metabolic engineering of muconic acid production in Saccharomyces cerevisiae. Metab. Eng. 15, 55–66. https://doi.org/10.1016/j.ymben.2012.10.003

D'Ambrosio, V., Dore, E., Di Blasi, R., van den Broek, M., Sudarsan, S., Horst, J. ter, Ambri, F., Sommer, M.O.A., Rugbjerg, P., Keasling, J.D., Mans, R., Jensen, M.K., 2020. Regulatory control circuits for stabilizing long-term anabolic product formation in yeast. Metab. Eng. 61, 369–380. https://doi.org/10.1016/j.ymben.2020.07.006

D'Ambrosio, V., Jensen, M.K., 2017. Lighting up yeast cell factories by transcription factor-based biosensors. FEMS Yeast Res. 17. https://doi.org/10.1093/femsyr/fox076

Damerow, P., 2012. Sumerian Beer: The Origins of Brewing Technology in Ancient Mesopotamia. Cuneiform Digital Library Journal 2, 20.

Damude, H.G., Gillies, P.J., Macool, D.J., Picataggio, S.K., Pollak, D.M.W., Ragghianti, J.J., Xue, Z., Yadav, N.S., Zhang, H., Zhu, Q.Q., 2011. High eicosapentaenoic acid producing strains of Yarrowia lipolytica. US7932077B2.

Davy, A.M., Kildegaard, H.F., Andersen, M.R., 2017. Cell Factory Engineering. Cell Syst. 4, 262–275. https://doi.org/10.1016/j.cels.2017.02.010

Deaner, M., Mejia, J., Alper, H.S., 2017. Enabling Graded and Large-Scale Multiplex of Desired Genes Using a Dual-Mode dCas9 Activator in *Saccharomyces cerevisiae*. ACS Synth. Biol. 6, 1931–1943. https://doi.org/10.1021/acssynbio.7b00163

Delépine, B., Duigou, T., Carbonell, P., Faulon, J.-L., 2018. RetroPath2.0: A retrosynthesis workflow for metabolic engineers. Metab. Eng. 45, 158–170. https://doi.org/10.1016/j.ymben.2017.12.002

Delvigne, F., Noorman, H., 2017. Scale-up/Scale-down of microbial bioprocesses: a modern light on an old issue. Microb. Biotechnol. 10, 685–687. https://doi.org/10.1111/1751-7915.12732

Domenzain, I., Sánchez, B., Anton, M., Kerkhoven, E.J., Millán-Oropeza, A., Henry, C., Siewers, V., Morrissey, J.P., Sonnenschein, N., Nielsen, J., 2022. Reconstruction of a catalogue of genome-scale metabolic models with enzymatic constraints using GECKO 2.0. Nat. Commun. 13, 3766. https://doi.org/10.1038/s41467-022-31421-1

Dong, N., Lin, H., 2021. Contribution of phenylpropanoid metabolism to plant development and plant–environment interactions. J. Integr. Plant Biol. 63, 180–209. https://doi.org/10.1111/jipb.13054

Dragosits, M., Mattanovich, D., 2013. Adaptive laboratory evolution – principles and applications for biotechnology. Microb. Cell Factories 12, 64. https://doi.org/10.1186/1475-2859-12-64

Du, J., Shao, Z., Zhao, H., 2011. Engineering microbial factories for synthesis of value-added products. J. Ind. Microbiol. Biotechnol. 38, 873–890. https://doi.org/10.1007/s10295-011-0970-3

Du, Y.-H., Wang, M.-Y., Yang, L.-H., Tong, L.-L., Guo, D.-S., Ji, X.-J., 2022. Optimization and Scale-Up of Fermentation Processes Driven by Models. Bioengineering 9, 473. https://doi.org/10.3390/bioengineering9090473

Dujon, B., Sherman, D., Fischer, G., Durrens, P., Casaregola, S., Lafontaine, I., de Montigny, J., Marck, C., Neuvéglise, C., Talla, E., Goffard, N., Frangeul, L., Aigle, M., Anthouard, V., Babour, A., Barbe, V., Barnay, S., Blanchin, S., Beckerich, J.-M., Beyne, E., Bleykasten, C., Boisramé, A., Boyer, J., Cattolico, L., Confanioleri, F., de Daruvar, A., Despons, L., Fabre, E., Fairhead, C., Ferry-Dumazet, H., Groppi, A., Hantraye, F., Hennequin, C., Jauniaux, N., Joyet, P., Kachouri, R., Kerrest, A., Koszul, R., Lemaire, M., Lesur, I., Ma, L., Muller, H., Nicaud, J.-M., Nikolski, M., Oztas, S., Ozier-Kalogeropoulos, O., Pellenz, S., Potier, S., Richard, G.-F., Straub, M.-L., Suleau, A., Swennen, D., Tekaia, F., Wésolowski-Louvel, M., Westhof, E., Wirth, B., Zeniou-Meyer, M., Zivanovic, I., Bolotin-Fukuhara, M., Thierry, A., Bouchier, C., Caudron, B., Scarpelli, C., Gaillardin, C., Weissenbach, J., Wincker, P., Souciet, J.-L., 2004. Genome evolution in yeasts. Nature 430, 35–44. https://doi.org/10.1038/nature02579

Duncan, K., Edwards, R.M., Coggins, J.R., 1987. The pentafunctional *arom* enzyme of *Saccharomyces cerevisiae* is a mosaic of monofunctional domains. Biochem. J. 246, 375–386. https://doi.org/10.1042/bj2460375

Egermeier, M., Russmayer, H., Sauer, M., Marx, H., 2017. Metabolic Flexibility of Yarrowia lipolytica Growing on Glycerol. Front. Microbiol. 8. https://doi.org/10.3389/fmicb.2017.00049

European Commission - Joint Research Centre, BTG Biomass Technology Group B.V., 2019. Insights into the European market for bio-based chemicals: factsheets for 10 biobased product categories. Publications Office, LU.

European Parliament, 2008. Regulation (EC) No 1334/2008 of the European Parliament and of the Council of 16 December 2008 on flavourings and certain food ingredients with

flavouring properties for use in and on foods and amending Council Regulation (EEC) No 1601/91, Regulations (EC) No 2232/96 and (EC) No 110/2008 and Directive 2000/13/EC (Text with EEA relevance), OJ L.

Evans, C.T., Scragg, A.H., Ratledge, C., 2005. A Comparative Study of Citrate Efflux from Mitochondria of Oleaginous and Non-oleaginous Yeasts. Eur. J. Biochem. 130, 195–204. https://doi.org/10.1111/j.1432-1033.1983.tb07136.x

Evolva, 2019. Veri-te Resveratrol. Evolva. [WWW Document]. URL https://veriteresveratrol.com/wp-content/uploads/2019/01/Veri-te-Resveratrol-Brochure.pdf (accessed 4.5.23).

Ewing, T.A., Nouse, N., van Lint, M., van Haveren, J., Hugenholtz, J., van Es, D.S., 2022. Fermentation for the production of biobased chemicals in a circular economy: a perspective for the period 2022–2050. Green Chem. 24, 6373–6405. https://doi.org/10.1039/D1GC04758B

FDA, 2023. Recently Published GRAS Notices and FDA Letters.

Fejzagić, A.V., Gebauer, J., Huwa, N., Classen, T., 2019. Halogenating Enzymes for Active Agent Synthesis: First Steps Are Done and Many Have to Follow. Molecules 24, 4008. https://doi.org/10.3390/molecules24214008

Feng, C., Chen, J., Ye, W., Liao, K., Wang, Z., Song, X., Qiao, M., 2022. Synthetic Biology-Driven Microbial Production of Resveratrol: Advances and Perspectives. Front. Bioeng. Biotechnol. 10, 833920. https://doi.org/10.3389/fbioe.2022.833920

Fernandes, P., 2010. Enzymes in Food Processing: A Condensed Overview on Strategies for Better Biocatalysts. Enzyme Res. 2010, 1–19. https://doi.org/10.4061/2010/862537

Fleischmann, R.D., Adams, M.D., White, O., Clayton, R.A., Kirkness, E.F., Kerlavage, A.R., Bult, C.J., Tomb, J.-F., Dougherty, B.A., Merrick, J.M., McKenney, K., Sutton, G., FitzHugh, W., Fields, C., Gocayne, J.D., Scott, J., Shirley, R., Liu, L., Glodek, A., Kelley, J.M., Weidman, J.F., Phillips, C.A., Spriggs, T., Hedblom, E., Cotton, M.D., Utterback, T.R., Hanna, M.C., Nguyen, D.T., Saudek, D.M., Brandon, R.C., Fine, L.D., Fritchman, J.L., Fuhrmann, J.L., Geoghagen, N.S.M., Gnehm, C.L., McDonald, L.A., Small, K.V., Fraser, C.M., Smith, H.O., Venter, J.C., 1995. Whole-Genome Random Sequencing and Assembly of *Haemophilus influenzae* Rd. Science 269, 496–512. https://doi.org/10.1126/science.7542800

Fleming, A., 1929. On the Antibacterial Action of Cultures of a Penicillium, with Special Reference to their Use in the Isolation of B. influenzæ. Br. J. Exp. Pathol. 10, 226.

Formenti, L.R., Nørregaard, A., Bolic, A., Hernandez, D.Q., Hagemann, T., Heins, A.-L., Larsson, H., Mears, L., Mauricio-Iglesias, M., Krühne, U., Gernaey, K.V., 2014. Challenges in industrial fermentation technology research. Biotechnol. J. 9, 727–738. https://doi.org/10.1002/biot.201300236

Fournier, P., Abbas, A., Chasles, M., Kudla, B., Ogrydziak, D.M., Yaver, D., Xuan, J.W., Peito, A., Ribet, A.M., Feynerol, C., 1993. Colocalization of centromeric and replicative functions on autonomously replicating sequences isolated from the yeast Yarrowia lipolytica. Proc. Natl. Acad. Sci. 90, 4912–4916. https://doi.org/10.1073/pnas.90.11.4912

Franck, H.-G., Stadelhofer, J.W., 1988. Industrial aromatic chemistry: raw materials, processes, products. Springer-Verlag, Berlin ; New York.

Francois, J.M., Alkim, C., Morin, N., 2020. Engineering microbial pathways for production of bio-based chemicals from lignocellulosic sugars: current status and perspectives. Biotechnol. Biofuels 13, 118. https://doi.org/10.1186/s13068-020-01744-6

Fried, J.H., 1972. Method of producing citric acid by fermentation. US3632476A.

Galanie, S., Thodey, K., Trenchard, I.J., Filsinger Interrante, M., Smolke, C.D., 2015. Complete biosynthesis of opioids in yeast. Science 349, 1095–1100. https://doi.org/10.1126/science.aac9373

Gambini, J., Inglés, M., Olaso, G., Lopez-Grueso, R., Bonet-Costa, V., Gimeno-Mallench, L., Mas-Bargues, C., Abdelaziz, K.M., Gomez-Cabrera, M.C., Vina, J., Borras, C., 2015. Properties of Resveratrol: *In Vitro* and *In Vivo* Studies about Metabolism,

Bioavailability, and Biological Effects in Animal Models and Humans. Oxid. Med. Cell. Longev. 2015, 1–13. https://doi.org/10.1155/2015/837042

Gao, S., Tong, Y., Wen, Z., Zhu, L., Ge, M., Chen, D., Jiang, Y., Yang, S., 2016. Multiplex gene editing of the *Yarrowia lipolytica* genome using the CRISPR-Cas9 system. J. Ind. Microbiol. Biotechnol. 43, 1085–1093. https://doi.org/10.1007/s10295-016-1789-8

García-Granados, R., Lerma-Escalera, J.A., Morones-Ramírez, J.R., 2019. Metabolic Engineering and Synthetic Biology: Synergies, Future, and Challenges. Front. Bioeng. Biotechnol. 7, 36. https://doi.org/10.3389/fbioe.2019.00036

Garrett, J.F., 1930. Lactic Acid. Ind. Eng. Chem. 22, 1153–1154. https://doi.org/10.1021/ie50251a011

Gay-Lussac, J.-L., 1815. Lettre à M. Clément sur l'analyse de l'alcool et de l'éther sulfurique et sur les produits de la fermentation. Ann. Chim. 311–318.

Gentry, C.L., Egleton, R.D., Gillespie, T., Abbruscato, T.J., Bechowski, H.B., Hruby, V.J., Davis, T.P., 1999. The effect of halogenation on blood–brain barrier permeability of a novel peptide drug☆. Peptides 20, 1229–1238. https://doi.org/10.1016/S0196-9781(99)00127-8

Gerebtzoff, G., Li-Blatter, X., Fischer, H., Frentzel, A., Seelig, A., 2004. Halogenation of Drugs Enhances Membrane Binding and Permeation. ChemBioChem 5, 676–684. https://doi.org/10.1002/cbic.200400017

Germann, S.M., Baallal Jacobsen, S.A., Schneider, K., Harrison, S.J., Jensen, N.B., Chen, X., Stahlhut, S.G., Borodina, I., Luo, H., Zhu, J., Maury, J., Forster, J., 2016. Glucose-based microbial production of the hormone melatonin in yeast *Saccharomyces cerevisiae*. Biotechnol. J. 11, 717–724. https://doi.org/10.1002/biot.201500143

GEVO, 2022. Isobutanol Is a Building Block for Advanced Renewable Fuels and More [WWW Document]. URL https://gevo.com/products/isobutanol/ (accessed 4.5.23).

Giani, A.M., Gallo, G.R., Gianfranceschi, L., Formenti, G., 2020. Long walk to genomics: History and current approaches to genome sequencing and assembly. Comput. Struct. Biotechnol. J. 18, 9–19. https://doi.org/10.1016/j.csbj.2019.11.002

Goeddel, D.V., Heyneker, H.L., Hozumi, T., Arentzen, R., Itakura, K., Yansura, D.G., Ross, M.J., Miozzari, G., Crea, R., Seeburg, P.H., 1979a. Direct expression in Escherichia coli of a DNA sequence coding for human growth hormone. Nature 281, 544–548. https://doi.org/10.1038/281544a0

Goeddel, D.V., Kleid, D.G., Bolivar, F., Heyneker, H.L., Yansura, D.G., Crea, R., Hirose, T., Kraszewski, A., Itakura, K., Riggs, A.D., 1979b. Expression in Escherichia coli of chemically synthesized genes for human insulin. Proc. Natl. Acad. Sci. 76, 106–110. https://doi.org/10.1073/pnas.76.1.106

Goffeau, A., Barrell, B.G., Bussey, H., Davis, R.W., Dujon, B., Feldmann, H., Galibert, F., Hoheisel, J.D., Jacq, C., Johnston, M., Louis, E.J., Mewes, H.W., Murakami, Y., Philippsen, P., Tettelin, H., Oliver, S.G., 1996. Life with 6000 Genes. Science 274, 546–567. https://doi.org/10.1126/science.274.5287.546

Grasa, E.T., Ögmundarson, Ó., Gavala, H.N., Sukumara, S., 2021. Commodity chemical production from third-generation biomass: a techno-economic assessment of lactic acid production. Biofuels Bioprod. Biorefining 15, 257–281. https://doi.org/10.1002/bbb.2160

Gregson, B.H., Metodieva, G., Metodiev, M.V., Golyshin, P.N., McKew, B.A., 2020. Protein expression in the obligate hydrocarbon-degrading psychrophile *Oleispira antarctica* RB-8 during alkane degradation and cold tolerance. Environ. Microbiol. 22, 1870–1883. https://doi.org/10.1111/1462-2920.14956

Groenewald, M., Boekhout, T., Neuvéglise, C., Gaillardin, C., van Dijck, P.W.M., Wyss, M., 2014. *Yarrowia lipolytica* : Safety assessment of an oleaginous yeast with a great industrial potential. Crit. Rev. Microbiol. 40, 187–206. https://doi.org/10.3109/1040841X.2013.770386

Gu, C., Kim, G.B., Kim, W.J., Kim, H.U., Lee, S.Y., 2019. Current status and applications of genome-scale metabolic models. Genome Biol. 20, 121. https://doi.org/10.1186/s13059-019-1730-3

Gu, Y., Ma, J., Zhu, Y., Ding, X., Xu, P., 2020. Engineering *Yarrowia lipolytica* as a Chassis for *De Novo* Synthesis of Five Aromatic-Derived Natural Products and Chemicals. ACS Synth. Biol. 9, 2096–2106. https://doi.org/10.1021/acssynbio.0c00185

Gueldener, U., 2002. A second set of loxP marker cassettes for Cre-mediated multiple gene knockouts in budding yeast. Nucleic Acids Res. 30, 23e–223. https://doi.org/10.1093/nar/30.6.e23

Guo, W., Huang, Q., Feng, Y., Tan, T., Niu, S., Hou, S., Chen, Z., Du, Z., Shen, Y., Fang, X., 2020. Rewiring central carbon metabolism for tyrosol and salidroside production in *Saccharomyces cerevisiae*. Biotechnol. Bioeng. 117, 2410–2419. https://doi.org/10.1002/bit.27370

Guo, Y., Su, L., Liu, Q., Zhu, Y., Dai, Z., Wang, Q., 2022. Dissecting carbon metabolism of Yarrowia lipolytica type strain W29 using genome-scale metabolic modelling. Comput. Struct. Biotechnol. J. 20, 2503–2511. https://doi.org/10.1016/j.csbj.2022.05.018

Gurdo, N., Volke, D.C., Nikel, P.I., 2022. Merging automation and fundamental discovery into the design–build–test–learn cycle of nontraditional microbes. Trends Biotechnol. 40, 1148–1159. https://doi.org/10.1016/j.tibtech.2022.03.004

Han, B.-Z., Rombouts, F.M., Nout, M.J.R., 2001. A Chinese fermented soybean food. Int. J. Food Microbiol. 65, 1–10. https://doi.org/10.1016/S0168-1605(00)00523-7

Han, J., Li, S., 2023. De novo biosynthesis of berberine and halogenated benzylisoquinoline alkaloids in Saccharomyces cerevisiae. Commun. Chem. 6, 27. https://doi.org/10.1038/s42004-023-00821-9

Hansen, A.S.L., Lennen, R.M., Sonnenschein, N., Herrgård, M.J., 2017. Systems biology solutions for biochemical production challenges. Curr. Opin. Biotechnol. 45, 85–91. https://doi.org/10.1016/j.copbio.2016.11.018

Hassanshahian, M., Tebyanian, H., Cappello, S., 2012. Isolation and characterization of two crude oil-degrading yeast strains, Yarrowia lipolytica PG-20 and PG-32, from the Persian Gulf. Mar. Pollut. Bull. 64, 1386–1391. https://doi.org/10.1016/j.marpolbul.2012.04.020

Hassing, E.-J., de Groot, P.A., Marquenie, V.R., Pronk, J.T., Daran, J.-M.G., 2019. Connecting central carbon and aromatic amino acid metabolisms to improve de novo 2-phenylethanol production in Saccharomyces cerevisiae. Metab. Eng. 56, 165–180. https://doi.org/10.1016/j.ymben.2019.09.011

Hatti-Kaul, R., Törnvall, U., Gustafsson, L., Börjesson, P., 2007. Industrial biotechnology for the production of bio-based chemicals – a cradle-to-grave perspective. Trends Biotechnol. 25, 119–124. https://doi.org/10.1016/j.tibtech.2007.01.001

He, Q., Szczepańska, P., Yuzbashev, T., Lazar, Z., Ledesma-Amaro, R., 2020. De novo production of resveratrol from glycerol by engineering different metabolic pathways in Yarrowia lipolytica. Metab. Eng. Commun. 11, e00146. https://doi.org/10.1016/j.mec.2020.e00146

Heinrich, M., Mah, J., Amirkia, V., 2021. Alkaloids Used as Medicines: Structural Phytochemistry Meets Biodiversity—An Update and Forward Look. Molecules 26, 1836. https://doi.org/10.3390/molecules26071836

Helmstaedt, K., Strittmatter, A., Lipscomb, W.N., Braus, G.H., 2005. Evolution of 3-deoxy-D-arabino-heptulosonate-7-phosphate synthase-encoding genes in the yeast *Saccharomyces cerevisiae*. Proc. Natl. Acad. Sci. 102, 9784–9789. https://doi.org/10.1073/pnas.0504238102

Herrmann, K.M., 1995. The Shikimate Pathway: Early Steps in the Biosynthesis of Aromatic Compounds. Plant Cell 907–919. https://doi.org/10.1105/tpc.7.7.907

Heslot, H., 1990. Genetics and genetic engineering of the industrial yeast Yarrowia lipolytica, in: Applied Molecular Genetics, Advances in Biochemical Engineering/Biotechnology. Springer-Verlag, Berlin/Heidelberg, pp. 43–73. https://doi.org/10.1007/BFb0009079

Hinnen, A., Hicks, J.B., Fink, G.R., 1978. Transformation of yeast. Proc. Natl. Acad. Sci. 75, 1929–1933. https://doi.org/10.1073/pnas.75.4.1929

Holkenbrink, C., Dam, M.I., Kildegaard, K.R., Beder, J., Dahlin, J., Belda, D.D., Borodina, I., 2018. EasyCloneYALI: CRISPR/Cas9-Based Synthetic Toolbox for Engineering of the Yeast Yarrowia lipolytica. Biotechnol. J. 13, 1700543. https://doi.org/10.1002/biot.201700543

Hollands, K., Baron, C.M., Gibson, K.J., Kelly, K.J., Krasley, E.A., Laffend, L.A., Lauchli, R.M., Maggio-Hall, L.A., Nelson, M.J., Prasad, J.C., Ren, Y., Rice, B.A., Rice, G.H., Rothman, S.C., 2019. Engineering two species of yeast as cell factories for 2′-fucosyllactose. Metab. Eng. 52, 232–242. https://doi.org/10.1016/j.ymben.2018.12.005

Hostetler, G.L., Ralston, R.A., Schwartz, S.J., 2017. Flavones: Food Sources, Bioavailability, Metabolism, and Bioactivity. Adv. Nutr. 8, 423–435. https://doi.org/10.3945/an.116.012948

Hu, Y., Zhu, Z., Nielsen, J., Siewers, V., 2018. Heterologous transporter expression for improved fatty alcohol secretion in yeast. Metab. Eng. 45, 51–58. https://doi.org/10.1016/j.ymben.2017.11.008

Hua, D., Xu, P., 2011. Recent advances in biotechnological production of 2-phenylethanol. Biotechnol. Adv. 29, 654–660. https://doi.org/10.1016/j.biotechadv.2011.05.001

Huang, J., Xu, C., Ridoutt, B.G., Wang, X., Ren, P., 2017. Nitrogen and phosphorus losses and eutrophication potential associated with fertilizer application to cropland in China. J. Clean. Prod. 159, 171–179. https://doi.org/10.1016/j.jclepro.2017.05.008

Huccetogullari, D., Luo, Z.W., Lee, S.Y., 2019. Metabolic engineering of microorganisms for production of aromatic compounds. Microb. Cell Factories 18, 41. https://doi.org/10.1186/s12934-019-1090-4

Hui, C., Guo, Y., Zhu, D., Li, L., Yi, J., Zhang, N., 2022a. Metabolic engineering of the violacein biosynthetic pathway toward a low-cost, minimal-equipment lead biosensor. Biosens. Bioelectron. 214, 114531. https://doi.org/10.1016/j.bios.2022.114531

Hui, C., Hu, S., Li, L., Yun, J., Zhang, Y., Yi, J., Zhang, N., Guo, Y., 2022b. Metabolic engineering of the carotenoid biosynthetic pathway toward a specific and sensitive inorganic mercury biosensor. RSC Adv. 12, 36142–36148. https://doi.org/10.1039/D2RA06764A

Iman, M.N., Herawati, E., Fukusaki, E., Putri, S.P., 2022. Metabolomics-driven strain improvement: A mini review. Front. Mol. Biosci. 9, 1057709. https://doi.org/10.3389/fmolb.2022.1057709

International Energy Agency, 2021. World Energy Outlook 2021.

Ishikawa, H., Colby, D.A., Seto, S., Va, P., Tam, A., Kakei, H., Rayl, T.J., Hwang, I., Boger, D.L., 2009. Total Synthesis of Vinblastine, Vincristine, Related Natural Products, and Key Structural Analogues. J. Am. Chem. Soc. 131, 4904–4916. https://doi.org/10.1021/ja809842b

Jensen, E.D., Ambri, F., Bendtsen, M.B., Javanpour, A.A., Liu, C.C., Jensen, M.K., Keasling, J.D., 2021. Integrating continuous hypermutation with high-throughput screening for optimization of *cis,cis* -muconic acid production in yeast. Microb. Biotechnol. 14, 2617–2626. https://doi.org/10.1111/1751-7915.13774

Jensen, E.D., Ferreira, R., Jakočiūnas, T., Arsovska, D., Zhang, J., Ding, L., Smith, J.D., David, F., Nielsen, J., Jensen, M.K., Keasling, J.D., 2017. Transcriptional reprogramming in yeast using dCas9 and combinatorial gRNA strategies. Microb. Cell Factories 16, 46. https://doi.org/10.1186/s12934-017-0664-2

Jensen, K., Broeken, V., Hansen, A.S.L., Sonnenschein, N., Herrgård, M.J., 2019. OptCouple: Joint simulation of gene knockouts, insertions and medium modifications for prediction of growth-coupled strain designs. Metab. Eng. Commun. 8, e00087. https://doi.org/10.1016/j.mec.2019.e00087

Jessop-Fabre, M.M., Jakočiūnas, T., Stovicek, V., Dai, Z., Jensen, M.K., Keasling, J.D., Borodina, I., 2016. EasyClone-MarkerFree: A vector toolkit for marker-less integration of genes into *Saccharomyces cerevisiae* via CRISPR-Cas9. Biotechnol. J. 11, 1110–1117. https://doi.org/10.1002/biot.201600147

Jiang, H., Wood, K.V., Morgan, J.A., 2005. Metabolic Engineering of the Phenylpropanoid Pathway in *Saccharomyces cerevisiae*. Appl. Environ. Microbiol. 71, 2962–2969. https://doi.org/10.1128/AEM.71.6.2962-2969.2005

Jinek, M., Chylinski, K., Fonfara, I., Hauer, M., Doudna, J.A., Charpentier, E., 2012. A Programmable Dual-RNA–Guided DNA Endonuclease in Adaptive Bacterial Immunity. Science 337, 816–821. https://doi.org/10.1126/science.1225829

Johnson, C.W., Salvachúa, D., Khanna, P., Smith, H., Peterson, D.J., Beckham, G.T., 2016. Enhancing muconic acid production from glucose and lignin-derived aromatic compounds via increased protocatechuate decarboxylase activity. Metab. Eng. Commun. 3, 111–119. https://doi.org/10.1016/j.meteno.2016.04.002

Johnston, J.E., Lim, E., Roh, H., 2019. Impact of upstream oil extraction and environmental public health: A review of the evidence. Sci. Total Environ. 657, 187–199. https://doi.org/10.1016/j.scitotenv.2018.11.483

Jossek, R., Bongaerts, J., Sprenger, G.A., 2001. Characterization of a new feedback-resistant 3-deoxy-d-arabino-heptulosonate 7-phosphate synthase AroF of *Escherichia coli*. FEMS Microbiol. Lett. 202, 145–148. https://doi.org/10.1111/j.1574-6968.2001.tb10795.x

Kapoore, R., Vaidyanathan, S., 2018. Quenching for Microalgal Metabolomics: A Case Study on the Unicellular Eukaryotic Green Alga Chlamydomonas reinhardtii. Metabolites 8, 72. https://doi.org/10.3390/metabo8040072

Karathia, H., Vilaprinyo, E., Sorribas, A., Alves, R., 2011. Saccharomyces cerevisiae as a Model Organism: A Comparative Study. PLoS ONE 6, e16015. https://doi.org/10.1371/journal.pone.0016015

Karim, A.S., Curran, K.A., Alper, H.S., 2013. Characterization of plasmid burden and copy number in *Saccharomyces cerevisiae* for optimization of metabolic engineering applications. FEMS Yeast Res. 13, 107–116. https://doi.org/10.1111/1567-1364.12016

Karković Marković, A., Torić, J., Barbarić, M., Jakobušić Brala, C., 2019. Hydroxytyrosol, Tyrosol and Derivatives and Their Potential Effects on Human Health. Molecules 24, 2001. https://doi.org/10.3390/molecules24102001

Kavšček, M., Bhutada, G., Madl, T., Natter, K., 2015a. Optimization of lipid production with a genome-scale model of Yarrowia lipolytica. BMC Syst. Biol. 9, 72. https://doi.org/10.1186/s12918-015-0217-4

Kavšček, M., Stražar, M., Curk, T., Natter, K., Petrovič, U., 2015b. Yeast as a cell factory: current state and perspectives. Microb. Cell Factories 14, 94. https://doi.org/10.1186/s12934-015-0281-x

Kawasse, F.M., Amaral, P.F., Rocha-Leão, M.H.M., Amaral, A.L., Ferreira, E.C., Coelho, M.A.Z., 2003. Morphological analysis of Yarrowia lipolytica under stress conditions through image processing. Bioprocess Biosyst. Eng. 25, 371–375. https://doi.org/10.1007/s00449-003-0319-z

Kell, D.B., Swainston, N., Pir, P., Oliver, S.G., 2015. Membrane transporter engineering in industrial biotechnology and whole cell biocatalysis. Trends Biotechnol. 33, 237–246. https://doi.org/10.1016/j.tibtech.2015.02.001

Kelly, T.J., Smith, H.O., 1970. A restriction enzyme from Hemophilus influenzae. J. Mol. Biol. 51, 393–409. https://doi.org/10.1016/0022-2836(70)90150-6

Kerkhoven, E.J., Pomraning, K.R., Baker, S.E., Nielsen, J., 2016. Regulation of amino-acid metabolism controls flux to lipid accumulation in Yarrowia lipolytica. Npj Syst. Biol. Appl. 2, 16005. https://doi.org/10.1038/npjsba.2016.5

Kerscher, S., Durstewitz, G., Casaregola, S., Gaillardin, C., Brandt, U., 2001. The Complete Mitochondrial Genome of *Yarrowia lipolytica*. Comp. Funct. Genomics 2, 80–90. https://doi.org/10.1002/cfg.72

Khanijou, J.K., Kulyk, H., Bergès, C., Khoo, L.W., Ng, P., Yeo, H.C., Helmy, M., Bellvert, F., Chew, W., Selvarajoo, K., 2022. Metabolomics and modelling approaches for systems metabolic engineering. Metab. Eng. Commun. 15, e00209. https://doi.org/10.1016/j.mec.2022.e00209

Khodayari, A., Maranas, C.D., 2016. A genome-scale Escherichia coli kinetic metabolic model k-ecoli457 satisfying flux data for multiple mutant strains. Nat. Commun. 7, 13806. https://doi.org/10.1038/ncomms13806

Kim, Y.-M., Petzold, C.J., Kerkhoven, E.J., Baker, S.E., 2021. Editorial: Multi-Omics Technologies for Optimizing Synthetic Biomanufacturing. Front. Bioeng. Biotechnol. 9, 818010. https://doi.org/10.3389/fbioe.2021.818010

Kliszcz, A., Danel, A., Puła, J., Barabasz-Krasny, B., Możdżeń, K., 2021. Fleeting Beauty—The World of Plant Fragrances and Their Application. Molecules 26, 2473. https://doi.org/10.3390/molecules26092473

Ko, Y.-S., Kim, J.W., Lee, J.A., Han, T., Kim, G.B., Park, J.E., Lee, S.Y., 2020. Tools and strategies of systems metabolic engineering for the development of microbial cell factories for chemical production. Chem. Soc. Rev. 49, 4615–4636. https://doi.org/10.1039/D0CS00155D

Korosh, T.C., Markley, A.L., Clark, R.L., McGinley, L.L., McMahon, K.D., Pfleger, B.F., 2017. Engineering photosynthetic production of L-lysine. Metab. Eng. 44, 273–283. https://doi.org/10.1016/j.ymben.2017.10.010

Kozaeva, E., Mol, V., Nikel, P.I., Nielsen, A.T., 2022. High-throughput colorimetric assays optimized for detection of ketones and aldehydes produced by microbial cell factories. Microb. Biotechnol. 15, 2426–2438. https://doi.org/10.1111/1751-7915.14097

Krebs, H.A., 1940. The citric acid cycle. Biochem. J. 34, 460–463. https://doi.org/10.1042/bj0340460

Krebs, H.A., Johnson, W.A., 1937a. Metabolism of ketonic acids in animal tissues. Biochem. J. 31, 645–660. https://doi.org/10.1042/bj0310645

Krebs, H.A., Johnson, W.A., 1937b. The role of citric acid in intermediate metabolism in animal tissues. Enzymologia 4, 148–156.

Kulagina, N., Guirimand, G., Melin, C., Lemos-Cruz, P., Carqueijeiro, I., De Craene, J., Oudin, A., Heredia, V., Koudounas, K., Unlubayir, M., Lanoue, A., Imbault, N., St-Pierre, B., Papon, N., Clastre, M., Giglioli-Guivarc'h, N., Marc, J., Besseau, S., Courdavault, V., 2021. Enhanced bioproduction of anticancer precursor vindoline by yeast cell factories. Microb. Biotechnol. 14, 2693–2699. https://doi.org/10.1111/1751-7915.13898

Kurtzman, C.P., 1998. Yarrowia van der Walt & von Arx, in: The Yeasts. Elsevier, pp. 420–421. https://doi.org/10.1016/B978-044481312-1/50059-9

Labbé, S., Thiele, D.J., 1999. [8] Copper ion inducible and repressible promoter systems in yeast, in: Methods in Enzymology. Elsevier, pp. 145–153. https://doi.org/10.1016/S0076-6879(99)06010-3

Lahtvee, P.-J., Sánchez, B.J., Smialowska, A., Kasvandik, S., Elsemman, I.E., Gatto, F., Nielsen, J., 2017. Absolute Quantification of Protein and mRNA Abundances Demonstrate Variability in Gene-Specific Translation Efficiency in Yeast. Cell Syst. 4, 495-504.e5. https://doi.org/10.1016/j.cels.2017.03.003

Lakrisenko, P., Weindl, D., 2021. Dynamic models for metabolomics data integration. Curr. Opin. Syst. Biol. 28, 100358. https://doi.org/10.1016/j.coisb.2021.100358

Lammens, T.M., Potting, J., Sanders, J.P.M., De Boer, I.J.M., 2011. Environmental Comparison of Biobased Chemicals from Glutamic Acid with Their Petrochemical Equivalents. Environ. Sci. Technol. 45, 8521–8528. https://doi.org/10.1021/es201869e

Larroude, M., Rossignol, T., Nicaud, J.-M., Ledesma-Amaro, R., 2018. Synthetic biology tools for engineering Yarrowia lipolytica. Biotechnol. Adv. 36, 2150–2164. https://doi.org/10.1016/j.biotechadv.2018.10.004

Larroude, M., Trabelsi, H., Nicaud, J.-M., Rossignol, T., 2020. A set of Yarrowia lipolytica CRISPR/Cas9 vectors for exploiting wild-type strain diversity. Biotechnol. Lett. 42, 773–785. https://doi.org/10.1007/s10529-020-02805-4

Lawrence, D., Coe, M., Walker, W., Verchot, L., Vandecar, K., 2022. The Unseen Effects of Deforestation: Biophysical Effects on Climate. Front. For. Glob. Change 5, 756115. https://doi.org/10.3389/ffgc.2022.756115

Lawson, C.E., Martí, J.M., Radivojevic, T., Jonnalagadda, S.V.R., Gentz, R., Hillson, N.J., Peisert, S., Kim, J., Simmons, B.A., Petzold, C.J., Singer, S.W., Mukhopadhyay, A., Tanjore, D., Dunn, J.G., Garcia Martin, H., 2021. Machine learning for metabolic engineering: A review. Metab. Eng. 63, 34–60. https://doi.org/10.1016/j.ymben.2020.10.005

Leavitt, J.M., Wagner, J.M., Tu, C.C., Tong, A., Liu, Y., Alper, H.S., 2017. Biosensor-Enabled Directed Evolution to Improve Muconic Acid Production in *Saccharomyces cerevisiae*. Biotechnol. J. 12, 1600687. https://doi.org/10.1002/biot.201600687

Ledesma-Amaro, R., Lazar, Z., Rakicka, M., Guo, Z., Fouchard, F., Coq, A.-M.C.-L., Nicaud, J.-M., 2016. Metabolic engineering of Yarrowia lipolytica to produce chemicals and fuels from xylose. Metab. Eng. 38, 115–124. https://doi.org/10.1016/j.ymben.2016.07.001

Lee, M.E., Aswani, A., Han, A.S., Tomlin, C.J., Dueber, J.E., 2013. Expression-level optimization of a multi-enzyme pathway in the absence of a high-throughput assay. Nucleic Acids Res. 41, 10668–10678. https://doi.org/10.1093/nar/gkt809

Lee, M.E., DeLoache, W.C., Cervantes, B., Dueber, J.E., 2015. A Highly Characterized Yeast Toolkit for Modular, Multipart Assembly. ACS Synth. Biol. 4, 975–986. https://doi.org/10.1021/sb500366v

Lee, S.Y., Kim, H.U., Chae, T.U., Cho, J.S., Kim, J.W., Shin, J.H., Kim, D.I., Ko, Y.-S., Jang, W.D., Jang, Y.-S., 2019. A comprehensive metabolic map for production of bio-based chemicals. Nat. Catal. 2, 18–33. https://doi.org/10.1038/s41929-018-0212-4

Lennen, R.M., Lim, H.G., Jensen, K., Mohammed, E.T., Phaneuf, P.V., Noh, M.H., Malla, S., Börner, R.A., Chekina, K., Özdemir, E., Bonde, I., Koza, A., Maury, J., Pedersen, L.E., Schöning, L.Y., Sonnenschein, N., Palsson, B.O., Nielsen, A.T., Sommer, M.O.A., Herrgård, M.J., Feist, A.M., 2023. Laboratory evolution reveals general and specific tolerance mechanisms for commodity chemicals. Metab. Eng. 76, 179–192. https://doi.org/10.1016/j.ymben.2023.01.012

Li, H., Gao, S., Zhang, S., Zeng, W., Zhou, J., 2021. Effects of metabolic pathway gene copy numbers on the biosynthesis of (2S)-naringenin in Saccharomyces cerevisiae. J. Biotechnol. 325, 119–127. https://doi.org/10.1016/j.jbiotec.2020.11.009

Li, H., Ma, W., Lyv, Y., Gao, S., Zhou, J., 2022. Glycosylation Modification Enhances (2 *S*)-Naringenin Production in *Saccharomyces cerevisiae*. ACS Synth. Biol. 11, 2339–2347. https://doi.org/10.1021/acssynbio.2c00065

Li, M., Kildegaard, K.R., Chen, Y., Rodriguez, A., Borodina, I., Nielsen, J., 2015. De novo production of resveratrol from glucose or ethanol by engineered Saccharomyces cerevisiae. Metab. Eng. 32, 1–11. https://doi.org/10.1016/j.ymben.2015.08.007

Li, M., Schneider, K., Kristensen, M., Borodina, I., Nielsen, J., 2016. Engineering yeast for high-level production of stilbenoid antioxidants. Sci. Rep. 6, 1–8. https://doi.org/10.1038/srep36827

Li, W., Ma, L., Shen, X., Wang, J., Feng, Q., Liu, L., Zheng, G., Yan, Y., Sun, X., Yuan, Q., 2019. Targeting metabolic driving and intermediate influx in lysine catabolism for high-level glutarate production. Nat. Commun. 10, 3337. https://doi.org/10.1038/s41467-019-11289-4

Li, Y., Li, S., Thodey, K., Trenchard, I., Cravens, A., Smolke, C.D., 2018. Complete biosynthesis of noscapine and halogenated alkaloids in yeast. Proc. Natl. Acad. Sci. 115, E3922–E3931. https://doi.org/10.1073/pnas.1721469115

Lian, J., Mishra, S., Zhao, H., 2018. Recent advances in metabolic engineering of Saccharomyces cerevisiae: New tools and their applications. Metab. Eng. 50, 85–108. https://doi.org/10.1016/j.ymben.2018.04.011

Lim, H.G., Rychel, K., Sastry, A.V., Bentley, G.J., Mueller, J., Schindel, H.S., Larsen, P.E., Laible, P.D., Guss, A.M., Niu, W., Johnson, C.W., Beckham, G.T., Feist, A.M., Palsson, B.O., 2022. Machine-learning from Pseudomonas putida KT2440 transcriptomes reveals its transcriptional regulatory network. Metab. Eng. 72, 297–310. https://doi.org/10.1016/j.ymben.2022.04.004

Liu, H., Song, Y., Fan, X., Wang, C., Lu, X., Tian, Y., 2021. Yarrowia lipolytica as an Oleaginous Platform for the Production of Value-Added Fatty Acid-Based Bioproducts. Front. Microbiol. 11, 608662. https://doi.org/10.3389/fmicb.2020.608662

Liu, L., Alper, H.S., 2014. Draft Genome Sequence of the Oleaginous Yeast Yarrowia lipolytica PO1f, a Commonly Used Metabolic Engineering Host. Genome Announc. 2, e00652-14. https://doi.org/10.1128/genomeA.00652-14

Liu, M., Wang, C., Ren, X., Gao, S., Yu, S., Zhou, J., 2022. Remodelling metabolism for high-level resveratrol production in Yarrowia lipolytica. Bioresour. Technol. 365, 128178. https://doi.org/10.1016/j.biortech.2022.128178

Liu, Q., Liu, Y., Chen, Y., Nielsen, J., 2020. Current state of aromatics production using yeast: achievements and challenges. Curr. Opin. Biotechnol. 65, 65–74. https://doi.org/10.1016/j.copbio.2020.01.008

Liu, Q., Yu, T., Li, X., Chen, Yu, Campbell, K., Nielsen, J., Chen, Yun, 2019. Rewiring carbon metabolism in yeast for high level production of aromatic chemicals. Nat. Commun. 10, 1–13. https://doi.org/10.1038/s41467-019-12961-5

Liu, T., Gou, Y., Zhang, B., Gao, R., Dong, C., Qi, M., Jiang, L., Ding, X., Li, C., Lian, J., 2022. Construction of ajmalicine and sanguinarine de novo biosynthetic pathways using stable integration sites in yeast. Biotechnol. Bioeng. 119, 1314–1326. https://doi.org/10.1002/bit.28040

Liu, Y., Nielsen, J., 2019. Recent trends in metabolic engineering of microbial chemical factories. Curr. Opin. Biotechnol. 60, 188–197. https://doi.org/10.1016/j.copbio.2019.05.010

Löbs, A.-K., Schwartz, C., Wheeldon, I., 2017. Genome and metabolic engineering in non-conventional yeasts: Current advances and applications. Synth. Syst. Biotechnol. 2, 198–207. https://doi.org/10.1016/j.synbio.2017.08.002

Loenen, W.A.M., Dryden, D.T.F., Raleigh, E.A., Wilson, G.G., Murray, N.E., 2014. Highlights of the DNA cutters: a short history of the restriction enzymes. Nucleic Acids Res. 42, 3–19. https://doi.org/10.1093/nar/gkt990

Loira, N., Dulermo, T., Nicaud, J.-M., Sherman, D.J., 2012. A genome-scale metabolic model of the lipid-accumulating yeast Yarrowia lipolytica. BMC Syst. Biol. 6, 35. https://doi.org/10.1186/1752-0509-6-35

Long, C.P., Antoniewicz, M.R., 2019. High-resolution 13C metabolic flux analysis. Nat. Protoc. 14, 2856–2877. https://doi.org/10.1038/s41596-019-0204-0

Lu, H., Cao, W., Liu, X., Sui, Y., Ouyang, L., Xia, J., Huang, M., Zhuang, Y., Zhang, S., Noorman, H., Chu, J., 2018. Multi-omics integrative analysis with genome-scale metabolic model simulation reveals global cellular adaptation of Aspergillus niger under industrial enzyme production condition. Sci. Rep. 8, 14404. https://doi.org/10.1038/s41598-018-32341-1

Lu, H., Li, F., Sánchez, B.J., Zhu, Z., Li, G., Domenzain, I., Marcišauskas, S., Anton, P.M., Lappa, D., Lieven, C., Beber, M.E., Sonnenschein, N., Kerkhoven, E.J., Nielsen, J., 2019. A consensus S. cerevisiae metabolic model Yeast8 and its ecosystem for comprehensively probing cellular metabolism. Nat. Commun. 10, 3586. https://doi.org/10.1038/s41467-019-11581-3

Luttik, M.A.H., Vuralhan, Z., Suir, E., Braus, G.H., Pronk, J.T., Daran, J.M., 2008. Alleviation of feedback inhibition in Saccharomyces cerevisiae aromatic amino acid biosynthesis: Quantification of metabolic impact. Metab. Eng. 10, 141–153. https://doi.org/10.1016/j.ymben.2008.02.002

Lv, Y., Marsafari, M., Koffas, M., Zhou, J., Xu, P., 2019. Optimizing Oleaginous Yeast Cell Factories for Flavonoids and Hydroxylated Flavonoids Biosynthesis. ACS Synth. Biol. 8, 2514–2523. https://doi.org/10.1021/acssynbio.9b00193

Mackiewicz, P., Kowalczuk, M., Mackiewicz, D., Nowicka, A., Dudkiewicz, M., Laszkiewicz, A., Dudek, M.R., Cebrat, S., 2002. How many protein-coding genes are there in theSaccharomyces cerevisiae genome? Yeast 19, 619–629. https://doi.org/10.1002/yea.865

Maddox, S.M., Nalbandian, C.J., Smith, D.E., Gustafson, J.L., 2015. A Practical Lewis Base Catalyzed Electrophilic Chlorination of Arenes and Heterocycles. Org. Lett. 17, 1042–1045. https://doi.org/10.1021/acs.orglett.5b00186

Madzak, C., 2021. Yarrowia lipolytica Strains and Their Biotechnological Applications: How Natural Biodiversity and Metabolic Engineering Could Contribute to Cell Factories Improvement. J. Fungi 7, 548. https://doi.org/10.3390/jof7070548

Madzak, C., Tréton, B., Blanchin-Roland, S., 2000. Strong hybrid promoters and integrative expression/secretion vectors for quasi-constitutive expression of heterologous proteins in the yeast Yarrowia lipolytica. J. Mol. Microbiol. Biotechnol. 2, 207–216.

Makkar, H.P.S., Siddhuraju, P., Becker, K., 2007. Plant Secondary Metabolites, Methods in Molecular Biology™. Humana Press, Totowa, NJ. https://doi.org/10.1007/978-1-59745-425-4

Malina, C., Larsson, C., Nielsen, J., 2018. Yeast mitochondria: an overview of mitochondrial biology and the potential of mitochondrial systems biology. FEMS Yeast Res. 18. https://doi.org/10.1093/femsyr/foy040

Matson, M.M., Cepeda, M.M., Zhang, A., Case, A.E., Kavvas, E.S., Wang, X., Carroll, A.L., Tagkopoulos, I., Atsumi, S., 2022. Adaptive laboratory evolution for improved tolerance of isobutyl acetate in Escherichia coli. Metab. Eng. 69, 50–58. https://doi.org/10.1016/j.ymben.2021.11.002

May, O.E., Herrick, H.T., 1930. Some Minor Industrial Fermentations. Ind. Eng. Chem. 22, 1172–1176. https://doi.org/10.1021/ie50251a017

McGovern, P., Jalabadze, M., Batiuk, S., Callahan, M.P., Smith, K.E., Hall, G.R., Kvavadze, E., Maghradze, D., Rusishvili, N., Bouby, L., Failla, O., Cola, G., Mariani, L., Boaretto, E., Bacilieri, R., This, P., Wales, N., Lordkipanidze, D., 2017. Early Neolithic wine of Georgia in the South Caucasus. Proc. Natl. Acad. Sci. 114. https://doi.org/10.1073/pnas.1714728114

McGovern, P.E., Zhang, J., Tang, J., Zhang, Z., Hall, G.R., Moreau, R.A., Nuñez, A., Butrym, E.D., Richards, M.P., Wang, Chen-shan, Cheng, G., Zhao, Z., Wang, Changsui, 2004. Fermented beverages of pre- and proto-historic China. Proc. Natl. Acad. Sci. 101, 17593–17598. https://doi.org/10.1073/pnas.0407921102

Meng, H., Wang, J., Xiong, Z., Xu, F., Zhao, G., Wang, Y., 2013. Quantitative Design of Regulatory Elements Based on High-Precision Strength Prediction Using Artificial Neural Network. PLoS ONE 8, e60288. https://doi.org/10.1371/journal.pone.0060288

Meng, H.-L., Xiong, Z.-Q., Song, S.-J., Wang, J., Wang, Y., 2016. Construction of polyketide overproducing *Escherichia coli* strains via synthetic antisense RNAs based on in silico fluxome analysis and comparative transcriptome analysis. Biotechnol. J. 11, 530–541. https://doi.org/10.1002/biot.201500351

Meyers, R.A. (Ed.), 2005. Handbook of petrochemicals production processes, McGraw-Hill handbooks. McGraw-Hill, New York.

Michely, S., Gaillardin, C., Nicaud, J.-M., Neuvéglise, C., 2013. Comparative Physiology of Oleaginous Species from the Yarrowia Clade. PLoS ONE 8, e63356. https://doi.org/10.1371/journal.pone.0063356

Milne, N., Thomsen, P., Mølgaard Knudsen, N., Rubaszka, P., Kristensen, M., Borodina, I., 2020. Metabolic engineering of Saccharomyces cerevisiae for the de novo production of psilocybin and related tryptamine derivatives. Metab. Eng. 60, 25–36. https://doi.org/10.1016/j.ymben.2019.12.007

Mir, R., Jallu, S., Singh, T.P., 2015. The shikimate pathway: Review of amino acid sequence, function and three-dimensional structures of the enzymes. Crit. Rev. Microbiol. 41, 172–189. https://doi.org/10.3109/1040841X.2013.813901

Mishra, P., Lee, N.-R., Lakshmanan, M., Kim, M., Kim, B.-G., Lee, D.-Y., 2018. Genome-scale model-driven strain design for dicarboxylic acid production in Yarrowia lipolytica. BMC Syst. Biol. 12, 12. https://doi.org/10.1186/s12918-018-0542-5

Mitri, S., Koubaa, M., Maroun, R.G., Rossignol, T., Nicaud, J.-M., Louka, N., 2022. Bioproduction of 2-Phenylethanol through Yeast Fermentation on Synthetic Media

and on Agro-Industrial Waste and By-Products: A Review. Foods 11, 109. https://doi.org/10.3390/foods11010109
Morgunov, I.G., Kamzolova, S.V., Perevoznikova, O.A., Shishkanova, N.V., Finogenova, T.V., 2004. Pyruvic acid production by a thiamine auxotroph of Yarrowia lipolytica. Process Biochem. 39, 1469–1474. https://doi.org/10.1016/S0032-9592(03)00259-0
Muñiz, C.C., Zelaya, T.E.C., Esquivel, G.R., Fernández, F.J., 2007. Penicillin and cephalosporin production: A historical perspective. Rev. Latinoam. Microbiol. 49, 88–98.
Nagata, S., Taira, H., Hall, A., Johnsrud, L., Streuli, M., Ecsödi, J., Boll, W., Cantell, K., Weissmann, C., 1980. Synthesis in E. coli of a polypeptide with human leukocyte interferon activity. Nature 284, 316–320. https://doi.org/10.1038/284316a0
Naseri, G., 2023. A roadmap to establish a comprehensive platform for sustainable manufacturing of natural products in yeast. Nat. Commun. 14, 1916. https://doi.org/10.1038/s41467-023-37627-1
Nasim, N., Sandeep, I.S., Mohanty, S., 2022. Plant-derived natural products for drug discovery: current approaches and prospects. The Nucleus 65, 399–411. https://doi.org/10.1007/s13237-022-00405-3
Nielsen, J., Keasling, J.D., 2016. Engineering Cellular Metabolism. Cell 164, 1185–1197. https://doi.org/10.1016/j.cell.2016.02.004
Nielsen, J., Larsson, C., van Maris, A., Pronk, J., 2013. Metabolic engineering of yeast for production of fuels and chemicals. Curr. Opin. Biotechnol. 24, 398–404. https://doi.org/10.1016/j.copbio.2013.03.023
Nielsen, J., Tillegreen, C.B., Petranovic, D., 2022. Innovation trends in industrial biotechnology. Trends Biotechnol. 40, 1160–1172. https://doi.org/10.1016/j.tibtech.2022.03.007
Niu, P., Soto, M.J., Yoon, B.-J., Dougherty, E.R., Alexander, F.J., Blaby, I., Qian, X., 2021. TRIMER: Transcription Regulation Integrated with Metabolic Regulation. iScience 24, 103218. https://doi.org/10.1016/j.isci.2021.103218
Nubel, R., Fitts, R., Findlay, G., 1979. Fermentation process for the production of citric acid. US4155811A.
Ohtake, T., Pontrelli, S., Laviña, W.A., Liao, J.C., Putri, S.P., Fukusaki, E., 2017. Metabolomics-driven approach to solving a CoA imbalance for improved 1-butanol production in Escherichia coli. Metab. Eng. 41, 135–143. https://doi.org/10.1016/j.ymben.2017.04.003
Olatunde, A., Mohammed, A., Ibrahim, M.A., Tajuddeen, N., Shuaibu, M.N., 2022. Vanillin: A food additive with multiple biological activities. Eur. J. Med. Chem. Rep. 5, 100055. https://doi.org/10.1016/j.ejmcr.2022.100055
Osbourn, A.E., Lanzotti, V. (Eds.), 2009. Plant-derived Natural Products: Synthesis, Function, and Application. Springer US, New York, NY. https://doi.org/10.1007/978-0-387-85498-4
Osman, C., Noriega, T.R., Okreglak, V., Fung, J.C., Walter, P., 2015. Integrity of the yeast mitochondrial genome, but not its distribution and inheritance, relies on mitochondrial fission and fusion. Proc. Natl. Acad. Sci. 112. https://doi.org/10.1073/pnas.1501737112
Palmer, C.M., Miller, K.K., Nguyen, A., Alper, H.S., 2020. Engineering 4-coumaroyl-CoA derived polyketide production in Yarrowia lipolytica through a β-oxidation mediated strategy. Metab. Eng. 57, 174–181. https://doi.org/10.1016/j.ymben.2019.11.006
Pan, P., Hua, Q., 2012. Reconstruction and In Silico Analysis of Metabolic Network for an Oleaginous Yeast, Yarrowia lipolytica. PLoS ONE 7, e51535. https://doi.org/10.1371/journal.pone.0051535
Parapouli, M., Vasileiadi, A., Afendra, A.-S., Hatziloukas, E., 1 Molecular Biology laboratory, Department of Biological applications and Technology, University of Ioannina, Ioannina, Greece, 2 Genetics laboratory, Department of Biological applications and Technology, University of Ioannina, Ioannina, Greece, # These two authors

contributed equally, 2020. Saccharomyces cerevisiae and its industrial applications. AIMS Microbiol. 6, 1–32. https://doi.org/10.3934/microbiol.2020001

Patterson, K., Yu, J., Landberg, J., Chang, I., Shavarebi, F., Bilanchone, V., Sandmeyer, S., 2018. Functional genomics for the oleaginous yeast Yarrowia lipolytica. Metab. Eng. 48, 184–196. https://doi.org/10.1016/j.ymben.2018.05.008

Payne, J.T., Valentic, T.R., Smolke, C.D., 2021. Complete biosynthesis of the bisbenzylisoquinoline alkaloids guattegaumerine and berbamunine in yeast. Proc. Natl. Acad. Sci. 118, e2112520118. https://doi.org/10.1073/pnas.2112520118

Pereira, R., Mohamed, E.T., Radi, M.S., Herrgård, M.J., Feist, A.M., Nielsen, J., Chen, Y., 2020. Elucidating aromatic acid tolerance at low pH in *Saccharomyces cerevisiae* using adaptive laboratory evolution. Proc. Natl. Acad. Sci. 117, 27954–27961. https://doi.org/10.1073/pnas.2013044117

Petrone, D.A., Ye, J., Lautens, M., 2016. Modern Transition-Metal-Catalyzed Carbon–Halogen Bond Formation. Chem. Rev. 116, 8003–8104. https://doi.org/10.1021/acs.chemrev.6b00089

Petzold, C.J., Chan, L.J.G., Nhan, M., Adams, P.D., 2015. Analytics for Metabolic Engineering. Front. Bioeng. Biotechnol. 3. https://doi.org/10.3389/fbioe.2015.00135

Pfeiffer, T., Morley, A., 2014. An evolutionary perspective on the Crabtree effect. Front. Mol. Biosci. 1. https://doi.org/10.3389/fmolb.2014.00017

Philp, J.C., Ritchie, R.J., Allan, J.E.M., 2013. Biobased chemicals: the convergence of green chemistry with industrial biotechnology. Trends Biotechnol. 31, 219–222. https://doi.org/10.1016/j.tibtech.2012.12.007

Pinu, F., Villas-Boas, S., Aggio, R., 2017. Analysis of Intracellular Metabolites from Microorganisms: Quenching and Extraction Protocols. Metabolites 7, 53. https://doi.org/10.3390/metabo7040053

Piskur, J., Rozpedowska, E., Polakova, S., Merico, A., Compagno, C., 2006. How did Saccharomyces evolve to become a good brewer? Trends Genet. 22, 183–186. https://doi.org/10.1016/j.tig.2006.02.002

Pittard, J., Yang, J., 2008. Biosynthesis of the Aromatic Amino Acids. EcoSal Plus 3, ecosalplus.3.6.1.8. https://doi.org/10.1128/ecosalplus.3.6.1.8

Pleissner, D., Kümmerer, K., 2018. Green Chemistry and Its Contribution to Industrial Biotechnology, in: Fröhling, M., Hiete, M. (Eds.), Sustainability and Life Cycle Assessment in Industrial Biotechnology, Advances in Biochemical Engineering/Biotechnology. Springer International Publishing, Cham, pp. 281–298. https://doi.org/10.1007/10_2018_73

Pomraning, K.R., Baker, S.E., 2015. Draft Genome Sequence of the Dimorphic Yeast Yarrowia lipolytica Strain W29. Genome Announc. 3, e01211-15. https://doi.org/10.1128/genomeA.01211-15

Pomraning, K.R., Kim, Y.-M., Nicora, C.D., Chu, R.K., Bredeweg, E.L., Purvine, S.O., Hu, D., Metz, T.O., Baker, S.E., 2016. Multi-omics analysis reveals regulators of the response to nitrogen limitation in Yarrowia lipolytica. BMC Genomics 17, 138. https://doi.org/10.1186/s12864-016-2471-2

Pontrelli, S., Chiu, T.-Y., Lan, E.I., Chen, F.Y.-H., Chang, P., Liao, J.C., 2018. Escherichia coli as a host for metabolic engineering. Metab. Eng. 50, 16–46. https://doi.org/10.1016/j.ymben.2018.04.008

Postma, E.D., Hassing, E.-J., Mangkusaputra, V., Geelhoed, J., de la Torre, P., van den Broek, M., Mooiman, C., Pabst, M., Daran, J.-M., Daran-Lapujade, P., 2022. Modular, synthetic chromosomes as new tools for large scale engineering of metabolism. Metab. Eng. 72, 1–13. https://doi.org/10.1016/j.ymben.2021.12.013

Prieto-Díaz, R., González-Gómez, M., Fojo-Carballo, H., Azuaje, J., El Maatougui, A., Majellaro, M., Loza, M.I., Brea, J., Fernández-Dueñas, V., Paleo, M.R., Díaz-Holguín, A., Garcia-Pinel, B., Mallo-Abreu, A., Estévez, J.C., Andújar-Arias, A., García-Mera, X., Gomez-Tourino, I., Ciruela, F., Salas, C.O., Gutiérrez-de-Terán, H., Sotelo, E., 2023. Exploring the Effect of Halogenation in a Series of Potent and Selective A_{2B} Adenosine

Receptor Antagonists. J. Med. Chem. 66, 890–912. https://doi.org/10.1021/acs.jmedchem.2c01768
Pujari, I., Thomas, A., Sankar Babu, V., 2021. Native and non-native host assessment towards metabolic pathway reconstructions of plant natural products. Biotechnol. Rep. 30, e00619. https://doi.org/10.1016/j.btre.2021.e00619
Qiao, K., Imam Abidi, S.H., Liu, H., Zhang, H., Chakraborty, S., Watson, N., Kumaran Ajikumar, P., Stephanopoulos, G., 2015. Engineering lipid overproduction in the oleaginous yeast Yarrowia lipolytica. Metab. Eng. 29, 56–65. https://doi.org/10.1016/j.ymben.2015.02.005
Qu, Y., Easson, M.L.A.E., Froese, J., Simionescu, R., Hudlicky, T., De Luca, V., 2015. Completion of the seven-step pathway from tabersonine to the anticancer drug precursor vindoline and its assembly in yeast. Proc. Natl. Acad. Sci. 112, 6224–6229. https://doi.org/10.1073/pnas.1501821112
Radi, M.S., SalcedoSora, J.E., Kim, S.H., Sudarsan, S., Sastry, A.V., Kell, D.B., Herrgård, M.J., Feist, A.M., 2022. Membrane transporter identification and modulation via adaptive laboratory evolution. Metab. Eng. 72, 376–390. https://doi.org/10.1016/j.ymben.2022.05.004
Rajgarhia, V., Dundon, C., Olson, S., Suominen, P., Hause, B., 2004. Methods and materials for the production of D-lactic acid in yeast. US20040029256A1.
Ramon, C., Gollub, M.G., Stelling, J., 2018. Integrating –omics data into genome-scale metabolic network models: principles and challenges. Essays Biochem. 62, 563–574. https://doi.org/10.1042/EBC20180011
Ratledge, C., 2010. Single Cell Oils for the 21st Century, in: Single Cell Oils. Elsevier, pp. 3–26. https://doi.org/10.1016/B978-1-893997-73-8.50005-0
Redding-Johanson, A.M., Batth, T.S., Chan, R., Krupa, R., Szmidt, H.L., Adams, P.D., Keasling, J.D., Soon Lee, T., Mukhopadhyay, A., Petzold, C.J., 2011. Targeted proteomics for metabolic pathway optimization: Application to terpene production. Metab. Eng. 13, 194–203. https://doi.org/10.1016/j.ymben.2010.12.005
Reichle, D.E., 2023. Anthropogenic alterations to the global carbon cycle and climate change, in: The Global Carbon Cycle and Climate Change. Elsevier, pp. 285–352. https://doi.org/10.1016/B978-0-443-18775-9.00002-4
Reifenrath, M., Boles, E., 2018. Engineering of hydroxymandelate synthases and the aromatic amino acid pathway enables de novo biosynthesis of mandelic and 4-hydroxymandelic acid with Saccharomyces cerevisiae. Metab. Eng. 45, 246–254. https://doi.org/10.1016/j.ymben.2018.01.001
Rienzo, M., Jackson, S.J., Chao, L.K., Leaf, T., Schmidt, T.J., Navidi, A.H., Nadler, D.C., Ohler, M., Leavell, M.D., 2021. High-throughput screening for high-efficiency small-molecule biosynthesis. Metab. Eng. 63, 102–125. https://doi.org/10.1016/j.ymben.2020.09.004
Rocke, A.J., 2015. It Began with a Daydream: The 150th Anniversary of the Kekulé Benzene Structure. Angew. Chem. Int. Ed. 54, 46–50. https://doi.org/10.1002/anie.201408034
Rodrigues, C.I.S., Wahl, A., Gombert, A.K., 2021. Aerobic growth physiology of *Saccharomyces cerevisiae* on sucrose is strain-dependent. FEMS Yeast Res. 21, foab021. https://doi.org/10.1093/femsyr/foab021
Rodriguez, A., Chen, Y., Khoomrung, S., Özdemir, E., Borodina, I., Nielsen, J., 2017a. Comparison of the metabolic response to over-production of p-coumaric acid in two yeast strains. Metab. Eng. 44, 265–272. https://doi.org/10.1016/j.ymben.2017.10.013
Rodriguez, A., Kildegaard, K.R., Li, M., Borodina, I., Nielsen, J., 2015. Establishment of a yeast platform strain for production of p-coumaric acid through metabolic engineering of aromatic amino acid biosynthesis. Metab. Eng. 31, 181–188. https://doi.org/10.1016/j.ymben.2015.08.003
Rodriguez, A., Strucko, T., Stahlhut, S.G., Kristensen, M., Svenssen, D.K., Forster, J., Nielsen, J., Borodina, I., 2017b. Metabolic engineering of yeast for fermentative production of

flavonoids. Bioresour. Technol. 245, 1645–1654. https://doi.org/10.1016/j.biortech.2017.06.043
Rönicke, V., Graulich, W., Mumberg, D., Müller, R., Funk, M., 1997. Use of conditional promoters for expression of heterologous proteins in Saccharomyces cerevisiae, in: Methods in Enzymology. Elsevier, pp. 313–322. https://doi.org/10.1016/S0076-6879(97)83025-X
Roostita, R., Fleet, G.H., 1996. Growth of yeasts in milk and associated changes to milk composition. Int. J. Food Microbiol. 31, 205–219. https://doi.org/10.1016/0168-1605(96)00999-3
Rorrer, N.A., Dorgan, J.R., Vardon, D.R., Martinez, C.R., Yang, Y., Beckham, G.T., 2016. Renewable Unsaturated Polyesters from Muconic Acid. ACS Sustain. Chem. Eng. 4, 6867–6876. https://doi.org/10.1021/acssuschemeng.6b01820
Rychel, K., Decker, K., Sastry, A.V., Phaneuf, P.V., Poudel, S., Palsson, B.O., 2021. iModulonDB: a knowledgebase of microbial transcriptional regulation derived from machine learning. Nucleic Acids Res. 49, D112–D120. https://doi.org/10.1093/nar/gkaa810
Ryu, J.Y., Kim, H.U., Lee, S.Y., 2019. Deep learning enables high-quality and high-throughput prediction of enzyme commission numbers. Proc. Natl. Acad. Sci. 116, 13996–14001. https://doi.org/10.1073/pnas.1821905116
Rywińska, A., Juszczyk, P., Wojtatowicz, M., Robak, M., Lazar, Z., Tomaszewska, L., Rymowicz, W., 2013. Glycerol as a promising substrate for Yarrowia lipolytica biotechnological applications. Biomass Bioenergy 48, 148–166. https://doi.org/10.1016/j.biombioe.2012.11.021
Sáez-Sáez, J., Wang, G., Marella, E.R., Sudarsan, S., Cernuda Pastor, M., Borodina, I., 2020. Engineering the oleaginous yeast Yarrowia lipolytica for high-level resveratrol production. Metab. Eng. 62, 51–61. https://doi.org/10.1016/j.ymben.2020.08.009
Sánchez, B.J., Zhang, C., Nilsson, A., Lahtvee, P., Kerkhoven, E.J., Nielsen, J., 2017. Improving the phenotype predictions of a yeast genome-scale metabolic model by incorporating enzymatic constraints. Mol. Syst. Biol. 13, 935. https://doi.org/10.15252/msb.20167411
Sandberg, T.E., Salazar, M.J., Weng, L.L., Palsson, B.O., Feist, A.M., 2019. The emergence of adaptive laboratory evolution as an efficient tool for biological discovery and industrial biotechnology. Metab. Eng. 56, 1–16. https://doi.org/10.1016/j.ymben.2019.08.004
Sanger, F., Nicklen, S., Coulson, A.R., 1977. DNA sequencing with chain-terminating inhibitors. Proc. Natl. Acad. Sci. 74, 5463–5467. https://doi.org/10.1073/pnas.74.12.5463
Sastry, A.V., Gao, Y., Szubin, R., Hefner, Y., Xu, S., Kim, D., Choudhary, K.S., Yang, L., King, Z.A., Palsson, B.O., 2019. The Escherichia coli transcriptome mostly consists of independently regulated modules. Nat. Commun. 10, 5536. https://doi.org/10.1038/s41467-019-13483-w
Sauer, M., 2016. Industrial production of acetone and butanol by fermentation—100 years later. FEMS Microbiol. Lett. 363, fnw134. https://doi.org/10.1093/femsle/fnw134
Sauer, U., 2006. Metabolic networks in motion: ^{13}C-based flux analysis. Mol. Syst. Biol. 2, 62. https://doi.org/10.1038/msb4100109
Schläger, S., Dräger, B., 2016. Exploiting plant alkaloids. Curr. Opin. Biotechnol. 37, 155–164. https://doi.org/10.1016/j.copbio.2015.12.003
Schleyer, P. von R., 2001. Introduction: Aromaticity. Chem. Rev. 101, 1115–1118. https://doi.org/10.1021/cr0103221
Schubert, O.T., Röst, H.L., Collins, B.C., Rosenberger, G., Aebersold, R., 2017. Quantitative proteomics: challenges and opportunities in basic and applied research. Nat. Protoc. 12, 1289–1294. https://doi.org/10.1038/nprot.2017.040
Schwann, Th., 1837. Vorläufige Mittheilung, betreffend Versuche über die Weingährung und Fäulniss. Ann. Phys. Chem. 117, 184–193. https://doi.org/10.1002/andp.18371170517

Shang, Y., Zhang, P., Wei, W., Li, J., Ye, B.-C., 2023. Metabolic engineering for the high-yield production of polydatin in Yarrowia lipolytica. Bioresour. Technol. 129129. https://doi.org/10.1016/j.biortech.2023.129129

Si, H.-M., Zhang, F., Wu, A.-N., Han, R.-Z., Xu, G.-C., Ni, Y., 2016. DNA microarray of global transcription factor mutant reveals membrane-related proteins involved in n-butanol tolerance in Escherichia coli. Biotechnol. Biofuels 9, 114. https://doi.org/10.1186/s13068-016-0527-9

Sibirny, A., Madzak, C., Fickers, P., 2015. Genetic engineering of nonconventional yeasts for the production of valuable compounds, in: Microbial Biotechnology. CRC Press.

Siewers, V., 2014. An Overview on Selection Marker Genes for Transformation of Saccharomyces cerevisiae, in: Mapelli, V. (Ed.), Yeast Metabolic Engineering, Methods in Molecular Biology. Springer New York, New York, NY, pp. 3–15. https://doi.org/10.1007/978-1-4939-0563-8_1

Sivakumar, T.V., Giri, V., Park, J.H., Kim, T.Y., Bhaduri, A., 2016. ReactPRED: a tool to predict and analyze biochemical reactions. Bioinformatics 32, 3522–3524. https://doi.org/10.1093/bioinformatics/btw491

Skjoedt, M.L., Snoek, T., Kildegaard, K.R., Arsovska, D., Eichenberger, M., Goedecke, T.J., Rajkumar, A.S., Zhang, J., Kristensen, M., Lehka, B.J., Siedler, S., Borodina, I., Jensen, M.K., Keasling, J.D., 2016. Engineering prokaryotic transcriptional activators as metabolite biosensors in yeast. Nat. Chem. Biol. 12, 951–958. https://doi.org/10.1038/nchembio.2177

Snoek, T., Romero-Suarez, D., Zhang, J., Ambri, F., Skjoedt, M.L., Sudarsan, S., Jensen, M.K., Keasling, J.D., 2018. An Orthogonal and pH-Tunable Sensor-Selector for Muconic Acid Biosynthesis in Yeast. ACS Synth. Biol. 7, 995–1003. https://doi.org/10.1021/acssynbio.7b00439

Soltanieh, M., Zohrabian, A., Gholipour, M.J., Kalnay, E., 2016. A review of global gas flaring and venting and impact on the environment: Case study of Iran. Int. J. Greenh. Gas Control 49, 488–509. https://doi.org/10.1016/j.ijggc.2016.02.010

Speight, J.G., 2016. Handbook of Petroleum Refining, 0 ed. CRC Press. https://doi.org/10.1201/9781315374079

Srinivasan, P., Smolke, C.D., 2021. Engineering cellular metabolite transport for biosynthesis of computationally predicted tropane alkaloid derivatives in yeast. Proc. Natl. Acad. Sci. 118, e2104460118. https://doi.org/10.1073/pnas.2104460118

Srinivasan, P., Smolke, C.D., 2020. Biosynthesis of medicinal tropane alkaloids in yeast. Nature 585, 614–619. https://doi.org/10.1038/s41586-020-2650-9

Suástegui, M., Yu Ng, C., Chowdhury, A., Sun, W., Cao, M., House, E., Maranas, C.D., Shao, Z., 2017. Multilevel engineering of the upstream module of aromatic amino acid biosynthesis in Saccharomyces cerevisiae for high production of polymer and drug precursors. Metab. Eng. 42, 134–144. https://doi.org/10.1016/j.ymben.2017.06.008

Sumita, T., Iida, T., Yamagami, S., Horiuchi, H., Takagi, M., Ohta, A., 2002. YlALK1 encoding the cytochrome P450ALK1 in Yarrowia lipolytica is transcriptionally induced by n-alkane through two distinct cis-elements on its promoter. Biochem. Biophys. Res. Commun. 294, 1071–1078. https://doi.org/10.1016/S0006-291X(02)00607-1

Sveshnikova, A., MohammadiPeyhani, H., Hatzimanikatis, V., 2022. ARBRE: Computational resource to predict pathways towards industrially important aromatic compounds. Metab. Eng. 72, 259–274. https://doi.org/10.1016/j.ymben.2022.03.013

Sweeney, W.A., Bryan, P.F., 2000. BTX Processing, in: John Wiley & Sons, Inc (Ed.), Kirk-Othmer Encyclopedia of Chemical Technology. Wiley. https://doi.org/10.1002/0471238961.02202419230505.a01

Tai, M., Stephanopoulos, G., 2013. Engineering the push and pull of lipid biosynthesis in oleaginous yeast Yarrowia lipolytica for biofuel production. Metab. Eng. 15, 1–9. https://doi.org/10.1016/j.ymben.2012.08.007

Talapatra, S.K., Talapatra, B., 2015. Chemistry of Plant Natural Products: Stereochemistry, Conformation, Synthesis, Biology, and Medicine, 1st ed. 2015. ed. Springer Berlin

Heidelberg : Imprint: Springer, Berlin, Heidelberg. https://doi.org/10.1007/978-3-642-45410-3

Tanaka, Y., Minggat, E., Roseli, W., 2021. The impact of tropical land-use change on downstream riverine and estuarine water properties and biogeochemical cycles: a review. Ecol. Process. 10, 40. https://doi.org/10.1186/s13717-021-00315-3

Taskesenligil, Y., Aslan, M., Cogurcu, T., Saracoglu, N., 2023. Directed C–H Functionalization of C3-Aldehyde, Ketone, and Acid/Ester-Substituted Free (NH) Indoles with Iodoarenes *via* a Palladium Catalyst System. J. Org. Chem. 88, 1299–1318. https://doi.org/10.1021/acs.joc.2c00716

Tehlivets, O., Scheuringer, K., Kohlwein, S.D., 2007. Fatty acid synthesis and elongation in yeast. Biochim. Biophys. Acta BBA - Mol. Cell Biol. Lipids 1771, 255–270. https://doi.org/10.1016/j.bbalip.2006.07.004

Teng, Y., Zhang, J., Jiang, T., Zou, Y., Gong, X., Yan, Y., 2022. Biosensor-enabled pathway optimization in metabolic engineering. Curr. Opin. Biotechnol. 75, 102696. https://doi.org/10.1016/j.copbio.2022.102696

Teoh, S.T., Putri, S., Mukai, Y., Bamba, T., Fukusaki, E., 2015. A metabolomics-based strategy for identification of gene targets for phenotype improvement and its application to 1-butanol tolerance in Saccharomyces cerevisiae. Biotechnol. Biofuels 8, 144. https://doi.org/10.1186/s13068-015-0330-z

Thiele, I., Palsson, B.Ø., 2010. A protocol for generating a high-quality genome-scale metabolic reconstruction. Nat. Protoc. 5, 93–121. https://doi.org/10.1038/nprot.2009.203

Thomik, T., Wittig, I., Choe, J., Boles, E., Oreb, M., 2017. An artificial transport metabolon facilitates improved substrate utilization in yeast. Nat. Chem. Biol. 13, 1158–1163. https://doi.org/10.1038/nchembio.2457

Tian, M., Reed, J.L., 2018. Integrating proteomic or transcriptomic data into metabolic models using linear bound flux balance analysis. Bioinformatics 34, 3882–3888. https://doi.org/10.1093/bioinformatics/bty445

Toledo-Pereyra, L.H., 2009. The Strange Little Animals of Antony van Leeuwenhoek Surgical Revolution. J. Invest. Surg. 22, 4–8. https://doi.org/10.1080/08941930802634439

Trassaert, M., Vandermies, M., Carly, F., Denies, O., Thomas, S., Fickers, P., Nicaud, J.-M., 2017. New inducible promoter for gene expression and synthetic biology in Yarrowia lipolytica. Microb. Cell Factories 16, 141. https://doi.org/10.1186/s12934-017-0755-0

Traube, M., 1858. Zur Theorie der Gährungs- und Verwesungs erscheinungen, wie der Fermentwirkungen überhaupt. Ann. Phys. Chem. 179, 331–344. https://doi.org/10.1002/andp.18581790211

Tzin, V., Galili, G., 2010a. The Biosynthetic Pathways for Shikimate and Aromatic Amino Acids in *Arabidopsis thaliana*. Arab. Book 8, e0132. https://doi.org/10.1199/tab.0132

Tzin, V., Galili, G., 2010b. New Insights into the Shikimate and Aromatic Amino Acids Biosynthesis Pathways in Plants. Mol. Plant 3, 956–972. https://doi.org/10.1093/mp/ssq048

Ukibe, K., Katsuragi, T., Tani, Y., Takagi, H., 2008. Efficient screening for astaxanthin-overproducing mutants of the yeast *Xanthophyllomyces dendrorhous* by flow cytometry. FEMS Microbiol. Lett. 286, 241–248. https://doi.org/10.1111/j.1574-6968.2008.01278.x

van der Hoek, S.A., Borodina, I., 2020. Transporter engineering in microbial cell factories: the ins, the outs, and the in-betweens. Curr. Opin. Biotechnol. 66, 186–194. https://doi.org/10.1016/j.copbio.2020.08.002

Vardon, D.R., Rorrer, N.A., Salvachúa, D., Settle, A.E., Johnson, C.W., Menart, M.J., Cleveland, N.S., Ciesielski, P.N., Steirer, K.X., Dorgan, J.R., Beckham, G.T., 2016. cis,cis-Muconic acid: separation and catalysis to bio-adipic acid for nylon-6,6 polymerization. Green Chem. 18, 3397–3413. https://doi.org/10.1039/C5GC02844B

Vasilakou, E., van Loosdrecht, M.C.M., Wahl, S.A., 2020. Escherichia coli metabolism under short-term repetitive substrate dynamics: adaptation and trade-offs. Microb. Cell Factories 19, 116. https://doi.org/10.1186/s12934-020-01379-0

Vogt, T., 2010. Phenylpropanoid Biosynthesis. Mol. Plant 3, 2–20. https://doi.org/10.1093/mp/ssp106

Volk, M.J., Tran, V.G., Tan, S.-I., Mishra, S., Fatma, Z., Boob, A., Li, H., Xue, P., Martin, T.A., Zhao, H., 2023. Metabolic Engineering: Methodologies and Applications. Chem. Rev. 123, 5521–5570. https://doi.org/10.1021/acs.chemrev.2c00403

Wagner, J.M., Liu, L., Yuan, S.-F., Venkataraman, M.V., Abate, A.R., Alper, H.S., 2018a. A comparative analysis of single cell and droplet-based FACS for improving production phenotypes: Riboflavin overproduction in Yarrowia lipolytica. Metab. Eng. 47, 346–356. https://doi.org/10.1016/j.ymben.2018.04.015

Wagner, J.M., Williams, E.V., Alper, H.S., 2018b. Developing a *piggyBac* Transposon System and Compatible Selection Markers for Insertional Mutagenesis and Genome Engineering in *Yarrowia lipolytica*. Biotechnol. J. 13, 1800022. https://doi.org/10.1002/biot.201800022

Wake, H., 2005. Oil refineries: a review of their ecological impacts on the aquatic environment. Estuar. Coast. Shelf Sci. 62, 131–140. https://doi.org/10.1016/j.ecss.2004.08.013

Wang, G., Øzmerih, S., Guerreiro, R., Meireles, A.C., Carolas, A., Milne, N., Jensen, M.K., Ferreira, B.S., Borodina, I., 2020. Improvement of cis,cis-Muconic Acid Production in Saccharomyces cerevisiae through Biosensor-Aided Genome Engineering. ACS Synth. Biol. 9, 634–646. https://doi.org/10.1021/acssynbio.9b00477

Wang, G., Tavares, A., Schmitz, S., França, L., Almeida, H., Cavalheiro, J., Carolas, A., Øzmerih, S., Blank, L.M., Ferreira, B.S., Borodina, I., 2022. An integrated yeast-based process for *cis* , *cis* -muconic acid production. Biotechnol. Bioeng. 119, 376–387. https://doi.org/10.1002/bit.27992

Wasylenko, T.M., Ahn, W.S., Stephanopoulos, G., 2015. The oxidative pentose phosphate pathway is the primary source of NADPH for lipid overproduction from glucose in Yarrowia lipolytica. Metab. Eng. 30, 27–39. https://doi.org/10.1016/j.ymben.2015.02.007

Watson, J.D., Crick, F.H.C., 1953. Molecular Structure of Nucleic Acids: A Structure for Deoxyribose Nucleic Acid. Nature 171, 737–738. https://doi.org/10.1038/171737a0

Wei, S., Jian, X., Chen, J., Zhang, C., Hua, Q., 2017. Reconstruction of genome-scale metabolic model of Yarrowia lipolytica and its application in overproduction of triacylglycerol. Bioresour. Bioprocess. 4, 51. https://doi.org/10.1186/s40643-017-0180-6

Wei, W., Zhang, P., Shang, Y., Zhou, Y., Ye, B.-C., 2020. Metabolically engineering of Yarrowia lipolytica for the biosynthesis of naringenin from a mixture of glucose and xylose. Bioresour. Technol. 314, 123726. https://doi.org/10.1016/j.biortech.2020.123726

Wolf, S., Becker, J., Tsuge, Y., Kawaguchi, H., Kondo, A., Marienhagen, J., Bott, M., Wendisch, V.F., Wittmann, C., 2021. Advances in metabolic engineering of *Corynebacterium glutamicum* to produce high-value active ingredients for food, feed, human health, and well-being. Essays Biochem. 65, 197–212. https://doi.org/10.1042/EBC20200134

Wong, L., Engel, J., Jin, E., Holdridge, B., Xu, P., 2017. YaliBricks, a versatile genetic toolkit for streamlined and rapid pathway engineering in Yarrowia lipolytica. Metab. Eng. Commun. 5, 68–77. https://doi.org/10.1016/j.meteno.2017.09.001

Wood, V., Rutherford, K.M., Ivens, A., Rajandream, M.-A., Barrell, B., 2001. A Re-Annotation of the *Saccharomyces cerevisiae* Genome. Comp. Funct. Genomics 2, 143–154. https://doi.org/10.1002/cfg.86

Woolston, B.M., Edgar, S., Stephanopoulos, G., 2013. Metabolic Engineering: Past and Future. Annu. Rev. Chem. Biomol. Eng. 4, 259–288. https://doi.org/10.1146/annurev-chembioeng-061312-103312

Wright, A.V., Nuñez, J.K., Doudna, J.A., 2016. Biology and Applications of CRISPR Systems: Harnessing Nature's Toolbox for Genome Engineering. Cell 164, 29–44. https://doi.org/10.1016/j.cell.2015.12.035

Wu, J., Wang, Z., Zhang, X., Zhou, P., Xia, X., Dong, M., 2019. Improving medium chain fatty acid production in Escherichia coli by multiple transporter engineering. Food Chem. 272, 628–634. https://doi.org/10.1016/j.foodchem.2018.08.102

Xie, N.-Z., Liang, H., Huang, R.-B., Xu, P., 2014. Biotechnological production of muconic acid: current status and future prospects. Biotechnol. Adv. 32, 615–622. https://doi.org/10.1016/j.biotechadv.2014.04.001

Xu, Y., Holic, R., Hua, Q., 2020. Comparison and Analysis of Published Genome-scale Metabolic Models of Yarrowia lipolytica. Biotechnol. Bioprocess Eng. 25, 53–61. https://doi.org/10.1007/s12257-019-0208-1

Xu, Z., Yang, Z., Liu, Y., Lu, Y., Chen, K., Zhu, W., 2014. Halogen Bond: Its Role beyond Drug–Target Binding Affinity for Drug Discovery and Development. J. Chem. Inf. Model. 54, 69–78. https://doi.org/10.1021/ci400539q

Xue, Z., Sharpe, P.L., Hong, S.-P., Yadav, N.S., Xie, D., Short, D.R., Damude, H.G., Rupert, R.A., Seip, J.E., Wang, J., Pollak, D.W., Bostick, M.W., Bosak, M.D., Macool, D.J., Hollerbach, D.H., Zhang, H., Arcilla, D.M., Bledsoe, S.A., Croker, K., McCord, E.F., Tyreus, B.D., Jackson, E.N., Zhu, Q., 2013. Production of omega-3 eicosapentaenoic acid by metabolic engineering of Yarrowia lipolytica. Nat. Biotechnol. 31, 734–740. https://doi.org/10.1038/nbt.2622

Xue, Z., Yadav, N.S., Zhu, Q.Q., 2009. Optimized strains of yarrowia lipolytica for high eicosapentaenoic acid production. US20090093543A1.

Yáñez Feliú, G., Earle Gómez, B., Codoceo Berrocal, V., Muñoz Silva, M., Nuñez, I.N., Matute, T.F., Arce Medina, A., Vidal, G., Vidal Céspedes, C., Dahlin, J., Federici, F., Rudge, T.J., 2021. Flapjack: Data Management and Analysis for Genetic Circuit Characterization. ACS Synth. Biol. 10, 183–191. https://doi.org/10.1021/acssynbio.0c00554

Yang, H.-C., Li, W., Sun, J., Gross, M.L., 2023. Advances in Mass Spectrometry on Membrane Proteins. Membranes 13, 457. https://doi.org/10.3390/membranes13050457

Yao, R., Li, J., Feng, L., Zhang, X., Hu, H., 2019. 13C metabolic flux analysis-guided metabolic engineering of Escherichia coli for improved acetol production from glycerol. Biotechnol. Biofuels 12, 29. https://doi.org/10.1186/s13068-019-1372-4

Yunus, I.S., Lee, T.S., 2022. Applications of targeted proteomics in metabolic engineering: advances and opportunities. Curr. Opin. Biotechnol. 75, 102709. https://doi.org/10.1016/j.copbio.2022.102709

Zamboni, N., Fendt, S.-M., Rühl, M., Sauer, U., 2009. 13C-based metabolic flux analysis. Nat. Protoc. 4, 878–892. https://doi.org/10.1038/nprot.2009.58

Zelasko, S., Palaria, A., Das, A., 2013. Optimizations to achieve high-level expression of cytochrome P450 proteins using Escherichia coli expression systems. Protein Expr. Purif. 92, 77–87. https://doi.org/10.1016/j.pep.2013.07.017

Zha, J., Wu, X., Gong, G., Koffas, M.A.G., 2019. Pathway enzyme engineering for flavonoid production in recombinant microbes. Metab. Eng. Commun. 9, e00104. https://doi.org/10.1016/j.mec.2019.e00104

Zhang, H., Zhang, L., Chen, H., Chen, Y.Q., Chen, W., Song, Y., Ratledge, C., 2014. Enhanced lipid accumulation in the yeast Yarrowia lipolytica by over-expression of ATP:citrate lyase from Mus musculus. J. Biotechnol. 192, 78–84. https://doi.org/10.1016/j.jbiotec.2014.10.004

Zhang, J., Hansen, L.G., Gudich, O., Viehrig, K., Lassen, L.M.M., Schrübbers, L., Adhikari, K.B., Rubaszka, P., Carrasquer-Alvarez, E., Chen, L., D'Ambrosio, V., Lehka, B., Haidar, A.K., Nallapareddy, S., Giannakou, K., Laloux, M., Arsovska, D., Jørgensen, M.A.K., Chan, L.J.G., Kristensen, M., Christensen, H.B., Sudarsan, S., Stander, E.A., Baidoo, E., Petzold, C.J., Wulff, T., O'Connor, S.E., Courdavault, V., Jensen, M.K., Keasling, J.D., 2022. A microbial supply chain for production of the anti-cancer drug vinblastine. Nature 609, 341–347. https://doi.org/10.1038/s41586-022-05157-3

Zhang, J., Petersen, S.D., Radivojevic, T., Ramirez, A., Pérez-Manríquez, A., Abeliuk, E., Sánchez, B.J., Costello, Z., Chen, Y., Fero, M.J., Martin, H.G., Nielsen, J., Keasling, J.D., Jensen, M.K., 2020. Combining mechanistic and machine learning models for predictive engineering and optimization of tryptophan metabolism. Nat. Commun. 11, 4880. https://doi.org/10.1038/s41467-020-17910-1

Zhang, X., Liu, X., Meng, Y., Zhang, L., Qiao, J., Zhao, G.-R., 2021. Combinatorial engineering of Saccharomyces cerevisiae for improving limonene production. Biochem. Eng. J. 176, 108155. https://doi.org/10.1016/j.bej.2021.108155

Zhang, Y., Adams, I.P., Ratledge, Colin., 2007. Malic enzyme: the controlling activity for lipid production? Overexpression of malic enzyme in Mucor circinelloides leads to a 2.5-fold increase in lipid accumulation. Microbiology 153, 2013–2025. https://doi.org/10.1099/mic.0.2006/002683-0

Zhang, Y., Nielsen, J., Liu, Z., 2017. Engineering yeast metabolism for production of terpenoids for use as perfume ingredients, pharmaceuticals and biofuels. FEMS Yeast Res. 17. https://doi.org/10.1093/femsyr/fox080

Zhang, Z., Moo-Young, M., Chisti, Y., 1996. Plasmid stability in recombinant Saccharomyces cerevisiae. Biotechnol. Adv. 14, 401–435. https://doi.org/10.1016/S0734-9750(96)00033-X

Zhu, Y., Zhou, C., Wang, Y., Li, C., 2020. Transporter Engineering for Microbial Manufacturing. Biotechnol. J. 15, 1900494. https://doi.org/10.1002/biot.201900494

CHAPTER 2

Engineering the oleaginous yeast *Yarrowia lipolytica* for high-level resveratrol production

This chapter contains a previously published article:

Sáez-Sáez, J., Wang, G., Marella, E.R., Sudarsan, S., Cernuda Pastor, M., Borodina, I., 2020.
Engineering the oleaginous yeast *Yarrowia lipolytica* for high-level resveratrol production. *Metabolic Engineering*. 62, 51–61.
DOI: 10.1016/j.ymben.2020.08.009

Abstract

Resveratrol is a plant secondary metabolite with multiple health-beneficial properties. Microbial production of resveratrol in model microorganisms requires extensive engineering to reach commercially viable levels. Here, we explored the potential of the non-conventional yeast *Yarrowia lipolytica* to produce resveratrol and several other shikimate pathway-derived metabolites (*p*-coumaric acid, *cis*,*cis*-muconic acid, and salicylic acid). The *Y. lipolytica* strain expressing a heterologous pathway produced 52.1 ± 1.2 mg/L resveratrol in a small-scale cultivation. The titer increased to 409.0 ± 1.2 mg/L when the strain was further engineered with feedback-insensitive alleles of the key genes in the shikimate pathway and with five additional copies of the heterologous biosynthetic genes. In controlled fed-batch bioreactor, the strain produced 12.4 ± 0.3 g/L resveratrol, the highest reported titer to date for *de novo* resveratrol production, with a yield on glucose of 54.4 ± 1.6 mg/g and a productivity of 0.14 ± 0.01 g/L/h. The study showed that *Y. lipolytica* is an attractive host organism for the production of resveratrol and possibly other shikimate-pathway derived metabolites.

Introduction

Resveratrol (3,5,4′-trihydroxy-*trans*-stilbene) is a stilbenoid naturally present in grapes, berries, Japanese knotweed, and peanuts (Burns et al., 2002). In plants, it serves as phytoalexin, produced in defense against injuries and microbial infections (Langcake and Pryce, 1976; Vestergaard and Ingmer, 2019). In the past two decades, over 1,500 studies have been published on the health effects of resveratrol (PubMed, 2020). Clinical trials have proven that resveratrol beneficially influences disease biomarkers of diabetes, cardiovascular diseases, and neurological disorders (Bhatt et al., 2012; Brasnyó et al., 2011; Tomé-Carneiro et al., 2012; Turner et al., 2015). Resveratrol is commercialized as food and cosmetics ingredient and is sold as food supplement. The current market is around $97.7 million and is expected to grow at a compound annual growth rate (CAGR) of 8.1% from 2018 to 2028 (Future Market Insights, 2019). Extraction from Japanese knotweed remains the main source of resveratrol, but chemical synthesis by DSM and microbial fermentation by Evolva are gaining ground in the market (DSM, 2014; Evolva, 2019; Future Market Insights,

2019). Microbial fermentation process of resveratrol production has a number of advantages, such as low cost, high purity of the product, and independence on season.

Resveratrol is biosynthesized in plants via the phenylpropanoids pathway, using as precursors the aromatic amino acids L-phenylananine (L-Phe) or L-tyrosine (L-Tyr) (Sparvoli et al., 1994; Rosler et al., 1997). The first biosynthetic step involves the deamination of L-Phe/L-Tyr by phenylalanine/tyrosine ammonia lyase (PAL/TAL). In the L-Phe branch, PAL activity yields *trans*-cinnamic acid, which is hydroxylated into *p*-coumaric acid by cinnamic acid hydroxylase (C4H), a cytochrome P450 enzyme (Winkel-Shirley, 2001). Alternatively, TAL activity in the L-Tyr branch results in *p*-coumaric acid in a single enzymatic step (Jendresen et al., 2015). Further, coenzyme A is attached to *p*-coumaric acid by 4-coumaroyl-CoA ligase (4CL), resulting in 4-coumaroyl-CoA. In a final step, resveratrol synthase, a type III polyketide synthase (PKS), incorporates three units of malonyl-CoA to synthesize resveratrol (Winkel-Shirley, 2001). Microbial production of resveratrol by heterologous expression of the plant pathway has been successfully carried out in several hosts (Table 1, Table S1) (Thapa et al., 2019). Extensive metabolic engineering strategies have also been implemented to improve resveratrol titers, mainly aiming at rewiring carbon metabolism towards shikimate pathway, increasing L-Tyr/L-Phe and malonyl-CoA precursor supply, alleviating feedback regulations, or tuning gene copy number in the heterologous pathway (Liu et al., 2019; Li et al., 2015, 2016; Lim et al., 2011). Despite the efforts, the *de novo* production levels reported in scientific publications are still low, with the highest titer of 0.8 g/L achieved in *S. cerevisiae* (Li et al., 2016). Gram per liter titers have only been reached in *E. coli* by co-feeding *p*-coumaric acid (Lim et al., 2011), however addition of *p*-coumaric acid is not an option for a large-scale fermentation.

Yarrowia lipolytica is an emerging industrial host for the production of lipids, polyunsaturated fatty acids, and organic acids. As an oleaginous yeast, *Y. lipolytica* is naturally endowed with high fluxes towards malonyl-CoA and the pentose phosphate pathway (PPP) (Wasylenko et al., 2015; Blank et al., 2005). These metabolic traits could be particularly relevant for the production of shikimate pathway-derived compounds and plant natural products requiring aromatic amino acids and malonyl-CoA-derived building blocks, such as phenylpropanoids. Indeed, this yeast was recently shown as an attractive host for the biosynthesis of several plant flavonoids,

including naringenin, eriodictyol, taxifolin, and other aromatic compounds (Lv et al., 2019; Palmer et al., 2020; Lv et al., 2020; Gu et al., 2020a, 2020b; Shang et al., 2020; Wei et al., 2020). Resveratrol in particular has also been produced in *Y. lipolytica*, first described by DuPont and more recently in studies exploring the ability of the non-conventional yeast as production chassis for different polyketides and aromatics (Table S1) (Huang et al., 2006; Palmer et al., 2020; Gu et al., 2020a).

In this work, we have investigated the potential of *Y. lipolytica* for the production of several shikimate pathway-derived metabolites: *p*-coumaric acid, resveratrol, *cis*,*cis*-muconic acid, and salicylic acid.

Table 1. Resveratrol production in microbial hosts. The table includes the top producing strains per microorganism, considering also cultivations in which pathway precursors were fed. *Cerulenin was supplemented to the cultivation. **Refer to publication for detailed list of genetic modifications. n/a: metric not available as cultivation time was not reported. *4CL*: 4-coumaroyl-CoA, *STS*: stilbene synthase, *PAL*: phenylalanine ammonia-lyase, *C4H*: cinnamate-4-hydroxylase, *VST*: resveratrol synthase, *ACS*: acetyl-CoA synthase, *ATR2*: cytochrome P450 reductase, *ARO4*: 3-deoxy-D-arabinoheptulosonate-7-phosphate (DAHP) synthase, *ARO7*: chorismate mutase, *CYB5*: cytochrome b5, *ACC1*: acetyl-CoA carboxylase 1, *ARO10*: transaminated amino acid decarboxylase, *PEX10*: peroxisomal biogenesis factor 10, *TAL*: tyrosine ammonia-lyase, *pks*: polyketide synthase, fbr: feedback-resistant.

Microbial host	Genetic modifications	Metrics	Substrate/ Precursor fed	Reference
E. coli	*4CL* (*A. thaliana*) *STS* (*V. vinifera*)	Titer: 2.3 g/L Yield: 1.01 g/g *p*-coumaric acid Productivity: 95.83 mg/L/h	Glycerol/*p*-coumaric acid*	(Lim et al., 2011)
S. cerevisiae	*PAL* (*A. thaliana*) *C4H* (*A. thaliana*) *4CL* (*A. thaliana*) *VST* (*V. vinifera*) *ACS* (*S. enterica*) *ATR2* (*A. thaliana*) Overexpression of *ARO4*^{fbr}, *ARO7*^{fbr}, *CYB5,* and *ACC1* *ΔARO10*	Titer: 812 mg/L Yield: 8.87 mg/g glucose Productivity: 7.38 mg/L/h	Glucose/none	(Li et al., 2016)
Y. lipolytica	*4CL* (*N. tabacum*) *STS* (*A. hypogaea*)	Titer: 48.7 mg/L Yield: 0.15 g/g *p*-coumaric acid	Glucose/*p*-coumaric acid	(Palmer et al., 2020)

	Overexpression of *PEX10* and *ACC1*	Productivity: 0.29 mg/L/h		
C. glutamicum	*STS* (*A. hypogaea*) *4CL* (*P. crispum*) **	Titer: 158 mg/L Yield: 0.19 g/g *p*-coumaric acid Productivity: 2.19 mg/L/h	Glucose/*p*-coumaric acid*	(Kallscheuer et al., 2016)
L. lactis	*TAL, 4CL, STS, ACC* (different sources)	Titer: 1.27 mg/L Yield: 0.13 mg/g glucose Productivity: n/a	Glucose/none	(Gaspar et al., 2016)
S. venezuelae	*STS* (*A. hypogaea*) *4CL* (*S. coelicolor*) Pikromycin *pks* deletion	Titer: 0.4 mg/L Yield: 0.002 g/g *p*-coumaric acid Productivity: 0.006 mg/L/h	Sucrose/*p*-coumaric acid	(Park et al., 2009)

Materials and methods

Strain construction and cultivation

All *Y. lipolytica* strains constructed in this study are derived from ST6512, a W29 (NRRL Y-63746) derived strain harboring Cas9 in *KU70 locus* (Marella et al., 2019). The complete list of strains, plasmids, biobricks, and primers used in this work are available in the supplementary information 2 (Tables S2-S5). The strains are available upon request. The strain ST9671 has been deposited with Euroscarf collection (accession number Y41418). Unless otherwise stated, for pre-culture, strain construction, propagation, and cryostocking, yeast strains were grown at 30°C and 250 rpm (Thermo Fisher Scientific MaxQ8000) in YPD medium (10 g/L yeast extract, 20 g/L peptone, 20 g/L D-glucose). Media for plates contained 20 g/L agar.

Plasmids required for genome engineering were constructed using the set of vectors from EasyCloneYALI as backbones (Holkenbrink et al., 2018). Integrative vector backbones were PCR-amplified with compatible USER overhangs, while guide-RNA (gRNA) vector backbones for gene deletion were linearized by digestion. Synthetic genes required for *p*-coumaric acid, resveratrol, *cis*,*cis*-muconic acid and salicylic acid production were codon-optimized for *Y. lipolytica* using Thermo Fisher Scientific webtool and ordered as GeneArt Strings DNA Fragments. The DNA sequence of the synthetic genes is available in the supplementary information 2 (Table S6). Plasmid assembly and cloning was performed according to EasyCloneYALI instructions (Holkenbrink et al., 2018). For gene deletions, DNA fragments consisting of 400-600 bp up- and downstream of the target gene were used as repair template (800-1200 bp

total). All constructed plasmids were verified by Sanger sequencing (Eurofins Scientific SE). Yeast transformations were performed using a lithium acetate-based protocol as previously described (Holkenbrink et al., 2018). Transformants were selected using natMX or hphMX resistance markers. YPD plates for natMX or hphMX selection contained 250 mg/L of nourseothricin (Jena Bioscience, AB-101) or 400 mg/L hygromycin B (Invitrogen, 10687010), respectively.

Small-scale production and degradation assays

Standard production and degradation assays were performed in mineral medium containing 20 g/L D-glucose as carbon source (pH 6.0, adjusted with KOH), as described in (Jensen et al., 2014).

Strains from cryostocks were streaked onto YPD plates and incubated for 48 h at 30°C. Three single colonies from the YPD plate were inoculated for pre-culture in 24 deep-well plates (Enzyscreen B.V., CR1424) containing 3 mL of mineral medium, and incubated at 30°C for 48 h and 300 rpm agitation at 5 cm orbit cast, reaching the stationary phase. An adequate volume of pre-culture to start with an initial optical density (OD_{600}) of 0.1 was transferred to a fresh 24 deep-well plate containing 3 mL of medium, which was incubated for 72 h under the same conditions, reaching the stationary phase. After 72 h of cultivation, OD_{600} measurements and samples for HPLC analysis were prepared according to the procedure described in *Analytical methods*.

In the initial screening of *p*-coumaric acid and resveratrol production, the medium was supplemented with 2 mM L-tyrosine. The degradation assays were performed following the same conditions, but supplementing the mineral medium in the 72 h cultivation with the target compound at different concentrations.

Medium optimization for resveratrol production was carried out using mineral medium, YNB and YP with either 20/80 g/L glucose or 20/80 g/L glycerol as carbon source. YP contained 10 g/L yeast extract, 20 g/L peptone; YNB contained 6.7 g/L Yeast Nitrogen Base Without Amino Acids (Sigma-Aldrich, Y0626) and was adjusted to pH 6.0 with KOH. Pre-culture was carried out in standard YPD for 48 h in 24 deep-well plates. Pre-cultivation samples were centrifuged for 5 min at 3,000 x g, washed twice with sterile Milli-Q® water. An adequate volume to start at an initial OD_{600} of 0.1 was used to inoculate each of the cultivations in a new 24 deep-well plate, which

was incubated for 96 h and sampled every 24 h. In the assay to assess the effect of antifoam on resveratrol production, antifoam 204 (Sigma-Aldrich, A6426) was added to the standard mineral medium with 20 g/L glucose at concentrations of 1%, 3% and 5% v/v.

Fed-batch fermentation in bioreactor

For seed culture preparation, strain from cryostock was streaked onto a YPD plate and grown at 30°C for 48 h. Biomass from the plate was transferred to 1 mL YPD in a 14 mL pre-culture tube and incubated at 30°C for 18 h. A pre-culture volume of 250 µL was used to inoculate 50 mL of YPD in a 250 mL baffled shake flask and incubated at 30°C for 24 h and 250 rpm. The content of the shake flask was centrifuged for 5 min at 5,000 x g, washed twice with mineral medium and concentrated in 5 mL volume. This cell suspension was used to inoculate the reactors to an initial OD_{600} of 1.0.

The fermentation was carried out in duplicate in 1 L bioreactors (BIOSTAT® Q plus, Sartorius, Goettingen, Germany) equipped with measurement probes for pH, dissolved oxygen (DO) and temperature. Aeration was achieved with a horseshoe sparger. Off-gas O_2 and CO_2 levels were logged with a Prima BT MS (Thermo Fisher Scientific). Fermentation was carried out at 30°C and pH was maintained at 6.0 by automatic addition of 5 M KOH. The reactors initially contained 400 mL of mineral medium. One liter of medium contained 5 g $(NH_4)_2SO_4$, 3 g KH_2PO_4, 0.5 g $MgSO_4 \cdot 7H_2O$, 40 g D-glucose, 2 mL trace metal solution, 1 mL vitamin solution, and 0.4 mL antifoam 204. The trace metal and vitamin solutions were prepared as in (Jensen et al., 2014). Stirring and aeration rate were initiated at 540 rpm and 0.5 standard liter per minute (SLPM), respectively. The feed addition started when DO decreased from the initial 100% to 35%. During the fed-batch phase, DO was maintained at 20% by a two-level cascade of stirring (between 540 and 1,200 rpm) and airflow (between 0.5 and 1.5 SLPM). The initial feed rate was 1.0 g/h, with an exponential increase of 0.05 h^{-1}. When stirring and airflow reached maximum setpoints, feeding was changed to a constant feed rate until the end of the fermentation. The feed medium contained 460 g/L of D-glucose and 0.6 mL/L of antifoam, while the rest of the medium components were the same as in batch mineral medium, but at 10-fold higher concentration. Additional sterile antifoam 204 was

manually added to the reactors when foaming was observed. Sampling was carried out three times per day to measure OD_{600}, cell dry weight, and resveratrol.

Analytical methods

OD_{600} measurements were performed in a NanoPhotometer® P-Class (Implen GmbH) with 1.5 mL volume and 1 cm path cuvettes (Brand GmbH). The cell dry weight measurements were performed using Whatman™ cellulose nitrate membrane filters disc with 0.45 µm pore size (VWR, 7184–004). 500 µL of reactor sample was centrifuged at 17,000 x g for 5 min. Cell pellet was resuspended in 1 mL deionized water and the suspension was loaded onto the filter placed on a filtration unit. Filters were washed with 5 mL deionized water through vacuum. Before and after loading the sample, filters were dried using a microwave and weighed, as previously described (Marella et al., 2019). Cell dry weight was calculated as the difference in filter weights before and after loading the cell suspension. Measurements were performed in duplicate for each of the reactors.

For salicylic acid and *cis*,*cis*-muconic acid quantification, cultivation samples were centrifuged at 17,000 x g for 5 min and the supernatant used for analysis. In the case of *p*-coumaric acid and resveratrol, cultivation samples were mixed with an equal volume of absolute ethanol, vortexed thoroughly for 10 sec, and centrifuged at 17,000 x g for 5 min. Supernatants were used for analysis. In the case of intracellular analysis of resveratrol, 1 mL of broth was centrifuged at 17,000 x g for 5 min and the cell pellet was washed twice with 1 mL 50% v/v ethanol. Cells were resuspended in 500 µL of water and transferred to 2 mL screwcap tubes filled with 300 µL of glass beads (212-300 µm particle size, Sigma-Aldrich, G1277). Cell suspensions were disrupted with Precellys® 24 (Bertin Instruments) for five cycles of 20 s shaking at 5,000 rpm with 5-min pauses between cycles, when the samples were placed on ice. 500 µL of absolute ethanol was added to the disrupted cells and vortexed thoroughly. Samples were centrifuged at 17,000 x g for 5 min and the supernatant was used for the analysis. The samples from small-scale cultivations were analyzed on HPLC the same day. Bioreactor samples were prepared for HPLC and stored at -20°C until analysis.

Quantification of all compounds was performed with Dionex UltiMate 3000 HPLC (Thermo Fisher Scientific), equipped with a DAD-3000 UV/Vis detector (Dionex) and

a RI-101 Refractive Index Detector (Dionex). HPLC-grade solvents were used for the mobile phase. Peaks corresponding to the target compounds were identified by comparison to prepared standards (Sigma-Aldrich). Peak areas were used for compound quantification using external standard calibration method. Analysis of HPLC results was performed using the software Chromeleon 7 (ThermoFisher Scientific).

For resveratrol and *p*-coumaric acid, the HPLC system was equipped with a Discovery HS F5 150 mm × 2.1 mm column, particle size 3 µm (Supelco, 567503-U). The column oven temperature was set at 30°C and the flow rate to 0.7 mL/min. 5 µL of sample was injected for the quantification. Solvent A was 10 mM ammonium formate (pH 3.0, adjusted by formic acid). Solvent B was acetonitrile. Solvent composition was initially A = 95.0%, and B = 5.0%, which was kept until 0.5 min. Then, solvent composition was changed following a linear gradient until A = 40.0%, and B = 60.0% at 7.0 min. These conditions were kept constant for 2.5 min (7.0-9.5 min). The solvent composition was returned linearly to the initial conditions (A = 95.0%, B = 5.0 %) at 9.6 min, and remained unchanged until the end of the run (9.6-12 min). *p*-Coumaric acid was detected at a retention time of 4.7 min, using the absorbance at 277 nm for the quantification. Resveratrol was detected at a retention time of 5.7 min, using the absorbance at 333 nm for the quantification.

For salicylic acid, the HPLC system was equipped with a Cortecs UPLC T3 2.1 x 150 mm column, particle size 1.6 µm, pore size 120 Å (Waters, 186008500). The column oven temperature was set at 30°C and the flow rate to 0.3 mL/min. Solvent A was 0.1% formic acid in Milli-Q® water; solvent B was acetonitrile. 5 µL of sample was injected for the quantification. The initial solvent composition was A = 90.0%, and B = 10.0%, which was kept until 0.5 min. Solvent composition was then changed following a linear gradient until % A = 5.0 and % B = 95.0 at 7 min. This solvent composition was returned linearly to the initial conditions (A = 90.0%, B = 10.0 %) at 7.1 min, and remained unchanged until the end of the run (7.1-10 min). Salicylic acid was detected at a retention time of 6.6 min, using the absorbance at 250 nm for the quantification.

Quantification of *cis*,*cis*-muconic acid and pathway intermediates was performed using previously described methods (Wang et al., 2020).

Quantification of glucose, glycerol and organic acids was carried out on Aminex HPX-87H column (Bio-Rad Laboratories, USA) as described before (Borja et al., 2019), but with a column temperature of 60°C.

Results

Yarrowia lipolytica was readily able to produce aromatics

Insufficient intracellular levels of malonyl-CoA are a known limitation for the production of phenylpropanoids (Johnson et al., 2017). As the native metabolic traits of *Y. lipolytica* overcome this limitation, we tested its potential to synthesize the stilbenoid resveratrol. Additionally, we also evaluated its ability to produce *cis*,*cis*-muconic acid and salicylic acid, compounds that do not require malonyl-CoA building blocks and branch off from different precursors upstream in the shikimate pathway (Figure 1).

For the biosynthesis of resveratrol, we first tested two different TAL enzymes from *Herpetosiphon aurantiacus* (HaTAL) and *Flavobacterium johnsoniae* (FjTAL) producing the intermediate *p*-coumaric acid that have been shown to perform best in *S. cerevisiae* (Jendresen et al., 2015). The pathway was further extended up to resveratrol with *At4CL1* from *Arabidopsis thaliana* and *VvVST1* from *Vitis vinifera*, genes that were also successfully expressed in *S. cerevisiae* (Li et al., 2015). In a similar fashion to Li et al. work, we used different combinations of promoters with strong and constitutive expression like *GPD* and *TEFintron* to assess the best performing strain, using mineral medium with 2 mM L-tyrosine for the cultivation (Li et al., 2015; Holkenbrink et al., 2018). We evaluated the performance of the genes and combinations of promoters both in terms of titer and specific yield (Figure 2a, Figure S1a).

The best production of *p*-coumaric acid was achieved in strain ST8951 harboring FjTAL, but the titer remained low (1.11 ± 0.01 mg/L). ST8952 containing HaTAL produced 0.21 ± 0.01 mg/L *p*-coumaric acid (Figure 2a, Figure S1a). Based on these results and due to the native ability of *Y. lipolytica* to utilize a wide range of substrates (Abdel-Mawgoud et al., 2018), we hypothesized that *p*-coumaric acid could be consumed. In order to evaluate this, we performed a degradation assay with the parental strain ST6512 by supplementing *p*-coumaric acid to mineral medium. After

72 h, no *p*-coumaric acid was detected in the medium, suggesting its complete consumption by *Y. lipolytica* (Fig 2b). This was not observed in the degradation assays for resveratrol (Figure 2b) or other aromatics (Figure S2), where only a minor decrease in the extracellular concentrations compared to control medium was seen.

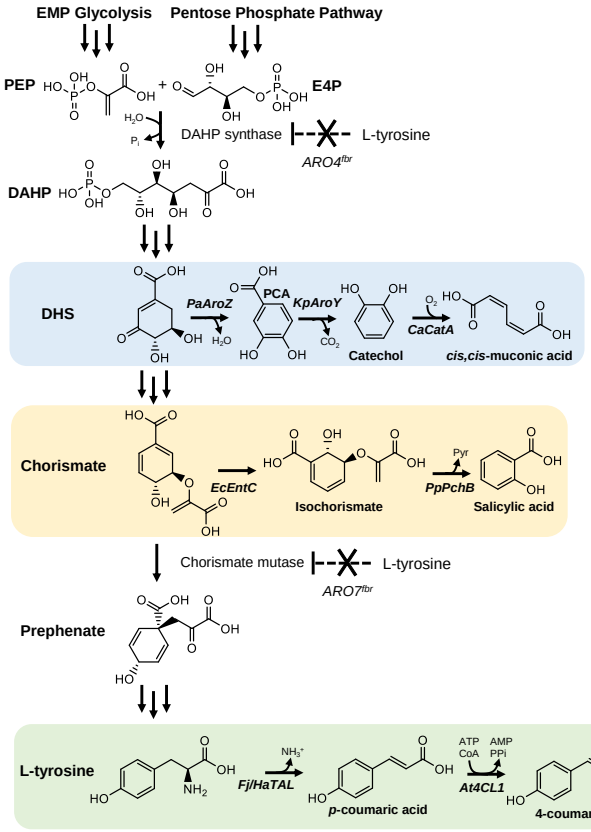

Heterologous genes		
Gene	**Protein name**	**Organism**
PaAroZ	DHS dehydratase	*Podospora anserina*
KpAroY.B	FMN prenyltransferase	*Klebsiella pneumoniae*
KpAroY.Ciso	PCA decarboxylase	*Klebsiella pneumoniae*
KpAroY.D	AroY subunit D	*Klebsiella pneumoniae*
CaCatA	Catechol 1,2-dioxygenase	*Candida albicans*
EcEntC	Isochorismate synthase	*Escherichia coli*
PpPchB	Isochorismate pyruvate-lyase	*Pseudomonas protegens Pf-5*
FjTAL	Tyrosine ammonia-lyase	*Flavobacterium johnsoniae*
HaTAL	Tyrosine ammonia-lyase	*Herpetosiphon aurantiacus*
At4CL1	4-coumaroyl-CoA ligase	*Arabidopsis thaliana*
VvVST1	Resveratrol synthase	*Vitis vinifera*

Figure 1. Biosynthetic pathways towards different aromatic compounds in engineered *Y. lipolytica*. The different aromatic metabolites are synthesized using either intermediates from the shikimate pathway or the aromatic amino acid L-tyrosine. Different colors show the different heterologous pathways. Multiple arrows represent multiple enzymatic steps, dashed arrows indicate feedback-regulated steps. PEP: phosphoenolpyruvate E4P: erythrose 4-phosphate, DAHP: 3-deoxy-D-arabinoheptulosonate 7-phosphate, DHS: 3-dehydroshikimate. PCA: protocatechuic acid, FMN: flavin mononucleotide. *ARO4*: DAHP synthase, *ARO7*: chorismate mutase, fbr: feedback-resistant.

Into the strains harboring TAL, the pathway towards resveratrol was integrated. Strains with FjTAL resulted in better titers than those expressing HaTAL (Figure 2a, Figure S1a). Among the strains harboring FjTAL, ST8953 reached the highest resveratrol titer (52.1 ± 1.2 mg/L), when *VvVST1* was expressed from the strong

constitutive promoter *TEFintron* (Figure 2a, Figure S1a) (Tai and Stephanopoulos, 2013; Holkenbrink et al., 2018).

Next, we constructed strains capable of producing *cis*,*cis*-muconic acid and salicylic acid. For *cis*,*cis*-muconic acid, we used biosynthetic genes that have been described to work in *S. cerevisiae* (Curran et al., 2013). The engineered strain ST8959 harbored *PaAroZ* from *Podospora anserina* encoding for DHS dehydratase, three genes from *K. pneumoniae* (*KpAroY.B*, encoding FMN prenyltransferase; *KpAroY.C*^{iso}, enconding PCA decarboxylase; *KpAroY*.D encoding a protein that may improve PCA decarboxylase activity), and *CaCatA* from *Candida albicans* encoding catechol 1,2-dioxygenase (Figure 1). Strain ST8959 produced 48.0 ± 6.4 mg/L *cis*,*cis*-muconic acid and 135.2 ± 0.1 mg/L of the intermediate protocatechuic acid (Figure 2c, Figure S1b), suggesting that enhanced PCA decarboxylase activity could improve production, as it does in *S. cerevisiae* (Curran et al., 2013; Skjoedt et al., 2016).

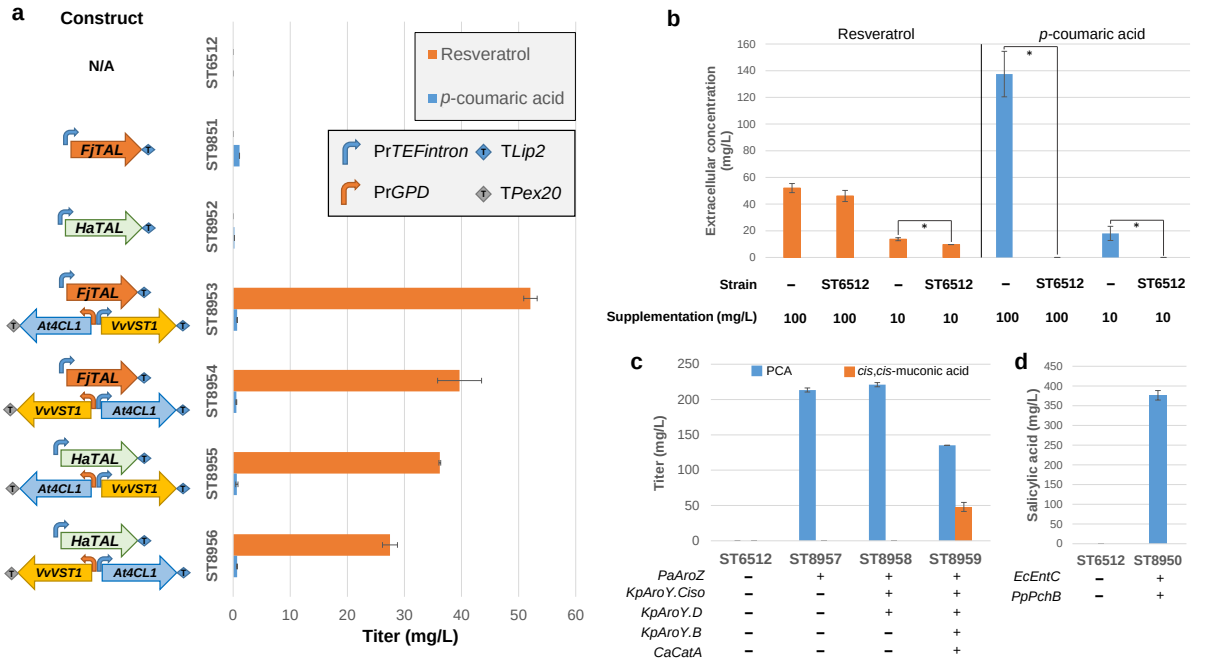

Figure 2. Titers of *p*-coumaric acid, resveratrol, *cis*,*cis*-muconic acid and salicylic in engineered *Y. lipolytica* strains. Cultivations were carried out for 72 h in 24 deep-well plates containing mineral medium with 20 g/L glucose. Extracellular content was subjected to HPLC analysis. Error bars represent standard deviation from at least three biological replicates. "-" and "+" symbols indicate absence or presence of the corresponding genetic modification, respectively. a) Production of *p*-coumaric acid and resveratrol with supplementation of 2 mM L-tyrosine. b) Degradation assays for *p*-coumaric acid and resveratrol in strain ST6512, at different supplementation concentrations. "-" represents a

medium control, non-inoculated. c) Production of *cis*,*cis*-muconic acid and the pathway intermediate protocatechuic acid (PCA). d) Production of salicylic acid. Statistical analysis was performed using Student's t-test (two-tailed; *P ≤ 0.05 two-sample unequal variance).

The salicylic acid producing strain was constructed by the expression of isochorismate synthase (*EcEntC*) from *E. coli* in combination with isochorismate pyruvate-lyase (*PpPchB*) from *Pseudomonas protegens* Pf-5 (Figure 1), as described in *E. coli* (Lin et al., 2013). This strain resulted in 376.4 ± 12.1 mg/L salicylic acid in the broth, while no additional peaks were detected on the HPLC chromatogram with respect to the control strain, suggesting no accumulation of isochorismate (Figure 2d, Figure S1c).

Among the strains described above, we observed that the titers for *cis*,*cis*-muconic acid and salicylic acid, shikimate pathway-derived products that do not require malonyl-CoA moieties, were comparable to titers in *S. cerevisiae* or *E. coli* (Curran et al., 2013; Wang et al., 2020; Lin et al., 2013). Conversely, resveratrol titers in ST8953 were 4.5 times higher than in a *S. cerevisiae* strain, when using similar biosynthetic genes and the same cultivation conditions (Li et al., 2015). These results suggest that *Y. lipolytica* has an advantage when producing compounds that require malonyl-CoA as one of the precursors, such as resveratrol. We then sought to further engineer resveratrol production in *Y. lipolytica*.

Feedback resistant *ARO4* and *ARO7* improved resveratrol production

Several metabolic engineering targets which have been proven to work in *S. cerevisiae* were selected (Li et al., 2015). First, we introduced feedback-insensitive versions of DAHP synthase (Aro4p) and chorismate mutase (Aro7p), enzymes that are otherwise allosterically regulated by L-tyrosine (Künzler et al., 1992; Brown and Dawes, 1990). In *S. cerevisiae*, the mutant alleles *ScARO4*^{K229L} and *ScARO7*^{G141S} are common engineering targets for shikimate pathway-derived products (Luttik et al., 2008; Gold et al., 2015; Mao et al., 2017; Rodriguez et al., 2015; Li et al., 2015). More recently, it has also been demonstrated that homologous *Y. lipolytica YlARO4*^{K221L} allele significantly increased naringenin titer (Palmer et al., 2020). Here, we simultaneously expressed feedback insensitive alleles from *Y. lipolytica* (*YlARO4*^{K221L} and *YlARO7*^{G139S} in strain ST9153) (Figure S3) or *S. cerevisiae* (*ScARO4*^{K229L} and *ScARO7*^{G141S} in strain

ST9178). The simultaneous introduction of mutated alleles for both genes from either of the two yeasts resulted in a similar effect, increasing resveratrol titer 2.2-fold to ca. 85 mg/L (Figure 3, Figure S4). Each gene individually contributed to the increase of titer, with *ARO4* showing a larger effect (Figure S5).

Next, we sought to increase L-Tyr precursor supply by deleting the genes involved in the conversion of aromatic amino acids into aromatic alcohols. *ARO10* and *PDC5* deletions have been demonstrated to increase *p*-coumaric acid titers by 2-fold in *S. cerevisiae* (Rodriguez et al., 2015). We identified the *Y. lipolytica* homologous genes YALI1_D08884g (*ARO10)* and YALI1_D12832g (*PDC5*) and carried out individual and double deletions. However, none of the deletions had a positive effect on resveratrol titer (Figure 3, Figure S4).

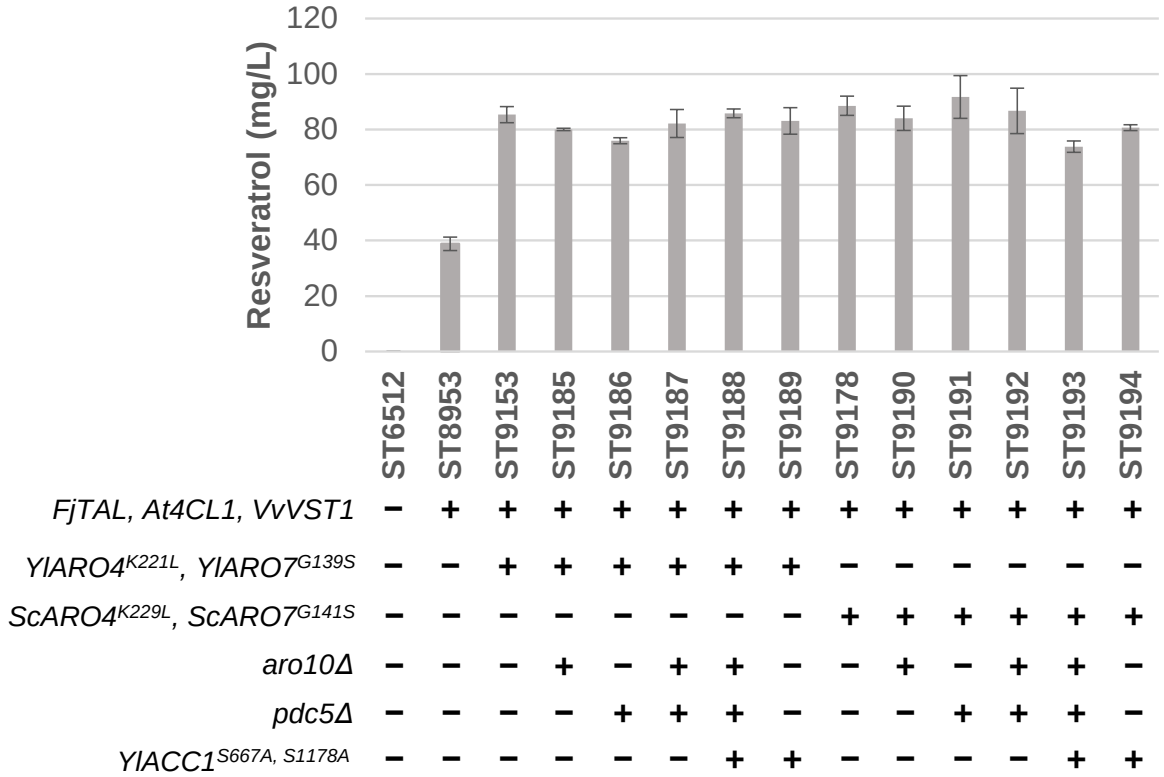

Figure 3. Resveratrol titer in engineered *Y. lipolytica* strains. Cultivations were carried out for 72 h in 24 deep-well plates containing mineral medium with 20 g/L glucose. Extracellular content was subjected to HPLC analysis. "-" and "+" symbols indicate absence or presence of the corresponding genetic modification, respectively. Error bars represent standard deviation from at least three biological replicates. *p*-Coumaric acid was not detected in any of the strains.

Lastly, we tried to increase malonyl-CoA supply by overexpressing *ACC1*. The last step of the pathway involves a type III PKS, which requires three malonyl-CoA units per resveratrol molecule. Thus, we hypothesized that intracellular malonyl-CoA levels could be limiting resveratrol biosynthesis. Acetyl-CoA carboxylase is the enzyme responsible for the conversion of acetyl-CoA to malonyl-CoA. In *S. cerevisiae*, acetyl-CoA carboxylase (ScAcc1p) can be phosphorylated by the kinase Snf1p in amino acids Ser659 and Ser1157, thus targeting it for degradation (Shirra et al., 2001). Two point mutations in those amino acids prevent its phosphorylation and hence results in higher malonyl-CoA supply (Shi et al., 2014). Based on homology with the *S. cerevisiae* protein, we decided to introduce the mutated *YlACC1*$^{S667A,\ S1178A}$ (Seip et al., 2013; Kerkhoven et al., 2016). Nonetheless, expression of this mutated version of *YlACC1* did not increase resveratrol titers (Figure 3, Figure S4).

Integration of multiple copies of resveratrol pathway led to increased resveratrol titers

Our results suggested that precursor supply was not a significant limitation for resveratrol production at the current stage. Thus, we hypothesized that resveratrol biosynthesis could be hampered by a low activity of the heterologous pathway, with impaired capacity to convert precursors to resveratrol, which could be overcome by the integration of multiple copies of the biosynthetic genes. We first examined the effect of expressing an extra copy on a strain harboring solely the initial integration of the pathway. Strain ST9663 carrying two copies of the biosynthetic genes in the pathway resulted in a 2.4-fold increase in resveratrol titers compared to strain ST8953 (Figure 4, Figure S6). We then integrated one to five additional copies of *FjTAL*, *At4CL1* and *VvVST1* into strains ST9153 and ST9178, already harboring a single copy of the pathway and feedback-resistant versions of *ARO4* and *ARO7* from *Y. lipolytica* or *S. cerevisiae*, respectively (Figure 4, Figure S6, Table S2).

In strains with *YlARO4*^{K221L}/*YlARO7*^{G139S} feedback-insensitive background, the integration of one to three extra copies led to a sharp increase in resveratrol levels: 195.2 ± 1.2 (ST9537), 265.8 ± 7.4 (ST9585), and 375.1 ± 11.2 mg/L (ST9616), respectively. Addition of a fourth and fifth additional copy showed a plateauing in the titers, with only a small improvement but still reaching 409.0 ± 1.2 mg/L in ST9671,

the top producing strain harboring a total of six copies. In strains expressing *S. cerevisiae* versions of the genes, improvement upon additional integrations was smaller, and saturation of the titers was observed earlier, only after two extra copies integrated. Indeed, the strain with three additional copies (ST9617, 176.8 ± 9.6 mg/L) performed worse than ST9537, with only one copy but with the mutant *ARO4*/*ARO7* sourced from *Y. lipolytica*. Taken together, these results demonstrate the higher activity of the feedback-insensitive *YlARO4*/*YlARO7* pair over its *S. cerevisiae* counterpart under this push-and-pull strategy.

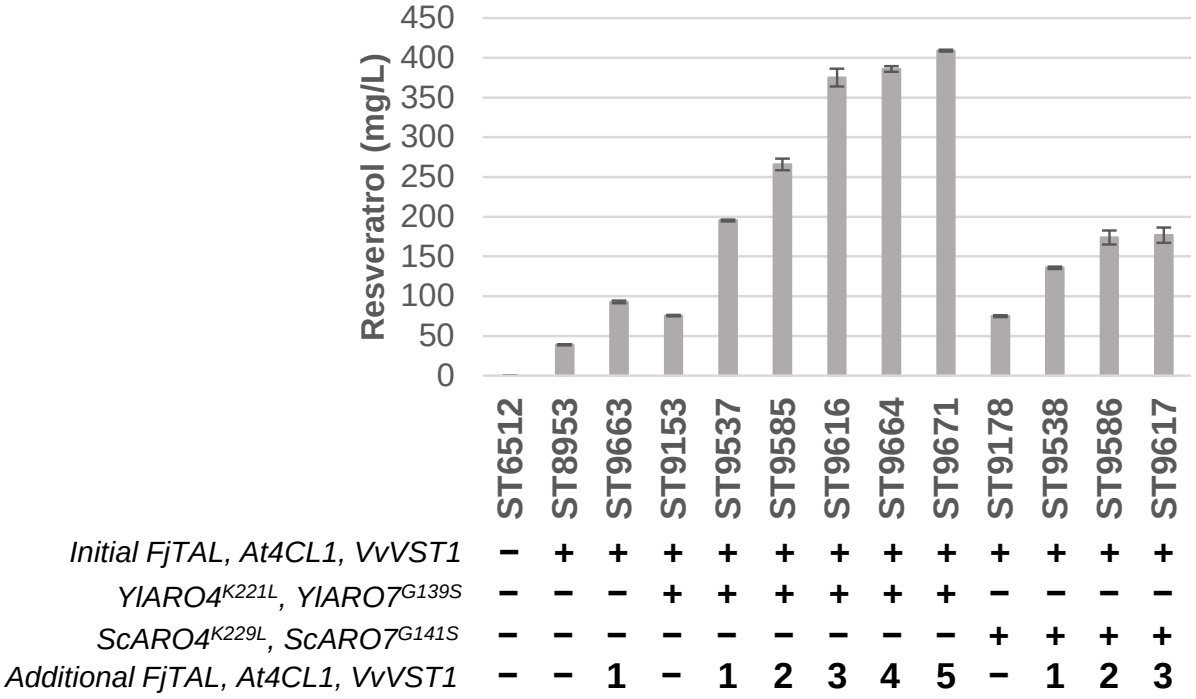

Figure 4. Effect on resveratrol titers of the integration of additional copies of the heterologous pathway. Cultivations were carried out for 72 h in 24 deep-well plates containing mineral medium with 20 g/L glucose. Extracellular content was subjected to HPLC analysis. "-" and "+" symbols indicate absence or presence of the corresponding genetic modification, respectively. Digits show the number of additional copies of resveratrol biosynthetic genes integrated. Error bars represent standard deviation from at least three biological replicates. *p*-Coumaric acid was not detected in any of the strains.

Resveratrol production was affected by carbon source and nutrient content

In *Y. lipolytica*, medium and particularly C/N ratio have been proven to be important factors for the production of several metabolites (Jacobsen et al., 2020; Ledesma-Amaro et al., 2016). Nitrogen limitation can halt the TCA and trigger lipogenesis through ATP citrate lyase, significantly altering the flux distribution in the cells (Ratledge and Wynn, 2002). Thus, we sought to increase the resveratrol titers of our best strain ST9671 by testing different media with different C/N ratios. We evaluated defined media (mineral medium and YNB), and the rich medium YP, each of them containing either glucose or glycerol at 20 or 80 g/L and evaluated titers and yields after 96 h (Figure 5, Figure S7). In addition, we assessed the cultivation profiles by sampling every 24 h (Figures S8-S10).

Overall, we observed that when carbon sources were supplemented at 80 g/L, only ca. 15-25 g/L were consumed after 96 h cultivation and that glucose performed better than glycerol for all types of media and concentrations (Figure 5, Figures S8-S10).

Cultivation in mineral medium resulted in 33-181% higher titers than in YNB medium, when comparing the experiments with the same carbon sources. The mineral medium contained 14.4 g/L of potassium phosphate monobasic, which serves as a pH buffer during the cultivation. In contrast, YNB medium contained only 1 g/L of this buffering agent and resulted in a bigger and a faster pH drop, which could have negatively influenced the growth, carbon source utilization, and resveratrol production (Figures S8-S9). The highest production levels were reached with rich YP with 80 g/L glucose (524.9 ± 75.1 mg/L), followed by mineral medium with 20 g/L glucose (402.2 ± 16.7 mg/L), standard medium we used for strain assessment above (Figure 5a). However, in terms of yield on glucose, all media with 20 g/L of this substrate and YP with 80 g/L presented similar results, ca. 20 mg resveratrol/g glucose (Figure 5b).

Interestingly, the intermediate *p*-coumaric acid was detected in significant amounts in all YP-based media, even at higher concentrations than resveratrol in most of the conditions. This was unexpected, as *p*-coumaric acid was never detected in our engineered strains in mineral medium, and was proven to be degraded in this medium by the parental strain ST6512 (Figure 2a).

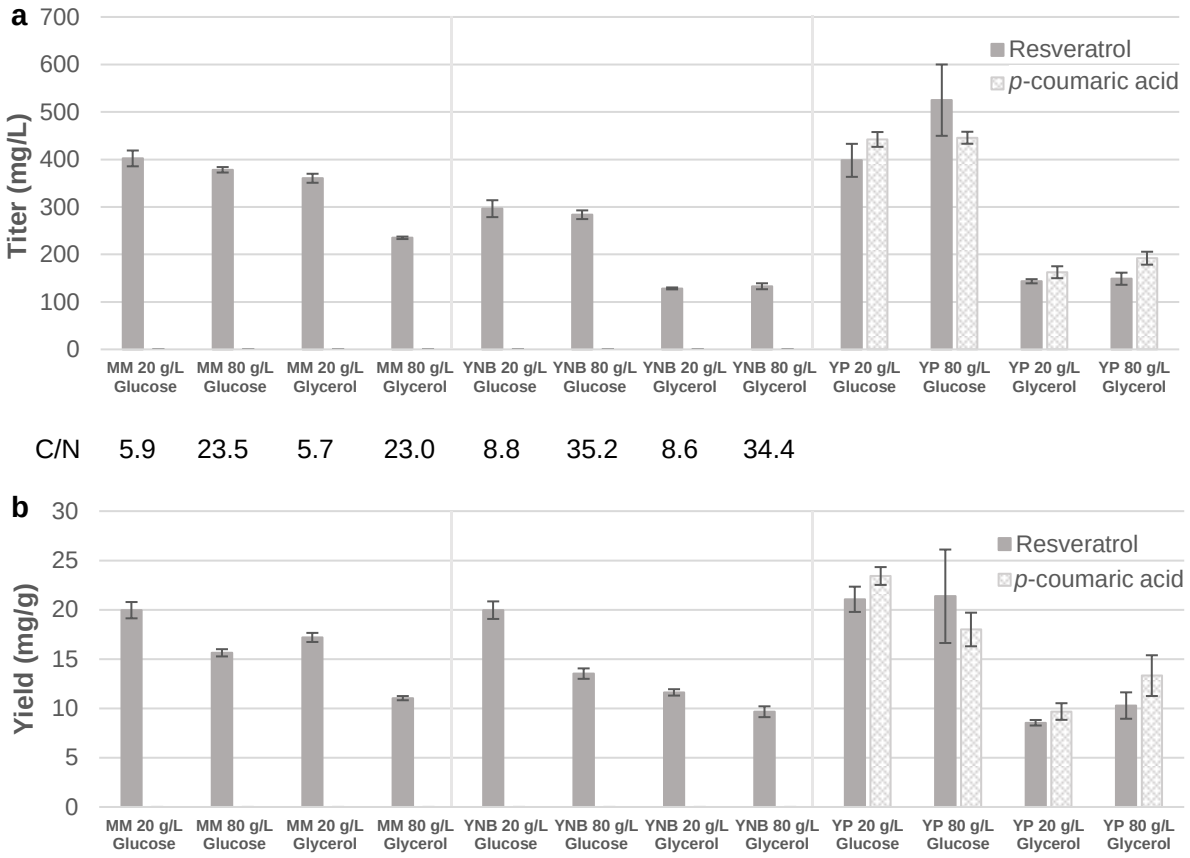

Figure 5. Resveratrol production in different media. Cultivations of strain ST9671 were carried out for 96 h in 24 deep-well plates using the media indicated for each condition. Extracellular content was subjected to HPLC analysis. Error bars represent standard deviation from at least three biological replicates. a) Titer after 96 h. b) Yield on carbon source after 96 h. MM: mineral medium, YNB: Yeast Nitrogen Base without amino acids. YP: Yeast extract Peptone. C/N stands for the molar carbon/nitrogen ratio in defined media.

Fed-batch fermentation enabled high-level resveratrol production

In order to demonstrate that *Y. lipolytica* could be an industrial production host for resveratrol, we carried out a fed-batch fermentation in 1 L bioreactors with the best producing strain (ST9671). Although with YP medium resveratrol titers seemed to be better in small-scale cultivations (Figure 5), we were concerned about *p*-coumaric acid accumulation over time (Figure S10), which could complicate the purification in an industrial production process. Moreover, complex medium is more expensive than mineral medium and has a higher tendency to foam. Therefore, we performed the

bioreactor experiment with mineral medium. With the aim of assessing whether quantification of intracellular resveratrol in fermentation samples would be relevant, we compared the extracellular and intracellular concentration of resveratrol in a small-scale cultivation using mineral medium. Most of the resveratrol was found in the extracellular fraction (391.17 ± 4.92 mg/L), compared to 34.12 ± 3.40 mg/L intracellularly (Figure S11). Thus, we only measured the extracellular fraction in our fermentation samples.

In bioreactors, cells showed a long lag phase of 22 h, probably due to the adaptation to mineral medium from YPD medium in the pre-culture. The fermentation was carried out with an exponential feeding profile, which was changed to a constant feed rate of 14 g/h for the last 14.3 h. This resulted in the addition of a total of 191.6 ± 0.8 g glucose over a span of 90 h. Controlled fermentation led to a resveratrol titer of 12.4 ± 0.3 g/L, with a yield on glucose of 54.4 ± 1.6 mg/g (15.3% of maximum theoretical yield) and a productivity of 0.14 ± 0.01 g/L/h (Figure 6, Figure S12, Figure S13) (Vos et al., 2015). Overall, these metrics represent an improvement over the previously reported values for resveratrol production in other microbial hosts (Table 1), especially for *de novo* production. Throughout the fermentation, only small amounts of by-products like citrate and α-ketoglutarate (<80 mg/L) were detected in the batch phase, while no *p*-coumaric acid was detected at any time point (Figure S13). The foaming was controlled by manual addition of antifoam and in total 32.7 ± 0.1 mL of antifoam was added per L reactor volume over the course of cultivation. As this amount of antifoam is relatively high, we questioned whether the antifoaming agent could have influenced the production of resveratrol. To assess the effect of antifoam, we carried out small-scale cultivations with addition of 1, 3, and 5% v/v antifoam. The antifoam addition had a negative effect on resveratrol production at all concentrations, with decreases on titer of 41-62%. (Figure S14).

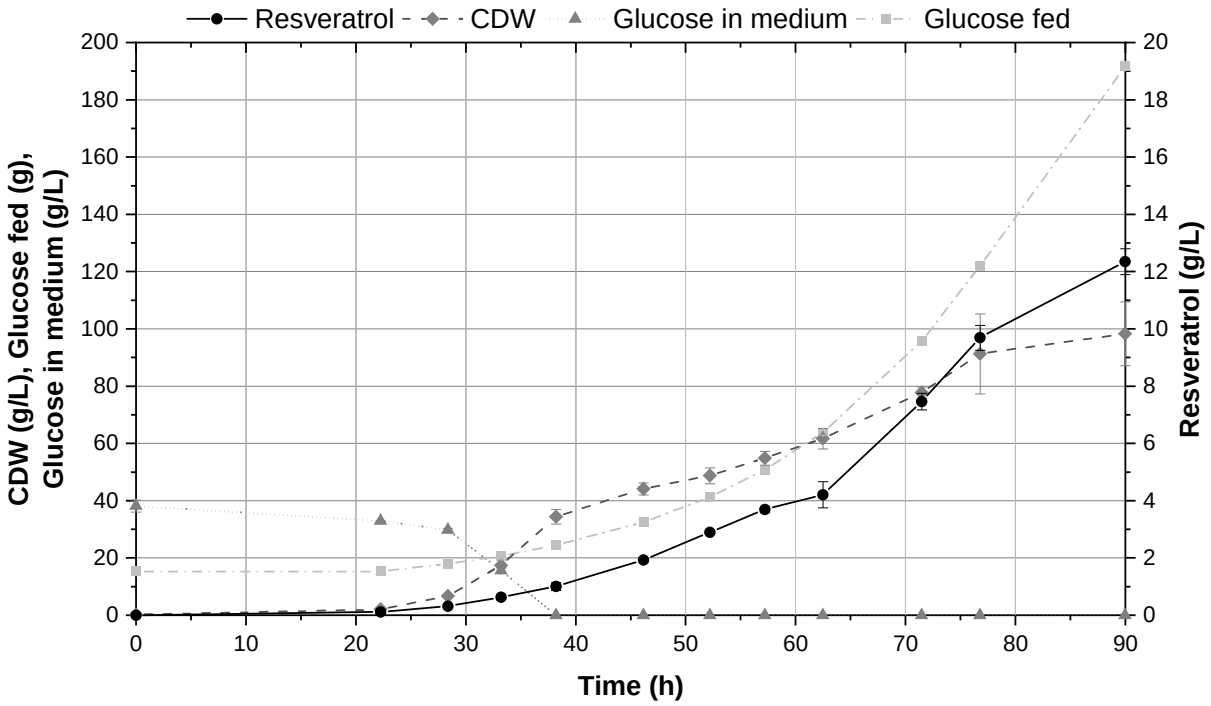

Figure 6. Fed-batch fermentation in bioreactor. Bioreactor cultivations with strain ST9671 were performed in duplicates. Data is presented as averages from both reactors, error bars represent standard deviation. Operational parameters for each of the reactors are shown in Figure S12. CDW: cell dry weight.

Discussion

In this study, high-level production of resveratrol was achieved in the emerging workhorse *Y. lipolytica*, attesting the potential of this oleaginous yeast for the production of plant secondary metabolites with a malonyl-CoA-derived structure. The strain was rationally engineered by the expression of feedback-alleviated versions of key genes in the shikimate pathway and multiple-copy integration of the genes in the heterologous pathway leading to resveratrol.

Our preliminary evaluation of the potential entailed the production of four aromatics (*p*-coumaric acid, resveratrol, salicylic acid, *cis*,*cis*-muconic acid) in the oleaginous yeast. When comparing the performance of *Y. lipolytica* with *S. cerevisiae* expressing the same pathways, a large difference was observed only for resveratrol (Figure 2, Figure S1) (Curran et al., 2013; Wang et al., 2020; Lin et al., 2013). This implied that the high PPP flux in *Y. lipolytica* did not enable a high concentration of shikimate pathway intermediates, which would favor a high production of derived products like

cis,*cis*-muconic acid or salicylic acid (Blank et al., 2005; Rodriguez et al., 2013). Therefore, a sufficient malonyl-CoA supply in the oleaginous yeast could explain the observed results with regards to resveratrol (Wasylenko et al., 2015). This initial result was in-line with recent studies that used *Y. lipolytica* to produce plant-derived flavonoids like naringenin (Lv et al., 2019; Palmer et al., 2020), achieving promising initial results and the highest reported titers to date upon strain engineering. All these secondary metabolites are phenylpropanoid polyketides requiring the action of type III PKS, enzymes involved in the incorporation of malonyl-CoA to the growing molecules (Lussier et al., 2013), which could be facilitated by the native oleaginous phenotype of *Y. lipolytica*.

An important finding in our initial strain engineering steps was the degradation of *p*-coumaric acid by *Y. lipolytica* (Figure 2b). (Palmer et al., 2020) demonstrated that concentrations up to 2 mM of *p*-coumaric acid do not affect the growth rate of *Y. lipolytica*, but they did not measure its degradation. In *S. cerevisiae*, it has been suggested that *p*-coumaric acid can be slowly converted into a range of less toxic compounds (Adeboye et al., 2015), while in other microorganisms it is transformed into *p*-hydroxybenzoic acid (Delneri et al., 1995). Since *p*-coumaric acid serves as precursor for resveratrol and many other plant phenylpropanoids, identification of the enzymes responsible for its degradation could improve the production of these metabolites. Understanding the effect of the rich medium on *p*-coumaric acid accumulation (Figure 5) would also be informative for further strain engineering. Given that the pH in YP media never reached values as low as in mineral medium or YNB (Figures S8-S10), it could be hypothesized that pH could affect the export of *p*-coumaric acid out of the cells. Moreover, the presence of complex nutrients in the rich YP medium could have attenuated *p*-coumaric acid degradation. In agreement with our findings, significant production of *p*-coumaric acid has been recently achieved in *Y. lipolytica* using YP-derived medium (Gu et al., 2020a).

The rational metabolic engineering strategies that we employed to further improve resveratrol production entailed the use of feedback insensitive versions of *ARO4/ARO7*, and multiple integration of resveratrol biosynthetic genes (Figure 3 and 4). Here, we showed that *YlARO4*^{K221L}*/YlARO7*^{G139S} performed better than the *S. cerevisiae* versions of these genes (Figure 4), which could be explained by a higher activity or a lower sensitivity to feedback regulation of the enzymes from *Y. lipolytica*.

In either case, this finding underlines the importance of testing several variants of key enzymes in the pathway. Our strain was further engineered by tuning the gene copy number of the heterologous pathway. Indeed, for many plant secondary metabolites, increased titers were obtained in *Y. lipolytica* by integrating multiple copies of heterologous pathway genes (Lv et al., 2019; Marella et al., 2019; Wang et al., 2016). This is most likely due to an overall low catalytic activity of the enzymes involved in secondary metabolites formation, as these compounds are typically synthesized in small amounts by the native host. With this motivation, we decided to add extra copies of the three heterologous genes, instead of examining the effect of individual genes. We also tried to increase resveratrol production by expressing a mutant version of *YlACC1* (Figure 3), but this did not improve the titer, contrary to improvement of naringenin production in *Y. lipolytica* in a study by (Lv et al., 2019). As we later confirmed by expressing additional copies of the heterologous pathway, a plausible explanation could be that malonyl-CoA was not a limiting precursor at that engineering stage or that malonyl-CoA was used for lipids production rather than for the biosynthesis of resveratrol. Another reason could be that the phosphorylation sites are not completely conserved in *Y. lipolytica* and the enzyme became inactive upon mutations (Pomraning et al., 2016). *ARO10* and *PDC5* deletions were also performed, with no positive effect on resveratrol levels (Figure 3), which could be caused by the low specificity of these enzymes (Vuralhan et al., 2005; Romagnoli et al., 2012) or the existence of isoenzymes.

Our top producing strain (ST9671) synthesized 409.0 ± 1.22 mg/L resveratrol *de novo* from glucose in small-scale cultivation, a 10-fold increase compared to our initial strain harboring only the biosynthetic pathway (Figure 4). (Palmer et al., 2020) have also recently demonstrated production of resveratrol in *Y. lipolytica*. In an *ACC1*/*PEX10* overexpression background, 48.7 mg/L were produced by feeding with 2 mM *p*-coumaric acid, in a strain lacking the *TAL* gene. When *TAL* was introduced, 8.8 mg/L of resveratrol were produced *de novo* from glucose. More recently, in a work aiming at developing a *Y. lipolytica* platform strain for the production of shikimate-pathway derived products, a titer of 12.67 mg/L resveratrol was achieved (Gu et al., 2020a). In this case, the strain was initially engineered for the production of 2-phenylethanol and subsequently tested for resveratrol production. Similar to our results, the use of feedback-insensitive versions of DAHP synthases was shown to be crucial to relieve allosteric regulation of the shikimate pathway.

The fed-batch fermentation of ST9671 resulted in 12.4 ± 0.3 g/L resveratrol and a yield of 54.4 ± 1.6 mg/g, representing 15.3% of the maximum theoretical yield on glucose (354.7 mg/g) (Vos et al., 2015) (Figure 6). This represents, to the best of our knowledge, the highest production of resveratrol and any *p*-coumaric acid-derived product in any microbial host (Thapa et al., 2019). Moreover, the fermentation was carried out in a cheap mineral medium without supplementation of any expensive aromatic intermediate or cerulenin, frequently used to inhibit lipids biosynthesis and increase malonyl-CoA pool (Lv et al., 2019; Marsafari and Xu, 2020). Further strain engineering aiming at enhancing precursors supply and a better control of foaming in the fermentation could improve the production (Figure 4, Figure S14). Collectively, these results illustrate the potential of *Y. lipolytica* for a high-level production of this family of compounds.

Conclusions

In this work, we engineered the oleaginous yeast *Y. lipolytica* for the production of the plant stilbenoid resveratrol. By the integration of feedback-resistant alleles for better precursor supply and multiple copies of the biosynthetic pathway, we reached the highest resveratrol production reported to date. This contrasts with other hosts, where extensive strain engineering is needed, and illustrates the suitability of the oleaginous yeast for the production of plant secondary metabolites with a polyketide structure.

Competing interests

The authors declare that they have no conflict of interest.

Acknowledgements

This project has received funding from the European Union's Horizon 2020 research and innovation programme under grant agreements No. 814408 (SHIKIFACTORY100 project) and No. 720770 (DAFIA project). IB also acknowledges the financial support from the Novo Nordisk Foundation (Grant agreement No. NNF10CC1016517) and from the European Research Council under the European

Union's Horizon 2020 research and innovation programme (YEAST-TRANS project, Grant Agreement No. 757384).

We thank NRRL Agricultural Research Service (ARS) Culture Collection for the gift of *Yarrowia lipolytica* Y-63746. The authors would like to thank Christoffer Knudsen for his help assembling the reactors. We thank Jonathan A Arnesen for the construction of EasyCloneYALI gRNA vectors with hphMX resistance markers. We thank Dr. Kanchana R Kildegaard (Biophero ApS, Denmark) for kindly providing plasmids pBP7995, pBP8003, pBP8006, and pBP8009. We thank Larissa RR Tramontin for kindly providing plasmid pCfB8681.

References

Abdel-Mawgoud, A.M., Markham, K.A., Palmer, C.M., Liu, N., Stephanopoulos, G., Alper, H.S., 2018. Metabolic engineering in the host Yarrowia lipolytica. Metabolic Engineering, Metabolic Engineering Host Organism Special Issue 50, 192–208. https://doi.org/10.1016/j.ymben.2018.07.016

Adeboye, P.T., Bettiga, M., Aldaeus, F., Larsson, P.T., Olsson, L., 2015. Catabolism of coniferyl aldehyde, ferulic acid and p-coumaric acid by Saccharomyces cerevisiae yields less toxic products. Microb Cell Fact 14. https://doi.org/10.1186/s12934-015-0338-x

Bhatt, J.K., Thomas, S., Nanjan, M.J., 2012. Resveratrol supplementation improves glycemic control in type 2 diabetes mellitus. Nutrition Research 32, 537–541. https://doi.org/10.1016/j.nutres.2012.06.003

Blank, L.M., Lehmbeck, F., Sauer, U., 2005. Metabolic-flux and network analysis in fourteen hemiascomycetous yeasts. FEMS Yeast Res 5, 545–558. https://doi.org/10.1016/j.femsyr.2004.09.008

Borja, G.M., Rodriguez, A., Campbell, K., Borodina, I., Chen, Y., Nielsen, J., 2019. Metabolic engineering and transcriptomic analysis of Saccharomyces cerevisiae producing p-coumaric acid from xylose. Microbial Cell Factories 18, 191. https://doi.org/10.1186/s12934-019-1244-4

Brasnyó, P., Molnár, G.A., Mohás, M., Markó, L., Laczy, B., Cseh, J., Mikolás, E., Szijártó, I.A., Mérei, Á., Halmai, R., Mészáros, L.G., Sümegi, B., Wittmann, I., 2011. Resveratrol improves insulin sensitivity, reduces oxidative stress and activates the Akt pathway in type 2 diabetic patients. british journal of nutrition 106, 383–389. https://doi.org/10.1017/S0007114511000316

Brown, J.F., Dawes, I.W., 1990. Regulation of chorismate mutase in Saccharomyces cerevisiae. Mol. Gen. Genet. 220, 283–288. https://doi.org/10.1007/bf00260495

Burns, J., Yokota, T., Ashihara, H., Lean, M.E.J., Crozier, A., 2002. Plant Foods and Herbal Sources of Resveratrol. J. Agric. Food Chem. 50, 3337–3340. https://doi.org/10.1021/jf0112973

Curran, K.A., Leavitt, J.M., Karim, A.S., Alper, H.S., 2013. Metabolic engineering of muconic acid production in Saccharomyces cerevisiae. Metabolic Engineering 15, 55–66. https://doi.org/10.1016/j.ymben.2012.10.003

Delneri, D., Degrassi, G., Rizzo, R., Bruschi, C.V., 1995. Degradation of trans-ferulic and p-coumaric acid by Acinetobacter calcoaceticus DSM 586. Biochim. Biophys. Acta 1244, 363–367. https://doi.org/10.1016/0304-4165(95)00021-3

DSM, 2014. resVida® Health benefit solution [WWW Document]. URL https://www.dsm.com/content/dam/dsm/human-nutrition/pdfs/resVida_A4_2pp_leaflet_08_09_2014_Final.pdf (accessed 6.26.20).

Evolva, 2019. Veri-te Resveratrol. Evolva. [WWW Document]. URL https://veriteresveratrol.com/wp-content/uploads/2019/01/Veri-te-Resveratrol-Brochure.pdf (accessed 4.5.23).

Future Market Insights, 2019. Resveratrol Market: Significant Health Benefits Attributed to Resveratrol to Drive Utilization in Dietary Supplements: Global Industry Analysis (2013 - 2017) & Opportunity Assessment (2018 - 2028) [WWW Document]. URL https://www.futuremarketinsights.com/reports/resveratrol-market (accessed 6.26.20).

Gaspar, P., Dudnik, A., Neves, A.R., Förster, J., 2016. Engineering Lactococcus lactis for stilbene production. Presented at the 28th International Conference on Polyphenols.

Gold, N.D., Gowen, C.M., Lussier, F.-X., Cautha, S.C., Mahadevan, R., Martin, V.J.J., 2015. Metabolic engineering of a tyrosine-overproducing yeast platform using targeted metabolomics. Microbial Cell Factories 14, 73. https://doi.org/10.1186/s12934-015-0252-2

Gu, Y., Ma, J., Zhu, Y., Ding, X., Xu, P., 2020a. Engineering Yarrowia lipolytica as a Chassis for De Novo Synthesis of Five Aromatic-Derived Natural Products and Chemicals. ACS Synth. Biol. https://doi.org/10.1021/acssynbio.0c00185

Gu, Y., Ma, J., Zhu, Y., Xu, P., 2020b. Refactoring Ehrlich Pathway for High-Yield 2-Phenylethanol Production in Yarrowia lipolytica. ACS Synth. Biol. 9, 623–633. https://doi.org/10.1021/acssynbio.9b00468

Holkenbrink, C., Dam, M.I., Kildegaard, K.R., Beder, J., Dahlin, J., Belda, D.D., Borodina, I., 2018. EasyCloneYALI: CRISPR/Cas9-Based Synthetic Toolbox for Engineering of the Yeast Yarrowia lipolytica. Biotechnology Journal 13, 1700543. https://doi.org/10.1002/biot.201700543

Huang, L.L., Xue, Z., Zhu, Q.Q., 2006. Method for the production of resveratrol in a recombinant oleaginous microorganism. WO2006125000A2.

Jacobsen, I.H., Ledesma-Amaro, R., Martinez, J.L., 2020. Recombinant β-Carotene Production by Yarrowia lipolytica – Assessing the Potential of Micro-Scale Fermentation Analysis in Cell Factory Design and Bioreaction Optimization. Front. Bioeng. Biotechnol. 8. https://doi.org/10.3389/fbioe.2020.00029

Jendresen, C.B., Stahlhut, S.G., Li, M., Gaspar, P., Siedler, S., Förster, J., Maury, J., Borodina, I., Nielsen, A.T., 2015. Highly Active and Specific Tyrosine Ammonia-Lyases from Diverse Origins Enable Enhanced Production of Aromatic Compounds in Bacteria and Saccharomyces cerevisiae. Appl. Environ. Microbiol. 81, 4458–4476. https://doi.org/10.1128/AEM.00405-15

Jensen, N.B., Strucko, T., Kildegaard, K.R., David, F., Maury, J., Mortensen, U.H., Forster, J., Nielsen, J., Borodina, I., 2014. EasyClone: method for iterative chromosomal integration of multiple genes Saccharomyces cerevisiae. FEMS Yeast Res 14, 238–248. https://doi.org/10.1111/1567-1364.12118

Johnson, A.O., Gonzalez-Villanueva, M., Wong, L., Steinbüchel, A., Tee, K.L., Xu, P., Wong, T.S., 2017. Design and application of genetically-encoded malonyl-CoA biosensors for metabolic engineering of microbial cell factories. Metabolic Engineering 44, 253–264. https://doi.org/10.1016/j.ymben.2017.10.011

Kallscheuer, N., Vogt, M., Stenzel, A., Gätgens, J., Bott, M., Marienhagen, J., 2016. Construction of a Corynebacterium glutamicum platform strain for the production of stilbenes and (2S)-flavanones. Metabolic Engineering 38, 47–55. https://doi.org/10.1016/j.ymben.2016.06.003

Kerkhoven, E.J., Pomraning, K.R., Baker, S.E., Nielsen, J., 2016. Regulation of amino-acid metabolism controls flux to lipid accumulation in Yarrowia lipolytica. npj Systems Biology and Applications 2, 1–7. https://doi.org/10.1038/npjsba.2016.5

Künzler, M., Paravicini, G., Egli, C.M., Irniger, S., Braus, G.H., 1992. Cloning, primary structure and regulation of the ARO4 gene, encoding the tyrosine-inhibited 3-deoxy-

D-arabino-heptulosonate-7-phosphate synthase from Saccharomyces cerevisiae. Gene 113, 67–74. https://doi.org/10.1016/0378-1119(92)90670-K

Langcake, P., Pryce, R.J., 1976. The production of resveratrol by Vitis vinifera and other members of the Vitaceae as a response to infection or injury. Physiological Plant Pathology 9, 77–86. https://doi.org/10.1016/0048-4059(76)90077-1

Ledesma-Amaro, R., Dulermo, R., Niehus, X., Nicaud, J.-M., 2016. Combining metabolic engineering and process optimization to improve production and secretion of fatty acids. Metabolic Engineering 38, 38–46. https://doi.org/10.1016/j.ymben.2016.06.004

Li, M., Kildegaard, K.R., Chen, Y., Rodriguez, A., Borodina, I., Nielsen, J., 2015. De novo production of resveratrol from glucose or ethanol by engineered Saccharomyces cerevisiae. Metabolic Engineering 32, 1–11. https://doi.org/10.1016/j.ymben.2015.08.007

Li, M., Schneider, K., Kristensen, M., Borodina, I., Nielsen, J., 2016. Engineering yeast for high-level production of stilbenoid antioxidants. Scientific Reports 6, 1–8. https://doi.org/10.1038/srep36827

Lim, C.G., Fowler, Z.L., Hueller, T., Schaffer, S., Koffas, M.A.G., 2011. High-Yield Resveratrol Production in Engineered Escherichia coli. Appl. Environ. Microbiol. 77, 3451–3460. https://doi.org/10.1128/AEM.02186-10

Lin, Y., Shen, X., Yuan, Q., Yan, Y., 2013. Microbial biosynthesis of the anticoagulant precursor 4-hydroxycoumarin. Nature Communications 4, 1–8. https://doi.org/10.1038/ncomms3603

Liu, Q., Yu, T., Li, X., Chen, Yu, Campbell, K., Nielsen, J., Chen, Yun, 2019. Rewiring carbon metabolism in yeast for high level production of aromatic chemicals. Nature Communications 10, 1–13. https://doi.org/10.1038/s41467-019-12961-5

Lussier, F.-X., Colatriano, D., Wiltshire, Z., Page, J.E., Martin, V.J.J., 2013. Engineering Microbes for Plant Polyketide Biosynthesis. Comput Struct Biotechnol J 3. https://doi.org/10.5936/csbj.201210020

Luttik, M.A.H., Vuralhan, Z., Suir, E., Braus, G.H., Pronk, J.T., Daran, J.M., 2008. Alleviation of feedback inhibition in Saccharomyces cerevisiae aromatic amino acid biosynthesis: Quantification of metabolic impact. Metabolic Engineering 10, 141–153. https://doi.org/10.1016/j.ymben.2008.02.002

Lv, Y., Gu, Y., Xu, J., Zhou, J., Xu, P., 2020. Coupling metabolic addiction with negative autoregulation to improve strain stability and pathway yield. Metabolic Engineering 61, 79–88. https://doi.org/10.1016/j.ymben.2020.05.005

Lv, Y., Marsafari, M., Koffas, M., Zhou, J., Xu, P., 2019. Optimizing Oleaginous Yeast Cell Factories for Flavonoids and Hydroxylated Flavonoids Biosynthesis. ACS Synth. Biol. 8, 2514–2523. https://doi.org/10.1021/acssynbio.9b00193

Mao, J., Liu, Q., Song, X., Wang, H., Feng, H., Xu, H., Qiao, M., 2017. Combinatorial analysis of enzymatic bottlenecks of l-tyrosine pathway by p-coumaric acid production in Saccharomyces cerevisiae. Biotechnol Lett 39, 977–982. https://doi.org/10.1007/s10529-017-2322-5

Marella, E.R., Dahlin, J., Dam, M.I., ter Horst, J., Christensen, H.B., Sudarsan, S., Wang, G., Holkenbrink, C., Borodina, I., 2019. A single-host fermentation process for the production of flavor lactones from non-hydroxylated fatty acids. Metabolic Engineering. https://doi.org/10.1016/j.ymben.2019.08.009

Marsafari, M., Xu, P., 2020. Debottlenecking mevalonate pathway for antimalarial drug precursor amorphadiene biosynthesis in Yarrowia lipolytica. Metabolic Engineering Communications 10, e00121. https://doi.org/10.1016/j.mec.2019.e00121

Palmer, C.M., Miller, K.K., Nguyen, A., Alper, H.S., 2020. Engineering 4-coumaroyl-CoA derived polyketide production in Yarrowia lipolytica through a β-oxidation mediated strategy. Metabolic Engineering 57, 174–181. https://doi.org/10.1016/j.ymben.2019.11.006

Park, S.R., Yoon, J.A., Paik, J.H., Park, J.W., Jung, W.S., Ban, Y.-H., Kim, E.J., Yoo, Y.J., Han, A.R., Yoon, Y.J., 2009. Engineering of plant-specific phenylpropanoids biosynthesis in

Streptomyces venezuelae. Journal of Biotechnology 141, 181–188. https://doi.org/10.1016/j.jbiotec.2009.03.013

Pomraning, K.R., Kim, Y.-M., Nicora, C.D., Chu, R.K., Bredeweg, E.L., Purvine, S.O., Hu, D., Metz, T.O., Baker, S.E., 2016. Multi-omics analysis reveals regulators of the response to nitrogen limitation in Yarrowia lipolytica. BMC Genomics 17, 138. https://doi.org/10.1186/s12864-016-2471-2

PubMed, 2020. PubMed results about resveratrol effects on health [WWW Document]. URL https://www.ncbi.nlm.nih.gov/pubmed?term=((resveratrol%5BTitle%5D)%20AND%20health) (accessed 6.4.20).

Ratledge, C., Wynn, J.P., 2002. The Biochemistry and Molecular Biology of Lipid Accumulation in Oleaginous Microorganisms, in: Laskin, A.I., Bennett, J.W., Gadd, G.M. (Eds.), Advances in Applied Microbiology, Advances in Applied Microbiology. Academic Press, pp. 1–52. https://doi.org/10.1016/S0065-2164(02)51000-5

Rodriguez, A., Kildegaard, K.R., Li, M., Borodina, I., Nielsen, J., 2015. Establishment of a yeast platform strain for production of p-coumaric acid through metabolic engineering of aromatic amino acid biosynthesis. Metabolic Engineering 31, 181–188. https://doi.org/10.1016/j.ymben.2015.08.003

Rodriguez, A., Martínez, J.A., Báez-Viveros, J.L., Flores, N., Hernández-Chávez, G., Ramírez, O.T., Gosset, G., Bolivar, F., 2013. Constitutive expression of selected genes from the pentose phosphate and aromatic pathways increases the shikimic acid yield in high-glucose batch cultures of an Escherichia coli strain lacking PTS and pykF. Microbial Cell Factories 12, 86. https://doi.org/10.1186/1475-2859-12-86

Romagnoli, G., Luttik, M.A.H., Kötter, P., Pronk, J.T., Daran, J.-M., 2012. Substrate Specificity of Thiamine Pyrophosphate-Dependent 2-Oxo-Acid Decarboxylases in Saccharomyces cerevisiae. Appl Environ Microbiol 78, 7538–7548. https://doi.org/10.1128/AEM.01675-12

Rosler, J., Krekel, F., Amrhein, N., Schmid, J., 1997. Maize Phenylalanine Ammonia-Lyase Has Tyrosine Ammonia-Lyase Activity. Plant Physiology 113, 175–179. https://doi.org/10.1104/pp.113.1.175

Seip, J., Jackson, R., He, H., Zhu, Q., Hong, S.-P., 2013. Snf1 Is a Regulator of Lipid Accumulation in Yarrowia lipolytica. Appl Environ Microbiol 79, 7360–7370. https://doi.org/10.1128/AEM.02079-13

Shang, Y., Wei, W., Zhang, P., Ye, B.-C., 2020. Engineering Yarrowia lipolytica for Enhanced Production of Arbutin. J. Agric. Food Chem. 68, 1364–1372. https://doi.org/10.1021/acs.jafc.9b07151

Shi, S., Chen, Y., Siewers, V., Nielsen, J., 2014. Improving Production of Malonyl Coenzyme A-Derived Metabolites by Abolishing Snf1-Dependent Regulation of Acc1. mBio 5. https://doi.org/10.1128/mBio.01130-14

Shirra, M.K., Patton-Vogt, J., Ulrich, A., Liuta-Tehlivets, O., Kohlwein, S.D., Henry, S.A., Arndt, K.M., 2001. Inhibition of Acetyl Coenzyme A Carboxylase Activity Restores Expression of the INO1 Gene in a snf1 Mutant Strain of Saccharomyces cerevisiae. Mol Cell Biol 21, 5710–5722. https://doi.org/10.1128/MCB.21.17.5710-5722.2001

Skjoedt, M.L., Snoek, T., Kildegaard, K.R., Arsovska, D., Eichenberger, M., Goedecke, T.J., Rajkumar, A.S., Zhang, J., Kristensen, M., Lehka, B.J., Siedler, S., Borodina, I., Jensen, M.K., Keasling, J.D., 2016. Engineering prokaryotic transcriptional activators as metabolite biosensors in yeast. Nature Chemical Biology 12, 951–958. https://doi.org/10.1038/nchembio.2177

Sparvoli, F., Martin, C., Scienza, A., Gavazzi, G., Tonelli, C., 1994. Cloning and molecular analysis of structural genes involved in flavonoid and stilbene biosynthesis in grape (Vitis vinifera L.). Plant Mol Biol 24, 743–755. https://doi.org/10.1007/BF00029856

Tai, M., Stephanopoulos, G., 2013. Engineering the push and pull of lipid biosynthesis in oleaginous yeast Yarrowia lipolytica for biofuel production. Metab. Eng. 15, 1–9. https://doi.org/10.1016/j.ymben.2012.08.007

Thapa, S.B., Pandey, R.P., Park, Y.I., Sohng, J.K., 2019. Biotechnological Advances in Resveratrol Production and its Chemical Diversity. Molecules 24. https://doi.org/10.3390/molecules24142571

Tomé-Carneiro, J., Gonzálvez, M., Larrosa, M., Yáñez-Gascón, M.J., García-Almagro, F.J., Ruiz-Ros, J.A., García-Conesa, M.T., Tomás-Barberán, F.A., Espín, J.C., 2012. One-Year Consumption of a Grape Nutraceutical Containing Resveratrol Improves the Inflammatory and Fibrinolytic Status of Patients in Primary Prevention of Cardiovascular Disease. American Journal of Cardiology 110, 356–363. https://doi.org/10.1016/j.amjcard.2012.03.030

Turner, R.S., Thomas, R.G., Craft, S., van Dyck, C.H., Mintzer, J., Reynolds, B.A., Brewer, J.B., Rissman, R.A., Raman, R., Aisen, P.S., 2015. A randomized, double-blind, placebo-controlled trial of resveratrol for Alzheimer disease. Neurology 85, 1383–1391. https://doi.org/10.1212/WNL.0000000000002035

Vestergaard, M., Ingmer, H., 2019. Antibacterial and antifungal properties of resveratrol. International Journal of Antimicrobial Agents 53, 716–723. https://doi.org/10.1016/j.ijantimicag.2019.02.015

Vos, T., de la Torre Cortés, P., van Gulik, W.M., Pronk, J.T., Daran-Lapujade, P., 2015. Growth-rate dependency of de novo resveratrolproduction in chemostat cultures of an engineered Saccharomycescerevisiae strain. Microbial Cell Factories 14, 133. https://doi.org/10.1186/s12934-015-0321-6

Vuralhan, Z., Luttik, M.A.H., Tai, S.L., Boer, V.M., Morais, M.A., Schipper, D., Almering, M.J.H., Kötter, P., Dickinson, J.R., Daran, J.-M., Pronk, J.T., 2005. Physiological Characterization of the ARO10-Dependent, Broad-Substrate-Specificity 2-Oxo Acid Decarboxylase Activity of Saccharomyces cerevisiae. Appl. Environ. Microbiol. 71, 3276–3284. https://doi.org/10.1128/AEM.71.6.3276-3284.2005

Wang, G., Øzmerih, S., Guerreiro, R., Meireles, A.C., Carolas, A., Milne, N., Jensen, M.K., Ferreira, B.S., Borodina, I., 2020. Improvement of cis,cis-Muconic Acid Production in Saccharomyces cerevisiae through Biosensor-Aided Genome Engineering. ACS Synth. Biol. 9, 634–646. https://doi.org/10.1021/acssynbio.9b00477

Wang, G., Xiong, X., Ghogare, R., Wang, P., Meng, Y., Chen, S., 2016. Exploring fatty alcohol-producing capability of Yarrowia lipolytica. Biotechnology for Biofuels 9, 107. https://doi.org/10.1186/s13068-016-0512-3

Wasylenko, T.M., Ahn, W.S., Stephanopoulos, G., 2015. The oxidative pentose phosphate pathway is the primary source of NADPH for lipid overproduction from glucose in Yarrowia lipolytica. Metabolic Engineering 30, 27–39. https://doi.org/10.1016/j.ymben.2015.02.007

Wei, W., Zhang, P., Shang, Y., Zhou, Y., Ye, B.-C., 2020. Metabolically engineering of Yarrowia lipolytica for the biosynthesis of naringenin from a mixture of glucose and xylose. Bioresource Technology 123726. https://doi.org/10.1016/j.biortech.2020.123726

Winkel-Shirley, B., 2001. Flavonoid biosynthesis. A colorful model for genetics, biochemistry, cell biology, and biotechnology. Plant Physiol. 126, 485–493. https://doi.org/10.1104/pp.126.2.485

Engineering the oleaginous yeast *Yarrowia lipolytica* for high-level resveratrol production

Supporting information

Supplementary information 1

Review of literature on microbial production of resveratrol

Supplementary Table S1. Microbial production of resveratrol in different hosts. Table shows different microorganisms engineered for the production of resveratrol, including metabolic engineering strategies used, titers obtained, and substrate or precursor fed. Abbreviations: *4CL*: 4-coumaroyl-CoA ligase, *STS*: stilbene synthase, *PAL*: phenylalanine ammonia-lyase, *ACC*: acetyl-CoA carboxylase, *TAL*: tyrosine ammonia-lyase; *matB*: malonyl-CoA synthetase, *matC*: malonate carrier protein, *fumC*: fumarate hydratase class II, *gapA*: glyceraldehyde-3-phosphate dehydrogenase A, *pgk*: phosphoglycerate kinase, PDH: pyruvate dehydrogenase, *fabD*: malonyl CoA-acyl carrier protein transacylase, *tktA/TKT*: transketolase 1/transketolase, *aroG*: 3-deoxy-7-phosphoheptulonate synthase, *pheA*: bifunctional chorismate mutase/prephenate dehydratase, *tyrR*: transcriptional regulatory protein, *trpE/D*: anthranilate synthase component 1/anthranilate phosphoribosyl transferase, *aroG/ARO3/4/5*: 3-deoxy-D-arabinoheptulosonate-7-phosphate (DAHP) synthase, *tyrA*: T-protein, *fabH*: 3-oxoacyl-[acyl-carrier-protein] synthase 3, *fabB*: 3-oxoacyl-[acyl-carrier-protein] synthase 1, *fabF*: 3-oxoacyl-[acyl-carrier-protein] synthase 2, *fabI*: enoyl-[acyl-carrier-protein] reductase [NADH] FabI, *pks*: polyketide synthase, *CPR*: cytochrome P450 reductase, *RS/VST*: resveratrol synthase, *ARO7*: chorismate mutase, *C4H*: cinnamate-4-hydroxylase, *ACS*: acetyl-CoA synthase *ATR2*: NADPH-cytochrome P450 reductase 2, *CYB5*: cytochrome b5, *ARO10*: transaminated amino acid decarboxylase, *PEX10*: peroxisomal biogenesis factor 10, *xfpK/xpkA*: phosphoketolase, *ARO1*: multifunctional AROM complex, *ARO2*: bifunctional chorismate synthase and flavin reductase, *ARO8*: aromatic aminotransferase I, *ARO9*: aromatic aminotransferase II, *TRP2*: anthranilate synthase, *TRP3*: indole-3-glycerol-phosphate synthase, *PYK*: pyruvate kinase, *PHA2*: prephenate dehydratase, fbr: feed-back resistant, *:multiple modifications, refer to publication.

Microbial host	Genetic modifications	Titer (mg/L)	Substrate/precursor	Reference
E. coli	*4CL* (*N. tabacum*) *STS* (*V. vinifera*)	16	*p*-coumaric acid	(Beekwilder et al., 2006)
E. coli	*4CL* (*A. thaliana*) *STS* (*A. hypogaea*)	100	*p*-coumaric acid	(Watts et al., 2006)
E. coli	*PAL* (*R. rubra*) *4CL* (*L. erythrorhizon*) *STS* (*A. hypogaea*) *ACC* (*C. glutamicum*)	37	L-tyrosine	(Katsuyama et al., 2007a)
E. coli	*4CL* (*L. erythrorhizon*) *STS* (*A. hypogaea*) *ACC* (*C. glutamicum*)	171	*p*-coumaric acid	(Katsuyama et al., 2007b)
E. coli	*TAL* (*S. espanaensis*)	1.4	*p*-coumaric acid	(Choi et al., 2011)

	4CL (*S. coelicolor*) *STS* (*A. hypogaea*)			
E. coli	*4CL* (*A. thaliana*) *STS* (*V. vinifera*)	2300	*p*-coumaric acid	(Lim et al., 2011)
E. coli	*TAL* (*R. glutinis*) *4CL* (*P. crispum*) *STS* (*V. vinifera*) *matB* and *matC* (*R. trifolii*)	35.02	L-tyrosine	(Wu et al., 2013)
E. coli	4CL (*A. thaliana*) STS (*V. vinifera*) *ΔfumC* Overexpression of *gapA*, *pgk*, PDH complex	1600	*p*-coumaric acid	(Bhan et al., 2013)
E. coli	*TAL* (*S. espanaensis*) *4CL* (*S. coelicolor*) *STS* (*A. hypogaea*)	5.2	Glucose	(Kang et al., 2014)
E. coli	*4CL* (*P. crispum*) *STS* (*V. vinifera*) *fabD* downregulation	268.2	*p*-coumaric acid	(Yang et al., 2015)
E. coli	*4CL* (*A. thaliana*) *STS* (*A. hypogaea*) (Fusion enzyme)	80.5	*p*-coumaric acid	(Zhang et al., 2015)
E. coli	*TAL* (*S. espanaensis*) *4CL* (*A. thaliana*) *STS* (*A. hypogaea*)	114.4	L-tyrosine	(Wang et al., 2015)
E. coli	*4CL* (*A. thaliana*) *STS* (*A. hypogaea*)	160	*p*-coumaric acid	(Afonso et al., 2015)
E. coli	*TAL* (R. glutinis) *4CL* (S. coelicolor) *STS* (V. vinifera) Overexpression of $tktA^{fbr}$ and $aroG^{fbr}$ *ΔpheA*	22.6	Glycerol	(Camacho-Zaragoza et al., 2016)
E. coli	*TAL* (*R. glutinis*) *4CL* (*P. crispum*) *STS* (*V. vinifera*) *ΔtyrR* and *ΔtrpED*	4.612	Glucose	(Liu et al., 2016)
E. coli	*TAL* (*T. cutaneum*) *4CL* (*P. crispum*) *STS* (*V. vinifera*) *matB* and *matC* (*R. trifolii*) $tyrA^{fbr}$ and $aroG^{fbr}$ (E. coli) Down-regulation of *fabD*, *fabH*, *fabB*, *fabF*, *fabI* Optimized expression of *TAL* mRNA secondary structure	304.5	Glucose	(Wu et al., 2017)
C. glutamicum	*STS* (*A. hypogaea*) *4CL* (*P. crispum*) *	158	*p*-coumaric acid	(Kallscheuer et al., 2016)
C. glutamicum	*TAL* (*F. johnsoniae*) *4CL* (*P. crispum*) *STS* (*A. hypogaea*) *aroH* (*E. coli*) *	12	Glucose	(Braga et al., 2018)
L. lactis	*TAL, 4CL, STS, ACC* (different sources)	1.27	Glucose	(Gaspar et al., 2016)
S. venezuelae	*STS* (*A. hypogaea*) *4CL* (*S. coelicolor*) Pikromycin *pks* deletion	0.4	*p*-coumaric acid	(Park et al., 2009)
S. cerevisiae	*4CL* (*Populus trichocarpa* × *Populus deltoids*) *STS* (*Vitis vinifera*)	1.45 (μg/L)	*p*-coumaric acid	(Becker et al., 2003)
S. cerevisiae	*4CL* (*N. tabacum*) *STS* (*V. vinifera*)	6	*p*-coumaric acid	(Beekwilder et al., 2006)
S. cerevisiae	*4CL* (*A. thaliana*) *STS* (*V. vinifera*) (fusion enzyme)	5.25	*p*-coumaric acid	(Zhang et al., 2006)

S. cerevisiae	*PAL*, *CPR* (*Populus trichocarpa* × *P. deltoides*) *C4H*, *4CL* (*Glycine max*) *RS* (*Vitis vinifera*)	0.31	*p*-coumaric acid	(Trantas et al., 2009)
S. cerevisiae	*4CL* (*A. thaliana*) *STS* (*V. vinifera*)	391	*p*-coumaric acid	(Sydor et al., 2010)
S. cerevisiae	*TAL* (*R. sphaeroides*) *4CL::STS (A. thaliana, V. vinifera; fusion enzyme)* *araE* (*E. coli*)	3.1	*p*-coumaric acid	(Wang et al., 2011)
S. cerevisiae	*4CL1* (*A. thaliana*) *STS* (*A. hypogaea*)	3.1	*p*-coumaric acid	(Shin et al., 2011)
S. cerevisiae	*PAL* (*R. toruloides*) *4CL* (*A. thaliana*) *STS* (*A. hypogaea*) *ACC1* overexpression	5.8	L-tyrosine	(Shin et al., 2012)
S. cerevisiae	*TAL* (*H. aurantiacus*) *4CL* (*A. thaliana*) *VST* (*V. vinifera*) *ARO4*^{fbr}, *ARO7*^{fbr}, *ACC1*	531.41	Ethanol	(Li et al., 2015)
S. cerevisiae	*PAL* (*A. thaliana*) *C4H* (*A. thaliana*) *4CL* (*A. thaliana*) *VST* (*V. vinifera*) *ACS* (*S. enterica*) *ATR2* (*A. thaliana*) Overexpression of *ARO4*^{fbr}, *ARO7*^{fbr}, *CYB5,* and *ACC1* *ΔARO10*	812	Glucose	(Li et al., 2016)
Y. lipolytica	*PAL* (*R. glutinis*) *4CL* (*S. coelicolor*) *STS* (*V. vinifera*)	1.4	L-tyrosine	(Huang et al., 2006)
Y. lipolytica	*4CL* (*N. tabacum*) *STS* (*A. hypogaea*) Overexpression of *PEX10* and *ACC1*	48.7	*p*-coumaric acid	(Palmer et al., 2020)
Y. lipolytica	*TAL* (*R. toruloides*) *4CL* (*P. crispum*) *VST* (*V. vinifera*) *ARO4*^{fbr} (*S. cerevisiae*) *aroG*^{fbr} (*E. coli*) *xfpK* (*B. breve*) *xpkA* (*A. capsulatum*) Overexpression of *ARO1*, *ARO2*, *ARO3*, *ARO4*, *ARO5*, *TKT* Deletion of *TRP2*, *TRP3*, *ARO8*, *ARO9*, *PYK*, *PHA2*	12.67	Glucose	(Gu et al., 2020)
Y. lipolytica	*TAL (F. johnsoniae)* *4CL (A. thaliana)* *VST (V. vinifera)* Overexpression *ARO4*^{fbr}, *ARO7*^{fbr}	12355	Glucose	This study

Supplementary information 2

Strains, plasmids, biobricks, primers and DNA fragments used in this study.

Supplementary Table S2. Strains used in this study.

Strain name	Genotype	Parent strain	Repair vector	gRNA vector	Source
ST6512	*MATa ku70Δ::PrTEF1-cas9-TTef12::PrGPD-dsdAMX-TLip2 (MATa ku70Δ::SpCas9-EcDsdAMX4)*	W29 (Y-63746)			(Marella et al., 2019)
ST8950	*MATa ku70Δ::SpCas9-EcDsdAMX4 IntC2::TPex20-PpPchB-PrGPD-PrTEFintron-EcEntC-TLip2*	ST6512	pCfB8811	pCfB6627	This study
ST8951	*MATa ku70Δ::SpCas9-EcDsdAMX4 IntC2::PrTEFintron-FjTAL-TLip2*	ST6512	pCfB8812	pCfB6627	This study
ST8952	*MATa ku70Δ::SpCas9-EcDsdAMX4 IntC2::PrTEFintron-HaTAL-TLip2*	ST6512	pCfB8815	pCfB6627	This study
ST8953	*MATa ku70Δ::SpCas9-EcDsdAMX4 IntC2::PrTEFintron-FjTAL-TLip2 IntC3::TPex20-At4CL1-PrGPD-PrTEFintron-VvVST1-TLip2*	ST8951	pCfB8816	pCfB6630	This study
ST8954	*MATa ku70Δ::SpCas9-EcDsdAMX4 IntC2::PrTEFintron-FjTAL IntC3::TPex20-VvVST1-PrGPD-PrTEFintron-At4CL1-TLip2*	ST8951	pCfB8817	pCfB6630	This study
ST8955	*MATa ku70Δ::SpCas9-EcDsdAMX4 IntC2::PrTEFintron-HaTAL-TLip2 IntC3::TPex20-At4CL1-PrGPD-PrTEFintron-VvVST1-TLip2*	ST8952	pCfB8816	pCfB6630	This study
ST8956	*MATa ku70Δ::SpCas9-EcDsdAMX4 IntC2::PrTEFintron-HaTAL IntC3::TPex20-VvVST1-PrGPD-PrTEFintron-At4CL1-TLip2*	ST8952	pCfB8817	pCfB6630	This study
ST8957	*MATa ku70Δ::SpCas9-EcDsdAMX4 IntC2::PrTEFintron-PaAroZ-TLip2*	ST6512	pCfB8813	pCfB6631	This study
ST8958	*MATa ku70Δ::SpCas9-EcDsdAMX4 IntC2::PrTEFintron-PaAroZ-TLip2 IntC3::TPex20-KpAroY.D-PrGPD-PrTEFintron-KpAroY.C^{Iso}-TLip2*	ST8957	pCfB8842	pCfB6631	This study
ST8959	*MATa ku70Δ::SpCas9-EcDsdAMX4 IntC2::PrTEFintron-PaAroZ-TLip2 IntC3::TPex20-KpAroY.D-PrGPD-PrTEFintron-KpAroY.C^{Iso}-TLip2 IntD1::TPex20-CaCatA-PrGPD-PrTEFintron-KpAroY.B-TLip2*	ST8958	pCfB8814	pCfB6631	This study
ST9153	*MATa ku70Δ::SpCas9-EcDsdAMX4 IntC2::PrTEFintron-FjTAL-TLip2 IntC3::TPex20-At4CL1-PrGPD-PrTEFintron-VvVST1-TLip2 IntE1::TPex20-YlARO7^{G139S}-PrGPD-PrTEFintron-YlARO4^{K221L}-TLip2*	ST8953	pCfB8977	pCfB6677	This study
ST9178	*MATa ku70Δ::SpCas9-EcDsdAMX4 IntC2::PrTEFintron-FjTAL-TLip2 IntC3::TPex20-At4CL1-PrGPD-PrTEFintron-VvVST1-TLip2 IntE1::TPex20-ScARO7^{G141S}-PrGPD-PrTEFintron-ScARO4^{K229L}-TLip2*	ST8953	pCfB9009	pCfB8858	This study
ST9185	*MATa ku70Δ::SpCas9-EcDsdAMX4 IntC2::PrTEFintron-FjTAL-TLip2 IntC3::TPex20-At4CL1-PrGPD-PrTEFintron-VvVST1-TLip2 IntE1::TPex20-YlARO7^{G139S}-PrGPD-PrTEFintron-YlARO4^{K221L}-TLip2 aro10Δ*	ST9153	BB4039	pCfB9010	This study
ST9186	*MATa ku70Δ::SpCas9-EcDsdAMX4 IntC2::PrTEFintron-FjTAL-TLip2 IntC3::TPex20-At4CL1-PrGPD-PrTEFintron-VvVST1-TLip2 IntE1::TPex20-YlARO7^{G139S}-PrGPD-PrTEFintron-YlARO4^{K221L}-TLip2 pdc5Δ*	ST9153	BB4042	pCfB9011	This study
ST9187	*MATa ku70Δ::SpCas9-EcDsdAMX4 IntC2::PrTEFintron-FjTAL-TLip2 IntC3::TPex20-At4CL1-PrGPD-PrTEFintron-VvVST1-TLip2 IntE1::TPex20-YlARO7^{G139S}-PrGPD-PrTEFintron-YlARO4^{K221L}-TLip2 aro10Δ pdc5Δ*	ST9186	BB4039	pCfB9015	This study
ST9188	*MATa ku70Δ::SpCas9-EcDsdAMX4 IntC2::PrTEFintron-FjTAL-TLip2 IntC3::TPex20-At4CL1-PrGPD-PrTEFintron-VvVST1-TLip2 IntE1::TPex20-YlARO7^{G139S}-PrGPD-PrTEFintron-YlARO4^{K221L}-TLip2 aro10Δ pdc5Δ IntD1::PrTEFintron-YlACC1^{S667A,S1178A}-TLip2*	ST9187	pCfB9035	pCfB6631	This study
ST9189	*MATa ku70Δ::SpCas9-EcDsdAMX4 IntC2::PrTEFintron-FjTAL-TLip2 IntC3::TPex20-At4CL1-PrGPD-PrTEFintron-VvVST1-TLip2 IntE1::TPex20-YlARO7^{G139S}-PrGPD-PrTEFintron-YlARO4^{K221L}-TLip2 IntD1::PrTEFintron-YlACC1^{S667A,S1178A}-TLip2*	ST9153	pCfB9035	pCfB6631	This study
ST9190	*MATa ku70Δ::SpCas9-EcDsdAMX4 IntC2::PrTEFintron-FjTAL-TLip2 IntC3::TPex20-At4CL1-PrGPD-PrTEFintron-VvVST1-TLip2 IntE1::TPex20-ScARO7^{G141S}-PrGPD-PrTEFintron-ScARO4^{K229L}-TLip2 aro10Δ*	ST9178	BB4039	pCfB9010	This study
ST9191	*MATa ku70Δ::SpCas9-EcDsdAMX4 IntC2::PrTEFintron-FjTAL-TLip2 IntC3::TPex20-At4CL1-PrGPD-PrTEFintron-VvVST1-TLip2 IntE1::TPex20-ScARO7^{G141S}-PrGPD-PrTEFintron-ScARO4^{K229L}-TLip2 pdc5Δ*	ST9178	BB4042	pCfB9011	This study

ST9192	*MATa ku70Δ::SpCas9-EcDsdAMX4 IntC2::PrTEFintron-FjTAL-TLip2 IntC3::TPex20-At4CL1-PrGPD-PrTEFintron-VvVST1-TLip2 IntE1::TPex20-ScARO7^{G141S}-PrGPD-PrTEFintron-ScARO4^{K229L}-TLip2 aro10Δ pdc5Δ*	ST9190	BB4042	pCfB9016	This study
ST9193	*MATa ku70Δ::SpCas9-EcDsdAMX4 IntC2::PrTEFintron-FjTAL-TLip2 IntC3::TPex20-At4CL1-PrGPD-PrTEFintron-VvVST1-TLip2 IntE1::TPex20-ScARO7^{G141S}-PrGPD-PrTEFintron-ScARO4^{K229L}-TLip2 aro10Δ pdc5Δ IntD1::PrTEFintron-YlACC1^{S667A,S1178A}-TLip2*	ST9192	pCfB9035	pCfB6631	This study
ST9194	*MATa ku70Δ::SpCas9-EcDsdAMX4 IntC2::PrTEFintron-FjTAL-TLip2 IntC3::TPex20-At4CL1-PrGPD-PrTEFintron-VvVST1-TLip2 IntE1::TPex20-ScARO7^{G141S}-PrGPD-PrTEFintron-ScARO4^{K229L}-TLip2 IntD1::PrTEFintron-YlACC1^{S667A,S1178A}-TLip2*	ST9178	pCfB9035	pCfB6631	This study
ST9537	*MATa ku70Δ::SpCas9-EcDsdAMX4 IntC2::PrTEFintron-FjTAL-TLip2 IntC3::TPex20-At4CL1-PrGPD-PrTEFintron-VvVST1-TLip2 IntE1::TPex20-YlARO7^{G139S}-PrGPD-PrTEFintron-YlARO4^{K221L}-TLip2 IntE4::TPex20-FjTAL-PrTEFintron-TPex20-At4CL1-PrGPD-PrTEFintron-VvVST1-TLip2*	ST9153	pCfB9178	pCfB6638	This study
ST9538	*MATa ku70Δ::SpCas9-EcDsdAMX4 IntC2::PrTEFintron-FjTAL-TLip2 IntC3::TPex20-At4CL1-PrGPD-PrTEFintron-VvVST1-TLip2 IntE1::TPex20-ScARO7^{G141S}-PrGPD-PrTEFintron-ScARO4^{K229L}-TLip2 IntE4::TPex20-FjTAL-PrTEFintron-TPex20-At4CL1-PrGPD-PrTEFintron-VvVST1-TLip2*	ST9178	pCfB9178	pCfB6638	This study
ST9585	*MATa ku70Δ::SpCas9-EcDsdAMX4 IntC2::PrTEFintron-FjTAL-TLip2 IntC3::TPex20-At4CL1-PrGPD-PrTEFintron-VvVST1-TLip2 IntE1::TPex20-YlARO7^{G139S}-PrGPD-PrTEFintron-YlARO4^{K221L}-TLip2 IntE4,D1::TPex20-FjTAL-PrTEFintron-TPex20-At4CL1-PrGPD-PrTEFintron-VvVST1-TLip2*	ST9537	pCfB9180	pCfB6631	This study
ST9586	*MATa ku70Δ::SpCas9-EcDsdAMX4 IntC2::PrTEFintron-FjTAL-TLip2 IntC3::TPex20-At4CL1-PrGPD-PrTEFintron-VvVST1-TLip2 IntE1::TPex20-ScARO7^{G141S}-PrGPD-PrTEFintron-ScARO4^{K229L}-TLip2 IntE4,D1::TPex20-FjTAL-PrTEFintron-TPex20-At4CL1-PrGPD-PrTEFintron-VvVST1-TLip2*	ST9538	pCfB9180	pCfB6631	This study
ST9616	*MATa ku70Δ::SpCas9-EcDsdAMX4 IntC2::PrTEFintron-FjTAL-TLip2 IntC3::TPex20-At4CL1-PrGPD-PrTEFintron-VvVST1-TLip2 IntE1::TPex20-YlARO7^{G139S}-PrGPD-PrTEFintron-YlARO4^{K221L}-TLip2 IntE4,D1,E3::TPex20-FjTAL-PrTEFintron-TPex20-At4CL1-PrGPD-PrTEFintron-VvVST1-TLip2*	ST9585	pCfB9179	pCfB6637	This study
ST9617	*MATa ku70Δ::SpCas9-EcDsdAMX4 IntC2::PrTEFintron-FjTAL-TLip2 IntC3::TPex20-At4CL1-PrGPD-PrTEFintron-VvVST1-TLip2 IntE1::TPex20-ScARO7^{G141S}-PrGPD-PrTEFintron-ScARO4^{K229L}-TLip2 IntE4,D1::TPex20-FjTAL-PrTEFintron-TPex20-At4CL1-PrGPD-PrTEFintron-VvVST1-TLip2*	ST9586	pCfB9179	pCfB6637	This study
ST9663	*MATa ku70Δ::SpCas9-EcDsdAMX4 IntC2::PrTEFintron-FjTAL-TLip2 IntC3::TPex20-At4CL1-PrGPD-PrTEFintron-VvVST1-TLip2 IntE4::TPex20-FjTAL-PrTEFintron-TPex20-At4CL1-PrGPD-PrTEFintron-VvVST1-TLip2*	ST8953	pCfB9178	pCfB6638	This study
ST9664	*MATa ku70Δ::SpCas9-EcDsdAMX4 IntC2::PrTEFintron-FjTAL-TLip2 IntC3::TPex20-At4CL1-PrGPD-PrTEFintron-VvVST1-TLip2 IntE1::TPex20-YlARO7^{G139S}-PrGPD-PrTEFintron-YlARO4^{K221L}-TLip2 IntE4,D1,E3,F3::TPex20-FjTAL-PrTEFintron-TPex20-At4CL1-PrGPD-PrTEFintron-VvVST1-TLip2*	ST9616	pCfB9316	pBP8003	This study
ST9671	*MATa ku70Δ::SpCas9-EcDsdAMX4 IntC2::PrTEFintron-FjTAL-TLip2 IntC3::TPex20-At4CL1-PrGPD-PrTEFintron-VvVST1-TLip2 IntE1::TPex20-YlARO7^{G139S}-PrGPD-PrTEFintron-YlARO4^{K221L}-TLip2 IntE4,D1,E3,F3,A1::TPex20-FjTAL-PrTEFintron-TPex20-At4CL1-PrGPD-PrTEFintron-VvVST1-TLip2*	ST9664	pCfB9315	pBP7995	This study
ST10246	*MATa ku70Δ::SpCas9-EcDsdAMX4 IntC2::PrTEFintron-FjTAL-TLip2 IntC3::TPex20-At4CL1-PrGPD-PrTEFintron-VvVST1-TLip2*	ST8953	pCfB8976	pCfB6633	This study
ST10247	*MATa ku70Δ::SpCas9-EcDsdAMX4 IntC2::PrTEFintron-FjTAL-TLip2 IntC3::TPex20-At4CL1-PrGPD-PrTEFintron-VvVST1-TLip2*	ST8953	pCfB9008	pCfB6633	This study

Supplementary Table S3: Plasmids used in this study.

Plasmid	Description	Parental vector	BioBricks	Source
pCfB826	X-4-*LoxP-HphMXsyn-ScARO7pm<-pTEF1-pPGK1->ScARO4pm*	See ref.	See ref.	(Rodriguez et al., 2015)
pCfB3405	*pORI1001-Nat-CEN1-USER*	See ref.	See ref.	(Holkenbrink et al., 2018)

pCfB6371	*pIntC_3-TPex20-TLip2*	See ref.	See ref.	(Holkenbrink et al., 2018)
pCfB6627	*pNat-YLgRNA2_IntC_2*	See ref.	See ref.	(Holkenbrink et al., 2018)
pCfB6630	*pNat-YLgRNA3_IntC_3*	See ref.	See ref.	(Holkenbrink et al., 2018)
pCfB6631	*pNat-YLgRNA2_IntD_1*	See ref.	See ref.	(Holkenbrink et al., 2018)
pCfB6633	*pNat-YLgRNA2_IntE_1*	See ref.	See ref.	(Holkenbrink et al., 2018)
pCfB6637	*pNat-YLgRNA2_IntE_3*	See ref.	See ref.	(Holkenbrink et al., 2018)
pCfB6638	*pNat-YLgRNA2_IntE_4*	See ref.	See ref.	(Holkenbrink et al., 2018)
pCfB6677	*pIntE_1-TPex20-TLip2*	See ref.	See ref.	(Holkenbrink et al., 2018)
pCfB6682	*pIntC_2-TPex20-TLip2*	See ref.	See ref.	(Holkenbrink et al., 2018)
pCfB6684	*pIntD_1-TPex20-TLip2*	See ref.	See ref.	(Holkenbrink et al., 2018)
pCfB6679	*pIntE_4-TPex20-TLip2*	See ref.	See ref.	(Holkenbrink et al., 2018)
pCfB6681	*pIntE_3-TPex20-TLip2*	See ref.	See ref.	(Holkenbrink et al., 2018)
pCfB8681	*pIntE_3-TPex20-PrTEFin->YlACC1->TLip2*	N/A	N/A	In-house (unpublished)
pCfB8811	*pIntC_2-TPex20<-PpPchB<-PrGPD::PrTEFin->EcEntC->TLip2*	pCfB6682	BB3855, BB3907, BB3909. BB3910	This study
pCfB8812	*pIntC_2-TPex20-PrTEFin->FjTAL->TLip2*	pCfB6682	BB3855, BB3908, BB3911	This study
pCfB8813	*pIntC_2-TPex20-PrTEFin->PaAroZ->TLip2*	pCfB6682	BB3855, BB3908, BB3917	This study
pCfB8814	*pIntD_1-TPex20<-CaCatA<-PrGPD::PrTEFin->KpAroY.B->TLip2*	pCfB6684	BB3857, BB3907, BB3918, BB3921	This study
pCfB8815	*pIntC_2-TPex20-PrTEFin->HaTAL->TLip2*	pCfB6682	BB3855, BB3908, BB3912	This study
pCfB8816	*pIntC_3-TPex20<-At4CL1<-PrGPD::PrTEFin->VvVST1->TLip2*	pCfB6371	BB3856, BB3907, BB3913, BB3914	This study
pCfB8817	*pIntC_3-TPex20<-VvVST1<-PrGPD::PrTEFin->At4CL1->TLip2*	pCfB6371	BB3856, BB3907, BB3915, BB3916	This study
pCfB8842	*pIntC_3-TPex20<-KpAroY.D<-PrGPD::PrTEFin->KpAroY.Ciso->TLip2*	pCfB6371	BB3856, BB3907, BB3919, BB3920	This study
pCfB8843	*pORI1001-Hyg-CEN1-USER*	N/A	N/A	In-house (unpublished)
pCfB8858	*pHphM-YLgRNA2_IntE_1*	N/A	N/A	In-house (unpublished)
pCfB8976	*pInt E_1-TPex20-PrTEFin->YlARO4_K221L->tLip2*	pCfB6677	BB4028, BB3908, BB4031	This study
pCfB8977	*pIntE_1-TPex20<-YlARO7G139S<-PrGPD::PrTEFin->YlARO4K221L->TLip2*	pCfB6677	BB4028, BB3907, BB4031, BB4034	This study
pCfB9008	*pIntE_1-TPex20-PrTEFin->ScARO4_K229L->TLip2*	pCfB6677	BB4028, BB3908, BB4035	This study
pCfB9009	*pIntE_1-TPex20<-ScARO7G141S<-PrGPD::PrTEFin->ScARO4K229L->TLip2*	pCfB6677	BB4028, BB3907, BB4035, BB4036	This study
pCfB9010	*pNat-gRNA-YALI1_D08884g*	pCfB3405	BB4050	This study
pCfB9011	*pNat-gRNA-YALI1_D12832g*	pCfB3405	BB4051	This study
pCfB9015	*pHphM-gRNA-YALI1_D08884g*	pCfB8843	BB4050	This study
pCfB9016	*pHphM-gRNA-YALI1_D12832g*	pCfB8843	BB4051	This study
pCfB9035	*pIntD_1-TPex20-PrTEFin->YlACC1_S667A+S1178A->TLip2*	pCfB6684	BB3857, BB4045, BB4049	This study
pCfB9178	*pIntE_4-TPex20<-FjTAL<-PrTEFin, <-TPex20<-At4CL1-PrGPD,PrTEFin->VvVST1->TLip2->*	pCfB6679	BB4154, BB4156, BB4157	This study
pCfB9179	*pIntE_3-TPex20<-FjTAL<-PrTEFin <-TPex20<-At4CL1-PrGPD,PrTEFin->VvVST1->TLip2->*	pCfB6681	BB4153, BB4156, BB4157	This study
pCfB9180	*pIntD_1-TPex20<-FjTAL<-PrTEFin, <-TPex20<-At4CL1-PrGPD,PrTEFin->VvVST1->TLip2->*	pCfB6684	BB3857, BB4156, BB4157	This study
pCfB9315	*pIntA_1-TPex20<-FjTAL<-PrTEFin, <-TPex20<-At4CL1-PrGPD,PrTEFin->VvVST1->TLip2->*	pBP8006	BB4322, BB4156, BB4157	This study
pCfB9316	*pIntF_3-TPex20<-FjTAL<-PrTEFin, <-TPex20<-At4CL1-PrGPD,PrTEFin->VvVST1->TLip2->*	pBP8009	BB4323, BB4156, BB4157	This study
pBP7995	*pNat-YLgRNA5-IntA_1*	N/A	N/A	BioPhero ApS
pBP8003	*pNat-YLgRNA4-IntF_3*	N/A	N/A	BioPhero ApS
pBP8006	*pIntA_1-TPex20-TLip2*	N/A	N/A	BioPhero ApS
pBP8009	*pIntF_3-TPex20-TLip2*	N/A	N/A	BioPhero ApS

Supplementary Table S4: Biobricks used in this study.

BioBrick	Description	PCR template	Forward primer	Reverse primer
BB3855	pIntC_2 backbone	pCfB6682	PR-23963	PR-23968
BB3856	pIntC_3 backbone	pCfB6371	PR-23963	PR-23968
BB3857	pIntD_1 backbone	pCfB6684	PR-23963	PR-23968
BB3905	*PrTEFin->*	gDNA ST6512	PR-23966	PR-23967
BB3906	*<-PrGPD*	gDNA ST6512	PR-23964	PR-23965
BB3907	*<-PrGPD::PrTEFin->*	BB3905+BB3906	PR-23965	PR-23967
BB3908	*PrTEFin->*	gDNA ST6512	PR-23995	PR-23967
BB3909	*<-PpPchB*	*PpPchB* GeneArt DNA String	PR-23973	PR-23974
BB3910	*EcEntC->* (*PrTEFin*)	*EcEntC* GeneArt DNA String	PR-24286	PR-23976
BB3911	*FjTAL->* (*PrTEFin*)	*FjTAL* GeneArt DNA String	PR-24287	PR-23997
BB3912	*HaTAL->* (*PrTEFin*)	*HaTAL* GeneArt DNA String	PR-24290	PR-23999
BB3913	*<-At4CL1*	*At4CL1* GeneArt DNA String	PR-23977	PR-23978
BB3914	*VvVST1->* (*PrTEFin*)	*VvVST1* GeneArt DNA String	PR-24291	PR-23980
BB3915	*<-VVVST1*	*VvVST1* GeneArt DNA String	PR-23983	PR-23984
BB3916	*At4CL1->* (*PrTEFin*)	*At4CL1* GeneArt DNA String	PR-24292	PR-23982
BB3917	*PaAroZ->* (*PrTEFin*)	*PaAroZ* GeneArt DNA String	PR-24288	PR-24002
BB3918	*KpAroY.B->* (*PrTEFin*)	*KpAroY.B* GeneArt DNA String	PR-24289	PR-23994
BB3919	*KpAroY.Ciso->* (*PrTEFin*)	*KpAroY.Ciso* GeneArt DNA String	PR-24293	PR-23989
BB3920	*<-KpAroY.D*	*KpAroY.D* GeneArt DNA String	PR-23986	PR-23987
BB3921	*<-CaCatA*	*CaCatA* GeneArt DNA String	PR-23991	PR-23992
BB4028	pIntE_1 backbone	pCfB6677	PR-23963	PR-23968
BB4029	*YlARO4K229L*, part 1	gDNA ST6512	PR-24549	PR-24550
BB4030	*YlARO4K229L*, part 2	gDNA ST6512	PR-24551	PR-24552
BB4031	*YlARO4K229L->* (*PrTEFin*)	BB4029+BB4030	PR-24549	PR-24552
BB4032	*YlARO7G139S*, part 1	gDNA ST6512	PR-24553	PR-24554
BB4033	*YlARO7G139S*, part 2	gDNA ST6512	PR-24555	PR-24556
BB4034	*<-YlARO7G139S*	BB4032+BB4033	PR-24553	PR-24556
BB4035	*ScARO4K229L->* (*PrTEFin*)	pCfB826	PR-24589	PR-24590
BB4036	*<-ScARO7G141S*	pCfB826	PR-24591	PR-24592
BB4037	*ARO10*_Up	gDNA ST6512	PR-24567	PR-24568
BB4038	*ARO10*_Down	gDNA ST6512	PR-24569	PR-24570
BB4039	*ARO10*_FullRepair	BB4037+BB4038	PR-24567	PR-24570
BB4040	*PDC5*_Up	gDNA ST6512	PR-24575	PR-24576
BB4041	*PDC5*_Down	gDNA ST6512	PR-24577	PR-24578
BB4042	*PDC5*_FullRepair	BB4040+BB4041	PR-24575	PR-24578
BB4043	PrTEFin+*YlACC1*-Ex1	pCfB8681	PR-23995	PR-24667
BB4044	*YlACC1*-Ex2	gDNA ST6512	PR-24668	PR-24669
BB4045	*PrTEFin*+*YlACC1*-Ex1-Ex2	BB4043+4044	PR-23995	PR-24669
BB4046	*YlACC1*-Ex3-Part1	gDNA ST6512	PR-24670	PR-18559
BB4047	*YlACC1*-Ex3-Part2	gDNA ST6512	PR-18558	PR-18561
BB4048	*YlACC1*-Ex3-Part3	gDNA ST6512	PR-18560	PR-24671
BB4049	*YlACC1*-Ex3-S667A,S1178A	BB4046+BB4047+BB4048	PR-24670	PR-24671
BB4050	gRNA-*ARO10*-single	BB1635+BB1636+PR-24565+PR-24566	PR-10607	PR-10604

BB4051	gRNA-*PDC5*-single	BB1635+BB1636+PR-24567+PR-24568	PR-10607	PR-10604
BB4153	pIntE_3 backbone	pCfB6681	PR-23963	PR-23968
BB4154	pIntE_4 backbone	pCfB6679	PR-23963	PR-23968
BB4155	pIntF_3 backbone	pBP8009	PR-23963	PR-23968
BB4156	<-*FjTAL-PrTEFin*	pCfB8812	PR-25054	PR-25055
BB4157	<*At4CL1-PrGPD*::*PrTEFin*->*VvVST1*->)	pCfB8816	PR-25056	PR-23980
BB4322	pIntA_1 backbone	pBP8006	PR-23963	PR-23968

Table S5: Primers used in this study.

Primer	Sequence	Description
PR-10604	CACGCGAUACCGTACCCACACAAAAAAAGCACCACCGACTC	Reverse primer for the amplification of crRNA-TRPR
PR-10607	CGTGCGAUAGTGAATCATTGCTAACAGATC	Forward primer for the amplification of PrtRNAGly
PR-15788	TAACCAACCUGCGCCGACCCGGAATCGAAC	Reverse primer for the amplification of PrtRNAGly
PR-15789	GTTTTAGAGCUAGAAATAGCAAGTTAAAATAAG	Forward primer for the amplification of crRNA-TRPR
PR-15790	AGTGCAGGUAGTGAATCATTGCTAACAGATC	Forward primer for the amplification of gRNA cassette in position 2
PR-15791	ACCTGCACUACCGTACCCACACAAAAAAAGCAC	Reverse primer for the amplification of gRNA cassette in position 2
PR-18558	ACCTCTTGCUGACGGTGGTATTCTGTGTCT	Forward primer for YlACC1 point mutation 1 in exon 3
PR-18559	AGCAAGAGGUCTAACTCCAATGTCGCATCG	Reverse primer for YlACC1 point mutation 1 in exon 3
PR-18560	ATGCCGTCUCCGACTTTTCGTACACCGTT	Forward primer for YlACC1 point mutation 2 in exon 3
PR-18561	AGACGGCAUCAGCTCGAGACACCGAGG	Reverse primer for YlACC1 point mutation 2 in exon 3
PR-23963	ATCGCACGUAAGTGTGGATGGGGAAGTGAGT	Forward primer for amplification of EasyCloneYALI integrative vectors
PR-23964	ATCAGTAGCUGACGCAGTAGGATGTCCTGCA	Forward primer for amplification of *PrGPD*, position 1. Double promoter
PR-23965	ACCTGCACUTGTTGATGTGTGTTTAATTCAAGAATGAAT	Reverse primer for amplification of *PrGPD*, position 1. Double promoter
PR-23966	AGCTACTGAUAGAGACCGGGTTGGCGGC	Forward primer for amplification of *PrTEFin*, position 2. Double promoter
PR-23967	AGTACTGCAAAAAGUGCTGGTCGGA	Reverse primer for amplification of *PrTEFin*, position 2. Double promoter
PR-23968	ATCGCGTGUCTTCTGTTCGGAATCAACCTCAAGG	Reverse primer for amplification of EasyCloneYALI integrative vectors
PR-23973	ACGTGCGAUTTACTCGTCCTGGGCGCCC	Reverse primer for amplification of *PpPchB* in position 1
PR-23974	AGTGCAGGUGCCACAATGAACTTCCCTCTGGTGGACC	Forward primer for amplification of *PpPchB* in position 1
PR-23976	ACACGCGAUTTAGTGCAGGCCGAACACGT	Reverse primer for amplification of *EcEntC* in position 2
PR-23977	AGTGCAGGUGCCACAATGGCTCCCCAAGAGCAGG	Forward primer for amplification of *At4CL1* in position 1
PR-23978	ACGTGCGAUTTACAGGCCGTTAGCCAGCT	Reverse primer for amplification of *At4CL1* in position 1
PR-23980	ACACGCGAUTTAGTTGGTCACGGTGGGCAC	Reverse primer for amplification of *VvVST1* in position 2
PR-23982	ACACGCGAUTTACAGGCCGTTAGCCAGCTT	Reverse primer for amplification of *At4CL1* in position 2
PR-23983	AGTGCAGGUGCCACAATGGCCTCTGTGGAAGAGTTCC	Forward primer for amplification of *VvVST1* in position 1
PR-23984	ACGTGCGAUTTAGTTGGTCACGGTGGGCA	Reverse primer for amplification of VvVST1 in position 1
PR-23986	AGTGCAGGUGCCACAATGATCTGTCCCCGATGCG	Forward primer for amplification of *KpAroY.D* in position 1
PR-23987	ACGTGCGAUTTATCGCTTGTCCTCGGGCAG	Reverse primer for amplification of *KpAroY.D* in position 1
PR-23989	ACACGCGAUTTACTTGGCAGAGCCCTGGT	Reverse primer for amplification of *KpAroY.Ciso* in position 2
PR-23991	AGTGCAGGUGCCACAATGTCTCAGGCCTTCACCGA	Forward primer for amplification *CaCatA* in position 1
PR-23992	ACGTGCGAUTTACAGCTTGATCTCGGCGTCC	Reverse primer for amplification of *CaCatA* in position 1
PR-23994	ACACGCGAUTTACTCGATCTCTTGGGCGAACTG	Reverse primer for amplification of *KpAroY.B* in position 2
PR-23995	ACGTGCGAUAGAGACCGGGTTGGCGGC	Forward primer for amplificatio of *PrTEFin* in position 2, single promoter

PR-23997	ACACGCGAUCTAGTTGTTAATCAGATGGTCCTTGACCTTC	Reverse primer for amplification of *FjTAL* in position 2
PR-23999	ACACGCGAUTTATCGGAACAGGATGATGGATCGC	Reverse primer for amplification of *HaTAL* in position 2
PR-24002	ACACGCGAUTTACAGGGCAGCAGACAGAGAC	Reverse primer for amplification of *PaAroZ* in position 2
PR-24286	ACTTTTTGCAGTACUAACCGCAGGACACCTCTCTGGCCGAAGAG	Forward primer for amplification of *EcEntC* in position 2, under control of *PrTEFin*
PR-24287	ACTTTTTGCAGTACUAACCGCAGAACACCATCAACGAGTACCTGTCT	Forward primer for amplification of *FjTAL* in position 2, under control of *PrTEFin*
PR-24288	ACTTTTTGCAGTACUAACCGCAGCCCTCTAAGCTGGCCATCAC	Forward primer for amplification of *PaAroZ* in position 2, under control of *PrTEFin*
PR-24289	ACTTTTTGCAGTACUAACCGCAGAAGCTGATCATCGGTATGACTGGT	Forward primer for amplification of *KpAroY.B* in position 2, under control of *PrTEFin*
PR-24290	ACTTTTTGCAGTACUAACCGCAGTCTACCACTCTGATCCTGACCGG	Forward primer for amplification of HaTAL in position 2, under control of PrTEFin
PR-24291	ACTTTTTGCAGTACUAACCGCAGGCCTCTGTGGAAGAGTTCCGA	Forward primer for amplification of *VvVST1* in position 2, under control of *PrTEFin*
PR-24292	ACTTTTTGCAGTACUAACCGCAGGCTCCCCAAGAGCAGGCC	Forward primer for amplification of *At4CL1* in position 2, under control of *PrTEFin*
PR-24293	ACTTTTTGCAGTACUAACCGCAGACCGCTCCTATCCAGGACC	Forward primer for amplification of *KpAroY.Ciso* in position 2, under control of *PrTEFin*
PR-24549	ACTTTTTGCAGTACUAACCGCAGTCCCGTTCCTCCTCTCCCAAC	Forward primer for amplification of *YlARO4* part 1 with point mutation
PR-24550	ACACCCAUGAAGTGGTGAGGGT	Reverse primer for amplification of *YlARO4* part 1 with point mutation
PR-24551	ATGGGTGUCACCCTGCAGGGTGTTGCCGCCATC	Forward primer for amplification of *YlARO4* part 2 with point mutation
PR-24552	ACACGCGAUTTAGTTCTTGTTTCGTCGCTCCT	Reverse primer for amplification of *YlARO4* part 2 with point mutation
PR-24553	AGTGCAGGUGCCACAATGGACTTCACTAAAGCCGACACC	Forward primer for amplification of *YlARO7* part 1 with point mutation
PR-24554	ACCGAGGAAUAGTTCTCGGGCTGATCTCCA	Reverse primer for amplification of *YlARO7* part 1 with point mutation
PR-24555	ATTCCTCGGUCATGGTGTGCGACATC	Forward primer for amplification of *YlARO7* part 2 with point mutation
PR-24556	ACGTGCGAUCTACTCCAACCGCCGGAGCA	Reverse primer for amplification of *YlARO7* part 2 with point mutation
PR-24565	GAAGTGGACTAAGTTGCTGGGTTTTAGAGCT	gRNA forward primer for *ARO10*
PR-24566	CCAGCAACTTAGTCCACTTCTAACCAACCT	gRNA reverse primer for *ARO10*
PR-24567	TGCATCTGGCTCTAAATGTCTCC	Forward primer for amplification of *ARO10* upstream homology arm
PR-24568	ATGTTGAUAGTCAAGTCACTGGAGAGATG	Reverse primer for amplification of *ARO10* upstream homology arm
PR-24569	ATCAACAUGATGAGATTGAGCGGAGCG	Forward primer for amplification of *ARO10* downstream homology arm
PR-24570	TCGGCTACCGGTTTGACTCAC	Reverse primer for amplification of *ARO10* downstream homology arm
PR-24573	TGTACAATGTCGACATGCGGGTTTTAGAGCT	gRNA forward primer for *PDC5*
PR-24574	CCGCATGTCGACATTGTACATAACCAACCT	gRNA reverse primer for *PDC5*
PR-24575	TCAGGCGTTGCTTTTGCTCC	Forward primer for amplification of *PDC5* upstream homology arm
PR-24576	ATGCTGGTUAGCAAGTCAAGTTAGGTTTTGGG	Reverse primer for amplification of *PDC5* upstream homology arm
PR-24577	AACCAGCAUTATAGATGAATCATTTAAAAAGAGATGACTTGTAG	Forward primer for amplification of *PDC5* downstream homology arm
PR-24578	TTCGCCATTCCCGCTCATTC	Reverse primer for amplification of *PDC5* downstream homology arm
PR-24589	ACTTTTTGCAGTACUAACCGCAGAGTGAATCTCCAATGTTCGCTGC	Forward primer for amplification of *ScARO4K229L* in position 2 with *PrTEFin*
PR-24590	ACACGCGAUTCATTTCTTGTTAACTTCTCTTCTTTGTCTGACAG	Reverse primer for amplification of *ScARO4K229L* in position 2 with *PrTEFin*
PR-24591	AGTGCAGGUGCCACAATGGATTTCACAAAACCAGAAACTGTTTTAAATC	Forward primer for amplification of *ScARO7G141S* in position 1
PR-24592	ACGTGCGAUTTACTCTTCCAACCTTCTTAGCAAGTATTCC	Reverse primer for amplification of *ScARO7G141S* in position 1
PR-24667	AGCCATACUGAAAAACCGACGTGTTAGTGTCC	Reverse primer for amplification of exon 1 in *YlACC1*
PR-24668	AGTATGGCUTCAGGATCTTCAACGC	Forward primer for amplification of exon 2 in *YlACC1*
PR-24669	ATGAGGACCUTGTTGATAACTGTATGACCTCCGTG	Reverse primer for amplification of exon 2 in *YlACC1*
PR-24670	AGGTCCTCAUCGCTAACAACGGTATTG	Forward primer for amplification of exon 3 in *YlACC1*
PR-24671	ACACGCGAUTCACAACCCCTTGAGCAGCTC	Reverse primer for amplification of exon 3 in *YlACC1*

PR-25054	ACGTGCGAUCTAGTTGTTAATCAGATGGTCCTT GACCTTC	Forward primer to amplify fused *PrTEFin-FjTAL*
PR-25055	AGCATAAGUAGAGACCGGGTTGGCGGC	Rerverse primer to amplify *fused PrTEFin-FjTAL*
PR-25056	ACTTATGCUACGCAACTAACATGAATGAATACG ATATACATC	Forward primer to amplify whole expression cassette from pCfB8816

Supplementary Table S6: Codon-optimized genes for *Y. lipolytica* used in this study.

HaTAL	ATGTCTACCACTCTGATCCTGACCGGCGAAGGCCTGGGCATCGACGACGTGGTGCGAGTGGCCCGACACCAGGACCGAGTC GAGCTGACCACCGATCCTGCCATTCTGGCCCAGATCGAGGCCTCTTGCGCCTACATCAACCAGGCCGTGAAGGAACACCAGC CTGTGTACGGCGTGACCACCGGCTTCGGCGGCATGGCCAACGTGATCATCTCTCCCGAGGAAGCCGCCGAGCTGCAGAACA ACGCCATCTGGTATCACAAGACCGGCGCTGGCAAGCTGCTGCCCTTCACCGACGTGCGAGCCGCCATGCTGCTGCGAGCCAA CTCTCACATGCGAGGTGCCTCTGGCATCCGACTCGAGATCATCCAGCGAATGGTGACCTTCCTGAACGCCAACGTCACCCCT CACGTGCGAGAGTTCGGCTCTATCGGCGCCTCTGGCGATCTGGTGCCCCTGATCTCTATCACCGGCGCTCTGCTGGGCACCG ACCAGGCTTTCATGGTGGACTTCAACGGCGAGACTCTGGACTGCATCTCTGCCCTCGAGCGACTGGGACTGCCCCGACTGCG ACTGCAGCCCAAGGAAGGACTGGCCATGATGAACGGCACCTCTGTGATGACCGGAATCGCCGCCAACTGCGTGCACGACGC CCGAATCCTGCTGGCCCTGGCTCTCGAGGCCCACGCTCTGATGATCCAGGGACTGCAGGGCACTAACCAGTCTTTTCACCCC TTCATCCACCGACACAAGCCCCACACCGGACAGGTGTGGGCCGCTGACCACATGCTCGAGCTGCAGGGCTCTCAGCTGT CTCGAAACGAGCTGGACGGCTCTCACGACTACCGAGATGGCGACCTGATTCAGGACCGATACTCTCTCCGATGTCTGCCCCA GTTCCTGGGACCTATCATCGACGGAATGGCCTTCATCTCTCACCATCTGCGAGTCGAGATCAACTCTGCCAACGACAACCCTC TGATCGACACCGCCTCTGCCGCCTCTTACCACGGCGGCAACTTTCTGGGACAGTACATCGGCGTCGGCATGGACCAGCTGCG GTACTACATGGGCCTGATGGCCAAGCACCTGGACGTGCAGATCGCCCTGCTGGTGTCTCCTCAGTTCAACAACGGACTGCCC GCCTCTCTGGTGGGCAACATTCAGCGAAAGGTGAACATGGGACTGAAGGGCCTGCAGCTGACCGCCAACTCTATTATGCCTA TCCTGACCTTTCTGGGCAACTCTCTGGCCGATCGATTCCCCACTCACGCCGAGCAGTTCAACCAGAACATCAACTCTCAAGGC TTCGGATCTGCCAACCTGGCTCGACAGACCATTCAGACCCTCCAGCAGTACATTGCTATCACCCTGATGTTCGGCGTGCAGG CCGTGGACCTGCGAACCCACAAGCTGGCCGGACACTACAACGCCGCTGAGCTGCTGTCTCCCCTGACCGCTAAGATCTACCA CGCCGTGCGATCTATCGTGAAGCACCCTCCTAGTCCTGAGCGACCCTACATCTGGAACGACGACGAGCAGGTCCTCGAGGCT CACATCTCTGCTCTGGCCCACGATATCGCCAACGACGGATCTCTGGTGTCTGCCGTCGAGCAGACCCTGTCTGGCCTGCGAT CCATCATCCTGTTCCGATAA
FjTAL	ATGAACACCATCAACGAGTACCTGTCTCTGGAAGAGTTCGAGGCCATCATCTTCGGCAACCAGAAGGTGACCATCTCTGACG TGGTGGTGAACCGAGTGAACGAGTCTTTCAACTTCCTGAAGGAATTCTCTGGCAACAAGGTGATCTACGGCGTGAACACCGG CTTCGGCCCCATGGCTCAGTACCGAATCAAGGAATCTGACCAGATCCAGCTGCAGTACAACCTGATCCGATCTCACTCTTCTG GCACCGGCAAGCCTCTGTCTCCCGTGTGCGCCAAGGCCGCCATTCTGGCCCGACTGAACACCCTGTCGCTGGGCAACTCTGG CGTGCACCCCTCTGTGATCAACCTGATGTCTGAGCTGATCAACAAGGACATTACCCCTCTGATCTTCGAGCACGGCGGCGTG GGCGCCTCTGGCGACCTGGTGCAGCTGTCTCACCTGGCTCTGGTGCTGATCGGCGAGGGCGAAGTGTTCTACAAGGGCGAG CGACGACCCACTCCTGAGGTGTTCGAGATCGAGGGACTGAAGCCCATCCAGGTCGAGATCCGAGAGGGACTCGCCCTGATC AACGGCACCTCCGTGATGACCGGCATCGGCGTGGTGAACGTGTACCACGCCAAGAAGCTGCTGGACTGGTCCCTGAAGTCC TCTTGCGCCATTAACGAGCTGGTGCAGGCCTACGACGACCACTTCTCTGCCGAGCTGAACCAGACCAAGCGACACAAGGGCC AGCAAGAGATCGCCCTGAAGATGCGACAGAACCTGTCTGACTCTACCCTGATTCGAAAGCGAGAGGACCACCTGTACTCTGG CGAGAACACCGAGGAAATCTTCAAGGAAAAGGTGCAAGAGTACTACTCTCTCCGATGCGTGCCCCAGATTCTGGGCCCCGTG CTGGAAACCATCAACAACGTGGCCTCTATTCTCGAGGACGAGTTCAACTCTGCCAACGACAACCCCATCATCGACGTGAAGA ACCAGCACGTCTACCACGGCGGCAACTTCCACGGCGACTACATCTCCCTCGAGATGGACAAGCTGAAGATCGTGATCACCAA GCTGACCATGCTGGCCGAGCGACAGCTGAACTACCTGCTGAACTCTAAGATCAACGAGCTGCTGCCTCCTTTCGTGAACCTG GGCACCCTGGGCTTCAACTTCGGCATGCAGGGCGTGCAGTTCACCGCCACCTCTACCACCGCCGAGTCTCAGATGCTGTCTA ACCCCATGTACGTGCACTCTATCCCCAACAACAACGATAACCAGGACATCGTGTCTATGGGCACCAACTCCGCCGTGATTACC TCTAAGGTGATCGAGAACGCCTTCGAGGTGCTGGCCATCGAGATGATCACCATCGTGCAGGCCATTGACTACCTGGGCCAGA AGGACAAGATCTCTTCTGTGTCTAAGAAGTGGTACGACGAGATTCGAAACATCATCCCCACCTTTAAGGAAGATCAGGTGAT GTACCCCTTCGTGCAGAAGGTCAAGGACCATCTGATTAACAACTAG
At4CL1	ATGGCTCCCCAAGAGCAGGCCGTGTCTCAGGTGATGGAAAAGCAGTCTAACAACAACAACTCTGACGTGATCTTCCGATCTA AGCTGCCCGACATCTACATCCCCAACCACCTGTCTCTGCACGACTACATCTTCCAGAACATCTCTGAGTTCGCCACCAAGCCT TGCCTGATCAACGGCCCCACCGGCCACGTGTACACCTACTCCGACGTCCACGTGATCTCTCGACAGATCGCCGCCAACTTCCA CAAGCTGGGCGTGAACCAGAACGACGTGGTGATGCTGCTGCTCCCAACTGTCCCGAGTTCGTGCTGTCTTTCCTGGCCGCC TCGTTCCGAGGCGCCACCGCTACCGCTGCTAACCCATTCTTCACCCCTGCCGAGATCGCCAAGCAGGCCAAGGCCTCTAACA CCAAGCTGATCATCACCGAGGCTCGATACGTGGACAAGATCAAGCCCCTGCAGAACGATGACGGCGTGGTGATCGTGTGCA TCGACGACAACGAGTCTGTGCCCATTCCTGAGGGCTGCCTGCGATTCACCGAGCTGACCCAGTCTACCACCGAGGCCTCTGA GGTGATCGACTCCGTCGAGATCTCTCCCGACGACGTTGTGGCTCTGCCCTACTCTTCTGGCACCACCGGACTGCCCAAGGGC GTGATGCTGACCCACAAGGGCCTCGTGACCTCTGTGGCCCAGCAGGTCGACGGCGAGAACCCCAACCTGTACTTCCACTCTG ACGACGTGATCCTGTGCGTGCTGCCCATGTTCCACATCTACGCCCTGAACTCTATCATGCTGTGCGGCCTGCGAGTGGGAGC CGCCATCCTGATCATGCCCAAGTTCGAGATCAACCTGCTGCTCGAGCTGATCCAGAGATGCAAGGTGACCGTGGCTCCTATG GTGCCTCCTATCGTGCTGGCCATTGCCAAGTCCTCTGAGACTGAGAAGTACGACCTGTCCTCTATCCGAGTGGTGAAGTCTG GCGCTGCTCCCCTCGGCAAGGAACTCGAGGACGCCGTGAACGCTAAGTTCCCCAACGCCAAGCTCGGACAAGGCTACGGCA TGACCGAGGCTGGCCCCGTCCTGGCCATGTCTCTGGGCTTCGCCAAGGAACCCTTTCCAGTCAAGTCCGGCGCCTGCGGCAC CGTGGTGCGAAACGCCGAGATGAAGATCGTGGACCCCGACACCGGCGACTCCCTGTCTCGAAACCAGCCTGGCGAGATCTG CATCCGAGGCCACCAGATCATGAAGGGCTACCTGAACAACCCCGCTGCCACCGCCGAGGACTATCGACAAGGACGGCTGGCT GCACACCGGTGACATCGGCCTGATTGACGACGACGATGAGCTGTTCATTGTGGACCGACTGAAGGAACTGATCAAGTACAA GGGCTTCCAGGTGGCTCCCGCCGAGCTTGAGGCCCTGCTGATCGGACACCCCGACATCACCGACGTGGCCGTGGTCGCCAT GAAGGAAGAGGCCGCTGGCGAGGTGCCCGTGGCCTTCGTGGTCAAGTCTAAGGACTCTGAGCTGTCTGAGGACGACGTCAA GCAGTTCGTGTCTAAGCAGGTCGTGTTCTACAAGCGAATCAACAAGGTGTTCTTCACCGAGTCTATCCCCAAGGCTCCCTCT GGCAAGATCCTGCGAAAGGACCTGCGAGCCAAGCTGGCTAACGGCCTGTAA
VvVST1	ATGGCCTCTGTGGAAGAGTTCCGAAACGCCCAGCGAGCCAAGGGACCCGCCACCATCCTGGCCATCGGCACCGCTACTCCCG ACCACTGCGTGTACCAGTCTGACTACGCCGACTACTACTTCCGAGTGACCAAGTCTGAGCACATGACCGAGCTGAAGAAGAA GTTCAACCGAATCTGCGACAAGTCTATGATCAAGAAGCGGTACATCCACCTGACCGAGGAAATGCTCGAGGAACACCCCAAC ATCGGCGCCTACATGGCCCCTTCTCTGAACATCCGACAAGAGATCATCACCGCCGAGGTGCCCCGACTGGGCCGAGATGCCG CTCTGAAGGCCCTGAAGGAATGGGGACAGCCCAAGTCCAAGATCACCCACCTGGTGTTCTGCACCACCTCTGGCGTCGAGAT GCCCGGTGCCGACTACAAGCTGGCCAACCTGCTGGGCCTCGAGACTTCTGTGCGACGAGTGATGCTGTACCACCAGGGCTG CTACGCTGGCGGCACCGTGCTGCGAACCGCCAAGGACCTGGCCGAGAACAACGCTGGCGCCCGAGTGCTGGTGGTGTGCTC TGAGATCACCGTGGTGACCTTCCGAGGTCCTTCTGAGGACGCCCTGGACTCTCTGGTCGGACAGGCCCTGTTCGGCGACGGA TCTTCTGCCGTGATCGTGGGCTCTGACCCCGACGTGTCTATCGAGCGACCCCTGTTCCAGCTGGTGTCTGCTGCCCAGACCT TCATTCCCAACTCTGCCGGCGCTATCGCCGGAAACCTGCGAGAGGTGGGCCTGACCTTCCACCTGTGGCCTAACGTGCCCAC TCTGATCTCTGAGAACATCGAGAAGTGTCTGACCCAGGCTTTCGACCCTCTGGGAATCTCTGACTGGAACTCTCTGTTCTGG

	ATCGCTCACCCCGGTGGACCCGCTATCCTGGACGCCGTCGAGGCCAAGCTGAACCTGGAAAAGAAGAAGCTGGAAGCTACC CGACACGTGCTGTCTGAGTACGGCAACATGTCCTCTGCCTGCGTGCTGTTCATTCTGGACGAGATGCGAAAGAAGTCTCTGA AGGGCGAGAAGGCCACCACCGGCGAGGGACTCGACTGGGGAGTGCTGTTCGGCTTCGGACCCGGCCTGACCATCGAGACTG TGGTGCTGCACTCTGTGCCCACCGTGACCAACTAA
EcEntC	ATGGACACCTCTCTGGCCGAAGAGGTGCAGCAGACCATGGCCACTCTGGCTCCCAACCGATTCTTCTTCATGTCTCCCTACCG ATCTTTCACCACCTCTGGCTGCTTCGCCCGATTCGACGAGCCCGCCGTGAACGGCGACTCTCCCGACTCGCCCTTCCAGCAGA AGCTGGCCGCTCTGTTCGCCGACGCCAAGGCTCAGGGCATCAAGAACCCCGTGATGGTGGGCGCTATCCCTTTCGACCCTCG ACAGCCCTCTTCTCTGTACATCCCCGAGTCTTGGCAGTCTTTCTCGCGACAAGAGAAGCAGGCCTCTGCTCGACGATTCACCC GATCTCAGTCTCTGAACGTGGTCGAGCGACAGGCTATCCCCGAGCAGACCACCTTCGAGCAGATGGTGGCCCGAGCCGCCG CTCTGACCGCTACTCCCCAGGTGGACAAGGTGGTGCTGTCTCGACTGATCGACATCACCACCGACGCCGCCATCGACTCTGG CGTGCTGCTCGAGCGACTGATTGCTCAGAACCCTGTGTCTTACAACTTCCACGTGCCTCTCGCCGACGGCGGAGTGCTGCTG GGCGCTTCTCCCGAGCTGCTGCTGCGAAAGGACGGCGAGCGATTCTCTTCTATTCCCCTGGCCGGCTCTGCCCGACGACAGC CCGACGAGGTGCTGGACCGAGAGGCCGGCAACCGACTGCTGGCCTCTGAGAAGGACCGACACGAGCACGAGCTGGTGACCC AGGCCATGAAGGAAGTGCTGCGAGAGCGATCTTCTGAGCTGCACGTGCCCTCTTCGCCCCAGCTGATCACCACTCCTACTCT GTGGCACCTGGCTACCCCTTTTGAAGGCAAGGCCAACTCTCAAGAGAACGCCCTGACTCTCGCCTGCCTGCTGCATCCCACG CCTGCTCTGTCTGGCTTCCCTCACCAGGCCGCCACTCAGGTGATCGCCGAGCTGGAACCCTTCGACCGAGAGCTGTTCGGCG GCATCGTCGGCTGGTGCGACTCTGAAGGCAACGGCGAGTGGGTCGTGACCATCCGATGCGCCAAGCTCCGAGAGAACCAGG TGCGACTGTTCGCTGGCGCCGGAATCGTGCCCGCCTCGTCGCCCCTCGGAGAGTGGCGAGAGACTGGCGTGAAGCTGTCTA CCATGCTGAACGTGTTCGGCCTGCACTAA
PpPchB	ATGAACTTCCCTCTGGTGGACCCCGACATGAAGACCCCTGAGCAGTGCTCTGGCCTGGACGACGTCCGATGCGGCATCGACG CCATGGACCAGCAGATCATTCAGGCCCTGGGCCGACGACTGGCCTACGTGAAGGCCGCTGCTCAGTTCAAGCCCACCGAGG ACTCTATCGCTGCTCCCGAGCGAGTGGCCGCCATGCTGCCCCAGCGACGACAGTGGGCCGAGCAGGCCTCTCTGGACCCCAT GTTCGTGGTGCCCCTGTTCGCCCAGATCATCCACTGGAACATTGCCCAGCAGGTCCGACACTGGCGACGGCAGCACGGCCTG GACCAGGGCGCCCAGGACGAGTAA
PaAroZ	ATGCCCTCTAAGCTGGCCATCACCTCTATGTCTCTGGGCCGATGCTACGCCGGCCACTCTTTCACCACCAAGCTGGACATGGC CCGAAAGTACGGCTACCAGGGCCTCGAGCTGTTCCACGAGGACCTGGCCGACGTGGCCTACCGACTGTCTGGCGAGACTCC CTCTCCTTGCGGCCCCTCGCCTGCCGCTCAGCTGTCTGCCGCTCGACAGATCCTGCGAATGTGCCAGGTGCGAAACATCGAG ATCGTGTGCCTGCAGCCTTTCTCGCAGTACGACGGCCTGCTGGACCGAGAGGAACACGAGCGACGACTCGAGCAGCTGGAA TTCTGGATCGAGCTGGCCCACGAGCTGGACACCGACATCATTCAGATCCCCGCCAACTTCCTGCCTGCCGAGGAAGTGACCG AGGACATCTCTCTGATCGTGTCTGACCTGCAAGAGGTGGCCGACATGGGACTGCAGGCTAACCCTCCTATCCGATTCGTGTA CGAGGCTCTGTGCTGGTCTACCCGAGTGGACACCTGGGAGCGATCTTGGGAAGTCGTGCAGCGAGTGAACCGACCTAACTT CGGCGTGTGTCTGGACACCTTCAACATTGCCGGCCGAGTGTACGCTGACCCCACCGTGGCCTCTGGACGAACCCCTAACGCC GAAGAGGCCATCCGAAAGTCTATCGCCCGACTGGTCGAGCGAGTGGACGTGTCTAAGGTGTTCTACGTGCAGGTCGTGGAC GCCGAGAAGCTGAAGAAGCCTCTGGTCCCCGGCCACCGATTCTACGACCCCGAGCAGCCCGCTCGAATGTCTTGGTCCCGAA ACTGCCGACTGTTCTACGGCGAGAAGGACCGAGGCGCCTACCTGCCTGTGAAGGAAATCGCCTGGGCCTTCTTCAACGGCCT GGGCTTCGAAGGCTGGGTGTCTCTGGAACTGTTCAACCGACGAATGTCTGACACCGGCTTCGGAGTGCCCGAGGAACTCGC CCGACGAGGCGCCGTGTCTTGGGCCAAGCTGGTGCGAGACATGAAGATCACCGTGGACTCTCCCACTCAGCAGCAGGCTAC CCAGCAGCCTATCCGAATGCTGTCTCTGTCTGCTGCCCTGTAA
KpAroY.B	ATGAAGCTGATCATCGGTATGACTGGTGCTACAGGTGCTCCATTGGGTGTTGCTTTGTTGCAAGCTTTGCGAGACATGCCCG AGGTCGAGACTCACCTGGTGATGTCTAAGTGGGCCAAGACCACCATCGAGCTGGAAACCCCTTGGACCGCTCGAGAGGTGG CCGCTCTGGCCGACTTCTCTCACTCTCCCGCCGACCAGGCCGCTACCATCTCTTCTGGATCTTTCCGAACCGACGGAATGATC GTGATCCCCTGCTCTATGAAGACCCTGGCTGGTATTAGAGCTGGTTATGCTGAAGGTTTGGTTGGTAGAGCTGCTGATGTTG TGCTGAAGGAAGGCCGAAAGCTGGTTCTGGTGCCCCGAGAGATGCCCCTGTCTACCATCCACCTCGAGAACATGCTGGCCCT GTCTCGAATGGGAGTCGCTATGGTGCCTCCTATGCCTGCCTACTACAACCATCCTGAGACTGTGGACGACATTACCAACCAC ATCGTGACCCGAGTGCTGGACCAGTTCGGCCTGGACTACCACAAGGCCCGACGATGGAACGGCCTGCGAACCGCCGAGCAG TTCGCCCAAGAGATCGAGTAA
KpAroY.C^{iso}	ATGACCGCTCCTATCCAGGACCTGCGAGATGCTATCGCCCTGCTCCAGCAGCACGACAACCAGTACCTCGAGACTGACCATC CTGTGGACCCCAACGCCGAGCTGGCCGGCGTGTACCGACACATCGGAGCCGGCGGAACCGTGAAGCGACCCACTCGAATCG GACCCGCCATGATGTTCAACAACATCAAGGGCTACCCTCACTCTCGAATCCTGGTGGGCATGCACGCCTCTCGACAGCGAGC CGCTCTGCTGCTGGGCTGCGAGGCTTCTCAGCTGGCCCTCGAGGTCGGCAAGGCCGTGAAGAAGCCCGTCGCTCCCGTCGT GGTGCCCGCCTCTTCTGCTCCCTGCCAAGAGCAGATCTTCCTGGCTGACGACCCCGACTTCGACCTGCGAACCCTGCTGCCT GCTCACACCAACACTCCTATCGACGCTGGCCCCTTCTTCTGCCTGGGACTCGCCCTGGCTTCTGACCCCGTGGACGCCTCTCT GACCGACGTGACCATCCACCGACTGTGCGTGCAGGGCCGAGATGAGCTGTCTATGTTCCTGGCCGCTGGCCGACACATTGA GGTGTTCCGACAGAAGGCCGAGGCTGCCGGCAAGCCCCTGCCTATCACCATCAACATGGGACTCGACCCCGCCATCTACATC GGCGCCTGCTTCGAGGCTCCCACCACTCCTTTCGGCTACAACGAGCTGGGCGTCGCTGGCGCCCTGCGACAGCGACCCGTCG AGCTGGTCCAGGGCGTGTCTGTGCCCGAGAAGGCCATTGCTCGAGCCGAGATCGTGATTGAGGGCGAGCTGCTGCCCGGCG TGCGAGTGCGAGAGGACCAGCACACCAACTCTGGCCACGCCATGCCTGAGTTCCCCGGCTACTGTGGCGGCGCTAACCCCTC TCTGCCCGTGATCAAGGTGAAGGCCGTCACCATGCGAAACAACGCCATCCTGCAGACCCTGGTCGGACCCGGCGAGGAACA CACTACCCTGGCCGGACTGCCCACCGAGGCCTCTATCTGGAACGCCGTCGAGGCCGCTATTCCCGGCTTCCTGCAGAACGTG TACGCCCACACCGCTGGCGGCGGAAAGTTCCTGGGAATCCTGCAGGTCAAGAAGCGACAGCCCGCCGACGAGGGCCGACAG GGCCAAGCTGCCCTGCTGGCCCTGGCCACCTACTCTGAGCTGAAGAACATCATTCTGGTGGACGAGGACGTGGACATCTTCG ACTCTGACGACATTCTGTGGGCCATGACTACCCGAATGCAGGGCGACGTGTCTATTACCACCATTCCTGGCATCCGAGGCCA CCAGCTGGACCCCTCTCAGACCCCTGAGTACTCGCCCTCTATCCGAGGCAACGGCATCTCTTGTAAGACCATTTTCGACTGCA CCGTGCCTTGGGCTCTGAAGTCTCACTTCGAGCGAGCCCCTTTCGCCGACGTGGACCCTCGACCTTTCGCTCCCGAGTACTTC GCCCGACTCGAGAAGAACCAGGGCTCTGCCAAGTAA
KpAroY.D	ATGATCTGTCCCCGATGCGCCGACGAGAAGATCGAGGTGATGGCCACCTCTCCTGTGAAGGGCGTGTGGACCGTGTACCAG TGCCAGCACTGCCTGTACACCTGGCGAGACACCGAGCCTCTGCGACGAACCTCGCGAGAGCACTACCCCGAGGCCTTCCGAA TGACCCAGAAGGACATCGACGAGGCTCCCCAGGTGCCTCACGTGCCTCCACTGCTGCCCGAGGACAAGCGATAA
CaCatA	ATGTCTCAGGCCTTCACCGAGTCTGTCAAGACCTCTCTGGGCCCCAACGCTACCCCTCGAGCCAAGAAGCTGATCGCCTCTCT GGTGCAGCACGTGCACGACTTCGCCCGAGAGAACCACCTGACCACCGAGGACTGGCTGTGGGGCGTCGACTTCATCAACCG AATCGGCCAGATGTCTGACTCTCGACGAAACGAGGGCATCCTGGTGTGCGACATCATCGGCCTCGAGACTCTGGTGGACGC CCTGACCAACGAGTCTGAGCAGTCTAACCACACCTCTTCCGCCATTCTGGGACCCTTCTACCTGCCTGACTCTCCTGTGTACC CCAACGGCGGCTCTATCGTGCAGAAGGCTATCCCCACCGACGTGAAGTGCTTCGTGCGAGGCAAGGTGACCGACACCGAGG GCAAGCCCCTCGGCGGAGCCCAGCTCGAGGTGTGGCAGTGCAACTCTGCCGGCTTCTACTCTCAGCAGGCCGACCACGACG GCCCCGAGTTCAACCTGCGAGGCACCTTCATCACCGACGACGAGGGAAACTACTCTTTCGAGTGTCTGCGACCTACTTCTTA CCCCATTCCTTACGACGGACCCGCTGGCGACCTGCTGAAGATCATGGATCGACACCCCAACCGACCTTCTCACATCCACTGGC GAGTGTCTCACCCCGGCTACCACACTCTGATCACCCAGATCTACGACGCCGAGTGTCCCTACACCAACAACGACTCTGTGTAC GCCGTGAAGGACGACATCATTGTGCACTTCGAGAAGGTGGACAACAAGGACAAGGACCTGGTCGGCAAGGTCGAGTACAAG CTGGACTACGACATCTCTCTGGCCACCGAGTCCTCTATCCAAGAGGCCCGAGCCGCCGCTAAGGCCCGACAGGACGCCGAGA TCAAGCTGTAA

Supplementary information 3

Specific yields for production assays (mg/L/OD_{600}), degradation assays for *cis*,*cis*-muconic acid and salicylic acid, medium optimization experiments, effect on resveratrol titers of feedback-resistant *ARO4* and *ARO7*, and additional information on selection of point mutations in Aro7p.

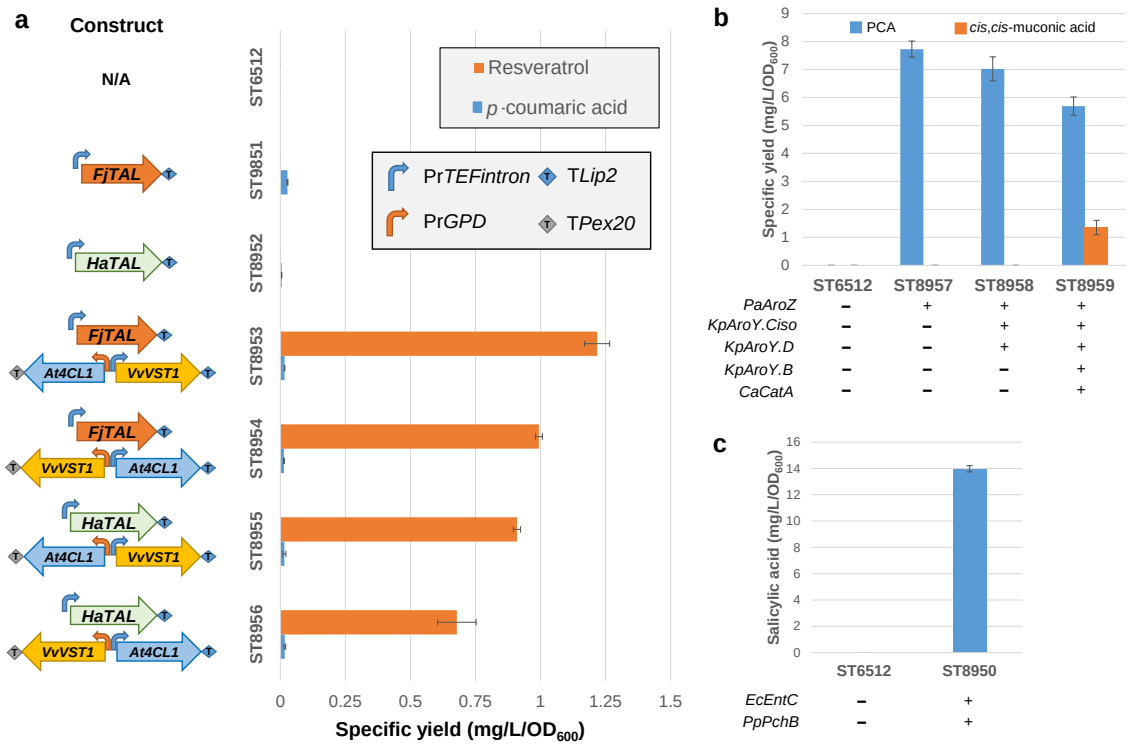

Supplementary Figure S1. Specific yields of *p*-coumaric acid, resveratrol, *cis*,*cis*-muconic acid and salicylic in engineered *Y. lipolytica* strains. Cultivations were carried out for 72 h in 24 deep-well plates containing mineral medium with 20 g/L glucose. Extracellular content was subjected to HPLC analysis. Error bars represent standard deviation from at least three biological replicates. "-" and "+" symbols indicate absence or presence of the corresponding genetic modification, respectively. A) Production of *p*-coumaric acid and resveratrol with supplementation of 2 mM L-tyrosine. B) Production of *cis*,*cis*-muconic acid and the pathway intermediate protocatechuic acid (PCA). C) Production of salicylic acid.

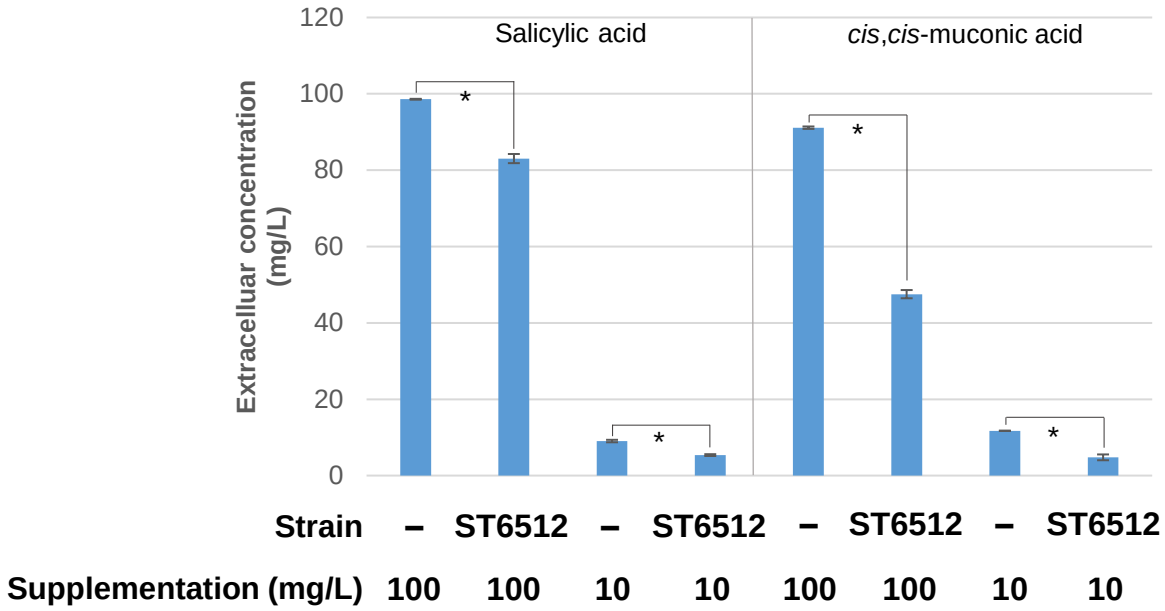

Supplementary Figure S2. Degradation assays for *cis*,*cis*-muconic acid and salicylic acid in strain ST6512, at different supplementation concentrations. "-" represents a medium control, non-inoculated. Error bars represent standard deviation from at least three biological replicates. Statistical analysis was performed using Student's t-test (two-tailed; *P ≤ 0.05 two-sample unequal variance).

```
Saccharomyces      1 MDFTKPETVLNLQNIRDELVRMEDSIIFKFIERSHFATC-PS--VYEA-N     46
                     |||||.:|||:|.||||.||||||:|:|..|||:.|  |  |  ||:| |
Yarrowia           1 MDFTKADTVLDLANIRDSLVRMEDTIVFNLIERAQF--CR-SEFVYKAGN     47

Saccharomyces     47 HPGLEIPNFKGSFLDW-AL--SNLE-IAHSRIRRFESPDE-TPFFPDKI-     90
                       . :||.||||:|||  |  |  | : |:::||:.:||| . ||||.:
Yarrowia          48 --S-DIPGFKGSYLDWF-LQES--EKV-HAKLRRYAAPDEQA-FFPDDLP     89

Saccharomyces     91 QKSFLPSINY-PQILAPYAPEVNYNDKIKKVYIEKIIPLI-SKRD-GDDK    137
                     : :.||.|:| | |||||:.||:.||:|||:|.:.|:||: :  . || :
Yarrowia          90 E-AILPPIDYAP-ILAPYSKEVSVNDEIKKIYTDDIVPLVCA--GTGD-Q    134

Saccharomyces    138 -NNFGSVAT-RDIECLQSLSRRIHFGKFVAEAKF-QSDIP-LYTKLIKSK    183
                      .|:||||..  |||.||:|||||||||||||:||  |:..  :|:|||:|
Yarrowia         135 PENYGSVMVC-DIETLQALSRRIHFGKFVAESKFL-SETER-FTELIKNK    181

Saccharomyces    184 DVEGIMK--NITNSAVEEKILERL-TKKAEV-YGVDPT-N-ESGER---R    224
                     |:.|| :   ||||.|||.||.||  :|| : ||.||| .  | :|   :
Yarrowia         182 DIAGI-EAA-ITNSKVEETILARLG-EKA-LAYGTDPTLRW-S-QRTQGK    225

Saccharomyces    225 I-TPEYLVK-IYKE-IVIPITKEVEVEYLLRRLEE    256
                     : : | :|| ||||  |||:||:|||:|||||||
Yarrowia          226 VDS-E-VVKRIYKEW-VIPLTKKVEVDYLLRRLE-    256
```

Supplementary Figure S3. Pairwise alignment between *S. cerevisiae* and *Y. lipolytica* Aro7p. Protein sequences were obtained from strains *S. cerevisiae* S288C (YPR060C) and *Y. lipolytica* CLIB89/W29 (YALI1_E20751p). In red, amino acid 141 that in *S. cerevisiae* confers feedback insensitivity when mutated from G to S (Luttik et al., 2008). Amino acid 139 in *Y. lipolytica* was subjected to the same replacement.

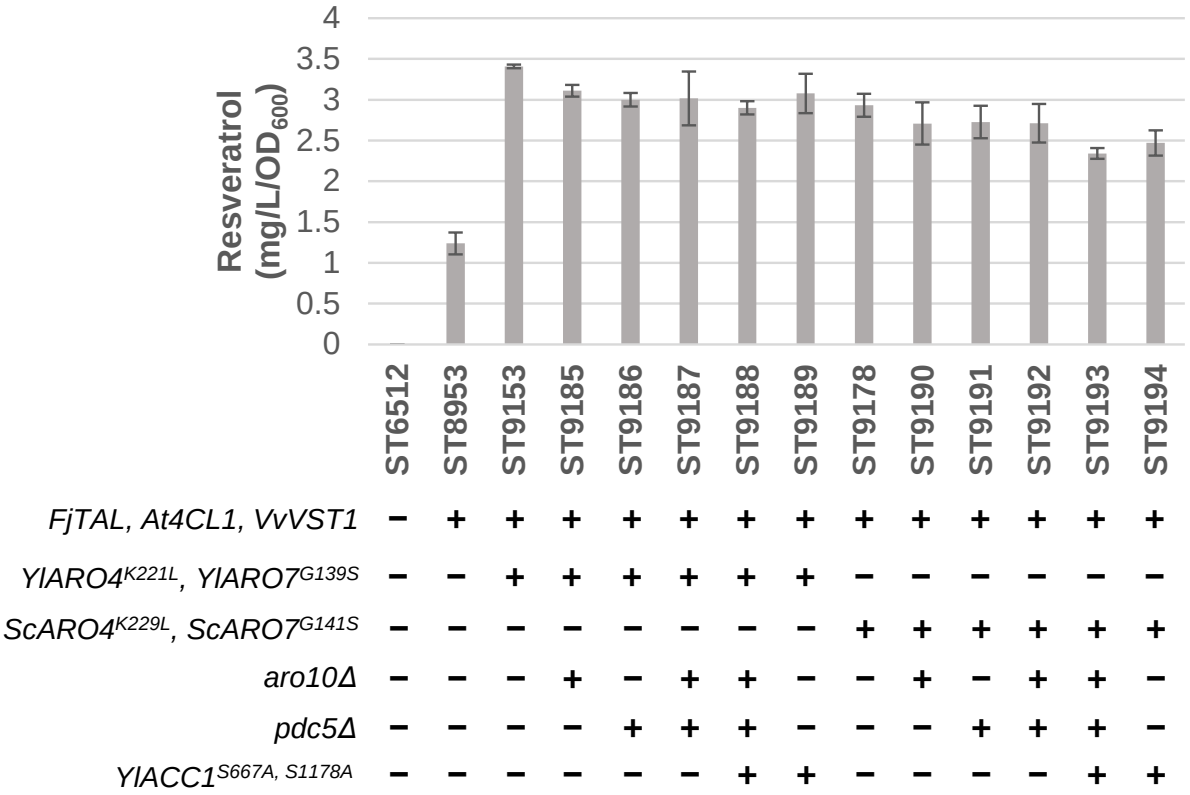

Supplementary Figure S4. Specific resveratrol yield in engineered *Y. lipolytica* strains. Cultivations were carried out for 72 h in 24 deep-well plates containing mineral medium with 20 g/L glucose. Extracellular content was subjected to HPLC analysis. "-" and "+" symbols indicate absence or presence of the corresponding genetic modification, respectively. Error bars represent standard deviation from at least three biological replicates. *p*-Coumaric acid was not detected in any of the strains.

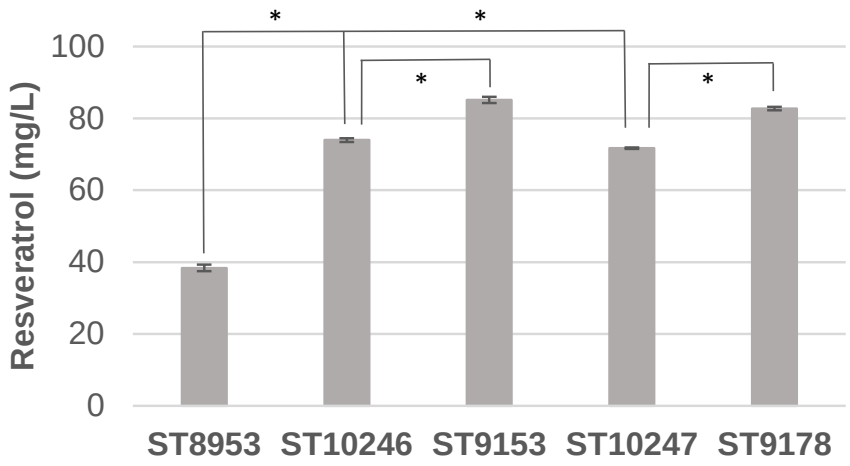

	ST8953	ST10246	ST9153	ST10247	ST9178
FjTAL, At4CL1, VvVST1	+	+	+	+	+
YlARO4^{K221L}	–	+	+	–	–
YlARO7^{G139S}	–	–	+	–	–
ScARO4^{K229L}	–	–	–	+	+
ScARO7^{G141S}	–	–	–	–	+

Supplementary Figure S5. Resveratrol titer in engineered *Y. lipolytica* strains expressing feedback insensitive alleles of *ARO4* and *ARO7*. Cultivations were carried out for 72 h in 24 deep-well plates containing mineral medium with 20 g/L glucose. Extracellular content was subjected to HPLC analysis. "-" and "+" symbols indicate absence or presence of the corresponding genetic modification, respectively. Error bars represent standard deviation from at least three biological replicates. *p*-Coumaric acid was not detected in any of the strains. Statistical analysis was performed using Student's t-test (two-tailed; *$P \leq 0.001$ two-sample unequal variance).

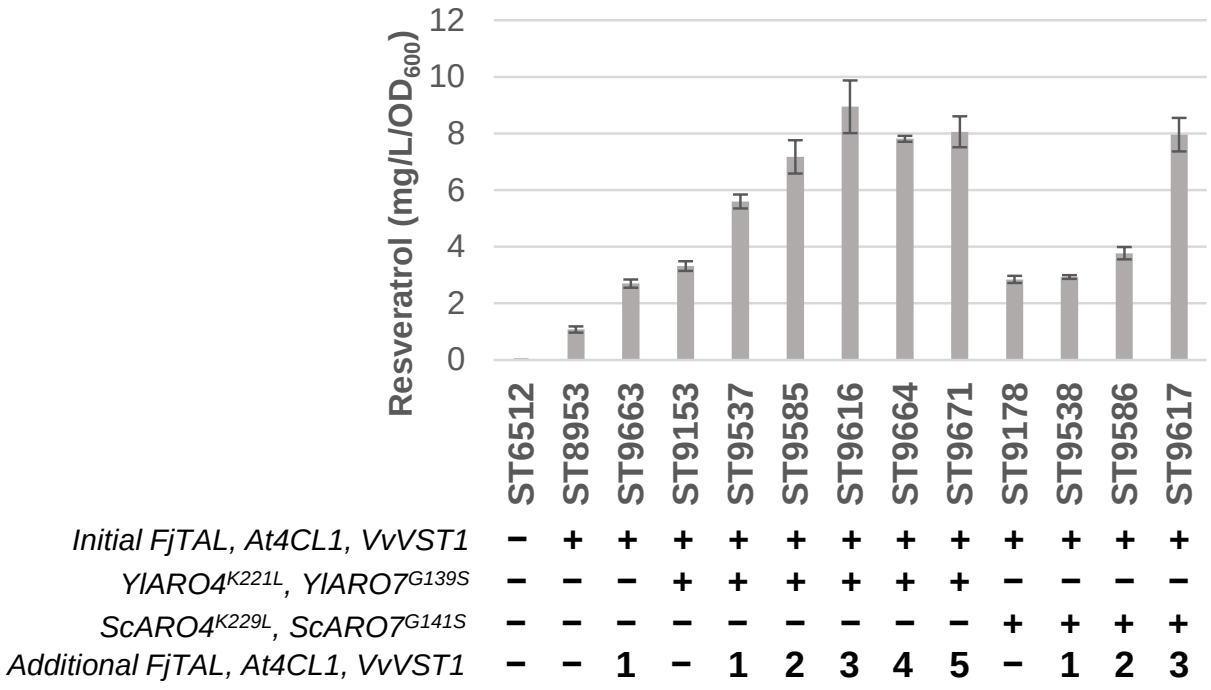

Supplementary Figure S6. Effect on specific resveratrol yield upon integration of multiple copies of resveratrol biosynthetic genes. Cultivations were carried out for 72 h in 24 deep-well plates containing mineral medium with 20 g/L glucose. Extracellular content was subjected to HPLC analysis. "-" and "+" symbols indicate absence or presence of the corresponding genetic modification, respectively. Digits show the number of additional copies of resveratrol biosynthetic genes integrated. Error bars represent standard deviation from at least three biological replicates. *p*-Coumaric acid was not detected in any of the strains.

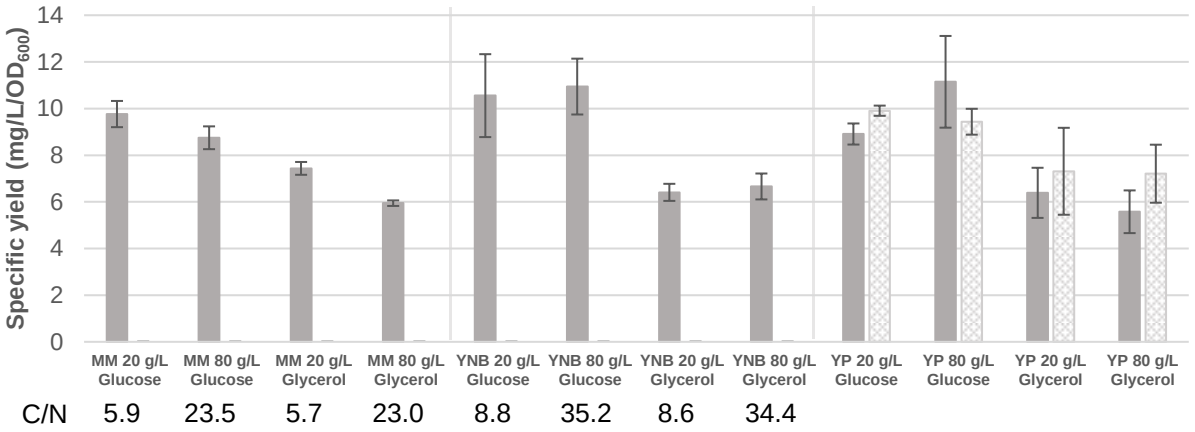

Supplementary Figure S7. Specific resveratrol yield of ST9671 in different media. Cultivations of strain ST9671 were carried out for 96 h in 24 deep-well plates using the media indicated for each condition. Extracellular content was subjected to HPLC analysis. Error bars represent standard deviation from at least three biological replicates. MM: mineral medium, YNB: Yeast Nitrogen Base without amino acids. YP: Yeast extract Peptone. C/N stands for the molar carbon/nitrogen ratio in defined media.

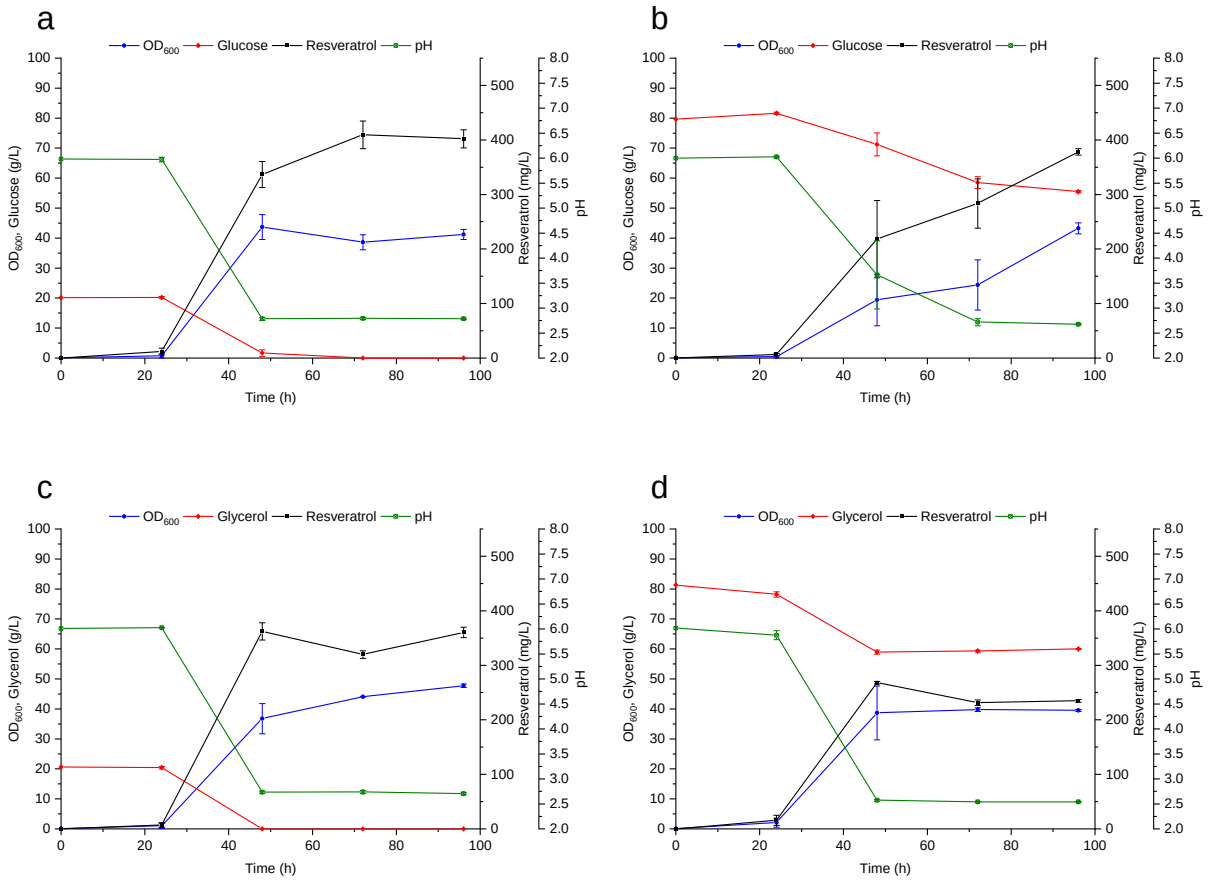

Supplementary Figure S8. Cultivation profile of ST9671 in mineral medium (MM). a) 20 g/L Glucose, b) 80 g/L glucose, c) 20 g/L glycerol, d) 80 g/L glycerol. Cultivations of strain ST9671 were carried out for 96 h in 24 deep-well plates and samples were taken every 24 h. Extracellular content was subjected to HPLC analysis. Error bars represent standard deviation from at least three biological replicates. No *p*-coumaric acid was detected.

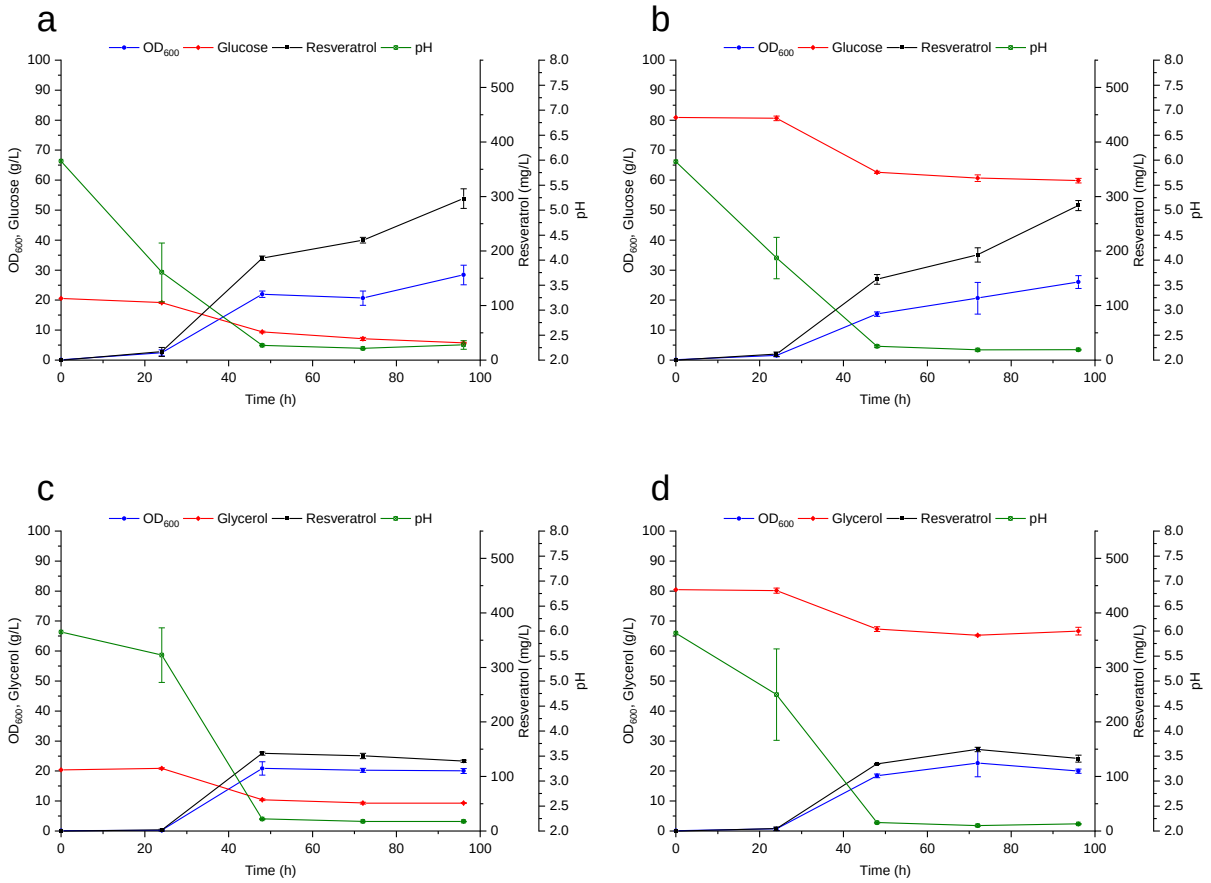

Supplementary Figure S9. Cultivation profile of ST9671 in Yeast Nitrogen Base without amino acids (YNB) medium. a) 20 g/L Glucose, b) 80 g/L glucose, c) 20 g/L glycerol, d) 80 g/L glycerol. Cultivations of strain ST9671 were carried out for 96 h in 24 deep-well plates and samples were taken every 24 h. Extracellular content was subjected to HPLC analysis. Error bars represent standard deviation from at least three biological replicates. No *p*-coumaric acid was detected.

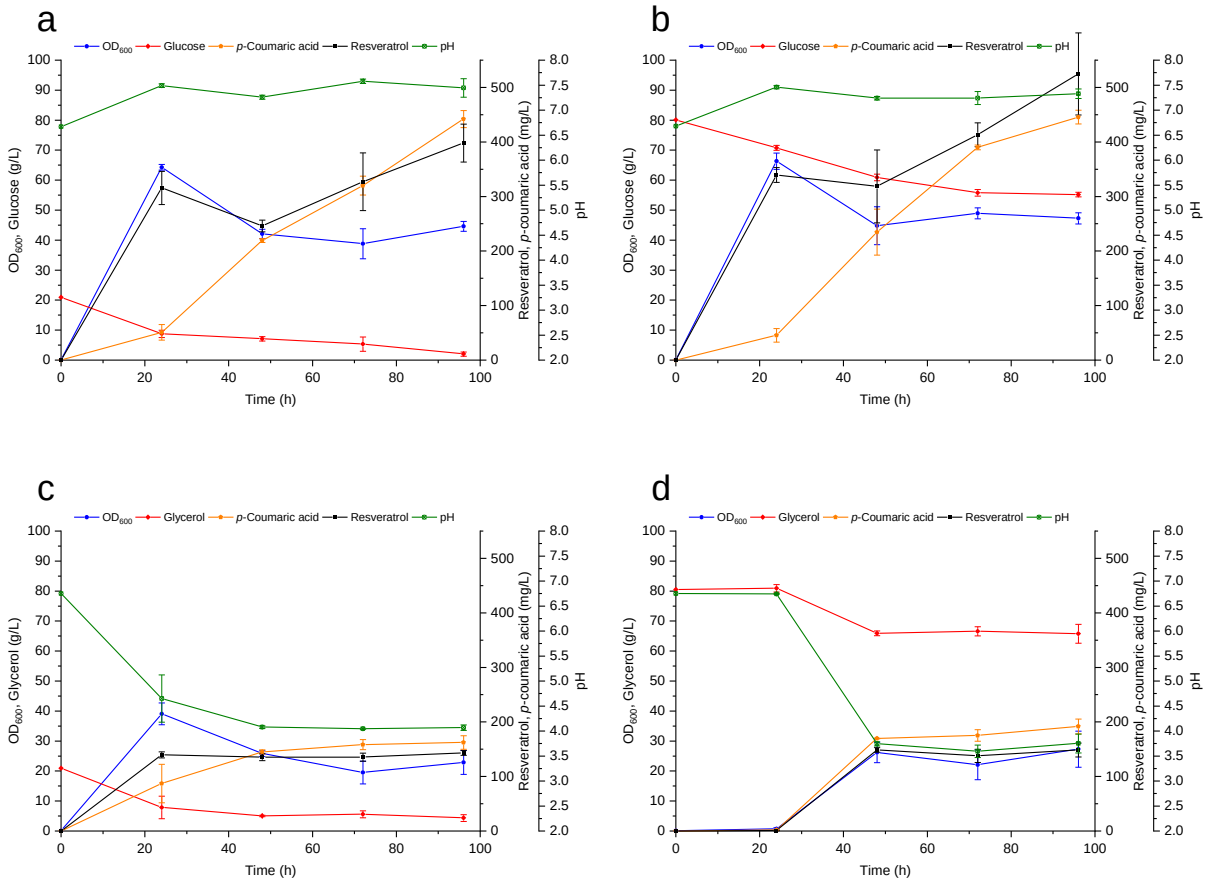

Supplementary Figure S10. Cultivation profile of ST9671 in Yeast Peptone (YP) medium. a) 20 g/L Glucose, b) 80 g/L glucose, c) 20 g/L glycerol, d) 80 g/L glycerol. Cultivations of strain ST9671 were carried out for 96 h in 24 deep-well plates and samples were taken every 24 h. Extracellular content was subjected to HPLC analysis. Error bars represent standard deviation from at least three biological replicates.

Supplementary information 4

Information related to the fed-batch experiment carried out in bioreactors and analysis of intracellular and extracellular resveratrol content of strain ST9671 in small-scale cultivation.

Selection of initial feed rate and exponential increase was selected as follows:

Exponential-feeding rate at time *t* follows the equation:

$$F(t) = F_o \cdot \exp(kt)$$

with k being the exponential constant (h^{-1}) and F_o the initial feeding rate (g-feed/h).

To create a carbon-limited condition, k should be well below the maximum growth rate (k

$<< \mu_{max}$), and glucose should be fed below the rate of its consumption at any time:

$F(t) \cdot C_{glc,feed} < r_{glc}(t)$, which also applies at the time of feeding start:

$F_o \cdot C_{glc,feed} < r_{glc,o} \Leftrightarrow F_o < r_{glc,o} / C_{glc,feed}$

Initial glucose consumption rate ($r_{glc,o}$) can be determined by multiplying cell growth rate when feeding starts (μ_o), the biomass yield on glucose ($1/Y_{SX}$), and the amount of cells at the start of the feeding ($X_o \cdot V_o$):

$r_{glc,o} = \mu_o \cdot (1/Y_{SX}) \cdot X_o \cdot V_o$

The following assumptions were made based on measurements and available data for *Y. lipolytica*:

- μ_o = 0.22 h^{-1} (growth rate at late exponential phase, measured)
- Y_{SX} = 0.43 g-cell/g-glucose (Kerkhoven et al., 2016)
- X_o = 10 g-cell/L (Marella et al., 2019)
- V_o = 0.4 L (the volume of batch culture)

These values give r_{glc} = 2.04 g-glucose/h. With glucose concentration in the feed, $C_{glc,feed}$ = 0.38 g-glucose/g-feed (calculated):

$F_O < r_{glc,o} / C_{glc,feed}$ = 5.42 g-feed/h

- An F_o of 1.0 g-feed/h was then selected to satisfy the above criteria.
- A k value of 0.05 h^{-1} was chosen to satisfy $k << \mu_{max}$ criteria.

Eventually, the fed-batch feeding rate followed the following equation:

$F(t)$ = 1.0 exp (0.05t)

F(t) was fixed when aeration & stirring rate reached maximum capacity.

For metrics calculations, the following parameters were considered:

Initial reactor volume: 400 mL

Feed medium added: 467.7 g = 383.3 mL

Volume extracted per sample: 3 mL

Base added: 68.7 ± 2.1 mL

Antifoam added: 27.6 mL

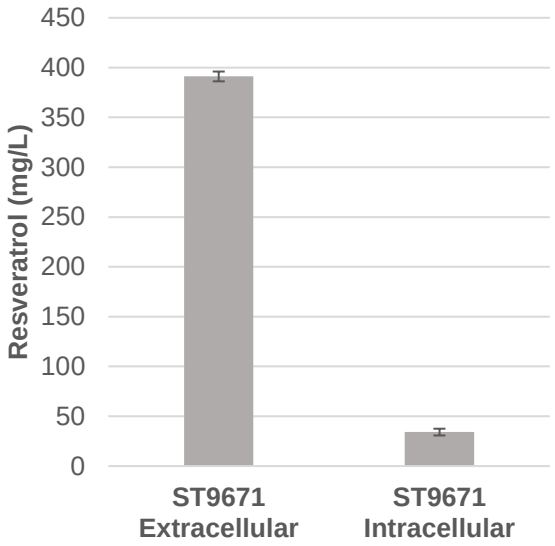

Supplementary Figure S11. Analysis of extracellular and intracellular resveratrol concentrations in the top-producing strain ST9671. Cultivations were carried out for 72 h in 24 deep-well plates containing mineral medium with 20 g/L glucose. Error bars represent standard deviation from at least three biological replicates. *p*-Coumaric acid was not detected in any of the strains.

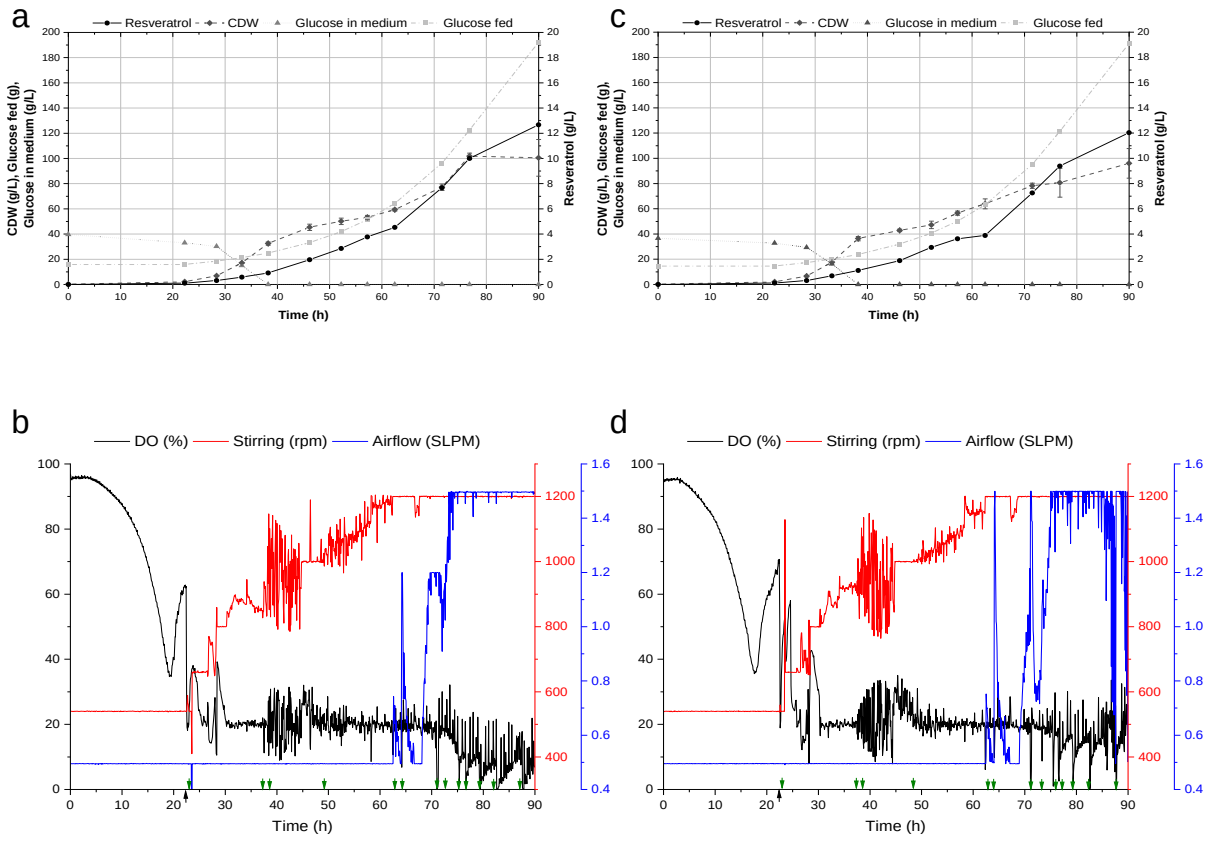

Supplementary Figure S12. Fed-batch fermentation in bioreactor of the highest producing strain ST9671. Individual graphs for each of the reactors. a) Fermentation profile for reactor 1, b) Operational parameters for reactor 1, c) Fermentation profile for reactor 2, d) Operational parameters for reactor 2. Error bars for CDW (cell dry weight) represent standard deviation from two measurements of the same bioreactor. *p*-Coumaric acid was not detected. Black arrow represents the start of the feeding (22.35 h). Green arrows indicate antifoam 204 addition. Severe foaming was a constant issue throughout the cultivation. Manual addition of defoamer was carried out at the following times, as indicated by the green arrows: 22.42 h (0.1 mL), 37.02 h (2 mL), 38.40 h (3 mL), 48.11 h (0.5 mL), 62.73 h (1 mL), 64.10 h (3 mL), 71.21 h (4 mL), 72.70 h (1 mL), 75.62 h (2 mL), 76.50 h (5 mL), 79.37 h (2 mL), 82.11 (2 mL), 87.80 h (2 mL).

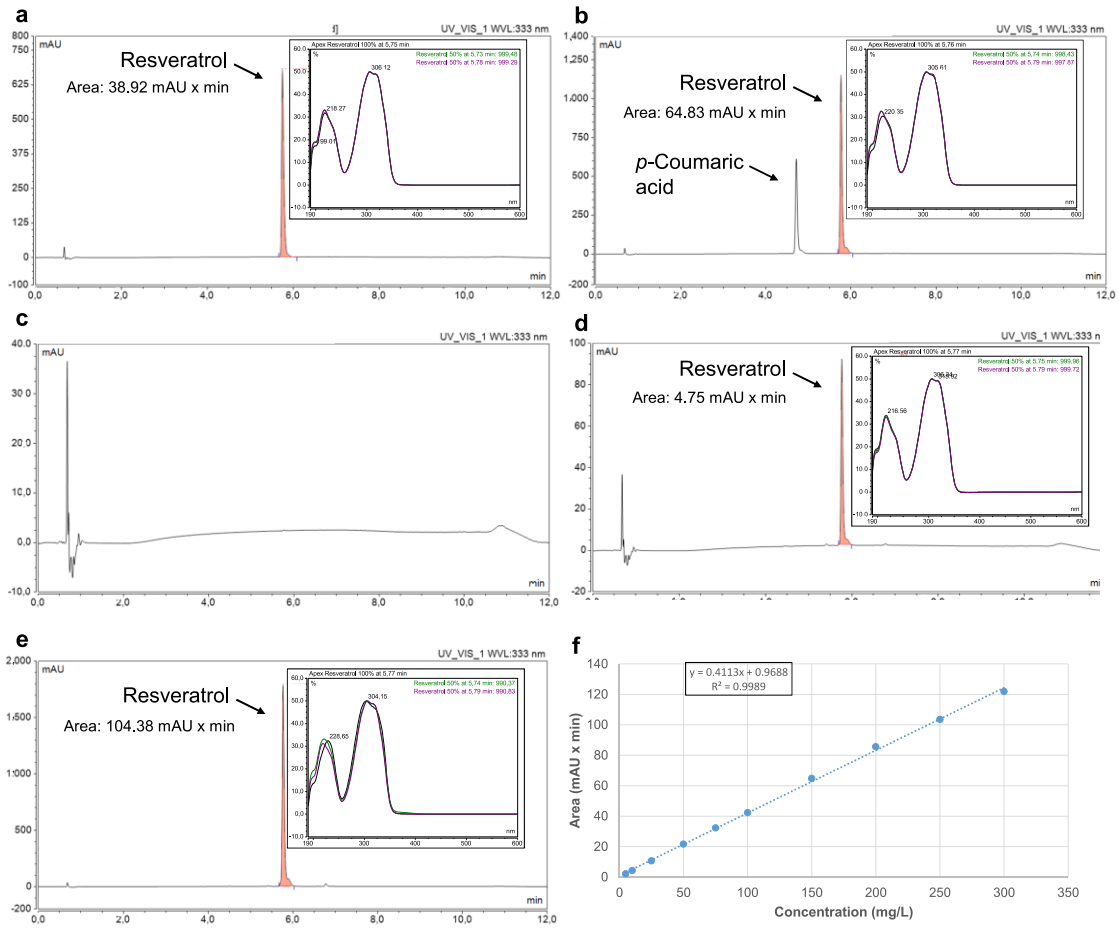

Supplementary Figure S13. HPLC analysis of fermentation samples for resveratrol quantification. Chromatograms (absorbance at 333 nm) and resveratrol UV-Vis spectra of a) Resveratrol standard (90 mg/L), b) Resveratrol and *p*-coumaric acid standard (150 mg/L each), c) Reactor 1 sample (0 h, 1/50 dilution), d) Reactor 1 sample (33.20 h, 1/50 dilution), e) Reactor 1 sample (89.96 h, 1/50 dilution). f) External calibration curve used for resveratrol quantification in reactor samples. The UV-Vis spectra show the characteristic maximum absorbance at 306 nm of *trans*-resveratrol (Nour et al., 2012).

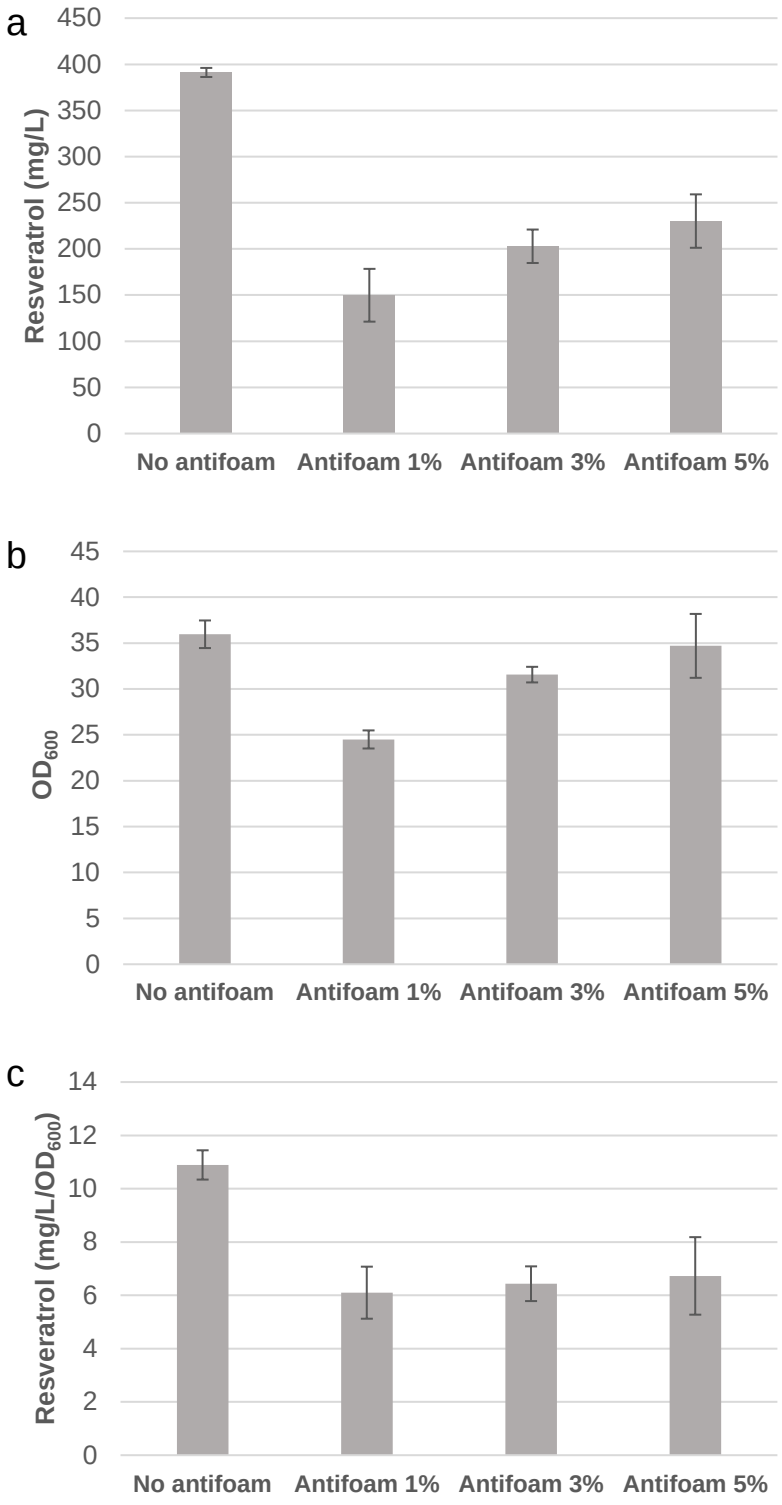

Supplementary Figure S14. Antifoam effect on resveratrol titers in the top-producing strain ST9671. Cultivations were carried out for 72 h in 24 deep-well plates containing mineral medium with 20 g/L glucose and the indicated v/v % of antifoam. Extracellular content was subjected to HPLC analysis. Error bars represent standard deviation from at least three biological replicates. a) Resveratrol titer. b) Optical density at 600 nm (OD_{600}). c) Specific resveratrol yield.

References

Afonso, M.S., Ferreira, S., Domingues, F.C., Silva, F., 2015. Resveratrol production in bioreactor: Assessment of cell physiological states and plasmid segregational stability. Biotechnology Reports 5, 7–13. https://doi.org/10.1016/j.btre.2014.10.008

Becker, J.V.W., Armstrong, G.O., van der Merwe, M.J., Lambrechts, M.G., Vivier, M.A., Pretorius, I.S., 2003. Metabolic engineering of Saccharomyces cerevisiae for the synthesis of the wine-related antioxidant resveratrol. FEMS Yeast Res 4, 79–85. https://doi.org/10.1016/S1567-1356(03)00157-0

Beekwilder, J., Wolswinkel, R., Jonker, H., Hall, R., Vos, C.H.R. de, Bovy, A., 2006. Production of Resveratrol in Recombinant Microorganisms. Appl. Environ. Microbiol. 72, 5670–5672. https://doi.org/10.1128/AEM.00609-06

Bhan, N., Xu, P., Khalidi, O., Koffas, M.A.G., 2013. Redirecting carbon flux into malonyl-CoA to improve resveratrol titers: Proof of concept for genetic interventions predicted by OptForce computational framework. Chemical Engineering Science, Synthetic Biology 103, 109–114. https://doi.org/10.1016/j.ces.2012.10.009

Braga, A., Oliveira, J., Silva, R., Ferreira, P., Rocha, I., Kallscheuer, N., Marienhagen, J., Faria, N., 2018. Impact of the cultivation strategy on resveratrol production from glucose in engineered Corynebacterium glutamicum. Journal of Biotechnology 265, 70–75. https://doi.org/10.1016/j.jbiotec.2017.11.006

Camacho-Zaragoza, J.M., Hernández-Chávez, G., Moreno-Avitia, F., Ramírez-Iñiguez, R., Martínez, A., Bolívar, F., Gosset, G., 2016. Engineering of a microbial coculture of Escherichia coli strains for the biosynthesis of resveratrol. Microbial Cell Factories 15, 163. https://doi.org/10.1186/s12934-016-0562-z

Choi, O., Wu, C.-Z., Kang, S.Y., Ahn, J.S., Uhm, T.-B., Hong, Y.-S., 2011. Biosynthesis of plant-specific phenylpropanoids by construction of an artificial biosynthetic pathway in Escherichia coli. J Ind Microbiol Biotechnol 38, 1657–1665. https://doi.org/10.1007/s10295-011-0954-3

Gaspar, P., Dudnik, A., Neves, A.R., Förster, J., 2016. Engineering Lactococcus lactis for stilbene production. Presented at the 28th International Conference on Polyphenols.

Gu, Y., Ma, J., Zhu, Y., Ding, X., Xu, P., 2020. Engineering Yarrowia lipolytica as a Chassis for De Novo Synthesis of Five Aromatic-Derived Natural Products and Chemicals. ACS Synth. Biol. https://doi.org/10.1021/acssynbio.0c00185

Holkenbrink, C., Dam, M.I., Kildegaard, K.R., Beder, J., Dahlin, J., Belda, D.D., Borodina, I., 2018. EasyCloneYALI: CRISPR/Cas9-Based Synthetic Toolbox for Engineering of the Yeast Yarrowia lipolytica. Biotechnology Journal 13, 1700543. https://doi.org/10.1002/biot.201700543

Huang, L.L., Xue, Z., Zhu, Q.Q., 2006. Method for the production of resveratrol in a recombinant oleaginous microorganism. WO2006125000A2.

Kallscheuer, N., Vogt, M., Stenzel, A., Gätgens, J., Bott, M., Marienhagen, J., 2016. Construction of a Corynebacterium glutamicum platform strain for the production of stilbenes and (2S)-flavanones. Metabolic Engineering 38, 47–55. https://doi.org/10.1016/j.ymben.2016.06.003

Kang, S.-Y., Lee, J.K., Choi, O., Kim, C.Y., Jang, J.-H., Hwang, B.Y., Hong, Y.-S., 2014. Biosynthesis of methylated resveratrol analogs through the construction of an artificial biosynthetic pathway in E. coli. BMC Biotechnology 14, 67. https://doi.org/10.1186/1472-6750-14-67

Katsuyama, Y., Funa, N., Horinouchi, S., 2007a. Precursor-directed biosynthesis of stilbene methyl ethers in Escherichia coli. Biotechnol. J. 2, 1286–1293. https://doi.org/10.1002/biot.200700098

Katsuyama, Y., Funa, N., Miyahisa, I., Horinouchi, S., 2007b. Synthesis of Unnatural Flavonoids and Stilbenes by Exploiting the Plant Biosynthetic Pathway in Escherichia coli. Chemistry & Biology 14, 613–621. https://doi.org/10.1016/j.chembiol.2007.05.004

Kerkhoven, E.J., Pomraning, K.R., Baker, S.E., Nielsen, J., 2016. Regulation of amino-acid metabolism controls flux to lipid accumulation in Yarrowia lipolytica. npj Systems Biology and Applications 2, 16005. https://doi.org/10.1038/npjsba.2016.5

Li, M., Kildegaard, K.R., Chen, Y., Rodriguez, A., Borodina, I., Nielsen, J., 2015. De novo production of resveratrol from glucose or ethanol by engineered Saccharomyces cerevisiae. Metabolic Engineering 32, 1–11. https://doi.org/10.1016/j.ymben.2015.08.007

Li, M., Schneider, K., Kristensen, M., Borodina, I., Nielsen, J., 2016. Engineering yeast for high-level production of stilbenoid antioxidants. Scientific Reports 6, 36827. https://doi.org/10.1038/srep36827

Lim, C.G., Fowler, Z.L., Hueller, T., Schaffer, S., Koffas, M.A.G., 2011. High-Yield Resveratrol Production in Engineered Escherichia coli. Appl. Environ. Microbiol. 77, 3451–3460. https://doi.org/10.1128/AEM.02186-10

Liu, X., Lin, J., Hu, H., Zhou, B., Zhu, B., 2016. De novo biosynthesis of resveratrol by site-specific integration of heterologous genes in Escherichia coli. FEMS Microbiol Lett 363. https://doi.org/10.1093/femsle/fnw061

Luttik, M.A.H., Vuralhan, Z., Suir, E., Braus, G.H., Pronk, J.T., Daran, J.M., 2008. Alleviation of feedback inhibition in Saccharomyces cerevisiae aromatic amino acid biosynthesis: Quantification of metabolic impact. Metabolic Engineering 10, 141–153. https://doi.org/10.1016/j.ymben.2008.02.002

Marella, E.R., Dahlin, J., Dam, M.I., ter Horst, J., Christensen, H.B., Sudarsan, S., Wang, G., Holkenbrink, C., Borodina, I., 2019. A single-host fermentation process for the production of flavor lactones from non-hydroxylated fatty acids. Metabolic Engineering. https://doi.org/10.1016/j.ymben.2019.08.009

Nour, V., Trandafir, I., Muntean, C., 2012. Ultraviolet Irradiation of Trans-Resveratrol and HPLC Determination of Trans-Resveratrol and Cis-Resveratrol in Romanian Red Wines. J Chromatogr Sci 50, 920–927. https://doi.org/10.1093/chromsci/bms091

Palmer, C.M., Miller, K.K., Nguyen, A., Alper, H.S., 2020. Engineering 4-coumaroyl-CoA derived polyketide production in Yarrowia lipolytica through a β-oxidation mediated strategy. Metabolic Engineering 57, 174–181. https://doi.org/10.1016/j.ymben.2019.11.006

Park, S.R., Yoon, J.A., Paik, J.H., Park, J.W., Jung, W.S., Ban, Y.-H., Kim, E.J., Yoo, Y.J., Han, A.R., Yoon, Y.J., 2009. Engineering of plant-specific phenylpropanoids biosynthesis in Streptomyces venezuelae. Journal of Biotechnology 141, 181–188. https://doi.org/10.1016/j.jbiotec.2009.03.013

Rodriguez, A., Kildegaard, K.R., Li, M., Borodina, I., Nielsen, J., 2015. Establishment of a yeast platform strain for production of p-coumaric acid through metabolic engineering of aromatic amino acid biosynthesis. Metabolic Engineering 31, 181–188. https://doi.org/10.1016/j.ymben.2015.08.003

Shin, S.-Y., Han, N.S., Park, Y.-C., Kim, M.-D., Seo, J.-H., 2011. Production of resveratrol from p-coumaric acid in recombinant Saccharomyces cerevisiae expressing 4-coumarate:coenzyme A ligase and stilbene synthase genes. Enzyme and Microbial Technology 48, 48–53. https://doi.org/10.1016/j.enzmictec.2010.09.004

Shin, S.-Y., Jung, S.-M., Kim, M.-D., Han, N.S., Seo, J.-H., 2012. Production of resveratrol from tyrosine in metabolically engineered Saccharomyces cerevisiae. Enzyme and Microbial Technology 51, 211–216. https://doi.org/10.1016/j.enzmictec.2012.06.005

Sydor, T., Schaffer, S., Boles, E., 2010. Considerable Increase in Resveratrol Production by Recombinant Industrial Yeast Strains with Use of Rich Medium. Appl. Environ. Microbiol. 76, 3361–3363. https://doi.org/10.1128/AEM.02796-09

Trantas, E., Panopoulos, N., Ververidis, F., 2009. Metabolic engineering of the complete pathway leading to heterologous biosynthesis of various flavonoids and stilbenoids in Saccharomyces cerevisiae. Metabolic Engineering 11, 355–366. https://doi.org/10.1016/j.ymben.2009.07.004

Wang, S., Zhang, S., Xiao, A., Rasmussen, M., Skidmore, C., Zhan, J., 2015. Metabolic engineering of Escherichia coli for the biosynthesis of various phenylpropanoid

derivatives. Metabolic Engineering 29, 153–159. https://doi.org/10.1016/j.ymben.2015.03.011

Wang, Y., Halls, C., Zhang, J., Matsuno, M., Zhang, Y., Yu, O., 2011. Stepwise increase of resveratrol biosynthesis in yeast Saccharomyces cerevisiae by metabolic engineering. Metabolic Engineering 13, 455–463. https://doi.org/10.1016/j.ymben.2011.04.005

Watts, K.T., Lee, P.C., Schmidt-Dannert, C., 2006. Biosynthesis of plant-specific stilbene polyketides in metabolically engineered Escherichia coli. BMC Biotechnology 6, 22. https://doi.org/10.1186/1472-6750-6-22

Wu, J., Liu, P., Fan, Y., Bao, H., Du, G., Zhou, J., Chen, J., 2013. Multivariate modular metabolic engineering of Escherichia coli to produce resveratrol from l-tyrosine. Journal of Biotechnology 167, 404–411. https://doi.org/10.1016/j.jbiotec.2013.07.030

Wu, J., Zhou, P., Zhang, X., Dong, M., 2017. Efficient de novo synthesis of resveratrol by metabolically engineered Escherichia coli. J Ind Microbiol Biotechnol 44, 1083–1095. https://doi.org/10.1007/s10295-017-1937-9

Yang, Y., Lin, Y., Li, L., Linhardt, R.J., Yan, Y., 2015. Regulating malonyl-CoA metabolism via synthetic antisense RNAs for enhanced biosynthesis of natural products. Metabolic Engineering 29, 217–226. https://doi.org/10.1016/j.ymben.2015.03.018

Zhang, E., Guo, X., Meng, Z., Wang, J., Sun, J., Yao, X., Xun, H., 2015. Construction, expression, and characterization of Arabidopsis thaliana 4CL and Arachis hypogaea RS fusion gene 4CL::RS in Escherichia coli. World J Microbiol Biotechnol 31, 1379–1385. https://doi.org/10.1007/s11274-015-1889-z

Zhang, Y., Li, S.-Z., Li, J., Pan, X., Cahoon, R.E., Jaworski, J.G., Wang, X., Jez, J.M., Chen, F., Yu, O., 2006. Using Unnatural Protein Fusions to Engineer Resveratrol Biosynthesis in Yeast and Mammalian Cells. J. Am. Chem. Soc. 128, 13030–13031. https://doi.org/10.1021/ja0622094

CHAPTER 3

Engineering *Saccharomyces cerevisiae* for the *de novo* production of halogenated tryptophan and tryptamine derivatives

This chapter contains a previously published article:

Milne, N., Sáez-Sáez, J., Nielsen, A.M., Dyekjær, J.D., Rago, D., Kristensen, M., Wulff, T., Borodina, I., 2023. Engineering *Saccharomyces cerevisiae* for the *de novo* production of halogenated tryptophan and tryptamine derivatives. *ChemistryOpen* 12, e202200266.
DOI: 10.1002/open.202200266

Abstract

The indole scaffold is a recurring structure in multiple bioactive heterocycles and natural products. Substituted indoles like the amino acid tryptophan serve as a precursor for a wide range of natural products with pharmaceutical or agrochemical applications. Inspired by the versatility of these compounds, medicinal chemists have for decades exploited indole as a core structure in the drug discovery process. With the aim of tuning the properties of lead drug candidates, regioselective halogenation of the indole scaffold is a common strategy. However, chemical halogenation is generally expensive, has a poor atom economy, lacks regioselectivity, and generates hazardous waste streams. As an alternative, in this work we engineer the industrial workhorse *Saccharomyces cerevisiae* for the *de novo* production of halogenated tryptophan and tryptamine derivatives. Functional expression of bacterial tryptophan halogenases together with a partner flavin reductase and a tryptophan decarboxylase resulted in the production of halogenated tryptophan and tryptamine with chlorine or bromine. Furthermore, by combining tryptophan halogenases, production of di-halogenated molecules was also achieved. Overall, this works paves the road for the production of new-to-nature halogenated natural products in yeast.

Introduction

Heterocycles are fundamental structural moieties present in more than half of the biologically active compounds found in nature (Pozharskii et al., 2011; Jampilek, 2019). Indole scaffolds in particular are a prominent example of a prevalent natural heterocycle with multi-disciplinary applications as pharmaceutical drugs or agrochemicals (Sravanthi and Manju, 2016). Indole is chemically constituted by a six-membered benzene ring fused to a five-membered pyrrole ring, and is produced by plants, fungi, and bacteria, which makes it ubiquitously present in nature (Chadha and Silakari, 2017; Lee and Lee, 2010). The prevalence of the indole scaffold in nature can be owed to the essential amino acid tryptophan, which is biosynthesized by the condensation of indole and serine (Dunn et al., 2008). Tryptophan in turn serves as a precursor for multiple natural bioactive compounds, like animal hormones (substituted tryptamines including serotonin and melatonin), plant hormones

(indole-3-acetic acid, indole-3-propionic acid), plant-derived marketed pharmaceuticals (vincristine, vinblastine), and psychedelics (psilocybin, ibogaine) (Richard et al., 2009; Mashiguchi et al., 2011; Almagro et al., 2015; Tylš et al., 2014; Mačiulaitis et al., 2008) (Figure 1). The versatility of the indole core makes it stand out as a so-called "privileged structure", a molecular scaffold that by the modification of functional groups can be converted into a variety of ligands with selective binding capacities against multiple biological targets (Wan et al., 2019). Indeed, medicinal chemists have for decades exploited indole as a core structure for drug discovery, resulting in multiple synthetic drugs used for the treatment of various disorders, including cancer, migraine, depression and hypertension (Chadha and Silakari, 2017; Watkins-Dulaney et al., 2020) (Figure 1).

In such drug discovery processes, halogenation is commonly used as a means to improve the properties of a lead drug candidate (Mendez et al., 2017), and consequently, the presence of halogens is frequent in drugs, with approximately 25% of all commercialized pharmaceuticals containing a halogen atom in their structure (Xu et al., 2014). Halogenation of drug candidates can increase membrane permeability (Gerebtzoff et al., 2004), enhance blood-brain barrier transport (Gentry et al., 1999), and strengthen the binding interactions between a ligand and its target, thereby increasing the ligand potency (Xu et al., 2014; Prieto-Díaz et al., 2023). The halogenation of the indole ring in particular has been proven to tune some properties of multiple cancer drug leads isolated from marine environments (Gul and Hamann, 2005). Furthermore, halogenated indoles serve as versatile precursors for the synthesis of more complex structures, as they facilitate cross-coupling reactions and other synthetic transformations (Sharma et al., 2017; J. Corr et al., 2017; Dachwitz et al., 2020).

Although multiple methods for the halogenation of indole heterocycles exist, these often involve the use of toxic reagents like transition metals (Petrone et al., 2016), generate significant amounts of by-products (Chung and Vanderwal, 2016), and the regioselectivity is mostly achieved only at the 2- and 3-positions on the indole ring (Taskesenligil et al., 2023). The addition of directing groups to the indole ring can also facilitate halogenation at the benzene ring, however, this strategy is associated with additional synthetic steps and reduced atom economy (Maddox et al., 2015; Rodriguez et al., 2014; Taskesenligil et al., 2023). Therefore, catalyst-controlled methods

employing enzymes that perform site-selective halogenations is emerging as a promising approach in synthetic chemistry, as they provide a means to overcome the electronic preference for substitution at the 2- and 3-positions (Latham et al., 2018). Among multiple classes of halogenating enzymes found in nature, flavin-dependent halogenases (FDHs) stand out for their marked substrate specificity and regioselectivity (van Pée and Patallo, 2006; Andorfer and Lewis, 2018). In addition to oxygen and halide ions, FDHs require input of $FADH_2$ provided by a partner flavin-reductase that performs NADH-driven reduction of FAD to $FADH_2$ (van Pée and Patallo, 2006). Tryptophan halogenases in particular are well-studied FDHs able to halogenate benzo positions of the indole ring in tryptophan, with multiple studies showing the use of these enzymes to halogenate tryptophan with chlorine or bromine in the 5-, 6- and 7-positions *in vitro* (Yeh et al., 2005; Zehner et al., 2005; Zeng and Zhan, 2011). However, an *in vitro* large-scale process is hindered by the low activity and stability of tryptophan halogenases as well as a need to add the expensive cofactors FAD, NADH, a partner reductase, and a cofactor-regenerating method based on additional enzymes (Frese and Sewald, 2015). The high cost of adding any of these cofactors would likely make the process economically infeasible.

Alternatively, *in vivo* production strategies using recombinant microorganisms circumvent some of these limitations and could be a preferred system. The bacterium *Corynebacterium glutamicum* has been engineered for the expression of tryptophan halogenases, tryptophan decarboxylase, and trytophanase, resulting in production of significant levels of 7-Br/Cl-tryptophan, 7-Br/Cl-tryptamine, and 7-Br/Cl-indole (Kerbs et al., 2022; Veldmann et al., 2019a, 2019b). More recently, *Escherichia coli* has been used as chassis for the production of the fabric dye Tyrian purple and other pigments, composed of a halogenated indole skeleton (Lee et al., 2020; Lai et al., 2021). While these studies show the potential of prokaryotic cell factories for the production of halogenated indoles, complex derivatives thereof with interesting properties could be challenging to produce, as these often entail the functional expression of cytochrome P450 enzymes, which remains a challenge in bacteria (Kandel et al., 2014; Hausjell et al., 2018). Conversely, the baker's yeast *Saccharomyces cerevisiae* is a preferred production chassis in the context of natural products, not only due to its eukaryotic cell nature that facilitates the expression of eukaryotic enzymes, but also supported by its scalability, its long industrial use as

production host and its minimal production of secondary metabolites (Ro et al., 2006; Brown et al., 2015; Li et al., 2018; Luo et al., 2019).

The current work represents a proof-of-concept for the *de novo* production of halogenated indole derivatives in *S. cerevisiae*, specifically halogenated tryptophan and tryptamine.

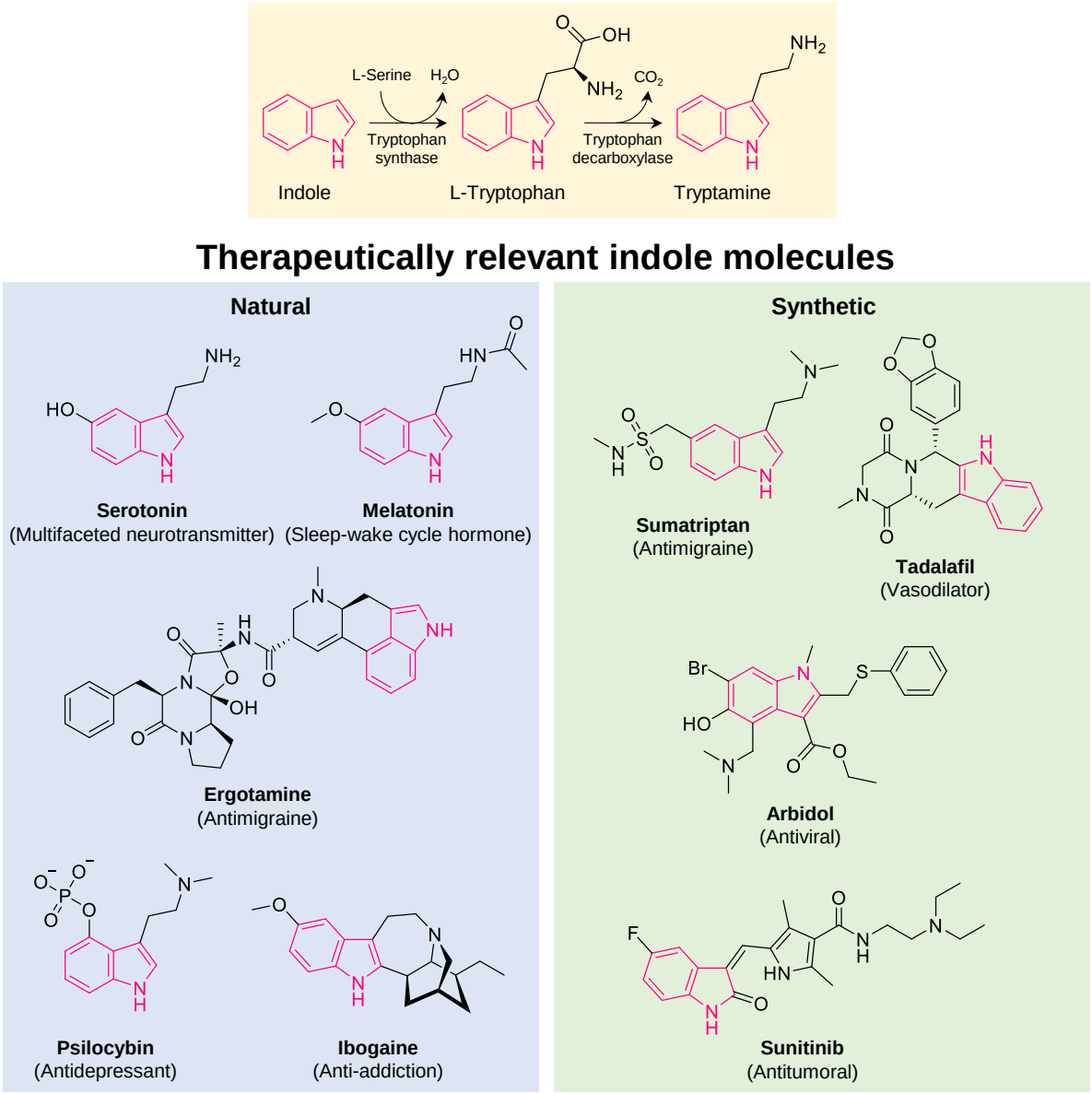

Figure 1. Schematic representation of tryptophan and tryptamine biosynthesis and the prevalence of the indole scaffold in naturally occurring and synthetic chemical compounds. The indole scaffold in different chemical structures is shown in pink. The therapeutic use of each of the compounds is described in brackets.

Materials and methods

Strains and media

Haploid *Saccharomyces cerevisiae* strain CEN.PK113-7D (MATa *URA3 HIS3 LEU2 TRP1 MAL2-8c SUC2*) was used as parental strain in this study (Entian and Kötter, 2007). *S. cerevisiae* cultures were grown in liquid Yeast Peptone Dextrose (YPD). The media were supplemented with 200 mg/L G418 for selection of the Cas9-plasmid and with 100 mg/L nourseothricin for selection of gRNA plasmids when required. Synthetic mineral medium for cultivation was prepared with 7.5 g/L $(NH_4)_2SO_4$, 14.4 g/L KH_2PO_4, 0.5 g/L $MgSO_4 \cdot 7H_2O$, 1 mL/L vitamins, 2mL/L trace elements and with 20 g/L glucose (Jensen et al., 2014). The pH was adjusted to 6.0 with NaOH. In the halogenation experiments, the media were supplemented with 25 mM KCl, 25 mM KBr or 1 mM tryptamine as required.

Escherichia coli DH5α was used for all plasmid cloning and propagation. *E. coli* strains were grown in Lysogeny Broth (LB) media supplemented with 100 mg/L ampicillin. Agar plates for both *S. cerevisiae* and *E. coli* cultivations were prepared as described above with addition of 20 g/L agar. Frozen stocks of *S. cerevisiae* and *E. coli* were prepared by adding glycerol to a final concentration of 25% (v/v) to overnight cultures and storing aliquots at −80 °C.

Construction of plasmids and strains

Relevant heterologous genes were codon-optimized for *S. cerevisiae* using the JCat online tool (Grote et al., 2005) and ordered as synthetic DNA strings from GeneArt (Thermo Fisher Scientific) (Table S3). The EasyClone-MarkerFree cloning system (Jessop-Fabre et al., 2016) was used to construct integration plasmids. Integration fragments and gRNA plasmids for CRISPR/Cas9-mediated integration were constructed as described by Jessop Fabre *et al.* BioBricks were amplified using USER-compatible primers and Phusion U Hot Start DNA Polymerase (Thermo Fisher Scientific). USER reactions were carried out according to New England Biolabs standard protocol. The USER reactions were then transformed into competent *E. coli DH5α* cells by heat shock for plasmid assembly and propagation. Plasmids were purified from *E. coli* cultures using NucleoSpin plasmid miniprep kit (Macherey Nagel) and correct plasmid assembly was verified by Sanger sequencing (Eurofins

Scientific). Integration fragments were linearized with FastDigest NotI restriction enzyme (Thermo Fisher Scientific). Integration fragments and gRNA plasmids when relevant were transformed into *S. cerevisiae* strains expressing Cas9 using the LiAc/SS carrier DNA/PEG method (Gietz and Schiestl, 2007). When involving nourseothricin selection, transformations were recovered in YPD + G418 media at 30 °C with 250 rpm shaking before plating. Transformations were plated on YPD supplemented with G418 and nourseothricin. Integrations of the vectors into the correct sites on the genome were verified by colony PCR using Red Taq (VWR Life Science) DNA polymerase. To prepare transformed strains for subsequent CRISPR/Cas9 mediated integrations, gRNAs were removed by re-streaking on YPD plates supplemented with G418 to maintain the selection for Cas9-vector and removal of the gRNAs was verified by replica plating. A list of all strains, plasmids, BioBricks and primers used and constructed in this study is available in the Supplementary information (Tables S4-S7).

Cultivation and extraction

Cultivations of *S. cerevisiae* strains were performed in synthetic mineral medium. Single colonies were inoculated into 400 µL media in 96-deep well plates with air-penetrable lids (Enzyscreen) and incubated for 48 hours at 30 °C and 300 rpm. From these pre-cultures, 10 µL were transferred to 490 µL media supplemented with relevant substrates when required and incubated for 72 hours in 96-deep well plates with air-penetrable lids at 30 °C and 300 rpm. Cultivations were performed in biological duplicates when metabolites were to be quantified.

For extraction of intracellular products, the cultivation broths were subjected to cell lysis, which was carried out by adding a small aliquot of acid-washed glass beads (212 - 300 µm, Sigma-Aldrich) and running the samples for two cycles of 20 sec at 5,500 rpm on a Precellys 24 Tissue Homogenizer (Bertin Instruments). The lysed cell broths were centrifuged at 17,000 g for 5 min and the supernatants were analyzed by LC-MS/MS. For the quantification of tryptamine and halogenated derivatives, the cultivation broths were centrifuged at 17,000 g for 5 min and the supernatants were analyzed by LC-MS/MS.

For the proteomics analysis, single colonies were inoculated in 2 mL of synthetic mineral medium and grown overnight in 13-mL pre-culture tubes. The next day, 24-deep well plates with air-penetrable lids (Enzyscreen) containing 2 mL of synthetic mineral medium were inoculated to an OD of ~0.1. Cultures were grown for 20 hours at 30 °C and 300 rpm. 400 µL of broth, corresponding to approximately 2 x 10^7 cells, was centrifuged at 3,000 g for 10 min, the supernatant was discarded and cell pellets were frozen at −80 °C until analysis.

Analytical methods

The LC-MS/MS analysis of the samples was performed on a Vanquish Duo UHPLC binary system (Thermo Fisher Scientific) coupled to IDX-Orbitrap Mass Spectrometer (Thermo Fisher Scientific, USA). The chromatographic separation was achieved using a Waters ACQUITY BEH C18 (10 cm × 2.1 mm, 1.7 µm) equipped with an ACQUITY BEH C18 guard column kept at 40 °C and using a flow rate of 0.35 mL/min as previously described (Kildegaard et al., 2021). A binary mobile phase system composed of 0.1% formic acid in MilliQ water (solvent A) and 0.1% formic acid in acetonitrile (solvent B) was employed. The gradient program began with 2% B for 0.8 minutes, followed by a linear increase to 5% B at 3.3 minutes. Subsequently, solvent B was increased until reaching 100% at 10 minutes, held for 1 minute, and then returned to the initial conditions. The column was allowed to re-equilibrate for 2.7 minutes before the next injection. The injection volume was 1 µL. The MS measurement was carried out in positive-heated electrospray ionization (HESI) mode with a voltage of 3500 V, the vaporizer temperature was set at 350 °C, the ion transfer tube temperature at 325 °C, and the sheath gas at 50 (a.u.). Acquisition was performed in full MS/MS spectra (Data dependent Acquisition-driven MS/MS) in the mass range of 70–1000 Da. The DDA acquisition settings were the following: automatic gain control (AGC) target value set at 4e5 for the full MS and 5e4 for the MS/MS spectral acquisition, the mass resolution was set to 120,000 for full scan MS and 60,000 for MS/MS events. Precursor ions were fragmented by stepped High-energy collision dissociation (HCD) using collision energies of 20, 40, and 60 eV. A lock mass of an internal calibrant was acquired throughout each injection to provide real-time adjustment of the instrument's m/z calibration. Peaks were integrated using QuanBrowser Thermo Xcalibur 4.2 (Thermo Fisher Scientific).

Analytical standards were purchased from Sigma-Aldrich (L-tryptophan, tryptamine), Carbosynth (5-chlorotryptophan, 6-chlorotryptophan, 5-bromotryptophan, 7-bromotryptophan, 5-chlorotryptamine hydrochloride, 6-chlorotryptamine, 7-chlorotryptamine hydrochloride, 6-bromotryptamine hydrochloride, 7-bromotryptamine hydrochloride), Toronto Research Chemicals (7-chlorotryptophan), BLDpharm (6-bromotryptophan), and VWR (5-bromotryptamine hydrochloride).

The calibration curves were generated using five concentration points per compound, over a concentration range of 0.04 to 6.25 mg/L, with the exception of tryptamine, which ranged from 1.72 to 160 mg/L. Each calibration point was determined through a single injection, which were randomly interspersed throughout the analytical run. The calibration curve data was modeled using ordinary least squares regression using the statsmodels 0.13.5 package in Python (Supplementary File 1).

The statistical significance of differences between measurements from biological replicate samples were calculated by using a two-tailed t-test assuming unequal variances.

Proteomic analysis

The frozen cell pellets derived from the cultivations were thawed on ice. Oxide beads (Glen Mills, NJ, USA) and 100 µL of 95 °C Guanidinium HCl (6 M Guanidinium hydrochloride (GuHCl), 5 mM tris(2-carboxyethyl)phosphine (TCEP), 10 mM chloroacetamide (CAA), 100 mM Tris–HCl pH 8.5) was added to all samples. Full disruption of the cells was achieved in a Mixer Mill (MM 400 Retsch, Haan, Germany) set at 25 Hz for 5 min at room temperature, followed by 10 min in a thermo mixer at 95 °C at 600 rpm. Cell debris was removed by centrifugation at 5,000 g for 10 min. A total of 100 µg protein were used for overnight tryptic digestion (constant shaking, 400 rpm, for 8 h), after which 10 µL of 10% TFA was added. Samples were then ready for de-salting using uSOLA C18 plate (Thermo Fisher Scientific).

Desalted samples were injected into Orbitrap Exploris 480 mass spectrometer (Thermo Fisher Scientific) using a CapLC system (Thermo Fisher Scientific). First, samples were captured at a flow of 10 µL/min on a precolumn (µ-precolumn C18 PepMap 100, 5 µm, 100 Å) and then at a flow of 1.2 µL/min the peptides were separated on a 15 cm C18 EASY-Spray column (PepMap RSLC C18 2 µm, 100Å, 150

µm x 15 cm). The applied gradient went from 4% acetonitrile in water (buffered with 0.1% formic acid) to 76% over a total of 60 minutes. While spraying the samples into the mass spectrometer the instrument operated in data dependent mode using the following settings: MS-level scans were performed with Orbitrap resolution set to 60,000; AGC Target 3.0e6; maximum injection time 50 ms; intensity threshold 5.0e3; dynamic exclusion 25 sec. Data dependent MS2 selection was performed in Top 20 Speed mode with HCD collision energy set to 28% (AGC target 1.0e4, maximum injection time 22 ms, Isolation window 1.2 m/z).

For analysis of the Thermo rawfiles, Proteome Discoverer 2.4 was used with the following settings: Fixed modifications: Carbamidomethyl (C) and Variable modifications: oxidation of methionine residues. First search mass tolerance 20 ppm and a MS/MS tolerance of 20 ppm. Trypsin as enzyme and allowing one missed cleavage. FDR was set at 0.1%. The Match between runs window was set to 0.7 min. Quantification was only based on unique peptides and normalization between samples was based on total peptide amount. For the searches, a protein database consisting of the *Saccharomyces cerevisiae* reference proteome (UP000002311) and the heterologous proteins was used.

Docking simulations

L-tryptophan, 5-Cl-L-tryptophan, 5-Br-L-tryptophan, 6-Cl-L-tryptophan, 6-Br-L-tryptophan, 7-Cl-L-tryptophan and 7-Br-L-tryptophan were docked to crystal structures of SrPyrH (PDBID 2WET:B), SttH (PDB ID 5HY5:A) and LaRebH (PDB ID 2E4G:B). L-tryptophan, tryptamine, 5-Cl-L-tryptophan, 5-Cl-tryptamine, 5-Br-L-tryptophan, 5-Br-tryptamine, 6-Cl-L-tryptophan, 6-Cl-tryptamine, 6-Br-L-tryptophan, 6-Br-tryptamine, 7-Cl-L-tryptophan, 7-Cl-tryptamine, 7-Br-L-tryptophan, and 7-Br-L-tryptamine were docked to CrTDC (PDB ID 6EEW:AB).

The ligands were based on structures of L-tryptophan (CHEBI_16828) and tryptamine (CHEBI_16765) by using MarvinSketch 19.19 (ChemAxon, https://www.chemaxon.com) to add Cl and Br at the 5-, 6-, and 7- positions, respectively, and calculate protonation state. The Optimize PyMOL plugin (The PyMOL Molecular Graphics System, Version 1.8 Schrödinger, LLC) was used to energy minimize the ligands, which finally were prepared for docking using AutoDockTools

version 1.5.6 to merge non-polar hydrogens, and add Gasteiger charges. The molecules were saved as rigid pdbqt files to retain their L-configuration (O'Boyle et al., 2011).

Co-crystallized ligands and water molecules were removed for the crystal structures of SrPyrH (PDBID 2WET:B), SttH (PDB ID 5HY5:A), LaRebH (PDB ID 2E4G:B) and CrTDC (PDB ID 6EEW:AB) and hydrogens were added with PyMOL. To mimic both chlorination and bromination, crystal structure Cl atoms were exchanged with Br. The positions of the active sites for SrPyrH, LaRebH and CrTDC were identified by calculating the center of mass of the bound L-tryptophan ligand. No ligand was bound in the SttH crystal structure, so the active site position was identified as the center of mass of the active site residues Lys79, Glu363, His96 and Phe98. The LaRebH crystal structure does contain FAD and Cl/Br, so co-factor and ions were added to the structure by superimposition with 2AR8. The structures were prepared for docking using AutoDockTools version 1.5.6 by merging non-polar hydrogens and adding Gasteiger charges. The structures were saved as rigid pdbqt files to retain the position of the active site Lys75 and Glu354 (SrPyrH numbering) amino acids.

The molecules were docked to the structures using AutoDock Vina 1.1.2 using a box size of 10x10x10 centered in the active site (Trott and Olson, 2010). The protein-ligand interactions were analyzed using binana 2.1 (Young et al., 2022).

Results

Expression of tryptophan halogenases in *S. cerevisiae* leads to the production of halogenated tryptophan

In nature, numerous bioactive compounds with halogenated indoles in their chemical structures have been discovered, leading to the characterization of several tryptophan FDHs able to act on the 5-, 6-, and 7-positions of the indole moiety of tryptophan.[21] Among several described tryptophan halogenases, SrPyrH (5-halogenase) from *Streptomyces rugosporus*, SttH (6-halogenase) from *Streptomyces toxytricini*, and LaRebH (7-halogenase) from *Lechevalieria aerocolonigenes* have been demonstrated to be functional in bacteria and plants when co-transformed with a partner flavin reductase, like LaRebF from *Lechevalieria aerocolonigenes* (Veldmann et al., 2019a; Fräbel et al., 2016; Runguphan et al., 2010). Additionally, in plants, the tryptophan decarboxylase CrTDC from *Catharanthus roseus* accepts halogenated tryptophan as a

substrate, leading to the production of halogenated tryptamine (Fräbel et al., 2016; Runguphan et al., 2010; Fräbel et al., 2018). Inspired by these works, we hypothesized that SttH, SrPyrH and LaRebH might also catalyze halogenation of tryptophan when co-expressed with LaRebF in *S. cerevisiae* and that introduction of the genes into a strain expressing CrTDC would lead to production of halogenated tryptamine (Figure 2a).

To attempt production of halogenated tryptophan, integrations of SrPyrH, SttH and LaRebH into *S. cerevisiae* strain ST7574 (CEN.PK113-7D + Cas9) were carried out with and without co-integration of the partner flavin reductase LaRebF. The same integrations were additionally performed in strain ST9336 expressing CrTDC in order to attempt production of halogenated tryptamine (Brown et al., 2015; Milne et al., 2020). A proteomic analysis confirmed high expression levels of the heterologous genes in multiple engineered strains (Figure S1, Supplementary File 1). Transformants were cultivated in synthetic mineral media supplemented with 25 mM KCl or 25 mM KBr (Figure 2b-c). We also performed computer-aided docking simulations to investigate the binding interactions between tryptophan, the different positional isomers of halotryptophan, and the tryptophan halogenases. Likewise, we evaluated the binding of halotryptophan and halotryptamine to CrTDC (Figures S2-S3 and Tables S1-S2).

Chlorotryptophan or bromotryptophan were present in all strains expressing a tryptophan halogenase and cultivated in a medium supplemented with the corresponding halide (Figures S4-S9), even in the absence of LaRebF. However, the levels of halogenated tryptophan were up to 100-fold higher when LaRebF was expressed, clearly demonstrating that $FADH_2$ supply was the limiting factor for the halogenation. Additionally, the intracellular tryptophan titers in the strains expressing halogenases did not demonstrate significant variations compared to the control strain, except for strain ST10290 harboring the 7-halogenase LaRebH and LaRebF. This indicates that, in general, only a limited proportion of tryptophan was halogenated, with a notable exception being the activity of LaRebH. Docking simulations suggested that indeed substrate is more favorably bound to LaRebH, potentially resulting in a higher activity (Figure S2, Table S1). Halogenation of tryptophan by SrPyrH resulted in the lowest titers, which is consistent with previously reported *in vitro* data on low activity and particularly low affinity for bromine. Specifically, previous studies have

shown that SrPyrH activity towards bromination is 75% lower than its activity towards chlorination (Runguphan et al., 2010). More interestingly, halogenated products from the kynurenine pathway, such as halogenated L-kynurenine, kynurenic acid, and xanthurenic acid were identified when expressing either of the halogenases, indicating that the native enzymes in yeast can incorporate halogenated tryptophan into the kynurenine pathway (Figures S10-S17).

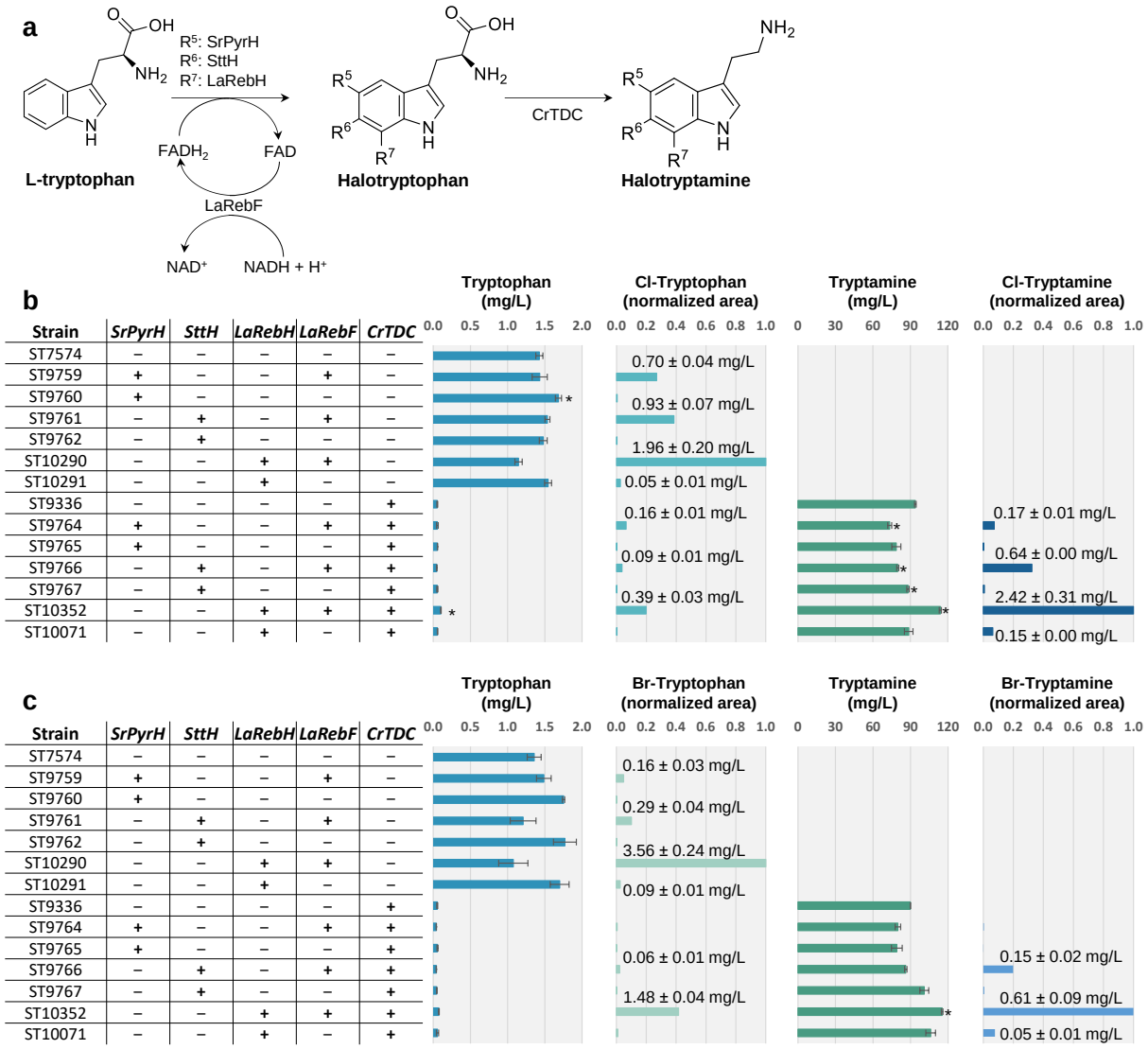

Figure 2. Production of halogenated tryptophan and tryptamine in recombinant yeast strains. a) Overview of heterologous biosynthesis of halogenated tryptophan and tryptamine in *S. cerevisiae* from the native precursor L-tryptophan. R^n groups in halotryptophan and halotryptamine represent a Cl or Br atom in the positions indicated by *n*. Production of halogenated compounds in synthetic mineral medium supplemented with b) 25 mM KCl or c) 25 mM KBr after 72 hours cultivation. "+" and "–" symbols indicate the presence or absence of the corresponding genetic modification, respectively. Cultivation broths of

strains lacking *CrTDC* were subjected to the intracellular extraction protocol. Cultivation broths of strains expressing *CrTDC* were centrifuged and the supernatants were used for the analysis. Titers of halogenated products are reported as normalized peak areas, meaning that areas matching the retention time, expected m/z, and fragmentation pattern of the metabolite of interest have been normalized with respect to the highest-producing strain of that metabolite. Titers of halogenated products not reported in mg/L were below the lowest calibration point (< 0.04 mg/L). Error bars/values represent the standard deviation from two biological replicates. Asterisk (*) indicates a p-value < 0.05 (two-tailed, unequal variance) between the strain and the control (ST7574 for strains lacking *CrTDC*, ST9336 for strains expressing *CrTDC*). Data available in the Supplementary File 1.

Strains expressing a tryptophan halogenase together with CrTDC and cultivated with the corresponding halide resulted in the production of chloro- or bromotryptamine (Figures S18-S23). The analytical standards allowed the determination of the regioselectivity and the quantification of products demonstrating an overall low catalytic activity of the enzymes. The highest titers obtained for halogenated tryptophan and tryptamine were 3.56 ± 0.24 mg/L 7-bromotryptophan and 2.42 ± 0.31 mg/L 7-chlorotryptamine. In addition, the strains producing brominated compounds were also able to perform chlorination, even though chloride was only present in trace amounts in the medium (0.15 mM) (Figure S24), indicating that chlorination could be favored, which is in line with the general consensus regarding flavin-dependent tryptophan halogenases (Schnepel and Sewald, 2017).

Tryptophan halogenases accept tryptamine as substrate

While in plants the sequence of reactions leading to halogenated tryptamine is assumed to begin with the halogenation of tryptophan, which is subsequently decarboxylated by CrTDC yielding halotryptamine (Fräbel et al., 2016; Runguphan et al., 2010), some tryptophan halogenases like LaRebH have been shown to present some substrate promiscuity, being able to act directly on tryptamine (Glenn et al., 2011; Payne et al., 2013). In order to assess whether the different halogenases we tested could accept tryptamine as substrate in *S. cerevisaie*, strains expressing individual tryptophan halogenases together with LaRebF were cultivated in synthetic mineral

medium supplemented with the corresponding halide and fed with 1 mM tryptamine (Figure 3).

Strain ID	*SrPyrH*	*SttH*	*LaRebH*	*LaRebF*	Halide	Tryptamine
ST7574	–	–	–	–	KCl	–
ST9759	+	–	–	+	KCl	–
ST9761	–	+	–	+	KCl	–
ST10290	–	–	+	+	KCl	–
ST7574	–	–	–	–	KCl	+
ST9759	+	–	–	+	KCl	+
ST9761	–	+	–	+	KCl	+
ST10290	–	–	+	+	KCl	+
ST7574	–	–	–	–	KBr	–
ST9759	+	–	–	+	KBr	–
ST9761	–	+	–	+	KBr	–
ST10290	–	–	+	+	KBr	–
ST7574	–	–	–	–	KBr	+
ST9759	+	–	–	+	KBr	+
ST9761	–	+	–	+	KBr	+
ST10290	–	–	+	+	KBr	+

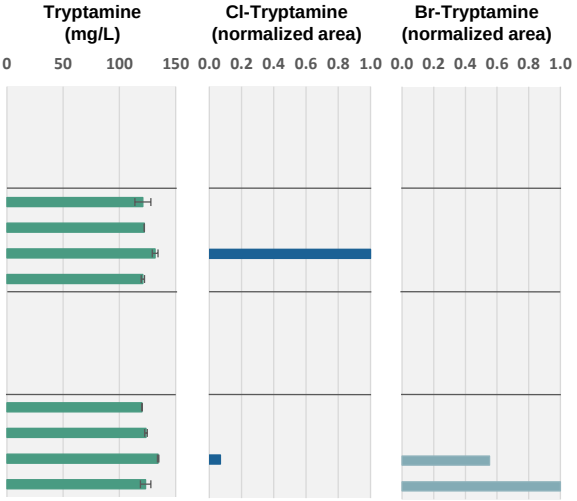

Figure 3. Direct halogenation of tryptamine in engineered *S. cerevisiae* strains expressing tryptophan halogenases. Cultivations were performed in synthetic mineral medium for 72 hours. "+" and "–" symbols indicate the presence or absence of the corresponding genetic modification, respectively. The "halide" column shows the halide compound added in the medium at a concentration of 25 mM, while the "tryptamine" column indicates the supplementation ("+") or absence ("–") of 1 mM tryptamine. Cultivation broths were centrifuged and the supernatants were used for the analysis. Titers of halogenated products are reported as normalized peak areas, meaning that areas matching the retention time, expected m/z, and fragmentation pattern of the metabolite of interest have been normalized with respect to the highest-producing strain of that metabolite. Titers of all halogenated products were below the lowest calibration point (< 0.04 mg/L). Error bars represent the standard deviation from two biological replicates. Data available in the Supplementary File 1.

Interestingly, SttH was able to halogenate tryptamine with both chlorine and bromine (Figures S25-S26), while LaRebH could only perform tryptamine bromination (Figure S27). The regioselectivity of the halogenation seemed to be maintained in all reactions (Figures S25-S27). This data suggests that the tryptamine halogenations in strains harboring CrTDC and SttH or LaRebH reported in Figure 2 were likely consequence of both the decarboxylation of halogenated tryptophan and the direct halogenation of tryptamine. In either case, both enzymatic reactions involve a non-native substrate, which has been shown to result in a poor catalytic activity. For example, the catalytic

efficiency of LaRebH is significantly lower when using tryptamine as a substrate, with a 59-fold reduction compared to tryptophan (Runguphan et al., 2010; Payne et al., 2013). This is reflected in the low titers of halotryptamine obtained by direct halogenation, which were found to be below 0.04 mg/L. Finally, halogenated tryptamine was not observed for strains expressing SrPyrH indicating that this enzyme is specific for tryptophan.

Co-expression of tryptophan halogenases results in the production of di-halogenated tryptophan

The expression of individual tryptophan halogenases and tryptophan decarboxylase resulted in the production of halotryptophan and halotryptamine. In order to investigate whether production of multi-halogenated tryptophan or tryptamine would be possible in *S. cerevisiae*, co-integrations of *SrPyrH*, *SttH*, *LaRebH* and *LaRebF* were carried out in strains ST7574 and ST9336, resulting in strains expressing several tryptophan halogenases with or without CrTDC.

In medium containing the corresponding halide, strains expressing two or three tryptophan halogenases and LaRebF produced a metabolite with mass and fragmentation pattern matching dichloro- or dibromotryptophan, suggesting that two tryptophan halogenases worked in conjunction to perform di-halogenation of tryptophan (Figures 4, S28-S31). However, no metabolite matching trihalotryptophan was detected in strains harboring three halogenases. Furthermore, when CrTDC was co-expressed, dihalotryptamine was not produced, indicating both that CrTDC cannot accept dihalotryptophan as substrate and that halotryptamine cannot be halogenated a second time by the remaining halogenases. Interestingly, strain ST9763 expressing two halogenases produced dichlorotryptophan, while ST9678 expressing the same halogenases in addition to CrTDC produced chlorotryptamine but not dichlorotryptophan, indicating a higher catalytic activity of CrTDC towards the shared substrate, namely chlorotryptophan. When these two strains were cultivated in KBr containing medium, dibromotryptophan was produced by strain ST9768, but surprisingly not by strain ST9763.

Strain	*SrPyrH*	*SttH*	*LaRebH*	*LaRebF*	*CrTDC*	Halide
ST7574	–	–	–	–	–	KCl
ST9336	–	–	–	–	+	KCl
ST9763	+	+	–	+	–	KCl
ST9768	+	+	–	+	+	KCl
ST10073	–	+	+	+	+	KCl
ST10072	+	+	+	+	+	KCl
ST7574	–	–	–	–	–	KBr
ST9336	–	–	–	–	+	KBr
ST9763	+	+	–	+	–	KBr
ST9768	+	+	–	+	+	KBr
ST10073	–	+	+	+	+	KBr
ST10072	+	+	+	+	+	KBr

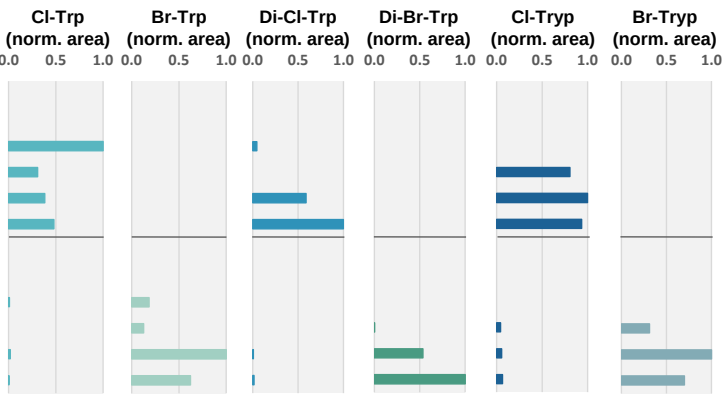

Figure 4. Production of dihalogenated tryptophan in engineered *S. cerevisiae* strains. Cultivations were performed in synthetic mineral medium for 72 hours. "+" and "–" symbols indicate the presence or absence of the corresponding genetic modification, respectively. The "halide" column shows the halide compound added in the medium at a concentration of 25 mM. Cultivation broths of strains lacking *CrTDC* were subjected to the intracellular extraction protocol. Cultivation broths of strains expressing *CrTDC* were centrifuged and the supernatants were used for the analysis. Titers of halogenated products are reported as normalized peak areas, meaning that areas matching the retention time (except for dihalotryptophan), expected m/z, and fragmentation pattern of the metabolite of interest have been normalized with respect to the highest-producing strain of that metabolite. Trp: tryptophan; Tryp: tryptamine. Data available in the Supplementary File 1.

Discussion

In this study, conceptual *de novo* production of a diverse range of halogenated tryptophan and tryptamine derivatives was achieved in the baker's yeast *S. cerevisiae* by the functional expression of bacterial tryptophan halogenases and a partner flavin reductase providing $FADH_2$. While the expression of the flavin reductase LaRebF was demonstrated to be fundamental for the production of halogenated metabolites, trace amounts were also detected even in the absence of LaRebF (Figure 2). The cofactor $FADH_2$ provided by LaRebF is natively produced in the citric acid cycle in *S. cerevisiae*, but as this takes place in the mitochondria and the halogenases are expressed in the cytosol, it is unlikely that the $FADH_2$ generated this way could be responsible for the observed halogenations (Kim and Winge, 2013). Other studies have similarly reported results indicating the presence of $FADH_2$ in the cytosol of *S. cerevisiae* without identifying the source (Enomoto et al., 2002; Bergdahl et al., 2014).

While the co-expression of tryptophan halogenases along with LaRebF and CrTDC resulted in the production of halogenated compounds, the low titers obtained and the concomitant accumulation of tryptophan and tryptamine suggested limited performance in *S. cerevisiae* (Figure 2). Indeed, as previously described in literature, the decarboxylation of halogenated tryptophan by CrTDC has been reported to be up to 30-fold lower in terms of catalytic efficiency compared to the native substrate tryptophan *in vitro* (Runguphan et al., 2010). Likewise, the direct halogenation of tryptamine has a turnover number 48-fold lower than tryptophan halogenation for LaRebH (Payne et al., 2013). Therefore, the use of enzyme variants with increased activity or shifted substrate specificity could help relieving sub-optimal enzymatic steps (Payne et al., 2015; Poor et al., 2014; Shepherd et al., 2015). In this regard, the noncanonical aromatic amino acid decarboxylase PcncAAAD from the hallucinogenic psilocybin mushroom *Psilocybe cubensis* has been demonstrated to display higher chlorotryptamine production than CrTDC (Torrens-Spence et al., 2018).

Similarly, the flavin reductase LaRebF has been systematically used in most of the works involving tryptophan halogenases, but many other flavin reductases have been characterized and could show better results in the reduction of FAD in yeast (Kendrew et al., 1995; Parry and Li, 1997; Galán et al., 2000; Lee and Zhao, 2007). The endogenous cytosolic supply of FAD in *S. cerevisiae* has also been demonstrated to be limiting the production of compounds whose biosynthesis requires this cofactor, which can be alleviated by overexpressing native genes involved in its biosynthesis (Nielsen et al., 2014). Another factor that could be affecting the halogenation reaction is the intracellular availability of Cl^- and Br^-, dependent on the transport kinetics for these anions (Jennings and Cui, 2008). The uptake kinetics of these anions into the cells has been shown to be affected by pH and temperature (Coury et al., 1999; Volkov, 2015). Thus, adjustments to these factors, as well as the overexpression of uptake transporters or the increase of halide concentrations in the medium, could improve their intracellular availability. In addition, engineering in the shikimate pathway has been proven to increase the titers of tryptophan-derived products (Milne et al., 2020; Zhang et al., 2020), which combined with the expression of engineered halogenase variants and a better cofactor supply could improve the production of halogenated compounds.

Although low titers were obtained, this study demonstrates the feasibility of *S. cerevisiae* as a production chassis for halogenated indoles. Some of the products obtained like 6-bromotryptamine could have direct applications in the pharmaceutical industry. The derivative 6-bromotryptamine A has been demonstrated to inhibit the activity of acetylcholinesterase *in vitro* and prevent scopolamine-induced short-term cognitive impairments in mice, thereby alleviating two main pathological events in the progress of Alzheimer's disease (Jin et al., 2020). Therefore, the biosynthesis of 6-bromotryptamine in *S. cerevisiae* would offer an alternative to the current chemical synthesis methods (Jin et al., 2020). Similarly, 5-bromotryptamine could be converted to 5-bromo-DMT, a metabolite found in marine sponges that has sedative properties (Kochanowska et al., 2008).

The identification of halogenated molecules within the kynurenine pathway presents opportunities for the manipulation of yeast to produce these compounds. This is of particular interest as imbalances in the kynurenine pathway have been associated with various psychiatric disorders, including depression and schizophrenia (Cervenka et al., 2017). 4-chloro-kynurenine, for example, has been found to have potential as a therapeutic prodrug for major depressive disorder (Vécsei et al., 2013). Additionally, other halogenated kynurenine derivatives such as bromo-kynurenine play a role in the striking green biofluorescence observed in certain species of shark (Park et al., 2019).

More importantly, tryptamine serves as a precursor for more than 3,000 secondary metabolites including monoterpenoid indole alkaloids (MIAs) like vinblastine or vincristine, important chemotherapy agents (O'Connor and Maresh, 2006). By feeding with halogenated indoles or expressing tryptophan halogenases in the medicinal plant *C. roseus*, production of multiple halogenated MIAs has been previously demonstrated *in vivo*, as most of the biosynthetic enzymes accept halogenated intermediates, while in some steps an engineered variant is required (Runguphan et al., 2010; Bernhardt et al., 2007; McCoy and O'Connor, 2006). In addition, functional expression of the enzymes leading to the MIA common intermediate strictosidine has been successfully achieved in yeast (Brown et al., 2015), which in combination with the results of the present work proves that *S. cerevisiae* could be a promising host for the production of new-to-nature halogenated natural products useful in drug discovery processes.

Conclusions

In this work, the successful production of various halogenated tryptophan and tryptamine derivatives was achieved in the industrial workhorse *Saccharomyces cerevisiae*. Functional expression of bacterial tryptophan halogenases together with a partner flavin reductase and a tryptophan decarboxylase resulted in the production of halogenated tryptophan and tryptamine with chlorine or bromine. Additionally, we showed that some tryptophan halogenases present some substrate promiscuity and can halogenate tryptamine directly and that the co-expression of two tryptophan halogenases results in the production of dihalotryptophan. Overall, this work demonstrates the suitability of *S. cerevisiae* for the production of halogenated natural products.

Acknowledgements

This project has received funding from the European Union's Horizon 2020 research and innovation programme under grant agreements No. 814408 (SHIKIFACTORY100 project) and No. 720770 (DAFIA project). IB also acknowledges the financial support from the Novo Nordisk Foundation (Grant agreement No. NNF20CC0035580, NNF20OC0060809, and NNF21OC0072559) and from the European Research Council under the European Union's Horizon 2020 research and innovation programme (YEAST-TRANS project, Grant Agreement No. 757384). The authors wish to thank Peter Kötter for the use of the CEN.PK.

Conflict of interest

NM and IB are inventors on patent application PCT/EP2020/075823. NM has a financial interest in Octarine Bio ApS.

References

Almagro, L., Fernández-Pérez, F., Pedreño, M.A., 2015. Indole Alkaloids from Catharanthus roseus: Bioproduction and Their Effect on Human Health. Molecules 20, 2973–3000. https://doi.org/10.3390/molecules20022973

Andorfer, M.C., Lewis, J.C., 2018. Understanding and Improving the Activity of Flavin-Dependent Halogenases via Random and Targeted Mutagenesis. Annu. Rev. Biochem. 87, 159–185. https://doi.org/10.1146/annurev-biochem-062917-012042

Bergdahl, B., Gorwa-Grauslund, M.F., van Niel, E.W., 2014. Physiological effects of over-expressing compartment-specific components of the protein folding machinery in xylose-fermenting Saccharomyces cerevisiae. BMC Biotechnol. 14, 28. https://doi.org/10.1186/1472-6750-14-28

Bernhardt, P., McCoy, E., O'Connor, S.E., 2007. Rapid Identification of Enzyme Variants for Reengineered Alkaloid Biosynthesis in Periwinkle. Chem. Biol. 14, 888–897. https://doi.org/10.1016/j.chembiol.2007.07.008

Brown, S., Clastre, M., Courdavault, V., O'Connor, S.E., 2015. De novo production of the plant-derived alkaloid strictosidine in yeast. Proc. Natl. Acad. Sci. 112, 3205–3210. https://doi.org/10.1073/pnas.1423555112

Cervenka, I., Agudelo, L.Z., Ruas, J.L., 2017. Kynurenines: Tryptophan's metabolites in exercise, inflammation, and mental health. Science 357, eaaf9794. https://doi.org/10.1126/science.aaf9794

Chadha, N., Silakari, O., 2017. Indoles as therapeutics of interest in medicinal chemistry: Bird's eye view. Eur. J. Med. Chem. 134, 159–184. https://doi.org/10.1016/j.ejmech.2017.04.003

Chung, W., Vanderwal, C.D., 2016. Stereoselective Halogenation in Natural Product Synthesis. Angew. Chem. Int. Ed. 55, 4396–4434. https://doi.org/10.1002/anie.201506388

Coury, L.A., McGeoch, J.E.M., Guidotti, G., Brodsky, J.L., 1999. The yeast Saccharomyces cerevisiae does not sequester chloride but can express a functional mammalian chloride channel. FEMS Microbiol. Lett. 179, 327–332. https://doi.org/10.1111/j.1574-6968.1999.tb08745.x

Dachwitz, S., Duwe, D.H., Wang, Y.H., Gruß, H., Hannappel, Y., Hellweg, T., Sewald, N., 2020. Suzuki–Miyaura Cross-Coupling of Bromotryptophan Derivatives at Ambient Temperature. Chem. – Eur. J. 26, 16357–16364. https://doi.org/10.1002/chem.202002454

Dunn, M.F., Niks, D., Ngo, H., Barends, T.R.M., Schlichting, I., 2008. Tryptophan synthase: the workings of a channeling nanomachine. Trends Biochem. Sci. 33, 254–264. https://doi.org/10.1016/j.tibs.2008.04.008

Enomoto, K., Arikawa, Y., Muratsubaki, H., 2002. Physiological role of soluble fumarate reductase in redox balancing during anaerobiosis in Saccharomyces cerevisiae. FEMS Microbiol. Lett. 215, 103–108. https://doi.org/10.1111/j.1574-6968.2002.tb11377.x

Entian, K.-D., Kötter, P., 2007. 25 Yeast Genetic Strain and Plasmid Collections, in: Stansfield, I., Stark, M.J. (Eds.), Methods in Microbiology, Yeast Gene Analysis. Academic Press, pp. 629–666. https://doi.org/10.1016/S0580-9517(06)36025-4

Fräbel, S., Krischke, M., Staniek, A., Warzecha, H., 2016. Recombinant flavin-dependent halogenases are functional in tobacco chloroplasts without co-expression of flavin reductase genes. Biotechnol. J. 11, 1586–1594. https://doi.org/10.1002/biot.201600337

Fräbel, S., Wagner, B., Krischke, M., Schmidts, V., Thiele, C.M., Staniek, A., Warzecha, H., 2018. Engineering of new-to-nature halogenated indigo precursors in plants. Metab. Eng. 46, 20–27. https://doi.org/10.1016/j.ymben.2018.02.003

Frese, M., Sewald, N., 2015. Enzymatic Halogenation of Tryptophan on a Gram Scale. Angew. Chem. Int. Ed. 54, 298–301. https://doi.org/10.1002/anie.201408561

Galán, B., Díaz, E., Prieto, M.A., García, J.L., 2000. Functional Analysis of the Small Component of the 4-Hydroxyphenylacetate 3-Monooxygenase of Escherichia coli W: a Prototype of a New Flavin:NAD(P)H Reductase Subfamily. J. Bacteriol. 182, 627–636. https://doi.org/10.1128/JB.182.3.627-636.2000

Gentry, C.L., Egleton, R.D., Gillespie, T., Abbruscato, T.J., Bechowski, H.B., Hruby, V.J., Davis, T.P., 1999. The effect of halogenation on blood–brain barrier permeability of a novel peptide drug☆. Peptides 20, 1229–1238. https://doi.org/10.1016/S0196-9781(99)00127-8

Gerebtzoff, G., Li-Blatter, X., Fischer, H., Frentzel, A., Seelig, A., 2004. Halogenation of Drugs Enhances Membrane Binding and Permeation. ChemBioChem 5, 676–684. https://doi.org/10.1002/cbic.200400017

Gietz, R.D., Schiestl, R.H., 2007. High-efficiency yeast transformation using the LiAc/SS carrier DNA/PEG method. Nat. Protoc. 2, 31–34. https://doi.org/10.1038/nprot.2007.13

Glenn, W.S., Nims, E., O'Connor, S.E., 2011. Reengineering a Tryptophan Halogenase To Preferentially Chlorinate a Direct Alkaloid Precursor. J. Am. Chem. Soc. 133, 19346–19349. https://doi.org/10.1021/ja2089348

Grote, A., Hiller, K., Scheer, M., Münch, R., Nörtemann, B., Hempel, D.C., Jahn, D., 2005. JCat: a novel tool to adapt codon usage of a target gene to its potential expression host. Nucleic Acids Res. 33, W526–W531. https://doi.org/10.1093/nar/gki376

Gul, W., Hamann, M.T., 2005. Indole alkaloid marine natural products: An established source of cancer drug leads with considerable promise for the control of parasitic, neurological and other diseases. Life Sci., NATURECEUTICALS (NATURAL PRODUCTS), NUTRACEUTICALS, HERBAL BOTANICALS, AND PSYCHOACTIVES: DRUG DISCOVERY AND DRUG-DRUG INTERACTIONS 78, 442–453. https://doi.org/10.1016/j.lfs.2005.09.007

Hausjell, J., Halbwirth, H., Spadiut, O., 2018. Recombinant production of eukaryotic cytochrome P450s in microbial cell factories. Biosci. Rep. 38. https://doi.org/10.1042/BSR20171290

Jampilek, J., 2019. Heterocycles in Medicinal Chemistry. Molecules 24, 3839. https://doi.org/10.3390/molecules24213839

J. Corr, M., V. Sharma, S., Pubill-Ulldemolins, C., T. Bown, R., Poirot, P., M. Smith, D.R., Cartmell, C., Fayad, A.A., M. Goss, R.J., 2017. Sonogashira diversification of unprotected halotryptophans, halotryptophan containing tripeptides; and generation of a new to nature bromo-natural product and its diversification in water. Chem. Sci. 8, 2039–2046. https://doi.org/10.1039/C6SC04423A

Jennings, M.L., Cui, J., 2008. Chloride Homeostasis in Saccharomyces cerevisiae: High Affinity Influx, V-ATPase-dependent Sequestration, and Identification of a Candidate Cl– Sensor. J. Gen. Physiol. 131, 379–391. https://doi.org/10.1085/jgp.200709905

Jensen, N.B., Strucko, T., Kildegaard, K.R., David, F., Maury, J., Mortensen, U.H., Forster, J., Nielsen, J., Borodina, I., 2014. EasyClone: method for iterative chromosomal integration of multiple genes Saccharomyces cerevisiae. FEMS Yeast Res. 14, 238–248. https://doi.org/10.1111/1567-1364.12118

Jessop-Fabre, M.M., Jakočiūnas, T., Stovicek, V., Dai, Z., Jensen, M.K., Keasling, J.D., Borodina, I., 2016. EasyClone-MarkerFree: A vector toolkit for marker-less integration of genes into *Saccharomyces cerevisiae* via CRISPR-Cas9. Biotechnol. J. 11, 1110–1117. https://doi.org/10.1002/biot.201600147

Jin, X., Wang, M., Shentu, J., Huang, C., Bai, Y., Pan, H., Zhang, D., Yuan, Z., Zhang, H., Xiao, X., Wu, X., Ding, L., Wang, Q., He, S., Cui, W., 2020. Inhibition of acetylcholinesterase activity and β-amyloid oligomer formation by 6-bromotryptamine A, a multi-target anti-Alzheimer's molecule. Oncol. Lett. 19, 1593–1601. https://doi.org/10.3892/ol.2019.11226

Kandel, S.E., Wienkers, L.C., Lampe, J.N., 2014. Chapter Twenty-Two - Cytochrome P450 Enzyme Metabolites in Lead Discovery and Development, in: Desai, M.C. (Ed.), Annual Reports in Medicinal Chemistry. Academic Press, pp. 347–359. https://doi.org/10.1016/B978-0-12-800167-7.00022-5

Kendrew, S.G., Harding, S.E., Hopwood, D.A., Marsh, E.N.G., 1995. Identification of a Flavin:NADH Oxidoreductase Involved in the Biosynthesis of Actinorhodin: PURIFICATION AND CHARACTERIZATION OF THE RECOMBINANT ENZYME. J. Biol. Chem. 270, 17339–17343. https://doi.org/10.1074/jbc.270.29.17339

Kerbs, A., Burgardt, A., Veldmann, K.H., Schäffer, T., Lee, J.-H., Wendisch, V.F., 2022. Fermentative Production of Halogenated Tryptophan Derivatives with

Corynebacterium glutamicum Overexpressing Tryptophanase or Decarboxylase Genes. ChemBioChem 23, e202200007. https://doi.org/10.1002/cbic.202200007

Kildegaard, K.R., Arnesen, J.A., Adiego-Pérez, B., Rago, D., Kristensen, M., Klitgaard, A.K., Hansen, E.H., Hansen, J., Borodina, I., 2021. Tailored biosynthesis of gibberellin plant hormones in yeast. Metab. Eng. 66, 1–11. https://doi.org/10.1016/j.ymben.2021.03.010

Kim, H.J., Winge, D.R., 2013. Emerging concepts in the flavinylation of succinate dehydrogenase. Biochim. Biophys. Acta BBA - Bioenerg. 1827, 627–636. https://doi.org/10.1016/j.bbabio.2013.01.012

Kochanowska, A.J., Rao, K.V., Childress, S., El-Alfy, A., Matsumoto, R.R., Kelly, M., Stewart, G.S., Sufka, K.J., Hamann, M.T., 2008. Secondary Metabolites from Three Florida Sponges with Antidepressant Activity. J. Nat. Prod. 71, 186–189. https://doi.org/10.1021/np070371u

Lai, H.-E., Obled, A.M.C., Chee, S.M., Morgan, R.M., Lynch, R., Sharma, S.V., Moore, S.J., Polizzi, K.M., Goss, R.J.M., Freemont, P.S., 2021. GenoChemetic Strategy for Derivatization of the Violacein Natural Product Scaffold. ACS Chem. Biol. 16, 2116–2123. https://doi.org/10.1021/acschembio.1c00483

Latham, J., Brandenburger, E., Shepherd, S.A., Menon, B.R.K., Micklefield, J., 2018. Development of Halogenase Enzymes for Use in Synthesis. Chem. Rev. 118, 232–269. https://doi.org/10.1021/acs.chemrev.7b00032

Lee, J., Kim, J., Song, J.E., Song, W.-S., Kim, E.-J., Kim, Y.-G., Jeong, H.-J., Kim, H.R., Choi, K.-Y., Kim, B.-G., 2020. Production of Tyrian purple indigoid dye from tryptophan in Escherichia coli. Nat. Chem. Biol. 1–9. https://doi.org/10.1038/s41589-020-00684-4

Lee, J.-H., Lee, J., 2010. Indole as an intercellular signal in microbial communities. FEMS Microbiol. Rev. 34, 426–444. https://doi.org/10.1111/j.1574-6976.2009.00204.x

Lee, J.-K., Zhao, H., 2007. Identification and Characterization of the Flavin:NADH Reductase (PrnF) Involved in a Novel Two-Component Arylamine Oxygenase. J. Bacteriol. 189, 8556–8563. https://doi.org/10.1128/JB.01050-07

Li, Y., Li, S., Thodey, K., Trenchard, I., Cravens, A., Smolke, C.D., 2018. Complete biosynthesis of noscapine and halogenated alkaloids in yeast. Proc. Natl. Acad. Sci. 115, E3922–E3931. https://doi.org/10.1073/pnas.1721469115

Luo, X., Reiter, M.A., d'Espaux, L., Wong, J., Denby, C.M., Lechner, A., Zhang, Y., Grzybowski, A.T., Harth, S., Lin, W., Lee, H., Yu, C., Shin, J., Deng, K., Benites, V.T., Wang, G., Baidoo, E.E.K., Chen, Y., Dev, I., Petzold, C.J., Keasling, J.D., 2019. Complete biosynthesis of cannabinoids and their unnatural analogues in yeast. Nature 567, 123–126. https://doi.org/10.1038/s41586-019-0978-9

Mačiulaitis, R., Kontrimavičiūtė, V., Bressolle, F., Briedis, V., 2008. Ibogaine, an anti-addictive drug: pharmacology and time to go further in development. A narrative review. Hum. Exp. Toxicol. 27, 181–194. https://doi.org/10.1177/0960327107087802

Maddox, S.M., Nalbandian, C.J., Smith, D.E., Gustafson, J.L., 2015. A Practical Lewis Base Catalyzed Electrophilic Chlorination of Arenes and Heterocycles. Org. Lett. 17, 1042–1045. https://doi.org/10.1021/acs.orglett.5b00186

Mashiguchi, K., Tanaka, K., Sakai, T., Sugawara, S., Kawaide, H., Natsume, M., Hanada, A., Yaeno, T., Shirasu, K., Yao, H., McSteen, P., Zhao, Y., Hayashi, K., Kamiya, Y., Kasahara, H., 2011. The main auxin biosynthesis pathway in Arabidopsis. Proc. Natl. Acad. Sci. 108, 18512–18517. https://doi.org/10.1073/pnas.1108434108

McCoy, E., O'Connor, S.E., 2006. Directed Biosynthesis of Alkaloid Analogs in the Medicinal Plant *Catharanthus roseus*. J. Am. Chem. Soc. 128, 14276–14277. https://doi.org/10.1021/ja066787w

Mendez, L., Henriquez, G., Sirimulla, S., Narayan, M., 2017. Looking Back, Looking Forward at Halogen Bonding in Drug Discovery. Molecules 22, 1397. https://doi.org/10.3390/molecules22091397

Milne, N., Thomsen, P., Mølgaard Knudsen, N., Rubaszka, P., Kristensen, M., Borodina, I., 2020. Metabolic engineering of Saccharomyces cerevisiae for the de novo production

of psilocybin and related tryptamine derivatives. Metab. Eng. 60, 25–36. https://doi.org/10.1016/j.ymben.2019.12.007

Nielsen, C.A., Folly, C., Hatsch, A., Molt, A., Schröder, H., O'Connor, S.E., Naesby, M., 2014. The important ergot alkaloid intermediate chanoclavine-I produced in the yeast Saccharomyces cerevisiae by the combined action of EasC and EasE from Aspergillus japonicus. Microb. Cell Factories 13, 95. https://doi.org/10.1186/s12934-014-0095-2

O'Boyle, N.M., Banck, M., James, C.A., Morley, C., Vandermeersch, T., Hutchison, G.R., 2011. Open Babel: An open chemical toolbox. J. Cheminformatics 3, 33. https://doi.org/10.1186/1758-2946-3-33

O'Connor, S.E., Maresh, J.J., 2006. Chemistry and biology of monoterpene indole alkaloid biosynthesis. Nat. Prod. Rep. 23, 532. https://doi.org/10.1039/b512615k

Park, H.B., Lam, Y.C., Gaffney, J.P., Weaver, J.C., Krivoshik, S.R., Hamchand, R., Pieribone, V., Gruber, D.F., Crawford, J.M., 2019. Bright Green Biofluorescence in Sharks Derives from Bromo-Kynurenine Metabolism. iScience 19, 1291–1336. https://doi.org/10.1016/j.isci.2019.07.019

Parry, R.J., Li, W., 1997. An NADPH:FAD Oxidoreductase from the Valanimycin Producer, Streptomyces viridifaciens: CLONING, ANALYSIS, AND OVEREXPRESSION*. J. Biol. Chem. 272, 23303–23311. https://doi.org/10.1074/jbc.272.37.23303

Payne, J.T., Andorfer, M.C., Lewis, J.C., 2013. Regioselective Arene Halogenation using the FAD-Dependent Halogenase RebH. Angew. Chem. Int. Ed. 52, 5271–5274. https://doi.org/10.1002/anie.201300762

Payne, J.T., Poor, C.B., Lewis, J.C., 2015. Directed Evolution of RebH for Site-Selective Halogenation of Large Biologically Active Molecules. Angew. Chem. Int. Ed. 54, 4226–4230. https://doi.org/10.1002/anie.201411901

Petrone, D.A., Ye, J., Lautens, M., 2016. Modern Transition-Metal-Catalyzed Carbon–Halogen Bond Formation. Chem. Rev. 116, 8003–8104. https://doi.org/10.1021/acs.chemrev.6b00089

Poor, C.B., Andorfer, M.C., Lewis, J.C., 2014. Improving the Stability and Catalyst Lifetime of the Halogenase RebH By Directed Evolution. ChemBioChem 15, 1286–1289. https://doi.org/10.1002/cbic.201300780

Pozharskii, A.F., Soldatenkov, A.T., Katritzky, A.R., 2011. Why Nature Prefers Heterocycles, in: Heterocycles in Life and Society. John Wiley & Sons, Ltd, Chichester, UK, pp. 11–33. https://doi.org/10.1002/9781119998372.ch2

Prieto-Díaz, R., González-Gómez, M., Fojo-Carballo, H., Azuaje, J., El Maatougui, A., Majellaro, M., Loza, M.I., Brea, J., Fernández-Dueñas, V., Paleo, M.R., Díaz-Holguín, A., Garcia-Pinel, B., Mallo-Abreu, A., Estévez, J.C., Andújar-Arias, A., García-Mera, X., Gomez-Tourino, I., Ciruela, F., Salas, C.O., Gutiérrez-de-Terán, H., Sotelo, E., 2023. Exploring the Effect of Halogenation in a Series of Potent and Selective A2B Adenosine Receptor Antagonists. J. Med. Chem. 66, 890–912. https://doi.org/10.1021/acs.jmedchem.2c01768

Richard, D.M., Dawes, M.A., Mathias, C.W., Acheson, A., Hill-Kapturczak, N., Dougherty, D.M., 2009. L-Tryptophan: Basic Metabolic Functions, Behavioral Research and Therapeutic Indications. Int. J. Tryptophan Res. IJTR 2, 45–60.

Ro, D.-K., Paradise, E.M., Ouellet, M., Fisher, K.J., Newman, K.L., Ndungu, J.M., Ho, K.A., Eachus, R.A., Ham, T.S., Kirby, J., Chang, M.C.Y., Withers, S.T., Shiba, Y., Sarpong, R., Keasling, J.D., 2006. Production of the antimalarial drug precursor artemisinic acid in engineered yeast. Nature 440, 940–943. https://doi.org/10.1038/nature04640

Rodriguez, R.A., Pan, C.-M., Yabe, Y., Kawamata, Y., Eastgate, M.D., Baran, P.S., 2014. Palau'chlor: A Practical and Reactive Chlorinating Reagent. J. Am. Chem. Soc. 136, 6908–6911. https://doi.org/10.1021/ja5031744

Runguphan, W., Qu, X., O'Connor, S.E., 2010. Integrating carbon–halogen bond formation into medicinal plant metabolism. Nature 468, 461–464. https://doi.org/10.1038/nature09524

Schnepel, C., Sewald, N., 2017. Enzymatic Halogenation: A Timely Strategy for Regioselective C–H Activation. Chem. – Eur. J. 23, 12064–12086. https://doi.org/10.1002/chem.201701209

Sharma, S.V., Tong, X., Pubill-Ulldemolins, C., Cartmell, C., Bogosyan, E.J.A., Rackham, E.J., Marelli, E., Hamed, R.B., Goss, R.J.M., 2017. Living GenoChemetics by hyphenating synthetic biology and synthetic chemistry in vivo. Nat. Commun. 8, 229. https://doi.org/10.1038/s41467-017-00194-3

Shepherd, S.A., Karthikeyan, C., Latham, J., Struck, A.-W., Thompson, M.L., Menon, B.R.K., Styles, M.Q., Levy, C., Leys, D., Micklefield, J., 2015. Extending the biocatalytic scope of regiocomplementary flavin-dependent halogenase enzymes. Chem. Sci. 6, 3454–3460. https://doi.org/10.1039/C5SC00913H

Sravanthi, T.V., Manju, S.L., 2016. Indoles — A promising scaffold for drug development. Eur. J. Pharm. Sci. 91, 1–10. https://doi.org/10.1016/j.ejps.2016.05.025

Taskesenligil, Y., Aslan, M., Cogurcu, T., Saracoglu, N., 2023. Directed C–H Functionalization of C3-Aldehyde, Ketone, and Acid/Ester-Substituted Free (NH) Indoles with Iodoarenes *via* a Palladium Catalyst System. J. Org. Chem. 88, 1299–1318. https://doi.org/10.1021/acs.joc.2c00716

Torrens-Spence, M.P., Liu, C.-T., Pluskal, T., Chung, Y.K., Weng, J.-K., 2018. Monoamine Biosynthesis via a Noncanonical Calcium-Activatable Aromatic Amino Acid Decarboxylase in Psilocybin Mushroom. ACS Chem. Biol. 13, 3343–3353. https://doi.org/10.1021/acschembio.8b00821

Trott, O., Olson, A.J., 2010. AutoDock Vina: improving the speed and accuracy of docking with a new scoring function, efficient optimization and multithreading. J. Comput. Chem. 31, 455–461. https://doi.org/10.1002/jcc.21334

Tylš, F., Páleníček, T., Horáček, J., 2014. Psilocybin – Summary of knowledge and new perspectives. Eur. Neuropsychopharmacol. 24, 342–356. https://doi.org/10.1016/j.euroneuro.2013.12.006

van Pée, K.-H., Patallo, E.P., 2006. Flavin-dependent halogenases involved in secondary metabolism in bacteria. Appl. Microbiol. Biotechnol. 70, 631–641. https://doi.org/10.1007/s00253-005-0232-2

Vécsei, L., Szalárdy, L., Fülöp, F., Toldi, J., 2013. Kynurenines in the CNS: recent advances and new questions. Nat. Rev. Drug Discov. 12, 64–82. https://doi.org/10.1038/nrd3793

Veldmann, K.H., Dachwitz, S., Risse, J.M., Lee, J.-H., Sewald, N., Wendisch, V.F., 2019a. Bromination of L-tryptophan in a Fermentative Process With Corynebacterium glutamicum. Front. Bioeng. Biotechnol. 7, 219. https://doi.org/10.3389/fbioe.2019.00219

Veldmann, K.H., Minges, H., Sewald, N., Lee, J.-H., Wendisch, V.F., 2019b. Metabolic engineering of Corynebacterium glutamicum for the fermentative production of halogenated tryptophan. J. Biotechnol. 291, 7–16. https://doi.org/10.1016/j.jbiotec.2018.12.008

Volkov, V., 2015. Quantitative description of ion transport via plasma membrane of yeast and small cells. Front. Plant Sci. 6.

Wan, Y., Li, Y., Yan, C., Yan, M., Tang, Z., 2019. Indole: A privileged scaffold for the design of anti-cancer agents. Eur. J. Med. Chem. 183, 111691. https://doi.org/10.1016/j.ejmech.2019.111691

Watkins-Dulaney, E., Straathof, S., Arnold, F., 2020. Tryptophan Synthase: Biocatalyst Extraordinaire. ChemBioChem cbic.202000379. https://doi.org/10.1002/cbic.202000379

Xu, Z., Yang, Z., Liu, Y., Lu, Y., Chen, K., Zhu, W., 2014. Halogen Bond: Its Role beyond Drug–Target Binding Affinity for Drug Discovery and Development. J. Chem. Inf. Model. 54, 69–78. https://doi.org/10.1021/ci400539q

Yeh, E., Garneau, S., Walsh, C.T., 2005. Robust in vitro activity of RebF and RebH, a two-component reductase/halogenase, generating 7-chlorotryptophan during

rebeccamycin biosynthesis. Proc. Natl. Acad. Sci. 102, 3960–3965. https://doi.org/10.1073/pnas.0500755102

Young, J., Garikipati, N., Durrant, J.D., 2022. BINANA 2: Characterizing Receptor/Ligand Interactions in Python and JavaScript. J. Chem. Inf. Model. 62, 753–760. https://doi.org/10.1021/acs.jcim.1c01461

Zehner, S., Kotzsch, A., Bister, B., Süssmuth, R.D., Méndez, C., Salas, J.A., van Pée, K.-H., 2005. A Regioselective Tryptophan 5-Halogenase Is Involved in Pyrroindomycin Biosynthesis in Streptomyces rugosporus LL-42D005. Chem. Biol. 12, 445–452. https://doi.org/10.1016/j.chembiol.2005.02.005

Zeng, J., Zhan, J., 2011. Characterization of a tryptophan 6-halogenase from Streptomyces toxytricini. Biotechnol. Lett. 33, 1607–1613. https://doi.org/10.1007/s10529-011-0595-7

Zhang, J., Petersen, S.D., Radivojevic, T., Ramirez, A., Pérez-Manríquez, A., Abeliuk, E., Sánchez, B.J., Costello, Z., Chen, Y., Fero, M.J., Martin, H.G., Nielsen, J., Keasling, J.D., Jensen, M.K., 2020. Combining mechanistic and machine learning models for predictive engineering and optimization of tryptophan metabolism. Nat. Commun. 11, 4880. https://doi.org/10.1038/s41467-020-17910-1

Engineering *Saccharomyces cerevisiae* for the *de novo* production of halogenated tryptophan and tryptamine derivatives

Supporting information

Table S1. Binana2 calculated interactions for docking of L-tryptophan and 5-halo-tryptophan in SrPyrH, L-Tryptophan and 6-halo-tryptophan in SttH, and L-tryptophan and 7-halo-tryptophan in LaRebH. Docking is carried out with either Br or Cl in each of the structures.

Protein	Interactions	Molecule	Molecule	Protein	Molecule	Molecule
SrPyrH-Br		**L-Tryptophan**	**5-Br-Tryptophan**	**SrPyrH-Cl**	**L-Tryptophan**	**5-Cl-Tryptophan**
	Hydrophobic	Phe49, Ile78, His92, Phe94, Phe451, Tyr454	Phe49, Thr51, His92, Phe94, Phe451, Tyr454		Phe49, Ile78, His92, Phe94, Phe451, Tyr454	Phe49, Thr51, His92, Phe94, Phe451, Tyr454
	Salt bridge	-	-		-	-
	Hydrogen bond	Amine N-Ser50 NH 3.4 Å Amine NH-Ser50 OG 3.4 Å	Amine NH-Ser50 OG 3.2 Å		Amine N-Ser50 NH 3.5 Å Amine NH-Ser50 OG 3.4 Å	Amine N-Ser50 NH 3.3 Å Amine NH-Ser50 OG 3.3 Å
	Halogen bond	-	Br-Ser355 OG 4.7 Å		-	Cl-Ser355 O 5.5 Å Cl-Ser355 OG 4.5 Å
	Cation-π-interaction	-	-		-	-
	π-π-stacking	Pyrrole-His92 4.3 Å Benzene-His92 4.7 Å	Benzene-His92 4.4 Å		Pyrrole-His92 4.3 Å Benzene-His92 4.7 Å	Benzene-His92 4.4 Å
	T-stacking	Pyrrole-Phe49 5.5 Å	Pyrrole-Phe49 5.4 Å		Pyrrole-Phe49 5.8 Å	Pyrrole-Phe49 5.4 Å
SttH-Br		**L-Tryptophan**	**6-Br-tryptophan**	**SttH-Cl**	**L-Tryptophan**	**6-Cl-tryptophan**
	Hydrophobic	Phe53, Ser54, Lys79, Val82, His96, Pro97, Phe98, Glu363, Pro461	Phe53, Ser54, Lys79, Val82, His96, Pro97, Phe98, Glu363, Pro461		Phe53, Ser54, Ala81, Val82, His96, Phe98, Glu363, Leu460, Tyr463	Phe53, Ser54,Lys79, Val82, His96, Pro97, Phe98, Glu363, Pro461
	Salt bridge	-	-			-
	Hydrogen bond	Carboxylate O-Tyr463 OH 2.5 Å	Carboxylate O-Tyr463 OH 2.5 Å		Carboxylate O-Tyr463 OH 3.1 Å	Carboxylate O-Tyr463 OH 2.5 Å
	Halogen bond	-	-		-	-
	Cation-π-interaction	Amine-Phe53 3.0 Å Pyrrole-His96 3.0 Å	Amine-Phe53 3.1 Å Pyrrole-His96 3.0 Å		Pyrrole-His96 3.0 Å Benzene-His96 3.2 Å	Amine-Phe93 3.1 Å Pyrrole-His96 3.0 Å
	π-π-stacking:	Pyrrole-His96 3.1 Å Benzene-His96 3.9 Å	Pyrrole-His96 3.1 Å Benzene-His96 3.9 Å		-	Pyrrole-His96 3.0 Å Benzene-His96 3.9 Å
	T-stacking:	Pyrrole-Phe98 5.0 Å	Pyrrole-Phe98 5.0 Å		-	Pyrrole-Phe98 5.0 Å
LaRebH-Br		**L-Tryptophan**	**7-Br-tryptophan**	**LaRebH-Cl**	**L-Tryptophan**	**7-Cl-tryptophan**
	Hydrophobic	Ile52, Lys79, Ile82, His109, Ser110, Phe111, Glu357, Ser358, Tyr454, Asn470	Ile52, Lys79, Ile82, His109, Ser110, Phe111, Glu357, Tyr454, Asn470		Ile52, Lys79, Ile82, His109, Ser110, Phe111, Glu357, Ser358, Tyr454, Asn470	Ile52, Lys79, Ile82, His109, Ser110, Phe111, Glu357, Tyr454, Asn470
	Salt bridge	Amine-Glu461 5.1 Å	Amine-Glu461 4.8 Å		Amine-Glu461 5.1 Å	Amine-Glu461 5.0 Å
	Hydrogen bond	Indole NH-His109 0 3.3 Å	Indole NH-His109 0 3.5 Å		Indole NH-His109 0 3.2 Å	Indole NH-His109 O 3.4 Å

	Halogen bond	-	Br-Ile82 N 4.8 Å	-	Br-Ile82 N 4.7Å
	Cation-π-interaction	Pyrrole-His109 3.4 Å	Pyrrole-His109 3.6 Å	Pyrrole-His109 3.5 Å	Pyrrole-His109 3.5 Å
	π-π-stacking:	Pyrrole-His109 3.6 Å Benzene His109 4.5 Å	Pyrrole-His109 3.6 Å Benzene His109 4.5 Å Benzene Phe111 4.5 Å	Pyrrole-His109 3.5Å Benzene His109 4.5 Å	Pyrrole-His109 3.6 Å Benzene His109 4.6 Å
	T-stacking:	-	-	-	-

Table S2: Binana2 calculated interactions for docking of 5-, 6- and 7-halo-tryptophan and 5-, 6- and 7-halo-tryptamine to CrTDC.

CrTDC	**5-Br-tryptophan**	**5-Br-tryptamine**	**5-Cl-tryptophan**	**5-Cl-tryptamine**
Hydrophobic	Trp92A, Phe100A, His318A, LLP319A, Val122B, Phe124B	Phe100A, Phe101A, Thr262A, His318A, Val122B, Phe124B, Thr369B, Gly370B	Phe100A, His318A, LLP319A, Leu325A, Val122B, Phe124B, Thr369B, Gly370B	Phe100A, His318A, LLP319A, Val122B, Phe124B, Thr369B, Gly370B
Salt bridge	-	-	-	-
Hydrogen bond	Indole N-Phe101A NH 3.6 Å Indole NH-Phe101 O 2.8 Å	Amine NH -Phe101A N 3.7 Å Indole NH-Gly370B N 3.7 Å	Indole NH-Gly370B N 3.1 Å	Indole NH-Gly370B N 3.6 Å Phe101A N Amine NH 3.9
Halogen bond	-	Br-Pro102A O 5.3 Å	Cl Pro102A O 4.8 Å Cl-Ala103A N 5.2 Å	Cl-Pro102A 5.0 Å Cl-Ala103A 5.4 Å
Cation-π-interaction	Pyrrole-LLP 4.6 Å Benzene-LLP 4.3 Å	Pyrrole-LLP 4.5Å Benzene-LLP 4.4 Å	-	Pyrrole-LLP 4.5 Å Benzene-LLP 4.4 Å
π-π-stacking:	-	Pyrrole-Phe124B 4.9 Å	-	Pyrrole-Phe124B 4.9 Å
T-stacking:	-	Pyrrole-LLP Pyridine 6.1 Å	-	Pyrrole-LLP Pyridine 6.3 Å
CrTDC	**6-Br-tryptophan**	**6-Br-tryptamine**	**6-Cl-tryptophan**	**6-Cl-tryptamine**
Hydrophobic	Phe101A, LLP319A, Val122B, Thr369B	Trp92A, Phe101A, His318A, LLP319A, Phe124B, Thr369B, Gly370B	Trp92A, Phe101A, LLP319A, Val122B, Thr369B	Trp92A, Phe100A, Phe101A, Thr262A, LLP319A, Val122B, Thr369B
Salt bridge	-	-	-	-
Hydrogen bond	Indole NH-Gly370B N 3.6 Å	-	-	Amine NH-Phe100A O 3.9 Å
Halogen bond	-	Br-His318A O 4.6 Å	Cl-Ala103A N 5.4 Å	-
Cation-π-interaction	Benzene-LLP319A 3.9 Å	Benzene-LLP319A 4.1 Å Amine-Phe124B 5.5 Å	Benzene-LLP319A 4.0 Å	Amine-Phe101A 4.1 Å Benzene-LLP319A 4.2 Å Pyrrole-LLP319A 4.3 Å
π-π-stacking:	-	-	-	-
T-stacking:	-	Pyrrole-LLP Pyridine 6.5Å	-	-
CrTDC	**7-Br-tryptophan**	**7-Br-tryptamine**	**7-Cl-tryptophan**	**7-Cl-tryptamine**
Hydrophobic	Phe101A, LLP319A, Val122B, Thr369B	Trp92A, Phe100A, Phe101A, His318A, LLP319A, Val122B, Phe124B, Thr369B	Phe101A, LLP319A, Val122B, Phe124B, Thr369B	Trp92A, Phe100A, Phe101A, His318A, LLP319A, Val122B, Phe124B, Thr369B
Salt bridge	-	-	-	-
Hydrogen bond	-	Amine NH-Phe101A N 3.8 Å Indole NH-Gly370B N 4.0 Å	-	Amine NH-Phe101A N 3.8Å Indole NH-Gly370B N 3.9 Å
Halogen bond	-	-	-	-
Cation-π-interaction	Benzene-LLP319A 3.9 Å	Benzene-LLP319A 4.5 Å Pyrrole-LLP319A 4.4 Å	Benzene-LLP319A 4.0 Å	Benzene-LLP319A 4.6 Å Pyrrole-LLP319A 4.4 Å
π-π-stacking:	-	Pyrrole-Phe124B 5.0 Å	-	Pyrrole-Phe124B 5.0 Å
T-stacking:	-	-	-	-

Table S3. DNA sequences of synthetic genes codon optimized for *S. cerevisiae*.

SrPyrH	ATGATCAGATCTGTTGTTATCGTTGGTGGTGGTACTGCTGGTTGGATGACTGCTTCTTACTTGAAGGCTG CTTTCGACGACAGAATCGACGTTACTTTGGTTGAATCTGGTAACGTTAGAAGAATCGGTGTTGGTGAAGC TACTTTCTCTACTGTTAGACACTTCTTCGACTACTTGGGTTTGGACGAAAGAGAATGGTTGCCAAGATGTG CTGGTGGTTACAAGTTGGGTATCAGATTCGAAAACTGGTCTGAACCAGGTGAATACTTCTACCACCCATTC GAAAGATTGAGAGTTGTTGACGGTTTCAACATGGCTGAATGGTGGTTGGCTGTTGGTGACAGAAGAACTT CTTTCTCTGAAGCTTGTTACTTGACTCACAGATTGTGTGAAGCTAAGAGAGCTCCAAGAATGTTGGACGGT TCTTTGTTCGCTTCTCAAGTTGACGAATCTTTGGGTAGATCTACTTTGGCTGAACAAAGAGCTCAATTCCC ATACGCTTACCACTTCGACGCTGACGAAGTTGCTAGATACTTGTCTGAATACGCTATCGCTAGAGGTGTTA GA CACGTTGTTGACGACGTTCAACACGTTGGTCAAGACGAAAGAGGTTGGATCTCTGGTGTTCACACTAAGC AACACGGTGAAATCTCTGGTGACTTGTTCGTTGACTGTACTGGTTTCAGAGGTTTGTTGATCAACCAAACT TTGGGTGGTAGATTCCAATCTTTCTCTGACGTTTTGCCAAACAACAGAGCTGTTGCTTTGAGAGTTCCAAG AGAAAACGACGAAGACATGAGACCATACACTACTGCTACTGCTATGTCTGCTGGTTGGATGTGGACTATC CCATTGTTCAAGAGAGACGGTAACGGTTACGTTTACTCTGACGAATTCATCTCTCCAGAAGAAGCTGAAA GAGAATTGAGATCTACTGTTGCTCCAGGTAGAGACGACTTGGAAGCTAACCACATCCAAATGAGAATCGG TAGAAACGAAAGAACTTGGATCAACAACTGTGTTGCTGTTGGTTTGTCTGCTGCTTTCGTTGAACCATTGG AATCTACTGGTATCTTCTTCATCCAACACGCTATCGAACAATTGGTTAAGCACTTCCCAGGTGAAAGATGG GACCCAGTTTTGATCTCTGCTTACAACGAAAGAATGGCTCACATGGTTGACGGTGTTAAGGAATTCTTGGT TTTGCACTACAAGGGTGCTCAAAGAGAAGACACTCCATACTGGAAGGCTGCTAAGACTAGAGCTATGCCA GACGGTTTGGCTAGAAAGTTGGAATTGTCTGCTTCTCACTTGTTGGACGAACAAACTATCTACCCATACTA CCACGGTTTCGAAACTTACTCTTGGATCACTATGAACTTGGGTTTGGGTATCGTTCCAGAAAGACCAAGAC CAGCTTTGTTGCACATGGACCCAGCTCCAGCTTTGGCTGAATTCGAAAGATTGAGAAGAGAAGGTGACGA ATTGATCGCTGCTTTGCCATCTTGTTACGAATACTTGGCTTCTATCCAATAG
SttH	ATGAACACTAGAAACCCAGACAAGGTTGTTATCGTTGGTGGTGGTACTGCTGGTTGGATGACTGCTTCTT ACTTGAAGAAGGCTTTCGGTGAAAGAGTTTCTGTTACTTTGGTTGAATCTGGTACTATCGGTACTGTTGGT GTTGGTGAAGCTACTTTCTCTGACATCAGACACTTCTTCGAATTCTTGGACTTGAGAGAAGAAGAATGGAT GCCAGCTTGTAACGCTACTTACAAGTTGGCTGTTAGATTCCAAGACTGGCAAAGACCAGGTCACCACTTCT ACCACCCATTCGAACAAATGAGATCTGTTGACGGTTTCCCATTGACTGACTGGTGGTTGCAAAACGGTCCA ACTGACAGATTCGACAGAGACTGTTTCGTTATGGCTTCTTTGTGTGACGCTGGTAGATCTCCAAGATACTT GAACGGTTCTTTGTTGCAACAAGAATTCGACGAAAGAGCTGAAGAACCAGCTGGTTTGACTATGTCTGAA CACCAAGGTAAGACTCAATTCCCATACGCTTACCACTTCGAAGCTGCTTTGTTGGCTGAATTCTTGTCTGG TTACTCTAAGGACAGAGGTGTTAAGCACGTTGTTGACGAAGTTTTGGAAGTTAAGTTGGACGACAGAGGT TGGATCTCTCACGTTGTTACTAAGGAACACGGTGACATCGGTGGTGACTTGTTCGTTGACTGTACTGGTTT CAGAGGTGTTTTGTTGAACCAAGCTTTGGGTGTTCCATTCGTTTCTTACCAAGACACTTTGCCAAACGACT CTGCTGTTGCTTTGCAAGTTCCATTGGACATGGAAGCTAGAGGTATCCCACCATACACTAGAGCTACTGCT AAGGAAGCTGGTTGGATCTGGACTATCCCATTGATCGGTAGAATCGGTACTGGTTACGTTTACGCTAAGG ACTACTGTTCTCCAGAAGAAGCTGAAAGAACTTTGAGAGAATTCGTTGGTCCAGAAGCTGCTGACGTTGA AGCTAACCACATCAGAATGAGAATCGGTAGATCTGAACAATCTTGGAAGAACAACTGTGTTGCTATCGGT TTGTCTTCTGGTTTCGTTGAACCATTGGAATCTACTGGTATCTTCTTCATCCACCACGCTATCGAACAATTG GTTAAGCACTTCCCAGCTGGTGACTGGCACCCACAATTGAGAGCTGGTTACAACTCTGCTGTTGCTAACGT TATGGACGGTGTTAGAGAATTCTTGGTTTTGCACTACTTGGGTGCTGCTAGAAACGACACTAGATACTGG AAGGACACTAAGACTAGAGCTGTTCCAGACGCTTTGGCTGAAAGAATCGAAAGATGGAAGGTTCAATTGC CAGACTCTGAAAACGTTTTCCCATACTACCACGGTTTGCCACCATACTCTTACATGGCTATCTTGTTGGGT ACTGGTGCTATCGGTTTGAGACCATCTCCAGCTTTGGCTTTGGCTGACCCAGCTGCTGCTGAAAAGGAATT CACTGCTATCAGAGACAGAGCTAGATTCTTGGTTGACACTTTGCCATCTCAATACGAATACTTCGCTGCTA TGGGTCAAAGAGTTTAG
LaRebH	ATGTCTGGTAAGATCGACAAGATCTTGATCGTTGGTGGTGGTACTGCTGGTTGGATGGCTGCTTCTTACT TGGGTAAGGCTTTGCAAGGTACTGCTGACATCACTTTGTTGCAAGCTCCAGACATCCCAACTTTGGGTGTT GGTGAAGCTACTATCCCAAACTTGCAAACTGCTTTCTTCGACTTCTTGGGTATCCCAGAAGACGAATGGAT GAGAGAATGTAACGCTTCTTACAAGGTTGCTATCAAGTTCATCAACTGGAGAACTGCTGGTGAAGGTACT TCTGAAGCTAGAGAATTGGACGGTGGTCCAGACCACTTCTACCACTCTTTCGGTTTGTTGAAGTACCACGA ACAAATCCCATTGTCTCACTACTGGTTCGACAGATCTTACAGAGGTAAGACTGTTGAACCATTCGACTACG CTTGTTACAAGGAACCAGTTATCTTGGACGCTAACAGATCTCCAAGAAGATTGGACGGTTCTAAGGTTACT AACTACGCTTGGCACTTCGACGCTCACTTGGTTGCTGACTTCTTGAGAAGATTCGCTACTGAAAAGTTGGG TGTTAGACACGTTGAAGACAGAGTTGAACACGTTCAAAGAGACGCTAACGGTAACATCGAATCTGTTAGA ACTGCTACTGGTAGAGTTTTCGACGCTGACTTGTTCGTTGACTGTTCTGGTTTCAGAGGTTTGTTGATCAA CAAGGCTATGGAAGAACCATTCTTGGACATGTCTGACCACTTGTTGAACGACTCTGCTGTTGCTACTCAAG TTCCACACGACGACGACGCTAACGGTGTTGAACCATTCACTTCTGCTATCGCTATGAAGTCTGGTTGGACT TGGAAGATCCCAATGTTGGGTAGATTCGGTACTGGTTACGTTTACTCTTCTAGATTCGCTACTGAAGACGA AGCTGTTAGAGAATTCTGTGAAATGTGGCACTTGGACCCAGAAACTCAACCATTGAACAGAATCAGATTC AGAGTTGGTAGAAACAGAAGAGCTTGGGTTGGTAACTGTGTTTCTATCGGTACTTCTTCTTGTTTCGTTGA ACCATTGGAATCTACTGGTATCTACTTCGTTTACGCTGCTTTGTACCAATTGGTTAAGCACTTCCCAGACA AGTCTTTGAACCCAGTTTTGACTGCTAGATTCAACAGAGAAATCGAAACTATGTTCGACGACACTAGAGAC TTCATCCAAGCTCACTTCTACTTCTCTCCAAGAACTGACACTCCATTCTGGAGAGCTAACAAGGAATTGAG ATTGGCTGACGGTATGCAAGAAAAGATCGACATGTACAGAGCTGGTATGGCTATCAACGCTCCAGCTTCT GACGACGCTCAATTGTACTACGGTAACTTCGAAGAAGAATTCAGAAACTTCTGGAACAACTCTAACTACTA CTGTGTTTTGGCTGGTTTGGGTTTGGTTCCAGACGCTCCATCTCCAAGATTGGCTCACATGCCACAAGCTA CTGAATCTGTTGACGAAGTTTTCGGTGCTGTTAAGGACAGACAAAGAAACTTGTTGGAAACTTTGCCATCT TTGCACGAATTCTTGAGACAACAACACGGTAGATAG
LaRebF	ATGACTATCGAATTCGACAGACCAGGTGCTCACGTTACTGCTGCTGACCACAGAGCTTTGATGTCTTTGTT CCCAACTGGTGTTGCTGTTATCACTGCTATCGACGAAGCTGGTACTCCACACGGTATGACTTGTACTTCTT TGACTTCTGTTACTTTGGACCCACCAACTTTGTTGGTTTGTTTGAACAGAGCTTCTGGTACTTTGCACGCT GTTAGAGGTGGTAGATTCGGTGTTAACTTGTTGCACGCTAGAGGTAGAAGAGCTGCTGAAGTTTTCTCTA

CTGCTGTTCAAGACAGATTCGGTGAAGTTAGATGGGAACACTCTGACGTTACTGGTATGCCATGGTTGGC
TGAAGACGCTCACGCTTTCGCTGGTTGTGTTGTTAGAAAGTCTACTGTTGTTGGTGACCACGAAATCGTTT
TGGGTGAAGTTCACGAAGTTGTTAGAGAACACGACTTGCCATTGTTGTACGGTATGAGAGAATTCGCTGT
TTGGACTCCAGAAGGTTAG

Table S4. List of *S. cerevisiae* strains used in this study.

Name	Parental strain	Added DNA element	Relevant genotype	Source
CEN.PK113-7D	-	-	Mata *MAL2-8c SUC2 URA3 HIS3 LEU2 TRP1*	(Entian and Kötter, 2007)
ST7574	CEN.PK113-7D	pCfB2312	*MAL2-8c SUC2 URA3 HIS3 LEU2 TRP1* + pCfB2312 (Cas9)	(Milne et al., 2020b)
ST9336	ST7574	pCfB8881	*MAL2-8c SUC2 URA3 HIS3 LEU2 TRP1 XI-3:: CrTDC*	This study
ST9759	ST7574	pCfB9331	*MAL2-8c SUC2 URA3 HIS3 LEU2 TRP1 XI-1:: SrPyrH, LaRebF*	This study
ST9760	ST7574	pCfB9332	*MAL2-8c SUC2 URA3 HIS3 LEU2 TRP1 XI-1:: SrPyrH*	This study
ST9761	ST7574	pCfB9333	*MAL2-8c SUC2 URA3 HIS3 LEU2 TRP1 XII-5:: SttH, LaRebF*	This study
ST9762	ST7574	pCfB9334	*MAL2-8c SUC2 URA3 HIS3 LEU2 TRP1 XII-5:: SttH*	This study
ST9763	ST7574	pCfB9332, pCfB9333	*MAL2-8c SUC2 URA3 HIS3 LEU2 TRP1 XI-1:: SrPyrH XII-5:: SttH, LaRebF*	This study
ST9764	ST9336	pCfB9331	*MAL2-8c SUC2 URA3 HIS3 LEU2 TRP1 XI-3:: CrTDC XI-1:: SrPyrH, LaRebF*	This study
ST9765	ST9336	pCfB9332	*MAL2-8c SUC2 URA3 HIS3 LEU2 TRP1 XI-3:: CrTDC XI-1:: SrPyrH*	This study
ST9766	ST9336	pCfB9333	*MAL2-8c SUC2 URA3 HIS3 LEU2 TRP1 XI-3:: CrTDC XII-5:: SttH, LaRebF*	This study
ST9767	ST9336	pCfB9334	*MAL2-8c SUC2 URA3 HIS3 LEU2 TRP1 XI-3:: CrTDC XII-5:: SttH*	This study
ST9768	ST9336	pCfB9332, pCfB9333	*MAL2-8c SUC2 URA3 HIS3 LEU2 TRP1 XI-3:: CrTDC XI-1:: SrPyrH XII-5:: SttH, LaRebF*	This study
ST10071	ST9336	pCfB9712	*MAL2-8c SUC2 URA3 HIS3 LEU2 TRP1 XI-3:: CrTDC XII-4: :LaRebH*	This study
ST10072	ST9768	pCfB9712	*MAL2-8c SUC2 URA3 HIS3 LEU2 TRP1 XI-3:: CrTDC XI-1:: SrPyrH XII-5:: SttH, LaRebF XII-4:: LaRebH*	This study
ST10073	ST9766	pCfB9712	*MAL2-8c SUC2 URA3 HIS3 LEU2 TRP1 XI-3:: CrTDC XII-5:: SttH, LaRebF XII-4:: LaRebH*	This study
ST10290	ST7574	pCfB9713	*MAL2-8c SUC2 URA3 HIS3 LEU2 TRP1 XII-4:: LaRebH, LaRebF*	This study
ST10352	ST9336	pCfB9713	*MAL2-8c SUC2 URA3 HIS3 LEU2 TRP1 XI-3:: CrTDC XII-4:: LaRebH, LaRebF*	This study

Table S5. List of plasmids used in this study.

Name	Parent plasmid, BioBricks	Relevant characteristics	Origin
		Templates for PCR amplification	
p1977	-	*pTDH3-pTEF1* fused promoters	(Jessop-Fabre et al., 2016)
pCfB8793	-	CrTDC template	(Milne et al., 2020a)
		gRNA plasmids for targeting genomic integration sites by CRISPR-Cas9	
pCfB3043	-	2µm ori NatMX pSNR52-XI-1- gRNA-tSUP4	(Jessop-Fabre et al., 2016)
pCfB3045	-	2µm ori NatMX pSNR52-XI-3 gRNA-tSUP4	(Jessop-Fabre et al., 2016)
pCfB3049	-	2µm ori NatMX pSNR52-XII-4 gRNA-tSUP4	(Jessop-Fabre et al., 2016)
pCfB3050	-	2µm ori NatMX pSNR52-XII-5 gRNA-tSUP4	(Jessop-Fabre et al., 2016)
pCfB9077	pTAJAK-71, BB3959, BB4027	2µm ori NatMX pSNR52-XI-1 gRNA-tSUP4 pSNR52-XII-5 gRNA-tSUP4	This study
		Episomal yeast expression plasmids	
pCfB2312		2µm ori *pTEF1->cas9* KanMX	(Jessop-Fabre et al., 2016)
pTAJAK-71		2µm ori NatMX	(Jessop-Fabre et al., 2016)
		Backbone plasmids for EasyClone-MarkerFree plasmid assembly	
pCfB2904	-	pXI-3-USER	(Jessop-Fabre et al., 2016)
pCfB2909	-	pXII-5-USER	(Jessop-Fabre et al., 2016)

pCfB3036	-	pXI-1-USER	(Jessop-Fabre et al., 2016)
pCfB3040	-	pXII-4-USER	(Jessop-Fabre et al., 2016)
Plasmids for integration into yeast genome			
pCfB8881	pCfB2904, BB3816, BB8	*XI-3:: CrTDC<-pTEF1*	This study
pCfB9331	pCfB3036, BB4336, BB464, BB4338	*XI-1:: SrPyrH<-pTDH3-pTEF1->LaRebF*	This study
pCfB9332	pCfB3036, BB4336, BB410	*XI-1:: SrPyrH<-pTDH3*	This study
pCfB9333	pCfB2909, BB4337, BB464, BB4338	*XII-5:: SttH<-pTDH3-pTEF1->LaRebF*	This study
pCfB9334	pCfB2909, BB410	*XII-5:: SttH<-pTDH3*	This study
pCfB9712	pCfB3040, BB4441, BB410	*XII-4:: LaRebH<-pTDH3*	This study
pCfB9713	pCfB3040, BB4441, BB464, BB4338	*XII-4:: LaRebH<-pTDH3-pTEF1->LaRebF*	This study

Table S6. List of BioBricks used in this study.

Name	Description	Fwd primer	Rev primer	Template
BB8	*TEF1* promoter	PR-5	PR-6	p1977
BB410	*TDH3* promoter	PR-1852	PR-1853	p1977
BB464	*TDH3-TEF1* fused promoters	PR-1853	PR-1565	p1977
BB3816	*CrTDC* gene	PR-23893	PR-23894	pCfB8793
BB3959	XI-1 gRNA	PR-10525	PR-10530	pCfB3043
BB4027	XII-5 gRNA	PR-10526	PR-10529	pCfB3050
BB4336	*SrPyrH* gene	PR-26290	PR-26291	Synthetic DNA (GeneArt)
BB4337	*SttH* gene	PR-26292	PR-26293	Synthetic DNA (GeneArt)
BB4338	*LaRebF* gene	PR-26294	PR-26295	Synthetic DNA (GeneArt)
BB4441	*LaRebH* gene	PR-26840	PR-26841	Synthetic DNA (GeneArt)

Table S7. List of primers used in this study.

Name	Sequence (5'→3')	Purpose
Primers for BioBrick amplification		
PR-5	ACCTGCACUTTGTAATTAAAACTTAG	Fwd primer to amplify BB8
PR-6	CACGCGAUGCACACACCATAGCTTC	Rev primer to amplify BB8
PR-1565	ATGACAGAUTTGTAATTAAAACTTAG	Fwd primer to amplify BB464
PR-1852	CACGCGAUATAAAAAACACGCTTTTTCAG	Fwd primer to amplify BB410
PR-1853	ACCTGCACUTTTGTTTGTTTATGTGTGTTTATTC	Rev primer to amplify BB0410 and BB0464
PR-10525	CGTGCGAUAGGGAACAAAAGCTGGAGCT	Fwd primer to amplify BB3959
PR-10526	AGTGCAGGUAGGGAACAAAAGCTGGAGCT	Fwd primer to amplify BB4027
PR-10529	CACGCGAUTAACTAATTACATGACTCGA	Rev primer to amplify BB4027
PR-10530	ACCTGCACUTAACTAATTACATGACTCGA	Rev primer to amplify BB3959
PR-23893	AGTGCAGGUAAAACAATGGGTTCTATTGATTCTACCAACG	Fwd primer to amplify BB3816
PR-23894	CGTGCGAUTCAGGCTTCTTTCAACAAGTC	Rev primer to amplify BB3816
PR-26290	AGTGCAGGUAAAACAATGATCAGATCTGTTGTTATCGTTGGTG	Fwd primer to amplify BB4336
PR-26291	CGTGCGAUCTATTGGATAGAAGCCAAGTATTCG	Rev primer to amplify BB4336
PR-26292	AGTGCAGGUAAAACAATGAACACTAGAAACCCAG	Fwd primer to amplify BB4337
PR-26293	CGTGCGAUCTAAACTCTTTGACCCATAGC	Rev primer to amplify BB4337
PR-26294	ATCTGTCAUAAAACAATGACTATCGAATTCGACAGACC	Fwd primer to amplify BB4338
PR-26295	CACGCGAUCTAACCTTCTGGAGTCCAAAC	Rev primer to amplify BB4338

PR-26840	AGTGCAGGUAAAACAATGTCTGGTAAGATCGACAAG	Fwd primer to amplify BB4441
PR-26841	CGTGCGAUCTATCTACCGTGTTGTTGTCTC	Rev primer to amplify BB4441
Primers for verification of correct EasyClone plasmid assembly		
PR-22955	GACGGTAGGTATTGATTGTAATTCTG	*pTDH3* Fwd diagnostic PCR primer
PR-339	GCTCATTAGAAAGAAAGCATAGC	*pTEF1* Fwd diagnostic PCR primer
PR-224	GAAATTCGCTTATTTAGAAGTGTC	*tADH1* Rev diagnostic PCR primer
PR-225	CTCCTTCCTTTTCGGTTAGAG	*tCYC1* Rev diagnostic PCR primer
PR-23875	ACTGTTGGGAAGGGCGATC	gRNA cassette Fwd diagnostic PCR primer
PR-23876	AGCGCCCAATACGCAAAC	gRNA cassette Rev diagnostic PCR primer
Primers for genotyping correct genomic integration of expression cassettes		
PR-2221	GTTGACACTTCTAAATAAGCGAATTTC	Universal Rev primer binding in *S. cerevisiae* integration cassettes
PR-897	GAACTGACGTCGAAGGCTCT	Fwd primer for diagnostic PCR of EasyClone plasmid integration at XII-4 site
PR-898	CGTGAAATCTCTTTGCGGTAG	Rev primer for diagnostic PCR of EasyClone plasmid integration at XII-4 site
PR-899	CCACCGAAGTTGATTTGCTT	Fwd primer for diagnostic PCR of EasyClone plasmid integration at XII-5 site
PR-900	GTGGGAGTAAGGGATCCTGT	Rev primer for diagnostic PCR of EasyClone plasmid integration at XII-5 site
PR-907	CTTAATGGGTAGTGCTTGACACG	Fwd primer for diagnostic PCR of EasyClone plasmid integration at XI-1 site
PR-908	GAAGACCCATGGTTCCAAGGA	Rev primer for diagnostic PCR of EasyClone plasmid integration at XI-1 site
PR-911	GTGCTTGATTTGCGTCATTC	Fwd primer for diagnostic PCR of EasyClone plasmid integration at XI-3 site
PR-912	CACATTGAGCGAATGAAACG	Rev primer for diagnostic PCR of EasyClone plasmid integration at XI-3 site

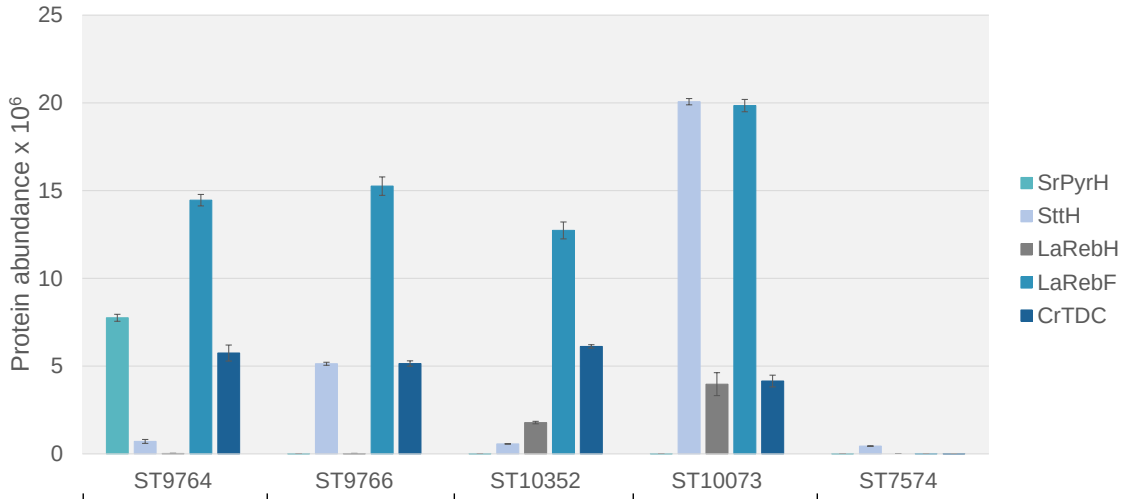

	ST9764	ST9766	ST10352	ST10073	ST7574
SrPyrH	+	–	–	–	–
SttH	–	+	–	+	–
LaRebH	–	–	+	+	–
LaRebF	+	+	+	+	–
CrTDC	+	+	+	+	–

Figure S1. Normalized protein abundance of heterologous proteins in multiple *S. cerevisiae* engineered strains. "+" and "–" symbols indicate the presence or absence of the corresponding genetic modification, respectively. Error bars represent the standard deviation from two biological replicates. Complete dataset, including normalized abundances of yeast native proteins within the proteome, is shown in the Supplementary File 1.

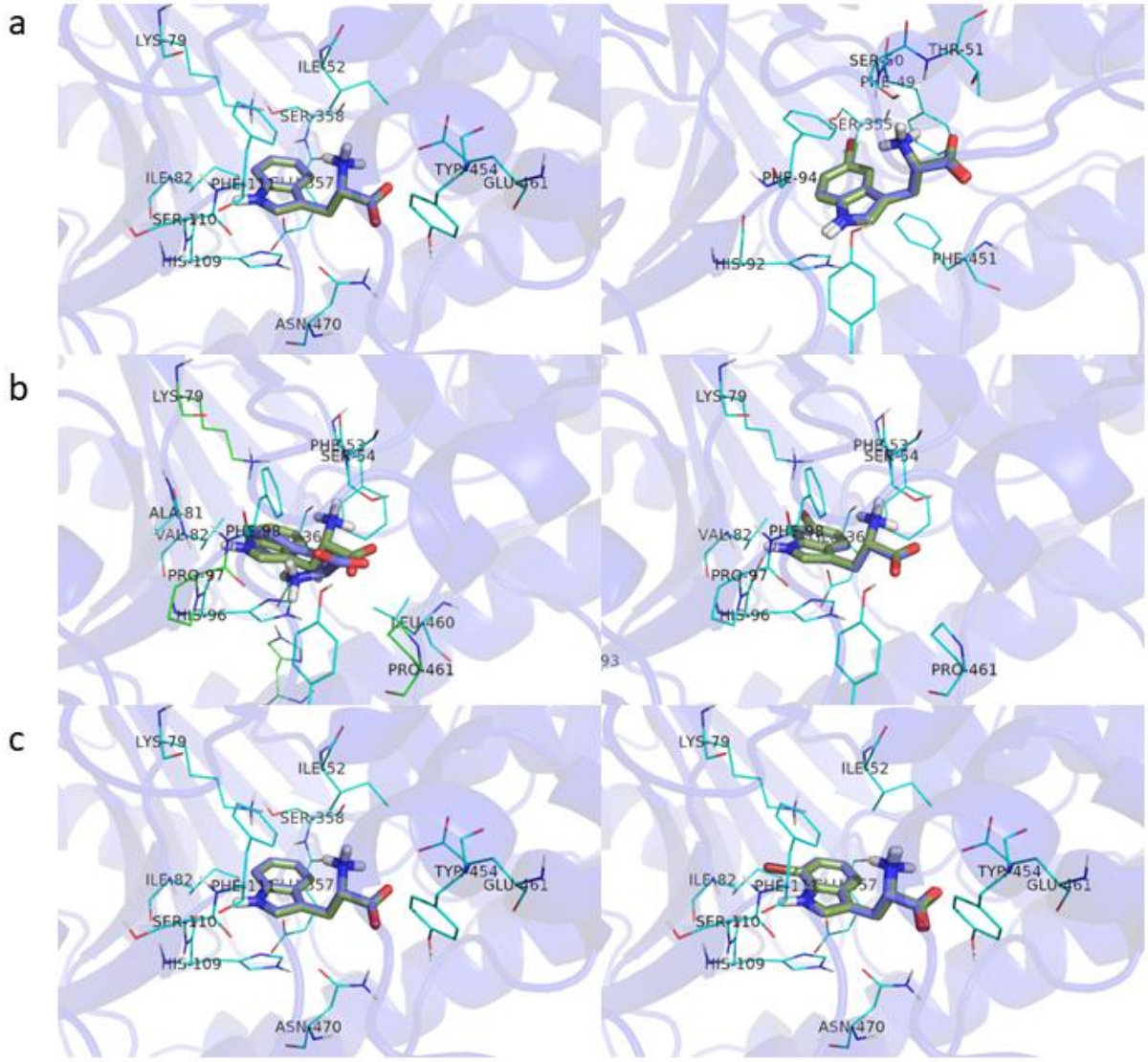

Figure S2. L-tryptophan and corresponding halotryptophan docked to a) SrPyrH, b) SttH, c) LaRebH. Chlorotryptophan is shown with green sticks and bromotryptophan is shown as slate blue.

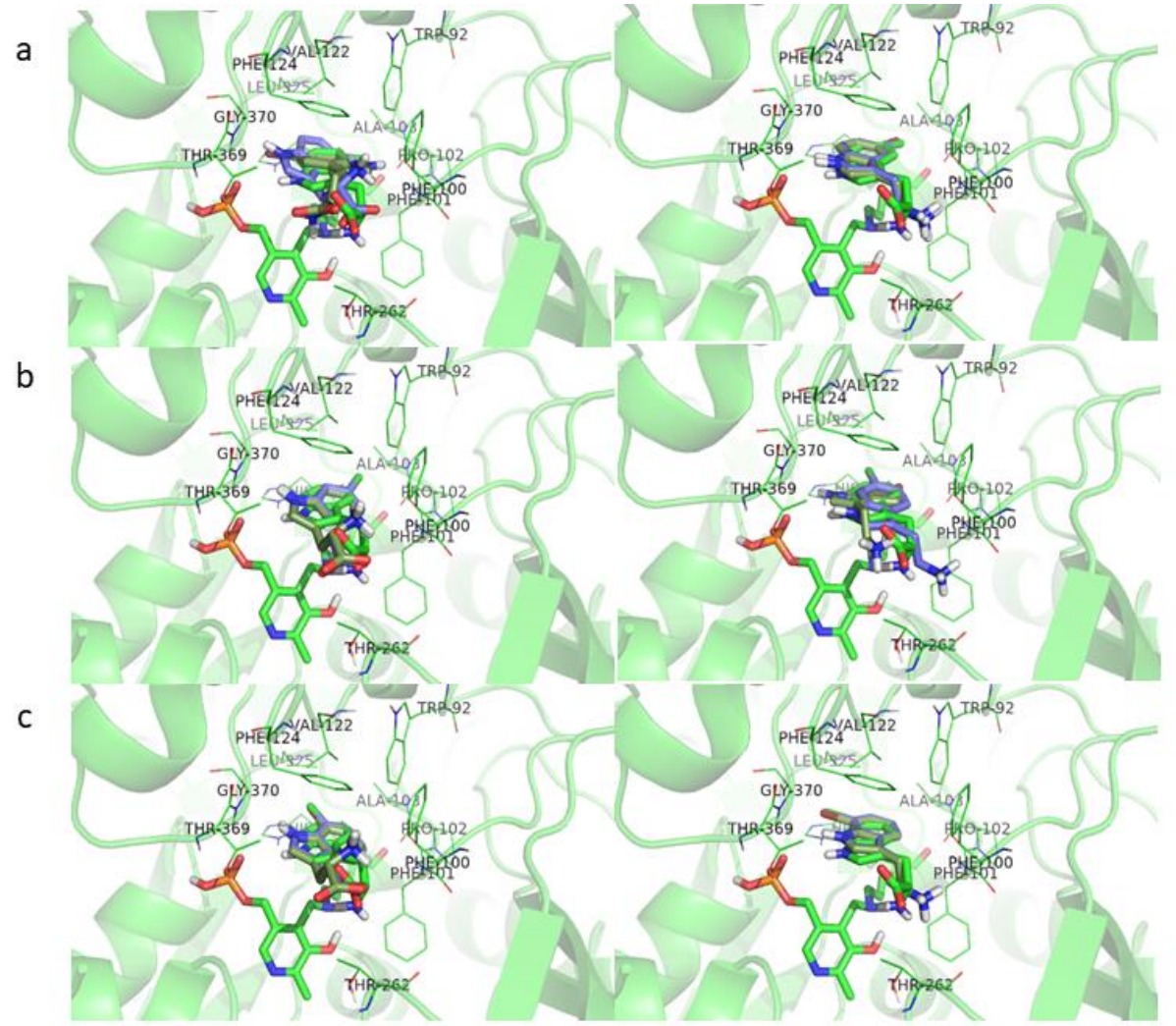

Figure S3. Docking of halotryptophan and halotryptamine to CrTDC. Chlorotryptophan is shown with green sticks and bromotryptophan is shown as slate blue. The crystal structure cofactor LLP and bound L-tryptophan is shown in bright green. a) 5-halotryptophan to the left-hand side, 5-halotryptamine to the right-hand side. b) 6-halotryptophan to the left-hand side, 6-halotryptamine to the right-hand side. c) 7-halotryptophan to the left-hand side, 7-halotryptamine to the right-hand side.

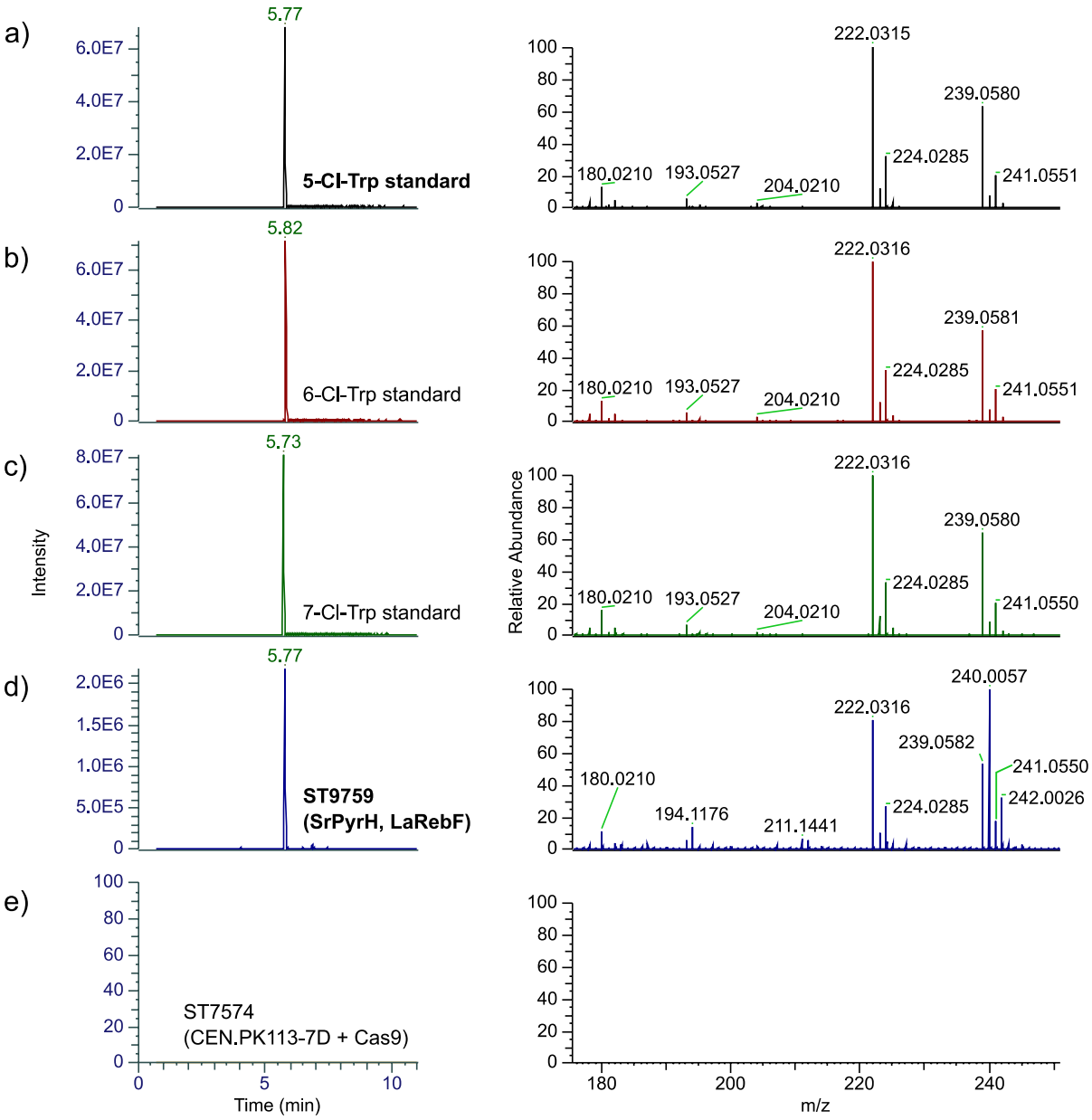

Figure S4. Production of 5-chlorotryptophan in engineered *S. cerevisiae* strains. LC-MS extracted ion chromatograms and corresponding mass spectra of the main peak for a) 5-chlorotryptophan standard, b) 6-chlorotryptophan standard, c) 7-chlorotryptophan standard, d) ST9759 (*SrPyrH*, *LaRebF*), e) ST7574 (Wild-type control, CEN.PK113-7D + Cas9). Theoretical m/z of $[M+H]^+$ and $[M+H-NH_3]^+$ adducts with ^{35}Cl and ^{37}Cl isotopes is 239.0582/222.0316 (most abundant) and 241.0552/224.0287, respectively. Note the presence of chlorinated xanthurenic acid as the main halogenated product, with observed m/z $[M+H]^+$ of 240.0057 (^{35}Cl) and 242.0026 (^{37}Cl).

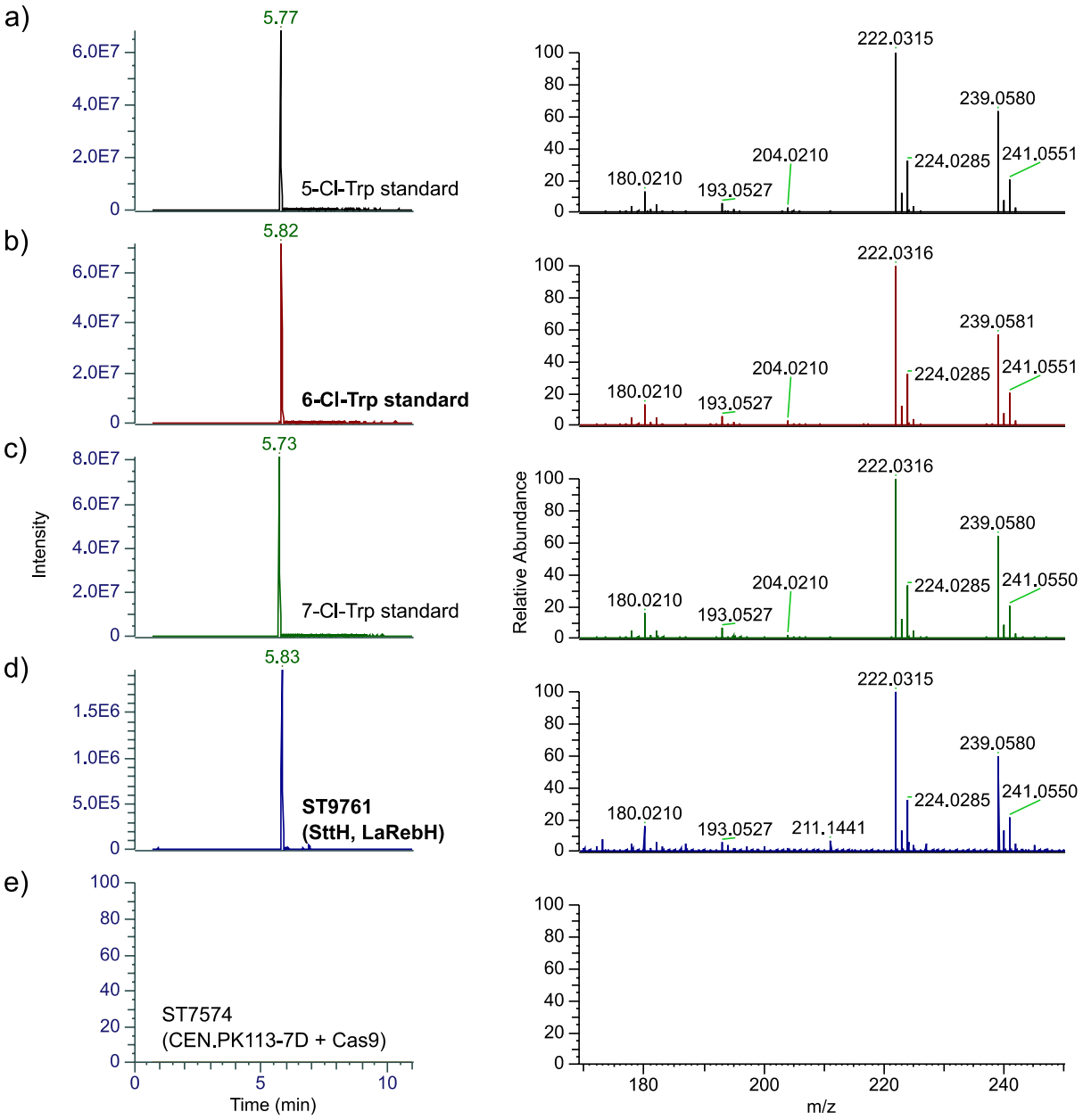

Figure S5. Production of 6-chlorotryptophan in engineered *S. cerevisiae* strains. LC-MS extracted ion chromatograms and corresponding mass spectra of the main peak for a) 5-chlorotryptophan standard, b) 6-chlorotryptophan standard, c) 7-chlorotryptophan standard, d) ST9761 (*SttH*, *LaRebF*), e) ST7574 (Wild-type control, CEN.PK113-7D + Cas9). Theoretical m/z of $[M+H]^+$ and $[M+H-NH_3]^+$ adducts with ^{35}Cl and ^{37}Cl isotopes is 239.0582/222.0316 (most abundant) and 241.0552/224.0287, respectively.

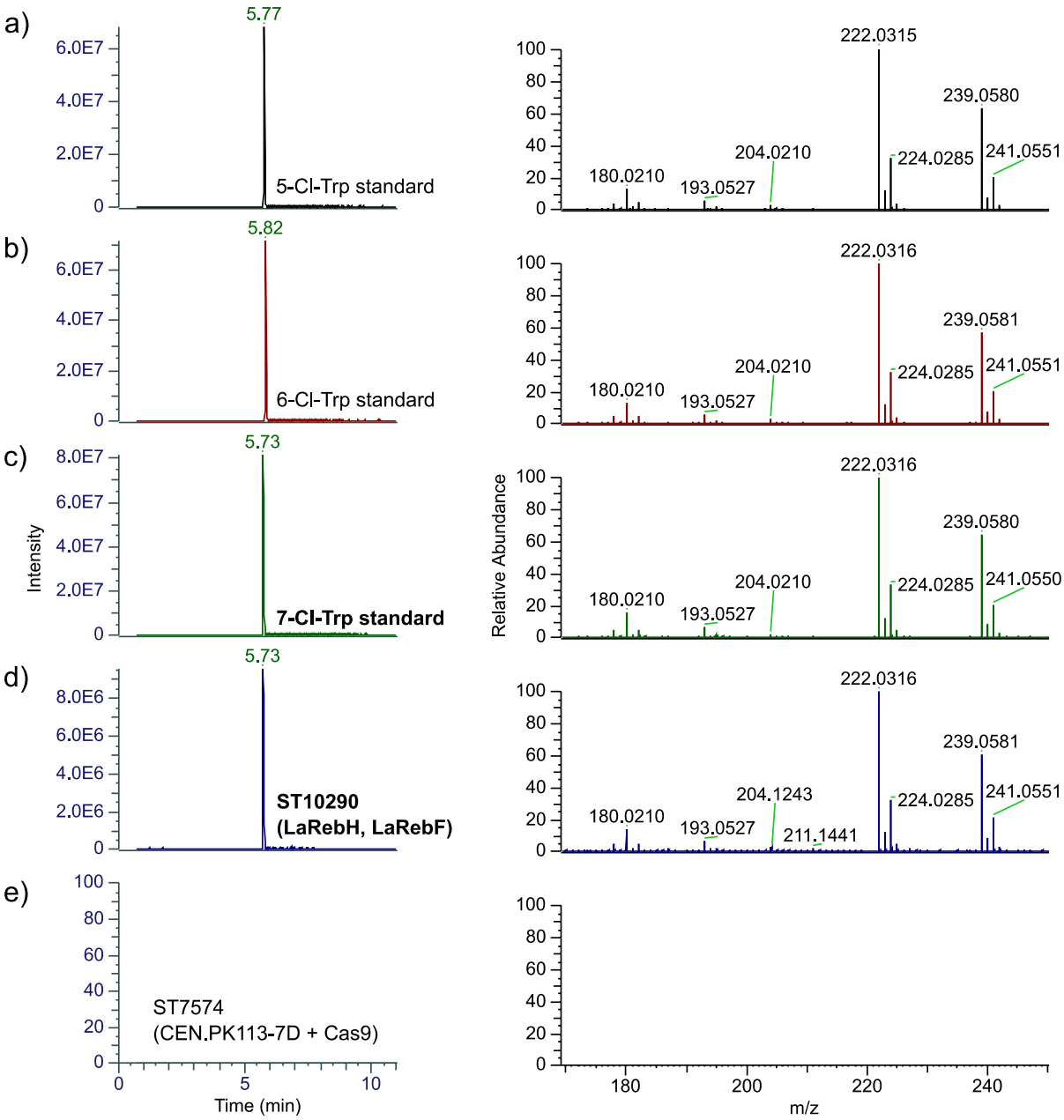

Figure S6. Production of 7-chlorotryptophan in engineered *S. cerevisiae* strains. LC-MS extracted ion chromatograms and corresponding mass spectra of the main peak for a) 5-chlorotryptophan standard, b) 6-chlorotryptophan standard, c) 7-chlorotryptophan standard, d) ST10290 (*LaRebH*, *LaRebF*), e) ST7574 (Wild-type control, CEN.PK113-7D + Cas9). Theoretical m/z of $[M+H]^+$ and $[M+H-NH_3]^+$ adducts with ^{35}Cl and ^{37}Cl isotopes is 239.0582/222.0316 (most abundant) and 241.0552/224.0287, respectively.

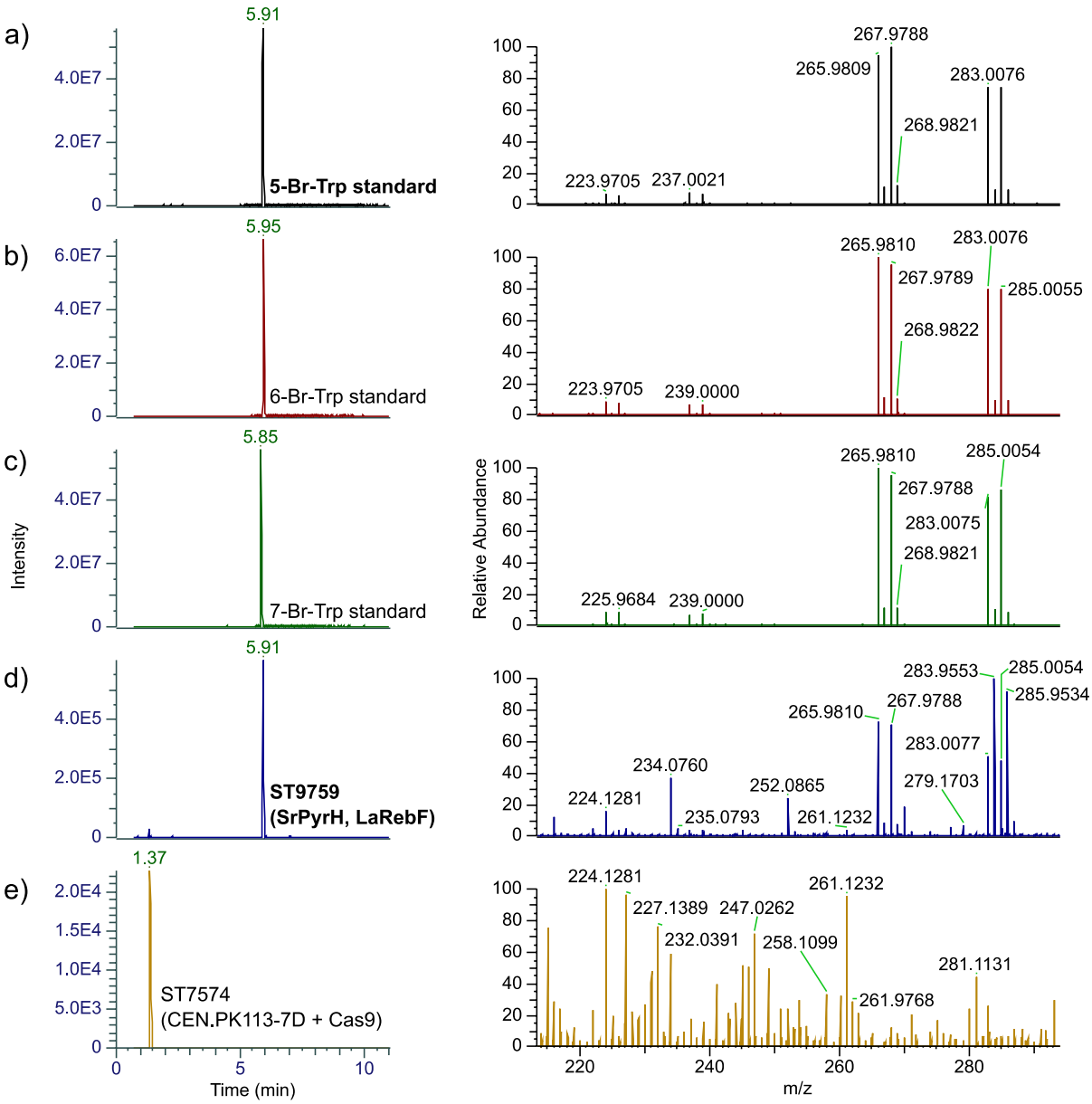

Figure S7. Production of 5-bromotryptophan in engineered *S. cerevisiae* strains. LC-MS extracted ion chromatograms and corresponding mass spectra of the main peak for a) 5-bromotryptophan standard, b) 6-bromotryptophan standard, c) 7-bromotryptophan standard, d) ST9759 (*SrPyrH*, *LaRebF*), e) ST7574 (Wild-type control, CEN.PK113-7D + Cas9). Theoretical m/z of $[M+H]^+$ and $[M+H-NH_3]^+$ adducts with ^{79}Br and ^{81}Br isotopes is 283.0077/265.9811 (most abundant) and 285.0056/267.9791, respectively. Note the presence of brominated xanthurenic acid as the main halogenated product, with observed $[M+H]^+$ m/z of 283.9553 (^{79}Br) and 285.9534 (^{81}Br).

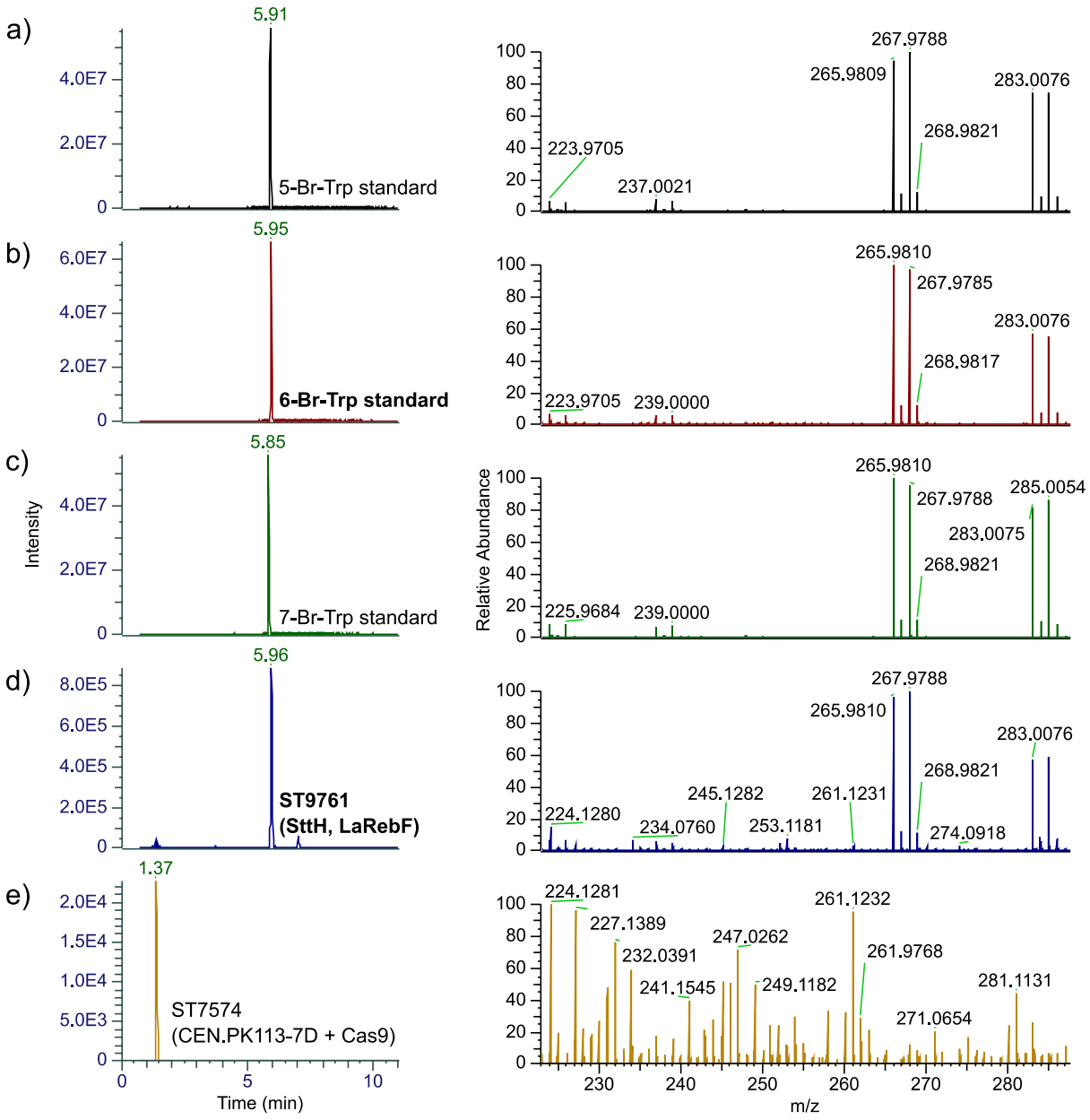

Figure S8. Production of 6-bromotryptophan in engineered *S. cerevisiae* strains. LC-MS extracted ion chromatograms and corresponding mass spectra of the main peak for a) 5-bromotryptophan standard, b) 6-bromotryptophan standard, c) 7-bromotryptophan standard, d) ST9761 (*SttH*, *LaRebF*), e) ST7574 (Wild-type control, CEN.PK113-7D + Cas9). Theoretical m/z of $[M+H]^+$ and $[M+H-NH_3]^+$ adducts with ^{79}Br and ^{81}Br isotopes is 283.0077/265.9811 (most abundant) and 285.0056/267.9791, respectively.

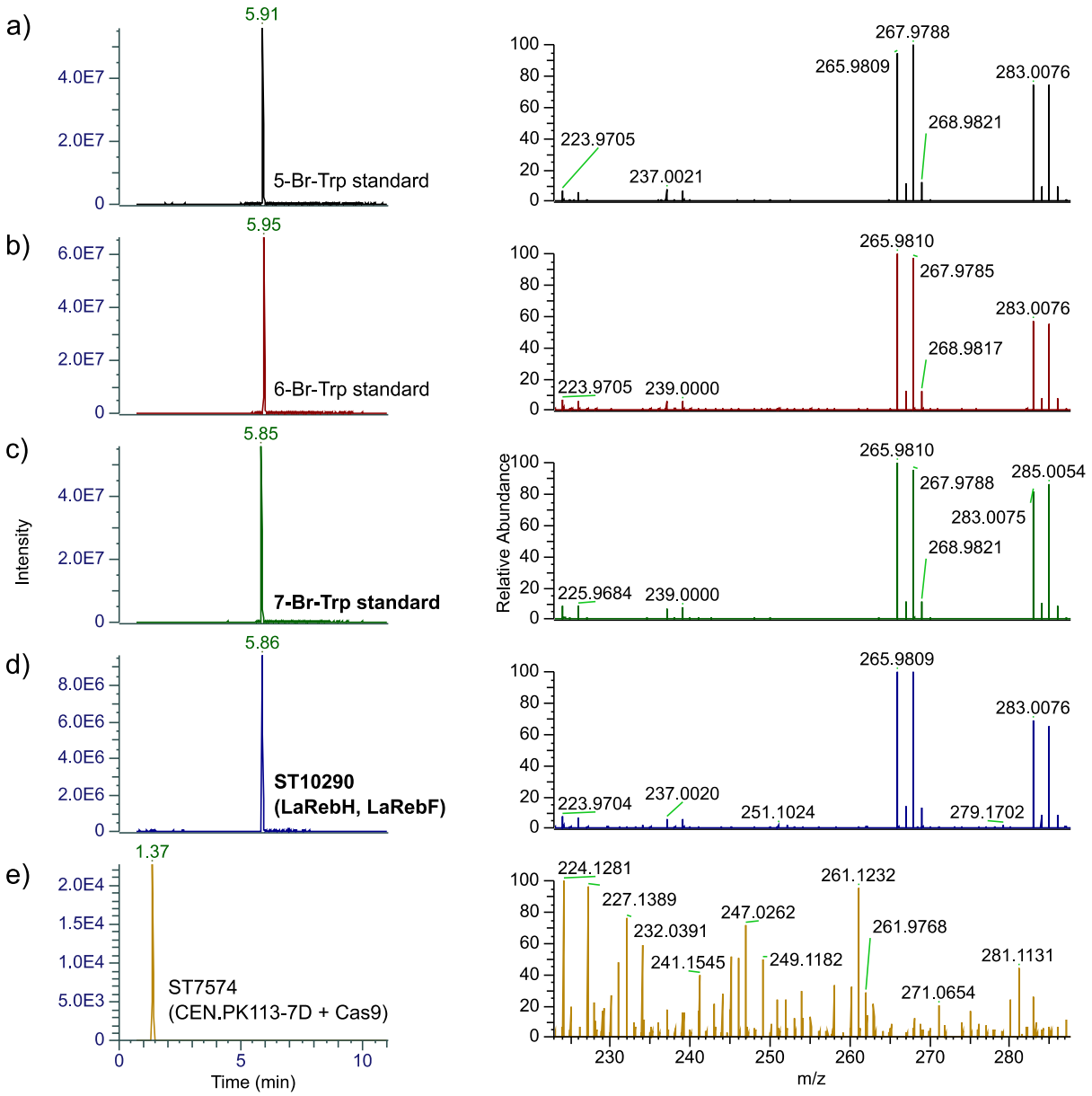

Figure S9. Production of 7-bromotryptophan in engineered *S. cerevisiae* strains. LC-MS extracted ion chromatograms and corresponding mass spectra of the main peak for a) 5-bromotryptophan standard, b) 6-bromotryptophan standard, c) 7-bromotryptophan standard, d) ST10290 (*LaRebH*, *LaRebF*), e) ST7574 (Wild-type control, CEN.PK113-7D + Cas9). Theoretical m/z of $[M+H]^+$ and $[M+H-NH_3]^+$ adducts with ^{79}Br and ^{81}Br isotopes is 283.0077/265.9811 (most abundant) and 285.0056/267.9791, respectively.

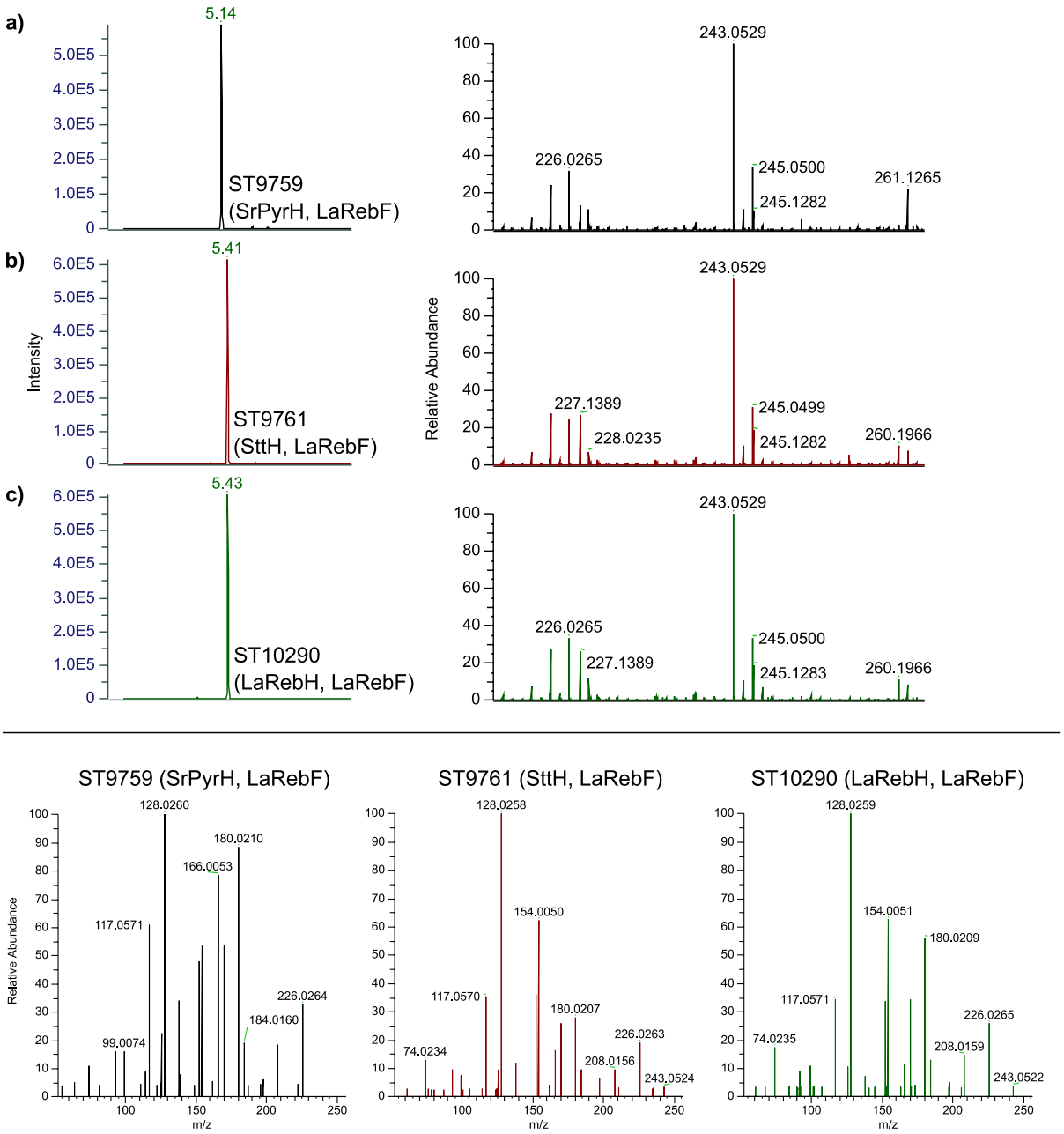

Figure S10. Production of chlorinated L-kynurenine in engineered *S. cerevisiae* strains. LC-MS extracted ion chromatograms and corresponding mass spectra of the main peak for a) ST9759 (*SrPyrH*, *LaRebF*), b) ST9761 (*SttH*, *LaRebF*), c) ST10290 (*LaRebH*, *LaRebF*). Theoretical m/z of $[M+H]^+$ adducts with ^{35}Cl and ^{37}Cl isotopes is 243.0537 (most abundant) and 245.0507, respectively. Bottom panel: MS^2 of precursor ion corresponding to $[M+H]^+$ adduct containing ^{35}Cl. n.d.: not detected or precursor ion not fragmented due to low intensity.

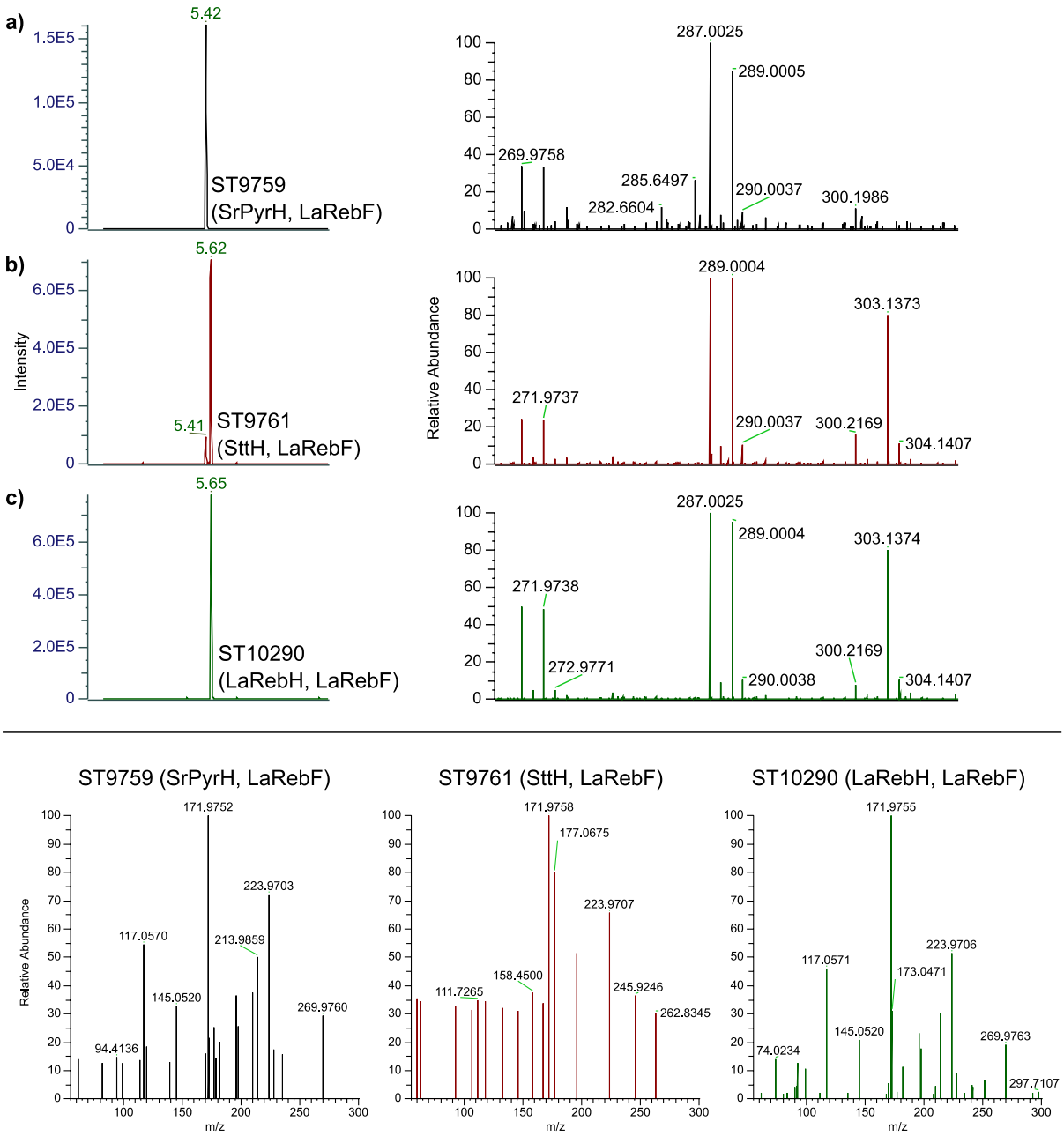

Figure S11. Production of brominated L-kynurenine in engineered *S. cerevisiae* strains. LC-MS extracted ion chromatograms and corresponding mass spectra of the main peak for a) ST9759 (*SrPyrH*, *LaRebF*), b) ST9761 (*SttH*, *LaRebF*), c) ST10290 (*LaRebH*, *LaRebF*). Theoretical m/z of $[M+H]^+$ adducts with ^{79}Br and ^{81}Br isotopes is 287.0031 (most abundant) and 289.0011, respectively. Bottom panel: MS^2 of precursor ion corresponding to $[M+H]^+$ adduct containing ^{79}Br. n.d.: not detected or precursor ion not fragmented due to low intensity.

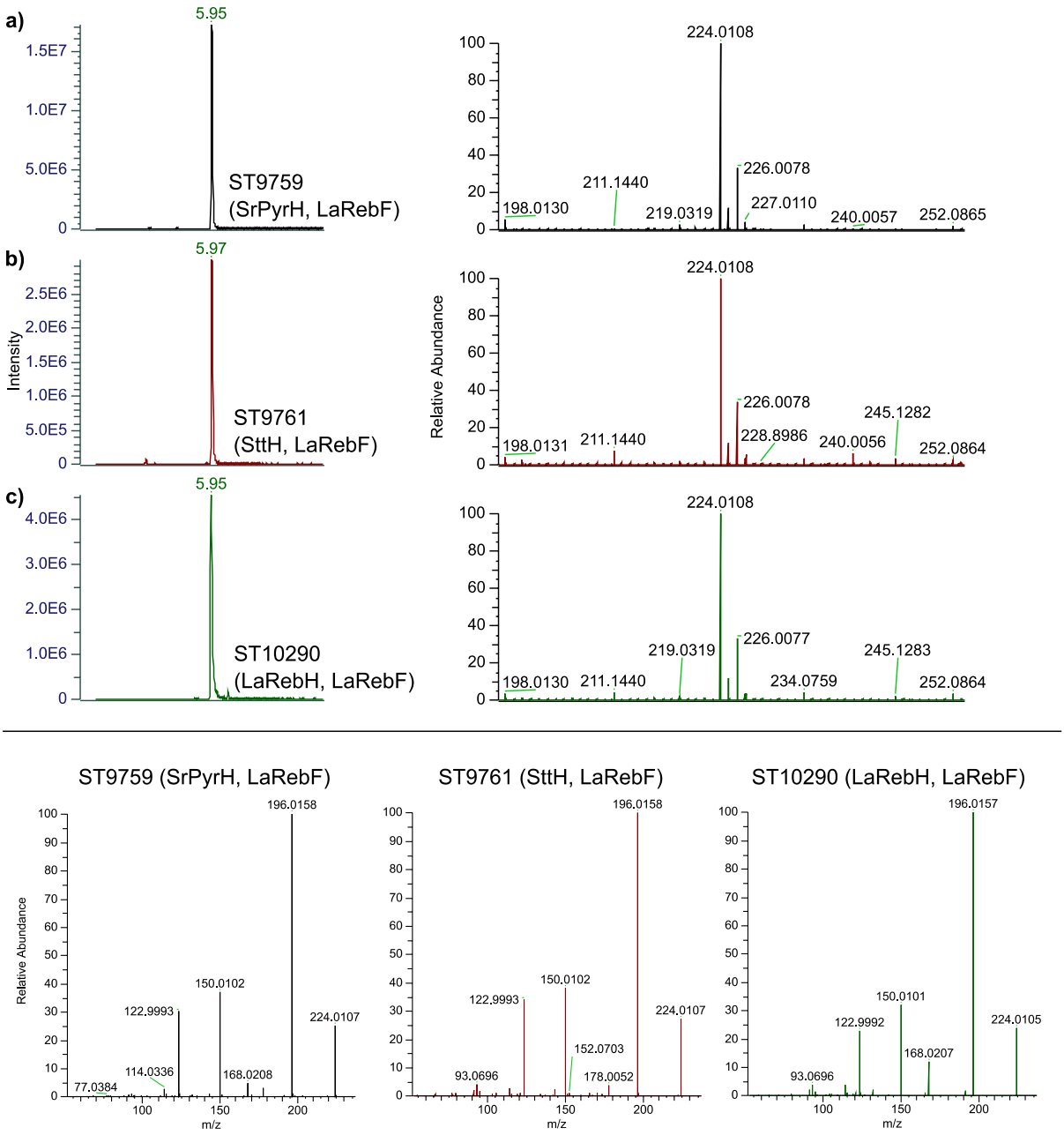

Figure S12. Production of chlorinated kynurenic acid in engineered *S. cerevisiae* strains. LC-MS extracted ion chromatograms and corresponding mass spectra of the main peak for a) ST9759 (*SrPyrH*, *LaRebF*), b) ST9761 (*SttH*, *LaRebF*), c) ST10290 (*LaRebH*, *LaRebF*). Theoretical m/z of $[M+H]^+$ adducts with ^{35}Cl and ^{37}Cl isotopes is 224.0115 (most abundant) and 226.0085, respectively. Bottom panel: MS^2 of precursor ion corresponding to $[M+H]^+$ adduct containing ^{35}Cl. n.d.: not detected or precursor ion not fragmented due to low intensity.

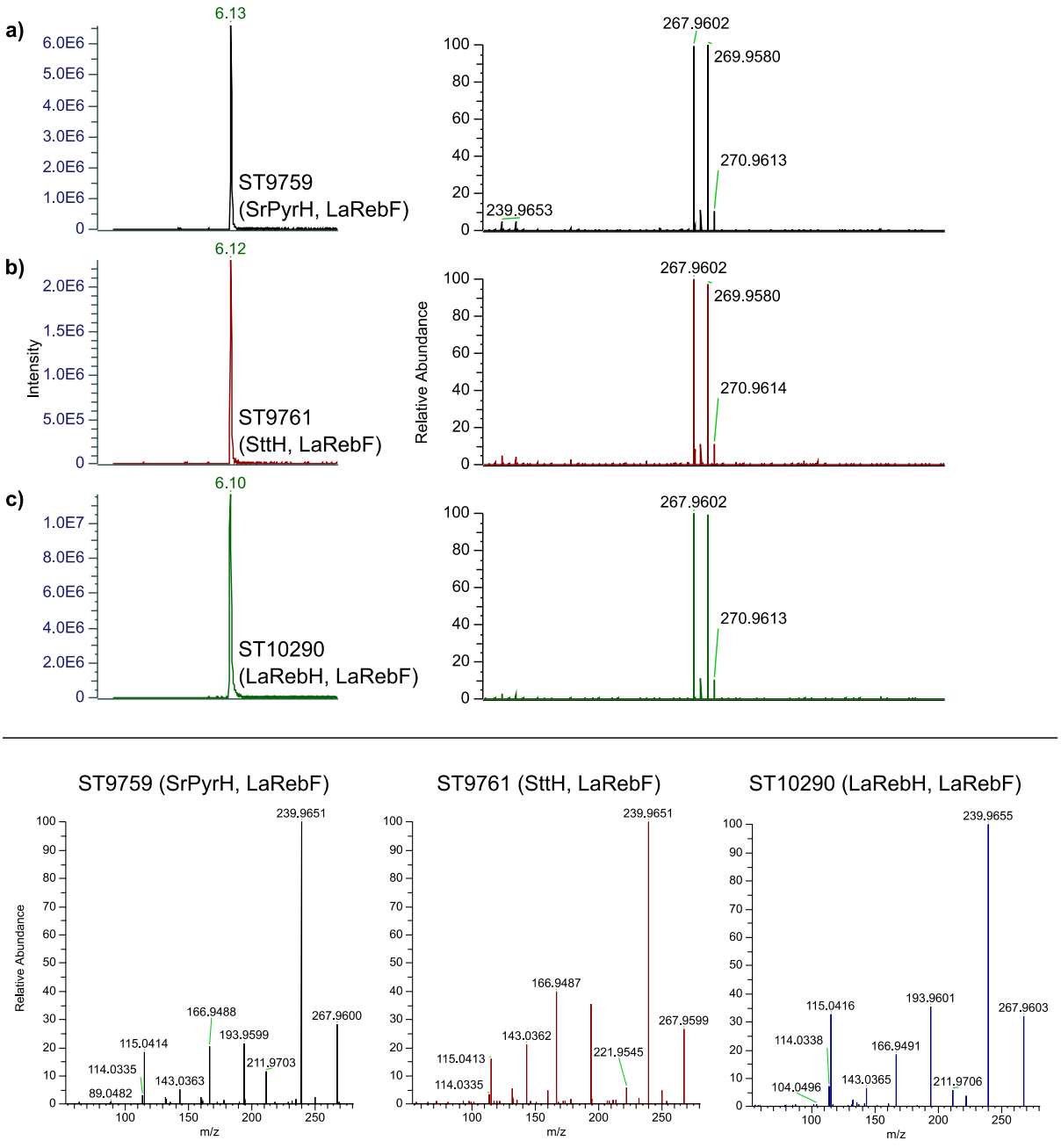

Figure S13. Production of brominated kynurenic acid in engineered *S. cerevisiae* strains. LC-MS extracted ion chromatograms and corresponding mass spectra of the main peak for a) ST9759 (*SrPyrH*, *LaRebF*), b) ST9761 (*SttH*, *LaRebF*), c) ST10290 (*LaRebH*, *LaRebF*). Theoretical m/z of $[M+H]^+$ adducts with ^{79}Br and ^{81}Br isotopes is 267.9609 (most abundant) and 269.9589, respectively. Bottom panel: MS^2 of precursor ion corresponding to $[M+H]^+$ adduct containing ^{79}Br. n.d.: not detected or precursor ion not fragmented due to low intensity.

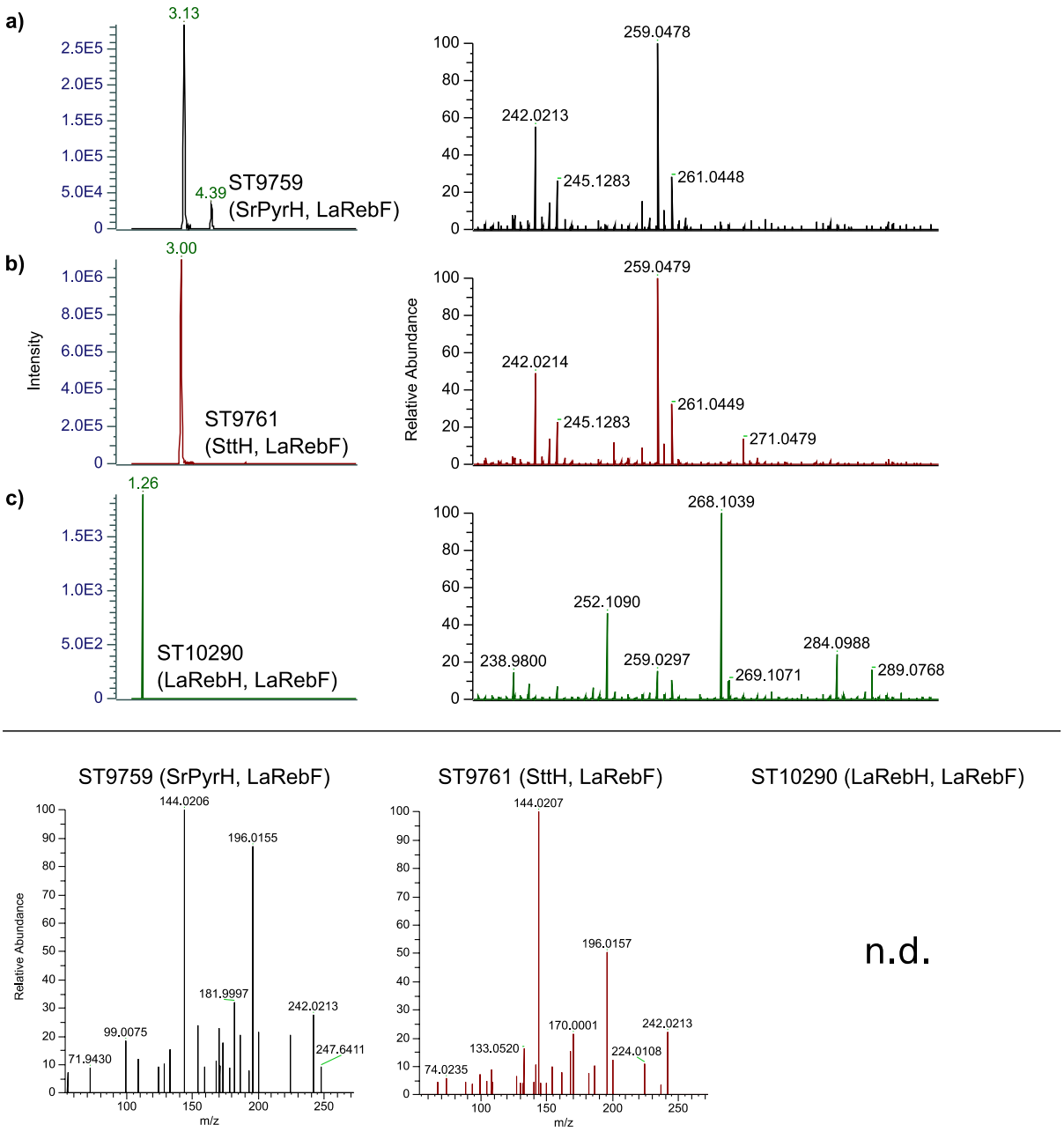

Figure S14. Production of chlorinated 3-hydroxy-L-kynurenine in engineered *S. cerevisiae* strains. LC-MS extracted ion chromatograms and corresponding mass spectra of the main peak for a) ST9759 (*SrPyrH*, *LaRebF*), b) ST9761 (*SttH*, *LaRebF*), c) ST10290 (*LaRebH*, *LaRebF*), compound not detected. Theoretical m/z of $[M+H]^+$ adducts with ^{35}Cl and ^{37}Cl isotopes is 259.0486 (most abundant) and 261.0456, respectively. Bottom panel: MS^2 of precursor ion corresponding to $[M+H]^+$ adduct containing ^{35}Cl. n.d.: not detected or precursor ion not fragmented due to low intensity.

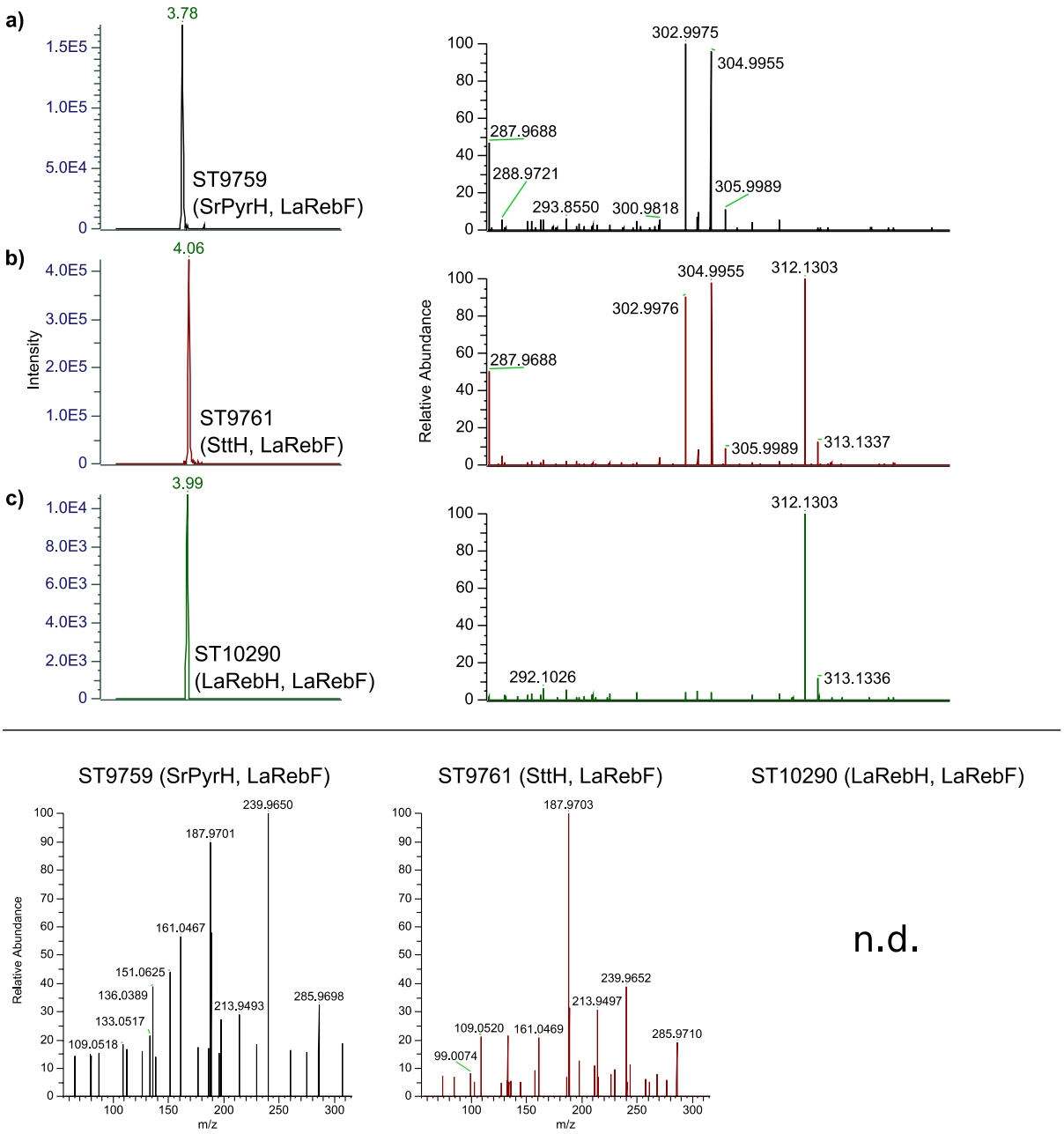

Figure S15. Production of brominated 3-hydroxy-L-kynurenine in engineered *S. cerevisiae* strains. LC-MS extracted ion chromatograms and corresponding mass spectra of the main peak for a) ST9759 (*SrPyrH*, *LaRebF*), b) ST9761 (*SttH*, *LaRebF*), c) ST10290 (*LaRebH*, *LaRebF*)), compound not detected. Theoretical m/z of $[M+H]^+$ adducts with ^{79}Br and ^{81}Br isotopes is 302.9980 (most abundant) and 304.9960, respectively. Bottom panel: MS^2 of precursor ion corresponding to $[M+H]^+$ adduct containing ^{79}Br. n.d.: not detected or precursor ion not fragmented due to low intensity.

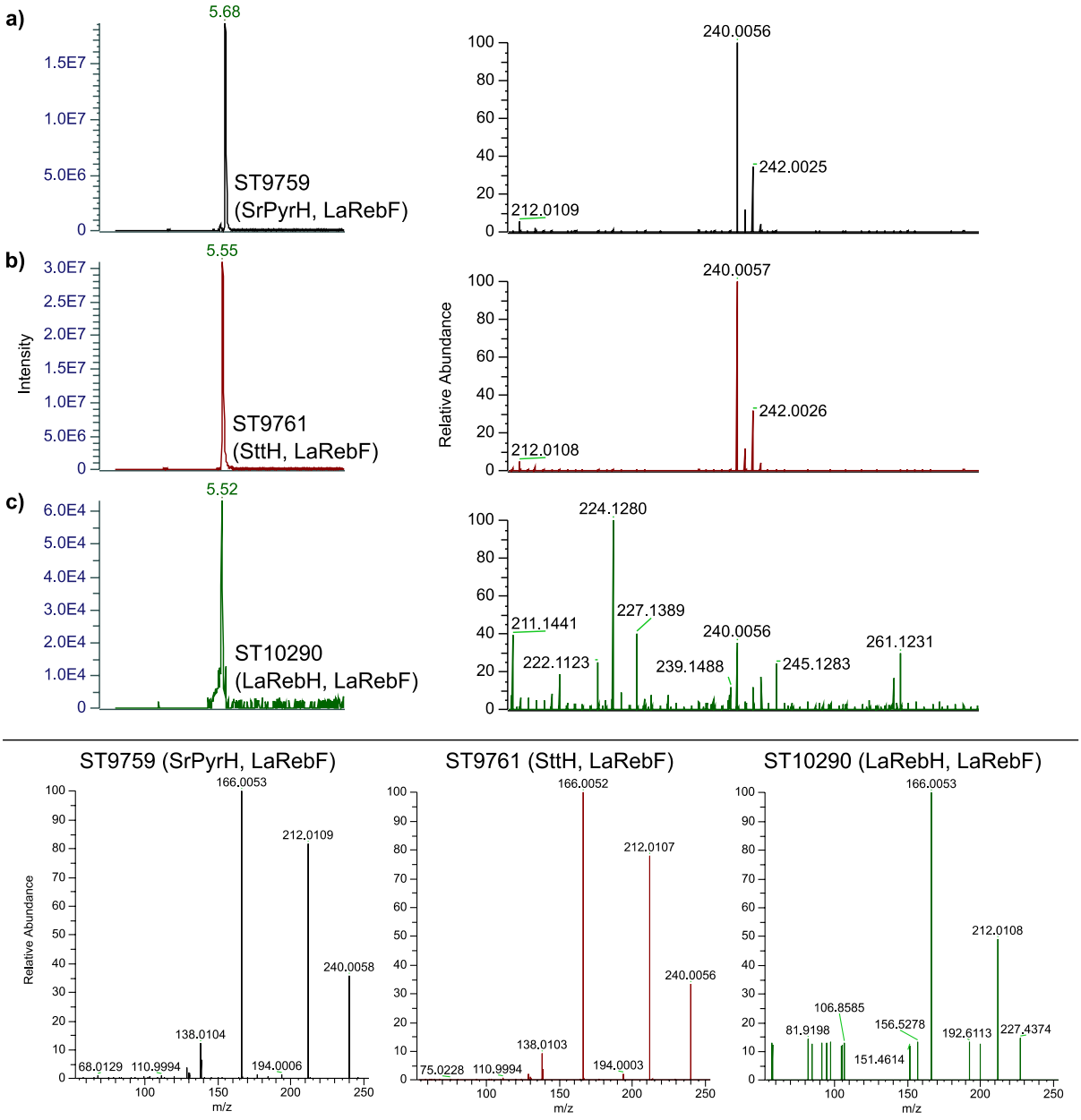

Figure S16. Production of chlorinated xanthurenic acid in engineered *S. cerevisiae* strains. LC-MS extracted ion chromatograms and corresponding mass spectra of the main peak for a) ST9759 (*SrPyrH*, *LaRebF*), b) ST9761 (*SttH*, *LaRebF*), c) ST10290 (*LaRebH*, *LaRebF*). Theoretical m/z of $[M+H]^+$ adducts with ^{35}Cl and ^{37}Cl isotopes is 240.0064 (most abundant) and 242.0034, respectively. Bottom panel: MS^2 of precursor ion corresponding to $[M+H]^+$ adduct containing ^{35}Cl. n.d.: not detected or precursor ion not fragmented due to low intensity.

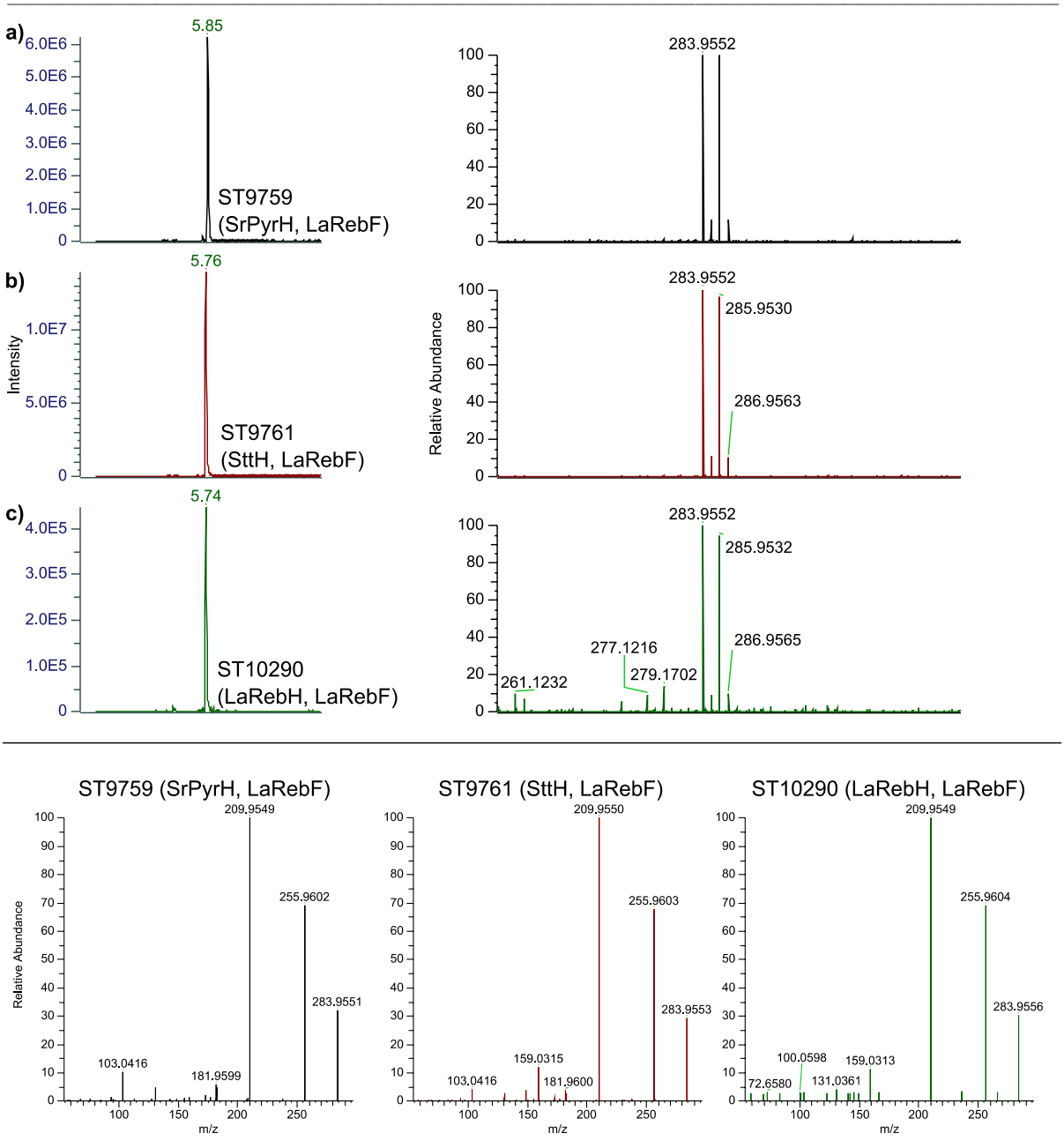

Figure S17. Production of brominated xanthurenic acid in engineered *S. cerevisiae* strains. LC-MS extracted ion chromatograms and corresponding mass spectra of the main peak for a) ST9759 (*SrPyrH*, *LaRebF*), b) ST9761 (*SttH*, *LaRebF*), c) ST10290 (*LaRebH*, *LaRebF*). Theoretical m/z of $[M+H]^+$ adducts with ^{79}Br and ^{81}Br isotopes is 283.9558 (most abundant) and 285.9538, respectively. Bottom panel: MS^2 of precursor ion corresponding to $[M+H]^+$ adduct containing ^{79}Br. n.d.: not detected or precursor ion not fragmented due to low intensity.

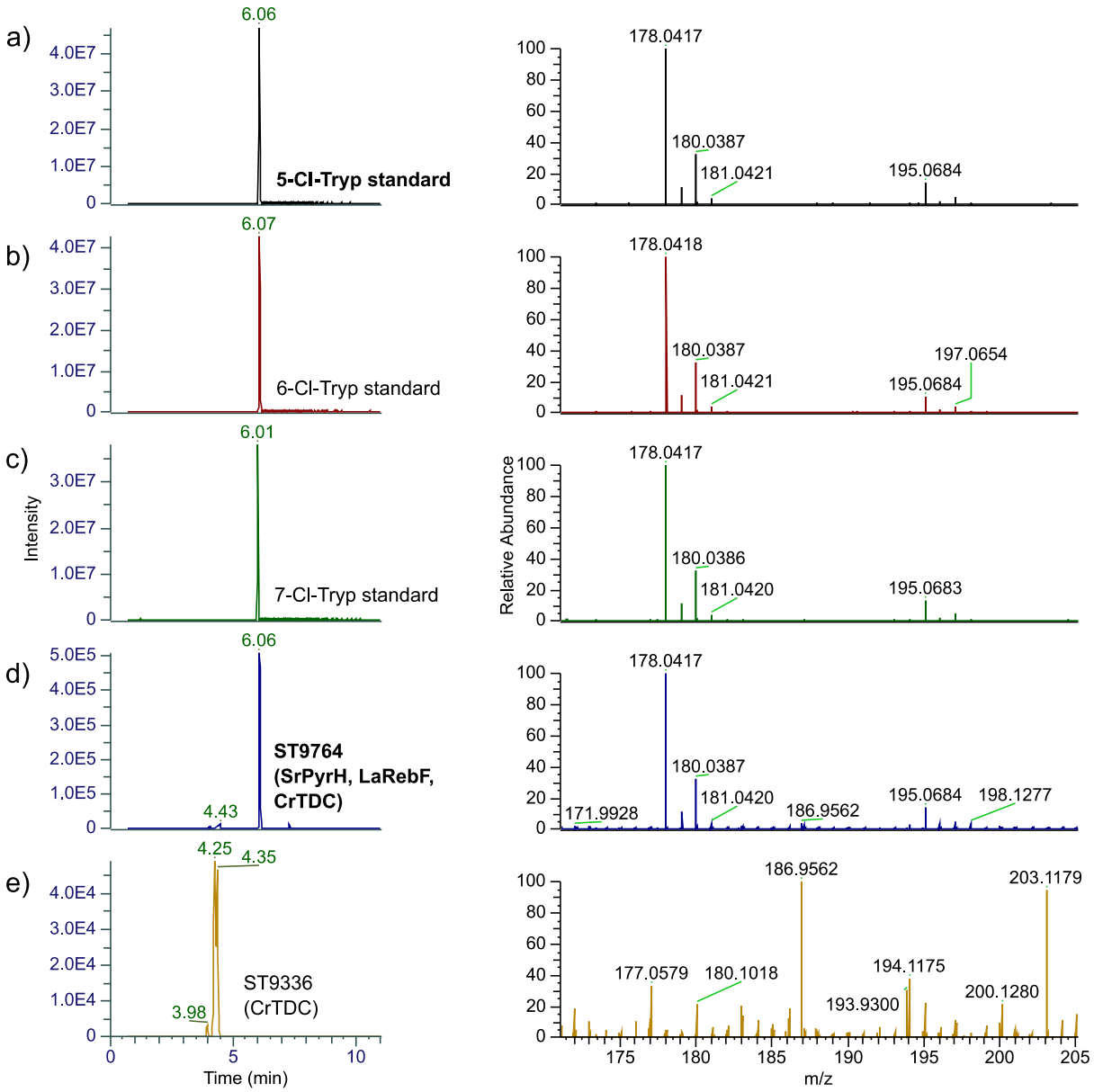

Figure S18. Production of 5-chlorotryptamine in engineered *S. cerevisiae* strains. LC-MS extracted ion chromatograms and corresponding mass spectra of the main peak for a) 5-chlorotryptamine standard, b) 6-chlorotryptamine standard, c) 7-chlorotryptamine standard, d) ST9764 (*SrPyrH*, *LaRebF*, *CrTDC*), e) ST9336 (Tryptamine control, *CrTDC*). Theoretical m/z of $[M+H]^+$ and $[M+H-NH_3]^+$ adducts with ^{35}Cl and ^{37}Cl isotopes is 195.0684/178.0418 (most abundant) and 197.0654/180.0389, respectively.

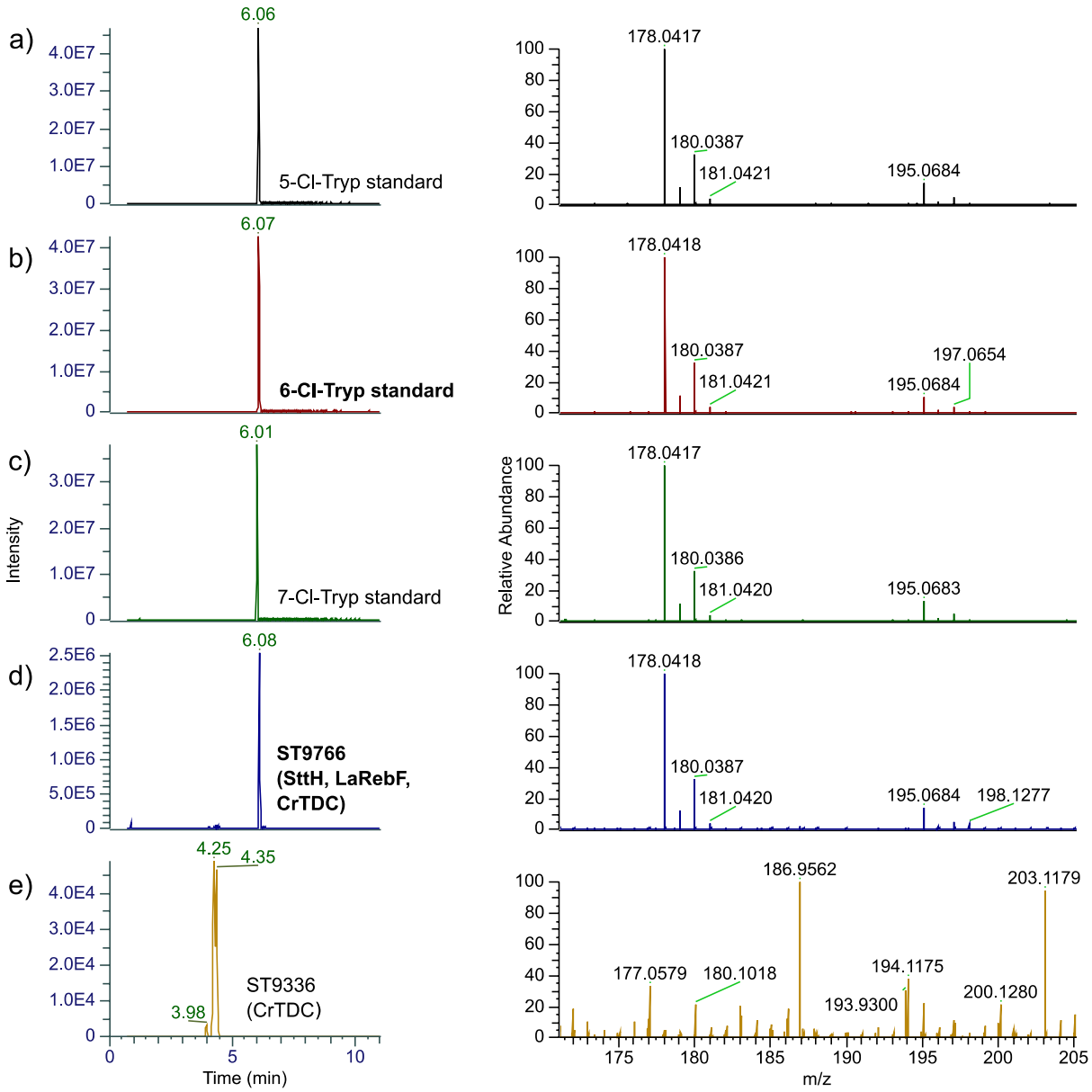

Figure S19. Production of 6-chlorotryptamine in engineered *S. cerevisiae* strains. LC-MS extracted ion chromatograms and corresponding mass spectra of the main peak for a) 5-chlorotryptamine standard, b) 6-chlorotryptamine standard, c) 7-chlorotryptamine standard, d) ST9766 (*SttH*, *LaRebF*, *CrTDC*), e) ST9336 (Tryptamine control, *CrTDC*). Theoretical m/z of $[M+H]^+$ and $[M+H-NH_3]^+$ adducts with ^{35}Cl and ^{37}Cl isotopes is 195.0684/178.0418 (most abundant) and 197.0654/180.0389, respectively.

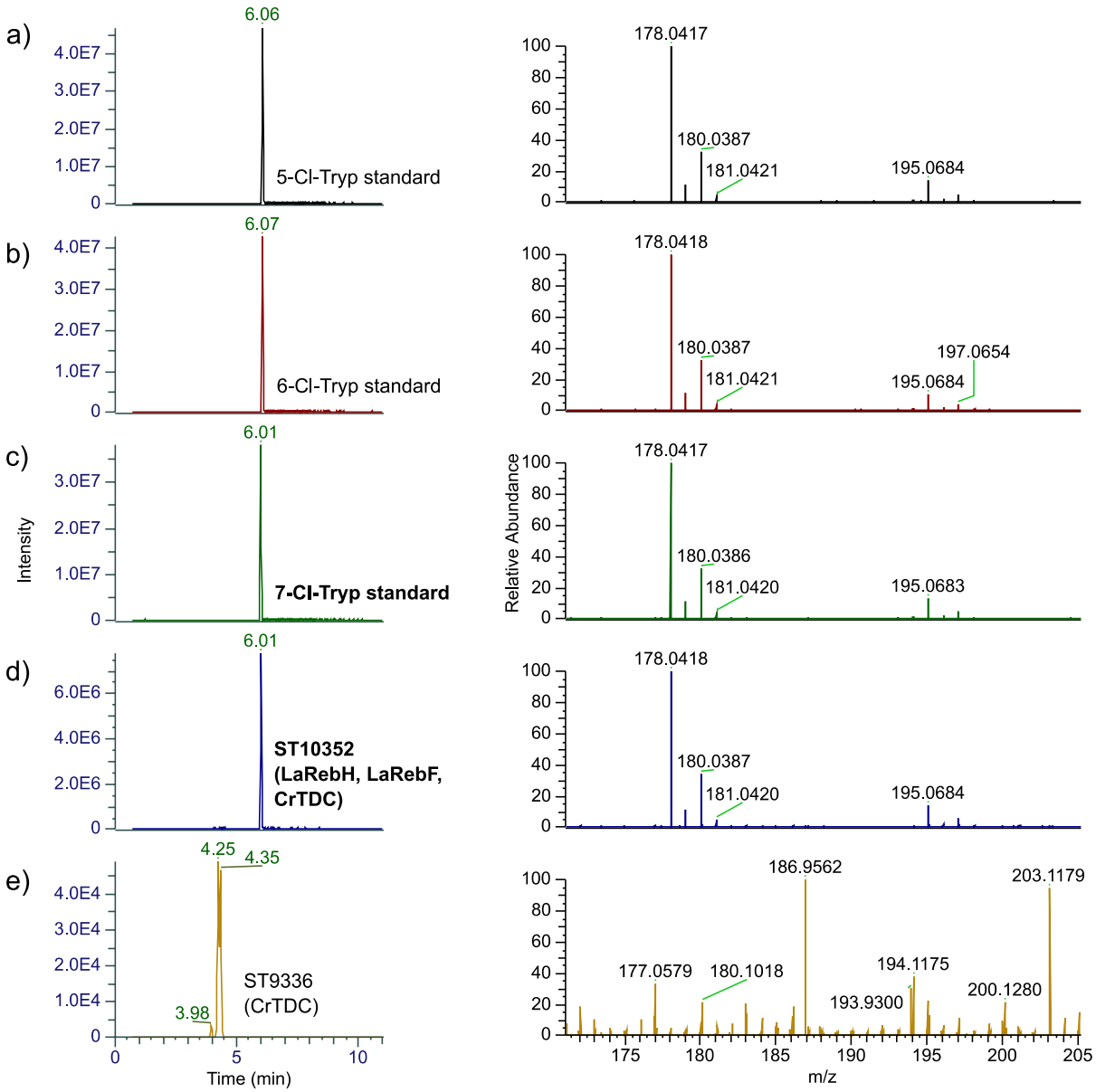

Figure S20. Production of 7-chlorotryptamine in engineered *S. cerevisiae* strains. LC-MS extracted ion chromatograms and corresponding mass spectra of the main peak for a) 5-chlorotryptamine standard, b) 6-chlorotryptamine standard, c) 7-chlorotryptamine standard, d) ST10352 (*LaRebH*, *LaRebF*, *CrTDC*), e) ST9336 (Tryptamine control, *CrTDC*). Theoretical m/z of $[M+H]^+$ and $[M+H-NH_3]^+$ adducts with ^{35}Cl and ^{37}Cl isotopes is 195.0684/178.0418 (most abundant) and 197.0654/180.0389, respectively.

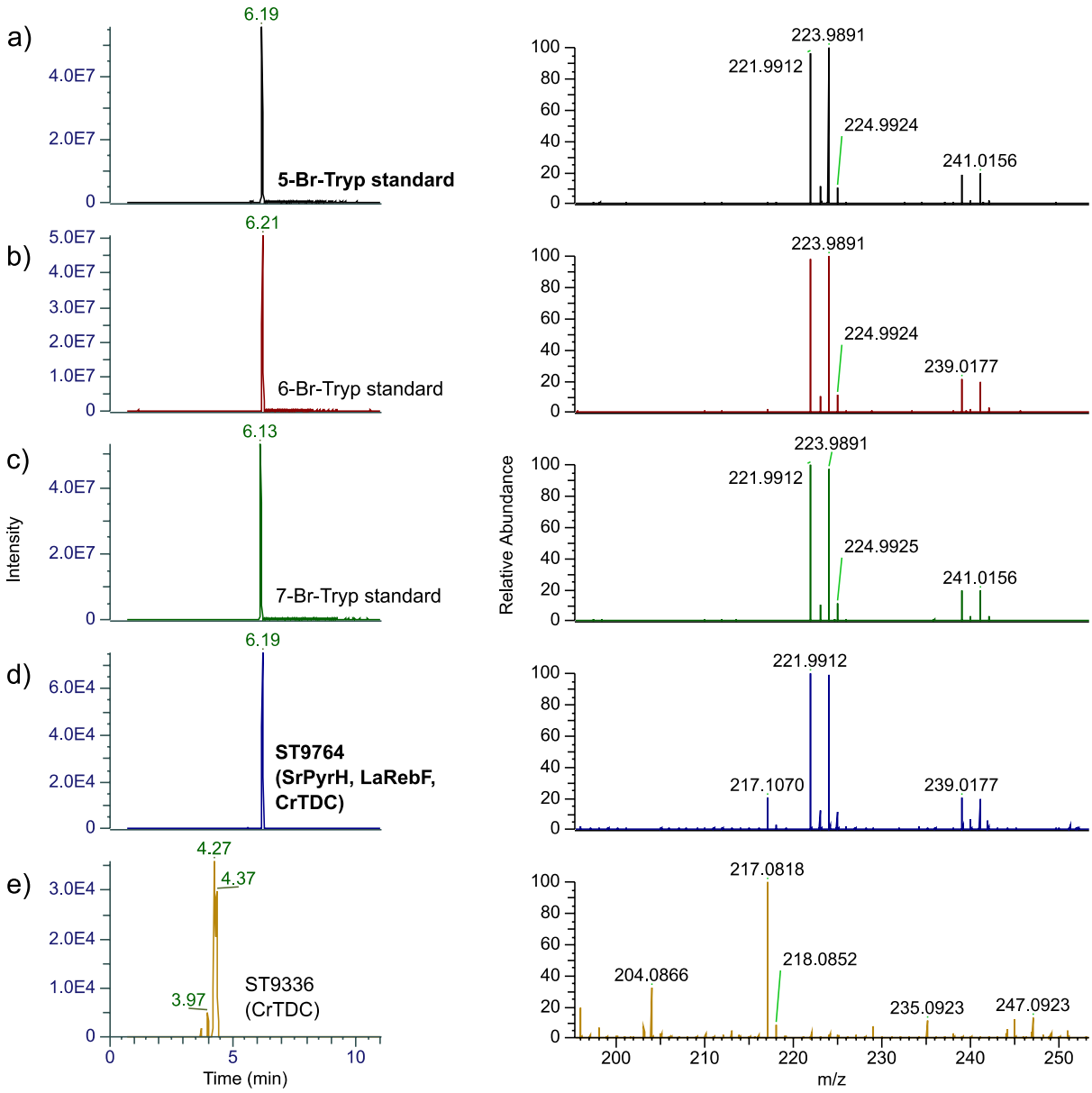

Figure S21. Production of 5-bromotryptamine in engineered *S. cerevisiae* strains. LC-MS extracted ion chromatograms and corresponding mass spectra of the main peak for a) 5-bromotryptamine standard, b) 6-bromotryptamine standard, c) 7-bromotryptamine standard, d) ST9764 (*SrPyrH*, *LaRebF*, *CrTDC*), e) ST9336 (Tryptamine control, *CrTDC*). Theoretical m/z of $[M+H]^+$ and $[M+H-NH_3]^+$ adducts with ^{79}Br and ^{81}Br isotopes is 239.0178/221.9913 (most abundant) and 241.0158/223.9832, respectively.

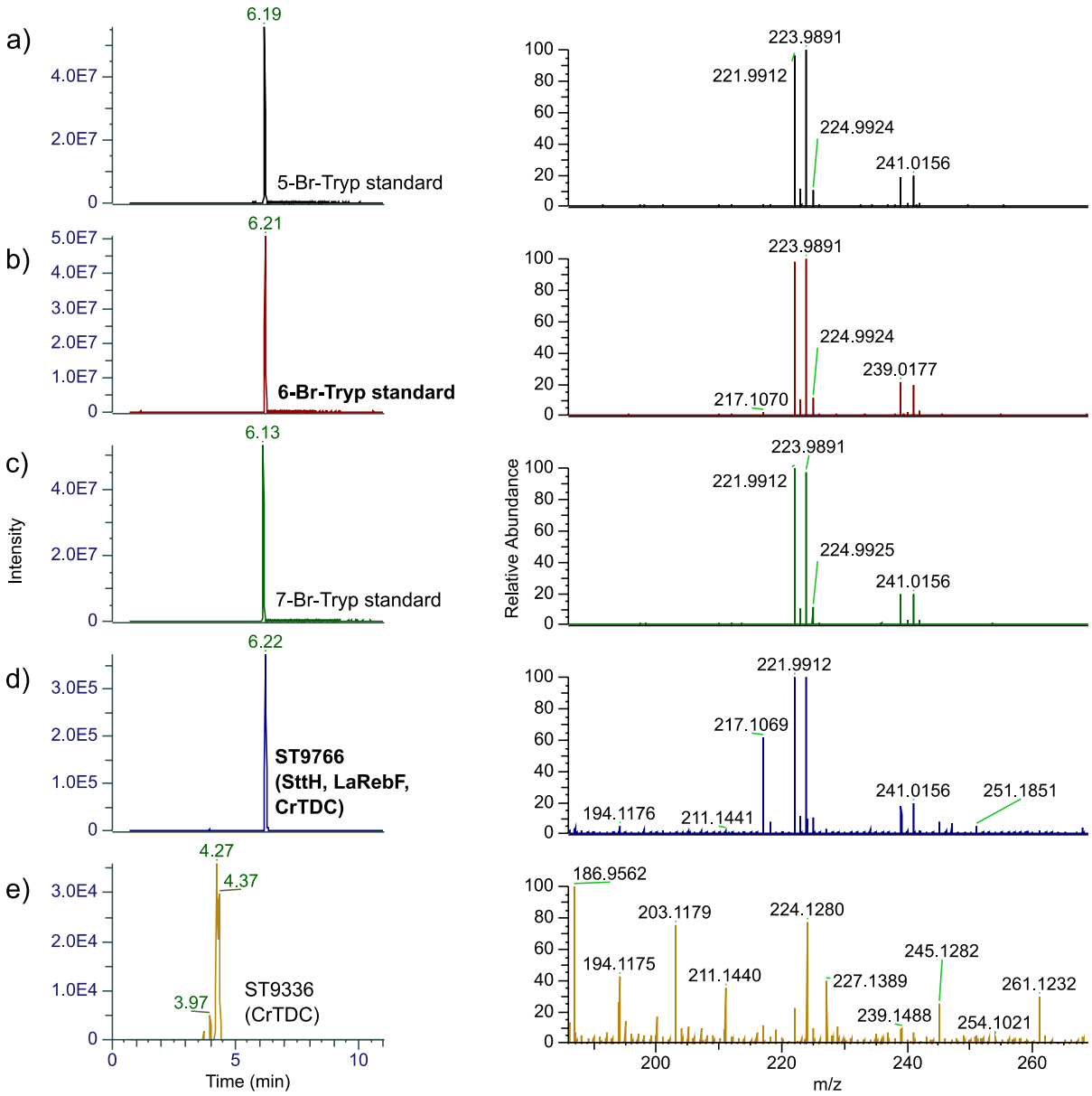

Figure S22. Production of 6-bromotryptamine in engineered *S. cerevisiae* strains. LC-MS extracted ion chromatograms and corresponding mass spectra of the main peak for a) 5-bromotryptamine standard, b) 6-bromotryptamine standard, c) 7-bromotryptamine standard, d) ST9766 (*SttH*, *LaRebF*, *CrTDC*), e) ST9336 (Tryptamine control, *CrTDC*). Theoretical m/z of $[M+H]^+$ and $[M+H-NH_3]^+$ adducts with ^{79}Br and ^{81}Br isotopes is 239.0178/221.9913 (most abundant) and 241.0158/223.9832, respectively.

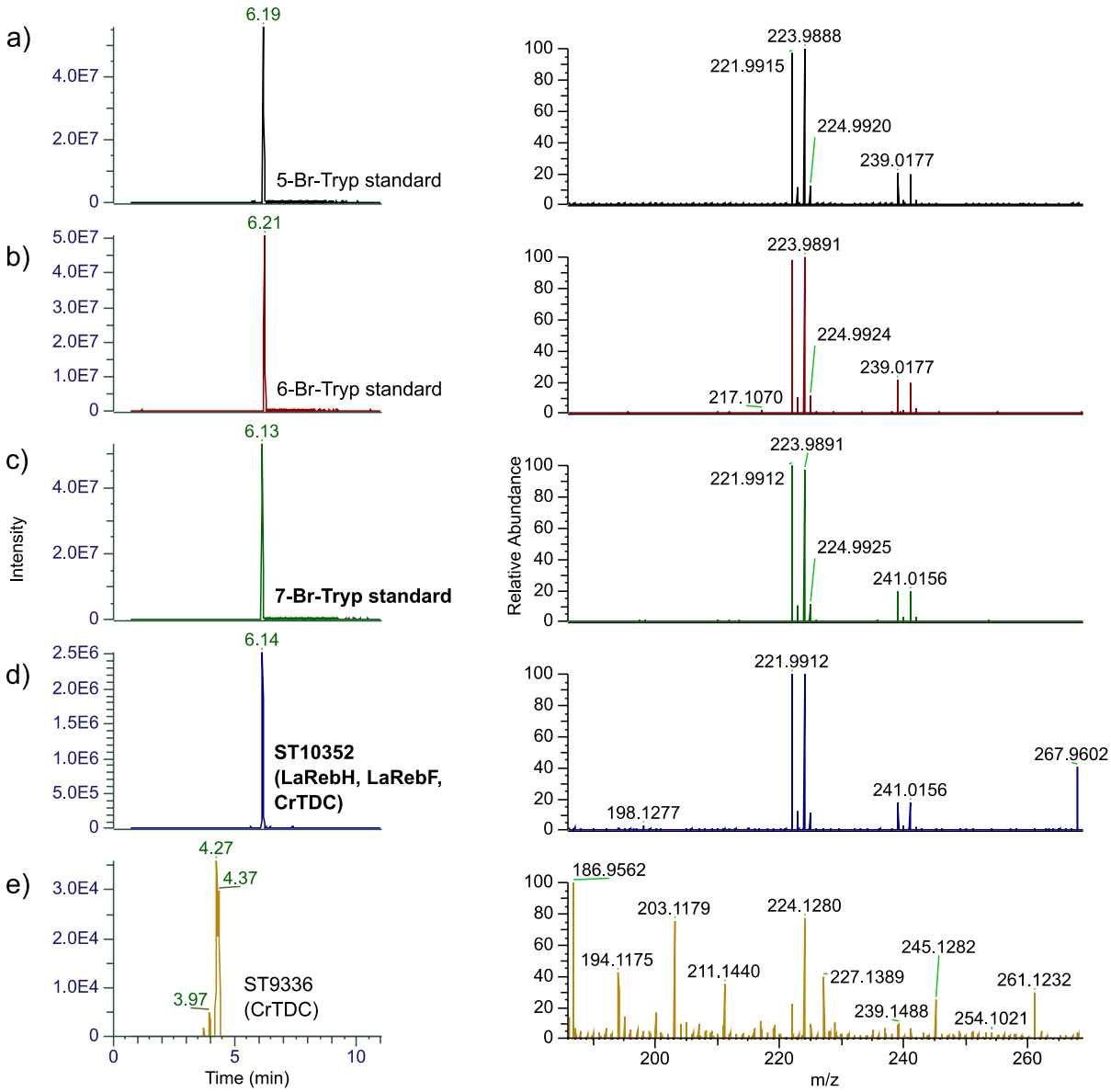

Figure S23. Production of 7-bromotryptamine in engineered *S. cerevisiae* strains. LC-MS extracted ion chromatograms and corresponding mass spectra of the main peak for a) 5-bromotryptamine standard, b) 6-bromotryptamine standard, c) 7-bromotryptamine standard, d) ST10352 (*LaRebH*, *LaRebF*, *CrTDC*), e) ST9336 (Tryptamine control, *CrTDC*). Theoretical m/z of $[M+H]^+$ and $[M+H-NH_3]^+$ adducts with ^{79}Br and ^{81}Br isotopes is 239.0178/221.9913 (most abundant) and 241.0158/223.9832, respectively.

a

Strain	*SrPyrH*	*SttH*	*LaRebH*	*LaRebF*	*CrTDC*
ST7574	–	–	–	–	–
ST9759	+	–	–	+	–
ST9760	+	–	–	–	–
ST9761	–	+	–	+	–
ST9762	–	+	–	–	–
ST10290	–	–	+	+	–
ST10291	–	–	+	–	–
ST9336	–	–	–	–	+
ST9764	+	–	–	+	+
ST9765	+	–	–	–	+
ST9766	–	+	–	+	+
ST9767	–	+	–	–	+
ST10352	–	–	+	+	+
ST10071	–	–	+	–	+

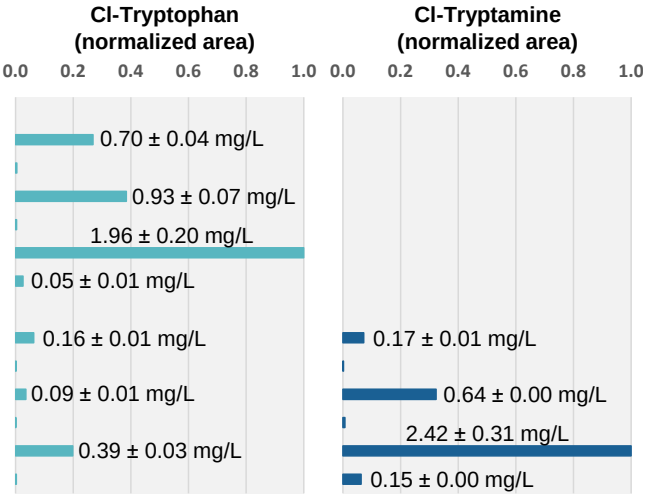

b

Strain	*SrPyrH*	*SttH*	*LaRebH*	*LaRebF*	*CrTDC*
ST7574	–	–	–	–	–
ST9759	+	–	–	+	–
ST9760	+	–	–	–	–
ST9761	–	+	–	+	–
ST9762	–	+	–	–	–
ST10290	–	–	+	+	–
ST10291	–	–	+	–	–
ST9336	–	–	–	–	+
ST9764	+	–	–	+	+
ST9765	+	–	–	–	+
ST9766	–	+	–	+	+
ST9767	–	+	–	–	+
ST10352	–	–	+	+	+
ST10071	–	–	+	–	+

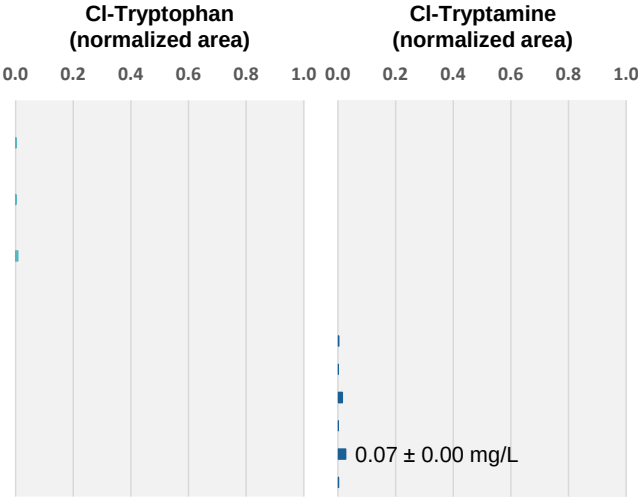

Figure S24. Production of chlorinated tryptophan and tryptamine in recombinant *S. cerevisiae* strains. Yeast strains were cultivated for 72 hours in synthetic mineral medium supplemented with a) 25 mM KCl or b) 25 mM KBr. "+" and "–" symbols indicate the presence or absence of the corresponding genetic modification, respectively. Cultivation broths of strains lacking *CrTDC* were subjected to the intracellular extraction protocol. Cultivation broths of strains expressing CrTDC were centrifuged and the supernatants were used for the analysis. Titers of halogenated products are reported as normalized peak areas, meaning that areas matching the retention time, expected m/z, and fragmentation pattern of the metabolite of interest have been normalized with respect to the highest-producing strain of that metabolite. Error values represent the standard deviation from two biological replicates. Data available in the Supplementary File 1.

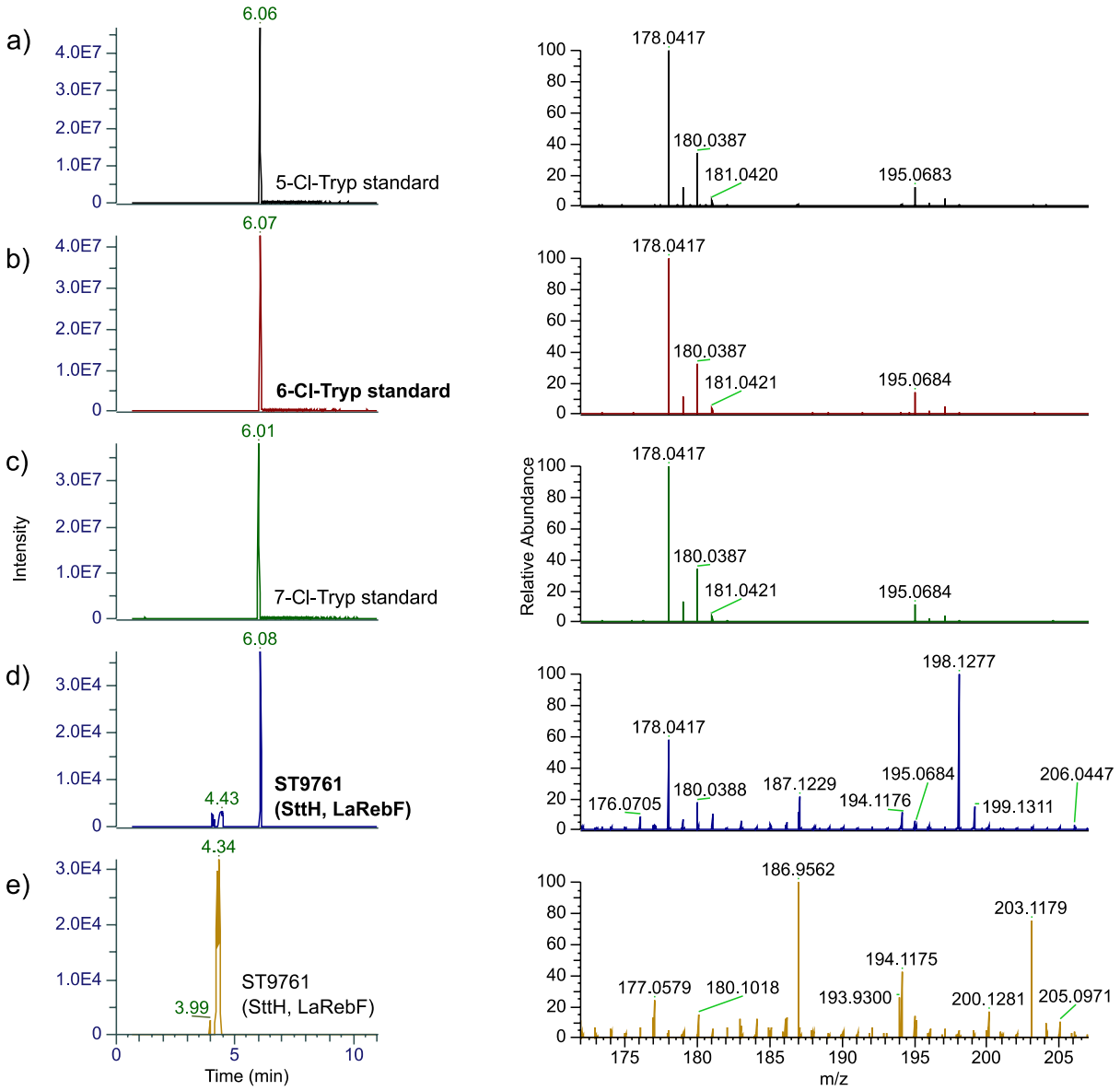

Figure S25. Direct chlorination of tryptamine in engineered *S. cerevisiae* strain expressing *SttH*. LC-MS extracted ion chromatograms and corresponding mass spectra of the main peak for a) 5-chlorotryptamine standard, b) 6-chlorotryptamine standard, c) 7-chlorotryptamine standard, d) ST9761 (*SttH*, *LaRebF*) fed with 1 mM tryptamine, e) ST9761 (*SttH*, *LaRebF*) without tryptamine feeding. Theoretical m/z of $[M+H]^+$ and $[M+H-NH_3]^+$ adducts with ^{35}Cl and ^{37}Cl isotopes is 195.0684/178.0418 (most abundant) and 197.0654/180.0389, respectively.

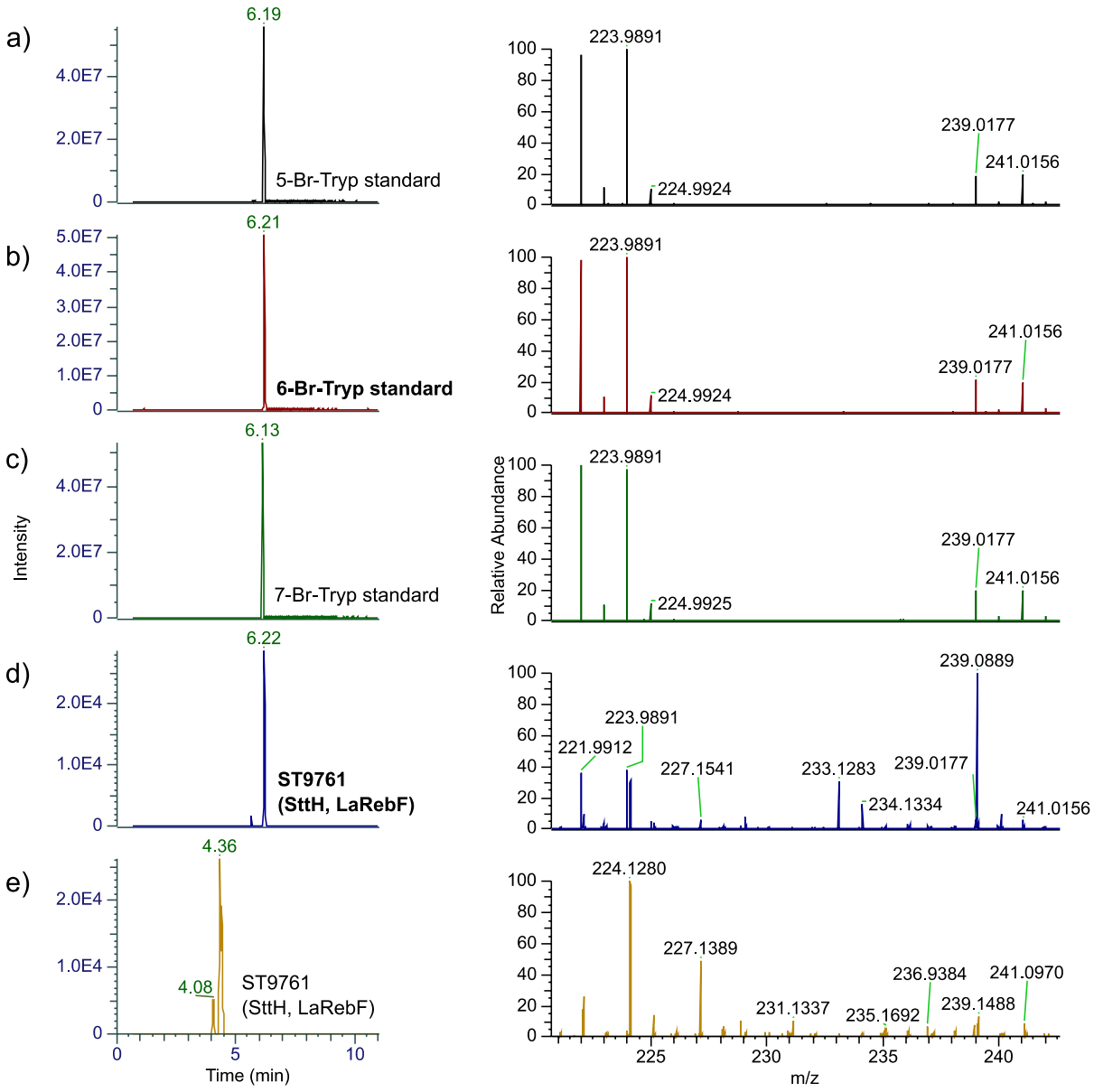

Figure S26. Direct bromination of tryptamine in engineered *S. cerevisiae* strain expressing *SttH*. LC-MS extracted ion chromatograms and corresponding mass spectra of the main peak for a) 5-bromotryptamine standard, b) 6-bromotryptamine standard, c) 7-bromotryptamine standard, ST9761 (*SttH*, *LaRebF*) fed with 1 mM tryptamine, e) ST9761 (*SttH*, *LaRebF*) without tryptamine feeding. Theoretical m/z of $[M+H]^+$ and $[M+H-NH_3]^+$ adducts with ^{79}Br and ^{81}Br isotopes is 239.0178/221.9913 (most abundant) and 241.0158/223.9832, respectively.

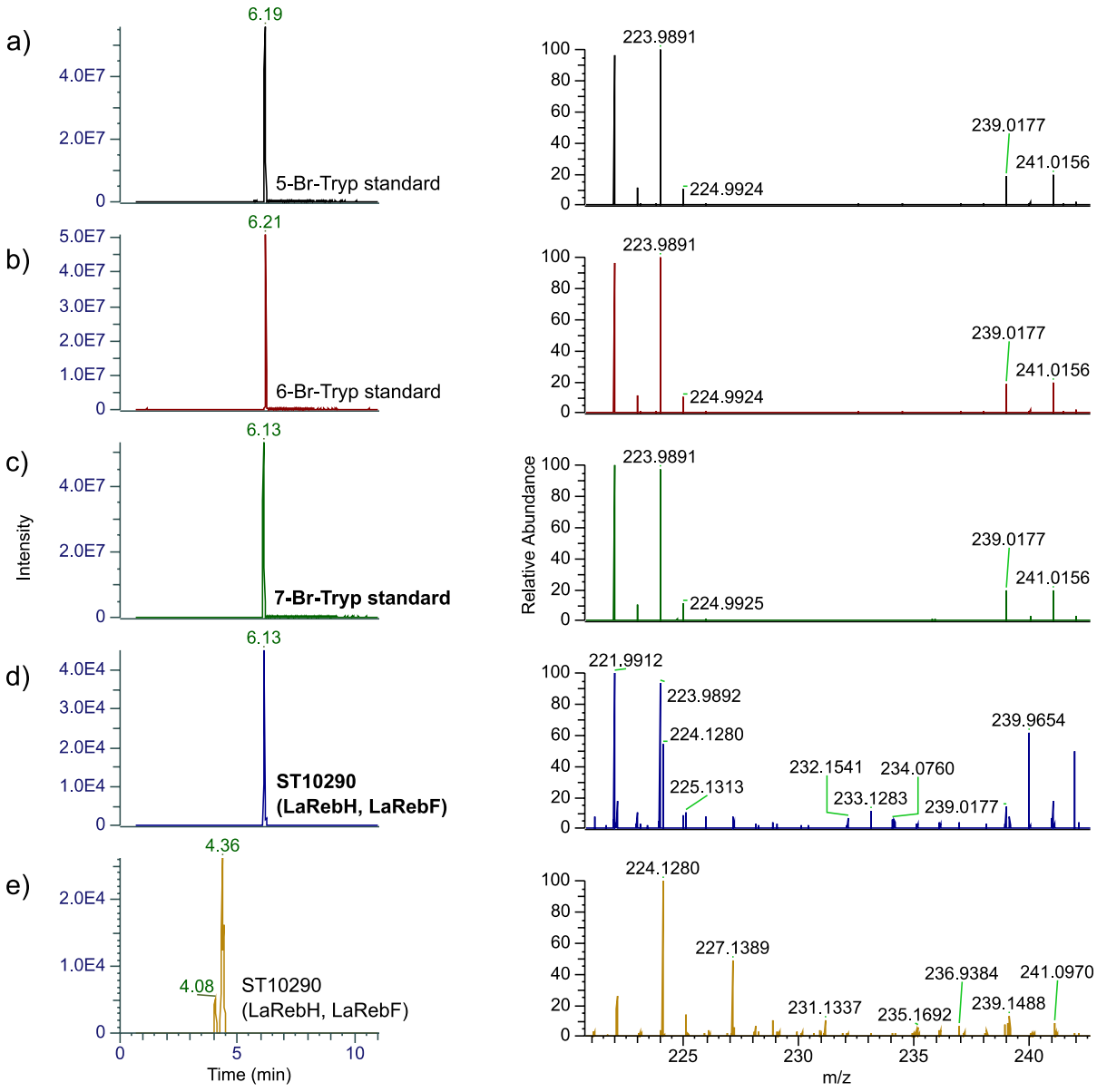

Figure S27. Direct bromination of tryptamine in engineered *S. cerevisiae* strain expressing *LaRebH*. LC-MS extracted ion chromatograms and corresponding mass spectra of the main peak for a) 5-bromotryptamine standard, b) 6-bromotryptamine standard, c) 7-bromotryptamine standard, ST10290 (*LaRebH*, *LaRebF*) fed with 1 mM tryptamine, e) ST10290 (*LaRebH*, *LaRebF*) without tryptamine feeding. . Theoretical m/z of $[M+H]^+$ and $[M+H-NH_3]^+$ adducts with ^{79}Br and ^{81}Br isotopes is 239.0178/221.9913 (most abundant) and 241.0158/223.9832, respectively.

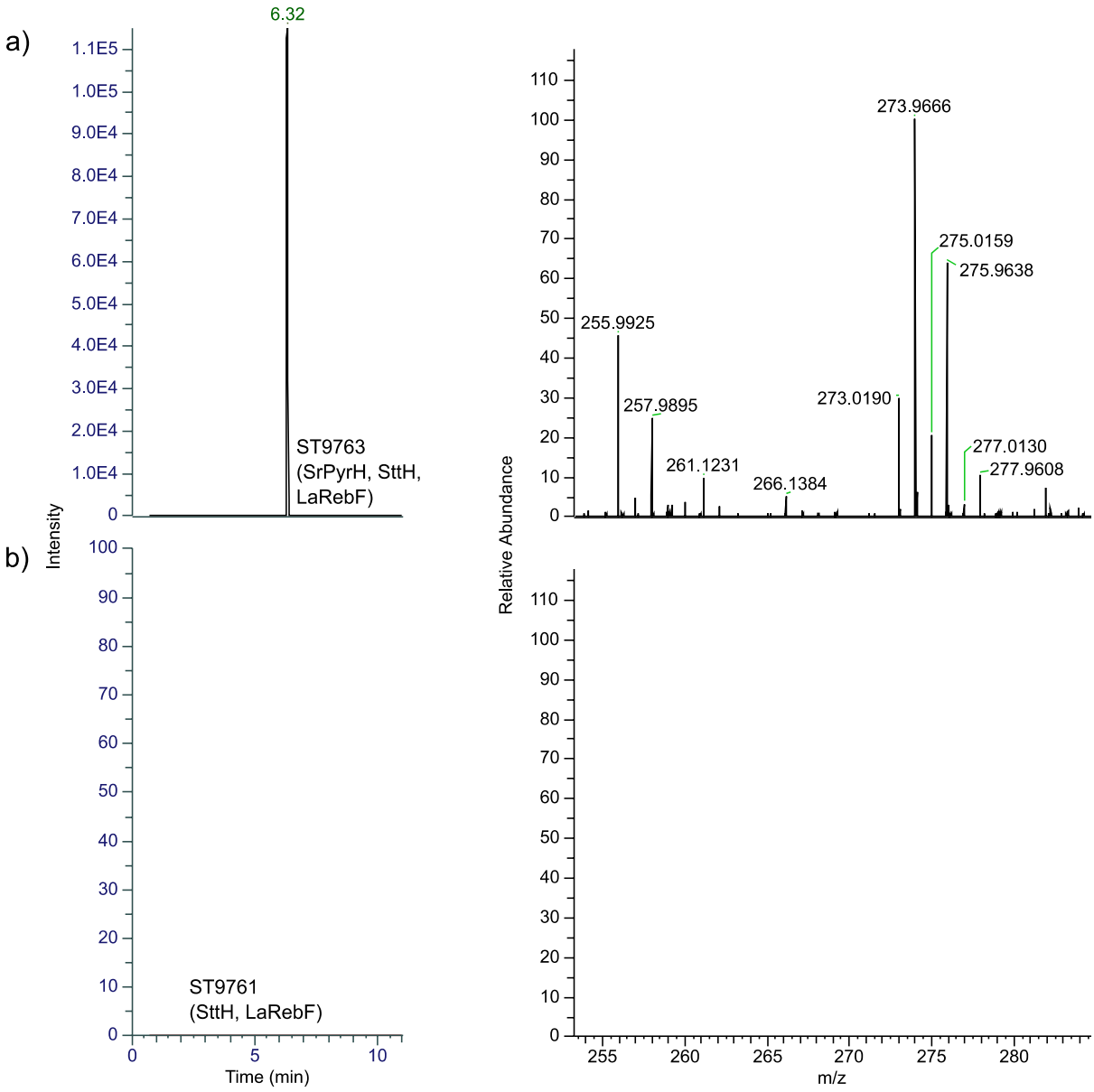

Figure S28. Production of 5,6-dichlorotryptophan in engineered *S. cerevisiae* strains. LC-MS extracted ion chromatograms and corresponding mass spectra of the main peak for a) ST9763 (*SrPyrH*, *SttH*, *LaRebF*), b) ST9761 (6-chlorotryptophan control, *SttH*, *LaRebF*). Theoretical m/z of $[M+H]^+$ and $[M+H-NH_3]^+$ adducts with $^{35}Cl/^{35}Cl$, $^{35}Cl/^{37}Cl$, and $^{37}Cl/^{37}Cl$ isotopes is 273.0192/255.9927 (most abundant), 275.0163/257.9897 and 277.0133/259.9868, respectively. Note the presence of a dichlorinated compound, likely dichlorinated xanthurenic acid, as the main halogenated product, with observed $[M+H]^+$ m/z of 273.9666 ($^{35}Cl/^{35}Cl$), 275.9698 ($^{35}Cl/^{37}Cl$), and 277.9608 ($^{37}Cl/^{37}Cl$).

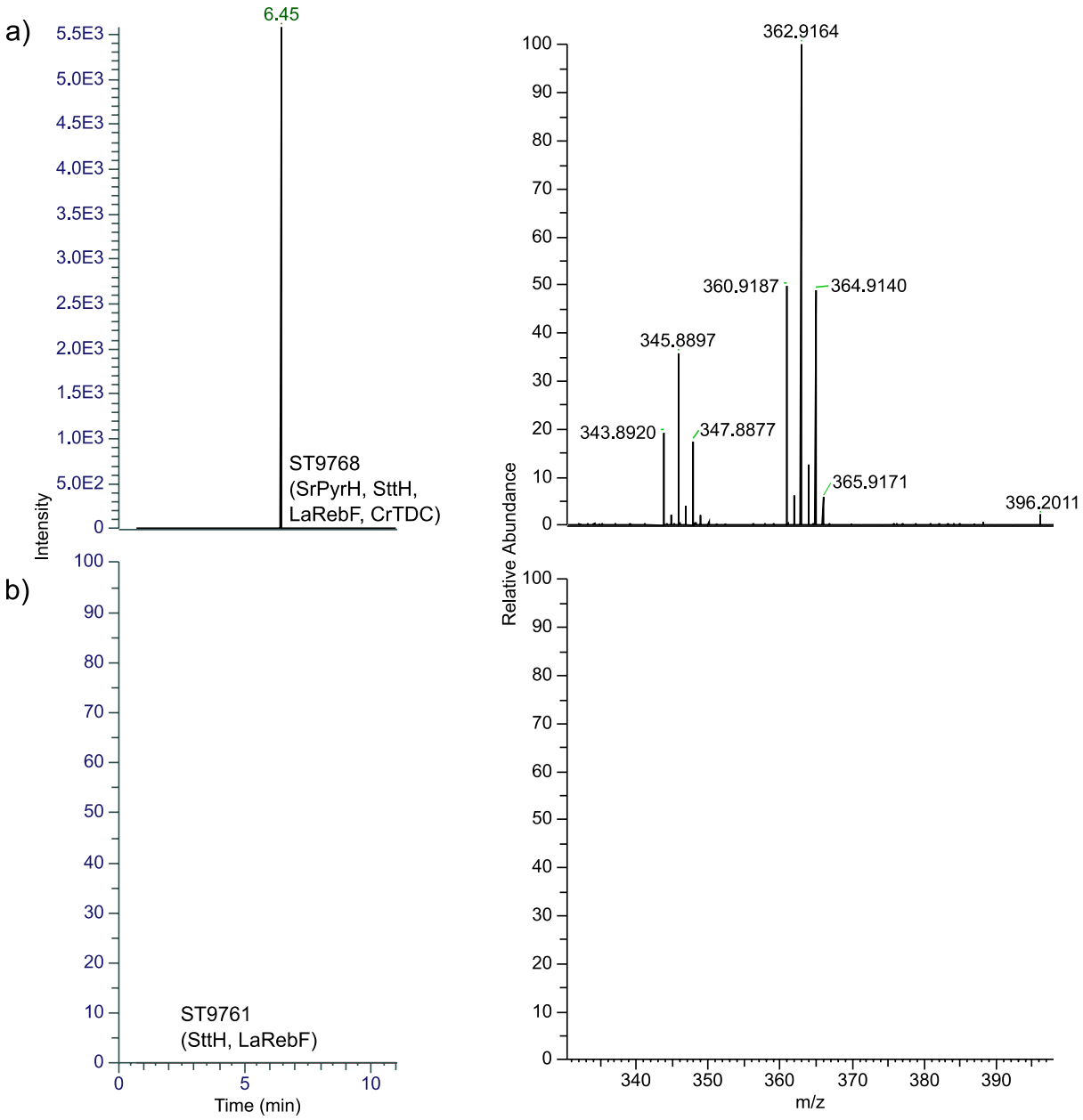

Figure S29. Production of 5,6-dibromotryptophan in engineered *S. cerevisiae* strains. LC-MS extracted ion chromatograms and corresponding mass spectra of the main peak for a) ST9768 (*SrPyrH*, *SttH*, *LaRebF*, *CrTDC*), b) ST9761 (6-chlorotryptophan control, *SttH*, *LaRebF*). Theoretical m/z of $[M+H]^+$ and $[M+H-NH_3]^+$ adducts with $^{79}Br/^{79}Br$, $^{79}Br/^{81}Br$, and $^{81}Br/^{81}Br$ isotopes is 360.9182/343.8916, 362.9161/345.8896 (most abundant), and 364.9141/347.8875, respectively.

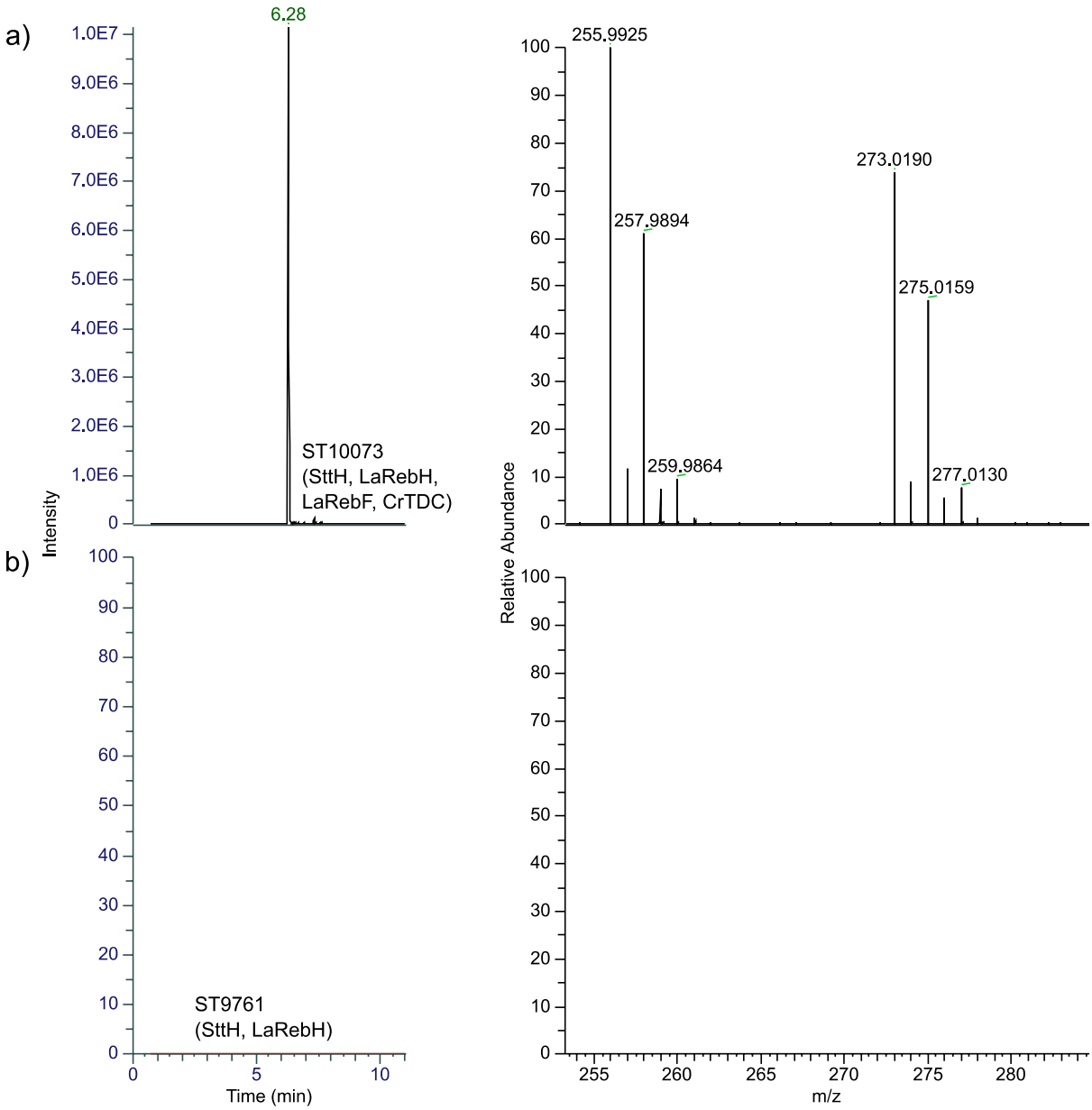

Figure S30. Production of 6,7-dichlorotryptophan in engineered *S. cerevisiae* strains. LC-MS extracted ion chromatograms and corresponding mass spectra of the main peak for a) ST10073 (*SttH*, *LaRebH*, *LaRebF*, *CrTDC*), b) ST9761 (6-chlorotryptophan control, *SttH*, *LaRebF*). Theoretical m/z of $[M+H]^+$ and $[M+H-NH_3]^+$ adducts with $^{35}Cl/^{35}Cl$, $^{35}Cl/^{37}Cl$, and $^{37}Cl/^{37}Cl$ isotopes is 273.0192/255.9927 (most abundant), 275.0163/257.9897 and 277.0133/259.9868, respectively.

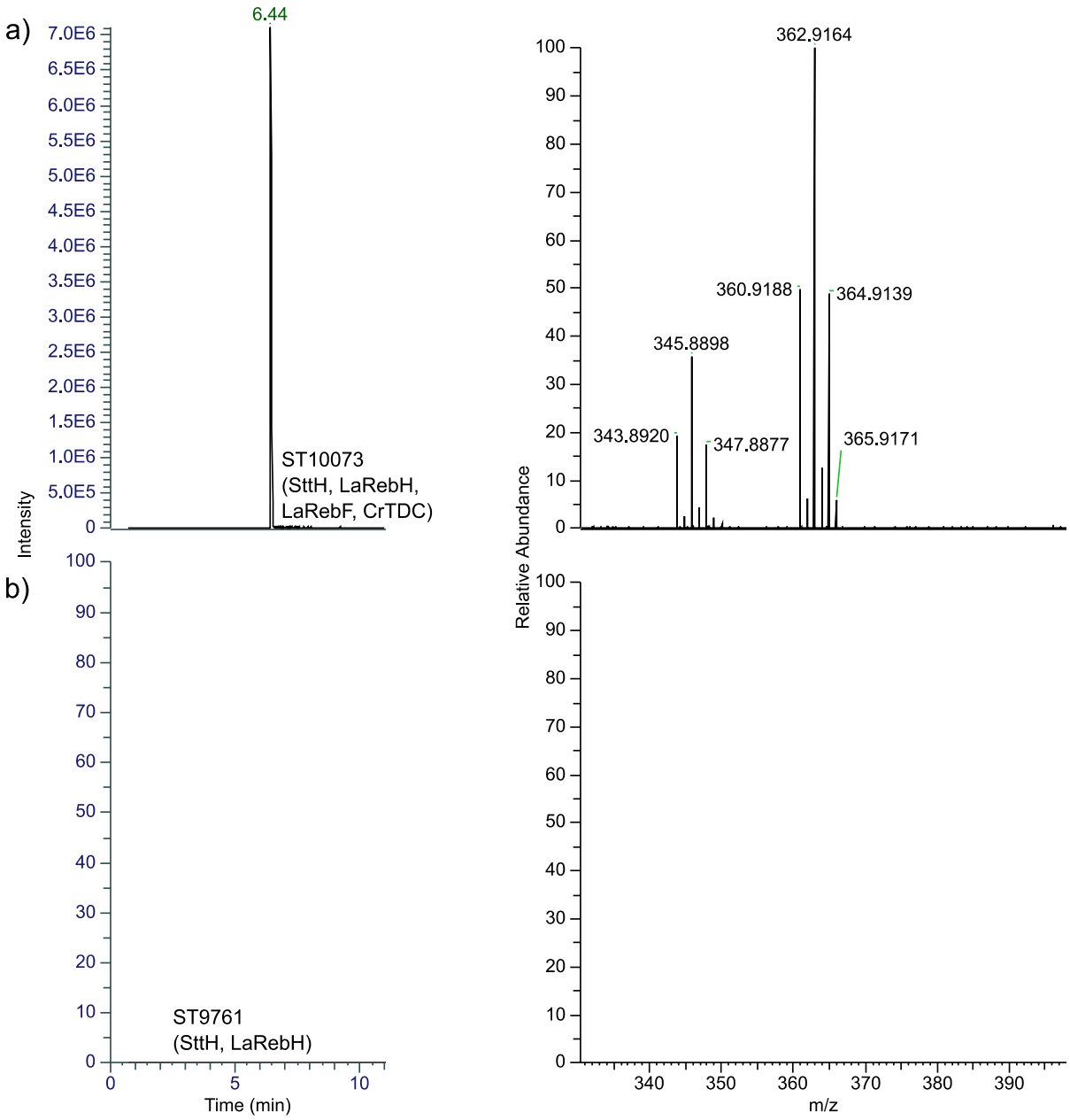

Figure S31. Production of 6,7-dibromotryptophan in engineered *S. cerevisiae* strains. LC-MS extracted ion chromatograms and corresponding mass spectra of the main peak for a) ST10073 (*SttH*, *LaRebH*, *LaRebF*, *CrTDC*), b) ST9761 (6-chlorotryptophan control, *SttH*, *LaRebF*). Theoretical m/z of $[M+H]^+$ and $[M+H-NH_3]^+$ adducts with $^{79}Br/^{79}Br$, $^{79}Br/^{81}Br$, and $^{81}Br/^{81}Br$ isotopes is 360.9182/343.8916, 362.9161/345.8896 (most abundant), and 364.9141/347.8875, respectively.

References

Entian, K.-D., Kötter, P., 2007. 25 Yeast Genetic Strain and Plasmid Collections, in: Methods in Microbiology. Elsevier, pp. 629–666. https://doi.org/10.1016/S0580-9517(06)36025-4

Jessop-Fabre, M.M., Jakočiūnas, T., Stovicek, V., Dai, Z., Jensen, M.K., Keasling, J.D., Borodina, I., 2016. EasyClone-MarkerFree: A vector toolkit for marker-less integration of genes into *Saccharomyces cerevisiae* via CRISPR-Cas9. Biotechnology Journal 11, 1110–1117. https://doi.org/10.1002/biot.201600147

Milne, N., Thomsen, P., Mølgaard Knudsen, N., Rubaszka, P., Kristensen, M., Borodina, I., 2020a. Metabolic engineering of Saccharomyces cerevisiae for the de novo production of psilocybin and related tryptamine derivatives. Metabolic Engineering 60, 25–36. https://doi.org/10.1016/j.ymben.2019.12.007

Milne, N., Tramontin, L.R.R., Borodina, I., 2020b. A teaching protocol demonstrating the use of EasyClone and CRISPR/Cas9 for metabolic engineering of Saccharomyces cerevisiae and Yarrowia lipolytica. FEMS Yeast Research 20. https://doi.org/10.1093/femsyr/foz062

CHAPTER 4

Identification of transporters involved in aromatic compounds tolerance through a deletion library screening

This chapter contains a manuscript in preparation:

Sáez-Sáez, J., Munro, L.J., Møller-Hansen, I., Kell, D.B., Borodina, I.

Abstract

Aromatic compounds are used in pharmaceutical, food, textile, and other industries. Increased demand has sparked interest in exploring biotechnological approaches for their sustainable production as an alternative to chemical synthesis from petrochemicals or plant extraction. These aromatic products may be toxic to microorganisms, which complicates their production in cell factories. In this study, we performed a broad analysis of the toxicity of 54 aromatics towards *Escherichia coli*, *Saccharomyces cerevisiae* and *Yarrowia lipolytica*, common production hosts for these compounds. Next, we selected a subset of toxic aromatics, namely 2-phenylethanol, 4-tyrosol, benzyl alcohol, berberine and vanillin, and screened them against a transporter deletion library in *E. coli* and *S. cerevisiae*, resulting in the identification of multiple transporters whose disruption increases or decreases in ability of the cells to tolerate these compounds. Lastly, based on the transporter targets we found for 2-phenylethanol in yeast, we showcased how transporter engineering can be applied to improve the metrics of 2-phenylethanol bioconversion from L-phenylalanine, with deletions of *YIA6*, *PTR2* or *MCH4* improving titer by 8-12% and specific yield by 38-57%. Our findings provide insights into the use of transporters as targets for improving the production of aromatic compounds in microbial cell factories.

Introduction

Aromatic compounds play a vital role in various facets of human life, including food, pharmaceuticals, and personal care (Berger, 2007; Welsch et al., 2010; Liu, 2022). Despite their widespread use and significance, the extraction of these compounds from natural plant producers is often hindered by low yields, and their chemical synthesis can be complex and generate hazardous waste (Hernandez and Sarlah, 2019; Kapadia et al., 2022). The rising demand for these compounds, combined with the limitations of traditional methods, has led to biotechnological manufacturing becoming an increasingly popular alternative (Averesch and Krömer, 2018; Huccetogullari et al., 2019; Liu et al., 2020).

Development of the microbial production of aromatic compounds has garnered extensive research in the scientific community, including the biosynthesis of complex

structures like flavonoids and alkaloids (Huccetogullari et al., 2019; Rodriguez et al., 2017; Zhang et al., 2022). Despite this, the number of aromatic compounds produced at an industrial scale through microbial fermentation remains limited. Notable examples include vanillin, a commonly used flavor in the food industry, and resveratrol, a food additive and supplement with health-promoting properties (Evolva, 2023a, 2023b; Sáez-Sáez et al., 2020). However, several challenges impede the broader adoption of a bio-based approach to the production of a greater diversity of aromatic compounds (Kim et al., 2023).

From a strain engineering perspective, product cytotoxicity is a common limitation (Mohedano et al., 2022). Many valuable aromatic compounds are naturally produced by plants as a defense mechanism and possess antimicrobial properties (Patra, 2012). Consequently, the production of aromatics in microbial cell factories often leads to a decline in cell fitness, robustness, and productivity. For example, vanillin and 2-phenylethanol have been reported to exhibit toxicity to yeast at concentrations below a gram per liter (Hansen et al., 2009; Hazelwood et al., 2006; Hassing et al., 2019). In order to overcome this challenge, tolerance adaptive laboratory evolution (TALE) has been widely adopted as the preferred method for generating tolerant phenotypes (Mohamed et al., 2020, 2017; Radi et al., 2022a; Sandberg et al., 2019). Through a gradual exposure of the strains to increasing levels of the toxic compound, phenotypes in the cell population with higher tolerance are selected and propagated. This process eventually results in the selection of cells resistant to high concentrations of the toxic product, leading to improved cell fitness and robustness (Dragosits and Mattanovich, 2013; Sandberg et al., 2019). In many instances, the underlying genetic basis of a tolerant phenotype can be attributed to mutations in transporter-encoding genes, which drive the exchange of the compound across the cell membrane (Lennen et al., 2023; Pereira et al., 2019, 2020; Radi et al., 2022a, 2022b; Kell, 2021). For example, in TALE experiments conducted with *E. coli* against different amino acids, mutations in genes encoding for membrane transporters were demonstrated to be responsible for improved amino acid tolerance. Implementation of the observed transporter modifications in an L-phenylalanine overproducer strain improved the product titers. Furthermore, fluorophore-based transport assays validated the role of the transporters in the amino acid exchange across the membrane, a function previously unknown for these transporters (Jindal et al., 2019; Radi et al., 2022b; Salcedo-Sora et al., 2021). These examples showcase the utility of TALE for generating tolerant

strains against toxic products and, more importantly, highlights a significant gap in the knowledge of molecule transport, even for well-known compounds such as amino acids. However, it is noteworthy that the evolved cells are not necessarily directly applicable as production hosts, as they often harbor multiple mutations, where some may be detrimental to the production of the toxic metabolite. Evolved strains may feature decreased transformation efficiencies, loss of heterologous pathways, or decreased transport of the product in general, both influx and efflux. Therefore, it is necessary to undergo a costly and time-consuming procedure of genome re-sequencing and reverse engineering to identify the causal mutations and then implement these in the production strain (Dragosits and Mattanovich, 2013; Sandberg et al., 2019).

Transporter engineering is a valuable strategy for enhancing the performance of microbial cell factories, offering multiple benefits beyond relieving product toxicity (Kell et al., 2015; Kell, 2018, 2021; Munro and Kell, 2021; van der Hoek and Borodina, 2020; Zhu et al., 2020). One potential advantage of transporter engineering is the ability to express transporters that uptake alternative, more cost-effective substrates (Thomik et al., 2017). In cases where the product exerts feedback inhibition, release into the media can alleviate this inhibition, which additionally reduces downstream processing costs (Korosh et al., 2017). Additionally, identifying appropriate transporters can prevent the leakage of pathway intermediates, further improving the economics of the bioprocess (Li et al., 2019). Despite the numerous benefits that transporter engineering can offer, it remains underutilized in strain engineering cycles due to a lack of knowledge regarding the relationship between substrates and corresponding transporters.

Multiple strategies have been utilized to associate substrates with their transporters, aside from TALE. Toxicity-based screening of transporter knockout or metagenomic libraries has been a commonly employed approach, where growth under toxic conditions is used as a selection criterion. This method has been applied in relevant microbial hosts to a range of compounds including amino acids, drugs, antibiotics, or the human hormone melatonin (Acton et al., 2017; Malla et al., 2022; Munro and Kell, 2022; Yang et al., 2022). More recently, the development of genetically encoded biosensors coupling intracellular compound concentrations to a detectable signal has enabled the discovery of new transporters for compounds such as thiamine, *cis*,*cis*-

muconic acid, and betaxanthins (Genee et al., 2016; Wang et al., 2021). While more specialized techniques, such as transporter expression in *Xenopus laevis* oocytes or solid-supported membrane-based electrophysiology, can provide valuable information, they typically require advanced expertise and have limited throughput (Bazzone et al., 2016; Nour-Eldin et al., 2006). Nevertheless, these techniques can achieve a deeper characterization of the transporters by performing more sophisticated transport assays (Bazzone et al., 2016).

As for many other families of compounds, the knowledge of the transport of aromatics in microorganisms is limited. Some research has been done on the transport of toxic aromatics generated during the valorization of lignocellulosic biomass or present in polluted areas with the prospect for bioremediation (Mutanda et al., 2022). However, transporter engineering has been sparsely applied in the context of microbial cell factories. Some successful examples within alkaloids production include the expression of exporters for the final product or importers for pathway intermediates, which can be utilized in co-culture systems involving two strains (Belew et al., 2020; Yamada et al., 2021; Dastmalchi et al., 2019).

In this study, we explore the potential of transporter engineering for improving the bioproduction of aromatics. Specifically, we evaluate the toxicity of 54 aromatic compounds in *E. coli*, *S. cerevisiae* and *Y. lipolytica*. We then use complete *E. coli* and *S. cerevisiae* transporter-knockout collections to screen against a subset of toxic aromatics, enabling us to identify transporter-encoding genes whose expression levels can improve or reduce product tolerance. Finally, we demonstrate the utility of transporter engineering for 2-phenylethanol production in of *S. cerevisiae*, resulting in improved process titer and specific yield.

Materials and methods

Strains and media

The initial toxicity assays were performed using *Saccharomyces cerevisiae* CEN.PK113-7D, *Yarrowia lipolytica* W29 (NRRL Y-63746), and *Escherichia coli* K-12 MG1655 and BL21(DE3) (Entian and Kötter, 2007; Gaillardin et al., 1973; Bachmann, 1972; Studier and Moffatt, 1986). For tolerance screenings against a selected group of toxic aromatics, isolates harboring single deletions in transporter-encoding genes

were obtained from the YKO (*S. cerevisiae* BY4741) and Keio (*E. coli* K-12 BW25113) deletion collections (Baba et al., 2006; Winzeler et al., 1999; Giaever et al., 2002). *S. cerevisiae* CEN.PK113-7D strain background was used for 2-phenylethanol overproduction and for testing the selected transporter candidates. All the strain genotypes are described in Table S1.

Yeast strains were cultivated in mineral medium containing (per L^{-1}) 7.5 g $(NH_4)_2SO_4$, 14.4 g KH_2PO_4, 0.5 g $MgSO_4 \cdot 7H_2O$, 20 g D-glucose, 2 mL trace metals solution, and 1 mL vitamins. The trace metals and vitamins solution were prepared as previously described (Jensen et al., 2014). The pH of the medium was adjusted to pH 6.0 with KOH. Auxotrophies of *S. cerevisiae* BY4741 derived strains were complemented by supplementing the medium with 380 mg/L leucine, 76 mg/L histidine, 76 mg/L methionine, and 76 mg/L uracil. In the production assays of 2-phenylethanol, 5 g/L of L-phenylalanine was added to the medium for bioconversion.

E. coli was grown in M9extra medium containing (per L^{-1}) 12.8 g $Na_2HPO_4 \cdot 7H_2O$, 3 g KH_2PO_4, 0.5 g NaCl, 1 g NH_4Cl, 0.24 g $MgSO_4$, 0.011 g $CaCl_2$, 20 g D-glucose, 1 mL $FeCl_3$ solution (50 mM $FeCl_3 \cdot 6H_2O$ in 100 mM citric acid monohydrate), and 500 µL of a trace elements solution, as previously described (Falkenberg et al., 2021). The pH of the medium was adjusted to pH 6.8 with NaOH.

Aromatic compounds in toxicity and tolerance screenings were added to the media and solubilized. The pH was then adjusted and the media were filter-sterilized. All the aromatic compounds were purchased from Sigma-Aldrich.

Strain construction

To construct integration plasmids for the overexpression of candidate transporter genes, we utilized the EasyClone-MarkerFree cloning system (Jessop-Fabre et al., 2016). Integration fragments and gRNA plasmids for CRISPR/Cas9-mediated genomic integration were constructed according to the protocol described by Jessop-Fabre et al. (Jessop-Fabre et al., 2016). BioBricks were amplified with Phusion U Hot Start DNA Polymerase (Thermo Fisher Scientific) and USER-compatible primers, and then subjected to USER reactions based on the standard protocol from New England Biolabs. The resulting products were transformed into competent *E. coli* DH5α cells to assemble and propagate the plasmids, which were then purified using the

NucleoSpin plasmid miniprep kit (Macherey Nagel) and sequenced by Eurofins Scientific to confirm the correct plasmid assembly. FastDigest NotI restriction enzyme (Thermo Fisher Scientific) was used to linearize the integration fragments, which were then transformed into *S. cerevisiae* strains expressing Cas9, along with the corresponding gRNA plasmids, using the LiAc/ssDNA/PEG method (Gietz and Schiestl, 2007). Transformations were recovered in YPD+G418 media at 30°C with 250 rpm shaking before plating on YPD supplemented with G418 and nourseothricin. We confirmed the integration of the vectors into the correct sites on the genome by performing colony PCR with RedTaq DNA polymerase (VWR Life Science). We provide a comprehensive list of all strains, plasmids, BioBricks, and primers used and constructed in this study in the Supporting Information (Tables S1–S4).

Cultivation procedure and conditions

In the toxicity experiments, 0.5 mL of medium in a 13 mL pre-culture tube was inoculated with wild-type strains, stored as cryostocks, using a 10 µL inoculation loop. The tubes were incubated at 30 (yeast) or 37 °C (*E. coli*) and 250 rpm for 20 (*E. coli*) or 24 hours (yeast). Next, 400 µL of broth was transferred to a 250 mL shake flask containing 10 mL of medium and incubated under the same conditions for 6-8 (*E. coli*) or 10-12 hours (yeast) until having exponentially growing cells. These cultures were then used as inoculum (<5 µL, initial $OD_{600} \approx 0.1$) for 96-well plates with transparent bottom (CR1496dg, EnzyScreen BV) containing 300 µL of medium per well. Plates were covered with a sandwich cover with pins (CR1396b, EnzyScreen BV).

To screen the transporter deletion library, 500 µL of medium in 96-deep well plates was inoculated with the library using a 96-pin replicator (CR1000, EnzyScreen BV). The plates were covered with an air penetrable lid (CR1296, EnzyScreen BV) and then incubated at 30 °C (yeast) or 37 °C (*E. coli*) and 300 rpm overnight. The following day, the resulting plates were mixed with 500 µL of glycerol. A 3 µL droplet of the broth and glycerol mixture was dispensed into the bottom of each well in 96-well plates with transparent bottom (CR1496dg, EnzyScreen BV). The loaded plates containing the propagated library were stored at −20 °C for up to 3 weeks, or at −80 °C for longer storage. To initiate the library screening, 297 µL of media was dispensed into the inoculated plates, which prior to incubation were covered with a sandwich cover with

pins (CR1396b, EnzyScreen BV). Glycerol mixing of pre-cultures, inoculation and media loading were performed using an Opentron OT-2 liquid handler, as previously described (Munro and Kell, 2022). Scripts for operating the OT-2 have been previously made available at https://github.com/ljm176/TransporterScreening.

For the validation of transporter candidates and in the 2-phenylethanol production assays, 96 deep-well plates containing 0.5 mL of medium were inoculated with the strains. The plates were covered with an air penetrable lid (CR1296, EnzyScreen BV) and incubated at 30 (*S. cerevisiae*) or 37 °C (*E. coli*) and 300 rpm for 18 (*E. coli*) or 20 hours (yeast). The following day, OD_{600} of the pre-cultures was measured and a volume corresponding to an initial OD_{600} of 0.1 was transferred to 96-well plates with a transparent bottom (CR1496dg, EnzyScreen BV), containing 300 µL of medium.

In all experiments, plates were incubated using the Growth Profiler 960 (EnzyScreen BV) at 30 °C/250 rpm for yeast and 37 °C/225 rpm for *E. coli*, following the manufacturer's recommended shaking settings. Images were captured at 15-20 minute intervals for *E. coli* and 20-30 minute intervals for yeast, with a shutter time of 5 ms. Cultivation times were at least 40 hours for *E. coli* and 60 hours for yeast to ensure adequate growth for the estimation of μ_{max}. Cultivations were performed in duplicate, with the exception of the validation of transporter-deletion candidates (n = 4) and the assessment of the effect of transporter engineering on 2-phenylethanol production (n = 3).

Microbial growth data analysis

Growth Profiler 960 pictures were processed using the manufacturer's software GP960Viewer to obtain G-values from the central pixels of each well. G-values were then converted to OD_{600} equivalents using calibration curves previously generated. Growth rates were determined from the growth data using custom Python scripts that calculate the slope of linear regression fits between ln-transformed OD_{600} and time. A minimum OD_{600} of 0.125 in *E. coli* and 0.3 in yeast was required to initiate growth rate calculations. A sliding window of 12 time points (corresponding to 180-240 minutes in *E. coli* and 240-360 minutes in yeast) was used to determine growth rates across the growth curves. The maximum specific growth rate (μ_{max}) was defined as the maximum slope within the growth profile having a correlation coefficient R^2 greater

than 0.98. Half maximal inhibitory concentrations (IC_{50}) were determined using GraphPad Prism 9 and a variable slope four-parameter model. During the screening of the transporter deletion library, any strains that were unable to grow in a control medium without the presence of any toxic aromatic compounds were excluded from further analysis. Additionally, any strains that displayed a coefficient of variation greater than 0.3 for their relative μ_{max} in the presence of aromatics compounds (μ_{max} strain/μ_{max} wild-type) were also excluded from the analysis. All growth data, raw and processed, is presented in the Supplementary File 1.

Quantification of 2-phenylethanol using high-pressure liquid chromatography

To quantify 2-phenylethanol, the supernatant of the yeast cultivation samples was used after centrifugation at 17,000 g for 5 min. The quantification was performed using a Dionex UltiMate 3000 high-pressure liquid chromatography (HPLC) system equipped with a DAD-3000 UV/Vis detector (Dionex). The stationary phase was a Discovery HS F5 150 mm × 2.1 mm column with a particle size of 3 µm, while the mobile phase was a binary system composed of 10 mM ammonium formate at pH 3.0, adjusted by formic acid (solvent A), and acetonitrile (solvent B). The flow rate was set to 0.7 mL/min, and 5 µL of the sample was injected for quantification. The solvent composition was initially set to A = 95.0% and B = 5.0%, which was maintained until 0.5 min. Thereafter, the solvent composition was changed following a linear gradient until A = 40.0% and B = 60.0% at 7.0 min, which was kept constant for 2.5 min (7.0–9.5 min). The solvent composition was then returned linearly to the initial conditions (A = 95.0%, B = 5.0%) at 9.6 min and remained unchanged until the end of the run (9.6-12 min).

2-Phenylethanol was detected at a retention time of 4.8 min, and the absorbance at 214 nm was used for quantification. Peaks corresponding to the target compounds were identified by comparison to prepared standards (Sigma-Aldrich). Peak areas were used for compound quantification using the external standard calibration method. Analysis of HPLC results was performed using the software Chromeleon 7 (Thermo Fisher Scientific).

Results

Toxicity evaluation of a broad range of aromatic compounds

The production of aromatic compounds via microbial fermentation has gained significant attention in recent years due to its potential for sustainable and efficient industrial processes. Over 50 different aromatic compounds that have been produced in cell factories have been listed in a recent literature review (Huccetogullari et al., 2019). However, although some studies have reported toxicity at low concentrations for specific products, a comprehensive evaluation of the overall toxicity of aromatics in multiple microbial hosts is lacking.

To address this gap, we conducted a rigorous assessment of the toxicity of multiple aromatic compounds. Our selection criteria encompassed a range of parameters, including diverse aromatic ring structures, distinct functional groups, commercial relevance, and the potential for production in cell factories, resulting in the inclusion of 54 aromatic compounds in our evaluation (Tables S5-S6). In order to conduct the toxicity assessment, we selected common production hosts for aromatics, namely, the bacterium *Escherichia coli* (strains BL21(DE3) and K-12 MG1655) and the baker's yeast *Saccharomyces cerevisiae* (Averesch and Krömer, 2018; Huccetogullari et al., 2019; Liu et al., 2020). We also included the non-conventional yeast *Yarrowia lipolytica*, which has demonstrated excellent potential as a host for aromatics production (Gu et al., 2020; Liu et al., 2022; Sáez-Sáez et al., 2020).

Our evaluation of compound toxicity was conducted in liquid cultivations, with each compound tested at five different concentrations (Table S7). To determine the inhibitory effects of the compounds on growth, we measured the maximum specific growth rate (μ_{max}) and used the half-maximal inhibitory concentration (IC_{50}) to quantify their potency (Figure 1, Figure S1).

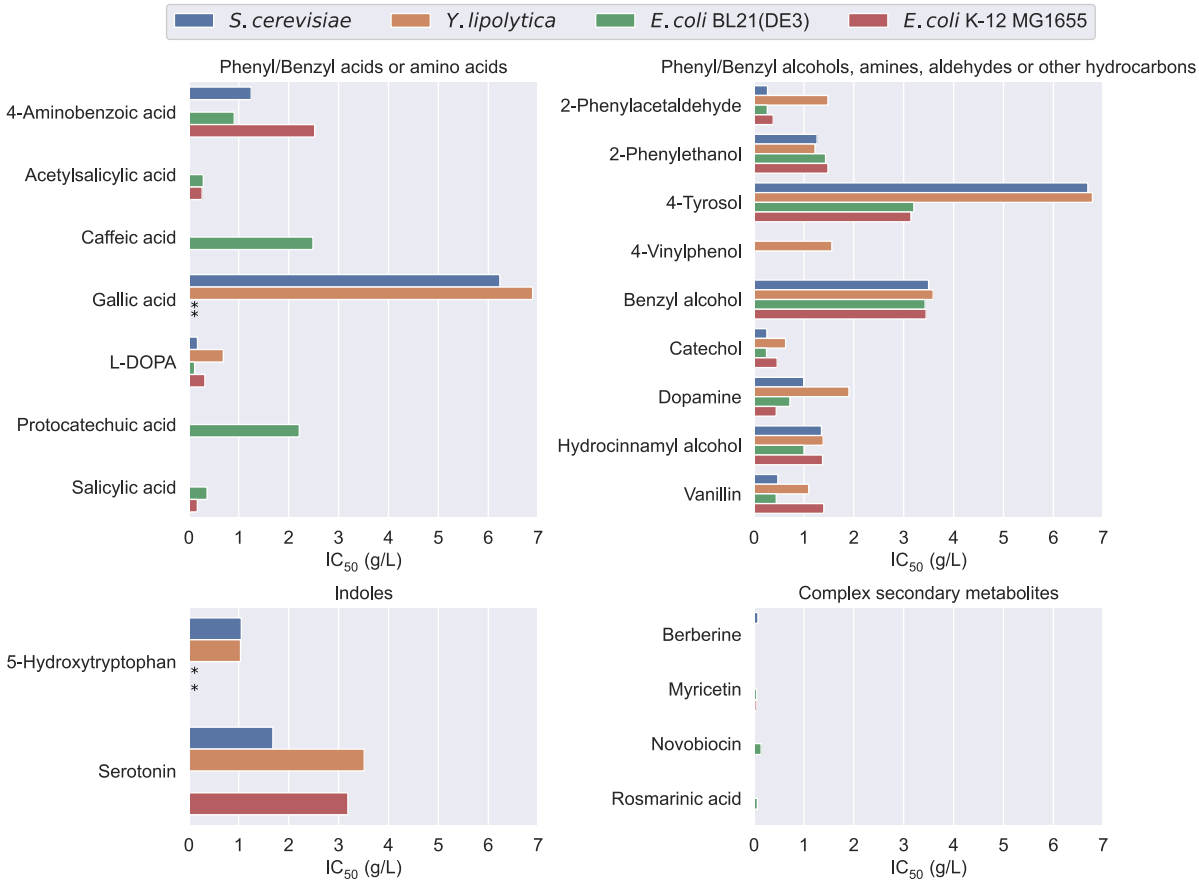

Figure 1: Comparison of estimated IC_{50} values for various toxic aromatic compounds on different microorganisms. A missing bar indicates that the IC_{50} value was not reached within the concentration range tested. *: toxicity could not be determined due to medium becoming black over time.

The toxicity evaluation resulted in the identification of 22 compounds that reduced μ_{max} to half in at least one of the four strains tested. Remarkably, 9 of these compounds exhibited toxicity towards all the strains, highlighting their antimicrobial effect against both yeast and *E. coli*. These aromatic compounds predominantly belong to the phenyl or benzyl alcohols, amines, or aldehyde classes, and exhibited an IC_{50} value mostly below 2 g/L. Complex aromatic compounds that belong to secondary metabolites typically have poor solubility in water and seldom exhibited toxicity before they reached their solubility limits.

In general, we found that there were no major differences in tolerance among the different microorganisms tested, and compounds that were toxic to only one host were rare occurrences. Notably, *Y. lipolytica* appeared to be equally or more tolerant than

S. cerevisiae, while *E. coli* strains showed similar tolerance levels, with some compounds like vanillin or 4-aminobenzoic acid exhibiting differential effects on the two strains. This is consistent with what can be a very substantial difference in accumulation of aromatic fluorophores for related *E. coli* strains (Salcedo-Sora et al., 2021).

Screening of transporter deletion libraries yields transporter deletions improving or reducing tolerance to aromatics

The identification of aromatic compounds that are toxic to common microbial production hosts prompted us to develop a strategy for generating tolerant strains against them. Given the evidence that transporter manipulation can confer resistance or sensitivity to toxic compounds, we screened a transporter deletion library to identify potential targets for engineering (Lennen et al., 2023; Pereira et al., 2019, 2020; Radi et al., 2022b). We employed strains harboring individual transporter-encoding gene knockouts derived from the *E. coli* Keio and *S. cerevisiae* YKO deletion collections. Specifically, our transporter deletion libraries comprised 444 *E. coli* and 305 *S. cerevisiae* individual transporter knockout strains, covering a significant proportion of the genes annotated as transporters in the two model microorganisms (Table S8, Figure S2) (Yang et al., 2022; Munro and Kell, 2022; Wang et al., 2021). Many of these were 'orphan' or in *E. coli* so-called y-genes, whose substrates were still not known (Ghatak et al., 2019).

The transporter deletion library was screened against a subset of aromatic compounds from those identified as toxic (Figure 1). Our selection criteria were based on multiple factors, including industrial relevance and reports of production and toxicity in cell factories. The compounds we selected were: 2-phenylethanol (used in fragrances, flavors, and cosmetics due to its pleasant floral aroma) (Hua and Xu, 2011); 4-tyrosol (a natural antioxidant with potential therapeutic applications for oxidative stress-related diseases) (Karković Marković et al., 2019); benzyl alcohol (a versatile compound used as a solvent, flavoring agent, and preservative) (del Olmo et al., 2017); berberine (used in traditional Chinese medicine and has shown potential as a therapeutic agent for various conditions) (Ai et al., 2021); and vanillin (a popular

flavoring agent used in the food industry, as well as in fragrances and cosmetics) (Martău et al., 2021).

As the genetic background of the parent strains from the Keio and YKO collections differed from those used in the toxicity screening, resulting in potential variations in tolerance, we reassessed the compound toxicity in the new backgrounds (Figure 2a-b). While the toxicity profiles of most compounds remained consistent, *S. cerevisiae* BY4741 exhibited increased tolerance to berberine and 4-tyrosol, the latter of which was non-toxic within the concentration range tested. Likewise, berberine was not toxic in *E. coli* K-12 BW25113, similar to what was observed in the previous background. For the library screening, we selected a compound concentration that resulted in an approximate halving of μ_{max}, with the aim of identifying transporter deletions that could improve or reduce product tolerance (Figure 2a-b, Table S9).

For each strain of the library, we analyzed the μ_{max} relative to the wild-type strain in the presence of each toxic compound. In general we observed a normal distribution of the library population, with most of the strains falling within ±2 standard deviations of the mean relative μ_{max} value. To identify potential transporters responsible for transporting aromatics, we selected for further validation the top 8 strains for each microorganism and compound with the highest and lowest product tolerance.

Although the library screening method allowed for identifying preliminary transporter deletions affecting product tolerance, it had some limitations that could have affected the μ_{max} determinations. The lack of a pre-culture step and the direct growth of cells from cryostocks, which could have led to differences in inoculum size and state, have been demonstrated to result in significant variations in μ_{max} in high-throughput screenings (Atolia et al., 2020). To address these limitations, in the validation step of the selected candidates, we used the same inocula size of exponentially growing cells for all strains, and we increased the number of replicates to ensure sufficient statistical power.

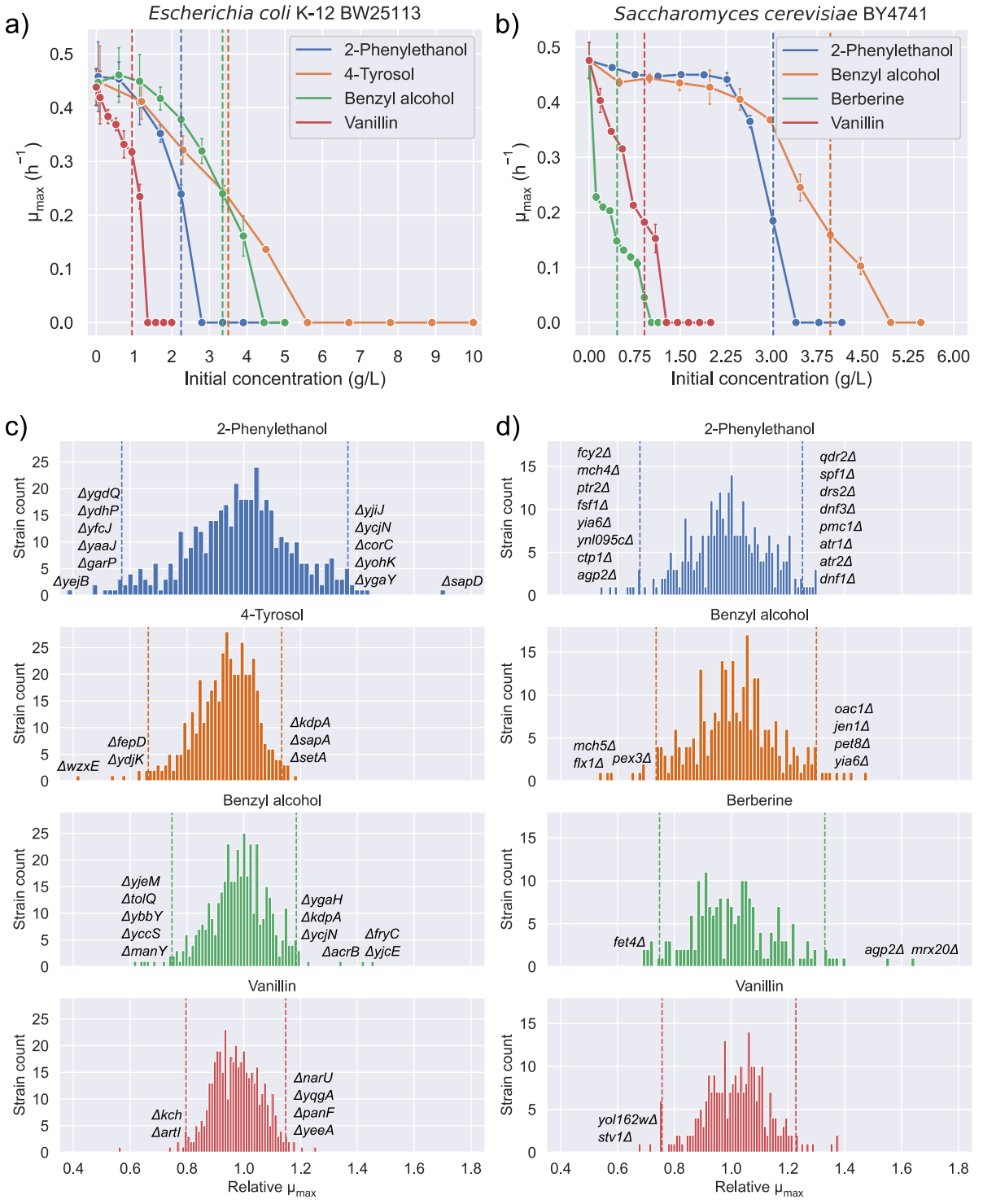

Figure 2. Screening the transporter deletion library for tolerance against toxic aromatic compounds. Panels a) and b) display the toxicity of each aromatic compound towards the parent strain of the transporters deletion library, with the dashed lines indicating the chosen concentration for subsequent library screening. Panels c) (*E. coli*) and d) (*S. cerevisiae*) depict the distribution of the library against each aromatic compound through histograms. The mean relative μ_{max} with respect to the wild-type control is used as distribution parameter. The relative μ_{max} cutoff value, indicated by dashed lines, was used to select the top

eight candidates with the highest and lowest product tolerance. Strains from each top 8 with validated effects are identified by labeled histogram bins (Figure 3).

To confirm that the effects observed in the relative μ_{max} were not due to a growth defect of the transporter deletion, we evaluated the impact of each candidate transporter deletion in the absence of any aromatic compound (Figure 3). Most transporter deletions did not cause significant differences in μ_{max} compared to the wild-type strain when grown in the control medium. However, marked differences were observed in the strains harboring deletions of *ygdQ*, *tolQ*, and *ybbY* in *E. coli* and deletions in *PTR2*, *YNL095C* and *FLX1* in *S. cerevisiae*, with up to ca. 25% reduction in μ_{max}. Next, we assessed the effect of the transporter deletions in the presence of toxic aromatics and confirmed a number of deletions resulting in improved or reduced tolerance for specific compounds (Figure 3, Figures S3-S4, Table S10). Transporter deletions were generally found to restore μ_{max} by app. 15 to 60% (Figure S3).

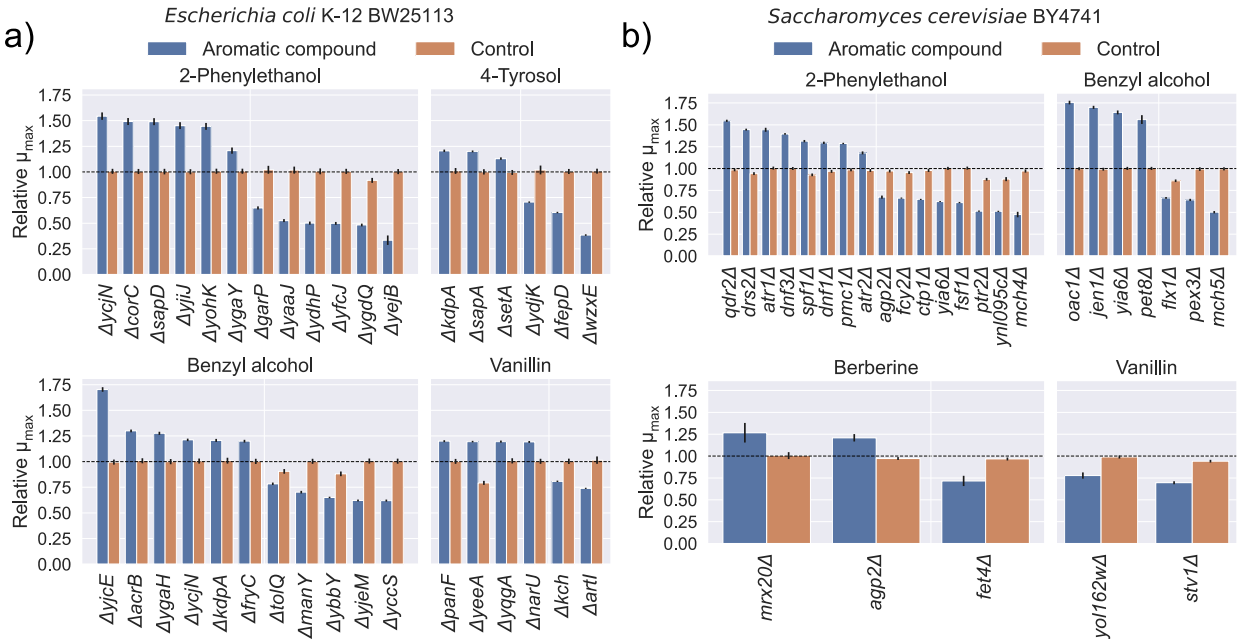

Figure 3. Validated transporter deletions that either improve or reduce the tolerance of a) *E. coli* and b) *S. cerevisiae* to multiple toxic aromatic compounds. *Control* represents μ_{max} with respect to the wild-type strain in control medium, lacking any toxic aromatic compound. *Aromatic compound* shows the μ_{max} with respect to the wild-type strain in the same medium but containing the aromatic compound indicated in each subplot, at the same concentration used in the library screening (Table S9). Error bars denote the estimated standard deviation of at least 4 biological replicates. The horizontal dashed line

indicates a value of 1, expected for strains not showing differences with respect to the wild-type control.

Interestingly, specific transporter deletions were found to affect the tolerance of more than one aromatic. For instance, *ΔycjN* in *E. coli* improved the tolerance of 2-phenylethanol and benzyl alcohol, while *ΔkdpA* enhanced the tolerance of 4-tyrosol and benzyl alcohol. In *S. cerevisiae*, *agp2Δ* enhanced the resistance to berberine while diminishing 2-phenylethanol tolerance, and a similar trend was observed for *yia6Δ* between benzyl alcohol and 2-phenylethanol.

Multi-compound analysis of the transporter deletion libraries suggests interrelationships between transporters

Following the identification of transporter deletions with similar or opposite effects in two different aromatics (Figure 3), we explored other potential interrelationships between transporters within the whole library dataset generated. We searched for transporter deletion pairs presenting similar trends in terms of μ_{max} for the four aromatic compounds tested, translated into a high correlation coefficient ($R^2 > 0.999$) and a p-value < 0.05 after applying a full Bonferroni correction. We found 44 transporter pairs in *E. coli* and 13 transporter pairs in *S. cerevisiae* that met these criteria (Figures S5-S6). The transporters set derived from all the pairs exhibited clustering patterns (Figure 4) that could provide insight into the function of transporters with unknown functions by comparison to those with known functions. For instance, the deletion of the transporter-encoding y-gene from *E. coli yifK* showed a high degree of correlation with the deletion of *argT* (Figure 4a, Figure S5), known to be involved in the uptake of multiple amino acids (Charlier and Bervoets, 2019). Therefore, *yifK* could potentially have some shared function or substrate specificity with *argT*.

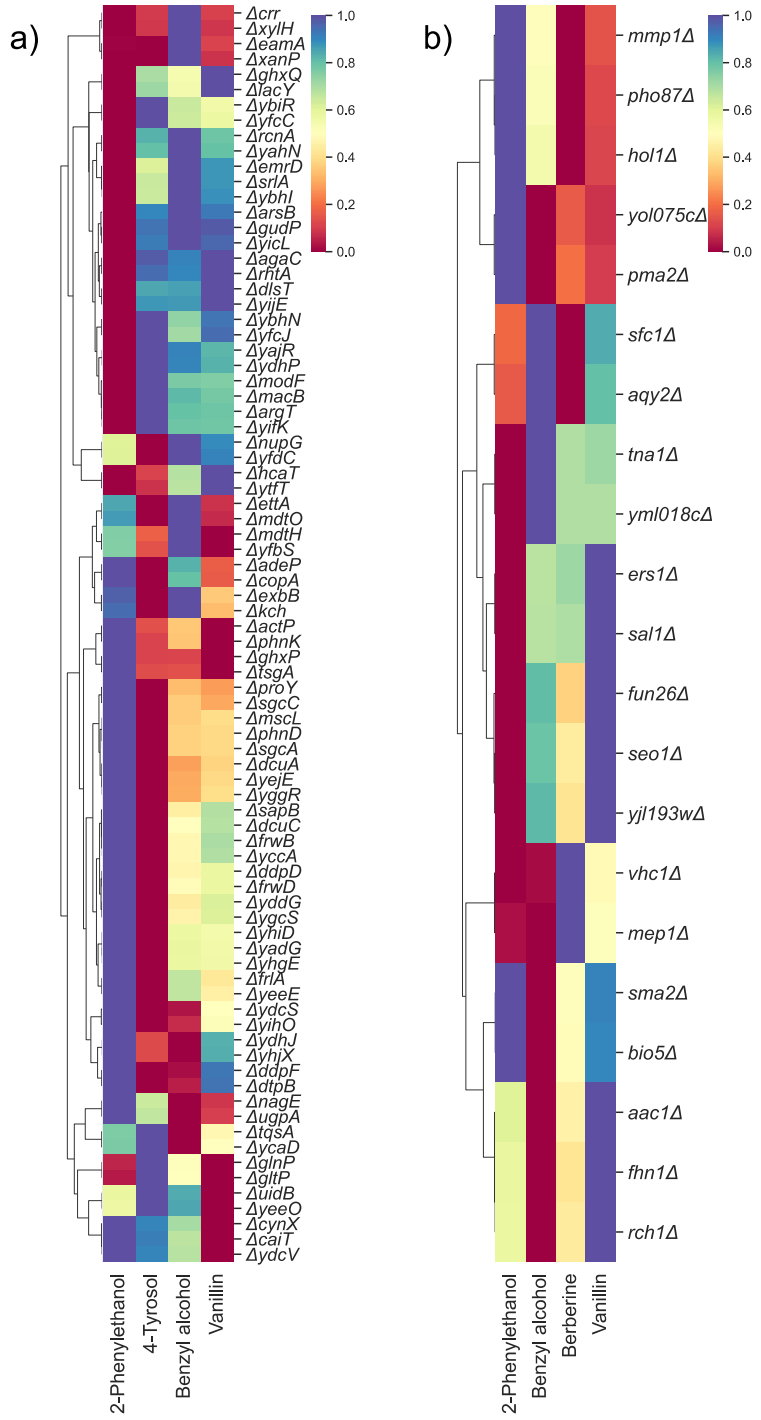

Figure 4. Clustermap showing highly correlated transporter deletions across four different aromatic compounds in (a) *E. coli* and (b) *S. cerevisiae*. The clustering parameter is the mean of relative and normalized μ_{max}, which compares the μ_{max} in the presence of the toxic aromatic compound to the wild-type control and normalizes it against the effect of the deletion in the absence of the compound. The heatmap values are scaled from 0 to 1 for better comparability and interpretation. For each transporter pair, the correlation scatterplots are presented in Figures S5-S6.

Transporter engineering modulates 2-phenylethanol production in *S. cerevisiae*

2-Phenylethanol is a naturally occurring metabolite synthesized by *S. cerevisiae* and other yeasts via the Ehrlich pathway, utilizing the aromatic amino acid L-phenylalanine as a precursor (Dai et al., 2021) (Figure 5a). This compound has garnered industrial attention for its application in the cosmetics and fragrance industries, in addition to its ability to impact the sensory properties of fermented alcoholic beverages such as wine (Cordente et al., 2021; Mitri et al., 2022).

Our transporters deletion library identified 16 transporter deletions altering the tolerance of *S. cerevisiae* to exogenously supplemented 2-phenylethanol (Figure 3b). Subsequently, we investigated whether these changes could also impact its production. Although 2-phenylethanol can be produced natively through the Ehrlich pathway, the production is typically low in wild-type strains and extensive genetic engineering is required to achieve significant titers (Hassing et al., 2019). Therefore, we sought an alternative approach and decided to use whole-cell bioconversion by supplementing L-phenylalanine to the medium. This approach has been shown to result in gram-per-liter titers and has been successfully used to produce 2-phenylethanol in other studies (Cui et al., 2011; Mitri et al., 2022). We tested the 16 deletion strains in the presence and absence of 5 g/L of L-phenylalanine. Also, with the hypothesis that the 8 transporter deletions leading to increased sensitivity could be 2-phenylethanol exporters, we overexpressed them in a strain with improved flux within the shikimate pathway (strain ST9599: CEN.PK113-7D + $ARO4^{K229L}$ + $ARO7^{G141S}$) (Luttik et al., 2008).

The deletion of *YIA6*, *PTR2*, and *MCH4* led to a significant improvement in titers, with up to a 12.4% increase, as well as specific yield, with an increase of up to 82.2% (Figure 5b). Disrupting *QDR2*, *DNF1*, and *SPF1* only improved specific yield. On the other hand, deletions of *DRS2*, *CTP1*, *FSF1*, and *AGP2* reduced 2-phenylethanol titers. Interestingly, strains with these deletions, especially *AGP2* and *CTP1*, exhibited significant growth impairment, an effect that was not observed in the control medium without L-phenylalanine (Figure S7). The overexpression of transporters did not lead to improvements in the measured metrics. In fact, overexpression of *FCY2*, *CTP1*, *FSF1*, *YNL095C*, and *MCH4* resulted in lower titers (Figure 5c).

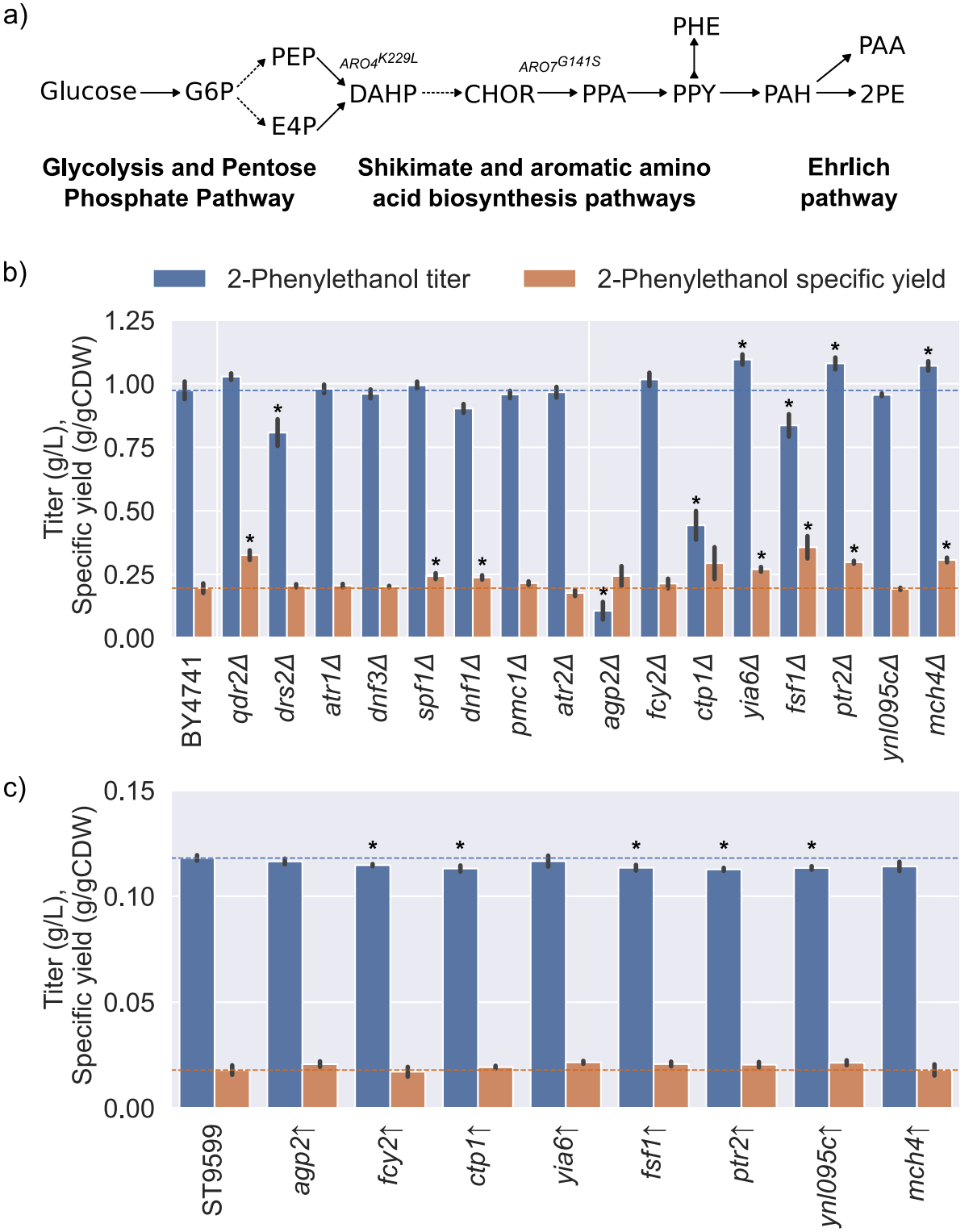

Figure 5. Effect of transporter engineering on 2-phenylethanol production in *S. cerevisiae*. a) Metabolic pathways leading to 2-phenylethanol biosynthesis in *S. cerevisiae*. Dashed lines indicate multiple enzymatic steps. G6P: glucose 6-phosphate; PEP: phosphoenolpyruvate; erythrose 4-phosphate; DAHP: 3-Deoxy-D-arabinoheptulosonate 7-phosphate; CHOR: chorismate; PPA: prephenate; PPY: phenylpyruvate; PHE: L-phenylalanine; PAH: phenylacetaldehyde; PAA: phenylacetate; 2PE: 2-phenylethanol. b)

Effect of transporters deletions on 2-phenylethanol bioconversion. c) Effect of transporters overexpressions on 2-phenylethanol bioconversion. L-phenylalanine was supplemented at a concentration of 5 g/L. Asterisks (*) indicate a *p*-value < 0.05 (two-sample unequal variance).

Discussion

In this study, the toxicity of a wide range of aromatic compounds towards industrial production microorganisms was evaluated. In addition, we screened *E. coli* and *S. cerevisiae* transporter deletion libraries against a subset of toxic aromatics, and identified a number of transporter deletions leading to increased tolerance or sensitivity. Lastly, we showed how transporter engineering applied to 2-phenylethanol can modulate its production in *S. cerevisiae*.

Although previous studies have documented the toxicity of several popular aromatics, such as 2-phenylethanol, vanillin, or catechol (Brochado et al., 2010; Dai et al., 2021; Song et al., 2022), there have not been many systematic reports analyzing the toxicity of a broad range of compounds, as was done in this study, allowing for comparisons between multiple hosts. Moreover, *Y. lipolytica*, which has recently emerged as a promising host for the production of various aromatics (Gu et al., 2020), has not been thoroughly investigated for its toxicity against this family of compounds.

The screening of the transporter-deletion libraries revealed a number of transporter deletions increasing compound tolerance or sensitivity, in some cases consistent with previously reported data on other compounds with aromatic rings. For instance, the deletion of *garP* sensitized *E. coli* towards 2-phenylethanol, an effect that was also observed for melatonin (Yang et al., 2022). In yeast, disruption of *QDR2* improved the tolerance towards 2-phenylethanol in this work, and was previously linked to the transport of other aromatics like betaxanthins (Savitskaya et al., 2019; Wang et al., 2021).

Although it may appear intuitive that transporters leading to increased tolerance are importers and those resulting in enhanced sensitivity are exporters, numerous studies have demonstrated that single gene deletions can have pleiotropic effects on the expression of multiple other genes (Cooper et al., 2007; Barrio-Hernandez et al., 2023; Featherstone and Broadie, 2002). Thus, follow-up validation experiments are necessary to confirm that the observed effect on tolerance results directly from altered

transport. Expression of the transporters in *Xenopus* oocytes and conducting transport assays would be valuable for validating this mechanism (Miller and Zhou, 2000; Wang et al., 2021). Note too that effluxers are far more likely to turn up in these kinds of assays since if multiple influxers exist the loss of one simply lets others 'take up the slack' (Mendes et al., 2020).

Regardless of the underlying mechanism of product tolerance, our method offers a valuable alternative to traditional approaches such as TALE. Recent TALE studies have shown how disruptions in transporter-encoding genes contribute significantly to the tolerant phenotype, which agrees with our observed results (Figure S3) (Babel and Krömer, 2020; Lennen et al., 2023). However, our approach offers a more streamlined and cost-effective solution by eliminating the need for laborious tasks such as serial transfers, genome sequencing, identification of mutations, and reverse engineering, which can be both time-consuming and expensive in the absence of automation equipment (Dragosits and Mattanovich, 2013; Mohamed et al., 2020, 2017; Radi et al., 2022a; Sandberg et al., 2019). This significantly reduces the associated labor and costs, allowing for a more efficient and effective approach to studying product tolerance.

The toxicity of 2-phenylethanol in *S. cerevisiae* and the identification of tolerance mechanisms has been the focus of several recent studies (Zhu et al., 2021; Xia et al., 2022). A missense mutation in *PDR1* was demonstrated to improve titers in a producing strain (Xia et al., 2022). *PDR1* is a transcription factor regulating the expression of multiple genes, and among them there are ATP-binding cassette (ABC) transporters like *PDR5*, *PDR15*, *PDR10*, *PDR12*, *PDR11*, *YOR1*, and *AUS1*, which confer resistance to several drugs (Buechel and Pinkett, 2020). Interestingly, our library screening did not reveal any of these transporter deletions affecting 2-phenylethanol tolerance, as probably a change in the expression of all transporters regulated by *PDR1* is required to observe a similar effect. However, among the transporter disruptions that we identified to alter product titer and specific yield, Ptr2p and Agp2p stand out due to their roles in peptide and amino acid import and nitrogen metabolism (Aouida et al., 2013, 2005; Becerra-Rodríguez et al., 2020; Sáenz et al., 2014). Agp2p, in particular, has been speculated to be involved in the uptake of L-phenylalanine (Schreve and Garrett, 2004), which could explain the impaired growth of the *agp2Δ* strain in the excess of extracellular L-phenylalanine (Table S10).

Studies of drug-transporter interactions can take two broad forms (Kell, 2018). In the first, the transporter is known and its possibly unknown substrates are identified ('de-orphanisation') (Gründemann et al., 2005; Munro and Kell, 2022). In the second, as here, the substrates are known and the transporters are sought, not least in order to enable protein engineering of the successful targets. In the event, a large number of y-genes in *E. coli* were here thereby detected and thus nominally de-orphanised; at the very least our data-driven 'discovery' strategy allowed specific hypotheses to be generated for more exact testing (Kell and Oliver, 2004). In summary, the findings from this study shed light on targets that could identify potential transport pathways and then be engineered to enhance the tolerance to aromatic compounds. These results lay the groundwork for subsequent follow-up validation experiments and further investigation of these targets.

Conclusions

A standard systems biology strategy first identifies genes relevant to process and then seeks to manipulate them. This study accordingly provides valuable insights into the toxicity of aromatics in common production hosts and identifies specific transporter-encoding genes involved in product tolerance. Our findings suggest that transporter engineering could be a promising strategy to improve the production of aromatic compounds in microbial cell factories. Further research can explore the potential of the identified transporters as targets for engineering.

Acknowledgements

This project has received funding from the European Union's Horizon 2020 research and innovation programme under grant agreements No. 814408 (SHIKIFACTORY100 project). IB also acknowledges the financial support from the Novo Nordisk Foundation (Grant agreement No. NNF20CC0035580, NNF20OC0060809, and NNF21OC0072559) and from the European Research Council under the European Union's Horizon 2020 research and innovation programme (YEAST-TRANS project, Grant Agreement No. 757384). DBK acknowledges financial support from the Novo Nordisk Foundation (Grant agreement No. NNF20CC0035580).

Conflict of interest

The authors declare that they have no conflicts of interest to disclose.

References

Acton, E., Lee, A.H.-Y., Zhao, P.J., Flibotte, S., Neira, M., Sinha, S., Chiang, J., Flaherty, P., Nislow, C., Giaever, G., 2017. Comparative functional genomic screens of three yeast deletion collections reveal unexpected effects of genotype in response to diverse stress. Open Biol. 7, 160330. https://doi.org/10.1098/rsob.160330

Ai, X., Yu, P., Peng, L., Luo, L., Liu, J., Li, S., Lai, X., Luan, F., Meng, X., 2021. Berberine: A Review of its Pharmacokinetics Properties and Therapeutic Potentials in Diverse Vascular Diseases. Front. Pharmacol. 12, 762654. https://doi.org/10.3389/fphar.2021.762654

Aouida, M., Leduc, A., Poulin, R., Ramotar, D., 2005. AGP2 Encodes the Major Permease for High Affinity Polyamine Import in Saccharomyces cerevisiae. J. Biol. Chem. 280, 24267–24276. https://doi.org/10.1074/jbc.M503071200

Aouida, M., Texeira, M.R., Thevelein, J.M., Poulin, R., Ramotar, D., 2013. Correction: Agp2, a Member of the Yeast Amino Acid Permease Family, Positively Regulates Polyamine Transport at the Transcriptional Level. PLoS ONE 8. https://doi.org/10.1371/annotation/ff0ad3b6-fff4-4783-8c2e-968a95283ab8

Atolia, E., Cesar, S., Arjes, H.A., Rajendram, M., Shi, H., Knapp, B.D., Khare, S., Aranda-Díaz, A., Lenski, R.E., Huang, K.C., 2020. Environmental and Physiological Factors Affecting High-Throughput Measurements of Bacterial Growth. mBio 11, e01378-20. https://doi.org/10.1128/mBio.01378-20

Averesch, N.J.H., Krömer, J.O., 2018. Metabolic Engineering of the Shikimate Pathway for Production of Aromatics and Derived Compounds—Present and Future Strain Construction Strategies. Front. Bioeng. Biotechnol. 6. https://doi.org/10.3389/fbioe.2018.00032

Baba, T., Ara, T., Hasegawa, M., Takai, Y., Okumura, Y., Baba, M., Datsenko, K.A., Tomita, M., Wanner, B.L., Mori, H., 2006. Construction of *Escherichia coli* K-12 in-frame, single-gene knockout mutants: the Keio collection. Mol. Syst. Biol. 2. https://doi.org/10.1038/msb4100050

Babel, H., Krömer, J.O., 2020. Evolutionary engineering of E. coli MG1655 for tolerance against isoprenol. Biotechnol. Biofuels 13, 183. https://doi.org/10.1186/s13068-020-01825-6

Bachmann, B.J., 1972. Pedigrees of some mutant strains of Escherichia coli K-12. Bacteriol. Rev. 36, 525–557. https://doi.org/10.1128/br.36.4.525-557.1972

Barrio-Hernandez, I., Schwartzentruber, J., Shrivastava, A., del-Toro, N., Gonzalez, A., Zhang, Q., Mountjoy, E., Suveges, D., Ochoa, D., Ghoussaini, M., Bradley, G., Hermjakob, H., Orchard, S., Dunham, I., Anderson, C.A., Porras, P., Beltrao, P., 2023. Network expansion of genetic associations defines a pleiotropy map of human cell biology. Nat. Genet. 55, 389–398. https://doi.org/10.1038/s41588-023-01327-9

Bazzone, A., Madej, M.G., Kaback, H.R., Fendler, K., 2016. pH Regulation of Electrogenic Sugar/H+ Symport in MFS Sugar Permeases. PLOS ONE 11, e0156392. https://doi.org/10.1371/journal.pone.0156392

Becerra-Rodríguez, C., Marsit, S., Galeote, V., 2020. Diversity of Oligopeptide Transport in Yeast and Its Impact on Adaptation to Winemaking Conditions. Front. Genet. 11, 602. https://doi.org/10.3389/fgene.2020.00602

Belew, Z.M., Crocoll, C., Møller-Hansen, I., Naesby, M., Borodina, I., Nour-Eldin, H.H., 2020. Identification and characterization of phlorizin transporter from *Arabidopsis thaliana*

and its application for phlorizin production in *Saccharomyces cerevisiae* (preprint). Molecular Biology. https://doi.org/10.1101/2020.08.14.248047

Berger, R.G. (Ed.), 2007. Flavours and Fragrances: Chemistry, Bioprocessing and Sustainability. Springer, Berlin, Heidelberg. https://doi.org/10.1007/978-3-540-49339-6

Brochado, A.R., Matos, C., Møller, B.L., Hansen, J., Mortensen, U.H., Patil, K.R., 2010. Improved vanillin production in baker's yeast through in silico design. Microb. Cell Factories 9, 84. https://doi.org/10.1186/1475-2859-9-84

Buechel, E.R., Pinkett, H.W., 2020. Transcription factors and ABC transporters: from pleiotropic drug resistance to cellular signaling in yeast. FEBS Lett. 594, 3943–3964. https://doi.org/10.1002/1873-3468.13964

Charlier, D., Bervoets, I., 2019. Regulation of arginine biosynthesis, catabolism and transport in Escherichia coli. Amino Acids 51, 1103–1127. https://doi.org/10.1007/s00726-019-02757-8

Cooper, T.F., Ostrowski, E.A., Travisano, M., 2007. A NEGATIVE RELATIONSHIP BETWEEN MUTATION PLEIOTROPY AND FITNESS EFFECT IN YEAST. Evolution 61, 1495–1499. https://doi.org/10.1111/j.1558-5646.2007.00109.x

Cordente, A.G., Espinase Nandorfy, D., Solomon, M., Schulkin, A., Kolouchova, R., Francis, I.L., Schmidt, S.A., 2021. Aromatic Higher Alcohols in Wine: Implication on Aroma and Palate Attributes during Chardonnay Aging. Molecules 26, 4979. https://doi.org/10.3390/molecules26164979

Cui, Z., Yang, X., Shen, Q., Wang, K., Zhu, T., 2011. Optimisation of biotransformation conditions for production of 2-phenylethanol by a *Saccharomyces cerevisiae* CWY132 mutant. Nat. Prod. Res. 25, 754–759. https://doi.org/10.1080/14786419.2010.529441

Dai, J., Xia, H., Yang, C., Chen, X., 2021. Sensing, Uptake and Catabolism of L-Phenylalanine During 2-Phenylethanol Biosynthesis via the Ehrlich Pathway in Saccharomyces cerevisiae. Front. Microbiol. 12, 601963. https://doi.org/10.3389/fmicb.2021.601963

Dastmalchi, M., Chang, L., Chen, R., Yu, L., Chen, X., Hagel, J.M., Facchini, P.J., 2019. Purine Permease-Type Benzylisoquinoline Alkaloid Transporters in Opium Poppy. Plant Physiol. 181, 916–933. https://doi.org/10.1104/pp.19.00565

del Olmo, A., Calzada, J., Nuñez, M., 2017. Benzoic acid and its derivatives as naturally occurring compounds in foods and as additives: Uses, exposure, and controversy. Crit. Rev. Food Sci. Nutr. 57, 3084–3103. https://doi.org/10.1080/10408398.2015.1087964

Dragosits, M., Mattanovich, D., 2013. Adaptive laboratory evolution – principles and applications for biotechnology. Microb. Cell Factories 12, 64. https://doi.org/10.1186/1475-2859-12-64

Entian, K.-D., Kötter, P., 2007. 25 Yeast Genetic Strain and Plasmid Collections, in: Stansfield, I., Stark, M.J. (Eds.), Methods in Microbiology, Yeast Gene Analysis. Academic Press, pp. 629–666. https://doi.org/10.1016/S0580-9517(06)36025-4

Evolva, 2023a. Evolva, flavors and fragrances [WWW Document]. URL https://evolva.com/business-segment/flavors-and-fragrances/

Evolva, 2023b. Evolva, health ingredients [WWW Document]. URL https://evolva.com/business-segment/health-ingredients/

Falkenberg, K.B., Mol, V., de la Maza Larrea, A.S., Pogrebnyakov, I., Nørholm, M.H.H., Nielsen, A.T., Jensen, S.I., 2021. The ProUSER2.0 Toolbox: Genetic Parts and Highly Customizable Plasmids for Synthetic Biology in *Bacillus subtilis*. ACS Synth. Biol. 10, 3278–3289. https://doi.org/10.1021/acssynbio.1c00130

Featherstone, D.E., Broadie, K., 2002. Wrestling with pleiotropy: Genomic and topological analysis of the yeast gene expression network. BioEssays 24, 267–274. https://doi.org/10.1002/bies.10054

Gaillardin, C.M., Charoy, V., Heslot, H., 1973. A study of copulation, sporulation and meiotic segregation in Candida lipolytica. Arch. Für Mikrobiol. 92, 69–83. https://doi.org/10.1007/BF00409513

Genee, H.J., Bali, A.P., Petersen, S.D., Siedler, S., Bonde, M.T., Gronenberg, L.S., Kristensen, M., Harrison, S.J., Sommer, M.O.A., 2016. Functional mining of transporters using synthetic selections. Nat. Chem. Biol. 12, 1015–1022. https://doi.org/10.1038/nchembio.2189

Ghatak, S., King, Z.A., Sastry, A., Palsson, B.O., 2019. The y-ome defines the 35% of *Escherichia coli* genes that lack experimental evidence of function. Nucleic Acids Res. 47, 2446–2454. https://doi.org/10.1093/nar/gkz030

Giaever, G., Chu, A.M., Ni, L., Connelly, C., Riles, L., Véronneau, S., Dow, S., Lucau-Danila, A., Anderson, K., André, B., Arkin, A.P., Astromoff, A., El Bakkoury, M., Bangham, R., Benito, R., Brachat, S., Campanaro, S., Curtiss, M., Davis, K., Deutschbauer, A., Entian, K.-D., Flaherty, P., Foury, F., Garfinkel, D.J., Gerstein, M., Gotte, D., Güldener, U., Hegemann, J.H., Hempel, S., Herman, Z., Jaramillo, D.F., Kelly, D.E., Kelly, S.L., Kötter, P., LaBonte, D., Lamb, D.C., Lan, N., Liang, H., Liao, H., Liu, L., Luo, C., Lussier, M., Mao, R., Menard, P., Ooi, S.L., Revuelta, J.L., Roberts, C.J., Rose, M., Ross-Macdonald, P., Scherens, B., Schimmack, G., Shafer, B., Shoemaker, D.D., Sookhai-Mahadeo, S., Storms, R.K., Strathern, J.N., Valle, G., Voet, M., Volckaert, G., Wang, C., Ward, T.R., Wilhelmy, J., Winzeler, E.A., Yang, Y., Yen, G., Youngman, E., Yu, K., Bussey, H., Boeke, J.D., Snyder, M., Philippsen, P., Davis, R.W., Johnston, M., 2002. Functional profiling of the Saccharomyces cerevisiae genome. Nature 418, 387–391. https://doi.org/10.1038/nature00935

Gietz, R.D., Schiestl, R.H., 2007. High-efficiency yeast transformation using the LiAc/SS carrier DNA/PEG method. Nat. Protoc. 2, 31–34. https://doi.org/10.1038/nprot.2007.13

Gründemann, D., Harlfinger, S., Golz, S., Geerts, A., Lazar, A., Berkels, R., Jung, N., Rubbert, A., Schömig, E., 2005. Discovery of the ergothioneine transporter. Proc. Natl. Acad. Sci. 102, 5256–5261. https://doi.org/10.1073/pnas.0408624102

Gu, Y., Ma, J., Zhu, Y., Ding, X., Xu, P., 2020. Engineering *Yarrowia lipolytica* as a Chassis for *De Novo* Synthesis of Five Aromatic-Derived Natural Products and Chemicals. ACS Synth. Biol. 9, 2096–2106. https://doi.org/10.1021/acssynbio.0c00185

Hansen, E.H., Møller, B.L., Kock, G.R., Bünner, C.M., Kristensen, C., Jensen, O.R., Okkels, F.T., Olsen, C.E., Motawia, M.S., Hansen, J., 2009. De Novo Biosynthesis of Vanillin in Fission Yeast (*Schizosaccharomyces pombe*) and Baker's Yeast (*Saccharomyces cerevisiae*). Appl. Environ. Microbiol. 75, 2765–2774. https://doi.org/10.1128/AEM.02681-08

Hassing, E.-J., de Groot, P.A., Marquenie, V.R., Pronk, J.T., Daran, J.-M.G., 2019. Connecting central carbon and aromatic amino acid metabolisms to improve de novo 2-phenylethanol production in Saccharomyces cerevisiae. Metab. Eng. 56, 165–180. https://doi.org/10.1016/j.ymben.2019.09.011

Hazelwood, L.A., Tai, S.L., Boer, V.M., de Winde, J.H., Pronk, J.T., Daran, J.M., 2006. A new physiological role for Pdr12p in *Saccharomyces cerevisiae* : export of aromatic and branched-chain organic acids produced in amino acid catabolism. FEMS Yeast Res. 6, 937–945. https://doi.org/10.1111/j.1567-1364.2006.00094.x

Hernandez, L.W., Sarlah, D., 2019. Empowering Synthesis of Complex Natural Products. Chem. – Eur. J. 25, 13248–13270. https://doi.org/10.1002/chem.201901808

Hua, D., Xu, P., 2011. Recent advances in biotechnological production of 2-phenylethanol. Biotechnol. Adv. 29, 654–660. https://doi.org/10.1016/j.biotechadv.2011.05.001

Huccetogullari, D., Luo, Z.W., Lee, S.Y., 2019. Metabolic engineering of microorganisms for production of aromatic compounds. Microb. Cell Factories 18, 41. https://doi.org/10.1186/s12934-019-1090-4

Jensen, N.B., Strucko, T., Kildegaard, K.R., David, F., Maury, J., Mortensen, U.H., Forster, J., Nielsen, J., Borodina, I., 2014. EasyClone: method for iterative chromosomal integration of multiple genes Saccharomyces cerevisiae. FEMS Yeast Res. 14, 238–248. https://doi.org/10.1111/1567-1364.12118

Jessop-Fabre, M.M., Jakočiūnas, T., Stovicek, V., Dai, Z., Jensen, M.K., Keasling, J.D., Borodina, I., 2016. EasyClone-MarkerFree: A vector toolkit for marker-less integration

of genes into Saccharomyces cerevisiae via CRISPR-Cas9. Biotechnol. J. 11, 1110–1117. https://doi.org/10.1002/biot.201600147

Jindal, S., Yang, L., Day, P.J., Kell, D.B., 2019. Involvement of multiple influx and efflux transporters in the accumulation of cationic fluorescent dyes by Escherichia coli. BMC Microbiol. 19, 195. https://doi.org/10.1186/s12866-019-1561-0

Kapadia, P., Newell, A.S., Cunningham, J., Roberts, M.R., Hardy, J.G., 2022. Extraction of High-Value Chemicals from Plants for Technical and Medical Applications. Int. J. Mol. Sci. 23, 10334. https://doi.org/10.3390/ijms231810334

Karković Marković, A., Torić, J., Barbarić, M., Jakobušić Brala, C., 2019. Hydroxytyrosol, Tyrosol and Derivatives and Their Potential Effects on Human Health. Molecules 24, 2001. https://doi.org/10.3390/molecules24102001

Kell, D.B., 2021. The Transporter-Mediated Cellular Uptake and Efflux of Pharmaceutical Drugs and Biotechnology Products: How and Why Phospholipid Bilayer Transport Is Negligible in Real Biomembranes. Molecules 26, 5629. https://doi.org/10.3390/molecules26185629

Kell, D.B., 2018. Control of Metabolite Efflux in Microbial Cell Factories, in: Fermentation Microbiology and Biotechnology, Fourth Edition. CRC Press, Fourth edition. | Boca Raton : Taylor & Francis, 2018. https://doi.org/10.1201/9780429506987

Kell, D.B., Oliver, S.G., 2004. Here is the evidence, now what is the hypothesis? The complementary roles of inductive and hypothesis-driven science in the post-genomic era. BioEssays 26, 99–105. https://doi.org/10.1002/bies.10385

Kell, D.B., Swainston, N., Pir, P., Oliver, S.G., 2015. Membrane transporter engineering in industrial biotechnology and whole cell biocatalysis. Trends Biotechnol. 33, 237–246. https://doi.org/10.1016/j.tibtech.2015.02.001

Kim, G.B., Choi, S.Y., Cho, I.J., Ahn, D.-H., Lee, S.Y., 2023. Metabolic engineering for sustainability and health. Trends Biotechnol. S0167779922003420. https://doi.org/10.1016/j.tibtech.2022.12.014

Korosh, T.C., Markley, A.L., Clark, R.L., McGinley, L.L., McMahon, K.D., Pfleger, B.F., 2017. Engineering photosynthetic production of L-lysine. Metab. Eng. 44, 273–283. https://doi.org/10.1016/j.ymben.2017.10.010

Lennen, R.M., Lim, H.G., Jensen, K., Mohammed, E.T., Phaneuf, P.V., Noh, M.H., Malla, S., Börner, R.A., Chekina, K., Özdemir, E., Bonde, I., Koza, A., Maury, J., Pedersen, L.E., Schöning, L.Y., Sonnenschein, N., Palsson, B.O., Nielsen, A.T., Sommer, M.O.A., Herrgård, M.J., Feist, A.M., 2023. Laboratory evolution reveals general and specific tolerance mechanisms for commodity chemicals. Metab. Eng. 76, 179–192. https://doi.org/10.1016/j.ymben.2023.01.012

Li, W., Ma, L., Shen, X., Wang, J., Feng, Q., Liu, L., Zheng, G., Yan, Y., Sun, X., Yuan, Q., 2019. Targeting metabolic driving and intermediate influx in lysine catabolism for high-level glutarate production. Nat. Commun. 10, 3337. https://doi.org/10.1038/s41467-019-11289-4

Liu, J.-K., 2022. Natural products in cosmetics. Nat. Prod. Bioprospecting 12, 40. https://doi.org/10.1007/s13659-022-00363-y

Liu, M., Wang, C., Ren, X., Gao, S., Yu, S., Zhou, J., 2022. Remodelling metabolism for high-level resveratrol production in Yarrowia lipolytica. Bioresour. Technol. 365, 128178. https://doi.org/10.1016/j.biortech.2022.128178

Liu, Q., Liu, Y., Chen, Y., Nielsen, J., 2020. Current state of aromatics production using yeast: achievements and challenges. Curr. Opin. Biotechnol. 65, 65–74. https://doi.org/10.1016/j.copbio.2020.01.008

Luttik, M.A.H., Vuralhan, Z., Suir, E., Braus, G.H., Pronk, J.T., Daran, J.M., 2008. Alleviation of feedback inhibition in Saccharomyces cerevisiae aromatic amino acid biosynthesis: Quantification of metabolic impact. Metab. Eng. 10, 141–153. https://doi.org/10.1016/j.ymben.2008.02.002

Malla, S., van der Helm, E., Darbani, B., Wieschalka, S., Förster, J., Borodina, I., Sommer, M.O.A., 2022. A Novel Efficient L-Lysine Exporter Identified by Functional

Metagenomics. Front. Microbiol. 13, 855736. https://doi.org/10.3389/fmicb.2022.855736

Martău, G.A., Călinoiu, L.-F., Vodnar, D.C., 2021. Bio-vanillin: Towards a sustainable industrial production. Trends Food Sci. Technol. 109, 579–592. https://doi.org/10.1016/j.tifs.2021.01.059

Mendes, P., Girardi, E., Superti-Furga, G., Kell, D.B., 2020. Why most transporter mutations that cause antibiotic resistance are to efflux pumps rather than to import transporters (preprint). Microbiology. https://doi.org/10.1101/2020.01.16.909507

Miller, A.J., Zhou, J.J., 2000. Xenopus oocytes as an expression system for plant transporters. Biochim. Biophys. Acta BBA - Biomembr. 1465, 343–358. https://doi.org/10.1016/S0005-2736(00)00148-6

Mitri, S., Koubaa, M., Maroun, R.G., Rossignol, T., Nicaud, J.-M., Louka, N., 2022. Bioproduction of 2-Phenylethanol through Yeast Fermentation on Synthetic Media and on Agro-Industrial Waste and By-Products: A Review. Foods 11, 109. https://doi.org/10.3390/foods11010109

Mohamed, E.T., Wang, S., Lennen, R.M., Herrgård, M.J., Simmons, B.A., Singer, S.W., Feist, A.M., 2017. Generation of a platform strain for ionic liquid tolerance using adaptive laboratory evolution. Microb. Cell Factories 16, 204. https://doi.org/10.1186/s12934-017-0819-1

Mohamed, E.T., Werner, A.Z., Salvachúa, D., Singer, C.A., Szostkiewicz, K., Rafael Jiménez-Díaz, M., Eng, T., Radi, M.S., Simmons, B.A., Mukhopadhyay, A., Herrgård, M.J., Singer, S.W., Beckham, G.T., Feist, A.M., 2020. Adaptive laboratory evolution of Pseudomonas putida KT2440 improves p-coumaric and ferulic acid catabolism and tolerance. Metab. Eng. Commun. 11, e00143. https://doi.org/10.1016/j.mec.2020.e00143

Mohedano, M.T., Konzock, O., Chen, Y., 2022. Strategies to increase tolerance and robustness of industrial microorganisms. Synth. Syst. Biotechnol. 7, 533–540. https://doi.org/10.1016/j.synbio.2021.12.009

Munro, L.J., Kell, D.B., 2022. Analysis of a Library of Escherichia coli Transporter Knockout Strains to Identify Transport Pathways of Antibiotics. Antibiotics 11, 1129. https://doi.org/10.3390/antibiotics11081129

Munro, L.J., Kell, D.B., 2021. Intelligent host engineering for metabolic flux optimisation in biotechnology. Biochem. J. 478, 3685–3721. https://doi.org/10.1042/BCJ20210535

Mutanda, I., Sun, J., Jiang, J., Zhu, D., 2022. Bacterial membrane transporter systems for aromatic compounds: Regulation, engineering, and biotechnological applications. Biotechnol. Adv. 59, 107952. https://doi.org/10.1016/j.biotechadv.2022.107952

Nour-Eldin, H.H., Nørholm, M.H., Halkier, B.A., 2006. Screening for plant transporter function by expressing a normalized Arabidopsis full-length cDNA library in Xenopus oocytes. Plant Methods 2, 17. https://doi.org/10.1186/1746-4811-2-17

Patra, A.K., 2012. An Overview of Antimicrobial Properties of Different Classes of Phytochemicals, in: Patra, Amlan K. (Ed.), Dietary Phytochemicals and Microbes. Springer Netherlands, Dordrecht, pp. 1–32. https://doi.org/10.1007/978-94-007-3926-0_1

Pereira, R., Mohamed, E.T., Radi, M.S., Herrgård, M.J., Feist, A.M., Nielsen, J., Chen, Y., 2020. Elucidating aromatic acid tolerance at low pH in *Saccharomyces cerevisiae* using adaptive laboratory evolution. Proc. Natl. Acad. Sci. 117, 27954–27961. https://doi.org/10.1073/pnas.2013044117

Pereira, R., Wei, Y., Mohamed, E., Radi, M., Malina, C., Herrgård, M.J., Feist, A.M., Nielsen, J., Chen, Y., 2019. Adaptive laboratory evolution of tolerance to dicarboxylic acids in Saccharomyces cerevisiae. Metab. Eng. 56, 130–141. https://doi.org/10.1016/j.ymben.2019.09.008

Radi, M.S., Munro, L.J., Salcedo-Sora, J.E., Kim, S.H., Feist, A.M., Kell, D.B., 2022a. Understanding Functional Redundancy and Promiscuity of Multidrug Transporters in E. coli under Lipophilic Cation Stress. Membranes 12, 1264. https://doi.org/10.3390/membranes12121264

Radi, M.S., SalcedoSora, J.E., Kim, S.H., Sudarsan, S., Sastry, A.V., Kell, D.B., Herrgård, M.J., Feist, A.M., 2022b. Membrane transporter identification and modulation via adaptive laboratory evolution. Metab. Eng. 72, 376–390. https://doi.org/10.1016/j.ymben.2022.05.004

Rodriguez, A., Strucko, T., Stahlhut, S.G., Kristensen, M., Svenssen, D.K., Forster, J., Nielsen, J., Borodina, I., 2017. Metabolic engineering of yeast for fermentative production of flavonoids. Bioresour. Technol. 245, 1645–1654. https://doi.org/10.1016/j.biortech.2017.06.043

Sáenz, D.A., Chianelli, M.S., Stella, C.A., 2014. L-Phenylalanine Transport in *Saccharomyces cerevisiae*: Participation of *GAP1, BAP2,* and *AGP1*. J. Amino Acids 2014, 1–9. https://doi.org/10.1155/2014/283962

Sáez-Sáez, J., Wang, G., Marella, E.R., Sudarsan, S., Cernuda Pastor, M., Borodina, I., 2020. Engineering the oleaginous yeast Yarrowia lipolytica for high-level resveratrol production. Metab. Eng. 62, 51–61. https://doi.org/10.1016/j.ymben.2020.08.009

Salcedo-Sora, J.E., Jindal, S., O'Hagan, S., Kell, D.B., 2021. A palette of fluorophores that are differentially accumulated by wild-type and mutant strains of Escherichia coli: surrogate ligands for profiling bacterial membrane transporters. Microbiology 167. https://doi.org/10.1099/mic.0.001016

Sandberg, T.E., Salazar, M.J., Weng, L.L., Palsson, B.O., Feist, A.M., 2019. The emergence of adaptive laboratory evolution as an efficient tool for biological discovery and industrial biotechnology. Metab. Eng. 56, 1–16. https://doi.org/10.1016/j.ymben.2019.08.004

Savitskaya, J., Protzko, R.J., Li, F.-Z., Arkin, A.P., Dueber, J.E., 2019. Iterative screening methodology enables isolation of strains with improved properties for a FACS-based screen and increased L-DOPA production. Sci. Rep. 9, 5815. https://doi.org/10.1038/s41598-019-41759-0

Schreve, J.L., Garrett, J.M., 2004. Yeast Agp2p and Agp3p function as amino acid permeases in poor nutrient conditions. Biochem. Biophys. Res. Commun. 313, 745–751. https://doi.org/10.1016/j.bbrc.2003.11.172

Song, G., Wu, F., Peng, Y., Jiang, X., Wang, Q., 2022. High-Level Production of Catechol from Glucose by Engineered Escherichia coli. Fermentation 8, 344. https://doi.org/10.3390/fermentation8070344

Studier, F.W., Moffatt, B.A., 1986. Use of bacteriophage T7 RNA polymerase to direct selective high-level expression of cloned genes. J. Mol. Biol. 189, 113–130. https://doi.org/10.1016/0022-2836(86)90385-2

Thomik, T., Wittig, I., Choe, J., Boles, E., Oreb, M., 2017. An artificial transport metabolon facilitates improved substrate utilization in yeast. Nat. Chem. Biol. 13, 1158–1163. https://doi.org/10.1038/nchembio.2457

van der Hoek, S.A., Borodina, I., 2020. Transporter engineering in microbial cell factories: the ins, the outs, and the in-betweens. Curr. Opin. Biotechnol. 66, 186–194. https://doi.org/10.1016/j.copbio.2020.08.002

Wang, G., Møller-Hansen, I., Babaei, M., D'Ambrosio, V., Christensen, H.B., Darbani, B., Jensen, M.K., Borodina, I., 2021. Transportome-wide engineering of Saccharomyces cerevisiae. Metab. Eng. 64, 52–63. https://doi.org/10.1016/j.ymben.2021.01.007

Welsch, M.E., Snyder, S.A., Stockwell, B.R., 2010. Privileged scaffolds for library design and drug discovery. Curr. Opin. Chem. Biol., Molecular Diversity 14, 347–361. https://doi.org/10.1016/j.cbpa.2010.02.018

Winzeler, E.A., Shoemaker, D.D., Astromoff, A., Liang, H., Anderson, K., Andre, B., Bangham, R., Benito, R., Boeke, J.D., Bussey, H., Chu, A.M., Connelly, C., Davis, K., Dietrich, F., Dow, S.W., El Bakkoury, M., Foury, F., Friend, S.H., Gentalen, E., Giaever, G., Hegemann, J.H., Jones, T., Laub, M., Liao, H., Liebundguth, N., Lockhart, D.J., Lucau-Danila, A., Lussier, M., M'Rabet, N., Menard, P., Mittmann, M., Pai, C., Rebischung, C., Revuelta, J.L., Riles, L., Roberts, C.J., Ross-MacDonald, P., Scherens, B., Snyder, M., Sookhai-Mahadeo, S., Storms, R.K., Véronneau, S., Voet, M., Volckaert, G., Ward, T.R., Wysocki, R., Yen, G.S., Yu, K., Zimmermann, K., Philippsen, P., Johnston, M., Davis, R.W., 1999. Functional Characterization of the *S. cerevisiae* Genome by Gene

Deletion and Parallel Analysis. Science 285, 901–906. https://doi.org/10.1126/science.285.5429.901

Xia, H., Kang, Y., Ma, Z., Hu, C., Yang, Q., Zhang, X., Yang, S., Dai, J., Chen, X., 2022. Evolutionary and reverse engineering in Saccharomyces cerevisiae reveals a Pdr1p mutation-dependent mechanism for 2-phenylethanol tolerance. Microb. Cell Factories 21, 269. https://doi.org/10.1186/s12934-022-01996-x

Yamada, Y., Urui, M., Oki, H., Inoue, K., Matsui, H., Ikeda, Y., Nakagawa, A., Sato, F., Minami, H., Shitan, N., 2021. Transport engineering for improving the production and secretion of valuable alkaloids in Escherichia coli. Metab. Eng. Commun. 13, e00184. https://doi.org/10.1016/j.mec.2021.e00184

Yang, L., Malla, S., Özdemir, E., Kim, S.H., Lennen, R., Christensen, H.B., Christensen, U., Munro, L.J., Herrgård, M.J., Kell, D.B., Palsson, B.Ø., 2022. Identification and Engineering of Transporters for Efficient Melatonin Production in Escherichia coli. Front. Microbiol. 13, 880847. https://doi.org/10.3389/fmicb.2022.880847

Zhang, J., Hansen, L.G., Gudich, O., Viehrig, K., Lassen, L.M.M., Schrübbers, L., Adhikari, K.B., Rubaszka, P., Carrasquer-Alvarez, E., Chen, L., D'Ambrosio, V., Lehka, B., Haidar, A.K., Nallapareddy, S., Giannakou, K., Laloux, M., Arsovska, D., Jørgensen, M.A.K., Chan, L.J.G., Kristensen, M., Christensen, H.B., Sudarsan, S., Stander, E.A., Baidoo, E., Petzold, C.J., Wulff, T., O'Connor, S.E., Courdavault, V., Jensen, M.K., Keasling, J.D., 2022. A microbial supply chain for production of the anti-cancer drug vinblastine. Nature 609, 341–347. https://doi.org/10.1038/s41586-022-05157-3

Zhu, L., Xu, S., Li, Y., Shi, G., 2021. Improvement of 2-phenylethanol production in Saccharomyces cerevisiae by evolutionary and rational metabolic engineering. PLOS ONE 16, e0258180. https://doi.org/10.1371/journal.pone.0258180

Zhu, Y., Zhou, C., Wang, Y., Li, C., 2020. Transporter Engineering for Microbial Manufacturing. Biotechnol. J. 15, 1900494. https://doi.org/10.1002/biot.201900494

Identification of transporters involved in aromatic compounds tolerance through a deletion library screening

Supporting information

Table S1. List of strains used in this study. Strains used in the transporters library screening are derived from the parent strains BY4741 (*S. cerevisiae*) and K-12 BW25113 (*E. coli*).

Microorganism	Strain	Genotype	Integrative vectors used	Reference
Saccharomyces cerevisiae	CEN.PK113-7D	MATa *URA3 TRP1 LEU2 HIS3*	n.a.	(Entian and Kötter, 2007)
Saccharomyces cerevisiae	BY4741	MATa *his3Δ1 leu2Δ0 met15Δ0 ura3Δ0*	n.a.	(Baker Brachmann et al., 1998)
Saccharomyces cerevisiae	ST9599	CEN.PK113-7D + *ARO4*^{K229L}↑ + *ARO7*^{G141S}↑	pCfB9114	This study
Saccharomyces cerevisiae	ST14058	ST9599 + *FCY2*↑	pCfB12380	This study
Saccharomyces cerevisiae	ST14059	ST9599 + *MCH4*↑	pCfB12381	This study
Saccharomyces cerevisiae	ST14060	ST9599 + *PTR2*↑	pCfB12382	This study
Saccharomyces cerevisiae	ST14061	ST9599 + *YIA6*↑	pCfB12383	This study
Saccharomyces cerevisiae	ST14062	ST9599 + *YNL095C*↑	pCfB12384	This study
Saccharomyces cerevisiae	ST14063	ST9599 + *CTP1*↑	pCfB12385	This study
Saccharomyces cerevisiae	ST14064	ST9599 + *AGP2*↑	pCfB12386	This study
Saccharomyces cerevisiae	ST14065	ST9599 + *FSF1*↑	pCfB12387	This study
Yarrowia lipolytica	W29, Y-63746	MATa	n.a.	(Gaillardin et al., 1973)
Escherichia coli	K-12 MG1655	*F- lambda- ilvG- rfb-50 rph-1*	n.a.	(Bachmann, 1972)
Escherichia coli	BL21(DE3)	*B dcm ompT hsdS(rB-mB-) gal*	n.a.	(Studier and Moffatt, 1986)
Escherichia coli	K-12 BW25113	*F- DE(araD-araB)567 lacZ4787(del)::rrnB-3 LAM- rph-1 DE(rhaD-rhaB)568 hsdR514*	n.a.	(Baba et al., 2006; Datsenko and Wanner, 2000)

Table S2. List of plasmids used in this study.

Plasmid	BioBricks	Description	Reference
pCfB3035	n.a.	Integrative vector for *locus* X-4	(Jessop-Fabre et al., 2016)
pCfB2909	n.a.	Integrative vector for *locus* XII-5	(Jessop-Fabre et al., 2016)
pCfB3042	n.a.	gRNA vector for *locus* X-4	(Jessop-Fabre et al., 2016)
pCfB3050	n.a.	gRNA vector for *locus* XII-5	(Jessop-Fabre et al., 2016)
pSP-GM1	n.a.	Plasmid backbone harboring *S. cerevisiae* promoters	(Partow et al., 2010)
pCfB9114	n.a.	Integrative vector for *locus* X-4, expression of *ARO4*K229L and *ARO7*G141S under control of promoter *TEF1* and *PGK1*, respectively	(Babaei et al., 2020)
pCfB12380	BB3034, BB8, BB6709	Integrative vector for *locus* XII-5, expression of *FCY2* under control of promoter *TEF1*	This study
pCfB12381	BB3034, BB8, BB6710	Integrative vector for *locus* XII-5, expression of *MCH4* under control of promoter *TEF1*	This study
pCfB12382	BB3034, BB8, BB6711	Integrative vector for *locus* XII-5, expression of *PTR2* under control of promoter *TEF1*	This study

pCfB12383	BB3034, BB8, BB6712	Integrative vector for *locus* XII-5, expression of *YIA6* under control of promoter *TEF1*	This study
pCfB12384	BB3034, BB8, BB6713	Integrative vector for *locus* XII-5, expression of *YNL095C* under control of promoter *TEF1*	This study
pCfB12385	BB3034, BB8, BB6714	Integrative vector for *locus* XII-5, expression of *CTP1* under control of promoter *TEF1*	This study
pCfB12386	BB3034, BB8, BB6715	Integrative vector for *locus* XII-5, expression of *AGP2* under control of promoter *TEF1*	This study
pCfB12387	BB3034, BB8, BB6716	Integrative vector for *locus* XII-5, expression of *FSF1* under control of promoter *TEF1*	This study

Table S3. List of BioBricks used in this study.

BioBrick	Amplification primer 1	Amplification primer 2	Template	Description
BB3034 (XII-5-MarkerFree)	PR-22420 (USER_backbone_1_Rev)	PR-22421 (USER_backbone_2_Fwd)	pCfB2909	USER-ready backbone of plasmid
BB8 (TEF1_U1)	PR-32768 (pTEF1_U1_fwd)	PR-1750 (PTEF1_fw)	pSP-GM1	*TEF1* promoter for position 1
BB6709 (FCY2_U1)	PR-32769 (FCY2_YER056C_U1_fwd)	PR-32770 (FCY2_YER056C_U1_rv)	CEN.PK113-7D gDNA	*FCY2* gene in position 1
BB6710 (MCH4_U1)	PR-32771 (MCH4_YOL119C_U1_rv)	PR-32772 (MCH4_YOL119C_U1_rv)	CEN.PK113-7D gDNA	*MCH4* gene in position 1
BB6711 (PTR2_U1)	PR-32773 (PTR2_YKR093W_U1_fwd)	PR-32774 (PTR2_YKR093W_U1_rv)	CEN.PK113-7D gDNA	*PTR2* gene in position 1
BB6712 (YIA6_U1)	PR-32775 (YIA6_YIL006W_U1_fwd)	PR-32776 (YIA6_YIL006W_U1_rv)	CEN.PK113-7D gDNA	*YIA6* gene in position 1
BB6713 (YNL095C_U1)	PR-32777 (YNL095C_U1_rv)	PR-32778 (YNL095C_U1_fwd)	CEN.PK113-7D gDNA	*YNL095C* gene in position 1
BB6714 (CTP1_U1)	PR-32779 (CTP1_YBR291C_U1_fwd)	PR-32780 (CTP1_YBR291C_U1_rv)	CEN.PK113-7D gDNA	*CTP1* gene in position 1
BB6715 (AGP2_U1)	PR-32781 (AGP2_YBR132C_U1_fwd)	PR-32782 (AGP2_YBR132C_U1_rv)	CEN.PK113-7D gDNA	*AGP2* gene in position 1
BB6716 (FSF1_U1)	PR-32783 (FSF1_YOR271C_U1_fwd)	PR-32784 (FSF1_YOR271C_U1_rv)	CEN.PK113-7D gDNA	*FSF1* gene in position 1

Table S4. List of primers used in this study.

Primer	Sequence	Use
PR-32768 (pTEF1_U1_fwd)	ACACGCGAUGCACACACCATAGCTTC	Amplification of TEF1 promoter for position 1
PR-1750 (PTEF1_fw)	ACCTGCACUTTGTAATTAAAACTTAGATTAGATTG	Amplification of TEF1 promoter for position 1
PR-22420 (USER_backbone_1_Rev)	ATCGCACGUGTAGATACGTTGTTGACACTTC	Amplification of EasyClone integrative vectors
PR-22421 (USER_backbone_2_Fwd)	ATCGCGTGUATCCGCTCTAACCGAAAAGGAAG	Amplification of EasyClone integrative vectors
PR-32769 (FCY2_YER056C_U1_fwd)	AGTGCAGGUAAAACAATGTTGGAAGAGGGAAATAATGTTTACG	Amplification of FCY2 promoter for position 1
PR-32770 (FCY2_YER056C_U1_rv)	ACGTGCGAUCTAACGACCGAAGTATTTCAATTCTAAAGG	Amplification of FCY2 promoter for position 1
PR-32771 (MCH4_YOL119C_U1_rv)	AGTGCAGGUAAAACAATGTTGAACATTCCCATAATTGCTAACTCC	Amplification of MCH4 promoter for position 1
PR-32772 (MCH4_YOL119C_U1_rv)	ACGTGCGAUTTAAAACTTACAAAGCTTCGCACCAAC	Amplification of MCH4 promoter for position 1

PR-32773 (PTR2_YKR093W_U1_fwd)	AGTGCAGGUAAAACAATGCTCAACCATCCCAGCC	Amplification of PTR2 promoter for position 1
PR-32774 (PTR2_YKR093W_U1_rv)	ACGTGCGAUCTAATATTTGGTGGTGGATCTTAGACTTTCC	Amplification of PTR2 promoter for position 1
PR-32775 (YIA6_YIL006W_U1_fwd)	AGTGCAGGUAAAACAATGACACAGACTGATAATCCTGTCCC	Amplification of YIA6 promoter for position 1
PR-32776 (YIA6_YIL006W_U1_rv)	ACGTGCGAUTTAAATTACCATAGTGCTAATATTTTCTAGGCGG	Amplification of YIA6 promoter for position 1
PR-32777 (YNL095C_U1_rv)	AGTGCAGGUAAAACAATGGTGCACATTACTCTGGGTC	Amplification of YNL095C promoter for position 1
PR-32778 (YNL095C_U1_fwd)	ACGTGCGAUTAAAGGTTCATCTGTACTTTCAGAAAGTAAG	Amplification of YNL095C promoter for position 1
PR-32779 (CTP1_YBR291C_U1_fwd)	ACGTGCGAUTCAGGCTAGCATAACTAAGACCTTTTCATAG	Amplification of CTP1 promoter for position 1
PR-32780 (CTP1_YBR291C_U1_rv)	AGTGCAGGUAAAACAATGTCCAGTAAAGCTACCAAAAGTGAC	Amplification of CTP1 promoter for position 1
PR-32781 (AGP2_YBR132C_U1_fwd)	AGTGCAGGUAAAACAATGACAAAGGAACGTATGACCATCG	Amplification of AGP2 promoter for position 1
PR-32782 (AGP2_YBR132C_U1_rv)	ACGTGCGAUTTATGCTTTGCTATAATATTGAAATTTTTCGAAGG	Amplification of AGP2 promoter for position 1
PR-32783 (FSF1_YOR271C_U1_fwd)	AGTGCAGGUAAAACAATGGCATCATCAGTCCCAGG	Amplification of FSF1 promoter for position 1
PR-32784 (FSF1_YOR271C_U1_rv)	ACGTGCGAUCTAAATACCTCTGTTAAAATAGACCTTTTCAATTGG	Amplification of FSF1 promoter for position 1

Table S5. List of 54 compounds evaluated for toxicity. Classes of compounds: A: Phenyl/Benzyl alcohols, amines, aldehydes or other hydrocarbons; B: Phenyl/Benzyl acids or amino acids; C: Indoles; D: Complex secondary metabolites; E: Dicarboxylic acid.

Compound	Class	Chemical structure
2-Phenylacetaldehyde	A	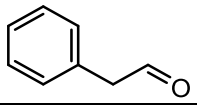
2-Phenylethanol	A	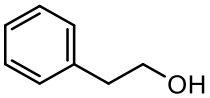
2-Phenylethylamine	A	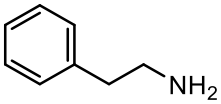
4-Aminobenzoic acid	B	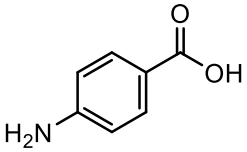
4-Coumaric acid	B	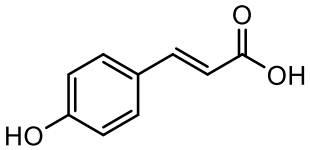
4-Tyrosol	A	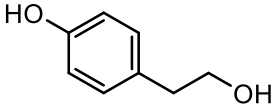
4-Vinylphenol	A	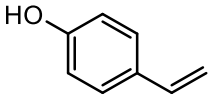

5-Hydroxytryptophan	C	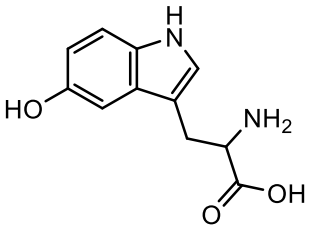
Acetylsalicylic acid	B	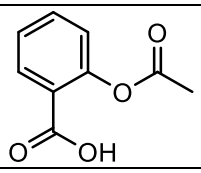
Aspartame	B	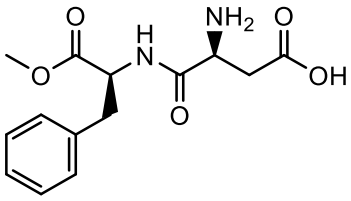
Atenolol	A	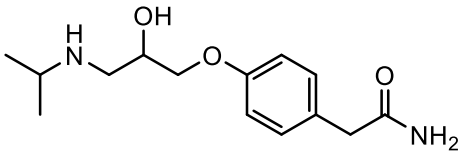
Benzyl alcohol	A	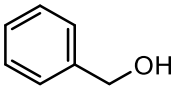
Berberine	D	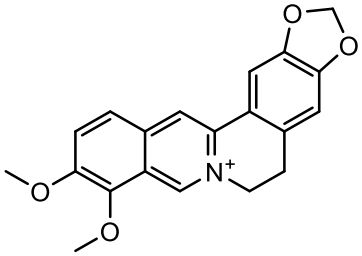
Caffeic acid	B	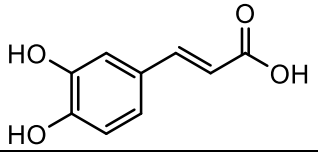
Catechin	D	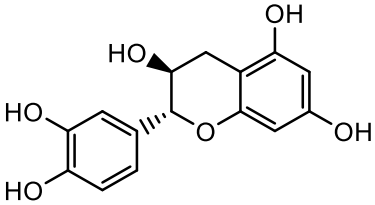
Catechol	A	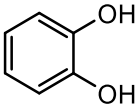

Colchicine	D	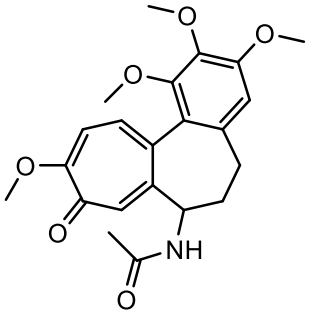
Dopamine	A	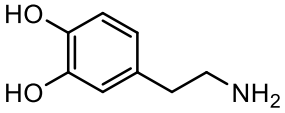
Ferulic acid	B	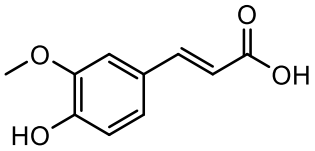
Gallic acid	B	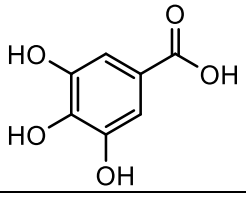
Gastrodin	A	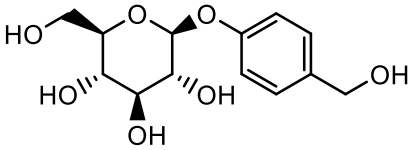
Hydrocinnamyl alcohol	A	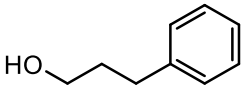
Isoeugenol	A	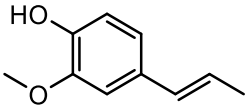
Kaempferol	D	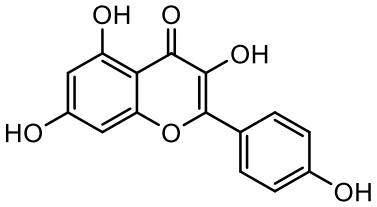
L-DOPA	B	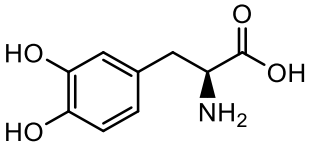
Mandelic acid	B	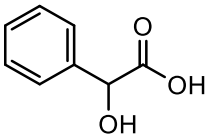

Melatonin	C	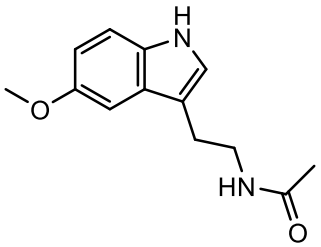
Methyleugenol	A	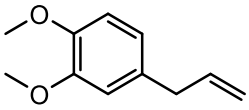
Myricetin	D	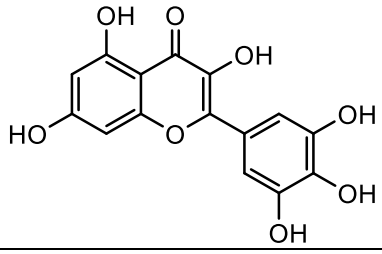
Naringenin	D	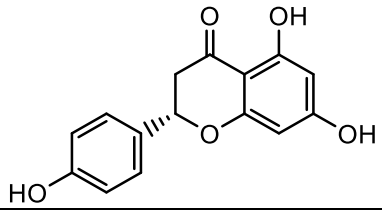
Neotame	A	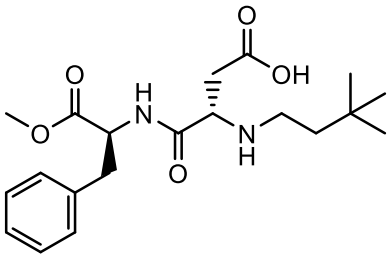
Novobiocin	D	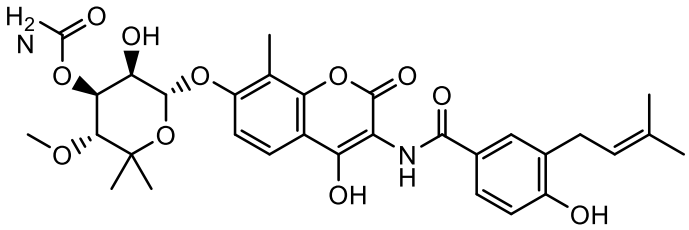
Papaverine	D	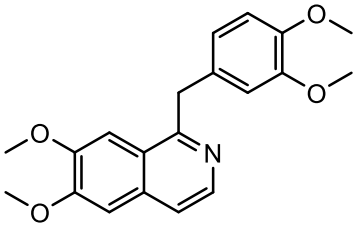
Phenylalanine	B	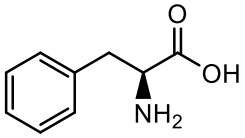
Phloretin	D	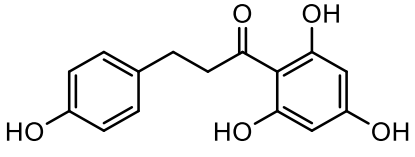

Protocatechuic acid	B	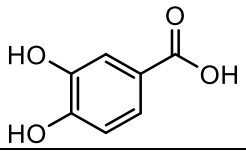
Quercetin	D	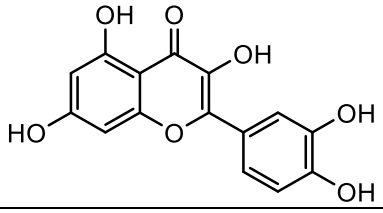
Quercetin 3-glucoside	D	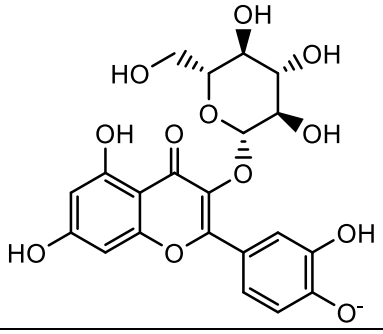
Quinine	D	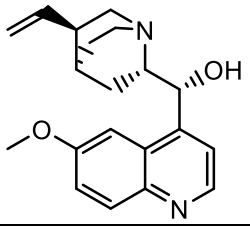
Resveratrol	D	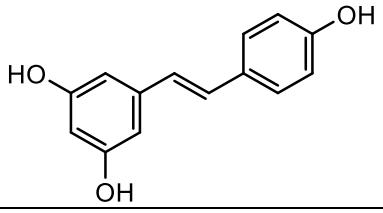
Rosmarinic acid	D	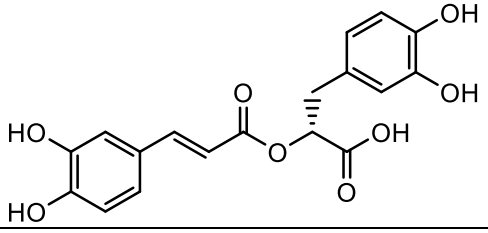
Rutin	D	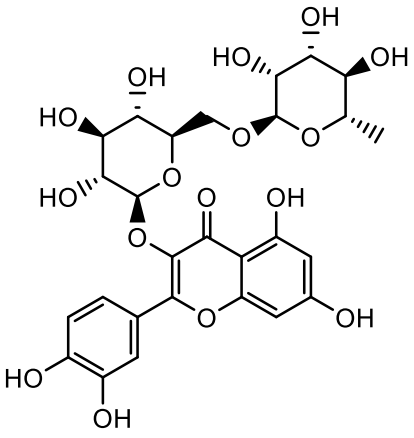

Salicylic acid	B	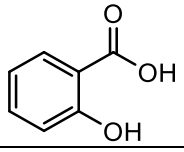
Serotonin	C	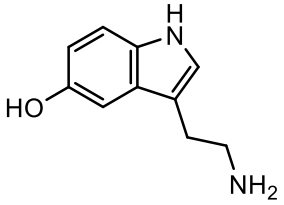
Shikimic acid	B	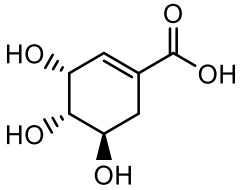
Styrene	A	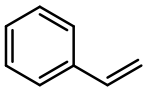
Tryptophan	C	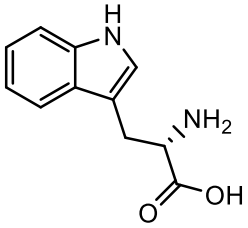
Tubocurarine	D	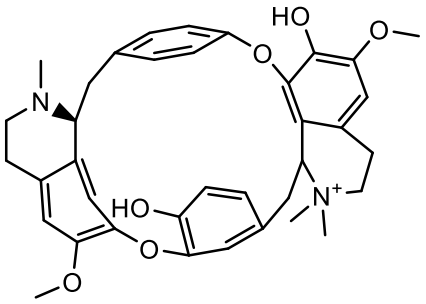
Tyrosine	B	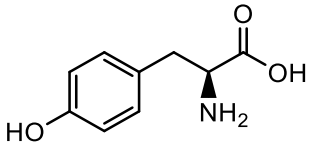
Vanillic acid	B	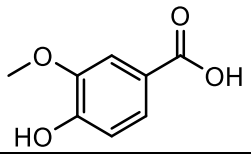
Vanillin	A	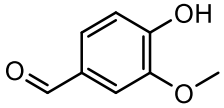
cis,cis-Muconic acid	E	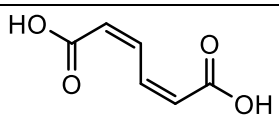
trans-Anethole	A	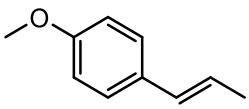

trans-Cinnamic acid B 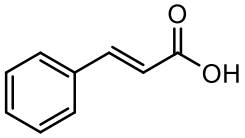

Table S6. Applications and uses of the 54 compounds evaluated for toxicity, including microbial production examples, when available. n.a.: not available.

Compound	Applications and uses	Example of microbial production
2-Phenylacetaldehyde	Cosmetics ingredient; floral odor	(Wang et al., 2023)
2-Phenylethanol	Cosmetics ingredient; rose-like odor	(Wang et al., 2019)
2-Phenylethylamine	Central nervous system stimulant	(Hamana and Niitsu, 1999)
4-Aminobenzoic acid	Building block for drugs and pesticides	(Averesch et al., 2016)
4-Coumaric acid	Food ingredient (antioxidant)	(Rodriguez et al., 2015)
4-Tyrosol	Food ingredient (antioxidant)	(Xu et al., 2020)
4-Vinylphenol	Food ingredient (aroma)	(Salgado et al., 2014)
5-Hydroxytryptophan	Antidepressant, appetite suppressant, and sleep aid	(Wang et al., 2018)
Acetylsalicylic acid	Anti-inflammatory drug	n.a.
Aspartame	Artificial sweetener	n.a.
Atenolol	Anti-hypertensive drug	n.a.
Benzyl alcohol	General solvent, bacteriostatic preservative for drugs, drug for the treatment of head lice	(Pugh et al., 2015)
Berberine	Natural yellow dye, supplement with blood-sugar-lowering properties	(Han and Li, 2023)
Caffeic acid	Food supplement used to boost the performance of athletes	(Zhou et al., 2021)
Catechin	Food supplement with antioxidant and antimicrobial properties	(Zhao et al., 2015)
Catechol	Building block for pesticides, perfumes and drugs	(Song et al., 2022)
Colchicine	Drug to treat gout and Behçet's disease	n.a.
Dopamine	Neuromodulatory substance	(Trenchard et al., 2015)
Ferulic acid	Cosmetics ingredient with antioxidant properties	(Lv et al., 2021)
Gallic acid	Tanning, ink dyes, and the manufacture of paper	(Aguilar-Zárate et al., 2015)
Gastrodin	Dietary supplement, drug to treat headache and migraine	(Yin et al., 2020)
Hydrocinnamyl alcohol	Flavoring agent	(Liu et al., 2021)
Isoeugenol	Food additive and cosmetics ingredient	(Wang et al., 2021)
Kaempferol	Dietary supplement with multiple health-promoting properties	(Lyu et al., 2019)
L-DOPA	Neurotransmitters precursor, used in the treatment of Parkinson's disease	(Fordjour et al., 2019)
Mandelic acid	Cosmetics ingredient	(Sun et al., 2011)
Melatonin	Dietary supplement used in the treatment of sleep disorders	(Zhang et al., 2021)
Methyleugenol	Food additive and cosmetics ingredient	n.a.
Myricetin	Dietary supplement with multiple health-promoting properties	(Leonard et al., 2006)
Naringenin	Food supplement with multiple health-promoting properties	(Wei et al., 2020)
Neotame	Artificial sweetener	n.a.
Novobiocin	Antibiotic	(Steffensky et al., 2000)
Papaverine	Drug for the treatment of visceral spasms and vasospasms	(Jamil et al., 2022)

Phenylalanine	Amino acid used for the treatment of vitiligo and other disorders	(Liu et al., 2019)
Phloretin	Dietary supplement with multiple health-promoting properties	(X. Liu et al., 2022)
Protocatechuic acid	Pharmacological applications as antioxidant, anti-inflammatory, and neuroprotective	(Li and Ye, 2021)
Quercetin	Dietary supplement with multiple health-promoting properties	(Rodriguez et al., 2017)
Quercetin 3-glucoside	Dietary supplement with multiple health-promoting properties	(De Bruyn et al., 2015)
Quinine	Drug used to treat malaria and babesiosis	n.a.
Resveratrol	Dietary supplement with multiple health-promoting properties	(M. Liu et al., 2022)
Rosmarinic acid	Dietary supplement with multiple health-promoting properties	(Babaei et al., 2020)
Rutin	Dietary supplement with multiple health-promoting properties	n.a.
Salicylic acid	Cosmetics ingredient for the treatment of many skin disorders	(Ahmadi et al., 2016)
Serotonin	Multifaceted hormone	(Mora-Villalobos and Zeng, 2018)
Shikimic acid	Precursor of antiviral drugs	(Martínez et al., 2015)
Styrene	Platform chemical for the manufacturing of latex, synthetic rubber, polystyrene resins, and other plastics	(Lee et al., 2019)
Tryptophan	Amino acid used in the treatment of sleep disorders	(Niu et al., 2019)
Tubocurarine	Adjunct for clinical anesthesia	n.a.
Tyrosine	Amino acid sold as dietary supplement	(Gold et al., 2015)
Vanillic acid	Flavoring agent with multiple biological activities	(Weiland et al., 2023)
Vanillin	Food additive and cosmetics ingredient	(Brochado et al., 2010)
cis,cis-Muconic acid	Platform chemical for manufacturing of plastics, resins, and pharmaceuticals	(Wang et al., 2022)
trans-Anethole	Flavoring agent and sweetener	n.a.
trans-Cinnamic acid	Food additive and cosmetics ingredient	(Vargas-Tah and Gosset, 2015)

Table S7. Concentration range tested for each compound.

Compound	C_1 (g/L)	C_2 (g/L)	C_3 (g/L)	C_4 (g/L)	C_5 (g/L)
2-Phenylacetaldehyde	2	1	0.5	0.25	0.125
2-Phenylethanol	5	2.5	1.25	0.625	0.3125
2-Phenylethylamine	2	1	0.5	0.25	0.125
4-Aminobenzoic acid	5	2.5	1.25	0.625	0.3125
4-Coumaric acid	0.8	0.4	0.2	0.1	0.05
4-Tyrosol	10	5	2.5	1.25	0.625
4-Vinylphenol	2	1	0.5	0.25	0.125
5-Hydroxytryptophan	3	1.5	0.75	0.375	0.1875
Acetylsalicylic acid	2.5	1.25	0.625	0.3125	0.15625
Aspartame	5	2.5	1.25	0.625	0.3125
Atenolol	0.2	0.1	0.05	0.025	0.0125
Benzyl alcohol	5	2.5	1.25	0.625	0.3125
Berberine	1.5	0.75	0.375	0.1875	0.09375
Caffeic acid	5	2.5	1.25	0.625	0.3125
Catechin	0.4	0.2	0.1	0.05	0.025
Catechol	1	0.5	0.25	0.125	0.0625

Colchicine	5	2.5	1.25	0.625	0.3125
Dopamine	4	2	1	0.5	0.25
Ferulic acid	0.5	0.25	0.125	0.0625	0.03125
Gallic acid	10	5	2.5	1.25	0.625
Gastrodin	5	2.5	1.25	0.625	0.3125
Hydrocinnamyl alcohol	5	2.5	1.25	0.625	0.3125
Isoeugenol	0.5	0.25	0.125	0.0625	0.03125
Kaempferol	0.05	0.025	0.0125	0.00625	0.003125
L-DOPA	3	1.5	0.75	0.375	0.1875
Mandelic acid	10	5	2.5	1.25	0.625
Melatonin	0.05	0.025	0.0125	0.00625	0.003125
Methyleugenol	0.4	0.2	0.1	0.05	0.025
Myricetin	0.05	0.025	0.0125	0.00625	0.003125
Naringenin	0.1	0.05	0.025	0.0125	0.00625
Neotame	5	2.5	1.25	0.625	0.3125
Novobiocin	0.5	0.25	0.125	0.0625	0.03125
Papaverine	0.5	0.25	0.125	0.0625	0.031
Phenylalanine	10	5	2.5	1.25	0.625
Phloretin	0.1	0.05	0.025	0.0125	0.00625
Protocatechuic acid	5	2.5	1.25	0.625	0.3125
Quercetin	0.05	0.025	0.0125	0.00625	0.003125
Quercetin 3-glucoside	0.2	0.1	0.05	0.025	0.0125
Quinine	0.3	0.15	0.075	0.0375	0.01875
Resveratrol	0.05	0.025	0.0125	0.00625	0.003125
Rosmarinic acid	0.1	0.05	0.025	0.0125	0.00625
Rutin	0.1	0.05	0.025	0.0125	0.00625
Salicylic acid	2.5	1.25	0.625	0.3125	0.15625
Serotonin	5	2.5	1.25	0.625	0.3125
Shikimic acid	5	2.5	1.25	0.625	0.3125
Styrene	0.2	0.1	0.05	0.025	0.0125
Tryptophan	10	5	2.5	1.25	0.625
Tubocurarine	5	2.5	1.25	0.625	0.3125
Tyrosine	0.4	0.2	0.1	0.05	0.025
Vanillic acid	1.25	0.625	0.3125	0.15625	0.078125
Vanillin	3	1.5	0.75	0.375	0.1875
cis,cis-Muconic acid	5	2.5	1.25	0.625	0.3125
trans-Anethole	0.1	0.05	0.025	0.0125	0.00625
trans-Cinnamic acid	0.4	0.2	0.1	0.05	0.025

Table S8. List of transporter-encoding genes included in the deletion library.

Microorganism	Individual transporter deletions in the library
Escherichia coli K-12 BW25113	*aaeA, acrB, acrD, acrF, actP, adeP, adeQ, adiC, agaC, agaV, alsC, alx, ampG, amtB, ansP, aqpZ, araE, araH, araJ, argO, argT, arnE, arnF, aroP, arsB, artI, artJ, artQ, ascF, atoE, atoS, atpB, atpI, barA, bcr, betT, bglF, brnQ, btuC, cadB, caiT, ccmC, chaA, chbC, citT, clcA, clcB, cmtA, cmtB, codB, copA, corA, corC, crr, cusA, cvrA, cycA, cydD, cynX, cysW, dauA, dctA, dcuA, dcuB, dcuC, dcuD, ddpB, ddpC, ddpD, ddpF, dgoT,*

	dhaM, dinF, dlsT, dppB, dsdX, dtpA, dtpB, dtpC, dtpD, eamA, eamB, emrB, emrD, emrY, entS, ettA, eutH, exbB, exbD, exuT, feoB, fepD, fetA, fetB, fieF, focA, focB, frlA, fruA, frvA, frvB, frwB, frwC, frwD, fryA, fryB, fryC, fsr, fucP, gabP, gadC, galP, garP, gdx, ghxP, ghxQ, glnP, glpF, glpT, gltK, gltP, gltS, glvB, glvC, gntP, gntT, gntU, gsiC, guaB, gudP, hcaT, hisM, hofC, hsrA, idnT, kch, kdgT, kdpA, kdpD, kefB, kefC, kgtP, kup, lacY, leuE, livH, livJ, livK, lldP, lplT, lptB, lsrA, lsrC, lysP, macB, malF, malX, manY, mdfA, mdlA, mdlB, mdtB, mdtD, mdtF, mdtG, mdtH, mdtI, mdtJ, mdtK, mdtL, mdtN, mdtO, melB, mepM, metI, mglC, mgtA, mhpT, mlaC, mlaE, mltF, mngA, modB, modF, mscK, mscL, mscM, mscS, mtlA, mtr, murP, nagE, nanT, narK, narU, nepI, nhaB, nikC, nimT, nirC, nlpA, nupG, nupX, oppB, panF, perM, pheP, phnD, phnK, phnL, phoR, pitA, plaP, potB, potE, potH, proP, proW, proY, pstC, psuT, ptsG, ptsI, ptsN, ptsP, putP, puuP, rarD, rbbA, rbsC, rcnA, rcnB, rhaT, rhmT, rhtA, rhtB, rhtC, rutG, sapA, sapB, sapC, sapD, sapF, sbp, sdaC, setA, setB, setC, sgcA, sgcB, sgcC, shiA, sotB, soxR, srlA, sstT, ssuC, sufB, tatC, tdcC, tehA, thiP, tnaB, tolQ, tolR, torT, tqsA, treB, trkH, tsgA, ttdT, tyrP, uacT, ugpA, uhpC, uhpT, uidB, ulaA, uraA, uup, wzxE, xanP, xanQ, xapB, xylE, xylH, yaaJ, yaaU, yadG, yadH, yadI, yadS, yahN, yajR, ybaE, ybaL, ybaT, ybbA, ybbP, ybbW, ybbY, ybhF, ybhG, ybhI, ybhN, ybhR, ybhS, ybiO, ybiR, ybiT, ybjJ, ybjL, ycaD, ycaM, yccA, yccS, ycfT, ycjN, ycjO, ycjP, ycjV, ydcO, ydcS, ydcT, ydcU, ydcV, ydcZ, yddA, yddB, yddG, ydeE, ydfJ, ydgI, ydhC, ydhJ, ydhK, ydhP, ydiK, ydiM, ydiN, ydjE, ydjK, ydjN, ydjX, yeaV, yebQ, yedA, yeeA, yeeE, yeeO, yegH, yegT, yehW, yehY, yejB, yejE, yfbS, yfcC, yfcJ, yfdC, yfdV, yfeH, yfeO, yfjD, ygaH, ygaY, ygaZ, ygbN, ygcS, ygdQ, yggR, yggT, yghD, yghE, yghF, ygiS, ygjI, yhbE, yhdP, yhdW, yhdX, yhdY, yhdZ, yheS, yhfK, yhgE, yhhJ, yhhS, yhhT, yhiD, yhjE, yhjV, yhjX, yiaM, yiaN, yiaV, yibH, yicG, yicJ, yicL, yidE, yidK, yifK, yihN, yihO, yihP, yijE, yjbB, yjcE, yjeH, yjeM, yjfF, yjhB, yjhF, yjiJ, yjjP, ykgG, yneE, ynfA, ynfM, ynjB, ynjC, ynjD, yoaE, yohK, yojI, yphD, yphE, yphF, ypjA, yqcE, yqeG, yqgA, yraQ, yrbG, ytfF, ytfL, ytfT, zitB, zntA, zntB, znuB, zupT
Saccharomyces cerevisiae BY4741	*YAL022C, YAL026C, YAL053W, YAL067C, YBL042C, YBL089W, YBL099W, YBL102W, YBR008C, YBR021W, YBR043C, YBR068C, YBR069C, YBR085W, YBR104W, YBR132C, YBR171W, YBR180W, YBR187W, YBR207W, YBR219C, YBR220C, YBR235W, YBR241C, YBR287W, YBR291C, YBR293W, YBR294W, YBR295W, YBR296C, YBR298C, YCL002C, YCL025C, YCL038C, YCL069W, YCR011C, YCR023C, YCR028C, YCR037C, YCR075C, YCR098C, YDL054C, YDL100C, YDL119C, YDL128W, YDL138W, YDL149W, YDL194W, YDL199C, YDL206W, YDL210W, YDL231C, YDR011W, YDR046C, YDR061W, YDR093W, YDR107C, YDR119W, YDR135C, YDR178W, YDR205W, YDR270W, YDR298C, YDR329C, YDR338C, YDR345C, YDR352W, YDR406W, YDR438W, YDR456W, YDR470C, YDR497C, YDR508C, YDR536W, YEL004W, YEL006W, YEL031W, YEL063C, YEL065W, YER019C-A, YER039C, YER053C, YER056C, YER060W, YER113C, YER119C, YER145C, YER154W, YER166W, YER185W, YFL011W, YFL040W, YFL050C, YFL054C, YFL055W, YFR045W, YGL006W, YGL077C, YGL084C, YGL114W, YGL140C, YGL186C, YGR033C, YGR055W, YGR062C, YGR096W, YGR121C, YGR131W, YGR138C, YGR181W, YGR213C, YGR217W, YGR224W, YGR257C, YGR260W, YGR281W, YGR289C, YHL008C, YHL016C, YHL035C, YHL036W, YHL040C, YHL047C, YHR032W, YHR048W, YHR050W, YHR092C, YHR094C, YHR096C, YIL006W, YIL013C, YIL023C, YIL088C, YIL120W, YIL121W, YIL134W, YIL166C, YIR028W, YJL059W, YJL062W, YJL093C, YJL107C, YJL108C, YJL129C, YJL133W, YJL163C, YJL193W, YJL198W, YJL214W, YJR001W, YJR077C, YJR095W, YJR106W, YJR121W, YJR124C, YJR135W-A, YJR152W, YKL050C, YKL120W, YKL146W, YKL174C, YKL175W, YKL188C, YKL217W, YKL221W, YKR039W, YKR050W, YKR052C, YKR093W, YKR103W, YKR104W, YKR105C, YKR106W, YLL015W, YLL028W, YLL043W,*

YLL048C, YLL052C, YLL053C, YLL055W, YLL061W, YLR004C, YLR034C, YLR046C, YLR081W, YLR083C, YLR092W, YLR130C, YLR138W, YLR152C, YLR188W, YLR220W, YLR237W, YLR292C, YLR295C, YLR348C, YML018C, YML038C, YML066C, YML081C-A, YML116W, YML123C, YMR011W, YMR034C, YMR054W, YMR056C, YMR088C, YMR155W, YMR162C, YMR166C, YMR177W, YMR221C, YMR241W, YMR243C, YMR253c, YMR279C, YMR319C, YNL003C, YNL065W, YNL070W, YNL083W, YNL095C, YNL101W, YNL121C, YNL125C, YNL142W, YNL268W, YNL270C, YNL275W, YNL291C, YNL318C, YNL321W, YNR013C, YNR039C, YNR055C, YNR056C, YNR062C, YNR070W, YNR072W, YOL020W, YOL060C, YOL075C, YOL077W-A, YOL092W, YOL103W, YOL119C, YOL122C, YOL137W, YOL158C, YOL162W, YOL163W, YOR011W, YOR045W, YOR049C, YOR071C, YOR079C, YOR087W, YOR092W, YOR100C, YOR130C, YOR153W, YOR161C, YOR192C, YOR222W, YOR270C, YOR271C, YOR273C, YOR291W, YOR306C, YOR307C, YOR316C, YOR328W, YOR332W, YOR334W, YOR348C, YOR378W, YPL006W, YPL036W, YPL058C, YPL060W, YPL078C, YPL092W, YPL134C, YPL147W, YPL189W, YPL224C, YPL244C, YPL264C, YPL265W, YPL270W, YPL271W, YPL274W, YPR003C, YPR011C, YPR021C, YPR036W, YPR058W, YPR128C, YPR138C, YPR149W, YPR156C, YPR192W, YPR194C, YPR198W, YPR201W

Table S9. Compound concentrations used in the library screening and subsequent validation experiments. Values reported in g/L.

Compound	*E. coli*	*S. cerevisiae*
2-Phenylethanol	2.25	3.03
4-Tyrosol	3.5	n.a.
Benzyl alcohol	3.35	3.97
Berberine	n.a.	0.46
Vanillin	0.95	0.91

Table S10. List of transporter deletions validated to improve or reduce product tolerance. Host: *Ec*: *E. coli*, *Sc*: *S. cerevisiae*; Arom: Toxic aromatic compound; 2PE: 2-Phenylethanol, 4Tyr: 4-Tyrosol; BenzOH: Benzyl alcohol; Van: Vanillin; Berb: Berberine; Tol: Tolerance; ↑: tolerance improved; ↓: tolerance reduced. Substrate, familiy name, transporter class and TC number have been retrieved from transportDB 2.0 (Elbourne et al., 2017).

Host	Name	Arom	Tol	Substrate	Family name	Transp. Class	TC #
Ec	*ycjN*	2PE	↑		The ATP-binding Cassette (ABC) Superfamily	ATP-Dependent	3.A.1
Ec	*corC*	2PE	↑				
Ec	*sapD*	2PE	↑		The ATP-binding Cassette (ABC) Superfamily	ATP-Dependent	3.A.1
Ec	*yjiJ*	2PE	↑	multidrug efflux	The Major Facilitator Superfamily (MFS)	Secondary Transporter	2.A.1
Ec	*yohK*	2PE	↑				
Ec	*ygaY*	2PE	↑				

Ec	*garP*	2PE	↓	D-glycerate D-glucarate galactarate	The Major Facilitator Superfamily (MFS)	Secondary Transporter	2.A.1
Ec	*yaaJ*	2PE	↓		The Alanine or Glycine:Cation Symporter (AGCS) Family	Secondary Transporter	2.A.25
Ec	*ydhP*	2PE	↓		The Major Facilitator Superfamily (MFS)	Secondary Transporter	2.A.1
Ec	*yfcJ*	2PE	↓		The Major Facilitator Superfamily (MFS)	Secondary Transporter	2.A.1
Ec	*ygdQ*	2PE	↓	tellurium ion efflux	The Tellurium Ion Resistance (TerC) Family	Unclassified	9.A.30
Ec	*yejB*	2PE	↓	ATP ADP phosphate peptide L-alanyl-gamma;-D-glutamyl-meso-diaminopimelate dipeptide	The ATP-binding Cassette (ABC) Superfamily	ATP-Dependent	3.A.1
Ec	*kdpA*	4Tyr	↑	ATP K+ phosphate ADP	The P-type ATPase (P-ATPase) Superfamily	ATP-Dependent	3.A.3
Ec	*sapA*	4Tyr	↑		The ATP-binding Cassette (ABC) Superfamily	ATP-Dependent	3.A.1
Ec	*setA*	4Tyr	↑	alpha;-lactose	The Major Facilitator Superfamily (MFS)	Secondary Transporter	2.A.1
Ec	*ydjK*	4Tyr	↓		The Major Facilitator Superfamily (MFS)	Secondary Transporter	2.A.1
Ec	*fepD*	4Tyr	↓	ATP ADP phosphate ferric enterobactin complex	The ATP-binding Cassette (ABC) Superfamily	ATP-Dependent	3.A.1
Ec	*wzxE*	4Tyr	↓	N-acetyl-alpha;-D-fucosyl-(1rarr;4)-N-acetyl-beta;-D-mannosaminouronyl-(1rarr;4)-N-acetyl-alpha;-D-glucosaminyl-diphospho-ditrans octacis-undecaprenol	The Multidrug/Oligosaccharidyl-lipid/Polysaccharide (MOP) Flippase Superfamily	Secondary Transporter	2.A.66
Ec	*yjcE*	BenzOH	↑		The Monovalent Cation:Proton Antiporter-1 (CPA1) Family	Secondary Transporter	2.A.36
Ec	*acrB*	BenzOH	↑	drug chenodeoxycholate	The Resistance-Nodulation-Cell Division (RND) Superfamily	Secondary Transporter	2.A.6
Ec	*ygaH*	BenzOH	↑	L-valine	The Branched Chain Amino Acid Exporter (LIV-E) Family	Secondary Transporter	2.A.78
Ec	*ycjN*	BenzOH	↑		The ATP-binding Cassette (ABC) Superfamily	ATP-Dependent	3.A.1
Ec	*kdpA*	BenzOH	↑	ATP K+ phosphate ADP	The P-type ATPase (P-ATPase) Superfamily	ATP-Dependent	3.A.3
Ec	*fryC*	BenzOH	↑		Sugar Specific PTS	Phosphotransferase System (PTS)	4.A
Ec	*tolQ*	BenzOH	↓		The H+- or Na+-translocating Bacterial Flagellar Motor 1ExbBD Outer Membrane Transport Energizer (Mo	Ion Channels	1.A.30
Ec	*manY*	BenzOH	↓	HPr - phosphorylated D-	Sugar Specific PTS	Phosphotransferase System (PTS)	4.A

				mannopyranose D-mannopyranose 6-phosphate			
Ec	*ybbY*	BenzOH	↓		The Nucleobase:Cation Symporter-2 (NCS2) Family	Secondary Transporter	2.A.40
Ec	*yjeM*	BenzOH	↓		The Amino Acid-Polyamine-Organocation (APC) Family	Secondary Transporter	2.A.3
Ec	*yccS*	BenzOH	↓	fusaric acid efflux?	The Aromatic Acid Exporter (ArAE) Family	Secondary Transporter	2.A.85
Ec	*yqgA*	Van	↑	nitrate nitrite	The Major Facilitator Superfamily (MFS)	Secondary Transporter	2.A.1
Ec	*narU*	Van	↑	Na+ (R)-pantothenate	The Solute:Sodium Symporter (SSS) Family	Secondary Transporter	2.A.21
Ec	*panF*	Van	↑	fusaric acid efflux?	The Aromatic Acid Exporter (ArAE) Family	Secondary Transporter	2.A.85
Ec	*yeeA*	Van	↑	K+	The Voltage-gated Ion Channel (VIC) Superfamily	Ion Channels	1.A.1
Ec	*kch*	Van	↓		The ATP-binding Cassette (ABC) Superfamily	ATP-Dependent	3.A.1
Ec	*artI*	Van	↓		The ATP-binding Cassette (ABC) Superfamily	ATP-Dependent	3.A.1
Sc	*QDR2*	2PE	↑	multidrug efflux?	The Major Facilitator Superfamily (MFS)	Secondary Transporter	2.A.1
Sc	*DRS2*	2PE	↑	Amino phospholipids	The P-type ATPase (P-ATPase) Superfamily	ATP-Dependent	3.A.3
Sc	*ATR1*	2PE	↑	Aminotriazole and 4-nitroquinoline resistance	The Major Facilitator Superfamily (MFS)	Secondary Transporter	2.A.1
Sc	*DNF3*	2PE	↑	calcium ion/phospholipid?	The P-type ATPase (P-ATPase) Superfamily	ATP-Dependent	3.A.3
Sc	*SPF1*	2PE	↑	Involved in sensitivity to Pichia killer toxin	The P-type ATPase (P-ATPase) Superfamily	ATP-Dependent	3.A.3
Sc	*DNF1*	2PE	↑	calcium ion	The P-type ATPase (P-ATPase) Superfamily	ATP-Dependent	3.A.3
Sc	*PMC1*	2PE	↑	Ca2+ (vacuolar) uptake	The P-type ATPase (P-ATPase) Superfamily	ATP-Dependent	3.A.3
Sc	*ATR2*	2PE	↑	aminotriazole ?	The Major Facilitator Superfamily (MFS)	Secondary Transporter	2.A.1
Sc	*AGP2*	2PE	↓	Amino acids (general)	The Amino Acid-Polyamine-Organocation (APC) Family	Secondary Transporter	2.A.3
Sc	*FCY2*	2PE	↓	Cytosine/purines	The Nucleobase:Cation Symporter-1 (NCS1) Family	Secondary Transporter	2.A.39
Sc	*CTP1*	2PE	↓	Citrate	The Mitochondrial Carrier (MC) Family	Secondary Transporter	2.A.29
Sc	*YIA6*	2PE	↓	Unclassified	The Mitochondrial Carrier (MC) Family	Secondary Transporter	2.A.29
Sc	*FSF1*	2PE	↓	Tricarboxylates	The Mitochondrial Tricarboxylate Carrier (MTC) Family	Secondary Transporter	2.A.54
Sc	*PTR2*	2PE	↓	Peptides	The Proton-dependent Oligopeptide Transporter (POT) Family	Secondary Transporter	2.A.17
Sc	*YNL095C*	2PE	↓	auxin efflux?	The Auxin Efflux Carrier (AEC) Family	Secondary Transporter	2.A.69
Sc	*MCH4*	2PE	↓	monocarboxylate?	The Major Facilitator Superfamily (MFS)	Secondary Transporter	2.A.1
Sc	*OAC1*	BenzOH	↑	oxaloacetate/ malonate/sulfate	The Mitochondrial Carrier (MC) Family	Secondary Transporter	2.A.29
Sc	*JEN1*	BenzOH	↑	Lactate?	The Major Facilitator Superfamily (MFS)	Secondary Transporter	2.A.1
Sc	*YIA6*	BenzOH	↑	Unclassified	The Mitochondrial Carrier (MC) Family	Secondary Transporter	2.A.29
Sc	*PET8*	BenzOH	↑	S-adenosylmethionine (SAM)	The Mitochondrial Carrier (MC) Family	Secondary Transporter	2.A.29
Sc	*FLX1*	BenzOH	↓	Unclassified	The Mitochondrial Carrier (MC) Family	Secondary Transporter	2.A.29

Sc	*PEX3*	BenzOH	↓				
Sc	*MCH5*	BenzOH	↓	monocarboxylate?	The Major Facilitator Superfamily (MFS)	Secondary Transporter	2.A.1
Sc	*MRX20*	Berb	↑	tricarboxylate	The Mitochondrial Carrier (MC) Family	Secondary Transporter	2.A.29
Sc	*AGP2*	Berb	↑	Amino acids (general)	The Amino Acid-Polyamine-Organocation (APC) Family	Secondary Transporter	2.A.3
Sc	*FET4*	Berb	↓	Fe2+ (uptake; low-affinity)	The Low Affinity Fe2+ Transporter (FeT) Family	Unclassified	9.A.9
Sc	*YOL162W*	Van	↓	allantoate?	The Major Facilitator Superfamily (MFS)	Secondary Transporter	2.A.1
Sc	*STV1*	Van	↓				

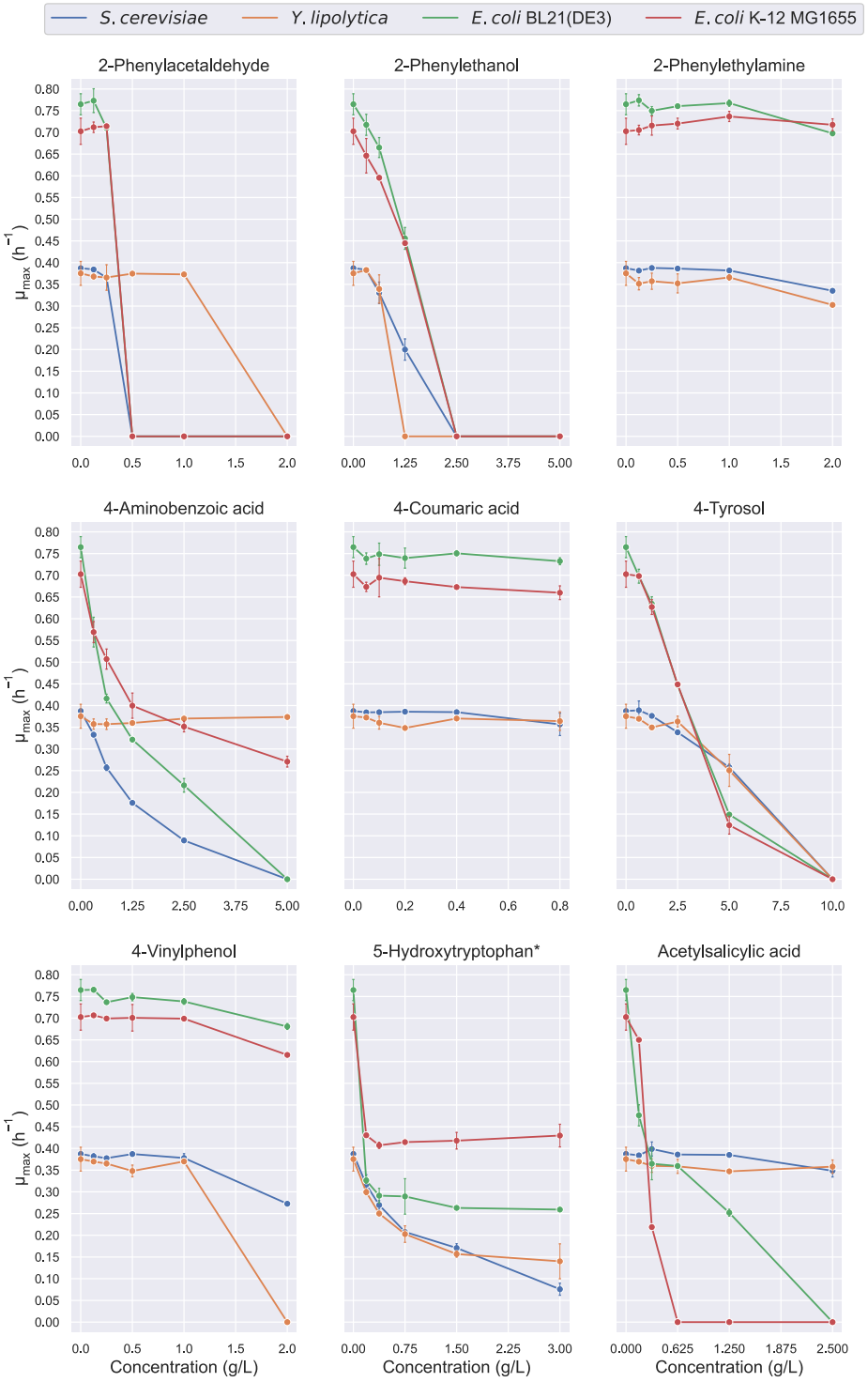
S. cerevisiae
Y. lipolytica
E. coli BL21(DE3)
E. coli K-12 MG1655
2-Phenylacetaldehyde
2-Phenylethanol
2-Phenylethylamine
4-Aminobenzoic acid
4-Coumaric acid
4-Tyrosol
4-Vinylphenol
5-Hydroxytryptophan*
Acetylsalicylic acid
μmax (h−1)
Concentration (g/L)

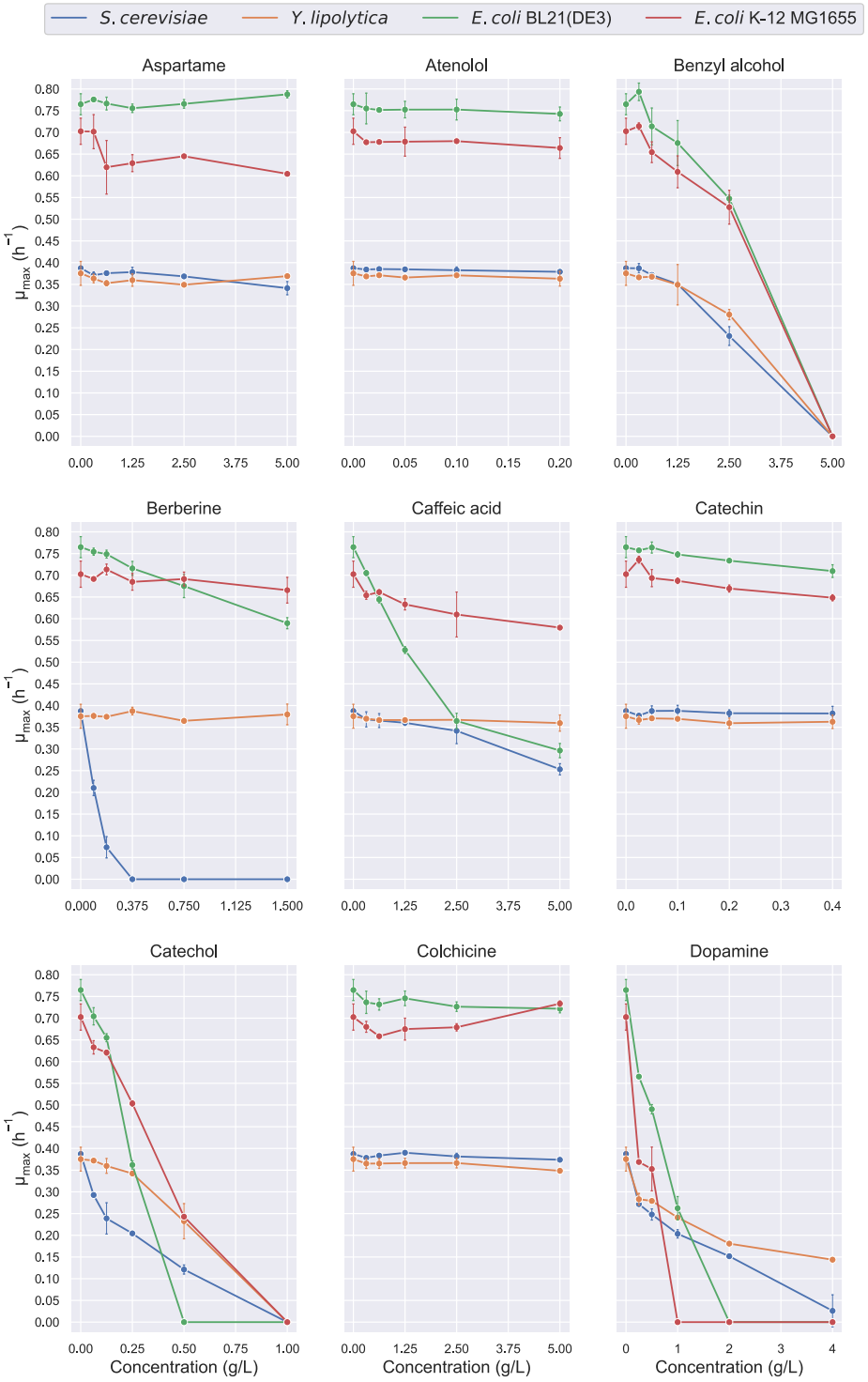
S. cerevisiae
Y. lipolytica
E. coli BL21(DE3)
E. coli K-12 MG1655
Aspartame
Atenolol
Benzyl alcohol
Berberine
Caffeic acid
Catechin
Catechol
Colchicine
Dopamine
μmax (h−1)
Concentration (g/L)

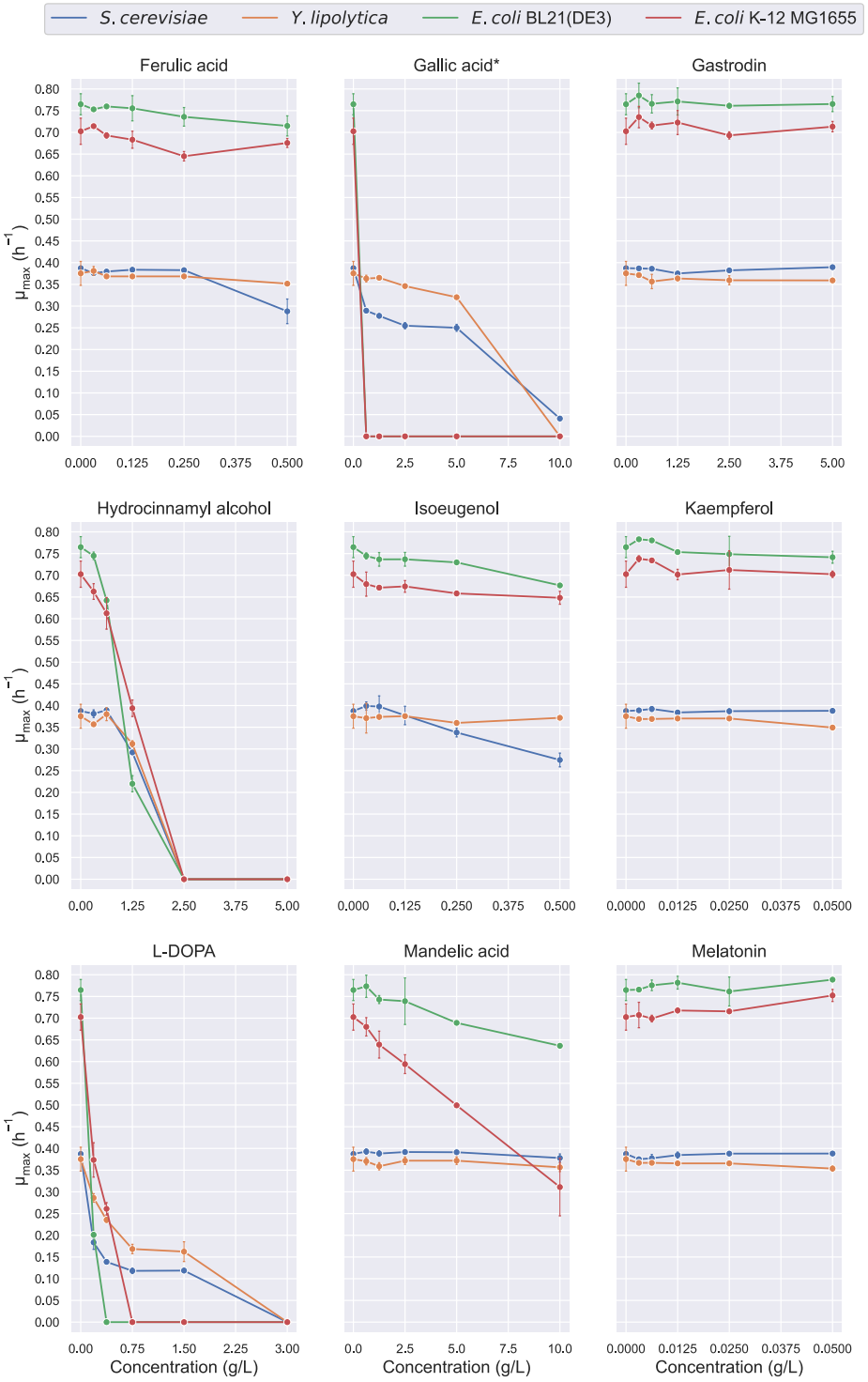
S. cerevisiae
Y. lipolytica
E. coli BL21(DE3)
E. coli K-12 MG1655
Ferulic acid
Gallic acid*
Gastrodin
Hydrocinnamyl alcohol
Isoeugenol
Kaempferol
L-DOPA
Mandelic acid
Melatonin
μmax (h−1)
Concentration (g/L)

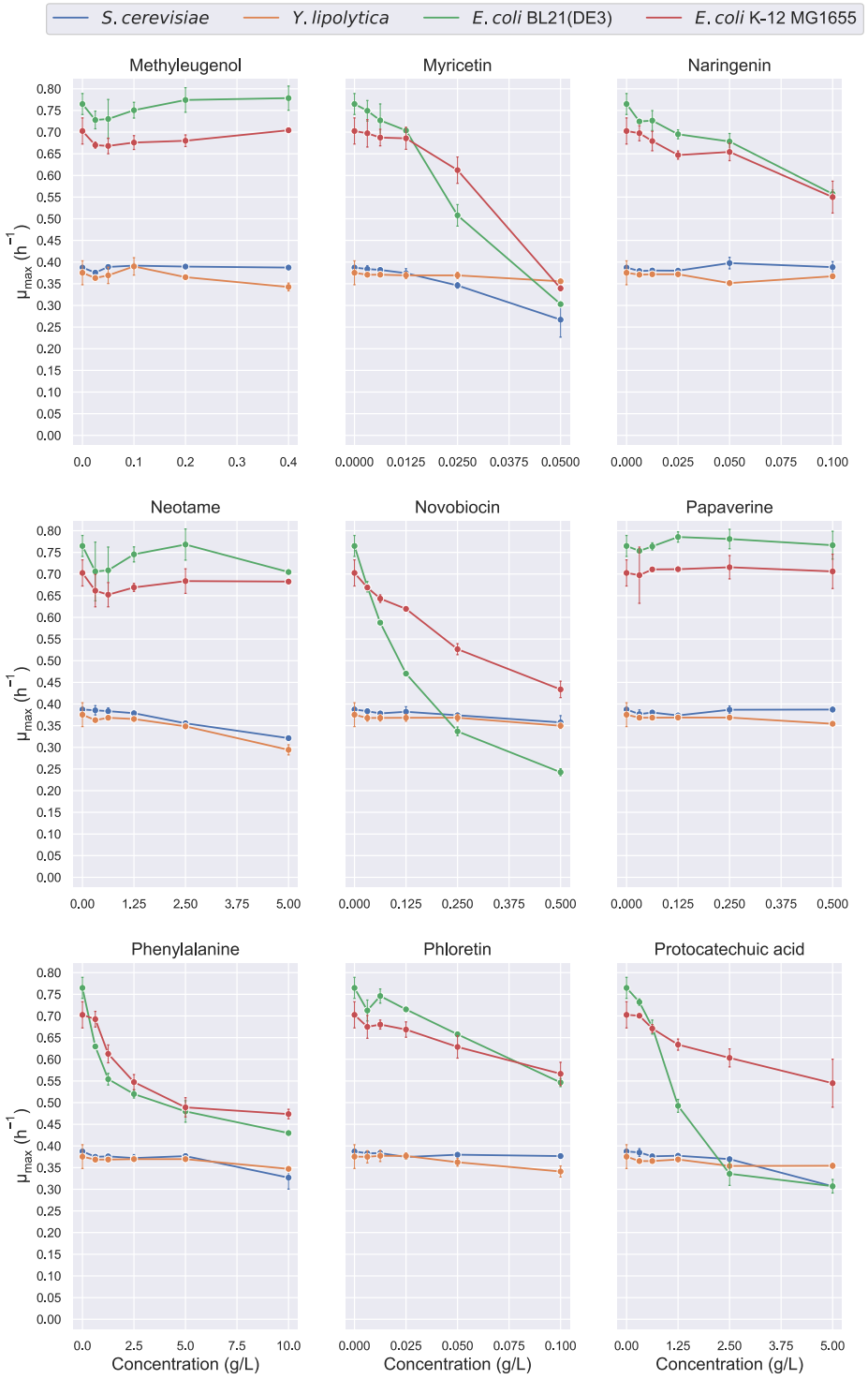
S. cerevisiae
Y. lipolytica
E. coli BL21(DE3)
E. coli K-12 MG1655
Methyleugenol
Myricetin
Naringenin
Neotame
Novobiocin
Papaverine
Phenylalanine
Phloretin
Protocatechuic acid
μmax (h−1)
Concentration (g/L)

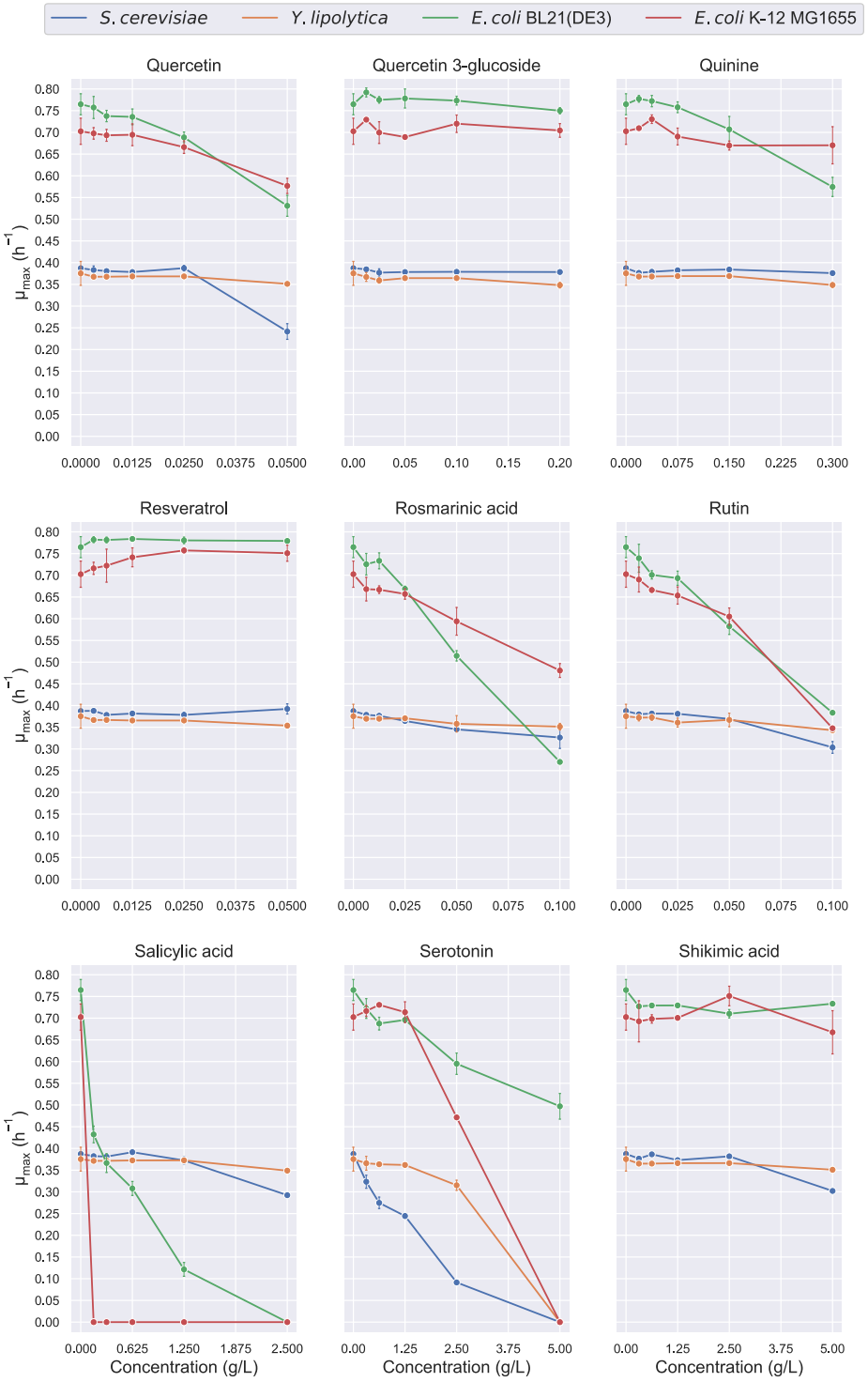
S. cerevisiae
Y. lipolytica
E. coli BL21(DE3)
E. coli K-12 MG1655
Quercetin
Quercetin 3-glucoside
Quinine
Resveratrol
Rosmarinic acid
Rutin
Salicylic acid
Serotonin
Shikimic acid
μmax (h−1)
Concentration (g/L)

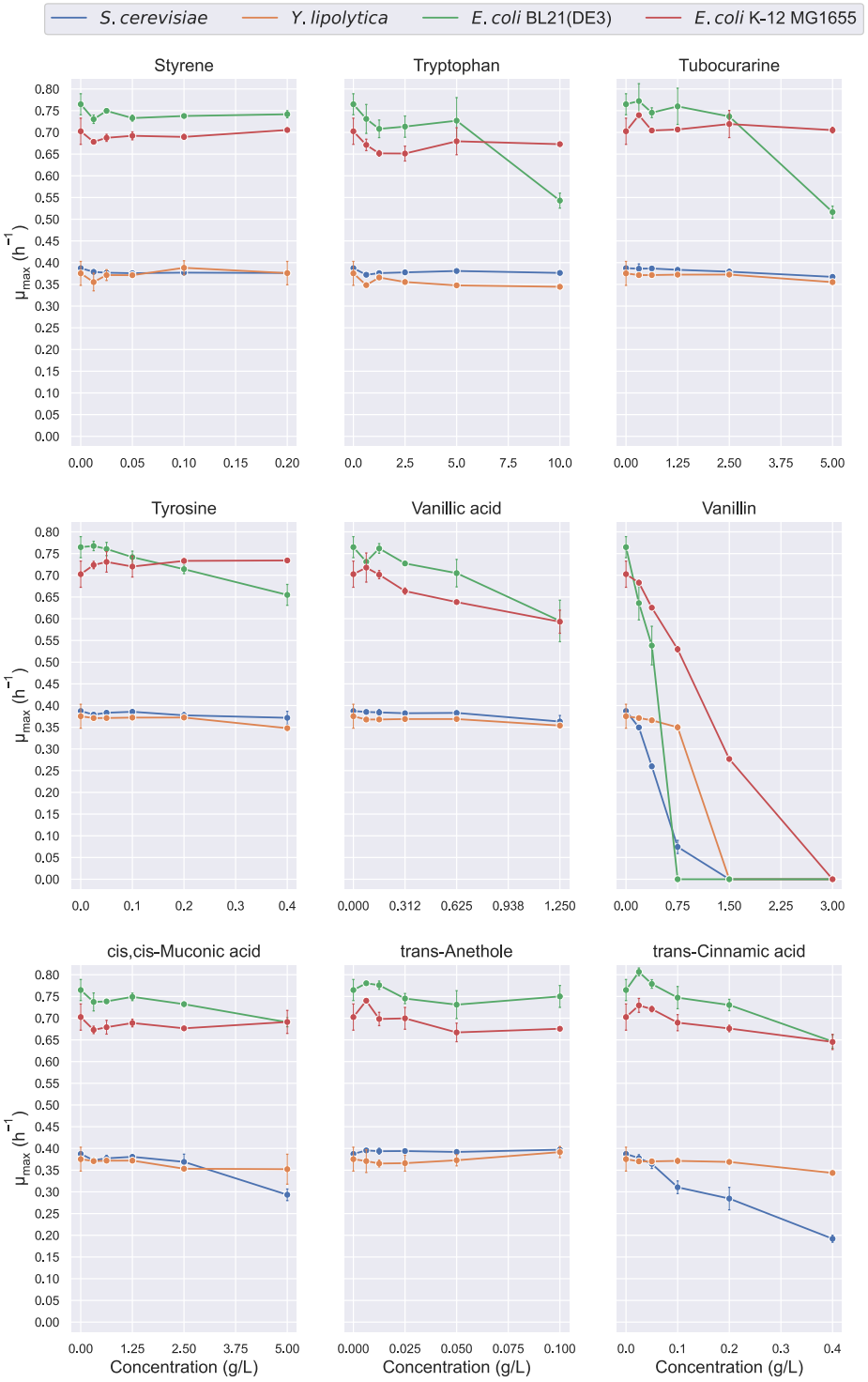

Figure S1. Toxicity of 54 aromatic compounds evaluated in *S. cerevisiae*, *Y. lipolytica* and *E. coli*. μ_{max} was determined as the highest slope of ln-transformed OD_{600} versus time within the exponential growth phase. The μ_{max} covered a window of 12 time points, and required a minimum R^2 value of 0.98. Error bars represent the standard deviation from two biological replicates. *: Addition of the given compound causes medium blackening and impedes μ_{max} estimation.

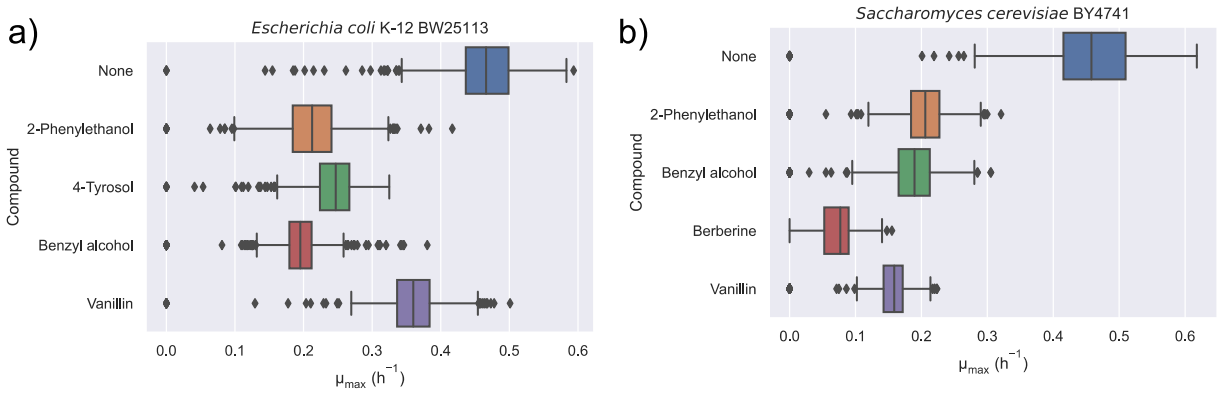

Figure S2. Box and Whisker diagram of transporters deletion library screening. Strains unable to grow in the control medium were excluded from the analysis, resulting in the selection of 444 strains in *E. coli* and 305 in *S. cerevisiae*. μ_{max} is calculated as the mean of two biological replicates.

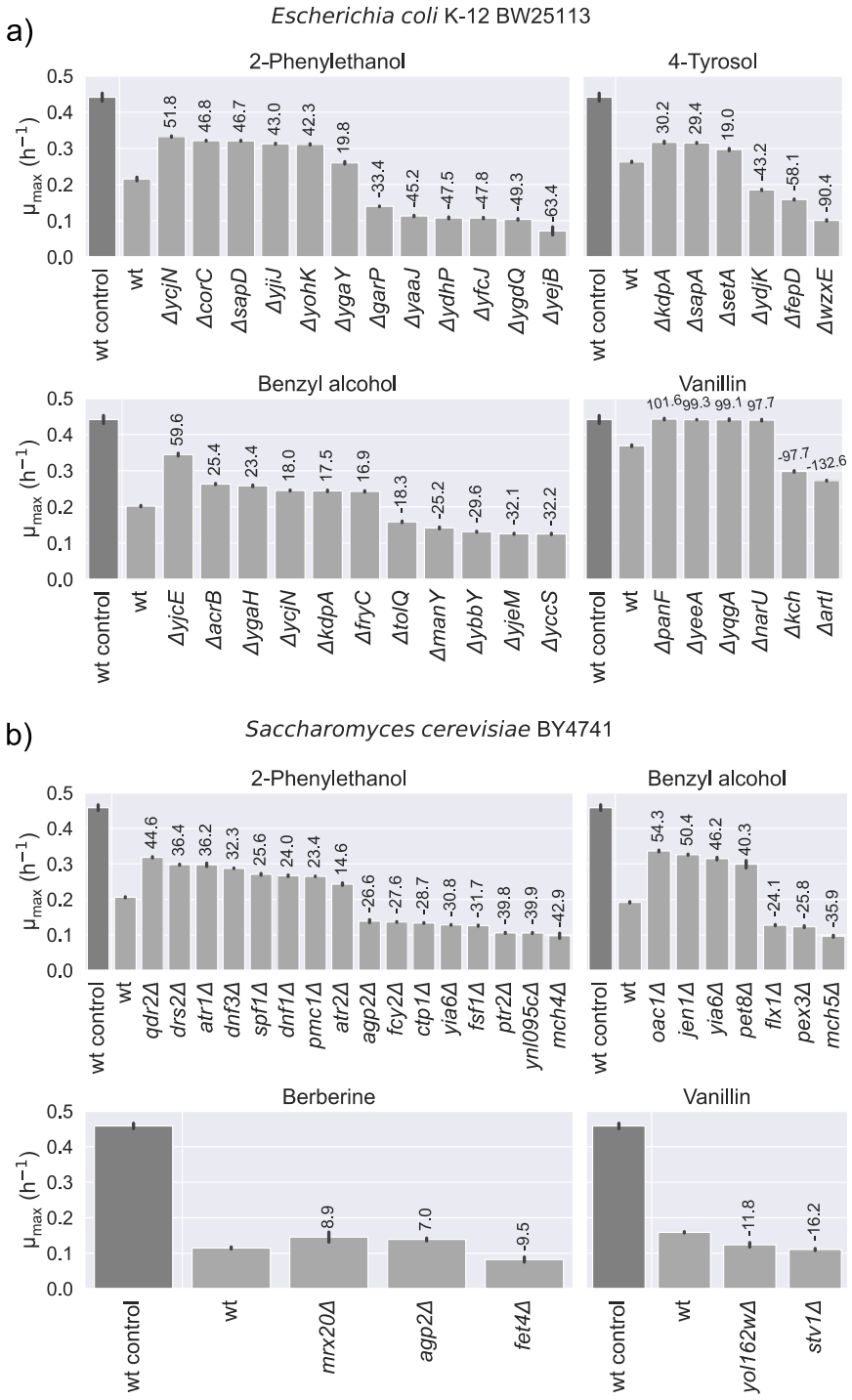

Figure S3. Contribution of transporter deletions to aromatics tolerance in a) *E. coli* and b) *S. cerevisiae*. Values on top of bars show the percentage of recovered tolerance, using as references the wild-type strain in the presence of the toxic aromatic compounds (wt, 0%) and the wild-type strain in the absence of aromatics (wt control, 100%). Error bars indicate the standard deviation of at least 4 biological replicates.

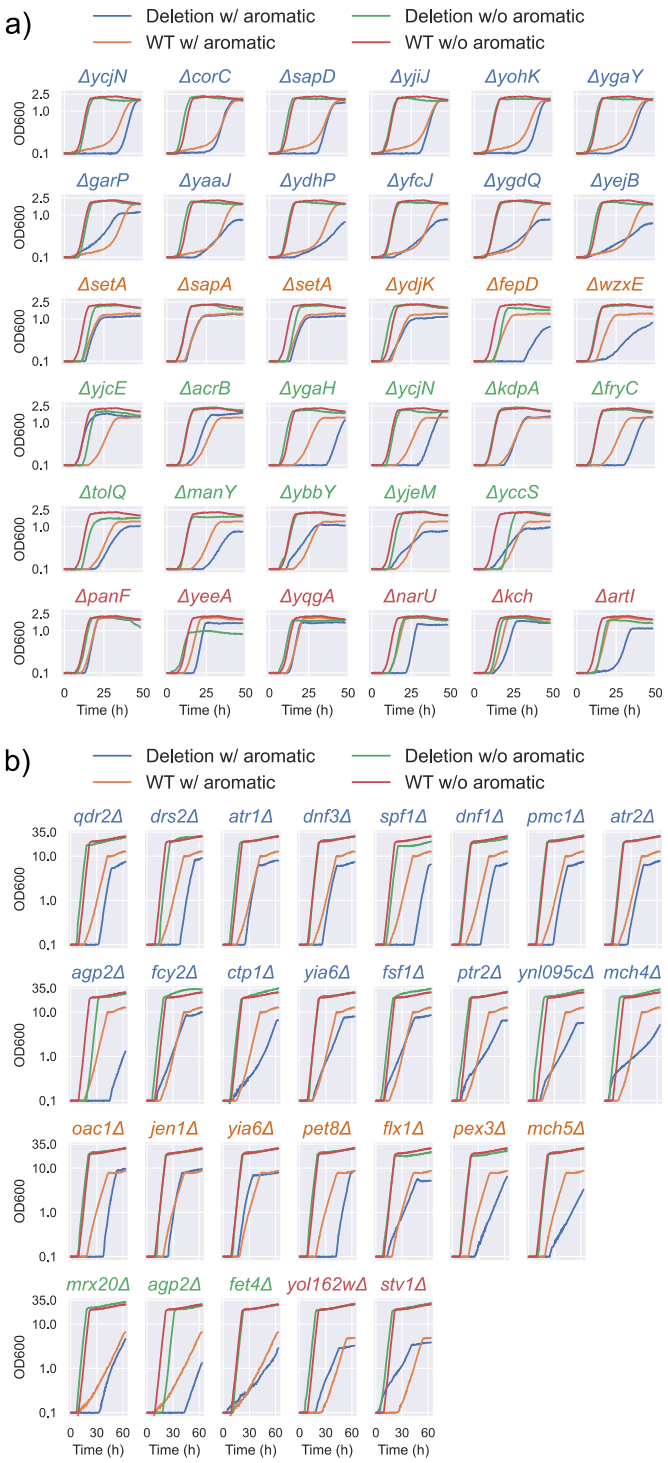

Figure S4. Growth profiles of validated transporter deletions improving or reducing tolerance. A representative growth curve per strain is shown. Font colors of deleted transporter-encoding genes represent the compound. a) *E. coli*. Blue: 2-phenylethanol; orange: 4-tyrosol; green: benzyl alcohol; red: vanillin. b) *S. cerevisiae*. Blue: 2-phenylethanol; orange: benzyl alcohol; green: berberine; red: vanillin.

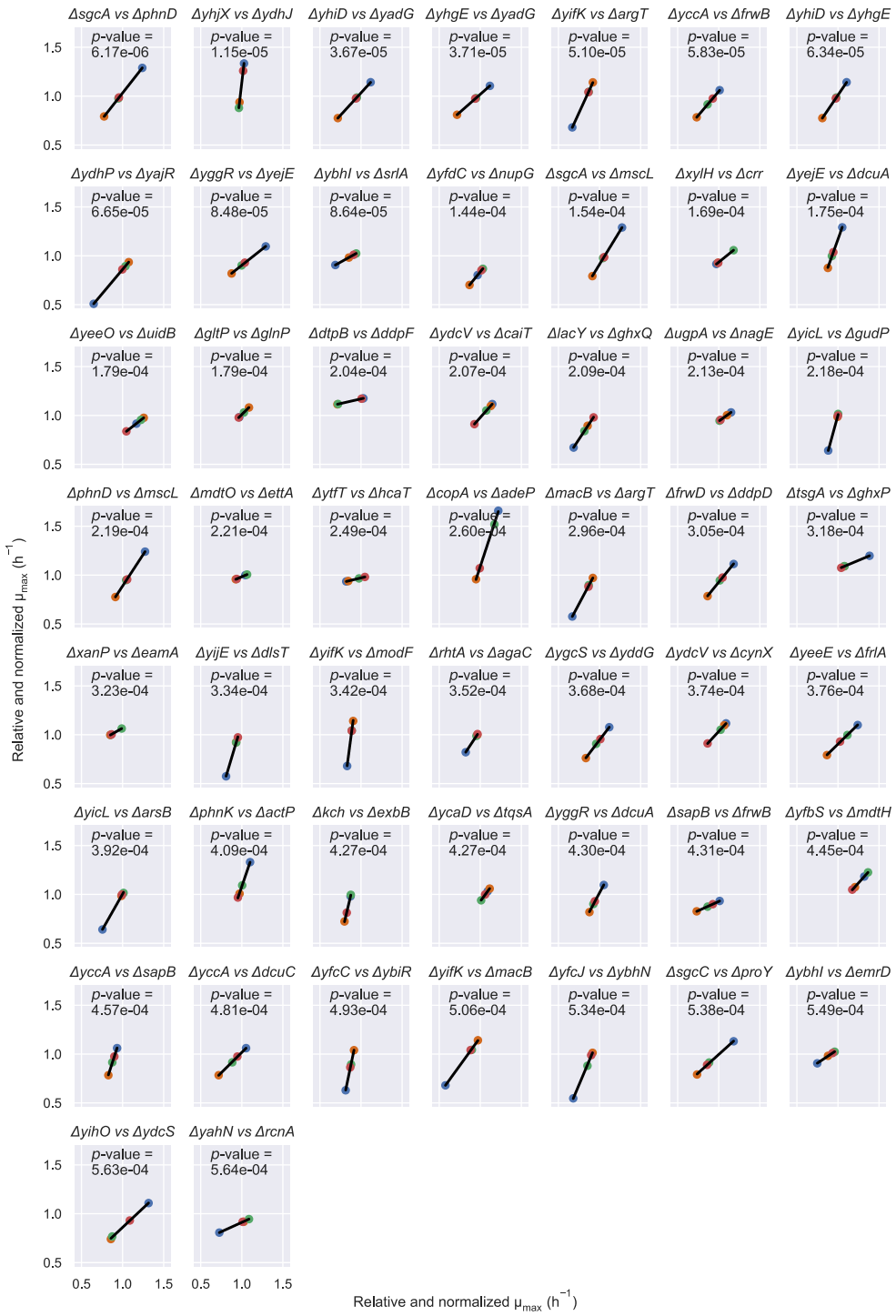

Figure S5. Pairs of transporters-encoding genes showing high degree of correlation in *E. coli*. The mean relative and normalized μ_{max} is used as correlation parameter. It compares the μ_{max} in the presence of the toxic aromatic compound to the wild-type control and normalizes it against the effect of the deletion in the absence of the compound. A R^2 coefficient higher than 0.999 and a p-value < 0.05 after a Bonferroni correction was enforced for the selection of the pairs. Colors indicate the different compounds: Blue: 2-phenylethanol; orange: 4-tyrosol; green: benzyl alcohol; red: vanillin.

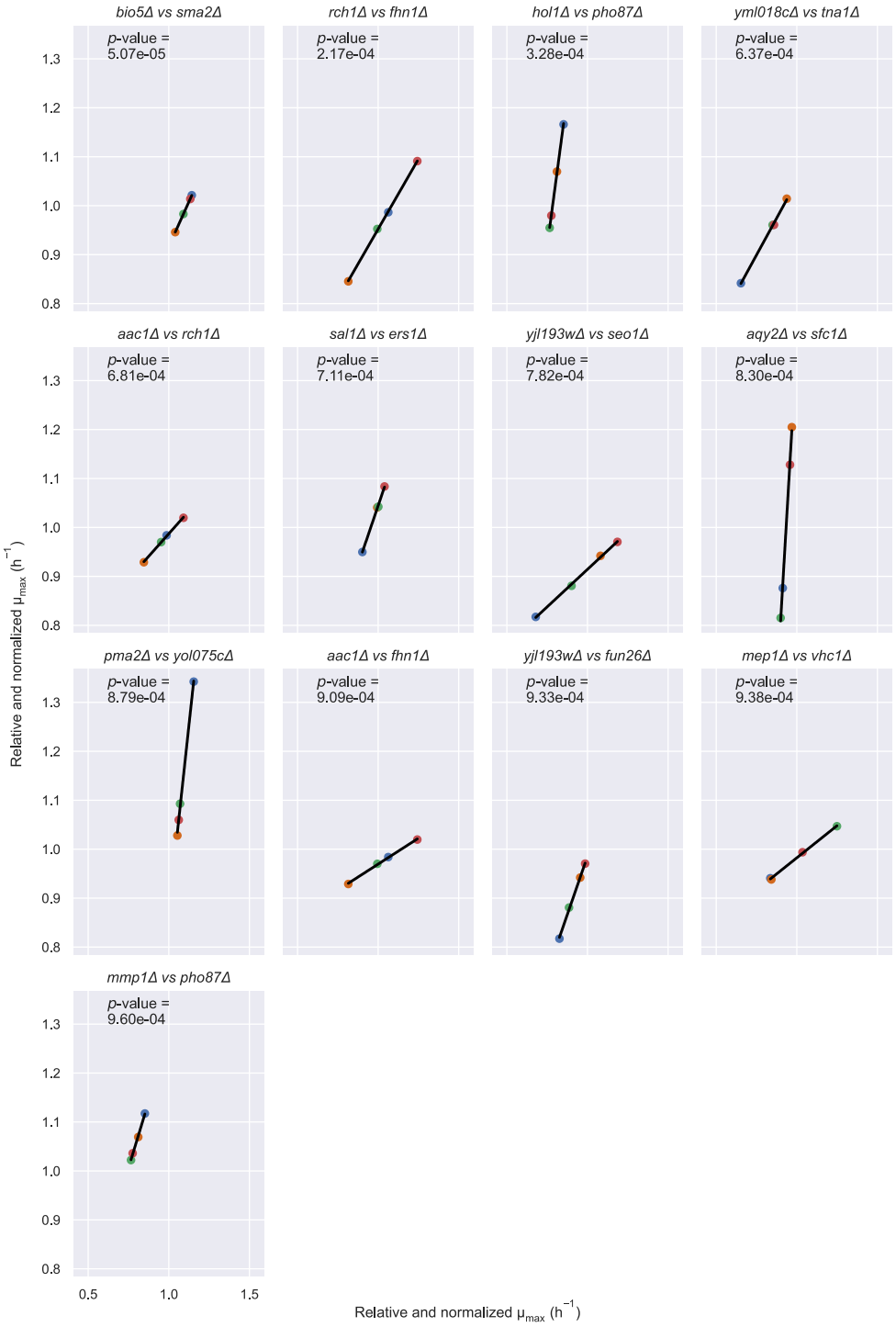

Figure S6. Pairs of transporters-encoding genes showing high degree of correlation in *S. cerevisiae*. The mean relative and normalized μ_{max} is used as correlation parameter. It compares the μ_{max} in the presence of the toxic aromatic compound to the wild-type control and normalizes it against the effect of the deletion in the absence of the compound. A R^2 coefficient higher than 0.999 and a p-value < 0.05 after a Bonferroni correction was enforced for the selection of the pairs. Colors indicate the different compounds: Blue: 2-phenylethanol; orange: benzyl alcohol; green: berberine; red: vanillin.

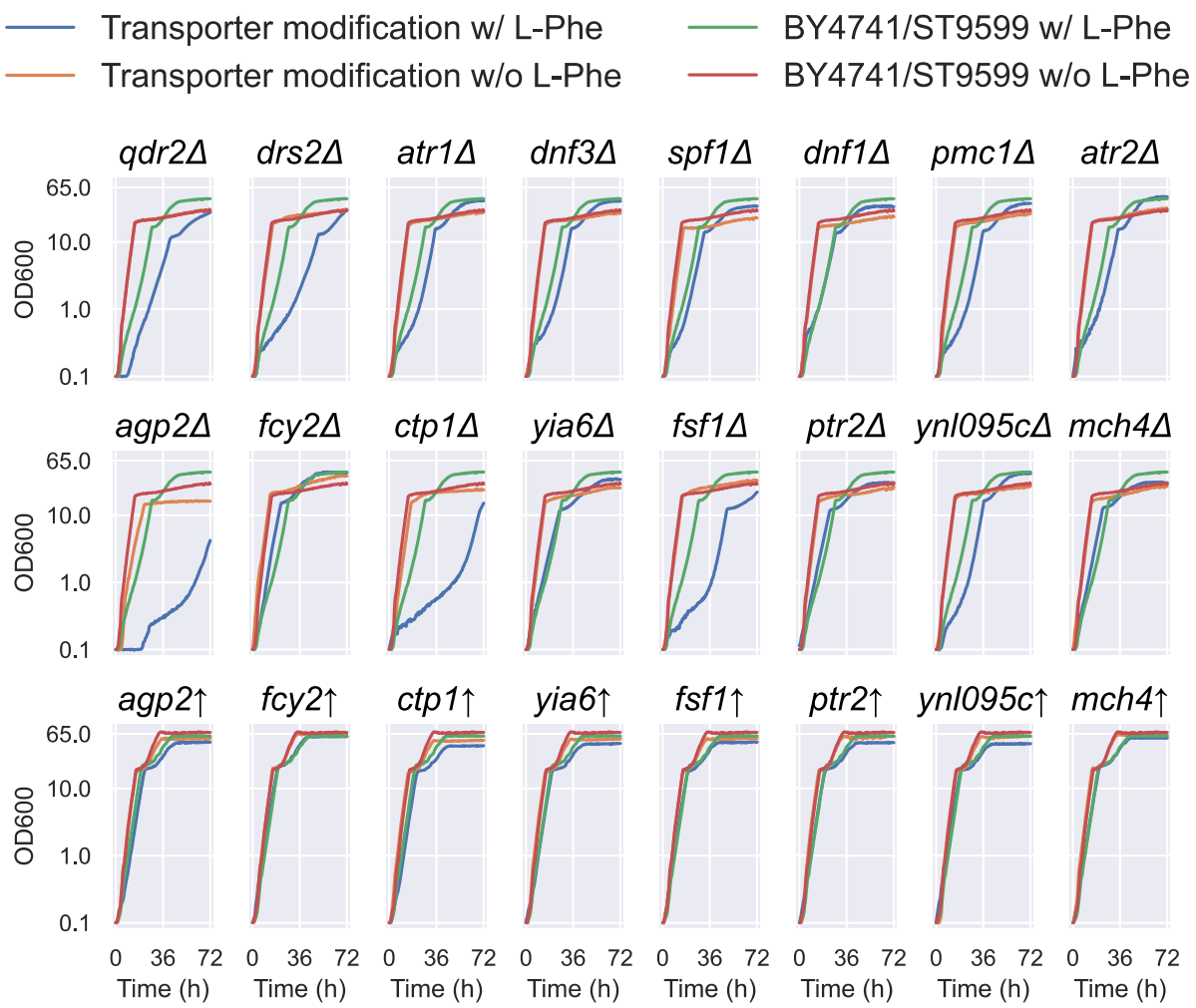

Figure S7. Growth profiles of transporter deletions improving or reducing 2-phenylethanol tolerance in an L-phenylalanine bioconversion process. A representative growth curve per strain is shown. L-phenylalanine was supplemented at a concentration of 5 g/L. Top panel: transporter deletions improving 2-phenylethanol tolerance. Middle panel: transporter deletions reducing 2-phenylethanol tolerance. Bottom panel: overexpression of transporters that upon deletion reduce 2-phenylethanol tolerance.

References

Aguilar-Zárate, P., Cruz, M.A., Montañez, J., Rodríguez-Herrera, R., Wong-Paz, J.E., Belmares, R.E., Aguilar, C.N., 2015. Gallic acid production under anaerobic submerged fermentation by two bacilli strains. Microb. Cell Factories 14, 209. https://doi.org/10.1186/s12934-015-0386-2

Ahmadi, M.K., Fang, L., Moscatello, N., Pfeifer, B.A., 2016. E. coli metabolic engineering for gram scale production of a plant-based anti-inflammatory agent. Metab. Eng. 38, 382–388. https://doi.org/10.1016/j.ymben.2016.10.001

Averesch, N.J.H., Winter, G., Krömer, J.O., 2016. Production of para-aminobenzoic acid from different carbon-sources in engineered Saccharomyces cerevisiae. Microb. Cell Factories 15, 89. https://doi.org/10.1186/s12934-016-0485-8

Baba, T., Ara, T., Hasegawa, M., Takai, Y., Okumura, Y., Baba, M., Datsenko, K.A., Tomita, M., Wanner, B.L., Mori, H., 2006. Construction of *Escherichia coli* K-12 in-frame, single-gene knockout mutants: the Keio collection. Mol. Syst. Biol. 2. https://doi.org/10.1038/msb4100050

Babaei, M., Borja Zamfir, G.M., Chen, X., Christensen, H.B., Kristensen, M., Nielsen, J., Borodina, I., 2020. Metabolic Engineering of *Saccharomyces cerevisiae* for Rosmarinic Acid Production. ACS Synth. Biol. 9, 1978–1988. https://doi.org/10.1021/acssynbio.0c00048

Bachmann, B.J., 1972. Pedigrees of some mutant strains of Escherichia coli K-12. Bacteriol. Rev. 36, 525–557. https://doi.org/10.1128/br.36.4.525-557.1972

Baker Brachmann, C., Davies, A., Cost, G.J., Caputo, E., Li, J., Hieter, P., Boeke, J.D., 1998. Designer deletion strains derived fromSaccharomyces cerevisiae S288C: A useful set of strains and plasmids for PCR-mediated gene disruption and other applications. Yeast 14, 115–132. https://doi.org/10.1002/(SICI)1097-0061(19980130)14:2<115::AID-YEA204>3.0.CO;2-2

Brochado, A.R., Matos, C., Møller, B.L., Hansen, J., Mortensen, U.H., Patil, K.R., 2010. Improved vanillin production in baker's yeast through in silico design. Microb. Cell Factories 9, 84. https://doi.org/10.1186/1475-2859-9-84

Datsenko, K.A., Wanner, B.L., 2000. One-step inactivation of chromosomal genes in *Escherichia coli* K-12 using PCR products. Proc. Natl. Acad. Sci. 97, 6640–6645. https://doi.org/10.1073/pnas.120163297

De Bruyn, F., Van Brempt, M., Maertens, J., Van Bellegem, W., Duchi, D., De Mey, M., 2015. Metabolic engineering of Escherichia coli into a versatile glycosylation platform: production of bio-active quercetin glycosides. Microb. Cell Factories 14, 138. https://doi.org/10.1186/s12934-015-0326-1

Elbourne, L.D.H., Tetu, S.G., Hassan, K.A., Paulsen, I.T., 2017. TransportDB 2.0: a database for exploring membrane transporters in sequenced genomes from all domains of life. Nucleic Acids Res. 45, D320–D324. https://doi.org/10.1093/nar/gkw1068

Entian, K.-D., Kötter, P., 2007. 25 Yeast Genetic Strain and Plasmid Collections, in: Stansfield, I., Stark, M.J. (Eds.), Methods in Microbiology, Yeast Gene Analysis. Academic Press, pp. 629–666. https://doi.org/10.1016/S0580-9517(06)36025-4

Fordjour, E., Adipah, F.K., Zhou, S., Du, G., Zhou, J., 2019. Metabolic engineering of Escherichia coli BL21 (DE3) for de novo production of l-DOPA from d-glucose. Microb. Cell Factories 18, 74. https://doi.org/10.1186/s12934-019-1122-0

Gaillardin, C.M., Charoy, V., Heslot, H., 1973. A study of copulation, sporulation and meiotic segregation in Candida lipolytica. Arch. Für Mikrobiol. 92, 69–83. https://doi.org/10.1007/BF00409513

Gold, N.D., Gowen, C.M., Lussier, F.-X., Cautha, S.C., Mahadevan, R., Martin, V.J.J., 2015. Metabolic engineering of a tyrosine-overproducing yeast platform using targeted metabolomics. Microb. Cell Factories 14, 73. https://doi.org/10.1186/s12934-015-0252-2

Hamana, K., Niitsu, M., 1999. Production of 2-phenylethylamine by decarboxylation of L-phenylalanine in alkaliphilic Bacillus cohnii. J. Gen. Appl. Microbiol. 45, 149–153. https://doi.org/10.2323/jgam.45.149

Han, J., Li, S., 2023. De novo biosynthesis of berberine and halogenated benzylisoquinoline alkaloids in Saccharomyces cerevisiae. Commun. Chem. 6, 27. https://doi.org/10.1038/s42004-023-00821-9

Jamil, O.K., Cravens, A., Payne, J.T., Kim, C.Y., Smolke, C.D., 2022. Biosynthesis of tetrahydropapaverine and semisynthesis of papaverine in yeast. Proc. Natl. Acad. Sci. 119, e2205848119. https://doi.org/10.1073/pnas.2205848119

Jessop-Fabre, M.M., Jakočiūnas, T., Stovicek, V., Dai, Z., Jensen, M.K., Keasling, J.D., Borodina, I., 2016. EasyClone-MarkerFree: A vector toolkit for marker-less integration of genes into Saccharomyces cerevisiae via CRISPR-Cas9. Biotechnol. J. 11, 1110–1117. https://doi.org/10.1002/biot.201600147

Lee, K., Bang, H.B., Lee, Y.H., Jeong, K.J., 2019. Enhanced production of styrene by engineered Escherichia coli and in situ product recovery (ISPR) with an organic solvent. Microb. Cell Factories 18, 79. https://doi.org/10.1186/s12934-019-1129-6

Leonard, E., Yan, Y., Koffas, M., 2006. Functional expression of a P450 flavonoid hydroxylase for the biosynthesis of plant-specific hydroxylated flavonols in Escherichia coli. Metab. Eng. 8, 172–181. https://doi.org/10.1016/j.ymben.2005.11.001

Li, J., Ye, B.-C., 2021. Metabolic engineering of Pseudomonas putida KT2440 for high-yield production of protocatechuic acid. Bioresour. Technol. 319, 124239. https://doi.org/10.1016/j.biortech.2020.124239

Liu, M., Wang, C., Ren, X., Gao, S., Yu, S., Zhou, J., 2022. Remodelling metabolism for high-level resveratrol production in Yarrowia lipolytica. Bioresour. Technol. 365, 128178. https://doi.org/10.1016/j.biortech.2022.128178

Liu, X., Liu, J., Lei, D., Zhao, G.-R., 2022. Modular metabolic engineering for production of phloretic acid, phloretin and phlorizin in Escherichia coli. Chem. Eng. Sci. 247, 116931. https://doi.org/10.1016/j.ces.2021.116931

Liu, X., Niu, H., Li, Q., Gu, P., 2019. Metabolic engineering for the production of l-phenylalanine in Escherichia coli. 3 Biotech 9, 85. https://doi.org/10.1007/s13205-019-1619-6

Liu, Z., Zhang, X., Lei, D., Qiao, B., Zhao, G.-R., 2021. Metabolic engineering of Escherichia coli for de novo production of 3-phenylpropanol via retrobiosynthesis approach. Microb. Cell Factories 20, 121. https://doi.org/10.1186/s12934-021-01615-1

Lv, H., Zhang, Y., Shao, J., Liu, H., Wang, Y., 2021. Ferulic acid production by metabolically engineered Escherichia coli. Bioresour. Bioprocess. 8, 70. https://doi.org/10.1186/s40643-021-00423-0

Lyu, X., Zhao, G., Ng, K.R., Mark, R., Chen, W.N., 2019. Metabolic Engineering of *Saccharomyces cerevisiae* for De Novo Production of Kaempferol. J. Agric. Food Chem. 67, 5596–5606. https://doi.org/10.1021/acs.jafc.9b01329

Martínez, J.A., Bolívar, F., Escalante, A., 2015. Shikimic Acid Production in Escherichia coli: From Classical Metabolic Engineering Strategies to Omics Applied to Improve Its Production. Front. Bioeng. Biotechnol. 3. https://doi.org/10.3389/fbioe.2015.00145

Mora-Villalobos, J.-A., Zeng, A.-P., 2018. Synthetic pathways and processes for effective production of 5-hydroxytryptophan and serotonin from glucose in Escherichia coli. J. Biol. Eng. 12, 3. https://doi.org/10.1186/s13036-018-0094-7

Niu, H., Li, R., Liang, Q., Qi, Q., Li, Q., Gu, P., 2019. Metabolic engineering for improving L-tryptophan production in *Escherichia coli*. J. Ind. Microbiol. Biotechnol. 46, 55–65. https://doi.org/10.1007/s10295-018-2106-5

Partow, S., Siewers, V., Bjørn, S., Nielsen, J., Maury, J., 2010. Characterization of different promoters for designing a new expression vector in Saccharomyces cerevisiae. Yeast 27, 955–964. https://doi.org/10.1002/yea.1806

Pugh, S., McKenna, R., Halloum, I., Nielsen, D.R., 2015. Engineering Escherichia coli for renewable benzyl alcohol production. Metab. Eng. Commun. 2, 39–45. https://doi.org/10.1016/j.meteno.2015.06.002

Rodriguez, A., Kildegaard, K.R., Li, M., Borodina, I., Nielsen, J., 2015. Establishment of a yeast platform strain for production of p-coumaric acid through metabolic engineering of

aromatic amino acid biosynthesis. Metab. Eng. 31, 181–188. https://doi.org/10.1016/j.ymben.2015.08.003

Rodriguez, A., Strucko, T., Stahlhut, S.G., Kristensen, M., Svenssen, D.K., Forster, J., Nielsen, J., Borodina, I., 2017. Metabolic engineering of yeast for fermentative production of flavonoids. Bioresour. Technol. 245, 1645–1654. https://doi.org/10.1016/j.biortech.2017.06.043

Salgado, J.M., Rodríguez-Solana, R., Curiel, J.A., de las Rivas, B., Muñoz, R., Domínguez, J.M., 2014. Bioproduction of 4-vinylphenol from corn cob alkaline hydrolyzate in two-phase extractive fermentation using free or immobilized recombinant E. coli expressing pad gene. Enzyme Microb. Technol. 58–59, 22–28. https://doi.org/10.1016/j.enzmictec.2014.02.005

Song, G., Wu, F., Peng, Y., Jiang, X., Wang, Q., 2022. High-Level Production of Catechol from Glucose by Engineered Escherichia coli. Fermentation 8, 344. https://doi.org/10.3390/fermentation8070344

Steffensky, M., Mühlenweg, A., Wang, Z.-X., Li, S.-M., Heide, L., 2000. Identification of the Novobiocin Biosynthetic Gene Cluster of *Streptomyces spheroides* NCIB 11891. Antimicrob. Agents Chemother. 44, 1214–1222. https://doi.org/10.1128/AAC.44.5.1214-1222.2000

Studier, F.W., Moffatt, B.A., 1986. Use of bacteriophage T7 RNA polymerase to direct selective high-level expression of cloned genes. J. Mol. Biol. 189, 113–130. https://doi.org/10.1016/0022-2836(86)90385-2

Sun, Z., Ning, Y., Liu, L., Liu, Y., Sun, B., Jiang, W., Yang, C., Yang, S., 2011. Metabolic engineering of the L-phenylalanine pathway in Escherichia coli for the production of S- or R-mandelic acid. Microb. Cell Factories 10, 71. https://doi.org/10.1186/1475-2859-10-71

Trenchard, I.J., Siddiqui, M.S., Thodey, K., Smolke, C.D., 2015. De novo production of the key branch point benzylisoquinoline alkaloid reticuline in yeast. Metab. Eng. 31, 74–83. https://doi.org/10.1016/j.ymben.2015.06.010

Vargas-Tah, A., Gosset, G., 2015. Production of Cinnamic and p-Hydroxycinnamic Acids in Engineered Microbes. Front. Bioeng. Biotechnol. 3. https://doi.org/10.3389/fbioe.2015.00116

Wang, G., Tavares, A., Schmitz, S., França, L., Almeida, H., Cavalheiro, J., Carolas, A., Øzmerih, S., Blank, L.M., Ferreira, B.S., Borodina, I., 2022. An integrated yeast-based process for *cis* , *cis* -muconic acid production. Biotechnol. Bioeng. 119, 376–387. https://doi.org/10.1002/bit.27992

Wang, G., Wang, M., Yang, J., Li, Q., Zhu, N., Liu, L., Hu, X., Yang, X., 2023. *De novo* Synthesis of 2-phenylethanol from Glucose by Metabolically Engineered *Escherichia coli*. J. Ind. Microbiol. Biotechnol. 49, kuac026. https://doi.org/10.1093/jimb/kuac026

Wang, H., Liu, W., Shi, F., Huang, L., Lian, J., Qu, L., Cai, J., Xu, Z., 2018. Metabolic pathway engineering for high-level production of 5-hydroxytryptophan in Escherichia coli. Metab. Eng. 48, 279–287. https://doi.org/10.1016/j.ymben.2018.06.007

Wang, Q., Wu, X., Lu, X., He, Y., Ma, B., Xu, Y., 2021. Efficient Biosynthesis of Vanillin from Isoeugenol by Recombinant Isoeugenol Monooxygenase from Pseudomonas nitroreducens Jin1. Appl. Biochem. Biotechnol. 193, 1116–1128. https://doi.org/10.1007/s12010-020-03478-5

Wang, Y., Zhang, H., Lu, X., Zong, H., Zhuge, B., 2019. Advances in 2-phenylethanol production from engineered microorganisms. Biotechnol. Adv. 37, 403–409. https://doi.org/10.1016/j.biotechadv.2019.02.005

Wei, W., Zhang, P., Shang, Y., Zhou, Y., Ye, B.-C., 2020. Metabolically engineering of Yarrowia lipolytica for the biosynthesis of naringenin from a mixture of glucose and xylose. Bioresour. Technol. 314, 123726. https://doi.org/10.1016/j.biortech.2020.123726

Weiland, F., Barton, N., Kohlstedt, M., Becker, J., Wittmann, C., 2023. Systems metabolic engineering upgrades Corynebacterium glutamicum to high-efficiency cis, cis-muconic acid production from lignin-based aromatics. Metab. Eng. 75, 153–169. https://doi.org/10.1016/j.ymben.2022.12.005

Xu, W., Yang, C., Xia, Y., Zhang, L., Liu, C., Yang, H., Shen, W., Chen, X., 2020. High-Level Production of Tyrosol with Noninduced Recombinant *Escherichia coli* by Metabolic Engineering. J. Agric. Food Chem. 68, 4616–4623. https://doi.org/10.1021/acs.jafc.9b07610

Yin, H., Hu, T., Zhuang, Y., Liu, T., 2020. Metabolic engineering of Saccharomyces cerevisiae for high-level production of gastrodin from glucose. Microb. Cell Factories 19, 218. https://doi.org/10.1186/s12934-020-01476-0

Zhang, Y., He, Y., Zhang, N., Gan, J., Zhang, S., Dong, Z., 2021. Combining protein and metabolic engineering strategies for biosynthesis of melatonin in Escherichia coli. Microb. Cell Factories 20, 170. https://doi.org/10.1186/s12934-021-01662-8

Zhao, S., Jones, J.A., Lachance, D.M., Bhan, N., Khalidi, O., Venkataraman, S., Wang, Z., Koffas, M.A.G., 2015. Improvement of catechin production in Escherichia coli through combinatorial metabolic engineering. Metab. Eng. 28, 43–53. https://doi.org/10.1016/j.ymben.2014.12.002

Zhou, P., Yue, C., Shen, B., Du, Y., Xu, N., Ye, L., 2021. Metabolic engineering of Saccharomyces cerevisiae for enhanced production of caffeic acid. Appl. Microbiol. Biotechnol. 105, 5809–5819. https://doi.org/10.1007/s00253-021-11445-1

CHAPTER 5

Understanding the physiology of *p*-coumaric acid production in *Saccharomyces cerevisiae*

This chapter contains a manuscript in preparation:

Sáez-Sáez, J.†, Hesselberg-Thomsen, V.†, Babaei, M., Borodina, I.

†These authors contributed equally to this work.

Abstract

Phenylpropanoids represent an important family of plant natural products with applications in multiple industries, including pharmaceuticals, food supplements or cosmetics. However, their low concentrations in plants and challenges associated with chemical synthesis make microbial production an attractive alternative. *p*-Coumaric acid, a common precursor for all phenylpropanoids, serves as an attractive target compound for the development of microbial platform strains for phenylpropanoids production. *Saccharomyces cerevisiae*, with its eukaryotic architecture, has emerged as a preferred host organism for this purpose. To achieve high *p*-coumaric acid production, in this study we implemented rational strategies derived from existing literature to construct multiple *p*-coumaric acid platform strains. Subsequently, a physiological characterization of these strains was conducted to gain insights into their performance. This work sets the foundation for further multi-omics characterization of these engineered strains, aiming to enhance our understanding of their metabolic capabilities and optimize phenylpropanoid production in microbial cell factories.

Introduction

Plant natural products are secondary metabolites serving essential physiological and ecological functions, including defense, stress resistance, and communication (Guo et al., 2022). Beyond their roles within natural plant producers, these compounds hold significant importance in human life and society. Phenylpropanoids, as notable constituents of plant natural products, exhibit a wide range of industrial applications across diverse sectors such as pharmaceuticals, fragrances, flavors, cosmetics, agrochemicals, and polymer industries (Cesarino et al., 2022).

Phenylpropanoids, however, are typically found in plants at low concentrations, thereby requiring substantial amounts of biomass for economically feasible production (Hostetler et al., 2017; Rodriguez et al., 2017). Moreover, the levels of these compounds can vary due to environmental factors, plant species, and tissue types (Dong and Lin, 2021). The purification of individual compounds from processed biomass is also challenging due to the presence of related products with similar structures (Jiang et al., 2005). Chemical synthesis of phenylpropanoids, especially for complex compounds, presents significant challenges and often necessitates

biotransformation processes (Chemler and Koffas, 2008). In addition, the use of toxic solvents and extreme reaction conditions can impact yield and scalability. In this regard, regulations restrict the use of chemically produced food additives, while there is also a growing preference for natural sources (European Parliament, 2008; Cortez et al., 2017). Consequently, chemical synthesis is not considered a practical alternative for their production.

Alternatively, microbial production of phenylpropanoids in cell factories is gaining momentum due to its numerous advantages, including scalability, cost-effectiveness, and sustainability (Cravens et al., 2019; Romero-Suarez et al., 2022). The common precursor for all subfamilies of phenylpropanoids, including stilbenoids, flavonoids or anthocyanins, is *p*-coumaric acid (Vogt, 2010). Prototroph microorganisms can biosynthesize *p*-coumaric acid through either a one-step or two-step enzymatic process. This is achieved by heterologously expressing ammonia lyases for the aromatic amino acids (AAA) L-tyrosine and L-phenylalanine. In the case of the L-phenylalanine route, a P450 enzyme, along with the corresponding cytochrome P450 reductase and cytochrome b_5, are also involved (Li et al., 2015, 2016; Liu et al., 2019). While *Escherichia coli* has been engineered for *p*-coumaric acid production, typically the baker's yeast *Saccharomyces cerevisiae* is a preferred production host due to its eukaryotic architecture that facilitates the expression of plant enzymes (Wang et al., 2015; Ro et al., 2006; Brown et al., 2015; Siddiqui et al., 2012).

There have been great efforts in developing targeted rational engineering strategies to rewire metabolic pathways toward high *p*-coumaric acid production in *S. cerevisiae*. Most of the strategies are based on the overexpression, deletion or fine-tuning of the expression of genes involved in the glycolysis, pentose phosphate, shikimate, AAA biosynthesis and degradation (Ehrlich) pathways (Lee and Wendisch, 2017; Averesch and Krömer, 2018; Huccetogullari et al., 2019; Cao et al., 2020). These strategies have been also successful in the *de novo* high-titer production of other AAA-derived compounds such as resveratrol and 2-phenylethanol (Li et al., 2015, 2016; Hassing et al., 2019).

In this study, we employ rational engineering strategies derived from existing literature to develop multiple *S. cerevisiae* platform strains for *p*-coumaric acid production. Subsequently, we conduct a physiological characterization of these

constructed strains. This preliminary step paves the way for an ongoing project, which aims to perform a multi-omics characterization of these strains.

Materials and methods

Strain construction and DNA materials

The yeast strain CEN.PK113-7D, containing the episomal vector pCfB2312 for Cas9 protein expression, served as the parent strain in this study (Milne et al., 2020). For Cas9 selection, all constructed strains (Table S1) were cultivated with 200 mg/L G418 (Sigma-Aldrich), except for production cultures. Gene knock in/out was performed using the EasyClone-MarkerFree toolbox (Jessop-Fabre et al., 2016). Yeast strains were transformed using the standard lithium acetate method (Gietz and Schiestl, 2007) and plated on YPD medium supplemented with antibiotics: nourseothricin (Jena Bioscience GmbH) at 100 mg/L and G418 (as mentioned earlier). Colony PCR with RedTaq® DNA polymerase (VWR, Belgium) was performed to confirm the correct integration of DNA fragments or gene deletions. Integrative and gRNA plasmids are listed in Table S2. Cloning was conducted using Uracil Specific Excision Reagent (USER®, New England Biolabs), as previously described (Babaei et al., 2020). BioBricks and primers used for their amplification and cloning are listed in Tables S3-S4. PCR were performed using USER-compatible Phusion U polymerase (Thermo Fisher Scientific). Fragments were purified using the NucleoSpin® Gel and PCR Clean-up kit (Macherey-Nagel). After USER treatment, the assembled vectors were transformed into competent *Escherichia coli* DH5α cells through heat shock at 42 °C for 45 seconds. The cultivations in *E. coli* were carried out at 37 °C in Lysogeny Broth (LB) broth or agar-plate supplemented with 100 mg/L ampicillin as selection marker. The correct assembly of integrative vectors was initially tested using colony PCR with 2xOneTaq® Master Mix (New England Biolabs) and later verified by sequencing (Mix2Seq kits, Eurofins Genomics, Germany).

The synthetic genes used for *p*-coumaric acid production were ordered as GeneStrings from GeneArt (Thermo Fisher Scientific) in codon-optimized variants for *S. cerevisiae*. The sequences of these genes is summarized in Table S5.

Cultivation of *S. cerevisiae* in small-scale in simulated fed-batch

For the production of *p*-coumaric under glucose-limited conditions, the strains were cultivated overnight in 5 mL YPD medium in 13-mL tubes at 30 °C and 250 rpm. The following day, adequate amount of cells were inoculated to 20 mL mineral medium in 120 mL unbaffled shake flasks, targeting an initial OD_{600} 0.1. The mineral medium composition is, per L: 7.5 g $(NH_4)_2SO4$, 14.4 g KH_2PO_4, 0.5 g $MgSO_4.7H_2O$, 2 mL trace metal (3.0 g/L $FeSO_4 \cdot 7H_2O$, 4.5 g/L $ZnSO_4 \cdot 7H_2O$, 4.5 g/L $CaCl_2 \cdot 2H_2O$, 0.84 g/L $MnCl_2 \cdot 2H_2O$, 0.3 g/L $CoCl_2 \cdot 6H_2O$, 0.3 g/L $CuSO_4 \cdot 5H_2O$, 0.4 g/L $Na_2MoO_4 \cdot 2H_2O$, 1.0 g/L H_3BO_3, 0.1 g/L KI, and 19.0 g/L $Na_2EDTA \cdot 2H_2O$), and 1 mL vitamin solutions (0.05 g/L D-biotin, 1.0 g/L D-pantothenic acid hemicalcium salt, 1.0 g/L thiamin–HCl, 1.0 g/L pyridoxin–HCl, 1.0 g/L nicotinic acid, 0.2 g/L *p*-aminobenzoic acid, and 25.0 g/L myo-inositol). To mimic fed-batch mode, six tablets of FeedBeads (SMFB08001, Kuhner Shaker, Basel, Switzerland) was used in each culture. The production experiments were run at 30 °C and 200 rpm. After 96 h, the culture broth was analyzed for cell dry weight (CDW) and metabolite titer.

Cultivation of *S. cerevisiae* in microfluidic bioreactor in fed-batch mode and physiological characterization

For seed train, strains from cryostocks were streaked out in YPD plates and grown for 48 hours at 30 °C. For each of the strains, a single colony was inoculated into 1 mL of mineral medium containing 6 g/L of glucose and cultivated for 10 hours and 250 rpm. An adequate amount of cells to target an initial OD_{600} = 0.1 was transferred to 1 mL of mineral medium with 4 g/L of glucose and incubated for 12 hours. Similarly, an inoculum corresponding to an initial OD_{600} = 0.1 was transferred to 8 wells per strain in the actual fed-batch fermentation plate.

The fed-batch fermentation was carried out in the microfluidic bioreactor Biolector Pro (m2p labs). A 32 wells microfluidic flower plate (MTP-MF32C-BOH2) was employed in the cultivation, filled with 800 µL of batch mineral medium per well. The glucose concentration in the batch media was 1.02 g/L for strain ST9402, 1.07 g/L for strain ST10248 and ST10283, and 1.29 g/L for ST10284. These glucose concentrations were determined in small-scale batch cultivations in order to match biomass concentrations for all strains at the end of the batch phase. The feed medium contained

93.75 g/L glucose for all strains, while the rest of medium components were the same as in batch mineral medium, but at 10-fold higher concentration. The reservoir wells were filled with 1800 µL of feed medium, each of them feeding 4 cultivation wells. Feeding was triggered after 14 h for strain ST9402, ST10248 and ST10283, while for ST10284 it started after 18 h, based on batch phase durations previously determined in small scale. The feeding profile was exponential, with an initial feeding rate of 1.23 µL/h following an exponential increase of 0.1 h^{-1}, according to the equation $F(t) = 1.23 \times e^{0.1t}$. The temperature was set at 30 °C, stirring at 1,300 rpm, 35% oxygen (enriched air), and humidity of 85%. pH was left uncontrolled during the whole cultivation.

For each strain, four samples were taken at the end of the feeding phase, covering a span of 7 hours. In each sampling round, two wells per strain were sampled, withdrawing 300 µL of broth. Wells were only sampled once as the volume withdrawn was significant and Biolector Pro does not adjust the feeding profile when samples are taken. Therefore, the samples from the four different time points are derived from two different wells each time. Samples were processed for OD_{600} measurement and quantification of *p*-coumaric acid, glucose, ethanol, glycerol, acetate, pyruvate, 2-ketoglutarate and succinate.

The biomass concentration in samples was determined from the OD_{600} measurements following the equation $CDW\ (g/L) = OD_{600}/0.1199$. Growth rates were determined by a linear fit of the natural logarithm of biomass against time. Yields were calculated as a linear fit of biomass against substrate or product. Specific production and consumption rates were calculated from the yields and growth rates. Errors are reported as the uncertainty associated to the slope of the linear fits or the expected uncertainties in the case of consumption and production rates.

Metabolite extraction and quantification

For the extraction of *p*-coumaric acid, 800 µL of culture was mixed 1:1 (v:v) with absolute ethanol supplemented with 0.01% w/v 3,5-di-tert-4-butylhydroxyltoluene (BHT). The mixture was then shaken vigorously using the Precellys T 24 homogenizer (Bertin Corp.) at 6500 rpm for 45 sec. The samples were then centrifuged for 30 min at 21,000 g, and the supernatant was used for metabolite quantification.

The authentic standard for *p*-coumaric acid was purchased from Sigma Aldrich with certified purity >96%. Quantification of *p*-coumaric acid was performed with Dionex Ultimate 3000 HPLC (Thermo Fisher Scientific), equipped with a Zorbax® C18 4.6 x 100 mm, particle size 3.5 µm column. The column oven temperature was maintained at 30 °C, with a flow rate of 1 mL/min and a sample injection volume of 10 µL. The HPLC method employed a mobile phase consisting of solvent A (0.1% formic acid) and solvent B (acetonitrile). Initially, the solvent composition was set at A = 80.0% and B = 20.0% until 1 min. Subsequently, a linear gradient was applied, gradually changing the solvent composition to A = 60.0% and B = 40.0% at 2.0 min. These conditions were maintained until 5.5 min. From 5.5 to 7.5 min, the solvent composition was linearly increased until A = 10.0% and B = 90.0%. This composition was maintained for 1.5 min (7.5 – 9 min), after which the solvent composition was returned to the initial conditions (A = 80.0%, B = 20.0%) at 9.2 min and remained constant until the end of the run (9.2-12 min).

For detection of *p*-coumaric acid, the retention time was 3.21 min, and the absorbance was measured at 310 nm. Peaks corresponding to the target compound were identified by comparison to prepared standards. Compound quantification was performed using the external standard calibration method, with peak area used for quantification. Analysis of the HPLC results was conducted using Chromeleon 7 software (Thermo Fisher Scientific).

Glucose, ethanol, glycerol, acetate, pyruvate, 2-ketoglutarate, and succinate were quantified in the supernatants of the cultivations. After centrifugation for 5 minutes at 21,000 g, the HPLC quantification method described previously (Sáez-Sáez et al., 2020) was employed.

Results

Establishing *p*-coumaric acid production in *S. cerevisiae*

As the initial step of this study, we incorporated the most promising rational engineering targets derived from literature to generate several platform strains with increased flux towards *p*-coumaric acid production (Figure 1a). To begin the strain construction, we first engineered the parent strain ST7574 by deleting the *ARO10* and *PDC5* genes (Koopman et al., 2012; Rodriguez et al., 2015). These modifications aimed

to block the degradation route for AAA. As a result, we obtained ST9402, onto which we introduced the heterologous pathway from L-tyrosine to *p*-coumaric acid by integrating *Flavobacterium johnsoniae*'s tyrosine ammonia-lyase (FjTAL) and *E. coli*'s heterologous shikimate kinase (EcAroL) (Rodriguez et al., 2015). This resulted in the strain ST10248, which reached a *p*-coumaric acid titer of 40.43 mg/L under glucose-limited conditions (Figure 1b).

The subsequent step towards improving the *p*-coumaric acid strain involved increasing and redirecting carbon flux towards the AAA pathway. This was achieved by expressing additional copies of the pathway genes *ARO1* (pentafunctional aromatic protein), *ARO2* (chorismate synthase), *ARO3* (DAHP synthase), *PHA2* (prephenate dehydrogenase), and incorporating the feedback-insensitive mutants *ARO4*^{K229L} and *ARO7*^{G141S}. These genetic modifications resulted in strain ST10283, which exhibited nearly three times higher *p*-coumaric acid production compared to its parent strain (ST10248), reaching a titer of 119.57 mg/L in simulated fed-batch cultivation.

Given the reported higher efficiency of *p*-coumaric acid production from L-phenylalanine compared to L-tyrosine (Liu et al., 2019), we incorporated the PAL pathway as well. This involved expressing phenylalanine ammonia lyase (AtPAL2), cinnamic acid hydroxylase (AtC4H), cytochrome P450 reductase (AtATR2) from *Arabidopsis thaliana*, and a cytochrome b_5 (*CYB5*) from *S. cerevisiae*. The combination of the PAL and TAL pathways synergistically increased *p*-coumaric acid titers. Furthermore, a previous metabolic flux analysis study revealed a significant differences in carbon flux between the two precursors of the shikimate pathway, with erythrose-4-phosphate (E4P) being 10 times lower than phosphoenolpyruvate (PEP) (Suástegui et al., 2016). To overcome this limitation, we implemented a strategy proposed by Liu et al., introducing a heterologous phosphoketolase enzyme from *Bifidobacterium breve* (Bbxfpk) (Bergman et al., 2019) to split fructose-6-phosphate into E4P and acetyl-phosphate (Liu et al., 2019). To mitigate the increase in acetate formation and growth inhibition caused by this phenotype (Meadows et al., 2016), we also deleted the native phosphatase GPP1 (glycerol-1-phosphatase) to prevent the conversion of acetyl-phosphate into acetate. Finally, to overcome the regulation of the native yeast prephenate dehydrogenase (Tyr1p) by high tyrosine concentrations, we expressed a variant from *Medicago truncatula* (MtPDH1). The resulting strain,

ST10284, exhibited the highest *p*-coumaric acid titer (578.56 mg/L) in a 30 g/L glucose-limited cultivation over 96 hours (Figure 2).

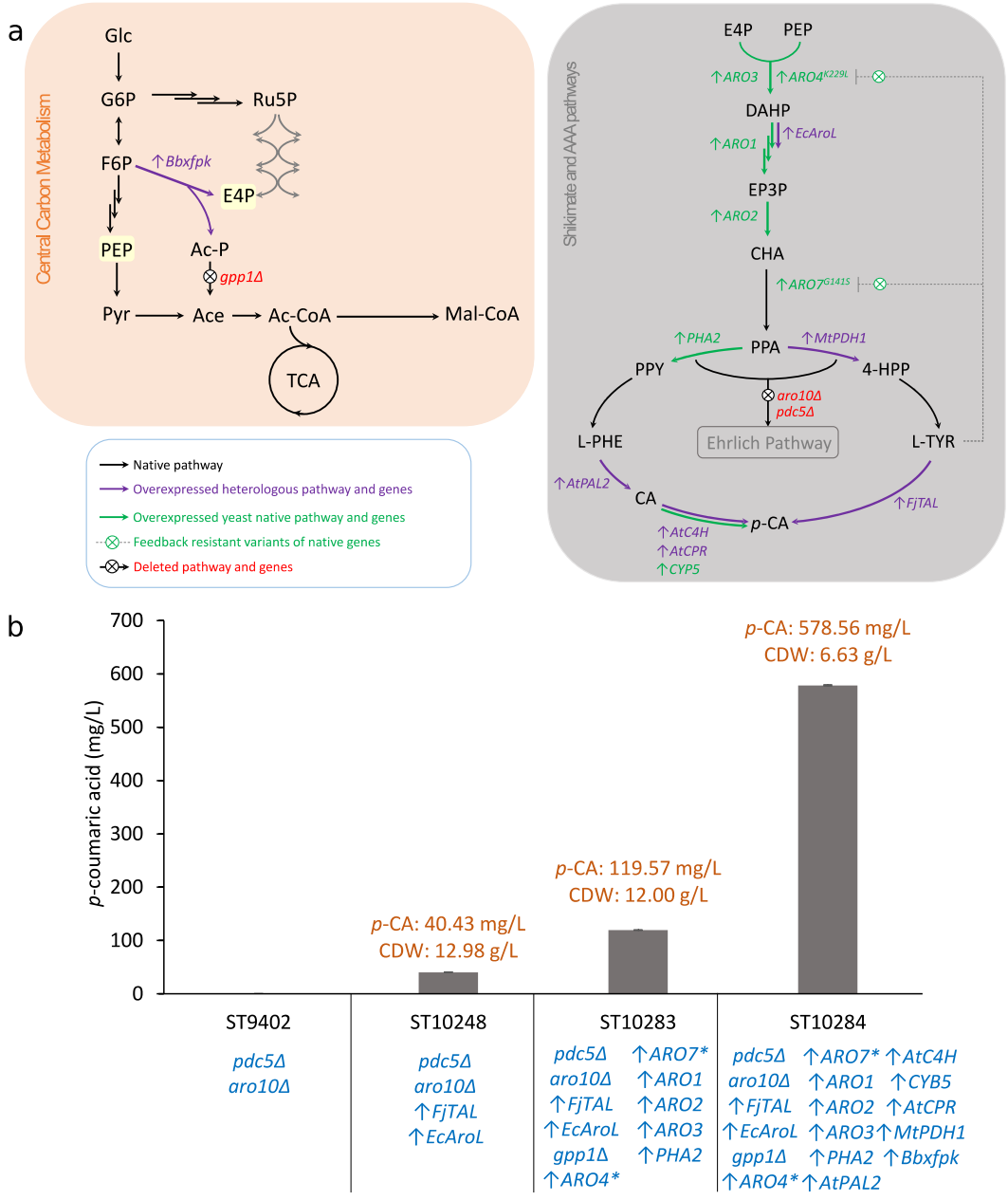

Figure 1. Strain engineering strategies for the production of *p*-coumaric acid in *S. cerevisiae*. a) Overview of pathways and targets engineered. Glc: glucose, G6P: glucose 6-phosphate, F6P: fructose 6-phosphate, PEP: phosphoenolpyruvate, Pyr: pyruvate, Ru5P: ribulose 5-phosphate, E4P: erythrose 4-phosphate, Ac-P: acetyl-phosphate, Ace: acetate, Ac-CoA: acetyl-CoA, Mal-CoA: malonyl-CoA, DAHP: 3-Deoxy-D-arabino-heptulosonic acid 7-phosphate, 5-enolpyruvylshikimate-3-phosphate, CHA: chorismic acid, PPA: prephenic acid, PPY: phenylpyruvic acid, L-PHE: L-phenylalanine, CA: cinnamic acid, *p*-CA: *p*-coumaric acid; 4-HPP: 4-hydroxyphenylpyruvic acid; L-TYR: L-tyrosine. b) Titers of *p*-coumaric acid and

biomass measurements in engineered *S. cerevisiae* strains after 96 hours cultivation in simulated fed-batch medium.

Physiological characterization of *p*-coumaric acid strains

The different constructed strains produced different levels of *p*-coumaric acid, showing incremental production titers and seemingly reduced biomass formation in simulated fed-batch cultivations over successive strain engineering rounds. To gain further insights into these strains, we opted to cultivate them under exponential fed-batch conditions using a microfluidic bioreactor system and assess basic physiological parameters. Using Biolector Pro, we selected a feeding profile that allows for sustained growth over 5 generations without encountering oxygen limitations, while simultaneously preventing the overflow metabolism. These conditions are essential to achieve a pseudo-steady state in the strains, enabling us to sample for multi-omics characterization. Additionally, they ensure the dilution of ^{13}C-unlabeled biomass, a crucial requirement for conducting fluxomics analysis.

In general, we observed a similar behavior between the different strains (Table 1). However, it was in the highest-producing strain, ST10284, where we observed a notable decrease in biomass yield compared to the non-producing control strain ST9402. Additionally, strain ST10284 exhibited a higher specific glucose uptake rate and a significant increase in specific *p*-coumaric acid yield compared to the other two producing strains. An interesting observation was the production of glycerol in the non-producing control strain ST9402, while the top-producing strain ST10284 showed some ethanol formation.

Table 1. Physiological parameters of shikimate chassis strains. n.a. not available (ST9402 is a non-producing control strain). *: production of metabolites detected at concentrations close to the detection limit at some time points, but not following a linear pattern.

Parameter	ST9402	ST10248	ST10283	ST10284
μ (h^{-1})	0.101 ± 0.003	0.099 ± 0.010	0.105 ± 0.010	0.097 ± 0.004
Y_{xs} (gDW/mmol Glucose)	0.097 ± 0.003	0.094 ± 0.008	0.097 ± 0.009	0.085 ± 0.003
q_s (mmol Glucose/gDW/h)	- 1.039 ± 0.040	-1.048 ± 0.137	-1.080 ± 0.147	-1.142 ± 0.058
q_p (mmol *p*-CA/gDW/h)	n.a.	0.001 ± 0.000	0.004 ± 0.000	0.085 ± 0.004
q_{EtOH} (mmol EtOH/gDW/h)	*	*	*	0.007 ± 0.002
$q_{Glycerol}$ (mmol Glycerol/gDW/h)	0.018 ± 0.002	*	*	*

Discussion and conclusions

The results hereby described represent the initial findings of an ongoing project aiming at a deeper characterization at the multi-omics level of several *p*-coumaric acid producing strains.

The strain construction revealed that *p*-coumaric acid production from L-tyrosine is limited despite overexpression of multiple genes from the shikimate pathway. However, the incorporation of the heterologous pathway for production from L-phenylalanine exhibited a synergistic effect. Additionally, the heterologous expressions of a phosphoketolase and a prephenate dehydrogenase played a crucial role in balancing the precursor supply and relieving enzymatic regulation. These findings align with previous reports on *p*-coumaric acid production in *S. cerevisiae* and validate the effectiveness of the employed genetic engineering strategies. Future enhancements of these strains could involve the use of inducible promoters or fine-tuning the expression of specific genes to further optimize production (Liu et al., 2019).

The physiological characterization of the strains revealed notable changes, including increased specific glucose uptake rates and reduced biomass yields, associated with *p*-coumaric acid production in the extensively engineered strain ST10284. These trends align with previous findings observed in a *S. cerevisiae* strain producing the stilbenoid resveratrol, a *p*-coumaric acid-derived product (Vos et al., 2015). It is important to note that the exo-metabolomics method utilized in this study did not account for other potential by-products, such as phloretic acid, which may be present in the broth due to the promiscuous activity of native enzymes on the heterologous pathway (Lehka et al., 2017). Additionally, the absence of measurements for CO_2 production and O_2 consumption in the Biolector Pro system limits a comprehensive understanding of the metabolic activity. Nevertheless, these simple physiological parameters proved sufficient for calibrating kinetic genome-scale metabolic models in an ongoing scientific collaboration aimed at validating model-guided strain designs. As the next steps of this project, we plan to transition to ambr250® bioreactor cultivations and perform multi-omics characterization. The acquired data will provide further insights into strain characterization and aid in generating new hypotheses to drive further improvements in the strains.

References

Averesch, N.J.H., Krömer, J.O., 2018. Metabolic Engineering of the Shikimate Pathway for Production of Aromatics and Derived Compounds—Present and Future Strain Construction Strategies. Front. Bioeng. Biotechnol. 6, 32. https://doi.org/10.3389/fbioe.2018.00032

Babaei, M., Borja Zamfir, G.M., Chen, X., Christensen, H.B., Kristensen, M., Nielsen, J., Borodina, I., 2020. Metabolic Engineering of *Saccharomyces cerevisiae* for Rosmarinic Acid Production. ACS Synth. Biol. 9, 1978–1988. https://doi.org/10.1021/acssynbio.0c00048

Bergman, A., Hellgren, J., Moritz, T., Siewers, V., Nielsen, J., Chen, Y., 2019. Heterologous phosphoketolase expression redirects flux towards acetate, perturbs sugar phosphate pools and increases respiratory demand in Saccharomyces cerevisiae. Microb. Cell Factories 18, 25. https://doi.org/10.1186/s12934-019-1072-6

Brown, S., Clastre, M., Courdavault, V., O'Connor, S.E., 2015. De novo production of the plant-derived alkaloid strictosidine in yeast. Proc. Natl. Acad. Sci. 112, 3205–3210. https://doi.org/10.1073/pnas.1423555112

Cao, M., Gao, M., Suástegui, M., Mei, Y., Shao, Z., 2020. Building microbial factories for the production of aromatic amino acid pathway derivatives: From commodity chemicals to plant-sourced natural products. Metab. Eng. 58, 94–132. https://doi.org/10.1016/j.ymben.2019.08.008

Cesarino, I., Eudes, A., Urbanowicz, B., Xie, M., 2022. Editorial: Phenylpropanoid Systems Biology and Biotechnology. Front. Plant Sci. 13, 866164. https://doi.org/10.3389/fpls.2022.866164

Chemler, J.A., Koffas, M.A., 2008. Metabolic engineering for plant natural product biosynthesis in microbes. Curr. Opin. Biotechnol. 19, 597–605. https://doi.org/10.1016/j.copbio.2008.10.011

Cortez, R., Luna-Vital, D.A., Margulis, D., Gonzalez de Mejia, E., 2017. Natural Pigments: Stabilization Methods of Anthocyanins for Food Applications. Compr. Rev. Food Sci. Food Saf. 16, 180–198. https://doi.org/10.1111/1541-4337.12244

Cravens, A., Payne, J., Smolke, C.D., 2019. Synthetic biology strategies for microbial biosynthesis of plant natural products. Nat. Commun. 10, 2142. https://doi.org/10.1038/s41467-019-09848-w

Dong, N., Lin, H., 2021. Contribution of phenylpropanoid metabolism to plant development and plant–environment interactions. J. Integr. Plant Biol. 63, 180–209. https://doi.org/10.1111/jipb.13054

European Parliament, 2008. Regulation (EC) No 1334/2008 of the European Parliament and of the Council of 16 December 2008 on flavourings and certain food ingredients with flavouring properties for use in and on foods and amending Council Regulation (EEC) No 1601/91, Regulations (EC) No 2232/96 and (EC) No 110/2008 and Directive 2000/13/EC (Text with EEA relevance), OJ L.

Gietz, R.D., Schiestl, R.H., 2007. High-efficiency yeast transformation using the LiAc/SS carrier DNA/PEG method. Nat. Protoc. 2, 31–34. https://doi.org/10.1038/nprot.2007.13

Guo, L., Yao, H., Chen, W., Wang, X., Ye, P., Xu, Z., Zhang, S., Wu, H., 2022. Natural products of medicinal plants: biosynthesis and bioengineering in post-genomic era. Hortic. Res. 9, uhac223. https://doi.org/10.1093/hr/uhac223

Hassing, E.-J., de Groot, P.A., Marquenie, V.R., Pronk, J.T., Daran, J.-M.G., 2019. Connecting central carbon and aromatic amino acid metabolisms to improve de novo 2-phenylethanol production in Saccharomyces cerevisiae. Metab. Eng. 56, 165–180. https://doi.org/10.1016/j.ymben.2019.09.011

Hostetler, G.L., Ralston, R.A., Schwartz, S.J., 2017. Flavones: Food Sources, Bioavailability, Metabolism, and Bioactivity. Adv. Nutr. 8, 423–435. https://doi.org/10.3945/an.116.012948

Huccetogullari, D., Luo, Z.W., Lee, S.Y., 2019. Metabolic engineering of microorganisms for production of aromatic compounds. Microb. Cell Factories 18, 41. https://doi.org/10.1186/s12934-019-1090-4

Jessop-Fabre, M.M., Jakočiūnas, T., Stovicek, V., Dai, Z., Jensen, M.K., Keasling, J.D., Borodina, I., 2016. EasyClone-MarkerFree: A vector toolkit for marker-less integration of genes into *Saccharomyces cerevisiae* via CRISPR-Cas9. Biotechnol. J. 11, 1110–1117. https://doi.org/10.1002/biot.201600147

Jiang, H., Wood, K.V., Morgan, J.A., 2005. Metabolic Engineering of the Phenylpropanoid Pathway in *Saccharomyces cerevisiae*. Appl. Environ. Microbiol. 71, 2962–2969. https://doi.org/10.1128/AEM.71.6.2962-2969.2005

Koopman, F., Beekwilder, J., Crimi, B., van Houwelingen, A., Hall, R.D., Bosch, D., van Maris, A.J., Pronk, J.T., Daran, J.-M., 2012. De novo production of the flavonoid naringenin in engineered Saccharomyces cerevisiae. Microb. Cell Factories 11, 155. https://doi.org/10.1186/1475-2859-11-155

Lee, J.-H., Wendisch, V.F., 2017. Biotechnological production of aromatic compounds of the extended shikimate pathway from renewable biomass. J. Biotechnol. 257, 211–221. https://doi.org/10.1016/j.jbiotec.2016.11.016

Lehka, B.J., Eichenberger, M., Bjørn-Yoshimoto, W.E., Vanegas, K.G., Buijs, N., Jensen, N.B., Dyekjær, J.D., Jenssen, H., Simon, E., Naesby, M., 2017. Improving heterologous production of phenylpropanoids in *Saccharomyces cerevisiae* by tackling an unwanted side reaction of Tsc13, an endogenous double bond reductase. FEMS Yeast Res. fox004. https://doi.org/10.1093/femsyr/fox004

Li, M., Kildegaard, K.R., Chen, Y., Rodriguez, A., Borodina, I., Nielsen, J., 2015. De novo production of resveratrol from glucose or ethanol by engineered Saccharomyces cerevisiae. Metab. Eng. 32, 1–11. https://doi.org/10.1016/j.ymben.2015.08.007

Li, M., Schneider, K., Kristensen, M., Borodina, I., Nielsen, J., 2016. Engineering yeast for high-level production of stilbenoid antioxidants. Sci. Rep. 6, 36827. https://doi.org/10.1038/srep36827

Liu, Q., Yu, T., Li, X., Chen, Yu, Campbell, K., Nielsen, J., Chen, Yun, 2019. Rewiring carbon metabolism in yeast for high level production of aromatic chemicals. Nat. Commun. 10, 1–13. https://doi.org/10.1038/s41467-019-12961-5

Meadows, A.L., Hawkins, K.M., Tsegaye, Y., Antipov, E., Kim, Y., Raetz, L., Dahl, R.H., Tai, A., Mahatdejkul-Meadows, T., Xu, L., Zhao, L., Dasika, M.S., Murarka, A., Lenihan, J., Eng, D., Leng, J.S., Liu, C.-L., Wenger, J.W., Jiang, H., Chao, L., Westfall, P., Lai, J., Ganesan, S., Jackson, P., Mans, R., Platt, D., Reeves, C.D., Saija, P.R., Wichmann, G., Holmes, V.F., Benjamin, K., Hill, P.W., Gardner, T.S., Tsong, A.E., 2016. Rewriting yeast central carbon metabolism for industrial isoprenoid production. Nature 537, 694–697. https://doi.org/10.1038/nature19769

Milne, N., Tramontin, L.R.R., Borodina, I., 2020. A teaching protocol demonstrating the use of EasyClone and CRISPR/Cas9 for metabolic engineering of Saccharomyces cerevisiae and Yarrowia lipolytica. FEMS Yeast Res. 20. https://doi.org/10.1093/femsyr/foz062

Ro, D.-K., Paradise, E.M., Ouellet, M., Fisher, K.J., Newman, K.L., Ndungu, J.M., Ho, K.A., Eachus, R.A., Ham, T.S., Kirby, J., Chang, M.C.Y., Withers, S.T., Shiba, Y., Sarpong, R., Keasling, J.D., 2006. Production of the antimalarial drug precursor artemisinic acid in engineered yeast. Nature 440, 940–943. https://doi.org/10.1038/nature04640

Rodriguez, A., Kildegaard, K.R., Li, M., Borodina, I., Nielsen, J., 2015. Establishment of a yeast platform strain for production of p-coumaric acid through metabolic engineering of aromatic amino acid biosynthesis. Metab. Eng. 31, 181–188. https://doi.org/10.1016/j.ymben.2015.08.003

Rodriguez, A., Strucko, T., Stahlhut, S.G., Kristensen, M., Svenssen, D.K., Forster, J., Nielsen, J., Borodina, I., 2017. Metabolic engineering of yeast for fermentative production of flavonoids. Bioresour. Technol. 245, 1645–1654. https://doi.org/10.1016/j.biortech.2017.06.043

Romero-Suarez, D., Keasling, J.D., Jensen, M.K., 2022. Supplying plant natural products by yeast cell factories. Curr. Opin. Green Sustain. Chem. 33, 100567. https://doi.org/10.1016/j.cogsc.2021.100567

Sáez-Sáez, J., Wang, G., Marella, E.R., Sudarsan, S., Cernuda Pastor, M., Borodina, I., 2020. Engineering the oleaginous yeast Yarrowia lipolytica for high-level resveratrol production. Metab. Eng. 62, 51–61. https://doi.org/10.1016/j.ymben.2020.08.009

Siddiqui, M.S., Thodey, K., Trenchard, I., Smolke, C.D., 2012. Advancing secondary metabolite biosynthesis in yeast with synthetic biology tools. FEMS Yeast Res. 12, 144–170. https://doi.org/10.1111/j.1567-1364.2011.00774.x

Suástegui, M., Guo, W., Feng, X., Shao, Z., 2016. Investigating strain dependency in the production of aromatic compounds in Saccharomyces cerevisiae. Biotechnol. Bioeng. 113, 2676–2685. https://doi.org/10.1002/bit.26037

Vogt, T., 2010. Phenylpropanoid Biosynthesis. Mol. Plant 3, 2–20. https://doi.org/10.1093/mp/ssp106

Vos, T., de la Torre Cortés, P., van Gulik, W.M., Pronk, J.T., Daran-Lapujade, P., 2015. Growth-rate dependency of de novo resveratrolproduction in chemostat cultures of an engineered Saccharomycescerevisiae strain. Microb. Cell Factories 14, 133. https://doi.org/10.1186/s12934-015-0321-6

Wang, S., Zhang, S., Xiao, A., Rasmussen, M., Skidmore, C., Zhan, J., 2015. Metabolic engineering of Escherichia coli for the biosynthesis of various phenylpropanoid derivatives. Metab. Eng. 29, 153–159. https://doi.org/10.1016/j.ymben.2015.03.011

Understanding the physiology of *p*-coumaric acid production in *Saccharomyces cerevisiae*

Supporting information

Table S1. List of strains used in this study.

Name	Parent	Added DNA Element(s)	Relevant Genotype	Source
CEN.PK 113-7D			MATa *MAL2-8c SUC2 URA3 HIS3 LEU2 TRP1*	(Entian and Kötter, 2007)
ST7574	CEN.PK 113-7D	pCfB2312	CEN.PK113-7D ↑*Cas9_KanMX*	(Milne et al., 2020)
ST9402	ST7574	PR-17720, PR-16208	CEN.PK113-7D ↑*Cas9_KanMX Daro10 Dpdc5*	This study
ST10248	ST9402	pCfB10022	CEN.PK113-7D ↑*Cas9, Δpdc5, Δaro10, ↑FjTAL, ↑EcAroL*	This study
ST10273	ST10248	PR-27237	CEN.PK113-7D ↑*Cas9, Δpdc5, Δaro10, ↑FjTAL, ↑EcAroL, Δgpp1*	This study
ST10283	ST10273	pCfB9114, pCfB10023, pCfB10026	CEN.PK113-7D ↑*Cas9, Δpdc5, Δaro10, ↑FjTAL, ↑EcAroL, Δgpp1, ↑Aro4^{K229L}, ↑Aro7^{G141S}, ↑Aro1, ↑Aro2, ↑Aro3, ↑PHA2*	This study
ST10284	ST10283	pCfB10098, pCfB9265, pCfB10108	CEN.PK113-7D ↑*Cas9, Δpdc5, Δaro10, ↑FjTAL, ↑EcAroL, Δgpp1, ↑Aro4^{K229L}, ↑Aro7^{G141S}, ↑Aro1, ↑Aro2, ↑Aro3, ↑PHA2, ↑AtPAL2, ↑AtC4H, ↑ScCYB5, ↑AtCPR, ↑MtPDH1, ↑Bbxfpk*	This study

Table S2. List of plasmids used in this study.

Plasmid	Parent vector	BioBricks	Source
Episomal plasmids			
pCfB2312(CEN/ARS_Cas9_kanMX)			(Stovicek et al., 2015)
gRNA plasmids for targeting genomic integration sites by CRISPR-Cas9			
pCfB3043 (p-gRNA XI-1)			(Jessop-Fabre et al., 2016)
pCfB10024 (NatMX_gRNA_GPP1-KO)	pCfB3043		This study
pCfB3052 (p-gRNA X-4 XI-3 XII-5)			(Jessop-Fabre et al., 2016)
pCfB3053 (p-gRNA X-2 XI-5 XII-4)			(Jessop-Fabre et al., 2016)
Plasmids for integration into yeast genome			
pCfB9114(X-4<-ScAro4pm-ScAro7pm->)			(Babaei et al., 2020)
pCfB9265(X-2_AtPAL2-AtC4H)	pCfB2899	BB0010, BB4261, BB4262	This study
pCfB10022 (XI-1_FjTAL-EcAroL)	pCfB3036	BB0010, BB380, BB4092	This study
pCfB10023 (XI-3_Aro1-Aro2)	pCfB2904	BB0010, BB4640, BB4641	This study
pCfB10026 (XII-5_Aro3-PHA2)	pCfB2909	BB0010, BB4642, BB4643	This study
pCfB10098 (XII-4_MtPDH1-Bbxfpk)	pCfB3040	BB0010, BB4683, BB4684	This study
pCfB10108 (XI-5_ScCYB5-AtCPR)	pCfB3037	BB0010, BB4263, BB4210	This study
Backbone plasmids for EasyClone-MarkerFree plasmid assembly			
pCfB2899 (X-2-MarkerFree)			(Jessop-Fabre et al., 2016)
pCfB2904 (XI-3-MarkerFree)			(Jessop-Fabre et al., 2016)
pCfB2909 (XII-5-MarkerFree)			(Jessop-Fabre et al., 2016)
pCfB3035 (X-4-MarkerFree)			(Jessop-Fabre et al., 2016)
pCfB3036 (XI-1-MarkerFree)			(Jessop-Fabre et al., 2016)
pCfB3037 (XI-5-MarkerFree)			(Jessop-Fabre et al., 2016)
pCfB3040 (XII-4-MarkerFree)			(Jessop-Fabre et al., 2016)
Templates for PCR amplification			
pSP-G1			(Partow et al., 2010)

Table S3. List of biobricks used in this study.

BioBrick	PCR template	Forward primer	Reverse primer
BB0010 (<-TEF1:PGK1->)	pSP-G1	PR-1750	PR-8
BB0380 (FjTAL<-)		PR-1691	PR-1692
BB4092 (EcAroL_U2)		PR-6785	PR-6786
BB4210 (ScCYB5_U1)		PR-25300	PR-25301
BB4261 (AtPAL2_U1)		PR-1588	PR-1589
BB4262 (AtC4H_U2)		PR-1546	PR-1547
BB4263 (AtATR2_U2)		PR-1554	PR-1555
BB4640 (ScAro1_U1)		PR-2173	PR-2174
BB4641 (ScAro2_U2)		PR-2179	PR-2180
BB4642 (ScAro3_U1)		PR-14640	PR-14641
BB4643 (PHA2_U2)		PR-27230	PR-27231
BB4683 (MtPDH1_U1)	Synthetic gene	PR-27232	PR-27233
BB4684 (Bbxfpk_U2)	Synthetic gene	PR-27234	PR-27235

Table S4. List of primers used in this study.

PR-10277(gRNArev)	GATCATTTATCTTTCACTGCGGAGAAG
PR-1388(aro4_U1_fw (ID1388))	AGTGCAGGU AAAACA ATGAGTGAATCTCCAATGTTCG
PR-1389(aro4_U1_rv (ID1389))	CGTGCGAU TCA TTTCTTGTTAACTTCTCTTCTTTG
PR-1390(aro7_U2_fw (ID1390))	ATCTGTCAU AAAACA ATGGATTTCACAAAACCAGAAAC
PR-1391(aro7_U2_rv (ID1391))	CACGCGAU TCA CTCTTCCAACCTTCTTAGCAAG
PR-14640(ID14640 (Sc_Aro3_1 Fw))	AGTGCAGGU AAA ACA ATGTTCATTAAAAACGATCACGC
PR-14641(ID14641 (Sc_Aro3_1 Rv))	CGTGCGAUCTATTTTTTCAAGGCCTTTCTTCTG
PR-1546(AtC4H_U2_fw (ID1546))	ATCTGTCAUAAAACAATGGACTTGTTGTTGTTG
PR-1547(AtC4H_U2_rv (ID1547))	CACGCGAUTCAACAGTTTCTTGGCTT
PR-1554(AtATR2_U2_fw (ID1554))	ATCTGTCAUAAAACAATGTCCTCCTCTTCTTCATCATCCACC
PR-1555(AtATR2_U2_rv (ID1555))	CACGCGAUTCACCAGACATCTCTCAA
PR-1588(4CL1-VST1 front part _U1_rv (ID1588))	AAACCGTUAGCCAACTTGGCTC
PR-1589(4CL1-VST1 latter part _U1_fw (ID1589))	AACGGTTUGGGTTCTGGTGCTTCCGTTGAAGAATTCAGAAACGC
PR-1691(FjTAL_U1_fw (ID1691))	AGTGCAGGUAAAACAATGAACACCATCAACGAATATCTGAGC
PR-1692(FjTAL_U1_rv (ID1692))	CGTGCGAUTTAATTGTTAATCAGGTG
PR-1750(PTEF1_fw (Xiao))	acctgcacuttgtaattaaaacttagattagattg
PR-2173(Aro1 1-Fw (2173))	AGTGCAGGUAAAACAATGGTGCAGTTAGCCAAAG
PR-2174(Aro1 1-Rv (2174))	CGTGCGAUCTACTCTTTCGTAACGGCATC
PR-2179(Aro2 2-Fw (2179))	ATCTGTCAUAAAACAATGTCAACGTTTGGGAAACTG
PR-2180(Aro2 2-Rv (2180))	CACGCGAUTTAATGAACCACGGATCTGGA
PR-25300 (ScCYB5_U1_fw)	AGTGCAGGU AAAACA ATG CCT AAA GTT TAC AGT TAC CAA
PR-25301 (ScCYB5_U1_rev)	CGTGCGAU TTA TTC GTT CAA CAA ATA ATA AGC AAC AC
PR-27230 (PHA2_U2_fw)	ATCTGTCAU AAAACA ATGGCCAGCAAGACTTTG
PR-27231 (PHA2_U2_rev)	CACGCGAU TTATTTGTGATAATATCTCTCATTTCTGG
PR-27232 (MtPDH1_U1_fw)	AGTGCAGGU AAAACA ATG TCT TCA TCT TCA AAA TC
PR-27233 (MtPDH1_U1_rev)	CGTGCGAU TAA GAT TCA GTT CTT TCT GG

PR-27234 (Bbxfpk_U2_fw)	ATCTGTCAU AAAACA ATG ACT AAC CCT GTA ATC GG
PR-27235 (Bbxfpk_U2_rev)	CACGCGAU TTA TTC ATT GTC ACC AGC AG
PR-27236 (GPP1_gRNA)	GGCCATGTCACGGGTACCAG GTTTTAGAGCTAGAA
PR-6785(Ec_AroL_2-Fw (6785))	ATCTGTCAUAAAACAATGACACAACCTCTTTTTCTGA
PR-6786(Ec_AroL_2-Rv (6786))	CACGCGAUTCAACAATTGATCGTCTGTGC
PR-8(PPGK1_rv)	atgacagauttgttttatatttgttg

Table S5. DNA sequences of synthetic genes used in this study.

Gene name	DNA sequence
FjTAL	ATGAACACCATCAACGAATATCTGAGCCTGGAAGAATTTGAAGCCATTATCTTTGGCAATCAGAAAGTG ACCATTAGTGATGTTGTTGTGAATCGCGTTAACGAGAGCTTTAACTTTCTGAAAGAATTTAGCGGCAAC AAAGTGATCTATGGTGTGAATACCGGTTTTGGTCCGATGGCACAGTATCGTATTAAAGAAAGCGATCAG ATTCAGCTGCAGTATAATCTGATTCGTAGCCATAGCAGCGGCACCGGTAAACCGCTGAGTCCGGTTTGT GCAAAAGCAGCAATTCTGGCACGTCTGAATACCCTGAGTCTGGGTAATAGCGGTGTTCATCCGAGCGTT ATTAATCTGATGAGCGAACTGATCAACAAAGATATCACACCGCTGATTTTTGAACATGGTGGTGTTGGT GCAAGCGGTGATCTGGTTCAGCTGAGCCATCTGGCACTGGTTCTGATTGGTGAAGGTGAAGTTTTCTAT AAAGGTGAACGTCGTCCGACACCGGAAGTTTTTGAAATTGAAGGTCTGAAACCGATCCAGGTGGAAATT CGCGAAGGTCTGGCCCTGATTAATGGCACCAGCGTTATGACCGGTATTGGTGTTGTTAATGTGTACCAT GCAAAAAAACTGCTGGATTGGAGCCTGAAAAGCAGCTGTGCAATTAATGAACTGGTTCAGGCATATGAT GATCACTTTAGCGCAGAACTGAATCAGACCAAACGTCATAAAGGTCAGCAAGAAATTGCACTGAAAATG CGTCAGAATCTGAGCGATAGCACCCTGATTCGCAAACGTGAAGATCATCTGTATAGCGGTGAAAACACC GAAGAAATCTTCAAAGAAAAAGTGCAAGAGTATTATAGCCTGCGTTGTGTTCCGCAGATTCTGGGTCCG GTTCTGGAAACCATTAACAATGTTGCAAGCATTCTGGAAGATGAATTTAACAGCGCAAACGATAACCCG ATCATCGATGTTAAAAACCAGCATGTTTATCACGGTGGCAATTTTCATGGTGATTATATCAGCCTGGAA ATGGATAAACTGAAAATCGTGATTACCAAACTGACCATGCTGGCAGAACGTCAGCTGAATTATCTGCTG AATAGCAAAATTAACGAACTGCTGCCTCCGTTTGTTAATCTGGGCACCCTGGGTTTTAACTTTGGTATGC AGGGTGTTCAGTTTACCGCAACCAGCACCACCGCAGAAAGCCAGATGCTGAGCAATCCGATGTATGTTC ATAGCATTCCGAACAATAATGATAACCAGGATATTGTTAGCATGGGCACCAATAGCGCAGTTATTACCA GCAAAGTTATCGAAAATGCCTTTGAAGTTCTGGCCATTGAAATGATTACCATTGTTCAGGCGATTGATT ATCTGGGCCAGAAAGATAAAATCAGCAGCGTTAGCAAAAAATGGTATGATGAAATCCGCAACATCATCC CGACCTTTAAAGAAGATCAGGTGATGTATCCGTTCGTGCAGAAAGTAAAAGACCACCTGATTAACAATT AA
EcAroL	ATGACACAACCTCTTTTTCTGATCGGGCCTCGGGGCTGTGGTAAAACAACGGTCGGAATGGCCCTTGCC GATTCGCTTAACCGTCGGTTTGTCGATACCGATCAGTGGTTGCAATCACAGCTCAATATGACGGTCGCG GAGATCGTCGAAAGGGAAGAGTGGGCGGGATTTCGCGCCAGAGAAACGGCGGCGCTGGAAGCGGTAA CTGCGCCATCCACCGTTATCGCTACAGGCGGCGGCATTATTCTGACGGAATTTAATCGTCACTTCATGCA AAATAACGGGATCGTGGTTTATTTGTGTGCGCCAGTATCAGTCCTGGTTAACCGACTGCAAGCTGCACC GGAAGAAGATTTACGGCCAACCTTAACGGGAAAACCGCTGAGCGAAGAAGTTCAGGAAGTGCTGGAAG AACGCGATGCGCTATATCGCGAAGTTGCGCATATTATCATCGACGCAACAAACGAACCCAGCCAGGTGA TTTCTGAAATTCGCAGCGCCCTGGCACAGACGATCAATTGTTGA
MtPDH1	ATGTCTTCATCTTCAAAATCATTGAAGATCGGTATCGTTGGTTTCGGTACATTCGGTCAATTCTTGGCAA ACACTATGATCAAGCAAGGTCATACTTTGACAGCTACTTCAAGAACAGATTACTCACAATTGTGTGATCA AATGGGTATTCATTTCTTTAGAGATATCACAGCATTTTTGGATGCTGATATGGATGTTATCTTGTTGTGT ACTTCTATTTCTTCATTATCAGAAGTTGTTGGTTCTATGCCATTGGCATGTTTGAAGAGACCAACATTGT TCGTTGATGTTTTGTCTGTTAAGGAACATCCTAAAAATTTGTTGTTGAAGGTTTTGCCAGAAGAATCAG ATATCTTGTGTACTCATCCAATGTTTGGTCCAGTTTCTGGTAAAAATGGTTGGCAAAATTTGACTTTTAT GTTCGATAAAGTTAGAATTAAAGATGAAGTTACTTGTTCAAAATTTTTACAAATTTTTGCATCTGAAGGT TGTAAAATGGTTGAAATGTCATGTGAAGAACATGATAAAGCTGCTGCTAAGTCTCAATTCATTACACAT ACTATCGGTAGAACATTGGCTGAAATGGATATCAAATCAACACCAATCGATACTAAGGGTTTCCAAACT TTGGTTGAATTGAAGAAACCAGTTATGGGTTGTTCATTCGATTTGTACTCTGGTTTGTTCGTTTACAACA GATTCGCAAGACAAGAATTAGAAAATTTGGAACATGCTTTGCATAAAGTTAAAGAAATGTTGGTTCAAA GAATTGATGAAGGTCAAAATCCAGAAAGAACTGAATCTTAA
Bbxfpk	TTGATCGCTGATCACCAACAAAACACCGTTTTTATAATGGGTCCAGGTCATGGTGGTCCAGCTGGTACT TCCCAAAGTTATGTTGACGGTACTTACACTGAATACTACCCAAACATAACAAAAGATGAAGCTGGTTTG CAAAAGTTTTTCAGACAATTCTCCTATCCAGGTGGTATCCCTAGTCATTTTGCACCAGAAACCCCTGGTT CAATTCACGAAGGTGGTGAATTGGGTTATGCTTTATCTCATGCTTACGGTGCAGTAATGAATAACCCAT CATTGTTTGTTCCTTGTATTATAGGTGACGGTGAAGCCGAAACAGGTCCATTAGCTACCGGTTGGCAAT CTAACAAATTGGTCAATCCAAGAACTGATGGTATCGTATTGCCTATCTTGCATTTGAACGGTTACAAGAT TGCAAATCCAACAATCTTGGCCAGAATATCTGATGAAGAATTACATGACTTTTTCCGTGGTATGGGTTAT CACCCTTACGAATTTGTTGCCGGTTTCGATAATGAAGACCACATGTCTATCCACAGAAGATTCGCTGAAT TGTTCGAAACTATCTTCGATGAAATTTGTGACATAAAAGCTGCTGCTCAAACCGATGACATGACTAGAC CATTCTACCCTATGTTGATTTTTAGAACTCCAAAGGGTTGGACATGCCCTAAGTTCATCGATGGTAAAAA GACAGAAGGTTCCTGGAGAGCACATCAAGTTCCATTAGCTAGTGCAAGAGATACCGAAGAACACTTTGA AGTCTTGAAAGGTTGGATGGAATCTTACAAGCCTGAAGAATTATTCAATGCAGATGGTTCAATTAAAGA TGACGTTACAGCCTTTATGCCAAAGGGTGAATTGAGAATAGGTGCCAATCCTAACGCTAATGGTGGTGT TATCAGAGAAGATTTGAAATTGCCAGAATTAGACCAATATGAAGTAACTGGTGTTAAGGAATACGGTCA TGGTTGGGGTCAAGTTGAAGCCCCTAGAGCTTTGGGTGCATATTGTAGAGATATCATTAAAAATAACCC AGACTCCTTTAGAATATTCGGTCCTGATGAAACAGCTAGTAACAGATTGAACGCAACTTATGAAGTAAC CGATAAGCAATGGGACAATGGTTACTTGTCTGGTTTAGTTGATGAACACATGGCAGTCACTGGTCAAGT

	AACAGAACAATTATCAGAACACCAATGCGAAGGTTTCTTGGAAGCATATTTGTTAACAGGTAGACATGG
	TATTTGGTCTTCATACGAATCTTTTGTACATGTTATCGATTCAATGTTGAACCAACACGCCAAATGGTTA
	GAAGCTACTGTTAGAGAAATACCTTGGAGAAAGCCTATCTCCAGTGTTAACTTGTTAGTCTCTTCACATG
	TATGGAGACAAGATCATAATGGTTTTTCTCACCAAGACCCAGGTGTCACATCATTGTTGATTAATAAGA
	CCTTCAATAACGATCACGTTACCAACATCTATTTTGCCACTGACGCTAACATGTTGTTGGCTATCTCTGA
	AAAGTGCTTCAAGTCAACTAACAAAATCAATGCAATATTCGCCGGTAAACAACCAGCACCTACATGGGT
	TACCTTGGATGAAGCCAGAGCTGAATTAGAAGCTGGTGCTGCTGAATGGAAATGGGCTTCTAATGCAG
	AAAATAACGATGAAGTTCAAGTTGTCTTGGCATCCGCCGGTGACGTCCCAACACAAGAATTGATGGCCG
	CTAGTGATGCTTTGAACAAAATGGGTATTAAGTTTAAAGTAGTTAACGTCGTAGATTTGTTGAAGTTAC
	AATCAAGAGAAAACAACGATGAAGCATTGACTGACGAAGAGTTTACTGAATTGTTTACTGCTGATAAAC
	CAGTATTGTTTGCATATCATTCCTACGCCCAAGATGTTAGAGGTTTGATCTATGATAGACCAAACCATGA
	CAATTTCCACGTTGTCGGTTACAAAGAACAAGGTTCAACCACTACACCTTTTGATATGGTCAGAGTAAAT
	GATATGGACAGATATGCATTGCAAGCAGCCGCTTTGAAGTTAATTGATGCAGACAAATACGCCGATAAG
	ATCGACGAATTAAACGCTTTTAGAAAGAAAGCATTTCAATTCGCAGTCGATAATGGTTATGACATTCCA
	GAGTTTACTGATTGGGTATACCCTGATGTTAAGGTTGATGAAACACAAATGTTGTCTGCTACTGCTGCT
	ACTGCTGGTGACAATGAATAA
	ATGTCCTCCTCTTCTTCATCATCCACCTCTATGATTGATTTGATGGCCGCTATTATCAAGGGTGAACCAG
	TTATAGTTTCTGATCCAGCTAATGCTTCTGCCTATGAATCTGTTGCTGCTGAATTATCCTCCATGTTGAT
	CGAAAACAGACAATTCGCTATGATCGTCACTACCTCTATTGCTGTTTTGATTGGTTGCATCGTTATGTTG
	GTTTGGAGAAGATCTGGTTCTGGTAACTCTAAAAGAGTCGAACCATTGAAGCCATTGGTTATCAAACCT
	AGAGAAGAAGAAATTGACGACGGTAGAAAGAAGGTTACCATTTTCTTTGGTACTCAAACCGGTACTGCT
	GAAGGTTTTGCTAAAGCTTTGGGTGAAGAAGCTAAAGCCAGATACGAAAAGACTAGATTCAAGATCGTT
	GACTTGGATGATTACGCTGCAGATGATGATGAATACGAAGAAAAGTTGAAGAAAGAAGATGTCGCCTT
	TTTCTTCTTGGCTACTTATGGTGATGGTGAACCTACTGATAATGCTGCTAGATTTTACAAGTGGTTCACC
	GAAGGTAATGATAGAGGTGAATGGTTGAAAAACTTGAAGTACGGTGTTTTCGGTTTGGGTAATAGACA
	ATACGAACACTTCAACAAGGTTGCCAAGGTTGTTGATGATATCTTGGTTGAACAAGGTGCCCAAAGATT
	GGTTCAAGTTGGTTTAGGTGATGATGACCAATGCATCGAAGATGATTTTACTGCTTGGAGAGAAGCTTT
	GTGGCCAGAATTGGATACAATCTTGAGAGAAGAAGGTGATACTGCTGTTGCTACTCCATATACTGCTGC
	TGTTTTAGAATACAGAGTTTCCATCCACGATTCCGAAGATGCTAAGTTCAACGATATTAACATGGCTAAC
	GGTAACGGTTACACCGTTTTTGATGCTCAACATCCATACAAGGCTAACGTTGCTGTTAAGAGAGAATTG
	CATACTCCAGAATCTGACAGATCCTGCATTCATTTGGAATTCGATATTGCTGGTTCCGGTTTGACTTACG
AtCPR	AAACTGGTGATCATGTTGGTGTTTTGTGCGATAACTTGTCTGAAACTGTTGATGAAGCCTTGAGATTAT
	TGGATATGTCTCCAGATACCTACTTCTCCTTGCATGCCGAAAAAGAAGATGGTACTCCAATCTCTTCATC
	TTTGCCACCACCATTTCCACCATGTAATTTGAGAACTGCTTTGACCAGATACGCTTGCTTGTTGTCATCT
	CCAAAAAAGTCTGCTTTGGTTGCTTTGGCTGCTCATGCTTCAGATCCAACTGAAGCTGAAAGATTGAAA
	CATTTGGCTTCTCCAGCTGGTAAGGATGAATATTCTAAATGGGTTGTTGAATCCCAAAGATCCTTGTTG
	GAAGTTATGGCTGAATTTCCATCTGCTAAACCACCATTGGGTGTTTTTTTTGCTGGTGTTGCTCCAAGAT
	TGCAACCTAGATTCTACTCTATTTCCTCCTCCCCAAAAATTGCCGAAACCAGAATTCATGTTACTTGCGC
	TTTGGTCTACGAAAAAATGCCAACTGGTAGAATCCATAAGGGTGTTTGTTCTACCTGGATGAAGAATGC
	TGTTCCTTACGAAAAGTCCGAAAACTGTTCTTCTGCTCCAATCTTCGTTAGACAATCCAATTTCAAGTTG
	CCATCCGATTCTAAGGTTCCAATTATCATGATTGGTCCAGGTACTGGTTTGGCTCCTTTTAGAGGTTTTT
	TACAAGAAAGATTGGCCTTGGTCGAATCCGGTGTTGAATTGGGTCCATCTGTTTTGTTTTTCGGTTGCA
	GAAACAGAAGAATGGACTTCATCTACGAAGAAGAATTACAAAGATTCGTCGAATCAGGTGCTTTGGCAG
	AATTGTCAGTTGCTTTTTCTAGAGAAGGTCCAACAAAAGAATACGTCCAACACAAGATGATGGATAAGG
	CTTCTGATATCTGGAACATGATTTCTCAAGGTGCCTACTTGTATGTTTGTGGTGATGCTAAAGGTATGG
	CCAGAGATGTTCATAGATCCTTGCATACAATTGCCCAAGAACAAGGTTCTATGGACTCTACAAAAGCAG
	AAGGTTTCGTCAAGAACTTGCAAACTTCTGGTAGATACTTGAGAGATGTCTGGTGA
	ATGGATCAAATCGAAGCTATGTTGTGTGGTGGTGGTGAAAAAACAAAAGTTGCTGTTACTACTAAGACC
	TTGGCCGATCCATTGAATTGGGGTTTGGCTGCTGATCAAATGAAGGGTTCTCATTTGGATGAAGTCAAG
	AAGATGGTCGAAGAATACAGAAGACCAGTTGTTAATTTGGGTGGTGAAACTTTGACTATTGGTCAAGTT
	GCTGCTATTTCTACTGTTGGTGGTTCTGTTAAGGTTGAATTGGCTGAAACTTCTAGAGCTGGTGTTAAG
	GCTTCTTCTGATTGGGTTATGGAATCTATGAACAAGGGTACTGATTCTTACGGTGTTACTACAGGTTTT
	GGTGCTACTTCTCATAGAAGAACTAAGAATGGTACTGCCTTGCAAACCGAATTGATCAGATTTTTGAAC
	GCCGGTATTTTCGGTAACACCAAAGAAACTTGTCATACCTTGCCACAATCTGCTACTAGAGCTGCTATGT
	TGGTTAGAGTTAACACTTTGTTGCAAGGTTACTCCGGTATCAGATTCGAAATTTTGGAAGCTATCACCTC
	CTTGTTGAACCATAACATTTCTCCATCTTTGCCATTGAGAGGTACTATTACTGCTTCTGGTGATTTGGTT
	CCATTGTCTTATATTGCTGGTTTGTTGACTGGTAGACCAAACTCTAAAGCTACTGGTCCAGATGGTGAA
	TCATTGACTGCTAAAGAAGCTTTTGAAAAGGCTGGTATCTCTACTGGTTTTTTTCGACTTGCAACCTAAAG
	AAGGTTTGGCTTTGGTTAATGGTACAGCTGTTGGTTCTGGTATGGCTTCTATGGTTTTGTTTGAAGCTA
	ACGTTCAAGCTGTTTTGGCCGAAGTTTTGTCTGCTATTTTTGCTGAAGTTATGTCCGGTAAGCCAGAATT
	CACTGATCATTTGACCCATAGATTGAAACATCACCCAGGTCAAATTGAAGCTGCTGCAATTATGGAACA
AtPAL2	TATCTTGGATGGTTCCTCTTACATGAAGTTGGCTCAAAAAGTTCACGAAATGGACCCATTGCAAAAGCC
	AAAACAAGATAGATACGCTTTGAGAACTTCTCCACAATGGTTGGGTCCACAAATAGAAGTTATTAGACA
	AGCCACCAAGTCCATCGAAAGAGAAATCAATTCTGTTAACGACAACCCATTGATCGACGTCAGTAGAAA
	CAAAGCTATTCATGGTGGTAACTTCCAAGGTACTCCAATTGGTGTTTCTATGGACAACACTAGATTGGC
	TATTGCTGCCATTGGTAAATTGATGTTCGCTCAATTCTCCGAATTGGTCAACGATTTTTACAACAACGGT
	TTGCCTTCTAACTTGACCGCTTCTTCTAATCCATCATTGGATTACGGTTTTAAGGGTGCTGAAATTGCTA
	TGGCTTCATACTGTTCTGAATTGCAATACTTGGCTAACCCAGTTACCTCTCATGTTCAATCTGCTGAACA
	ACACAATCAAGACGTTAACTCCTTGGGTTTGATCTCTTCTAGAAAGACTTCTGAAGCCGTTGACATCTTG
	AAGTTGATGTCTACTACATTCTTGGTCGGTATTTGCCAAGCTGTTGATTTGAGACATTTGGAAGAAAAC
	TTGAGACAAACCGTCAAGAACACCGTTTCACAAGTTGCTAAGAAAGTTTTGACCACCGGTATTAACGGT
	GAATTGCATCCATCTAGATTCTGCGAAAAGGATTTGTTGAAGGTCGTTGATAGAGAACAAGTTTTCACC
	TACGTTGATGATCCATGTTCTGCTACTTATCCATTGATGCAAAGATTGAGACAAGTCATCGTTGATCATG
	CTTTGTCTAATGGTGAAACCGAAAAGAACGCTGTTACCTCCATTTTCCAAAAGATTGGTGCTTTCGAAG
	AAGAATTGAAGGCCGTTTTGCCAAAAGAAGTTGAAGCAGCTAGAGCAGCTTACGGTAACGGTACTGCTC
	CAATTCCAAATAGAATCAAAGAATGCAGATCCTACCCATTATACAGATTCGTTAGAGAAGAATTAGGTA

	CTAAGTTGTTGACCGGTGAAAAGGTTGTTTCTCCAGGTGAAGAATTCGATAAGGTTTTCACTGCTATGT GCGAAGGTAAATTGATCGATCCATTGATGGACTGCTTGAAAGAATGGAATGGTGCTCCTATTCCTATCT GCTGA
AtC4H	ATGGACTTGTTGTTGTTGGAAAAGTCCTTGATTGCTGTTTTCGTTGCTGTTATTTTGGCCACCGTTATCT CTAAATTGAGAGGTAAGAAATTGAAGTTGCCACCAGGTCCAATTCCAATCCCAATTTTTGGTAATTGGT TGCAAGTTGGTGATGACTTGAACCACAGAAACTTGGTTGATTACGCTAAAAAGTTCGGTGATTTGTTCT TGTTGAGAATGGGTCAAAGAAATTTGGTCGTTGTTTCCTCACCAGACTTGACCAAAGAAGTTTTGTTGA CTCAAGGTGTCGAATTCGGTTCCAGAACTAGAAATGTTGTTTTCGATATCTTCACCGGTAAGGGTCAAG ATATGGTTTTTACTGTTTACGGTGAACATTGGAGAAAGATGAGAAGAATTATGACCGTTCCATTCTTCA CCAACAAGGTTGTCCAACAAAACAGAGAAGGTTGGGAATTTGAAGCTGCTTCTGTTGTTGAAGATGTCA AGAAGAATCCAGATTCTGCTACTAAGGGTATCGTTTTGAGAAAAAGATTGCAATTGATGATGTACAACA ACATGTTCAGAATCATGTTCGACAGAAGATTTGAATCCGAAGATGACCCTTTGTTTTTGAGATTGAAGG CTTTGAACGGTGAAAGATCTAGATTGGCTCAATCCTTCGAATACAACTACGGTGATTTCATCCCAATCTT AAGACCATTCTTGAGAGGTTACTTGAAGATCTGCCAAGATGTTAAGGATAGAAGAATCGCCTTGTTCAA AAAGTACTTCGTTGACGAAAGAAAGCAAATCGCTTCTTCTAAACCTACTGGTTCTGAAGGTTTGAAGTG CGCCATTGATCATATTTTGGAAGCTGAACAAAAGGGTGAAATCAACGAAGATAACGTCTTGTACATCGT CGAAAACATTAACGTTGCTGCTATTGAAACTACCTTGTGGTCTATTGAATGGGGTATTGCTGAATTGGT TAATCACCCAGAAATCCAATCCAAGTTGAGAAACGAATTGGATACTGTTTTGGGTCCAGGTGTTCAAGT TACTGAACCTGACTTGCATAAGTTGCCATACTTGCAAGCTGTTGTAAAAGAAACCTTGAGATTAAGAAT GGCCATCCCTTTGTTGGTTCCACATATGAACTTGCATGATGCTAAATTGGCCGGTTATGATATTCCAGCC GAATCCAAGATTTTGGTTAATGCTTGGTGGTTGGCTAACAATCCAAATTCTTGGAAAAAGCCAGAAGAA TTCAGACCAGAAAGATTTTTCGAAGAAGAAAGTCACGTTGAAGCCAACGGTAATGATTTTAGATACGTT CCATTTGGTGTTGGTAGAAGATCTTGTCCAGGTATTATCTTGGCTTTGCCAATTTTGGGTATTACCATCG GTAGAATGGTCCAAAACTTCGAATTATTGCCACCACCTGGTCAATCTAAGGTTGATACTTCTGAAAAGG GTGGTCAATTCTCCTTGCATATTTTGAACCACTCCATCATCGTTATGAAGCCAAGAAACTGTTGA

References

Babaei, M., Borja Zamfir, G.M., Chen, X., Christensen, H.B., Kristensen, M., Nielsen, J., Borodina, I., 2020. Metabolic Engineering of *Saccharomyces cerevisiae* for Rosmarinic Acid Production. ACS Synth. Biol. 9, 1978–1988. https://doi.org/10.1021/acssynbio.0c00048

Entian, K.-D., Kötter, P., 2007. 25 Yeast Genetic Strain and Plasmid Collections, in: Stansfield, I., Stark, M.J. (Eds.), Methods in Microbiology, Yeast Gene Analysis. Academic Press, pp. 629–666. https://doi.org/10.1016/S0580-9517(06)36025-4

Jessop-Fabre, M.M., Jakočiūnas, T., Stovicek, V., Dai, Z., Jensen, M.K., Keasling, J.D., Borodina, I., 2016. EasyClone-MarkerFree: A vector toolkit for marker-less integration of genes into *Saccharomyces cerevisiae* via CRISPR-Cas9. Biotechnol. J. 11, 1110–1117. https://doi.org/10.1002/biot.201600147

Milne, N., Tramontin, L.R.R., Borodina, I., 2020. A teaching protocol demonstrating the use of EasyClone and CRISPR/Cas9 for metabolic engineering of Saccharomyces cerevisiae and Yarrowia lipolytica. FEMS Yeast Res. 20. https://doi.org/10.1093/femsyr/foz062

Partow, S., Siewers, V., Bjørn, S., Nielsen, J., Maury, J., 2010. Characterization of different promoters for designing a new expression vector in Saccharomyces cerevisiae. Yeast 27, 955–964. https://doi.org/10.1002/yea.1806

Stovicek, V., Borodina, I., Forster, J., 2015. CRISPR–Cas system enables fast and simple genome editing of industrial Saccharomyces cerevisiae strains. Metab. Eng. Commun. 2, 13–22. https://doi.org/10.1016/j.meteno.2015.03.001

CHAPTER 6

Perspectives

Non-conventional hosts in metabolic engineering

The exploration of employing *Y. lipolytica* for the production of aromatic compounds yielded the highest bioprocess performance metrics reported for resveratrol in scientific publications (Sáez-Sáez et al., 2020). In a more recent study, further enhancements in the metrics were obtained using also an engineered *Y. lipolytica* strain, reaching up to 22.5 g/L resveratrol with a yield on glucose of 65.5 mg/g (M. Liu et al., 2022). Liu et al.'s publication unveiled additional genetic engineering targets that could enhance strain performance. Furthermore, it demonstrated the significant impact of pH, dissolved oxygen percentage (DO%), and carbon-to-nitrogen ratio (C/N) on the resveratrol titers. Although these factors were not considered in our study, incorporating them could potentially improve our results.

Several studies conducted by multiple research groups over the past 3-4 years have consistently emphasized and confirmed the significant potential of *Y. lipolytica* in aromatic compound production, specifically phenylpropanoids with a polyketide structure that rely on malonyl-CoA as a precursor. Compounds such as polydatin, naringenin, eriodictyol, taxifolin, scutellarin, and liquiritigenin have been successfully engineered for production in *Y. lipolytica*, demonstrating exceptional production levels and establishing new records in scientific literature (Gu et al., 2020; Lv et al., 2019; Palmer et al., 2020; Akram et al., 2021; Wang et al., 2022; Wei et al., 2020).

The high-level production of resveratrol and other phenylpropanoid-derived polyketides has been a long-standing goal in the model yeast *S. cerevisiae*. However, the significant disparity in precursors' pathways fluxes poses challenges in achieving efficient native precursor supply for production. Particularly, the flux difference between the glycolysis and PPP, respectively yielding PEP and E4P is notable, with the latter exhibiting a flux up to one order of magnitude lower (Suástegui et al., 2016). Additionally, the low intracellular levels of malonyl-CoA further contribute to these challenges. Notably, our genetic engineering strategies for *Y. lipolytica* were entirely adapted from a prior study in *S. cerevisiae* (Li et al., 2015). The *Y. lipolytica* strain exhibited remarkable improvements following similar genetic modifications. These results emphasize the critical importance of matching the target product with the native metabolic capabilities of the production host and the bioprocess conditions. *Candida tropicalis*, similar to *Y. lipolytica*, exhibits a balanced metabolic flux between glycolysis and the PPP and possesses an oleaginous phenotype (Blank et al., 2005).

Therefore, considering purely its native metabolic traits *C. tropicalis* could serve as a suitable host for resveratrol production (Chattopadhyay et al., 2020; L. Zhang et al., 2022). Interestingly, as early as the 1960s, British Petroleum (BP) developed bioprocesses for single-cell protein production where the chosen hosts were both *C. tropicalis* and *Y. lipolytica* (Groenewald et al., 2014).

The question of whether conventional hosts should undergo extensive engineering to meet specific requirements or if it is more effective to develop novel host microorganisms tailored to desired objectives remains a debate in metabolic engineering. Historically, *E. coli*, *C. glutamicum*, and *S. cerevisiae* have been the favored hosts for various bioprocesses due to our comprehensive understanding of their metabolism, genetics, and physiology, as well as the availability of synthetic biology tools for manipulation (Nielsen and Keasling, 2016). However, *Yarrowia lipolytica* has witnessed a substantial surge in usage both in academia and industry over the past 15 years, evident from the increasing number of publications and patents. A recent survey involving ten companies employing *Y. lipolytica* highlighted its ability to grow at high cell densities, broad substrate utilization capacity, and robustness, characteristics that may be limited in *S. cerevisiae* (Park and Ledesma-Amaro, 2023). Beyond the typical product families like organic acids, lipids, and terpenoids, some answers from the survey highlighted the growing interest in amino acids as potential target products in the near future. Notably, *Y. lipolytica* has demonstrated superior performance in ergothioneine production, an uncommon antioxidant amino acid, even with minimal engineering, surpassing the capabilities of *S. cerevisiae* (van der Hoek et al., 2022a, 2022b).

Nevertheless, certain characteristics in the aforementioned hosts can still pose challenges in terms of engineering. For example, properties including tolerance to chemical and physical stresses, high growth and substrate uptake rates, efficient utilization of a wide range of carbon sources, and functional expression of specific enzymes remain challenging (Blombach et al., 2022). These challenges stem primarily from the complexity of these traits and the limited understanding of their underlying biochemical mechanisms. In this context, novel production hosts possessing such innate capabilities might offer promising alternatives to overcome these challenges and unlock new possibilities in metabolic engineering and bioprocess optimization (Karaalioğlu and Yüceer, 2021; Blombach et al., 2022; Geijer et al., 2022).

For instance, the production of fungal secondary metabolites like polyketides and non-ribosomal peptides requires the expression of mega-enzymes. In a report using *S. cerevisiae* as production host, almost half of the constructed strains did not produce any detectable amount of product upon expression of the fungal biosynthetic gene clusters (Harvey et al., 2018). Some of the reasons could be attributed to incorrect protein folding, modification, and trafficking. Exploring novel yeast hosts that are phylogenetically closer to the sources of these enzymes could potentially enhance the production of such secondary metabolites.

Non-conventional hosts might also play a role in the development of bioprocesses using alternative substrate in a biocircular economy. The current reliance on carbohydrate-based substrates in biobased production faces challenges due to competition with food production and potential price increases. To overcome these issues, the utilization of non-food feedstocks such as lignocellulosic or municipal waste hydrolysates is being explored (Yaashikaa et al., 2020; Calvo-Flores and Martin-Martinez, 2022). However, this requires microbial systems with higher chemical tolerance and versatile metabolism. Notably, *Pseudomonas taiwanensis* exhibits desirable characteristics, including high chemical tolerance, efficient carbon utilization, and the ability to assimilate non-traditional carbon sources (Nies et al., 2020; Sivapuratharasan et al., 2022; Wordofa and Kristensen, 2018; Wynands et al., 2019). Additionally, yeasts like *Kluyveromyces marxianus* and *Debaryomyces hansenii* have shown promise in this regard (Baptista and Domingues, 2022; Lane and Morrissey, 2010; Navarrete et al., 2022).

In summary, the focus of exploring new microbial hosts has shifted from their inherent ability to produce specific chemicals (e.g., *Pseudomonas denitrificans* and vitamin B12 (Fang et al., 2017)) to their natural capacity in performing challenging tasks that are difficult to engineer in commonly used hosts in metabolic engineering. However, it is important to acknowledge that employing novel microbial hosts presents limitations in terms of knowledge regarding handling and cultivation, genetic manipulation, availability of synthetic biology toolboxes, genetic stability, and cellular heterogeneity. To address these challenges, various approaches can be employed, such as analyzing metagenomic data, constructing genome-scale metabolic models that integrate multi-omics data, and utilizing machine learning techniques (Chen et al., 2020; McElhinney et al., 2022; Mol et al., 2021; Pappu and Gummadi, 2017). These methods can assist

in the discovery, development, and optimization of unconventional organisms, providing valuable insights into their metabolic capabilities and potential as biocatalysts.

Production of new-to-nature halogenated natural products in yeast

Our work on *in vivo* halogenation in *S. cerevisiae* demonstrated that the indole ring of tryptophan could undergo halogenation at positions 5-, 6-, 7- utilizing either chlorine or bromine as halogen sources. Moreover, we successfully demonstrated the decarboxylation process of halogenated tryptophan into halogenated tryptamine, a crucial intermediate in the synthesis of biologically active natural products with therapeutic potential.

The generated molecules, halotryptophan and halotryptamine, have the potential to be purified and utilized in synthetic chemistry for cross-coupling reactions, yielding more complex halogenated compounds (Sharma et al., 2017). Another particularly captivating opportunity lies in integrating them into biosynthetic pathways of plant natural products, which can be implemented in yeast to facilitate the production of halogenated secondary metabolites. To pursue the former approach, it is essential to enhance the strains performance. Our proof-of-principle strains utilized only expressed the minimal enzymes necessary for halogenation. Incorporating genetic targets employed in Chapter 5 for *p*-coumaric acid production would likely enhance the titers. Nonetheless, it should be noted that halogenated tryptophan mainly resides intracellularly, posing challenges for downstream processing. Certain studies have successfully employed *C. glutamicum* to achieve gram-per-liter titers of halogenated tryptophan and tryptamine, serving as a promising starting point for purification and use in synthetic chemistry (Kerbs et al., 2022; Veldmann et al., 2019a, 2019b).

Hence, a more logical approach in yeast would be to introduce biosynthetic pathways capable of converting the halogenated compounds into valuable end products. Among these, the production of monoterpene indole alkaloids (MIAs) emerges as an especially intriguing compound family, given that certain members of this family possess a substantial market worth of billions of dollars annually (O'Connor and Maresh, 2006; J. Zhang et al., 2022). However, it is evident that incorporating halogenated compounds into the MIAs pathway presents challenges, starting with the suboptimal

decarboxylation of halotryptophan into halotryptamine, resulting in significant substrate accumulation. In order to overcome this limitation, several studies have utilized protein engineering techniques to modify both the substrate specificity and regioselectivity of the tryptophan 7-halogenase LaRebH. Some enzyme variants shifted the enzyme specificity towards tryptamine while also targeting other positions within the indole ring (Andorfer et al., 2016; Glenn et al., 2011). These enzyme variants could potentially be expressed in yeast to relieve this suboptimal enzymatic step. From halogenated tryptamine, in plants the enzymes of the MIAs pathway seem to be able to cope with most of the different halogenated intermediates. In particular, studies in *Catharanthus roseus* have demonstrated how halogenated tryptamine can be processed into a range of late MIAs intermediates and products (McCoy and O'Connor, 2006; Runguphan et al., 2010). Several MIAs biosynthetic enzymes have undergone *in vitro* characterization to evaluate their substrate promiscuity (McCoy et al., 2006; Yerkes et al., 2008). For strictosidine synthase in particular, a mutant enzyme is required for the processing of 5-chlorotryptamine (Bernhardt et al., 2007), while strictosidine-β-glucosidase is more tolerant towards substituted substrates (Yerkes et al., 2008). Refactoring MIAs pathways in yeast has been achieved to varying degrees of success, with recent breakthroughs in the production of vindoline and catharanthine, which require the functional expression of tens of biosynthetic genes (Brown et al., 2015; Qu et al., 2015; Kulagina et al., 2021; T. Liu et al., 2022; J. Zhang et al., 2022). Although challenging, the *in vivo* production of halogenated MIAs products in yeast appears feasible and will likely be demonstrated in the near future. In cases where the expressed enzymes fail to process halogenated intermediates, directed evolution, rational protein engineering, and machine learning have demonstrated their utility in enhancing enzyme promiscuity towards substituted substrates (Korendovych, 2018; Ogawa et al., 2023; Rix et al., 2020).

In addition to MIAs, there are alternative metabolites derived from tryptophan with shorter biosynthetic pathways that hold greater potential for successful production in yeast. Violacein, a natural pigment renowned for its vivid violet color and possessing antimicrobial, antiviral, and anticancer properties, requires the expression of five genes within its biosynthetic pathway (Ahmed et al., 2021). Recently, halogenated violacein was successfully produced in *E. coli* without the need for protein engineering, and crude extracts were employed in synthetic chemistry cross-coupling reactions to generate intricate halogenated structures (Lai et al., 2021). Furthermore, tryptamine

alkaloids like psilocybin and melatonin exhibit relatively simple pathways and have been previously biosynthesized in *S. cerevisiae* (Germann et al., 2016; Milne et al., 2020). Although it remains unclear whether the enzymes involved can act on halogenated substrates, it is worth noting that certain halogenated forms of melatonin have demonstrated efficacy in the treatment of primary insomnia (Zemlan et al., 2005).

Enhancing product tolerance in microbial cell factories through transporter engineering

Through our investigation of screening transporter deletion libraries in *E. coli* and *S. cerevisiae*, we successfully identified multiple transporter-encoding genes whose deletion resulted in increased product tolerance. Enhancing product tolerance is a key objective in tolerance adaptive laboratory evolution (TALE), and in comparison, screening transporter deletion libraries offers a significantly faster approach for achieving this goal.

The initial step in the screening of the transporter deletion library is based on the hypothesis that mutations in transporter-encoding genes contribute significantly to the tolerance phenotype, which is supported by multiple studies employing tolerance adaptive laboratory evolution (TALE) approaches (Mohamed et al., 2017; Srivastava et al., 2021; Radi et al., 2022; Lennen et al., 2023). This assumption yields a transporter deletion library comprising approximately 300-450 deletion strains for *S. cerevisiae* and *E. coli*, a size deemed suitable for evaluating the growth of the library in liquid medium in duplicate using Growth Profiler 960 at its full capacity. One could also consider evaluating the effect of deleting other groups of genes, like regulatory, stress response, chaperones, or signaling pathways genes. Deletion strains for those families of genes could be extracted from the YKO and Keio collections and organized into subsets for systematic analysis.

The preliminary assessment of the transporter-deletion library and subsequent validation of promising candidates normally require no more than two weeks for a single compound. TALE experiments typically require a timespan ranging from a few weeks to several months (Kildegaard et al., 2014; Pereira et al., 2019; Matson et al., 2022), and performing nearly daily transfers during the experiment can be laborious

and time-consuming, especially without the aid of automated liquid handlers (Dragosits and Mattanovich, 2013). Genome sequencing of the evolved populations and the subsequent reverse engineering process to confirm the mutations underlying the tolerant phenotype may also require a minimum of one to two months, assuming an optimistic scenario.

The screening of knockout libraries offers a compelling alternative for rapidly identifying deletion targets that enhance product tolerance. However, it should be noted that TALE studies generally yield a greater degree of tolerance, as a single deletion of a transporter, while beneficial for tolerance improvement, typically exhibits enhanced efficacy when combined with other genomic mutations, resulting in synergistic effects. For instance, in a study performing TALE in *E. coli* against glutamate and adipate, only after deleting 3 transporter-encoding genes, 85% and 60% of the tolerance of the evolved strains could be reconstructed, respectively (Lennen et al., 2023).

Although library screenings facilitate the identification of transporter-encoding genes that potentially influence product tolerance, they do not guarantee their direct involvement in compound transport. Cell-based assays, such as the one employed in this study, offer advantages in terms of rapidity and high-throughput capabilities. However, these assays can introduce significant background transporter activity due to the redundancy of transporters (Mans et al., 2017; Alon Cudkowicz and Schuldiner, 2019). Moreover, our understanding of the potential involvement of transporters in specific transport processes is limited, primarily due to the lack of knowledge regarding transporters and their associated substrates (Kell et al., 2011; Kell, 2021). Even annotated transporters with assigned functions and substrates, such as Tpo2p in *S. cerevisiae*, have recently been assigned new substrates (Wang et al., 2021). In the case of the transporters we identified to affect aromatic compounds tolerance, detailed annotations were lacking in transportDB (Elbourne et al., 2017). Therefore, further experiments are necessary to determine whether the observed effects on tolerance can be attributed directly to transport activity of the toxic compounds.

In light of this, an effective approach would involve utilizing *Xenopus laevis* oocytes as an expression system for the candidate transporters *Xenopus* oocytes possess minimal inherent transport activity, and their capability to easily express cRNAs of transporters and localize them to the plasma membrane makes them an excellent

platform for transporter characterization (Romero et al., 1998; Miller and Zhou, 2000). While this system does have inherent limitations regarding throughput, it still falls within an appropriate range for evaluating the 10-16 transporters that we identified as influential in product tolerance for specific aromatic compounds.

Multi-omics data to guide strain engineering

The last experimental chapter of this thesis represents an initial step of an ongoing project aiming at performing a multi-omics characterization (transcriptomics, proteomics, metabolomics, fluxomics) of several *S. cerevisiae* strains that produce *p*-coumaric acid. Initially, our plan was to utilize the microfluidic bioreactor Biolector Pro (m2p-labs) as the cultivation platform for multi-omics characterization of yeast strains in fed-batch mode. However, we encountered limitations that ultimately led us to abandon this system for multi-omics analysis and use ambr250® (Sartorius) instead.

The primary limitations were associated with the restricted cultivation volume, which impeded multiple samplings from the same culture for different omics analyses. Additionally, the inherent configuration of the automated sampling system caused the cultivation to enter a pause mode during sampling, halting the feeding process. Consequently, time-sensitive omics analyses, such as endometabolomics, were significantly affected, as inconsistencies were observed in the measurement of metabolites from the central carbon metabolism. While Biolector has proven valuable in bioprocess development and media optimization (Rohe et al., 2012; Wewetzer et al., 2015; Jacobsen et al., 2020), we believe that using it for multi-omics analysis stretches its capabilities. Enhancements, such as increased customization of cultivation parameters and sampling, would make multi-omics analysis more feasible with this system. Alternatively, opting for conventional bioreactor systems such as ambr250®, as utilized in our ongoing study, or other benchtop bioreactors would still be a favorable approach.

Although the experimental work involved in multi-omics studies can be laborious, the processing and analysis of data constitute the more time-consuming phase. Over the past years, the emergence of various user-friendly tools like Galaxy, KBase, and INCA, which do not necessitate coding expertise, has simplified the data analysis process for

most wet-lab scientists (Arkin et al., 2018; Jalili et al., 2020; Young, 2014; Rahim et al., 2022). However, these tools often have limitations, and the assistance of bioinformaticians with specialized knowledge remains crucial to optimize the time invested in this phase. As we proceed with the analysis phase, it raises the question of whether the substantial investment in terms of time and financial resources will ultimately be worthwhile and result in valuable engineering targets. Specifically, in the context of an "open-question" multi-omics study like this one, where we are not seeking specific answers to predefined problems, it will become crucial to evaluate whether the expenditure is justified and if it will yield meaningful engineering targets.

References

Ahmed, A., Ahmad, A., Li, R., AL-Ansi, W., Fatima, M., Mushtaq, B.S., Basharat, S., Li, Y., Bai, Z., 2021. Recent Advances in Synthetic, Industrial and Biological Applications of Violacein and Its Heterologous Production. J. Microbiol. Biotechnol. 31, 1465–1480. https://doi.org/10.4014/jmb.2107.07045

Akram, M., Rasool, A., An, T., Feng, X., Li, C., 2021. Metabolic engineering of Yarrowia lipolytica for liquiritigenin production. Chem. Eng. Sci. 230, 116177. https://doi.org/10.1016/j.ces.2020.116177

Alon Cudkowicz, N., Schuldiner, S., 2019. Deletion of the major Escherichia coli multidrug transporter AcrB reveals transporter plasticity and redundancy in bacterial cells. PLOS ONE 14, e0218828. https://doi.org/10.1371/journal.pone.0218828

Andorfer, M.C., Park, H.J., Vergara-Coll, J., Lewis, J.C., 2016. Directed evolution of RebH for catalyst-controlled halogenation of indole C–H bonds. Chem. Sci. 7, 3720–3729. https://doi.org/10.1039/C5SC04680G

Arkin, A.P., Cottingham, R.W., Henry, C.S., Harris, N.L., Stevens, R.L., Maslov, S., Dehal, P., Ware, D., Perez, F., Canon, S., Sneddon, M.W., Henderson, M.L., Riehl, W.J., Murphy-Olson, D., Chan, S.Y., Kamimura, R.T., Kumari, S., Drake, M.M., Brettin, T.S., Glass, E.M., Chivian, D., Gunter, D., Weston, D.J., Allen, B.H., Baumohl, J., Best, A.A., Bowen, B., Brenner, S.E., Bun, C.C., Chandonia, J.-M., Chia, J.-M., Colasanti, R., Conrad, N., Davis, J.J., Davison, B.H., DeJongh, M., Devoid, S., Dietrich, E., Dubchak, I., Edirisinghe, J.N., Fang, G., Faria, J.P., Frybarger, P.M., Gerlach, W., Gerstein, M., Greiner, A., Gurtowski, J., Haun, H.L., He, F., Jain, R., Joachimiak, M.P., Keegan, K.P., Kondo, S., Kumar, V., Land, M.L., Meyer, F., Mills, M., Novichkov, P.S., Oh, T., Olsen, G.J., Olson, R., Parrello, B., Pasternak, S., Pearson, E., Poon, S.S., Price, G.A., Ramakrishnan, S., Ranjan, P., Ronald, P.C., Schatz, M.C., Seaver, S.M.D., Shukla, M., Sutormin, R.A., Syed, M.H., Thomason, J., Tintle, N.L., Wang, D., Xia, F., Yoo, H., Yoo, S., Yu, D., 2018. KBase: The United States Department of Energy Systems Biology Knowledgebase. Nat. Biotechnol. 36, 566–569. https://doi.org/10.1038/nbt.4163

Baptista, M., Domingues, L., 2022. Kluyveromyces marxianus as a microbial cell factory for lignocellulosic biomass valorisation. Biotechnol. Adv. 60, 108027. https://doi.org/10.1016/j.biotechadv.2022.108027

Bernhardt, P., McCoy, E., O'Connor, S.E., 2007. Rapid Identification of Enzyme Variants for Reengineered Alkaloid Biosynthesis in Periwinkle. Chem. Biol. 14, 888–897. https://doi.org/10.1016/j.chembiol.2007.07.008

Blombach, B., Grünberger, A., Centler, F., Wierckx, N., Schmid, J., 2022. Exploiting unconventional prokaryotic hosts for industrial biotechnology. Trends Biotechnol. 40, 385–397. https://doi.org/10.1016/j.tibtech.2021.08.003

Brown, S., Clastre, M., Courdavault, V., O'Connor, S.E., 2015. De novo production of the plant-derived alkaloid strictosidine in yeast. Proc. Natl. Acad. Sci. 112, 3205–3210. https://doi.org/10.1073/pnas.1423555112

Calvo-Flores, F.G., Martin-Martinez, F.J., 2022. Biorefineries: Achievements and challenges for a bio-based economy. Front. Chem. 10, 973417. https://doi.org/10.3389/fchem.2022.973417

Chattopadhyay, A., Gupta, A., Maiti, M.K., 2020. Engineering an oleaginous yeast Candida tropicalis SY005 for enhanced lipid production. Appl. Microbiol. Biotechnol. 104, 8399–8411. https://doi.org/10.1007/s00253-020-10830-6

Chen, L.-X., Anantharaman, K., Shaiber, A., Eren, A.M., Banfield, J.F., 2020. Accurate and complete genomes from metagenomes. Genome Res. 30, 315–333. https://doi.org/10.1101/gr.258640.119

Dragosits, M., Mattanovich, D., 2013. Adaptive laboratory evolution – principles and applications for biotechnology. Microb. Cell Factories 12, 64. https://doi.org/10.1186/1475-2859-12-64

Elbourne, L.D.H., Tetu, S.G., Hassan, K.A., Paulsen, I.T., 2017. TransportDB 2.0: a database for exploring membrane transporters in sequenced genomes from all domains of life. Nucleic Acids Res. 45, D320–D324. https://doi.org/10.1093/nar/gkw1068

Fang, H., Kang, J., Zhang, D., 2017. Microbial production of vitamin B12: a review and future perspectives. Microb. Cell Factories 16, 15. https://doi.org/10.1186/s12934-017-0631-y

Geijer, C., Ledesma-Amaro, R., Tomás-Pejó, E., 2022. Unraveling the potential of non-conventional yeasts in biotechnology. FEMS Yeast Res. 22, foab071. https://doi.org/10.1093/femsyr/foab071

Germann, S.M., Baallal Jacobsen, S.A., Schneider, K., Harrison, S.J., Jensen, N.B., Chen, X., Stahlhut, S.G., Borodina, I., Luo, H., Zhu, J., Maury, J., Forster, J., 2016. Glucose-based microbial production of the hormone melatonin in yeast *Saccharomyces cerevisiae*. Biotechnol. J. 11, 717–724. https://doi.org/10.1002/biot.201500143

Glenn, W.S., Nims, E., O'Connor, S.E., 2011. Reengineering a Tryptophan Halogenase To Preferentially Chlorinate a Direct Alkaloid Precursor. J. Am. Chem. Soc. 133, 19346–19349. https://doi.org/10.1021/ja2089348

Groenewald, M., Boekhout, T., Neuvéglise, C., Gaillardin, C., van Dijck, P.W.M., Wyss, M., 2014. *Yarrowia lipolytica* : Safety assessment of an oleaginous yeast with a great industrial potential. Crit. Rev. Microbiol. 40, 187–206. https://doi.org/10.3109/1040841X.2013.770386

Gu, Y., Ma, J., Zhu, Y., Ding, X., Xu, P., 2020. Engineering *Yarrowia lipolytica* as a Chassis for *De Novo* Synthesis of Five Aromatic-Derived Natural Products and Chemicals. ACS Synth. Biol. 9, 2096–2106. https://doi.org/10.1021/acssynbio.0c00185

Harvey, C.J.B., Tang, M., Schlecht, U., Horecka, J., Fischer, C.R., Lin, H.-C., Li, J., Naughton, B., Cherry, J., Miranda, M., Li, Y.F., Chu, A.M., Hennessy, J.R., Vandova, G.A., Inglis, D., Aiyar, R.S., Steinmetz, L.M., Davis, R.W., Medema, M.H., Sattely, E., Khosla, C., St. Onge, R.P., Tang, Y., Hillenmeyer, M.E., 2018. HEx: A heterologous expression platform for the discovery of fungal natural products. Sci. Adv. 4, eaar5459. https://doi.org/10.1126/sciadv.aar5459

Jacobsen, I.H., Ledesma-Amaro, R., Martinez, J.L., 2020. Recombinant β-Carotene Production by Yarrowia lipolytica – Assessing the Potential of Micro-Scale Fermentation Analysis in Cell Factory Design and Bioreaction Optimization. Front. Bioeng. Biotechnol. 8, 29. https://doi.org/10.3389/fbioe.2020.00029

Jalili, V., Afgan, E., Gu, Q., Clements, D., Blankenberg, D., Goecks, J., Taylor, J., Nekrutenko, A., 2020. The Galaxy platform for accessible, reproducible and collaborative biomedical analyses: 2020 update. Nucleic Acids Res. 48, W395–W402. https://doi.org/10.1093/nar/gkaa434

Karaalioğlu, O., Yüceer, Y.K., 2021. Nonconventional yeasts to produce aroma compounds by using agri-food waste materials. FEMS Yeast Res. 21, foab063. https://doi.org/10.1093/femsyr/foab063

Kell, D.B., 2021. The Transporter-Mediated Cellular Uptake and Efflux of Pharmaceutical Drugs and Biotechnology Products: How and Why Phospholipid Bilayer Transport Is Negligible in Real Biomembranes. Molecules 26, 5629. https://doi.org/10.3390/molecules26185629

Kell, D.B., Dobson, P.D., Oliver, S.G., 2011. Pharmaceutical drug transport: the issues and the implications that it is essentially carrier-mediated only. Drug Discov. Today 16, 704–714. https://doi.org/10.1016/j.drudis.2011.05.010

Kerbs, A., Burgardt, A., Veldmann, K.H., Schäffer, T., Lee, J.-H., Wendisch, V.F., 2022. Fermentative Production of Halogenated Tryptophan Derivatives with Corynebacterium glutamicum Overexpressing Tryptophanase or Decarboxylase Genes. ChemBioChem 23, e202200007. https://doi.org/10.1002/cbic.202200007

Kildegaard, K.R., Hallström, B.M., Blicher, T.H., Sonnenschein, N., Jensen, N.B., Sherstyk, S., Harrison, S.J., Maury, J., Herrgård, M.J., Juncker, A.S., Forster, J., Nielsen, J., Borodina, I., 2014. Evolution reveals a glutathione-dependent mechanism of 3-hydroxypropionic acid tolerance. Metab. Eng. 26, 57–66. https://doi.org/10.1016/j.ymben.2014.09.004

Korendovych, I.V., 2018. Rational and Semirational Protein Design, in: Bornscheuer, U.T., Höhne, M. (Eds.), Protein Engineering, Methods in Molecular Biology. Springer New York, New York, NY, pp. 15–23. https://doi.org/10.1007/978-1-4939-7366-8_2

Kulagina, N., Guirimand, G., Melin, C., Lemos-Cruz, P., Carqueijeiro, I., De Craene, J., Oudin, A., Heredia, V., Koudounas, K., Unlubayir, M., Lanoue, A., Imbault, N., St-Pierre, B., Papon, N., Clastre, M., Giglioli-Guivarc'h, N., Marc, J., Besseau, S., Courdavault, V., 2021. Enhanced bioproduction of anticancer precursor vindoline by yeast cell factories. Microb. Biotechnol. 14, 2693–2699. https://doi.org/10.1111/1751-7915.13898

Lai, H.-E., Obled, A.M.C., Chee, S.M., Morgan, R.M., Lynch, R., Sharma, S.V., Moore, S.J., Polizzi, K.M., Goss, R.J.M., Freemont, P.S., 2021. GenoChemetic Strategy for Derivatization of the Violacein Natural Product Scaffold. ACS Chem. Biol. 16, 2116–2123. https://doi.org/10.1021/acschembio.1c00483

Lane, M.M., Morrissey, J.P., 2010. Kluyveromyces marxianus: A yeast emerging from its sister's shadow. Fungal Biol. Rev. 24, 17–26. https://doi.org/10.1016/j.fbr.2010.01.001

Lennen, R.M., Lim, H.G., Jensen, K., Mohammed, E.T., Phaneuf, P.V., Noh, M.H., Malla, S., Börner, R.A., Chekina, K., Özdemir, E., Bonde, I., Koza, A., Maury, J., Pedersen, L.E., Schöning, L.Y., Sonnenschein, N., Palsson, B.O., Nielsen, A.T., Sommer, M.O.A., Herrgård, M.J., Feist, A.M., 2023. Laboratory evolution reveals general and specific tolerance mechanisms for commodity chemicals. Metab. Eng. 76, 179–192. https://doi.org/10.1016/j.ymben.2023.01.012

Li, M., Kildegaard, K.R., Chen, Y., Rodriguez, A., Borodina, I., Nielsen, J., 2015. De novo production of resveratrol from glucose or ethanol by engineered Saccharomyces cerevisiae. Metab. Eng. 32, 1–11. https://doi.org/10.1016/j.ymben.2015.08.007

Liu, M., Wang, C., Ren, X., Gao, S., Yu, S., Zhou, J., 2022. Remodelling metabolism for high-level resveratrol production in Yarrowia lipolytica. Bioresour. Technol. 365, 128178. https://doi.org/10.1016/j.biortech.2022.128178

Liu, T., Gou, Y., Zhang, B., Gao, R., Dong, C., Qi, M., Jiang, L., Ding, X., Li, C., Lian, J., 2022. Construction of ajmalicine and sanguinarine de novo biosynthetic pathways using stable integration sites in yeast. Biotechnol. Bioeng. 119, 1314–1326. https://doi.org/10.1002/bit.28040

Lv, Y., Marsafari, M., Koffas, M., Zhou, J., Xu, P., 2019. Optimizing Oleaginous Yeast Cell Factories for Flavonoids and Hydroxylated Flavonoids Biosynthesis. ACS Synth. Biol. 8, 2514–2523. https://doi.org/10.1021/acssynbio.9b00193

Mans, R., Hassing, E.-J., Wijsman, M., Giezekamp, A., Pronk, J.T., Daran, J.-M., van Maris, A.J.A., 2017. A CRISPR/Cas9-based exploration into the elusive mechanism for lactate

export in Saccharomyces cerevisiae. FEMS Yeast Res. 17. https://doi.org/10.1093/femsyr/fox085
Matson, M.M., Cepeda, M.M., Zhang, A., Case, A.E., Kavvas, E.S., Wang, X., Carroll, A.L., Tagkopoulos, I., Atsumi, S., 2022. Adaptive laboratory evolution for improved tolerance of isobutyl acetate in Escherichia coli. Metab. Eng. 69, 50–58. https://doi.org/10.1016/j.ymben.2021.11.002
McCoy, E., Galan, M.C., O'Connor, S.E., 2006. Substrate specificity of strictosidine synthase. Bioorg. Med. Chem. Lett. 16, 2475–2478. https://doi.org/10.1016/j.bmcl.2006.01.098
McCoy, E., O'Connor, S.E., 2006. Directed Biosynthesis of Alkaloid Analogs in the Medicinal Plant *Catharanthus roseus*. J. Am. Chem. Soc. 128, 14276–14277. https://doi.org/10.1021/ja066787w
McElhinney, J.M.W.R., Catacutan, M.K., Mawart, A., Hasan, A., Dias, J., 2022. Interfacing Machine Learning and Microbial Omics: A Promising Means to Address Environmental Challenges. Front. Microbiol. 13, 851450. https://doi.org/10.3389/fmicb.2022.851450
Miller, A.J., Zhou, J.J., 2000. Xenopus oocytes as an expression system for plant transporters. Biochim. Biophys. Acta BBA - Biomembr. 1465, 343–358. https://doi.org/10.1016/S0005-2736(00)00148-6
Milne, N., Thomsen, P., Mølgaard Knudsen, N., Rubaszka, P., Kristensen, M., Borodina, I., 2020. Metabolic engineering of Saccharomyces cerevisiae for the de novo production of psilocybin and related tryptamine derivatives. Metab. Eng. 60, 25–36. https://doi.org/10.1016/j.ymben.2019.12.007
Mohamed, E.T., Wang, S., Lennen, R.M., Herrgård, M.J., Simmons, B.A., Singer, S.W., Feist, A.M., 2017. Generation of a platform strain for ionic liquid tolerance using adaptive laboratory evolution. Microb. Cell Factories 16, 204. https://doi.org/10.1186/s12934-017-0819-1
Mol, V., Bennett, M., Sánchez, B.J., Lisowska, B.K., Herrgård, M.J., Nielsen, A.T., Leak, D.J., Sonnenschein, N., 2021. Genome-scale metabolic modeling of P. thermoglucosidasius NCIMB 11955 reveals metabolic bottlenecks in anaerobic metabolism. Metab. Eng. 65, 123–134. https://doi.org/10.1016/j.ymben.2021.03.002
Navarrete, C., Estrada, M., Martínez, J.L., 2022. Debaryomyces hansenii: an old acquaintance for a fresh start in the era of the green biotechnology. World J. Microbiol. Biotechnol. 38, 99. https://doi.org/10.1007/s11274-022-03280-x
Nielsen, J., Keasling, J.D., 2016. Engineering Cellular Metabolism. Cell 164, 1185–1197. https://doi.org/10.1016/j.cell.2016.02.004
Nies, S.C., Alter, T.B., Nölting, S., Thiery, S., Phan, A.N.T., Drummen, N., Keasling, J.D., Blank, L.M., Ebert, B.E., 2020. High titer methyl ketone production with tailored Pseudomonas taiwanensis VLB120. Metab. Eng. 62, 84–94. https://doi.org/10.1016/j.ymben.2020.08.003
O'Connor, S.E., Maresh, J.J., 2006. Chemistry and biology of monoterpene indole alkaloid biosynthesis. Nat. Prod. Rep. 23, 532. https://doi.org/10.1039/b512615k
Ogawa, Y., Saito, Y., Yamaguchi, H., Katsuyama, Y., Ohnishi, Y., 2023. Engineering the Substrate Specificity of Toluene Degrading Enzyme XylM Using Biosensor XylS and Machine Learning. ACS Synth. Biol. 12, 572–582. https://doi.org/10.1021/acssynbio.2c00577
Palmer, C.M., Miller, K.K., Nguyen, A., Alper, H.S., 2020. Engineering 4-coumaroyl-CoA derived polyketide production in Yarrowia lipolytica through a β-oxidation mediated strategy. Metab. Eng. 57, 174–181. https://doi.org/10.1016/j.ymben.2019.11.006
Pappu, S.M.J., Gummadi, S.N., 2017. Artificial neural network and regression coupled genetic algorithm to optimize parameters for enhanced xylitol production by Debaryomyces nepalensis in bioreactor. Biochem. Eng. J. 120, 136–145. https://doi.org/10.1016/j.bej.2017.01.010
Park, Y.-K., Ledesma-Amaro, R., 2023. What makes Yarrowia lipolytica well suited for industry? Trends Biotechnol. 41, 242–254. https://doi.org/10.1016/j.tibtech.2022.07.006

Pereira, R., Wei, Y., Mohamed, E., Radi, M., Malina, C., Herrgård, M.J., Feist, A.M., Nielsen, J., Chen, Y., 2019. Adaptive laboratory evolution of tolerance to dicarboxylic acids in Saccharomyces cerevisiae. Metab. Eng. 56, 130–141. https://doi.org/10.1016/j.ymben.2019.09.008

Qu, Y., Easson, M.L.A.E., Froese, J., Simionescu, R., Hudlicky, T., De Luca, V., 2015. Completion of the seven-step pathway from tabersonine to the anticancer drug precursor vindoline and its assembly in yeast. Proc. Natl. Acad. Sci. 112, 6224–6229. https://doi.org/10.1073/pnas.1501821112

Radi, M.S., SalcedoSora, J.E., Kim, S.H., Sudarsan, S., Sastry, A.V., Kell, D.B., Herrgård, M.J., Feist, A.M., 2022. Membrane transporter identification and modulation via adaptive laboratory evolution. Metab. Eng. 72, 376–390. https://doi.org/10.1016/j.ymben.2022.05.004

Rahim, M., Ragavan, M., Deja, S., Merritt, M.E., Burgess, S.C., Young, J.D., 2022. INCA 2.0: A tool for integrated, dynamic modeling of NMR- and MS-based isotopomer measurements and rigorous metabolic flux analysis. Metab. Eng. 69, 275–285. https://doi.org/10.1016/j.ymben.2021.12.009

Rix, G., Watkins-Dulaney, E.J., Almhjell, P.J., Boville, C.E., Arnold, F.H., Liu, C.C., 2020. Scalable continuous evolution for the generation of diverse enzyme variants encompassing promiscuous activities. Nat. Commun. 11, 5644. https://doi.org/10.1038/s41467-020-19539-6

Rohe, P., Venkanna, D., Kleine, B., Freudl, R., Oldiges, M., 2012. An automated workflow for enhancing microbial bioprocess optimization on a novel microbioreactor platform. Microb. Cell Factories 11, 144. https://doi.org/10.1186/1475-2859-11-144

Romero, M.F., Kanai, Y., Gunshin, H., Hediger, M.A., 1998. [2] Expression cloning using Xenopus laevis oocytes, in: Methods in Enzymology. Elsevier, pp. 17–52. https://doi.org/10.1016/S0076-6879(98)96004-9

Runguphan, W., Qu, X., O'Connor, S.E., 2010. Integrating carbon–halogen bond formation into medicinal plant metabolism. Nature 468, 461–464. https://doi.org/10.1038/nature09524

Sharma, S.V., Tong, X., Pubill-Ulldemolins, C., Cartmell, C., Bogosyan, E.J.A., Rackham, E.J., Marelli, E., Hamed, R.B., Goss, R.J.M., 2017. Living GenoChemetics by hyphenating synthetic biology and synthetic chemistry in vivo. Nat. Commun. 8, 229. https://doi.org/10.1038/s41467-017-00194-3

Sivapuratharasan, V., Lenzen, C., Michel, C., Muthukrishnan, A.B., Jayaraman, G., Blank, L.M., 2022. Metabolic engineering of Pseudomonas taiwanensis VLB120 for rhamnolipid biosynthesis from biomass-derived aromatics. Metab. Eng. Commun. 15, e00202. https://doi.org/10.1016/j.mec.2022.e00202

Srivastava, V., Amanna, R., Rowden, S.J.L., Sengupta, S., Madhu, S., Howe, C.J., Wangikar, P.P., 2021. Adaptive laboratory evolution of the fast-growing cyanobacterium Synechococcus elongatus PCC 11801 for improved solvent tolerance. J. Biosci. Bioeng. 131, 491–500. https://doi.org/10.1016/j.jbiosc.2020.11.012

Suástegui, M., Guo, W., Feng, X., Shao, Z., 2016. Investigating strain dependency in the production of aromatic compounds in Saccharomyces cerevisiae. Biotechnol. Bioeng. 113, 2676–2685. https://doi.org/10.1002/bit.26037

van der Hoek, S.A., Rusnák, M., Jacobsen, I.H., Martínez, J.L., Kell, D.B., Borodina, I., 2022a. Engineering ergothioneine production in *Yarrowia lipolytica*. FEBS Lett. 596, 1356–1364. https://doi.org/10.1002/1873-3468.14239

van der Hoek, S.A., Rusnák, M., Wang, G., Stanchev, L.D., de Fátima Alves, L., Jessop-Fabre, M.M., Paramasivan, K., Jacobsen, I.H., Sonnenschein, N., Martínez, J.L., Darbani, B., Kell, D.B., Borodina, I., 2022b. Engineering precursor supply for the high-level production of ergothioneine in Saccharomyces cerevisiae. Metab. Eng. 70, 129–142. https://doi.org/10.1016/j.ymben.2022.01.012

Veldmann, K.H., Dachwitz, S., Risse, J.M., Lee, J.-H., Sewald, N., Wendisch, V.F., 2019a. Bromination of L-tryptophan in a Fermentative Process With Corynebacterium glutamicum. Front. Bioeng. Biotechnol. 7. https://doi.org/10.3389/fbioe.2019.00219

Veldmann, K.H., Minges, H., Sewald, N., Lee, J.-H., Wendisch, V.F., 2019b. Metabolic engineering of Corynebacterium glutamicum for the fermentative production of halogenated tryptophan. J. Biotechnol. 291, 7–16. https://doi.org/10.1016/j.jbiotec.2018.12.008

Wang, G., Møller-Hansen, I., Babaei, M., D'Ambrosio, V., Christensen, H.B., Darbani, B., Jensen, M.K., Borodina, I., 2021. Transportome-wide engineering of Saccharomyces cerevisiae. Metab. Eng. 64, 52–63. https://doi.org/10.1016/j.ymben.2021.01.007

Wang, Yina, Liu, Xiaonan, Chen, B., Liu, W., Guo, Z., Liu, Xiangyu, Zhu, X., Liu, J., Zhang, J., Li, J., Zhang, L., Gao, Y., Zhang, G., Wang, Yan, Choudhary, M.I., Yang, S., Jiang, H., 2022. Metabolic engineering of Yarrowia lipolytica for scutellarin production. Synth. Syst. Biotechnol. 7, 958–964. https://doi.org/10.1016/j.synbio.2022.05.009

Wei, W., Zhang, P., Shang, Y., Zhou, Y., Ye, B.-C., 2020. Metabolically engineering of Yarrowia lipolytica for the biosynthesis of naringenin from a mixture of glucose and xylose. Bioresour. Technol. 123726. https://doi.org/10.1016/j.biortech.2020.123726

Wewetzer, S.J., Kunze, M., Ladner, T., Luchterhand, B., Roth, S., Rahmen, N., Kloß, R., Costa e Silva, A., Regestein, L., Büchs, J., 2015. Parallel use of shake flask and microtiter plate online measuring devices (RAMOS and BioLector) reduces the number of experiments in laboratory-scale stirred tank bioreactors. J. Biol. Eng. 9, 9. https://doi.org/10.1186/s13036-015-0005-0

Wordofa, G.G., Kristensen, M., 2018. Tolerance and metabolic response of Pseudomonas taiwanensis VLB120 towards biomass hydrolysate-derived inhibitors. Biotechnol. Biofuels 11, 199. https://doi.org/10.1186/s13068-018-1192-y

Wynands, B., Otto, M., Runge, N., Preckel, S., Polen, T., Blank, L.M., Wierckx, N., 2019. Streamlined *Pseudomonas taiwanensis* VLB120 Chassis Strains with Improved Bioprocess Features. ACS Synth. Biol. 8, 2036–2050. https://doi.org/10.1021/acssynbio.9b00108

Yaashikaa, P.R., Kumar, P.S., Saravanan, A., Varjani, S., Ramamurthy, R., 2020. Bioconversion of municipal solid waste into bio-based products: A review on valorisation and sustainable approach for circular bioeconomy. Sci. Total Environ. 748, 141312. https://doi.org/10.1016/j.scitotenv.2020.141312

Yerkes, N., Wu, J.X., McCoy, E., Galan, M.C., Chen, S., O'Connor, S.E., 2008. Substrate specificity and diastereoselectivity of strictosidine glucosidase, a key enzyme in monoterpene indole alkaloid biosynthesis. Bioorg. Med. Chem. Lett. 18, 3095–3098. https://doi.org/10.1016/j.bmcl.2007.11.063

Young, J.D., 2014. INCA: a computational platform for isotopically non-stationary metabolic flux analysis. Bioinformatics 30, 1333–1335. https://doi.org/10.1093/bioinformatics/btu015

Zemlan, F.P., Mulchahey, J.J., Scharf, M.B., Mayleben, D.W., Rosenberg, R., Lankford, A., 2005. The Efficacy and Safety of the Melatonin Agonist beta-Methyl-6-Chloromelatonin in Primary Insomnia: A Randomized, Placebo-Controlled, Crossover Clinical Trial. J. Clin. Psychiatry 66, 384–390. https://doi.org/10.4088/JCP.v66n0316

Zhang, J., Hansen, L.G., Gudich, O., Viehrig, K., Lassen, L.M.M., Schrübbers, L., Adhikari, K.B., Rubaszka, P., Carrasquer-Alvarez, E., Chen, L., D'Ambrosio, V., Lehka, B., Haidar, A.K., Nallapareddy, S., Giannakou, K., Laloux, M., Arsovska, D., Jørgensen, M.A.K., Chan, L.J.G., Kristensen, M., Christensen, H.B., Sudarsan, S., Stander, E.A., Baidoo, E., Petzold, C.J., Wulff, T., O'Connor, S.E., Courdavault, V., Jensen, M.K., Keasling, J.D., 2022. A microbial supply chain for production of the anti-cancer drug vinblastine. Nature 609, 341–347. https://doi.org/10.1038/s41586-022-05157-3

Zhang, L., Yang, H., Xia, Y., Shen, W., Liu, L., Li, Q., Chen, X., 2022. Engineering the oleaginous yeast Candida tropicalis for α-humulene overproduction. Biotechnol. Biofuels Bioprod. 15, 59. https://doi.org/10.1186/s13068-022-02160-8

Engineering microbial hosts for the production of aromatic compounds

PhD thesis by Javier Sáez Sáez

Main supervisor: Prof. Irina Borodina

Co-supervisors: Dr. Mahsa Babaei, Dr. Sheila Ingemann Jensen

The Novo Nordisk Foundation Center for Biosustainability

Technical University of Denmark

The Novo Nordisk Foundation Center for Biosustainability
Technical University of Denmark

Building 220, Kemitorvet
2800 Kgs. Lyngby, Denmark
(+45) 45 25 80 00
biosustain@biosustain.dtu.dk

DTU

The Novo Nordisk Foundation
Center for Biosustainability